



Stephen P. Radzevich

# Geometry of Surfaces

A Practical Guide for  
Mechanical Engineers

*Second Edition*



Springer

# Geometry of Surfaces

Stephen P. Radzevich

# Geometry of Surfaces

A Practical Guide for Mechanical Engineers

Second Edition

Stephen P. Radzevich  
Southfield Innovation Center  
Eaton Corporation  
Southfield, MI, USA

ISBN 978-3-030-22183-6      ISBN 978-3-030-22184-3 (eBook)  
<https://doi.org/10.1007/978-3-030-22184-3>

1<sup>st</sup> edition: © John Wiley & Sons, Ltd. 2013

2<sup>nd</sup> edition: © Springer Nature Switzerland AG 2020

This work is subject to copyright. All rights are reserved by the Publisher, whether the whole or part of the material is concerned, specifically the rights of translation, reprinting, reuse of illustrations, recitation, broadcasting, reproduction on microfilms or in any other physical way, and transmission or information storage and retrieval, electronic adaptation, computer software, or by similar or dissimilar methodology now known or hereafter developed.

The use of general descriptive names, registered names, trademarks, service marks, etc. in this publication does not imply, even in the absence of a specific statement, that such names are exempt from the relevant protective laws and regulations and therefore free for general use.

The publisher, the authors and the editors are safe to assume that the advice and information in this book are believed to be true and accurate at the date of publication. Neither the publisher nor the authors or the editors give a warranty, expressed or implied, with respect to the material contained herein or for any errors or omissions that may have been made. The publisher remains neutral with regard to jurisdictional claims in published maps and institutional affiliations.

This Springer imprint is published by the registered company Springer Nature Switzerland AG  
The registered company address is: Gewerbestrasse 11, 6330 Cham, Switzerland



*This book is dedicated to my wife Natasha*

# Preface

This book is about geometry of part surfaces, their generation, and interaction with one another.

Written by a mechanical engineer, this book is *not* on differential geometry of surfaces. Instead, the book is devoted to the application of methods those developed in differential geometry of surfaces, for the purposes of solving problems in mechanical engineering.

A paradox exists in our current understanding of geometry of surfaces: We know everything about ideal (perfect) surfaces, which do not exist in reality, and our knowledge about real surfaces that exist physically is limited. Therefore, one of the main goals of the book is to adjust our knowledge of ideal surfaces for the purposes of better understanding of geometry of real surfaces. In other words: the goal of the book is to bridge a gap between ideal and real surfaces.

One of the significant advantages of the book is due to that it is written *not* by a mathematician, but it is written by a mechanical engineer, and for mechanical engineers.

Southfield, MI, USA

Stephen P. Radzevich

# Acknowledgements

I would like to share the credit for any research success with my numerous doctoral students with whom I have tested the proposed ideas and applied them in the industry. The contributions of many friends, colleagues, and students in overwhelming number cannot be acknowledged individually, and as much as our benefactors have contributed, even though their kindness and help must go unrecorded.

My thanks also go to those at *Springer* who took over the final stages and who will have to cope with the marketing and sales of the fruit of my efforts.

# Introduction

Performance of parts depends in much on geometry of the interacting surfaces. An in-depth investigation of geometry of smooth regular part surfaces is undertaken in this book. Analytical description of the surfaces, methods of their generation, along with an analytical approach for description of the geometry of contact of the interacting part surfaces are covered in the book.

This book is comprised of three parts and appendices.

Specification of part surfaces in terms of corresponding nominal smooth regular surface is considered in Part I of the book.

Geometry of part surfaces is discussed in Chap. 1 of the book. The discussion begins with an analytical description of perfect (ideal) surfaces. Here, in this text ideal surface is interpreted as a zero-thickness film. Then difference between *Classical Differential Geometry* and *Engineering Geometry of Surfaces* is analyzed. This analysis is followed by an analytical description of real part surfaces, which is based on much of the analytical description of the corresponding ideal surface. It is shown that while remained unknown, real part surface is located in between two boundary surfaces. The said boundary surfaces are represented by two perfect surfaces of the upper tolerance and of the lower tolerance. Specification of surfaces ends with the discussion of the natural representation of a desired part surface. This consideration involves the first and the second fundamental forms of a smooth regular part surface. For an analytically specified surface, elements of its local geometry are outlined. This consideration includes but is not limited to analytical representation of unit tangent vectors, tangent plane, unit normal vector, unit vectors of principal directions on a part surface, and so forth. Ultimately, design parameters of part surface curvature are discussed. Mostly, equations for principal surface curvatures along with normal curvatures at a surface point are considered. In addition to that mean curvature, *Gaussian* curvature, absolute curvature, shape operator, and curvedness of a surface at a point are considered. The classification of local part surface patches is proposed in this section of the book. The classification is followed by a circular chart comprised of all possible kinds of local part surface patches.

Chapter 2 is devoted to the analysis of a possibility of classification of part surfaces. Regardless of no scientific classification of smooth regular surfaces in

global sense is feasible in nature, local part surface patches can be classified. For the investigation of geometry of local part surface patches, planar characteristic images are employed. In this analysis, *Dupin* indicatrix, curvature indicatrix, and circular diagrams at a part surface point are covered in detail. Based on the obtained results of the analysis, two more circular charts are developed. One of them employs the part surface curvature indicatrices, while another one is based on the properties of circular diagrams at a current part surface point. This section of the book ends with a brief consideration of one more useful characteristic curve, which can be helpful for analytical description of geometry of a part surface locally.

In Part II, geometry of contact of two smooth regular part surfaces is considered. This part of the book is comprised of four chapters.

In Chap. 3, the discussion begins with review of earlier works in the field of contact geometry of surfaces. This includes order of contact of two surfaces, local relative orientation of the surfaces at a point of their contact, the first-order and the second-order analysis. The first-order analysis is limited just to the common tangent plane. The second-order analysis begins with the author's comments on analytical description of the local geometry of contacting surfaces loaded by a normal force: *Hertz's* proportional assumption. Then, the surface of relative normal curvature is considered. *Dupin* indicatrix and curvature indicatrix of the surface of relative normal curvature are discussed. This analysis is followed by the discussion of the surface of relative normal radii of curvature, normalized relative normal curvature along with a characteristic curve  $Ir_k(\mathcal{R})$  of novel kind.

This section of the monograph is followed by Chap. 4, in which an analytical method based on second fundamental forms of the contacting part surfaces is discussed. It is shown there that the resultant deviation of one of the contacting surfaces from the other contacting surface expressed in terms of the second fundamental forms of the contacting surfaces could be the best possible criterion for the analytical description of the contact geometry of two smooth regular surfaces. Such a criterion is legitimate, but it is computationally impractical. Thus, other analytical methods are required to be developed for this purpose.

In Chap. 5, a novel kind of characteristic curve for the purposes of analytical description of the contact geometry of two smooth regular part surfaces in the first order of tangency is discussed in detail. The discussion begins with preliminary remarks and follows with introduction and with derivation of an equation of the indicatrix of conformity  $Cnf_R(P_1/P_2)$  of two part surfaces. Then, directions of extremum degree of conformity of two part surfaces in contact are specified and are described analytically. This analysis is followed by determination and by derivation of corresponding equations of asymptotes of the indicatrix of conformity  $Cnf_R(P_1/P_2)$ . Capabilities of the indicatrix of conformity  $Cnf_R(P_1/P_2)$  of two smooth regular part surfaces  $P_1$  and  $P_2$  in the first order of tangency are compared with the corresponding capabilities of "*Dupin indicatrix Dup* ( $\mathcal{R}$ )" of the surface of relative curvature  $\mathcal{R}$ . Important properties of the indicatrix of conformity of two smooth regular part surfaces are outlined. Ultimately, the converse indicatrix of conformity  $Cnf_R^{cnv}(P_1/P_2)$  of two regular part surfaces in the first order of tangency is introduced and is briefly discussed as an alternative to the regular indicatrix of conformity  $Cnf_R(P_1/P_2)$ .

In Chap. 6, more characteristic curves are derived on the premises of “*Plücker conoid*” constructed at a point of a smooth regular part surface. At the beginning, main properties of the surface of “*Plücker conoid*” are briefly outlined. This includes but not limited to basics, analytical representation, and local properties along with auxiliary formulae. This analysis is followed by analytical description of local geometry of a smooth regular part surface. Ultimately, expressions for two more characteristic curves are derived. These newly introduced characteristic curves are referred to as *Plücker curvature indicatrix* and  $\mathcal{M}_R(P_1)$ -indicatrix of a part surface. The performed analysis makes it possible derivation of equations for two more planar characteristic curves for analytical description of the contact geometry of two smooth regular part surfaces  $P_1$  and  $P_2$  at a point of their contact. One of the newly derived characteristic curves is referred to as “ $\mathcal{M}_R(P_1/P_2)$ -relative indicatrix of the first kind” of two contacting part surfaces  $P_1$  and  $P_2$ . Another one is a curve inverse to the characteristic curve  $\mathcal{M}_R(P_1/P_2)$ . This second characteristic curve is referred to as “ $\mathcal{M}_k(P_1/P_2)$ -relative indicatrix of the second kind.” Main properties of both the characteristic curves are briefly discussed in this section of the monograph.

Feasible kinds of contact of two smooth regular part surfaces in the first order of tangency are discussed in Chap. 7. Analytical description of contact geometry of two smooth regular surfaces begins with investigation of a possibility of implementation of the indicatrix of conformity for the purposes of identification of actual kind of contact of two smooth regular part surfaces. Then, impact of accuracy of the computation of the parameters of the indicatrix of conformity  $Cnf_R(P_1/P_2)$  of two part surfaces is investigated. Ultimately, a classification of all possible kinds of contact of two smooth regular part surfaces in the first order of tangency is developed.

Various kinds of mapping of a part surface onto another part surface are discussed in Part III of the monograph. The discussion in this part of the monograph begins with a novel kind of the surfaces mapping, the so-called  $\mathbb{R}$ -mapping of the interacting part surfaces.

In Chap. 8, a novel method of the surfaces mapping, namely  $\mathbb{R}$ -mapping of the interacting part surfaces is disclosed. The preliminary remarks on the developed approach is followed by an in-detail consideration of the concept underlying in the  $\mathbb{R}$ -mapping of the interacting part surfaces. Then, principal features of  $\mathbb{R}$ -mapping of a part surface  $P_1$  onto another part surface  $P_2$  are disclosed. Due to  $\mathbb{R}$ -mapping of surface returns an equation of the mapped surface in natural representation, namely, in terms of fundamental magnitudes of the first and of the second order, the derived equation of the mapped surface is required been reconstructed and been represented in a convenient reference system. This issue got a comprehensive discussion in this chapter of the monograph. Consideration in the chapter ends with two examples of implementation of the discussed method of part surfaces mapping.

General consideration of generation of enveloping surface is discussed in Chap. 9. The consideration begins with the analysis of generation of an envelope to successive positions of a moving planar curve. Then, the discussion is extended to generation of the enveloping surface to successive positions of a moving smooth regular part surface. Enveloping surfaces to one-parametric as well as to two-parametric family of surfaces are covered in this section of the monograph. Further, the “*kinematic*

*method*” for generation of enveloping surfaces is introduced. The method was developed in 1940 by Dr. V. A. Shishkov. Implementation of the kinematic method for generation of one-parametric enveloping surfaces is disclosed. Then, the approach is extended to multi-parametric motion of a smooth regular part surface.

In Chap. 10, special cases of generation of enveloping surfaces are disclosed. For this purpose, a concept of reversibly enveloping surfaces is introduced. For the generation of reversibly enveloping surfaces, a novel method is proposed. This method is illustrated by an example of generation of reversibly enveloping surfaces in case tooth flanks for geometrically accurate (ideal) crossed-axis gear pairs. The performed analysis makes it possible a conclusion that two *Olivier principles* of generation of enveloping surfaces:

- in general case are not valid and
- in a degenerate case these two principles are useless

Ultimately, there is no sense to apply *Olivier principles* for the purpose of generation of reversibly enveloping smooth regular part surfaces.

Part surfaces those allow for sliding over themselves are considered as a particular degenerated case of enveloping surfaces.

Appendices’ section contains reference material that is useful in practical applications.

Elements of vector algebra are briefly outlined in Appendix A.

In Appendix B, elements of coordinate system transformation are represented. This section of the book also includes direct transformation of the surface fundamental forms. The latter makes it possible to avoid calculation of the first and of the second derivatives of the part surface equation, after the equation is represented in a new reference system.

Formulae for changing of surface parameters are represented in Appendix C.

In Appendix D, the closest distance of approach between two smooth regular surfaces is discussed.

A book of this size is likely to contain omissions and errors. If you have any constructive suggestions, please communicate them to the author via e-mail: [sp\\_radzevich@yahoo.com](mailto:sp_radzevich@yahoo.com).

Sterling Heights, MI, USA

Stephen P. Radzevich

# Contents

## Part I Part Surfaces

<b>1</b>	<b>Geometry of a Part Surface</b>	<b>3</b>
1.1	On Analytical Description of Perfect Surfaces	3
1.1.1	General Form of Representation of Smooth Regular Part Surfaces	6
1.1.2	Essentials of Piecewise Approximation of Sculptured Part Surfaces	7
1.1.3	Algebraic and Geometric Form	8
1.1.4	Significance of the Unit Tangent Vectors	10
1.2	On the Difference Between “ <i>Classical Differential Geometry</i> ” and “ <i>Engineering Geometry of Surfaces</i> ”	11
1.3	On the Analytical Description of Part Surfaces	13
1.4	Boundary Surfaces for Actual Part Surface	15
1.5	Natural Representation of Desired Part Surface	17
1.5.1	First Fundamental Form of a Desired Part Surface	18
1.5.2	Second Fundamental Form of a Desired Part Surface	20
1.5.3	Illustrative Example	23
1.6	Elements of Local Geometry of Desired Part Surface	26
1.6.1	Unit Vectors of Principal Directions at Point on Part Surface	27
1.6.2	Principal Curvatures at Point of Part Surface	28
1.6.3	Other Parameters of Part Surface Curvature	30
	References	33
<b>2</b>	<b>On a Possibility of Classification of Part Surfaces</b>	<b>35</b>
2.1	Sculptured Part Surfaces	35
2.1.1	Local Patches of Perfect Part Surfaces	36
2.1.2	Local Patches of Real Part Surfaces	37



2.2	Planar Characteristic Images . . . . .	43
2.2.1	Dupin Indicatrix . . . . .	43
2.2.2	Curvature Indicatrix . . . . .	47
2.2.3	Circular Chart of Curvature Indicatrices for Local Patches of Smooth Regular Part Surfaces. . . . .	49
2.3	Circular Diagrams at a Surface Point . . . . .	51
2.3.1	Circular Diagrams . . . . .	51
2.3.2	Circular Chart of Circular Diagrams for Local Patches of Smooth Regular Part Surfaces. . . . .	62
2.4	One More Useful Characteristic Curve . . . . .	62
	References . . . . .	64

## Part II Contact Geometry of Part Surfaces

<b>3</b>	<b>Early Works in the Field of Contact Geometry of Surfaces . . . . .</b>	<b>67</b>
3.1	Order of Contact. . . . .	67
3.2	Contact Geometry of Part Surfaces . . . . .	69
3.3	Local Relative Orientation of Contacting Part Surfaces . . . . .	69
3.4	First-Order Analysis: Common Tangent Plane . . . . .	75
3.5	Second-Order Analysis . . . . .	76
3.5.1	Comments on Analytical Description of Local Geometry of Contacting Surfaces Loaded by a Normal Force: “ <i>Hertz Proportional Assumption</i> ” . . . . .	76
3.5.2	Surface of Normal Relative Curvature . . . . .	79
3.5.3	“ <i>Dupin Indicatrix</i> ” at a Point of Surface of Relative Normal Curvature. . . . .	83
3.5.4	Matrix Representation of Equation of “ <i>Dupin Indicatrix</i> ” at a Point of Surface of Relative Normal Curvature. . . . .	84
3.5.5	Surface of Relative Normal Radii of Curvature . . . . .	85
3.5.6	Normalized Relative Normal Curvature . . . . .	85
3.5.7	Curvature Indicatrix of Surface of Relative Normal Curvature. . . . .	86
3.6	A Characteristic Curve $\Im\Re_k(\mathcal{R})$ of a Novel Kind. . . . .	89
	References . . . . .	90
<b>4</b>	<b>An Analytical Method Based on the Second Fundamental Forms of Contacting Part Surfaces . . . . .</b>	<b>91</b>
	Reference . . . . .	95
<b>5</b>	<b>Indicatrix of Conformity at Point of Contact of Two Smooth Regular Part Surfaces in the First Order of Tangency . . . . .</b>	<b>97</b>
5.1	Preliminary Remarks . . . . .	97
5.2	“ <i>Indicatrix of Conformity</i> ” at Point of Contact of Two Smooth Regular Part Surfaces in the First Order of Tangency . . . . .	101

5.3	Directions of Extremum Degree of Conformity of Two Part Surfaces in Contact . . . . .	109
5.4	Asymptotes of the Indicatrix of Conformity $Cnf_R(P_1/P_2)$ . . . . .	112
5.5	Comparison of the Capabilities of the “ <i>Indicatrix of Conformity</i> $Cnf_R(P_1/P_2)$ ” and of the “ <i>Dupin Indicatrix Dup (R)</i> ” of the Surface of Relative Curvature . . . . .	113
5.6	Important Properties of the Indicatrix of Conformity $Cnf_R(P/T)$ at Point of Contact of Two Smooth Regular Part Surfaces . . . . .	114
5.7	The “ <i>Converse Indicatrix of Conformity</i> ” at Point of Contact of Two Regular Part Surfaces in the First Order of Tangency . . . . .	115
	References . . . . .	117
<b>6</b>	<b>“<i>Plücker Conoid</i>”: More Characteristic Curves . . . . .</b>	<b>119</b>
6.1	“ <i>Plücker Conoid</i> ” . . . . .	119
6.1.1	Basics . . . . .	120
6.1.2	Analytical Representation . . . . .	120
6.1.3	Local Properties . . . . .	122
6.1.4	Auxiliary Formulae . . . . .	123
6.2	On Analytical Description of Local Geometry of Smooth Regular Part Surface . . . . .	123
6.2.1	Preliminary Remarks . . . . .	124
6.2.2	The “ <i>Plücker Conoid</i> ” . . . . .	125
6.2.3	“ <i>Plücker Curvature Indicatrix</i> ” . . . . .	127
6.2.4	$\mathcal{H}_R(P_1)$ -Indicatrix at a Point of a Part Surface . . . . .	129
6.3	Relative Characteristic Curve . . . . .	131
6.3.1	On a Possibility of Implementation of Two “ <i>Plücker Conoids</i> ” . . . . .	131
6.3.2	“ $\mathcal{H}_R(P_1/P_2)$ -Relative Indicatrix” at Point of Contact of Two Part Surfaces $P_1$ and $P_2$ . . . . .	133
	References . . . . .	136
<b>7</b>	<b>Possible Kinds of Contact of Two Smooth Regular Part Surfaces in the First Order of Tangency . . . . .</b>	<b>137</b>
7.1	On a Possibility of Implementation of the Indicatrix of Conformity for the Purposes of Identification of the Actual Kind of Contact of Two Smooth Regular Part Surfaces . . . . .	137
7.1.1	Impact of Accuracy of Computation on the Parameters of the Indicatrices of Conformity $Cnf_R(P_1/P_2)$ . . . . .	141
7.1.2	Classification of Possible Kinds of Contact of Two Smooth Regular Part Surfaces . . . . .	143
	Reference . . . . .	150

## Part III Mapping of Contacting Part Surfaces

<b>8</b>	<b><math>\mathbb{R}</math>-Mapping of Interacting Part Surfaces</b>	153
8.1	Preliminary Remarks	153
8.2	On the Concept of $\mathbb{R}$ -Mapping of Interacting Part Surfaces	155
8.3	$\mathbb{R}$ -Mapping of a Part Surface $P_1$ onto Part Surface $P_2$	157
8.4	Reconstruction of Mapped Part Surface	161
8.5	Illustrative Examples of Calculation of Design Parameters of Mapped Part Surface	162
	References	165
<b>9</b>	<b>Generation of Enveloping Surfaces: General Consideration</b>	167
9.1	Envelope for Successive Positions of a Moving Planar Curve	167
9.2	Envelope for Successive Positions of Moving Surface	170
9.2.1	Envelope for One-Parametric Family of Surfaces	171
9.2.2	Envelope for Two-Parametric Family of Surfaces	173
9.3	“ <i>Kinematic Method</i> ” for Determining Enveloping Surfaces	176
9.4	Peculiarities of Implementation of the “ <i>Kinematic Method</i> ” in Cases of Multi-parametric Relative Motion of Surfaces	188
	References	189
<b>10</b>	<b>Generation of Enveloping Surfaces: Special Cases</b>	191
10.1	Part Surfaces that Allow for “ <i>Sliding Over Themselves</i> ”	191
10.2	Reversibly Enveloping Surfaces: Introductory Remarks	194
10.3	Generation of Reversibly Enveloping Surfaces	206
10.3.1	Kinematics of Crossed-Axes Gearing	206
10.3.2	Base Cones in Crossed-Axes Gear Pairs	208
10.3.3	Tooth Flanks in Perfect Crossed-Axes Gear Pairs	212
10.3.4	Tooth Flank of a Gear in Crossed-Axes Gear Pair	218
10.4	On Looseness of Two “ <i>Olivier Principles</i> ”	223
10.4.1	An Example of Implementation of the “ <i>First Olivier Principle</i> ” for Generation of Enveloping Surfaces in a Degenerate Case	228
10.4.2	An Example of Implementation of the “ <i>Second Olivier Principle</i> ” for Generation of Enveloping Surfaces in a Degenerate Case	230
10.4.3	Concluding Remarks	231
	References	232
	<b>Conclusion</b>	233
	<b>Appendix A: Elements of Vector Calculus</b>	237
	<b>Appendix B: Applied Coordinate Systems and Linear Transformations</b>	243

**Appendix C: Change of Surface Parameters . . . . . 281**

**Appendix D: Closest Distance of Approach Between Two Part  
Surfaces . . . . . 283**

**Glossary . . . . . 291**

**Bibliography . . . . . 295**

**Index . . . . . 301**

## About the Author



**Dr. Stephen P. Radzevich** is Professor of Mechanical Engineering and Professor of Manufacturing Engineering. He received the M.Sc. (1976), the Ph.D. (1982), and the Dr.(Eng)Sc. (1991) all in mechanical engineering. He has extensive industrial experience in gear design and manufacture. He has developed numerous software packages dealing with CAD and CAM of precise gear finishing for a variety of industrial sponsors. His main research interest is *kinematic geometry of surface generation*, particularly with the focus on (a) precision gear design, (b) high-power-density gear trains, (c) torque share in multi-flow gear trains, (d) design of special purpose gear cutting/finishing tools, (e) design and machining (finishing) of precision gears for low-noise/noiseless transmissions of cars, light trucks, *etc.* He has spent about 40 years developing software, hardware, and other processes for gear design an optimization. Besides his work for industry, he trains engineering students at universities and gear engineers in companies. He authored and co-authored over 30 monographs, handbooks, and textbooks. The monographs entitled *Generation of Surfaces* (2001), *Kinematic Geometry of Surface Machining* (CRC Press, 2008), *CAD/CAM of Sculptured Surfaces on Multi-Axis NC Machine: The DG/K-Based Approach* (M&C Publishers, 2008), *Gear Cutting Tools: Fundamentals of Design and Computation* (CRC Press, 2010, 2nd edition 2017), *Precision Gear Shaving* (Nova Science Publishers, 2010), *Dudley's Handbook of Practical Gear Design and Manufacture* (CRC Press, 2012, 2nd edition 2016), *Theory of Gearing: Kinematics,*

*Geometry, and Synthesis* (CRC Press, 2012, 2nd edition 2018), *Geometry of Surfaces: A Practical Guide for Mechanical Engineers* (2013) are among the recently published volumes. He also authored and co-authored about 350 scientific papers and holds over 260 patents on inventions in the field of his scientific interests, both, USA patents on inventions, and International.

# Notations

$A_{P_1}$	Is the apex of the base cone of the part surface $P_1$
$A_{P_2}$	Is the apex of the base cone of the part surface $P_2$
$A_{pa}$	Is the plane-of-action apex
$C$	Is the center distance
$C_{1.P_1}, C_{2.P_1}$	Are the first and second principal plane sections of the traveling part surface $P_1$
$C_{1.P_2}, C_{2.P_2}$	Are the first and second principal plane sections of the generated part surface $P_2$ (the enveloping surface)
$Cnf_R(P_1/P_2)$	Is the indicatrix of conformity at a point of contact of two smooth regular part surfaces $P_1$ and $P_2$
$Cnf_k(P_1/R_2)$	Is the indicatrix of conformity that is converse to the indicatrix $Cnf_R(P_1/P_2)$
$E$	Is the characteristic line
$E_{P_1}, F_{P_1}, G_{P_1}$	Are the fundamental magnitudes of the first order of the smooth regular part surface $P_1$
$E_{P_2}, F_{P_2}, G_{P_2}$	Are the fundamental magnitudes of the first order of the smooth regular part surface $P_2$
$G_P$	Is the full curvature of a part surface $P$ at a point $m$
$M_P$	Is the mean curvature of a surface $P$ at a point $m$
$K$	Is the point of contact of two smooth regular part surfaces $P_1$ and $P_2$ (or a point within a line of contact of the part surfaces $P_1$ and $P_2$ )
$LC$	Is the line of contact between two regular part surfaces $P_1$ and $P_2$
$L_{P_1}, M_{P_1}, N_{P_1}$	Are the fundamental magnitudes of the second order of the smooth regular part surface $P_1$
$L_{P_2}, M_{P_2}, N_{P_2}$	Are the fundamental magnitudes of the second order of the smooth regular part surface $P_2$
$O_{P_1}$	Is the axis of rotation of the part surface $P_1$
$O_{P_2}$	Is the axis of rotation of the part surface $P_2$
$O_{pa}$	Is the axis of rotation of the plane of action, $PA$

$PA$	Is the plane of action
$P_{ln}$	Is the axis of instant rotation of two regular part surfaces $P_1$ and $P_2$ in relation to one another
$\mathbf{Rc}(PA \mapsto G)$	Is the operator of rolling/sliding (the operator of transition from the plane of action, $PA$ , to the gear, $G$ , in crossed-axes gearing)
$\mathbf{Rc}(PA \mapsto P)$	Is the operator of rolling/sliding (the operator of transition from the plane of action, $PA$ , to the pinion, $P$ , in crossed-axes gearing)
$\mathbf{Rl}_x(\varphi_y, Y)$	Is the operator of rolling over a plane ( $Y$ -axis is the axis of rotation, $X$ -axis is the axis of translation)
$\mathbf{Rl}_z(\varphi_y, Y)$	Is the operator of rolling over a plane ( $Y$ -axis is the axis of rotation, $Z$ -axis is the axis of translation)
$\mathbf{Rl}_y(\varphi_x, X)$	Is the operator of rolling over a plane ( $X$ -axis is the axis of rotation, $Y$ -axis is the axis of translation)
$\mathbf{Rl}_z(\varphi_x, X)$	Is the operator of rolling over a plane ( $X$ -axis is the axis of rotation, $Z$ -axis is the axis of translation)
$\mathbf{Rl}_x(\varphi_z, Z)$	Is the operator of rolling over a plane ( $Z$ -axis is the axis of rotation, $X$ -axis is the axis of translation)
$\mathbf{Rl}_y(\varphi_z, Z)$	Is the operator of rolling over a plane ( $Z$ -axis is the axis of rotation, $Y$ -axis is the axis of translation)
$\mathbf{Rr}_u(\varphi, Z)$	Is the operator of rolling of two coordinate systems
$\mathbf{Rs}(A \mapsto B)$	Is the operator of the resultant coordinate system transformation, say from a coordinate system $A$ to a coordinate system $B$
$\mathbf{Rt}(\varphi_x, X)$	Is the operator of rotation through an angle $\varphi_x$ about $X$ -axis
$\mathbf{Rt}(\varphi_y, Y)$	Is the operator of rotation through an angle $\varphi_y$ about $Y$ -axis
$\mathbf{Rt}(\varphi_z, Z)$	Is the operator of rotation through an angle $\varphi_z$ about $Z$ -axis
$R_{1.P1}, R_{2.P1}$	Are the first and the second principal radii of the gear tooth flank $P_1$
$R_{1.P2}, R_{2.P2}$	Are the first and the second principal radii of the gear tooth flank $P_2$
$\mathbf{Sc}_x(\varphi_x, p_x)$	Is the operator of screw motion about the $X$ -axis
$\mathbf{Sc}_y(\varphi_y, p_y)$	Is the operator of screw motion about the $Y$ -axis
$\mathbf{Sc}_z(\varphi_z, p_z)$	Is the operator of screw motion about the $Z$ -axis
$\mathbf{Tr}(a_x, X)$	Is the operator of translation at a distance $a_x$ along the $X$ -axis
$\mathbf{Tr}(a_y, Y)$	Is the operator of translation at a distance $a_y$ along the $Y$ -axis
$\mathbf{Tr}(a_z, Z)$	Is the operator of translation at a distance $a_z$ along the $Z$ -axis
$U_{P1}, V_{P1}$	Is the curvilinear (gaussian) coordinates of a point of a smooth regular part surface $P_1$
$U_{P2}, V_{P2}$	Is the curvilinear (gaussian) coordinates of a point of a smooth regular part surface $P_2$
$\mathbf{U}_{P1}, \mathbf{V}_{P1}$	Are the tangent vectors to curvilinear coordinate lines on a smooth regular part surface $P_1$
$\mathbf{U}_{P2}, \mathbf{V}_{P2}$	Are the tangent vectors to curvilinear coordinate lines on a smooth regular part surface $P_2$



$\mathbf{V}_\Sigma$	Is the linear velocity vector of the resultant motion of the smooth regular part surface $P_1$ in relation to a reference system, which the smooth regular part surface $P_2$ will be associated with
$d_{\text{cnf}}^{\min}$	Is the minimal diameter of the indicatrix of conformity, $\text{Cnf}_R(P_1/P_2)$ , for two smooth regular part surfaces $P_1$ and $P_2$ at a current contact point $K$
$k_{1.P1}, k_{2.P1}$	Are the first and second principal curvatures at a point of the smooth regular part surface $P_1$
$k_{1.P2}, k_{2.P2}$	Are the first and second principal curvatures at a point of the smooth regular part surface $P_2$
$\mathbf{n}_P$	Is the unit normal vector to a smooth regular part surface $P$
$p_{\text{sc}}$	Is the screw parameter (reduced pitch) of instant screw motion of the part surface $P_1$ in relation to the part surface $P_2$
$\mathbf{r}_{P1}$	Is the position vector of a point of a smooth regular part surface $P_1$
$r_{\text{cnf}}$	Is the position vector of a point of the indicatrix of conformity $\text{Cnf}_R(P_1/P_2)$ at a point of contact of two smooth regular part surfaces $P_1$ and $P_2$
$\mathbf{t}_{1.P1}, \mathbf{t}_{2.P1}$	Are the unit tangent vectors of principal directions at a point of the smooth regular part surface $P_1$
$\mathbf{t}_{1.P2}, \mathbf{t}_{2.P2}$	Are the unit tangent vectors of principal directions at a point of the smooth regular part surface $P_2$
$\mathbf{u}_{P1}, \mathbf{v}_{P1}$	Are the unit tangent vectors to curvilinear coordinate lines at a point of the smooth regular part surface $P_1$
$\mathbf{u}_{P2}, \mathbf{v}_{P2}$	Are the unit tangent vectors to curvilinear coordinate lines at a point of the smooth regular part surface $P_2$
$x_P y_P z_P$	Is the local <i>cartesian</i> coordinate system having its origin at a current point of contact of the part surfaces $P_1$ and $P_2$

## Greek Symbols

$\Phi_{1.P1}, \Phi_{2.P1}$	Are the first and second fundamental forms of the smooth regular part surface $P_1$
$\Phi_{1.P2}, \Phi_{2.P2}$	Are the first and second fundamental forms of the smooth regular part surface $P_2$
$\phi_{t,\omega}$	Is the transverse pressure angle
$\mu$	Is the angle of the part surfaces $P_1$ and $P_2$ local relative orientation
$\omega_{P1}$	Is the rotation vector of the regular part surface $P_1$
$\omega_{P2}$	Is the rotation vector of the part surface $P_2$
$\omega_{pl}$	Is the vector of instant rotation of the part surfaces $P_1$ and $P_2$ in relation to one another

## Subscripts

$\text{cnf}$	Conformity
$\text{max}$	Maximum
$\text{min}$	Minimum
$t$	Tangential
$\text{opt}$	Optimal

# Part I

## Part Surfaces

Design, production, and implementation of parts for products are common practice for most of the mechanical and manufacturing engineers. Any part can be viewed as a solid bounded by a certain number of surfaces. Two kinds of the bounding surfaces are recognized in this text; namely, they can be either “*working surfaces*” of a part, or they can be “not working surfaces” of a part. “*Working part surfaces*” interact either with one another or with the environment (with gas, air, fluids, or substances like sand). “*Not working part surfaces*” do not interact neither with one another, nor with the environment. The consideration below is mostly focused on the geometry of working part surfaces.

All part surfaces are reproduced on a solid. Appropriate manufacturing methods are used for these purposes. Due to that, part surfaces are often referred to as “*engineering surfaces*” in contrast to the surfaces that cannot be reproduced on a solid and which can exist only virtually [1–6].

Interaction with environment is the main purpose of all working part surfaces. Because of that, working part surfaces are also referred to as “*dynamic part surfaces*.” Air, gases, fluids, solids, and powders are perfect examples of environments which part surfaces are commonly interacting with. Moreover, part surfaces may interact with light, with electromagnetic fields of other nature, with sound waves, and so forth. Favorable parameters of part surface geometry are usually an output of a solution to complex problems in aerodynamics, hydrodynamics, contact interaction of solids with other solids, or solids with powder, as well as others.

In order to design and producing products with favorable performance, designing and manufacturing of part surfaces having favorable geometry are of critical importance. An appropriate analytical description of part surfaces is the first step to a better understanding of what do we need to design and how a desired part surface can be reproduced on a solid or, in other words, how a desired part surface can be manufactured.

Part I of the book is comprised of two chapters.

Chapter 1 is titled “Geometry of a Part Surface.”

Chapter 2 is titled “On a Possibility of Classification of Part Surfaces.”

## References

1. Radzevich, S. P. (2008). *CAD/CAM of sculptured surfaces on multi-axis NC machine: The DG/K-based approach* (p. 114). San Rafael, California: M&C Publishers.
2. Radzevich, S. P. (1991). *Differential-geometrical method of surface generation*, Doctoral Thesis, Tula, Tula Polytechnic Institute (p. 300).
3. Radzevich, S. P. (2001). *Fundamentals of surface generation* (Monograph, p. 592). Kiev: Rastan.
4. Radzevich, S. P. (2008). *Kinematic geometry of surface machining* (p. 536). Boca Raton Florida: CRC Press.
5. Radzevich, S. P. (1991). *Sculptured surface machining on multi-axis NC machine* (Monograph, p. 192). Kiev: Vishcha Schola.
6. Radzevich, S. P. (2014). *Generation of surfaces: Kinematic geometry of surface machining* (Monograph, p. 738). Boca Raton Florida: CRC Press.

# Chapter 1

## Geometry of a Part Surface



Variety of kinds of part surfaces approaches infinity. Plane surface, surfaces of revolution, surfaces of translation (that is, cylinders of general type, including, but not limited just to cylinders of revolution), and screw surfaces of a constant axial pitch can be found out in the design of all parts produced in the nowadays industry. Examples of part surfaces are illustrated in Fig. 1.1. As shown in Fig. 1.1, part surfaces feature a simple geometry. Most of the surfaces of these types allow for “*sliding over themselves*” [1].

Part surfaces of complex geometry are extensively used in the practice as well. Working surface of an impeller blade is a perfect example of the part surface having a complex geometry. Part surfaces of this kind are commonly referred to as the “*sculptured part surfaces*” or “*free form part surfaces*.” Example of a sculptured part surface is depicted in Fig. 1.2. Figure 1.3 [2] gives an insight into the origin of the term “*sculptured part surfaces*.” Commonly, a diagram similar to that shown in Fig. 1.4 is used to depict a sculptured part surface patch.

Sculptured part surfaces do not allow for “*sliding over themselves*.” Moreover, the design parameters of the local geometry of a sculptured part surface at any two infinitesimally close points within the surface patch differ from each other.

More examples of part surfaces of complex geometry can be found out in various industries, in the field of design and in production of gear cutting tools in particular [3].

### 1.1 On Analytical Description of Perfect Surfaces

In this section of the book, some important design parameters of perfect part surfaces are briefly outlined.

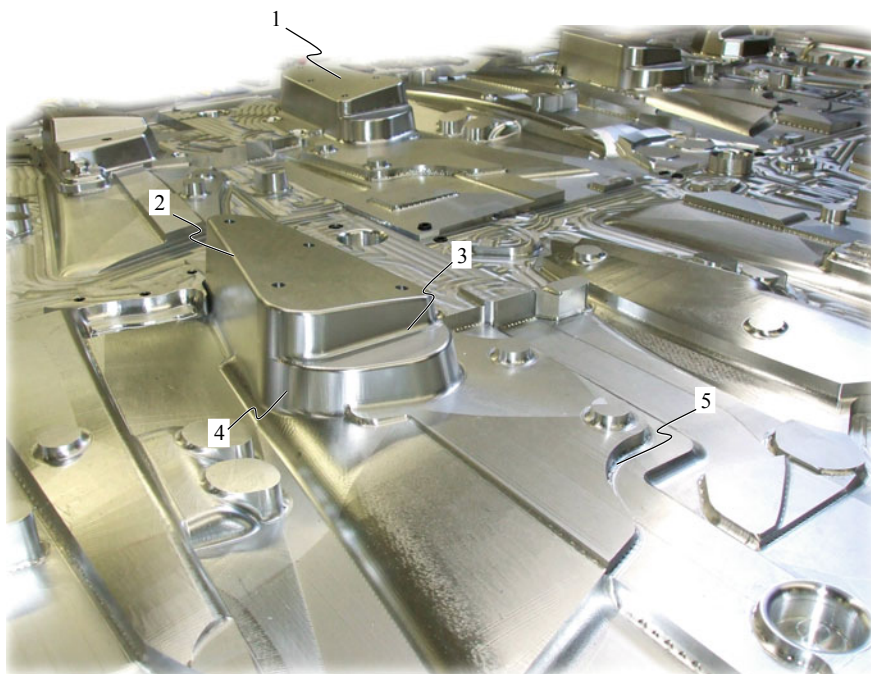


**Fig. 1.1** Examples of smooth regular part surfaces: a plane (1), an outer cylinder of revolution (2), an inner cylinder of revolution (3), a cone of revolution (4), and a torus (5), used in the design of a die



**Fig. 1.2** Working surface of impeller is a perfect example of a smooth regular sculptured part surface

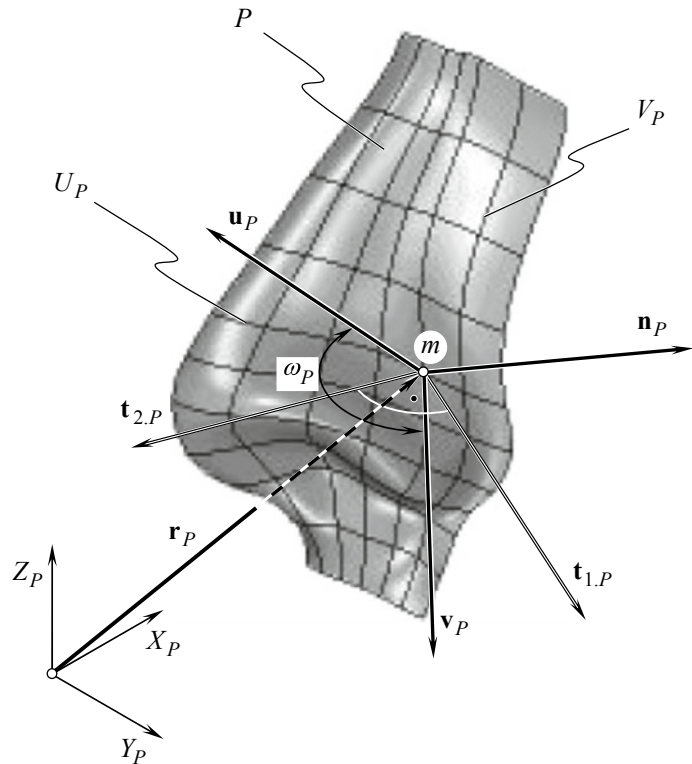


Fig. 1.3 On the origination of the term “sculptured part surface” Adapted from [2]

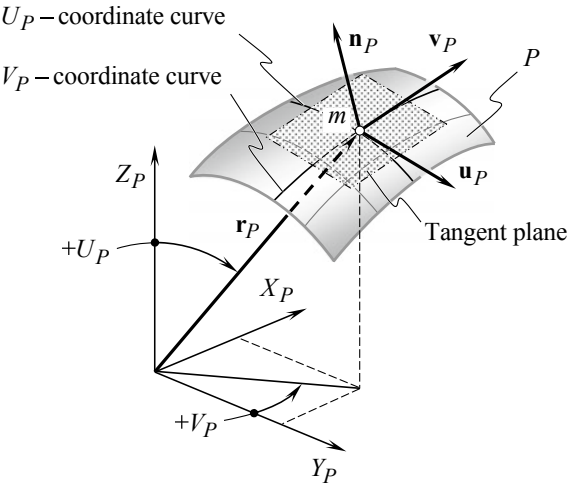


Fig. 1.4 On analytical description of a perfect part surface,  $P$

### 1.1.1 General Form of Representation of Smooth Regular Part Surfaces

A smooth regular surface could be uniquely specified by two independent variables. Therefore, we give a surface  $P$  (Fig. 1.4), in most cases, by expressing its rectangular coordinates  $X_P$ ,  $Y_P$ , and  $Z_P$ , as functions of two “Gaussian coordinates,”  $U_P$  and  $V_P$ , in a certain closed interval:

$$\mathbf{r}_P = \mathbf{r}_P(U_P, V_P) = \begin{bmatrix} X_P(U_P, V_P) \\ Y_P(U_P, V_P) \\ Z_P(U_P, V_P) \\ 1 \end{bmatrix}; \quad (U_{1.P} \leq U_P \leq U_{2.P}; V_{1.P} \leq V_P \leq V_{2.P}) \quad (1.1)$$

Here is designated:

- $\mathbf{r}_P$  is the position vector of point of the part surface  $P$
- $U_P$  and  $V_P$  are the curvilinear (Gaussian) coordinates of point of the part surface  $P$
- $X_P, Y_P, Z_P$  are the “Cartesian coordinates” of point of the part surface  $P$
- $U_{1.P}, U_{2.P}$  are the boundary values of the closed interval of the  $U_P$ —parameter
- $V_{1.P}, V_{2.P}$  are the boundary values of the closed interval of the  $V_P$ —parameter.

The parameters,  $U_P$  and  $V_P$ , must enter independently, which means that the matrix:

$$\mathbf{M} = \begin{bmatrix} \frac{\partial X_P}{\partial U_P} & \frac{\partial Y_P}{\partial U_P} & \frac{\partial Z_P}{\partial U_P} \\ \frac{\partial X_P}{\partial V_P} & \frac{\partial Y_P}{\partial V_P} & \frac{\partial Z_P}{\partial V_P} \end{bmatrix} \quad (1.2)$$

has rank 2. Positions where the rank is 1 or 0 are singular points; when the rank at all points is 1, then Eq. (1.1) represents a curve.

The following notations are proven being convenient in the consideration below.

The first derivatives of the position vector  $\mathbf{r}_P$  with respect to “Gaussian coordinates,”  $U_P$  and  $V_P$ , are designated as:

$$\frac{\partial \mathbf{r}_P}{\partial U_P} = \mathbf{U}_P \quad (1.3)$$

$$\frac{\partial \mathbf{r}_P}{\partial V_P} = \mathbf{V}_P \quad (1.4)$$

and for the unit tangent vectors:

$$\mathbf{u}_P = \frac{\mathbf{U}_P}{|\mathbf{U}_P|} \quad (1.5)$$



$$\mathbf{v}_P = \frac{\mathbf{V}_P}{|\mathbf{V}_P|} \quad (1.6)$$

correspondingly.

A direction of a tangent line to a  $U_P$ —coordinate curve through a point of interest,  $m$ , on a sculptured surface,  $P$ , is specified by the unit tangent vector,  $\mathbf{u}_P$  (as well as by the tangent vector  $\mathbf{U}_P$ ). Similarly, a direction of a tangent line to a  $V_P$ —coordinate curve through that same point of interest,  $m$ , on a sculptured surface,  $P$ , is specified by the unit tangent vector,  $\mathbf{v}_P$  (as well as by the corresponding tangent vector,  $\mathbf{V}_P$ ).

### 1.1.2 Essentials of Piecewise Approximation of Sculptured Part Surfaces

The discussed equations (see Eqs. 1.1–1.6) are valid for with respect to any and all surfaces expressed analytically. However, not all kinds of part surfaces parametrization are convenient in practice. Therefore, surfaces of a special kind are developed for engineering needs. These surfaces are commonly referred to as “*spline surfaces*” [4]. The important features of spline surfaces allow a perfect piecewise approximation of large portions of sculptured part surfaces along with simple expressions for the first and the second derivatives of the position point of point with respect to the “*Gaussian parameters*” of the part surface patch.

Key features of piecewise spline approximation of sculptured part surfaces are briefly outlined below.

A part surface “*patch*” is the simplest mathematical element that is used to model a part surface.<sup>1</sup> A “*patch*” can be defined as a curve bounded collection of points whose coordinates are given by continuous, two-parameter, single-valued mathematical functions of them [4]:

$$\begin{cases} X_P = X_P(u, w) \\ Y_P = Y_P(u, w) \\ Z_P = Z_P(u, w) \end{cases} \quad (1.7)$$

The parametric variables<sup>2</sup>  $u$  and  $w$  are constrained to the values  $u \in [0, 1]$  and  $w \in [0, 1]$ .

Fixing the value of one of the parametric variables results in a curve on the patch in terms of the other variable, which remains free. By continuing this process first for one variable and then the other for any number of arbitrary values in the allowed

<sup>1</sup> For a more in detail discussion on spline surface, the interested reader is referred to a perfect book by Mortenson [4], as well as to other advanced sources.

<sup>2</sup>It is important to point out here that it is a common practice in the technic of spline surface approximation to denote the “*Gaussian parameters*” of the surface patch by  $u$  and  $w$ , and not by  $U$  and  $V$ , as is in geometry of surfaces in a more general sense.

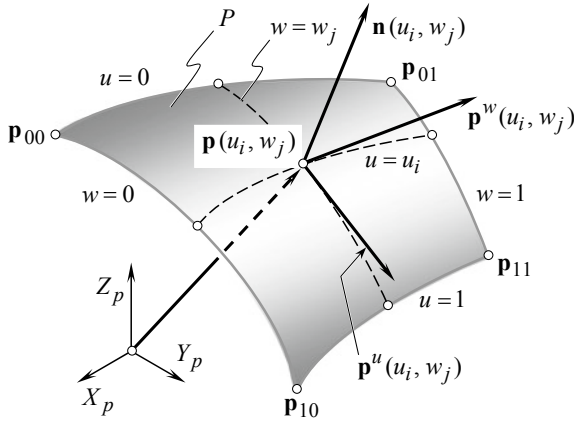


**Fig. 1.5** Parametric part surface patch,  $P$

interval, a parametric net of two one-parameter family of curves on the patch is formed so that just one curve of each family passes through each point  $\mathbf{p}(u, w)$ . Again, the positive sense on any curve is the sense in which the free parameter increases.

Referring to Fig. 1.5, a set of “*boundary conditions*” is associated with every point. The most obvious of these are the four corner points and the four curves defining the edges. Other of importance is the tangent vectors and twist vectors, which will be discussed later. For an ordinary patch  $P$ , there are always four and only four corner points and edge curves. This follows from the possible combinations of the two limits of the two parametric variables. The corner points can be found by substituting these four combinations of 0 and 1 into  $\mathbf{p}(u, w)$  to obtain  $\mathbf{p}(0, 0)$ ,  $\mathbf{p}(0, 1)$ ,  $\mathbf{p}(1, 0)$ , and  $\mathbf{p}(1, 1)$ . On the other hand, the edges or boundary curves are functions of one of two parametric variables. These are obtained by allowing one of the variables to remain free while fixing the other to its limiting values. This procedure results in four and only four possible combinations yielding the functions of the four parametric boundary curves  $\mathbf{p}(u, 0)$ ,  $\mathbf{p}(u, 1)$ ,  $\mathbf{p}(0, w)$ , and  $\mathbf{p}(1, w)$ .

### 1.1.3 Algebraic and Geometric Form

The algebraic form of a bicubic surface patch is given by:

$$\mathbf{p}(u, w) = \sum_{i=0}^3 \sum_{j=0}^3 \mathbf{a}_{ij} u^i w^j \quad (1.8)$$

The restriction on the parametric variables is  $u \in [0, 1]$  and  $w \in [0, 1]$ .

The  $\mathbf{a}_{ij}$  vectors are called the “*algebraic coefficients*” of the surface  $P$ . The reason for the term “*bicubic*” is obvious since both parametric variables can be cubic terms.

The parametric variables  $u$  and  $w$  are restricted by definition to values in the interval 0 to 1, inclusive. The restriction makes the surface  $P$  bounded in a regular way.

Equation (1.8) can be expanded, and the terms can be arranged in descending order:

$$\begin{aligned} \mathbf{p}(u, w) = & \mathbf{a}_{33}u^3w^3 + \mathbf{a}_{32}u^3w^2 + \mathbf{a}_{31}u^3w + \mathbf{a}_{30}u^3 \\ & + \mathbf{a}_{23}u^2w^3 + \mathbf{a}_{22}u^2w^2 + \mathbf{a}_{21}u^2w + \mathbf{a}_{20}u^2 \\ & + \mathbf{a}_{13}uw^3 + \mathbf{a}_{12}uw^2 + \mathbf{a}_{11}uw + \mathbf{a}_{10}u \\ & + \mathbf{a}_{03}w^3 + \mathbf{a}_{02}w^2 + \mathbf{a}_{01}w + \mathbf{a}_{00} \end{aligned} \quad (1.9)$$

This sixteen-term polynomial in  $u$  and  $w$  defines the set of app points lying on the part surface  $P$ . It is the algebraic form of a bicubic patch. Since each of the vector coefficients  $\mathbf{a}$  has three independent components, there is a total of 48 algebraic coefficients, or 48 degrees of freedom. Thus, each vector component is simply:

$$X_P(u, w) = a_{33x}u^3w^3 + a_{32x}u^3w^2 + a_{31x}u^3w + a_{30x}u^3 + \cdots + a_{00x} \quad (1.10)$$

There are similar expressions for  $Y_P(u, w)$  and  $Z_P(u, w)$ .

The algebraic form in matrix notation is:

$$\mathbf{p} = \mathbf{U}\mathbf{A}\mathbf{W}^T \quad (1.11)$$

where

$$\mathbf{U} = [u^3 \ u^2 \ u \ 1] \quad (1.12)$$

$$\mathbf{W} = [w^3 \ w^2 \ w \ 1] \quad (1.13)$$

$$\mathbf{A} = \begin{bmatrix} \mathbf{a}_{33} & \mathbf{a}_{32} & \mathbf{a}_{31} & \mathbf{a}_{30} \\ \mathbf{a}_{23} & \mathbf{a}_{22} & \mathbf{a}_{21} & \mathbf{a}_{20} \\ \mathbf{a}_{13} & \mathbf{a}_{12} & \mathbf{a}_{11} & \mathbf{a}_{10} \\ \mathbf{a}_{03} & \mathbf{a}_{02} & \mathbf{a}_{01} & \mathbf{a}_{00} \end{bmatrix} \quad (1.14)$$

Note that the subscripts of the vector elements in the  $\mathbf{A}$  matrix correspond to those in Eq. (1.9). They have no direct relationship to the normal indexing convention for matrices. Since the  $\mathbf{a}$  elements are three-component vectors, the  $\mathbf{A}$  matrix is a  $4 \times 4 \times 3$  array.

The algebraic coefficients of a patch determine its shape and position in space. However, patches of the same size and shape have a different set of coefficients if they occupy a different position in space. Change any one of 48 coefficients and a

completely different patch results. A point on the patch is generated each time when a specific pair of  $u$ ,  $w$  is inserted into Eq. (1.11). And, although the  $u$ ,  $w$  values are restricted by the expressions  $u \in [0, 1]$  and  $w \in [0, 1]$ , the range of the object-space variables  $X_P$ ,  $Y_P$ , and  $Z_P$  is unrestricted because the range of the algebraic coefficients is unrestricted.

A patch consists of an infinite number of points given by their  $X_P$ ,  $Y_P$ , and  $Z_P$  coordinates. There are also an infinite number of pairs of  $u$ ,  $w$  values in the corresponding parametric space. Clearly, there is a unique pair of  $u$ ,  $w$  values associated with each point in object space.

Observe that a bicubic surface patch is bounded by four curves and each boundary curve is obviously a parametric cubic curve, that is, a *pc*—curve (that is, “*parametric cubic curve*”). Each of these curves is named as follows:  $u_0$ ,  $u_1$ ,  $w_0$ ,  $w_1$  (for  $u = 0$ ,  $u = 1$ ,  $w = 0$ , and  $w = 1$ ) because they arise at the constant limiting values of the parametric variables. Another way of noting the boundary curves is by appropriately subscripted vector  $\mathbf{p}$ . Thus, the notation  $\mathbf{p}_{0w}$ ,  $\mathbf{p}_{1w}$ ,  $\mathbf{p}_{0u}$ , and  $\mathbf{p}_{1u}$  is also used for labeling the boundary curves. Their interpretation should be obvious. There are also for unique corner points  $\mathbf{p}_{00}$ ,  $\mathbf{p}_{10}$ ,  $\mathbf{p}_{01}$ ,  $\mathbf{p}_{11}$ .

As with the *pc*—curve, reversing the sequence of  $u$ ,  $w$  parameterization does not change the shape of a surface. And, aside from problem-specific computation constraints (for example, the direction of surface normals), almost complete freedom to assign  $u$ ,  $w = 0$  or  $1$  to the boundary curves is observed. The exception is that  $\mathbf{p}_{0w}$  must be opposite  $\mathbf{p}_{1w}$ , and  $\mathbf{p}_{0u}$  opposite  $\mathbf{p}_{1u}$ .

### 1.1.4 Significance of the Unit Tangent Vectors

Significance of the unit tangent vectors,  $\mathbf{u}_P$  and  $\mathbf{v}_P$ , becomes evident from the considerations immediately following.

First, unit tangent vectors,  $\mathbf{u}_P$  and  $\mathbf{v}_P$ , allow for an equation of the tangent plane to a surface  $P$  at  $m$ :

$$\text{Tangent plane} \quad \Rightarrow \quad \begin{bmatrix} [\mathbf{r}_{t,p} - \mathbf{r}_P^{(m)}] \\ \mathbf{u}_P \\ \mathbf{v}_P \\ 1 \end{bmatrix} = 0 \quad (1.15)$$

Here is designated:

$\mathbf{r}_{t,p}$  is the position vector of point of the tangent plane to the part surface,  $P$ , at point of interest,  $m$

$\mathbf{r}_P^{(m)}$  is the position vector of point of interest,  $m$ , on the part surface  $P$ .

Second, unit tangent vectors,  $\mathbf{u}_P$  and  $\mathbf{v}_P$ , allow for an equation of the perpendicular,  $\mathbf{N}_P$ , and of the unit normal vector,  $\mathbf{n}_P$ , to the sculptured part surface,  $P$ , at point of interest,  $m$ :

$$\mathbf{N}_P = \mathbf{U}_P \times \mathbf{V}_P \quad (1.16)$$

$$\mathbf{n}_P = \frac{\mathbf{N}_P}{|\mathbf{N}_P|} = \frac{\mathbf{U}_P \times \mathbf{V}_P}{|\mathbf{U}_P \times \mathbf{V}_P|} = \mathbf{u}_P \times \mathbf{v}_P \quad (1.17)$$

When order of multipliers in Eq. (1.16) [as well as in Eq. (1.17)] is chosen properly, then the unit normal vector,  $\mathbf{n}_P$ , is pointed outward of the bodily side bounded by the surface,<sup>3</sup>  $P$ .

In a case of bicubic function, the tangent vectors are:

$$\mathbf{p}_{uw}^u = \frac{\partial \mathbf{p}(u, w)}{\partial u} \quad (1.18)$$

$$\mathbf{p}_{uw}^w = \frac{\partial \mathbf{p}(u, w)}{\partial w} \quad (1.19)$$

Finally, at any point  $\mathbf{p}(u, w)$  on a basic patch, a vector normal (that is, perpendicular) to the patch can be constructed. A unit normal vector  $\mathbf{n}(u, w)$  can be easily found by computing the vector product of the tangent vectors  $\mathbf{p}^u$  and  $\mathbf{p}^w$  at the point:

$$\mathbf{n}(u, w) = \frac{\mathbf{p}^u \times \mathbf{p}^w}{|\mathbf{p}^u \times \mathbf{p}^w|} \quad (1.20)$$

The order in which the vector product is taken determines the direction of  $\mathbf{n}(u, w)$ .

The unit normal is indispensable in almost all phases of geometric modeling, and in most applications, a consistent normal direction is required.

## 1.2 On the Difference Between “Classical Differential Geometry” and “Engineering Geometry of Surfaces”

Classical differential geometry is developed mainly for the purpose of investigation of smooth regular surfaces. Engineering geometry also deals with smooth regular surfaces. What is the difference between these two geometries?

The difference between classical differential geometry and engineering geometry of surfaces is due mainly to that how surfaces are interpreted.

Only “phantom surfaces” are investigated in classical differential geometry. Surfaces of this kind do not exist physically. They can be understood as a zero-thickness film of an appropriate shape. Such a film can be accessed from both sides of the surface. The following indefiniteness is caused by this.

---

<sup>3</sup>It should be pointed out here that the unit tangent vectors,  $\mathbf{u}_P$  and  $\mathbf{v}_P$ , as well as the unit normal vector,  $\mathbf{n}_P$ , are dimensionless parameters of the geometry of the sculptured part surface  $P$ . This feature of the unit vectors  $\mathbf{u}_P$ ,  $\mathbf{v}_P$ , and  $\mathbf{n}_P$ , is convenient when performing practical calculations.

As an example, consider a surface, at a certain point  $m$  with Gaussian curvature  $\mathcal{G}_P$  of the surface having a positive value ( $\mathcal{G}_P > 0$ ). Classical differential geometry gives no answer to the question of whether the surface  $P$  is convex or concave in the vicinity of a point of interest  $m$ . In the first case (when the surface  $P$  is convex) the “mean curvature  $\mathcal{M}_P$ ” at the surface  $P$  point of interest  $m$  is of a positive value,  $\mathcal{M}_P > 0$ , while in the second case (when the surface  $P$  is concave), the mean curvature  $\mathcal{M}_P$  at the surface  $P$  point of interest  $m$  is of a negative value,  $\mathcal{M}_P < 0$ .

A similar is observed when “Gaussian curvature,  $\mathcal{G}_P$ ” at a certain surface point is of a negative value ( $\mathcal{G}_P < 0$ ).

In classical differential geometry, the answer to the question of whether a surface is convex or concave in the vicinity of a certain point  $m$  can be given only by convention.

In turn, surfaces that are treating in engineering geometry bound a solid—a “machine part” (or a “machine element”). This part can be called a “real object” (Figs. 1.1 and 1.2). The real object is the bearer of the surface shape.

Surfaces that bound real object are accessible only from one side as it is schematically illustrated in Fig. 1.6. We refer to this side of the surface as to “open side of part surface”. The opposite side of the surface  $P$  is not accessible. Because of this, we refer to the opposite side of the surface  $P$  as to “closed side of part surface.”

The positively directed normal unit vector  $+\mathbf{n}_P$  is pointed outward of the part body, that is, it is pointed from the bodily side to the void side. The negative normal unit vector  $-\mathbf{n}_P$  is pointed oppositely to  $+\mathbf{n}_P$ .

The existence of the open and closed sides of a part surface  $P$  eliminates the problem of identifying whether a surface is convex or concave. No convention is required in this respect. The latter is important in the development of CAD/CAM systems.

The description of a smooth regular surface in differential geometry of surfaces and in engineering geometry provides more differences between surfaces treated in these two different branches of geometry.

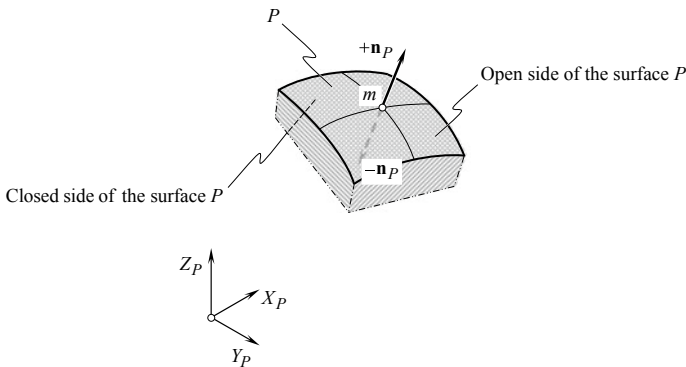


**Fig. 1.6** Open and closed sides of a part surface,  $P$

### 1.3 On the Analytical Description of Part Surfaces

Another principal difference in this respect is due to the nature of the real object. We should point out here again that a real object is the bearer of surface shape. No real object can be machined/manufactured precisely with zero deviations of its actual shape from the desired shape of the real object. Smaller or larger deviations in the shape of the real object from its desired shape are inevitable in nature. We won't go into detail here on the nature of the deviations. We should just simply realize that such deviations are inevitable and always exist.

As an example, let us consider how the surface of a round cylinder is specified in differential geometry of surfaces, and compare it with that in engineering geometry.

In differential geometry of surfaces, the coordinates of a point of interest  $m$  of the surface of a cylinder of revolution can be specified by the position vector  $\mathbf{r}_m$  of the point  $m$  (Fig. 1.7a). In the case under consideration, the position vector  $\mathbf{r}_m$  of a point within the surface of a cylinder of a radius  $r$ , and having  $Z$ -axis as its axis of rotation, can be expressed in matrix form as:

$$\mathbf{r}_m(\varphi, Z_m) = \begin{bmatrix} r \cos \varphi \\ r \sin \varphi \\ Z_m \\ 1 \end{bmatrix} \quad (1.21)$$

Here, the surface curvilinear coordinates are denoted by  $\varphi$  and  $Z_m$  accordingly. They are equivalents of the curvilinear coordinates  $U_P$  and  $V_P$  in Eq. (1.1).

Mechanical engineers have no other option rather than to treat a desired (nominal) part surface  $P$ , which is given by the part blueprint, and which is specified by the tolerance for the surface  $P$  accuracy.

As manufacturing errors are inevitable, the current surface point  $m^{\text{act}}$  actually deviates from its desired location  $m$ . The position vector  $\mathbf{r}_m^{\text{act}}$  of a current point  $m^{\text{act}}$  of the actual part surface deviates from that  $\mathbf{r}_m$  for a perfect surface point  $m$ . Without loss of generality, the surfaces deviations in the direction of the  $Z$ -axis are ignored. Instead, the surfaces deviations in the directions of the  $X$ - and  $Y$ -axis are considered.

The deviation of a point  $m^{\text{act}}$  from the corresponding surface point  $m$  that is measured perpendicular to the desired part surface,  $P$ , is designated as  $\delta_m$  (Fig. 1.7b). Formally, the position vector  $\mathbf{r}_m^{\text{act}}$  of a current point  $m^{\text{act}}$  of the actual part surface can be described analytically in matrix form as:

$$\mathbf{r}_m^{\text{act}}(\varphi, Z_m) = \begin{bmatrix} (r + \delta_m) \cos \varphi \\ (r + \delta_m) \sin \varphi \\ Z_m \\ 1 \end{bmatrix} \quad (1.22)$$

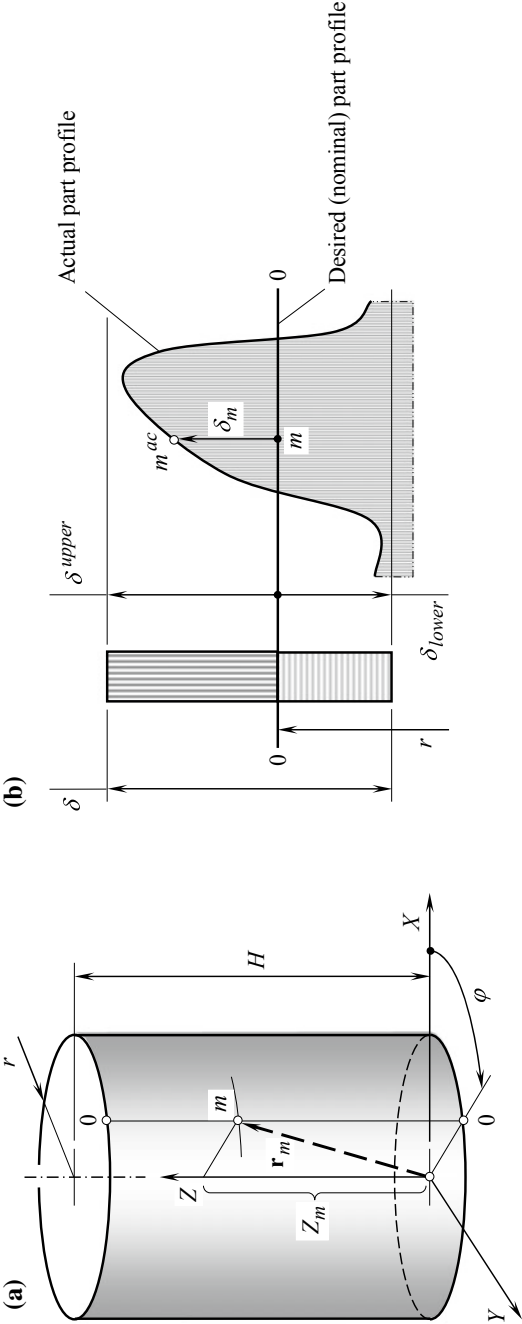


Fig. 1.7 Specification of **a** an perfect (ideal), and **b** a real part surface



where the deviation  $\delta_m$  is understood as a signed value. It is positive for the points  $m^{\text{act}}$ , those located outside the surface (see Eq. 1.21), and negative for the points  $m^{\text{act}}$  located inside the surface (see Eq. 1.21).

Unfortunately, the actual value of the deviation  $\delta_m$  is never known. Thus, Eq. (1.22) cannot be used for the purpose of analytical description of real part surfaces.

In practice, the permissible deviations  $\delta_m$  of surfaces in engineering geometry are limited to a certain tolerance bend. An example of a tolerance band is schematically shown in Fig. 1.7b. The positive deviation  $\delta_m$  must not exceed the upper limit  $\delta^{\text{upper}}$ , and the negative deviation  $\delta_m$  must not be greater than the lower limit  $\delta_{\text{lower}}$ . That is, in order to meet the requirements specified by the blueprint, the deviation  $\delta_m$  must be within the tolerance bend:

$$\delta_{\text{lower}} \leq \delta_m \leq \delta^{\text{upper}} \quad (1.23)$$

The total width of the tolerance band is equal to  $\delta_m = \delta^{\text{upper}} + \delta_{\text{lower}}$ . In this expression for the deviation  $\delta_m$ , both limits,  $\delta^{\text{upper}}$  and  $\delta_{\text{lower}}$ , are signed values. They can be either of a positive value, or of a negative value, as well as equal to zero.

Under such the scenario, the desired part surface  $P_{\text{des}}$  not only meets the requirements specified by the part blueprint, but any and all actual part surfaces  $P^{\text{ac}}$  located within the tolerance band  $\delta_{\text{lower}} \leq \delta \leq \delta^{\text{upper}}$  meet the requirements given by the blueprint. In other words, if a surface  $P_{\delta}^+$  is specified by a tolerance band  $\delta^{\text{upper}}$ , and a surface  $P_{\delta}^-$  is specified by a tolerance band  $\delta_{\text{lower}}$ , then an actual part surface  $P^{\text{ac}}$  is always located between the surfaces  $P_{\delta}^+$  and  $P_{\delta}^-$ . And, of course, the actual part surface  $P^{\text{ac}}$  always differs from the desired part surface  $P_{\text{des}}$ . However, the deviation of the surface  $P^{\text{ac}}$  from the surface  $P_{\text{des}}$  is always within the tolerance band  $\delta_{\text{lower}} \leq \delta \leq \delta^{\text{upper}}$ .

An intermediate summarization is as follows: We know everything about perfect (ideal) surfaces, which do not exist in reality, and we know nothing about real surfaces those exist physically (or, at least, our knowledge about real part surfaces is very limited).

In addition, the entire endless surface of the cylinder of revolution is not considered in engineering geometry. Only a portion of this surface is of importance in practice. Therefore, in the axial direction, the length of the cylinder is limited to an interval  $0 \leq Z_m \leq H$ , where  $H$  is a prespecified length of the cylinder of revolution.

With that said, we can now proceed with a more general consideration of the analytical representation of surfaces in engineering geometry.

## 1.4 Boundary Surfaces for Actual Part Surface

Owing to the deviations, an actual part surface  $P^{\text{act}}$  deviates from its nominal (desired) surface  $P_{\text{des}}$  (Fig. 1.8). However, the deviations are within the prespecified tolerance bands. Otherwise, the real object could get useless. In practice, this particular problem

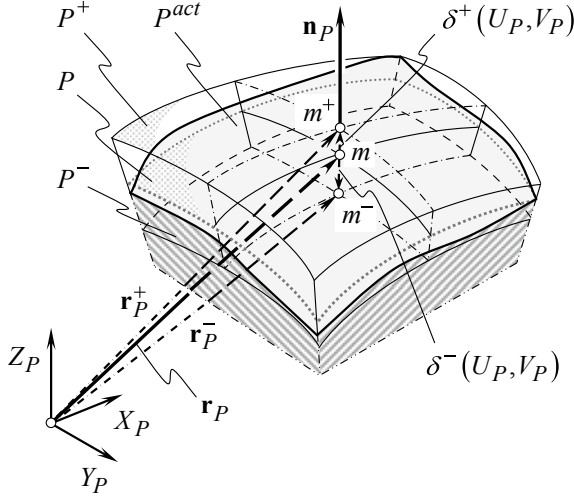


**Fig. 1.8** Analytical description of an actual part surface  $P^{\text{act}}$  located between the boundary surfaces  $P^+$  and  $P^-$

is easily solved by selecting appropriate tolerance bands for the shape and dimensions of the actual surface  $P^{\text{act}}$ .

Similar to measuring deviations, the tolerances are also measured in the direction of the unit normal vector  $\mathbf{n}_P$  to the desired (nominal) part surface  $P$ . Positive tolerance  $\delta^+$  is measured along the positive direction of the vector  $\mathbf{n}_P$ , while negative tolerance  $\delta^-$  is measured along the negative direction of the vector  $\mathbf{n}_P$ . In a particular case, one of the tolerances, either  $\delta^+$  or  $\delta^-$ , can be zero.

Often, the value of the tolerance bands  $\delta^+$  and  $\delta^-$  are of a constant value within the entire patch of the surface  $P$ . However, in special cases, for example, when machining a sculptured part surface on a multi-axis NC machine, the actual value of the tolerances  $\delta^+$  and  $\delta^-$  can be set as functions of the coordinates of the current point  $m$  on the surface  $P$ . This results in the tolerances being represented in terms of  $U_P$ —and  $V_P$ —parameters of the surface  $P$ , say in the form:

$$\delta^+ = \delta^+(U_P, V_P) \quad (1.24)$$

$$\delta^- = \delta^-(U_P, V_P). \quad (1.25)$$

The endpoint of the vector  $\delta^+ \cdot \mathbf{n}_P$  at a surface point of interest  $m$  produces the point  $m^+$ . Similarly, the endpoint of the vector  $\delta^- \cdot \mathbf{n}_P$  produces the corresponding point  $m^-$ .

The surface  $P^+$  of the upper tolerance is represented by the loci of the points  $m^+$  (that is, by the loci of the endpoints of the vector  $\delta^+ \cdot \mathbf{n}_P$ ). This makes possible to have an analytical representation of the surface  $P^+$  of upper tolerance in the form:

$$\mathbf{r}_P^+(U_P, V_P) = \mathbf{r}_P + \delta^+ \cdot \mathbf{n}_P \quad (1.26)$$

Usually, the surface  $P^+$  of upper tolerance is located above the nominal part surface  $P$ .

Similarly, the surface  $P^-$  of lower tolerance is represented by the loci of the points  $m^-$  (that is, by the loci of the endpoints of the vector  $\delta^- \cdot \mathbf{n}_P$ ). This also makes possible to have an analytical representation of the surface  $P^-$  of lower tolerance in the form:

$$\mathbf{r}_P^-(U_P, V_P) = \mathbf{r}_P + \delta^- \cdot \mathbf{n}_P \quad (1.27)$$

Commonly, the surface  $P^-$  of lower tolerance is located beneath the nominal part surface  $P$ .

The surfaces  $P^+$  and  $P^-$  are the boundary surfaces. The actual part surface  $P^{\text{act}}$  is located between the surfaces  $P^+$  and  $P^-$  as illustrated schematically in Fig. 1.8.

The actual part surface  $P^{\text{act}}$  cannot be represented analytically.<sup>4</sup> Moreover, the parameters of the local topology of the surface  $P$  considered above cannot be calculated for the surface,  $P^{\text{act}}$ . However, owing to the tolerances  $\delta^+$  and  $\delta^-$  being small enough compared to the normal radii of curvature of the nominal surfaces  $P$ , it is assumed below that the surface  $P^{\text{act}}$  possesses that same geometrical properties as the surface  $P$ , and that the difference between corresponding geometrical parameters of the surfaces  $P^{\text{act}}$  and  $P$  is negligibly small. In further consideration, this allows for a replacement of the actual surface  $P^{\text{act}}$  with the nominal surface  $P$ , which is much more convenient for performing calculations.

The consideration in this section illustrates the second principal difference between classical differential geometry and engineering geometry of surfaces.

Because of these differences, engineering geometry of surfaces often presents problems that were not envisioned in classical (pure) differential geometry of surfaces.

## 1.5 Natural Representation of Desired Part Surface

Specification of a surface in terms of the first and the second fundamental forms is commonly called as the “*natural kind of surface representation*.” In general form, it can be represented by a set of two equations:

---

<sup>4</sup>Actually, the surface  $P^{\text{act}}$  is unknown—any surface that is located between the surfaces of upper tolerance  $P^+$  and lower tolerance  $P^-$  meets the requirements to the part blueprint, and thus, every such surface can be considered as an actual surface  $P^{\text{act}}$ . The equation of the surface  $P^{\text{act}}$  cannot be represented in the form  $\mathbf{r}_P^{\text{act}} = \mathbf{r}_P + \delta^{\text{act}} \cdot \mathbf{n}_P$  because the actual value of the deviation  $\delta^{\text{act}}$  at the current surface point is not known. *MM* data yields only an approximation for  $\delta^{\text{act}}$  as well as the corresponding approximation for  $P^{\text{act}}$ .

$$\begin{aligned}
 & \left. \begin{array}{l} \text{Natural form of surface } P \\ \text{parameterization} \end{array} \right| \Rightarrow P \\
 & = P(\Phi_{1,P}, \Phi_{2,P}) \left\{ \begin{array}{l} \Phi_{1,P} = \Phi_{1,P}(E_P, F_P, G_P) \\ \Phi_{2,P} = \Phi_{2,P}(E_P, F_P, G_P, L_P, M_P, N_P) \end{array} \right. \quad (1.28)
 \end{aligned}$$

It was proven by *Bonnet*<sup>5</sup> (1867) that specification of the first and the second fundamental forms determines a unique surface if the *Gaussian*<sup>6</sup> characteristic equation<sup>7</sup> and the *Codazzi–Mainardi*<sup>8,9</sup> relationships of compatibility<sup>10</sup> are fulfilled, and those two surfaces that have an identical first and second fundamental forms must be congruent to one another<sup>11</sup> [5]. This statement is commonly considered as the main theorem in the theory of surfaces. The main theorem in the theory of surfaces is commonly called “*Bonnet theorem*.”

It is the right point to make clear what the first and the second fundamental forms of a surface stand for. Both of them relate to intrinsic geometry in differential vicinity of a surface point.

### 1.5.1 First Fundamental Form of a Desired Part Surface

Metric properties of a smooth regular surface  $P$  are described by the first fundamental form. Usually, the first fundamental form  $\Phi_{1,P}$  is represented as the quadratic form:

$$\Phi_{1,P} \Rightarrow ds_P^2 = E_P dU_P^2 + 2F_P dU_P dV_P + G_P dV_P^2 \quad (1.29)$$

Here, in Eq. (1.29) is designated:

$s_P$  is the linear element of the surface  $P$  ( $s_P$  is equal to the length of a segment of a certain curve line on the surface  $P$ )

$E_P, F_P, G_P$  are the fundamental magnitudes of first order.

Equation (1.29) is known from many advanced sources.

In engineering geometry of surfaces, another form of analytical representation of the first fundamental form  $\Phi_{1,P}$  is proven to be useful:

<sup>5</sup> *Pierre Ossian Bonnet* (December 22, 1819–June 22, 1892)—a French mathematician.

<sup>6</sup> *Johan Carl Friedrich Gauss* (April 30, 1777–February 23, 1855)—a famous German mathematician and physical scientist.

<sup>7</sup> *Gauss* equation of compatibility that follows from his famous “*theorema egregium*” is considered in detail below in Chap. 8.

<sup>8</sup> *Delfino Codazzi* (March 7, 1824–July 21, 1873)—an Italian mathematician.

<sup>9</sup> *Gaspare Mainardi* (June 27, 1800–March 9, 1879)—an Italian mathematician.

<sup>10</sup> “*Codazzi–Mainardi equations of compatibility*” are considered in detail below in Chap. 8.

<sup>11</sup> It should be mentioned here that two surfaces with identical first and second fundamental forms might also be symmetrical to one another. The interested reader is referred to special literature on the differential geometry of surfaces for details about this issue.

$$\Phi_{1,P} \Rightarrow ds_P^2 = [dU_P \ dV_P \ 0 \ 0] \cdot \begin{bmatrix} E_P & F_P & 0 & 0 \\ F_P & G_P & 0 & 0 \\ 0 & 0 & 1 & 0 \\ 0 & 0 & 0 & 1 \end{bmatrix} \cdot \begin{bmatrix} dU_P \\ dV_P \\ 0 \\ 0 \end{bmatrix} \quad (1.30)$$

This kind of analytical representation of the first fundamental form  $\Phi_{1,P}$  was proposed by Prof. *Radzevich* [6]. The practical advantage of Eq. (1.30) is that it can easily be incorporated into computer programs in which multiple coordinate system transformations are used. The latter is vital for many *CAD/CAM* applications.

The fundamental magnitudes of the first order  $E_P$ ,  $F_P$ , and  $G_P$  can be calculated from the following equations:

$$E_P = \mathbf{U}_P \cdot \mathbf{U}_P = \frac{\partial \mathbf{r}_P}{\partial U_P} \cdot \frac{\partial \mathbf{r}_P}{\partial U_P} \quad (1.31)$$

$$F_P = \mathbf{U}_P \cdot \mathbf{V}_P = \frac{\partial \mathbf{r}_P}{\partial U_P} \cdot \frac{\partial \mathbf{r}_P}{\partial V_P} \quad (1.32)$$

$$G_P = \mathbf{V}_P \cdot \mathbf{V}_P = \frac{\partial \mathbf{r}_P}{\partial V_P} \cdot \frac{\partial \mathbf{r}_P}{\partial V_P} \quad (1.33)$$

The fundamental magnitudes,  $E_P$ ,  $F_P$ , and  $G_P$ , of the first order are functions of  $U_P$ —and  $V_P$ —parameters of the surface  $P$ . In general, these relationships can be represented in the form:

$$E_P = E_P(U_P, V_P) \quad (1.34)$$

$$F_P = F_P(U_P, V_P) \quad (1.35)$$

$$G_P = G_P(U_P, V_P) \quad (1.36)$$

The fundamental magnitudes  $E_P$  and  $G_P$  are always positive ( $E_P > 0$ ,  $G_P > 0$ ), while the fundamental magnitude  $F_P$  can be equal to zero ( $F_P \geq 0$ ). This results in that the first fundamental form always being nonnegative ( $\Phi_{1,P} \geq 0$ ).

The first fundamental form  $\Phi_{1,P}$  yields calculation of the following major parameters of geometry of the surface  $P$ :

- (a) length of a curve-line segment on the surface  $P$ ,
- (b) square of the surface  $P$  portion bounded by a closed curve on the surface,
- (c) angle between any two directions on the surface  $P$ .

Owing to the first fundamental form representing the length of a curve-line segment, it is always nonnegative, that is, the inequality  $\Phi_{1,P} \geq 0$  is always observed.

The discriminant  $H_P$  of the first fundamental form  $\Phi_{1,P}$  can be calculated from the equation:

$$H_P = \sqrt{E_P G_P - F_P^2} \quad (1.37)$$

It is assumed here and below that the discriminant  $H_P$  is always nonnegative, that is,  $H_P = +\sqrt{E_P G_P - F_P^2}$ .

Having the fundamental magnitudes of the first order  $E_P$ ,  $F_P$ , and  $G_P$  calculated, makes the possible easy calculation of the following parameters of geometry of a part surface  $P$ .

The length  $s$  of a curve-line segment  $U_P = U_P(t)$ ,  $V_P = V_P(t)$ ,  $t_0 \leq t \leq t_1$  is given by the equation:

$$s = \int_{t_0}^t \sqrt{E_P \left( \frac{dU_P}{dt} \right)^2 + 2F_P \frac{dU_P}{dt} \frac{dV_P}{dt} + G_P \left( \frac{dV_P}{dt} \right)^2} dt \quad (1.38)$$

The value of the angle  $\theta$  between two specified directions through a certain point  $m$  on the surface  $P$  can be calculated from one of the following equations:

$$\cos \theta = \frac{F_P}{\sqrt{E_P G_P}} \quad (1.39)$$

$$\sin \theta = \frac{H_P}{\sqrt{E_P G_P}} \quad (1.40)$$

$$\tan \theta = \frac{H_P}{F_P} \quad (1.41)$$

For the calculation of square  $S_P$  of a surface patch  $\Sigma$ , which is bounded by a closed line on the surface  $P$ , the following equation is commonly used:

$$S_P = \iint_{\Sigma} \sqrt{E_P G_P - F_P^2} dU_P dV_P \quad (1.42)$$

The fundamental form  $\Phi_{1,P}$  remains the same while the surface is bending. This is another important feature of the first fundamental form  $\Phi_{1,P}$ . The feature can be employed to design 3D cams for finishing of a turbine blade with an abrasive strip as a cutting tool.

### 1.5.2 Second Fundamental Form of a Desired Part Surface

The curvature of a smooth regular surface  $P$  can be described by the second fundamental form  $\Phi_{2,P}$ .

Consider a point  $K$  on a smooth regular part surface  $P$  (Fig. 1.9). Location of

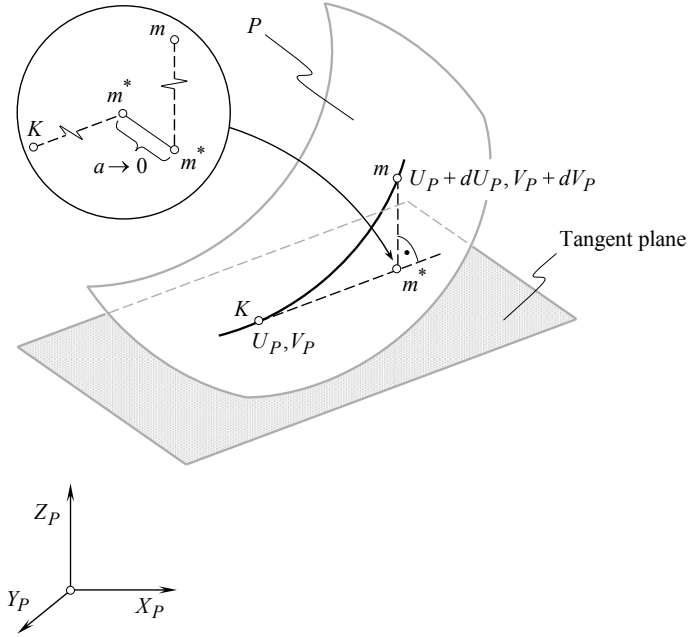


**Fig. 1.9** Definition of the second fundamental form,  $\Phi_{2,P}$ , at point of a smooth regular part surface  $P$

the point  $K$  is specified by to coordinates  $U_P$  and  $V_P$ . A line through the point  $K$  is entirely located within the surface  $P$ . A nearby point  $m$  is located within the line through the point  $K$ . The location of the point  $m$  is specified by the coordinates  $U_P + dU_P$  and  $V_P + dV_P$  as it is infinitesimally close to the point  $K$ . The closest distance of approach of the point  $m$  to the tangent plane through the point  $K$  is expressed by the second fundamental form  $\Phi_{2,P}$ . Torsion of the curve  $Km$  is ignored. Therefore, the distance  $a$  is assumed equal to zero ( $a = 0$ ).

Usually, it is represented as the quadratic form (Fig. 1.9)

$$\Phi_{2,P} \Rightarrow -d\mathbf{r}_P \cdot d\mathbf{n}_P = L_P dU_P^2 + 2M_P dU_P dV_P + N_P dV_P^2 \quad (1.43)$$

Equation (1.43) is known from many advanced sources.

In engineering geometry of surfaces, another form of analytical representation of the second fundamental form  $\Phi_{2,P}$  is proven to be useful:

$$\Phi_{2,P} \Rightarrow [dU_P \ dV_P \ 0 \ 0] \cdot \begin{bmatrix} L_P & M_P & 0 & 0 \\ M_P & N_P & 0 & 0 \\ 0 & 0 & 1 & 0 \\ 0 & 0 & 0 & 1 \end{bmatrix} \cdot \begin{bmatrix} dU_P \\ dV_P \\ 0 \\ 0 \end{bmatrix} \quad (1.44)$$

This kind of analytical representation of the second fundamental form  $\Phi_{2,P}$  was proposed by Radzevich [6]. Similar to Eq. (1.30), the practical advantage of Eq. (1.44) is that it can be easily incorporated into computer programs in which multiple coordinate system transformations are used. The latter is vital for many CAD/CAM applications.

Here, in Eq. (1.44), the parameters  $L_P$ ,  $M_P$ , and  $N_P$  designate fundamental magnitudes of the second order.

Fundamental magnitudes of the second order can be computed from the following equations:

$$L_P = \frac{\frac{\partial \mathbf{U}_P}{\partial U_P} \times \mathbf{U}_P \cdot \mathbf{V}_P}{\sqrt{E_P G_P - F_P^2}} \quad (1.45)$$

$$M_P = \frac{\frac{\partial \mathbf{U}_P}{\partial V_P} \times \mathbf{U}_P \cdot \mathbf{V}_P}{\sqrt{E_P G_P - F_P^2}} = \frac{\frac{\partial \mathbf{V}_P}{\partial U_P} \times \mathbf{U}_P \cdot \mathbf{V}_P}{\sqrt{E_P G_P - F_P^2}} \quad (1.46)$$

$$N_P = \frac{\frac{\partial \mathbf{V}_P}{\partial V_P} \times \mathbf{U}_P \cdot \mathbf{V}_P}{\sqrt{E_P G_P - F_P^2}} \quad (1.47)$$

The fundamental magnitudes  $L_P$ ,  $M_P$ , and  $N_P$  of the second order are also functions of  $U_P$ —and  $V_P$ —parameters of the surface  $P$ . These relationships in general form can be represented as follows:

$$L_P = L_P(U_P, V_P) \quad (1.48)$$

$$M_P = M_P(U_P, V_P) \quad (1.49)$$

$$N_P = N_P(U_P, V_P) \quad (1.50)$$

The discriminant  $T_P$  of the second fundamental form  $\Phi_{2,P}$  can be calculated from the equation:

$$T_P = \sqrt{L_P N_P - M_P^2} \quad (1.51)$$

Implementation of the first,  $\Phi_{1,P}$ , and of the second,  $\Phi_{2,P}$ , fundamental forms of a smooth regular part surface  $P$  makes possible a significant simplification when performing calculations of the parameters of the surface geometry.





$$\mathbf{U}_g = \begin{bmatrix} \cos \psi_{b.g} \sin V_g \\ -\cos \psi_{b.g} \cos V_g \\ -\sin \psi_{b.g} \\ 1 \end{bmatrix} \quad (1.53)$$

$$\mathbf{V}_g = \begin{bmatrix} -r_{b.g} \sin V_g + U_g \cos \psi_{b.g} \cos V_g \\ r_{b.g} \cos V_g + U_g \cos \psi_{b.g} \sin V_g \\ r_{b.g} \tan \psi_{b.g} \\ 1 \end{bmatrix} \quad (1.54)$$

Substituting the calculated vectors  $\mathbf{U}_g$  [see Eq. (1.53)] and  $\mathbf{V}_g$  [see Eq. (1.54)] into Eqs. (1.31)–(1.33), one can come up with formulae for the calculation of fundamental magnitudes of the first order:

$$E_g = 1 \quad (1.55)$$

$$F_g = -\frac{r_{b.g}}{\cos \psi_{b.g}} \quad (1.56)$$

$$G_g = \frac{U_g^2 \cos^4 \psi_{b.g} + r_{b.g}^2}{\cos^2 \psi_{b.g}} \quad (1.57)$$

These equations can be substituted directly to Eq. (1.29) for the first fundamental form:

$$\Phi_{1.g} \Rightarrow dU_g^2 - 2\frac{r_{b.g}}{\cos \psi_{b.g}}dU_g dV_g + \frac{U_g^2 \cos^4 \psi_{b.g} + r_{b.g}^2}{\cos^2 \psi_{b.g}}dV_g^2 \quad (1.58)$$

The calculated values of the fundamental magnitudes  $E_g$ ,  $F_g$ , and  $G_g$  can also be substituted to Eq. (1.30) for the quadratic form  $\Phi_{1.g}$ . In this way, the matrix representation of the first fundamental form  $\Phi_{1.g}$  can be obtained. The interested reader may wish to complete this formulae transformation on his/her own.

The discriminant  $H_g$  of the first fundamental form  $\Phi_{1.g}$  of the surface  $\mathcal{G}$  is can be calculated from the formula:

$$H_g = U_g \cos \psi_{b.g} \quad (1.59)$$

In order to derive an equation for the second fundamental form  $\Phi_{2.g}$  of the gear tooth surface  $\mathcal{G}$ , the second derivatives of  $\mathbf{r}_g(U_g, V_g)$  with respect to  $U_g$ —and  $V_g$ —parameters are required. The equations for the vectors  $\mathbf{U}_g$  and  $\mathbf{V}_g$  derived above make possible calculation of the required derivatives:

$$\frac{\partial \mathbf{U}_g}{\partial U_P} = \begin{bmatrix} 0 \\ 0 \\ 0 \\ 1 \end{bmatrix} \quad (1.60)$$

$$\frac{\partial \mathbf{U}_g}{\partial V_g} \equiv \frac{\partial \mathbf{V}_g}{\partial U_g} = \begin{bmatrix} \cos \psi_{b,g} \cos V_g \\ \cos \psi_{b,g} \sin V_g \\ 0 \\ 1 \end{bmatrix} \quad (1.61)$$

$$\frac{\partial \mathbf{V}_g}{\partial V_g} = \begin{bmatrix} -r_{b,g} \cos V_g - U_g \cos \psi_{b,g} \sin V_g \\ -r_{b,g} \sin V_g + U_g \cos \psi_{b,g} \cos V_g \\ 0 \\ 1 \end{bmatrix} \quad (1.62)$$

Further, substitute these derivatives (see Eqs. 1.60–1.62) and Eq. (1.37) into Eqs. (1.45)–(1.47). After the necessary formulae transformations are complete, Eqs. (1.45)–(1.47) cast into a set of formulae for the calculation of fundamental magnitudes of the second order of the screw involute surface  $\mathcal{G}$ :

$$L_g = 0 \quad (1.63)$$

$$M_g = 0 \quad (1.64)$$

$$N_g = -U_g \sin \psi_{b,g} \cos \psi_{b,g} \quad (1.65)$$

After substituting of Eqs. (1.63)–(1.65) into Eqs. (1.45)–(1.47), one can obtain an equation for the calculation of the second fundamental form of the screw involute surface  $\mathcal{G}$  of a gear tooth:

$$\Phi_{2,g} \Rightarrow -d\mathbf{r}_g \cdot d\mathbf{N}_g = -U_g \sin \psi_{b,g} \cos \psi_{b,g} dV_g^2 \quad (1.66)$$

Similarly, to the derivation of Eq. (1.58), the calculated values of the fundamental magnitudes  $L_g$ ,  $M_g$ , and  $N_g$  can be substituted into Eq. (1.44) for the quadratic form  $\Phi_{2,g}$ . In this way, the matrix representation of the second fundamental form  $\Phi_{2,g}$  can be calculated as well. The interested reader may wish to complete this formulae transformation on his/her own.

The discriminant  $T_g$  of the second fundamental form  $\Phi_{2,g}$  of the screw involute surface  $\mathcal{G}$  is equal to:

$$T_g = \sqrt{L_g M_g - N_g^2} = 0 \quad (1.67)$$

The derived set of six equations for the calculation of the fundamental magnitudes:

$E_g = 1$	$L_g = 0$
$F_g = -\frac{r_{b,g}}{\cos \psi_{b,g}}$	$M_g = 0$
$G_g = \frac{U_g^2 \cos^4 \psi_{b,g} + r_{b,g}^2}{\cos^2 \psi_{b,g}}$	$N_g = -U_g \sin \psi_{b,g} \cos \psi_{b,g}$

represents a natural kind of parameterization of the part surface  $P$ . All the major elements of geometry of the gear tooth surface can be calculated based on the fundamental magnitudes of the first  $\Phi_{1,g}$  and of the second  $\Phi_{2,g}$  order. Location and orientation of the surface  $\mathcal{G}$  are the two parameters that remain indefinite yet.

Once a surface is represented in natural form, that is, it is expressed in terms of six fundamental magnitudes of the first and of the second order, then further calculation of parameters of the surface  $P$  gets much easier. In order to demonstrate a significant simplification of the calculation of the parameters of the geometry of the surface  $P$ , numerous useful equations are presented below within the body of the text as an example.

## 1.6 Elements of Local Geometry of Desired Part Surface

Part surfaces of various complexities are used in present practice. Some part surfaces feature simple geometry such as cylinders of revolution, cones of revolution, planes, some kinds of surfaces of revolution, and some kinds of screw surfaces. Other parts, for example, sculptured part surfaces, feature complex geometry. It often happens that the analytical description of the local geometry of sculptured part surfaces works perfectly when evaluating their performance capability. Bearing this in mind, the main elements of a surface local geometry are outlined briefly below.

The local geometry at a point of interest  $m$  on the desired part surface  $P$  is described by a set of the parameters. Some of the parameters of surface geometry are already discussed in this chapter. They are as follows: tangent vectors  $\mathbf{U}_P$  and  $\mathbf{V}_P$  to Gauss coordinate lines through point  $m$  on the surface  $P$  (see Eqs. 1.3 and 1.4); unit tangent vectors  $\mathbf{u}_P$  and  $\mathbf{v}_P$  to Gauss coordinate lines through point  $m$  on the surface  $P$  (see Eqs. 1.5 and 1.6); a plane that is tangent to the surface  $P$  at point of interest  $m$  (see Eq. 1.15); and unite normal vector  $\mathbf{n}_P$  at point  $m$  (see Eq. 1.17). The rest of parameters of local geometry at point  $m$  on the surface  $P$  are concisely outlined below.

### 1.6.1 Unit Vectors of Principal Directions at Point on Part Surface

At any point  $m$  on a smooth regular part surface  $P$  there exist two directions, in which normal curvature of the surface reaches extreme values. These directions are commonly called the “*principal directions*” at a point on part surface  $P$ .

Commonly, the vectors of the principal directions are designated as  $\mathbf{T}_{1,P}$  and  $\mathbf{T}_{2,P}$ . The vectors  $\mathbf{T}_{1,P}$  and  $\mathbf{T}_{2,P}$  are located within a tangent plane through the point  $m$ . They are perpendicular to one another ( $\mathbf{T}_{1,P} \perp \mathbf{T}_{2,P}$ ).

The normal curvature of the surface  $P$  in the direction specified by the tangent vector  $\mathbf{T}_{1,P}$  is of a maximum value, while the normal curvature of that same surface in the direction specified by the tangent vector  $\mathbf{T}_{2,P}$  is of a minimum value.

For the calculation of the vectors  $\mathbf{T}_{1,P}$  and  $\mathbf{T}_{2,P}$  of principal directions through a given point  $m$  on the part surface  $P$ , the fundamental magnitudes of the first order  $E_P, F_P, G_P$ , and of the second order  $L_P, M_P, N_P$  are used.

The vectors  $\mathbf{T}_{1,P}$  and  $\mathbf{T}_{2,P}$  of principal directions can be calculated as the roots of the equation:

$$\begin{vmatrix} E_P dU_P + F_P dV_P & F_P dU_P + G_P dV_P \\ L_P dU_P + M_P dV_P & M_P dU_P + N_P dV_P \end{vmatrix} = 0 \quad (1.68)$$

The first principal plane section  $C_{1,P}$  is orthogonal to  $P$  at  $m$ , and passes through the vector  $\mathbf{T}_{1,P}$  of the first principal direction. The second principal plane section  $C_{2,P}$  is orthogonal to  $P$  at  $m$ , and passes through the vector  $\mathbf{T}_{2,P}$  of the second principal direction. The first and the second principal sections  $C_{1,P}$  and  $C_{2,P}$  are always perpendicular to one another.

In engineering geometry of surfaces, it is often preferred to treat the unit tangent vectors  $\mathbf{t}_{1,P}$  and  $\mathbf{t}_{2,P}$  of the principal directions instead of use the tangent vectors  $\mathbf{T}_{1,P}$  and  $\mathbf{T}_{2,P}$  themselves. The unit tangent vectors  $\mathbf{t}_{1,P}$  and  $\mathbf{t}_{2,P}$  are calculated from the following equations:

$$\mathbf{t}_{1,P} = \frac{\mathbf{T}_{1,P}}{|\mathbf{T}_{1,P}|} \quad (1.69)$$

$$\mathbf{t}_{2,P} = \frac{\mathbf{T}_{2,P}}{|\mathbf{T}_{2,P}|} \quad (1.70)$$

respectively.

The unit normal vector,  $\mathbf{n}_P$  (see Eq. 1.17), at a point of a part surface  $P$  together with the unit tangent vectors  $\mathbf{t}_{1,P}$  and  $\mathbf{t}_{2,P}$  (see Eqs. 1.69 and 1.70) of the principal directions forms a set of unit vectors  $\mathbf{n}_P \mathbf{t}_{1,P} \mathbf{t}_{2,P}$  of a local reference system. This reference system  $\mathbf{n}_P \mathbf{t}_{1,P} \mathbf{t}_{2,P}$  is commonly called as the “*Darboux<sup>12</sup> trihadron*.”

---

<sup>12</sup>Jean-Gaston **Darboux** (August 14, 1842–February 23, 1917)—a French mathematician.

### 1.6.2 Principal Curvatures at Point of Part Surface

Two normal curvatures of a surface  $P$  in the principal plane sections  $C_{1,P}$  and  $C_{2,P}$  are commonly referred to as “*principal curvatures*” of the surface. Principal curvatures at a point of interest of a smooth regular surface  $P$  are denoted by  $k_{1,P}$  and  $k_{2,P}$  accordingly. We should stress here that the inequality:

$$k_{1,P} > k_{2,P} \quad (1.71)$$

is always observed at any and all regular points on part surface  $P$ .

In reduced cases of part surfaces, that is, at all points on a sphere, as well as at all points on a plane, all normal curvatures at a surface point are equal to one another. In these reduced cases, principal directions at a surface point cannot be identified.

At a specified point  $m$  on a smooth regular part surface  $P$ , the principal curvatures  $k_{1,P}$  and  $k_{2,P}$  of the surface are calculated as roots of square equation:

$$\begin{vmatrix} L_P - E_P k_P & M_P - F_P k_P \\ M_P - F_P k_P & N_P - G_P k_P \end{vmatrix} = 0 \quad (1.72)$$

In expanded form, Eq. (1.72) can be rewritten as follows:

$$(E_P G_P - F_P^2) k_P^2 - (E_P N_P - 2F_P M_P + G_P L_P) k_P + (L_P N_P - M_P^2) = 0 \quad (1.73)$$

The principal radii of curvature  $R_{1,P}$  and  $R_{2,P}$  are reciprocal to the corresponding principal curvatures  $k_{1,P}$  and  $k_{2,P}$  of the surface  $P$  at that same point  $m$ . Thus, the principal radii of curvature  $R_{1,P}$  and  $R_{2,P}$  can be expressed in terms of the corresponding principal curvatures  $k_{1,P}$  and  $k_{2,P}$  accordingly:

$$R_{1,P} = \frac{1}{k_{1,P}} \quad (1.74)$$

$$R_{2,P} = \frac{1}{k_{2,P}} \quad (1.75)$$

The use of Eqs. (1.74) and (1.75) makes possible to compose an equation for the calculation of principal radii of curvature  $R_{1,P}$  and  $R_{2,P}$  similar to Eq. (1.72) that is used for the calculation of the principal curvatures  $k_{1,P}$  and  $k_{2,P}$  of the surface  $P$  at a point  $m$ . In expanded form, such the equation can be rewritten as<sup>13</sup>:

$$R_P^2 - \frac{E_P N_P - 2F_P M_P + G_P L_P}{T_P} R_P + \frac{H_P}{T_P} = 0 \quad (1.76)$$

---

<sup>13</sup>Reminder: algebraic values of the radii of principal curvature  $R_{1,P}$  and  $R_{2,P}$  are related to each other as  $R_{2,P} > R_{1,P}$ .

Here,  $H_P$  is the discriminant of the first order (see Eq. 1.37), and  $T_P$  is the discriminant of the second order (see Eq. 1.51) of the surface  $P$  at a point  $m$ .

The normal curvature  $k_P$  at a point on a surface  $P$  at an arbitrary direction through a point  $m$  can be calculated from the equation:

$$k_P = \frac{\Phi_{2,P}}{\Phi_{1,P}} \quad (1.77)$$

In case an angle  $\theta$  between a normal plane section  $C_P$  through the point  $m$  and the first principal plane  $C_{1,P}$  is known, then “Euler<sup>14</sup> equation” for the calculation of  $k_P$ :

$$k_P = k_{1,P} \cos^2 \theta + k_{2,P} \sin^2 \theta \quad (1.78)$$

can conveniently be used (here,  $\theta$  is the angle that the normal plane section  $C_P$  forms with the first principal plane section  $C_{1,P}$ ; in other words,  $\theta = \angle(\mathbf{t}_P, \mathbf{t}_{1,P})$  with  $\mathbf{t}_P$  designating the unit tangent vector within the normal plane section  $C_P$ ).

Equation (1.78) can also be rewritten in the form:

$$k_P = H_P + \frac{k_{1,P} - k_{2,P}}{2} \cos 2\theta \quad (1.79)$$

One more equation is of practical importance:

$$\tau_P = (k_{2,P} - k_{1,P}) \sin \theta \cos \theta \quad (1.80)$$

This equation is commonly called the “Sophie Germain equation” (or “Bertrand<sup>15</sup> equation,” in other interpretation). In this equation, the torsion  $\tau_P$  of the surface at a point  $m$  is expressed in terms of the principal curvatures  $k_{1,P}$  and  $k_{2,P}$ , and of the angle  $\theta$ .

The curvature of a surface in a plane section at an angle  $\nu$  in relation to the corresponding normal plane section can be calculated from “Meusnier<sup>16</sup> formula:”

$$k_{P,\nu} = \frac{k_P}{\cos \nu} \quad (1.81)$$

This equation can also be expressed in terms of corresponding radii of curvature:

$$R_{P,\nu} = R_P \cos \nu \quad (1.82)$$

---

<sup>14</sup>Leonhard **Euler** (April 15, 1707–September 18, 1783)—a famous Swiss mathematician and physicist.

<sup>15</sup>Joseph Louis François **Bertrand** (March 11, 1822–April 5, 1900)—a French mathematician.

<sup>16</sup>de La Place Jean Baptiste Marie **Meusnier** (June 19, 1754–June 13, 1793)—a French mathematician.

A few more expressions to mention here.

### 1.6.3 Other Parameters of Part Surface Curvature

In addition to the normal curvature  $k_P$  and to principal curvatures  $k_{1,P}$  and  $k_{2,P}$  at a point  $m$  of a smooth regular part surface  $P$ , several other parameters of curvature of a part surface are used in practice

#### 1.6.3.1 Mean Curvature at a Surface Point

The “mean curvature,  $\mathcal{M}_P$ ,” at a surface point is defined as half the sum<sup>17</sup> of the principal curvatures at that same surface point  $m$ . By definition, the mean curvature  $\mathcal{G}_P$  is equal to:

$$\mathcal{M}_P = \frac{k_{1,P} + k_{2,P}}{2} \quad (1.83)$$

The mean curvature can also be expressed in terms of fundamental magnitudes of the first and second order:

$$\mathcal{M}_P = \frac{E_P N_P - 2F_P M_P + G_P L_P}{2(E_P G_P - F_P^2)} \quad (1.84)$$

The “mean curvature,  $\mathcal{M}_P$ ,” is invariant with respect to a reference system the part surface  $P$  is analytically described in.

#### 1.6.3.2 Gaussian Curvature at a Surface Point

The “Gaussian curvature” (or, in other words, “full curvature”) at a surface point is defined as product of the principal curvatures at that same surface point  $m$ . By definition the “Gaussian curvature,  $\mathcal{G}_P$ ,” is equal to:

$$\mathcal{G}_P = k_{1,P} \cdot k_{2,P} \quad (1.85)$$

The “Gaussian curvature” can also be expressed in terms of fundamental magnitudes of the first and second order:

---

<sup>17</sup>Some researchers prefer to define mean curvature at a surface point as the sum of principal curvatures at a surface point  $m$ , and not as half the sum. Under such a scenario mean curvature  $\mathcal{M}_P$  is specified as  $\mathcal{M}_P = k_{1,P} + k_{2,P}$ . An equation for  $\mathcal{M}_P$  that is equivalent to Eq. (1.84) can be rewritten in the form  $\mathcal{M}_P = \frac{E_P N_P - 2F_P M_P + G_P L_P}{(E_P G_P - F_P^2)}$ .



$$\mathcal{G}_P = \frac{L_P N_P - M_P^2}{E_P G_P - F_P^2} \quad (1.86)$$

Equation (1.84) for “mean curvature,  $\mathcal{M}_P$ ,” together with Eq. (1.86) for “Gaussian curvature,  $\mathcal{G}_P$ ,” makes yield composing a quadratic equation:

$$k_P^2 - 2\mathcal{M}_P k_P + \mathcal{G}_P = 0 \quad (1.87)$$

for the calculation of principal curvatures  $k_{1,P}$  and  $k_{2,P}$ .

On solution of Eq. (1.87) with respect to  $k_{1,P}$  and  $k_{2,P}$ , the principal curvatures  $k_{1,P}$  and  $k_{2,P}$  can be expressed in terms of the “mean curvature,  $\mathcal{M}_P$ ,” and of the “Gaussian curvature,  $\mathcal{G}_P$ :”

$$k_{1,P} = \mathcal{M}_P + \sqrt{\mathcal{M}_P^2 - \mathcal{G}_P} \quad (1.88)$$

$$k_{2,P} = \mathcal{M}_P - \sqrt{\mathcal{M}_P^2 - \mathcal{G}_P} \quad (1.89)$$

The “Gaussian curvature,  $\mathcal{G}_P$ ,” is invariant with respect to a reference system the part surface  $P$  is analytically described in.

### 1.6.3.3 Absolute Curvature at a Surface Point

In certain applications, it is reasonable to specify local geometry of a surface by means of “absolute curvature.” By definition, “absolute curvature,  $\tilde{A}_P$ ,” at a point  $m$  of a smooth regular part surface  $P$  is equal:

$$\tilde{A}_P = |k_{1,P}| + |k_{2,P}| \quad (1.90)$$

The “absolute curvature,  $\tilde{A}_P$ ,” at a point  $m$  of a smooth regular part surface  $P$  can be expressed in terms of fundamental magnitudes of the first and second order, as well as in terms of the “mean curvature,  $\mathcal{M}_P$ ,” and “Gaussian curvature,  $\mathcal{G}_P$ ,” at a surface point  $m$  (see Eqs. 1.88 and 1.89).

### 1.6.3.4 Shape Operator of a Surface

The “shape operator”<sup>18</sup> is a generalized measure of concavity and convexity of a surface point  $m$ . Weingarten<sup>19</sup> is credited with the concept of shape operator of a surface.

<sup>18</sup> The “shape operator” is also often referred to as the “shape index” or “Weingarten map.”

<sup>19</sup> Julius Weingarten (March 2, 1836–June 16, 1910)—a German mathematician.

The differential structure of a surface is captured by the local “*Hessian matrix*,” which may be approximated in terms of surface normals by the expression:

$$\mathcal{H} = \begin{bmatrix} -\left(\frac{\partial \mathbf{n}_P}{\partial x}\right)_x & -\left(\frac{\partial \mathbf{n}_P}{\partial x}\right)_y \\ -\left(\frac{\partial \mathbf{n}_P}{\partial y}\right)_x & -\left(\frac{\partial \mathbf{n}_P}{\partial y}\right)_y \end{bmatrix} \quad (1.91)$$

where subscripts “ $x$ ” and “ $y$ ” denote the  $x$  and  $y$  components of the parameterized vector velocity.

The principal curvatures of the part surface are the eigenvalues of the “*Hessian matrix*,” found out by solving the equation:

$$|\mathcal{H} - k\mathbf{I}| = 0 \quad (1.92)$$

for  $k$ , where  $\mathbf{I}$  is the identity matrix.

By definition, the “*shape operator*,  $\mathcal{S}_P$ ,” is the differential of “*Gauss map*” of the surface. The “*shape operator*,  $\mathcal{S}_P$ ,” is a generalized measure of concavity and convexity.

The determinant of the “*shape operator*” at a point is the “*Gaussian curvature*,” but it also contains other information, since the mean curvature is half the trace of the shape operator. The eigenvectors and eigenvalues of the shape operator at every surface point determine the directions in which the surface bands at each point.

*Koenderink* and *van Doorn* developed a single value, angular measure to describe the local surface topology in terms of the principal curvatures.

The “*shape operator*” is given in terms of the components of the first and second fundamental forms by “*Weingarten equation*.”

$$\mathcal{S}_P = \frac{\begin{vmatrix} G_P L_P - F_P M_P & G_P M_P - F_P N_P \\ E_P M_P - F_P L_P & E_P N_P - F_P M_P \end{vmatrix}}{E_P G_P - F_P^2} \quad (1.93)$$

The shape operator can also be expressed in terms of principal curvatures at a surface point  $m$ :

$$\mathcal{S}_P = -\frac{2}{\pi} \arctan \frac{k_{1,P} + k_{2,P}}{k_{1,P} - k_{2,P}} \quad (1.94)$$

and may be expressed in terms of the surface normal:

$$\mathcal{S}_P = -\frac{2}{\pi} \arctan \frac{\left(\frac{\partial \mathbf{n}_P}{\partial x}\right)_x + \left(\frac{\partial \mathbf{n}_P}{\partial x}\right)_y}{\sqrt{\left[\left(\frac{\partial \mathbf{n}_P}{\partial x}\right)_x - \left(\frac{\partial \mathbf{n}_P}{\partial x}\right)_y\right]^2 + 4\left(\frac{\partial \mathbf{n}_P}{\partial x}\right)_y \left(\frac{\partial \mathbf{n}_P}{\partial x}\right)_x}} \quad (1.95)$$

The shape operator varies from  $-1$  to  $+1$ . It describes the local shape at a surface point independent of the scale of the surface. A shape operator value of  $+1$  corresponds to a concave local portion of the surface  $P$  for which the principal directions are unidentified, and thus, the normal radii of curvature in all directions are identical to each other. A shape operator of  $0$  corresponds to a saddle-like local portion of the surface  $P$  with principal curvatures of equal magnitude but opposite sign.

### 1.6.3.5 Curvedness of a Surface

The “*surface curvedness*” is another measure that is derived from the surface principal curvatures. By definition, the “*surface curvedness*,  $\mathfrak{R}_P$ ,” is equal to:

$$\mathfrak{R}_P = \sqrt{\frac{k_{1,P}^2 + k_{2,P}^2}{2}} \quad (1.96)$$

The curvedness describes the scale of the surface  $P$ , independent of its shape.

These quantities  $\mathcal{S}_P$  and  $\mathfrak{R}_P$  are the primary differential properties of a smooth regular part surface. Note that they are properties of the surface itself and do not depend upon its parameterization except for a possible change of sign.

In order to get a profound understanding of differential geometry of surfaces, the interested reader may wish to go to advanced monographs in the field. Systematic discussion of the topic is available from many sources. The author would like to turn the reader’s attention to the monographs by *doCarmo* [9], *Struik* [10], and others.

The elements of a surface local geometry considered briefly above make it possible to introduce a definition to the term “*sculptured part surface P*:”

**Definition 1.1** The sculptured part surface  $P$  is a smooth regular surface, whose major parameters of local geometry differ from each other in differential vicinity of any two points infinitely close to each other.

The given definition to the term “*sculptured part surface, P*” is of critical importance for further discussion.

It is instructive to point out here that a sculptured part surface  $P$  does not allow for “*sliding over itself*.”

## References

1. Radzevich, S. P. (1991). *Differential-geometrical method of surface generation* (300 p.) (Doctoral Thesis) Tula Polytechnic Institute, Tula.
2. Radzevich, S. P. (2017) *Generation of surfaces: Kinematic geometry of surface machining* (738 p.). Boca Raton, Florida: CRC Press.
3. Radzevich, S. P. (2010). *Gear cutting tools: Fundamentals of design and computation* (p. 786). Boca Raton, Florida: CRC Press.

4. Mortenson, M. E.: *Geometric modeling* (763 p.). New York: Wiley, Inc.
5. Bonnet, P. O. (1867) *Journ. Ec. Polytch.*, xiii, 31.
6. Radzevich, S. P. (2002). Conditions of proper sculptured surface machining. *Computer-Aided Design*, 34(10), 727–740.
7. Radzevich, S. P. (2001). *Fundamentals of surface generation* (p. 592). Monograph: Kiev, Rastan.
8. Radzevich, S. P. (2008). *Kinematic geometry of surface machining* (p. 536). Boca Raton, Florida: CRC Press.
9. doCarmo, M. P. (1976) *Differential geometry of curves and surfaces* (503 p.). Englewood Cliffs, NJ: Prentice-Hall.
10. Struik, D. J. (1961). *Lectures on classical differential geometry* (2nd ed., p. 232). Massachusetts: Addison-Wesley Publishing Company Inc.

## Chapter 2

# On a Possibility of Classification of Part Surfaces



An enormous number of kinds of part surfaces are used in the present-day engineering practice. A systematic investigation of surfaces for the purposes of practical application is of critical importance. With this intent, a scientific classification of part surfaces is desired to be developed. It is important to point out here that no classification of surfaces in global sense is feasible: No scientific classification of surfaces “*globally*” can be developed at all. Hence, other approaches for systematic study of part surfaces should be investigated.

### 2.1 Sculptured Part Surfaces

It makes sense to begin the analysis of a possibility of developing of a scientific classification of surfaces from the consideration of sculptured part surfaces, as such part surfaces represent the most general case featuring the most complex geometry.

Many products are designed with aesthetic sculptured surfaces to enhance their appearance, an important factor in customer satisfaction, especially for automotive and consumer electronics products. In other cases, products have sculptured surfaces to meet functional requirements. Examples of functional surfaces can be easily found in aero-, gas-, and hydrodynamic applications (turbine blades), optical (lamp reflector), and medical (parts of anatomical reproduction) applications, manufacturing surfaces (molding die, die face), and so forth. Functional surfaces interact with the environment or with another surface. Therefore, functional surfaces also can be called “*dynamic surface*”.

Functional surfaces do not allow for “*sliding over themselves*.”

In this text, a “*local surface patch,  $P$* ” is understood in the sense of a surface patch that is located in infinitesimal vicinity of point of the part surface  $P$ .

### 2.1.1 Local Patches of Perfect Part Surfaces

Geometrical features of local patches of perfect part surfaces can be expressed in terms of the “*Gaussian curvature*,  $\mathcal{G}_P$ ,” at a specified point of the surface. With that said, perfect local surface patches may feature either positive “*Gaussian curvature*” (in this particular case  $\mathcal{G}_P > 0$ ), or zero “*Gaussian curvature*” ( $\mathcal{G}_P = 0$ ), or finally negative “*Gaussian curvature*” ( $\mathcal{G}_P < 0$ ).

Specific values of the principal curvatures  $k_{1,P}$  and  $k_{2,P}$  are also used for making a decision regarding the actual shape features of a perfect local part surface patch.

The mean curvature  $\mathcal{M}_P$  of a perfect (an ideal) local part surface patch  $P$  can be employed for this purpose only by convention as there is no objective  $\mathcal{M}_P$ -based criterion for deciding whether a local part surface patch is convex or concave.

Commonly, five kinds of perfect local part surface patches are recognized (Fig. 2.1), as listed below.

First, in a case of positive “*Gaussian curvature*” ( $\mathcal{G}_P > 0$ ), the perfect local part surface patch is called an “*elliptical*” perfect local part surface patch. An example of an elliptical perfect local part surface patch is schematically depicted in Fig. 2.1a. The

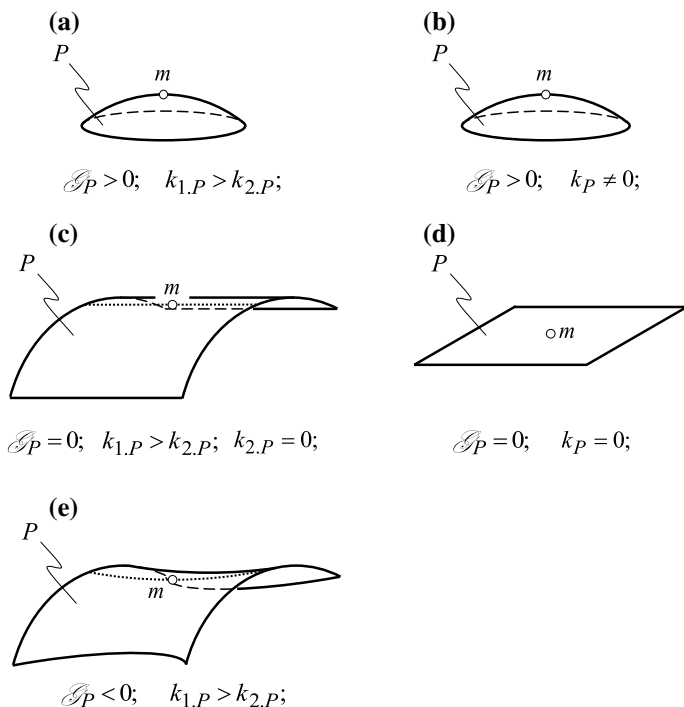


**Fig. 2.1** Five kinds of local surface patches of a perfect sculptured part surface  $P$ : **a** elliptical, **b** umbilical, **c** parabolical, **d** hyperbolic, and **e** planar

principal curvatures  $k_{1,P}$  and  $k_{2,P}$  of a perfect local surface patch of this particular kind relate to one another to meet the inequality  $k_{1,P} > k_{2,P}$ .

Second, when the “*Gaussian curvature*” is of a positive value ( $\mathcal{G}_P > 0$ ), the perfect local part surface patch may feature equally all normal curvatures in plane sections through a specified point  $m$  within the part surface  $P$ . In this particular case, principal directions at a surface point  $m$  cannot be identified. Thus, no principal curvatures of the perfect local part surface patch can be specified. A perfect local surface patch of this particular kind is called an “*umbilical*” perfect local part surface patch. An example of an elliptic perfect local part surface patch is schematically depicted in Fig. 2.1b. All normal curvatures  $k_P$  of the local surface patch of this particular kind are equal to one another, and all of them are of nonzero value ( $k_P \neq 0$ ).

Third, in a case of zero “*Gaussian curvature*” ( $\mathcal{G}_P = 0$ ), the perfect local part surface patch is called a “*parabolical*” perfect local part surface patch. An example of a parabolical perfect local part surface patch is schematically depicted in Fig. 2.1c. The principal curvatures  $k_{1,P}$  and  $k_{2,P}$  of a perfect local surface patch of this particular kind relate to one another to fulfill the inequality  $k_{1,P} > k_{2,P}$ . The second principal curvature  $k_{2,P}$  of a parabolical local surface patch is always zero ( $k_{2,P} = 0$ ).

Fourth, in a case of zero “*Gaussian curvature*” ( $\mathcal{G}_P = 0$ ), the perfect local part surface patch may feature equally all normal curvatures in plane sections through a specified point  $m$  within the part surface  $P$ . In this particular case, principal directions at a surface point  $m$  cannot be identified. Thus, no principal curvatures of the perfect local part surface patch can be specified. A perfect local surface patch of this particular kind is called a “*planar*” perfect local part surface patch. An example of planar perfect local part surface patch is schematically depicted in Fig. 2.1d. All normal curvatures  $k_P$  of a perfect local surface patch of this particular kind are equal to one another, and all of them are of a zero value ( $k_P \equiv 0$ ).

Fifth, in a case of negative “*Gaussian curvature*” ( $\mathcal{G}_P < 0$ ), the perfect local part surface patch is called a “*hyperbolical*” perfect local part surface patch. An example of a hyperbolical perfect local part surface patch is schematically depicted in Fig. 2.1e. The principal curvatures  $k_{1,P}$  and  $k_{2,P}$  of a perfect local surface patch of this particular kind relate to one another to meet the inequality  $k_{1,P} > k_{2,P}$ .

Local patches of perfect part surfaces of no other kind are recognized in differential geometry of surfaces, in addition to those five kinds just discussed above.

### 2.1.2 Local Patches of Real Part Surfaces

A real part surface bounds a solid: The solid is the “*bearer*” of the shape of the surface. This is one of the principal differences between perfect surfaces and real part surfaces. This difference makes it easy to distinguish whether a part surface is convex, concave, or of saddle type.

The performed analysis of the geometry of local patches of “*perfect*” part surfaces (see Fig. 2.1) makes allows proceeding to the corresponding local patches of “*real*”

part surfaces. Then, the following ten kinds of local patches of a real part surface are distinguished (Fig. 2.2).

1. “Convex local patch of elliptic kind” of a real part surface  $P$ . A convex local patch of elliptic kind is schematically shown in Fig. 2.2a. Local surface patches of this kind feature positive “Gaussian curvature” ( $\mathcal{G}_P > 0$ ) and positive mean

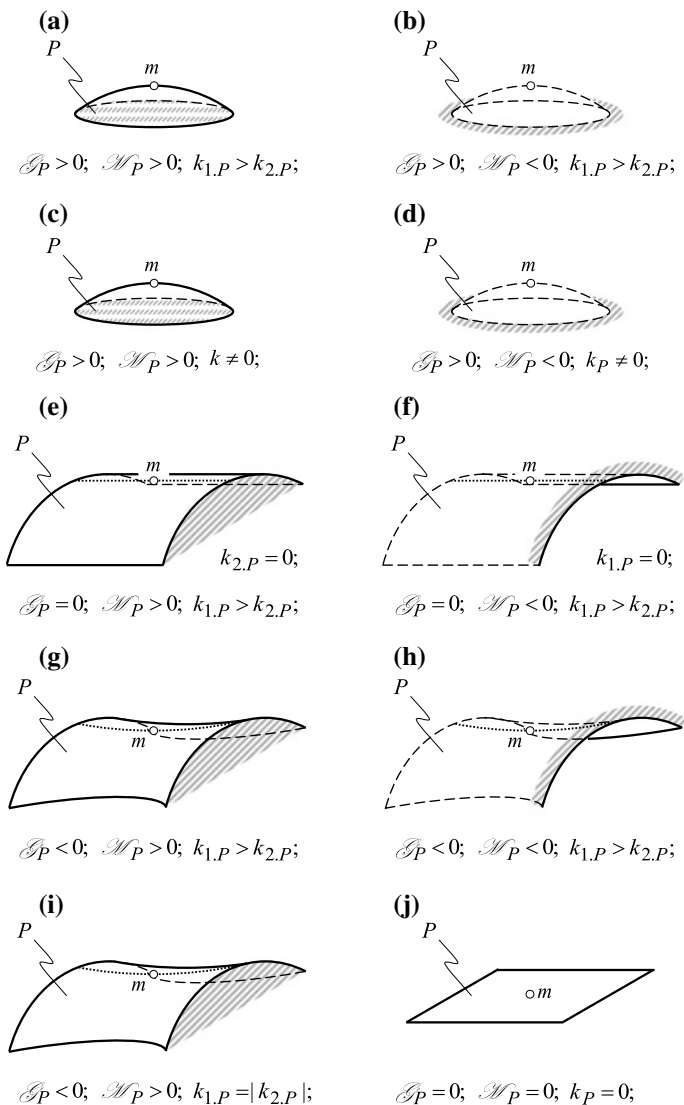


**Fig. 2.2** Ten kinds of local patches of real sculptured part surfaces (After Prof. S. P. Radzevich, 1991)



curvature ( $\mathcal{M}_P > 0$ ). At a point of interest  $m$ , the principal curvatures  $k_{1,P}$  and  $k_{2,P}$  for a convex local patch of elliptic kind relate to one another to meet the inequality  $k_{1,P} > k_{2,P} > 0$ . The body side of a convex local patch of elliptic kind is located entirely on one side in relation to the surface tangent plane through the point of interest  $m$ .

2. “*Concave local patch of elliptic kind*” of a real part surface  $P$ . A concave local patch of elliptic kind is schematically shown in Fig. 2.2b. Local surface patches of this kind feature positive “*Gaussian curvature*” ( $\mathcal{G}_P > 0$ ) and negative mean curvature ( $\mathcal{M}_P < 0$ ). At a point of interest  $m$ , the principal curvatures  $k_{1,P}$  and  $k_{2,P}$  for a concave local patch of elliptic kind relate to one another to fulfill the inequality  $k_{1,P} > k_{2,P} < 0$ . The body side of a concave local patch of elliptic kind is located on both sides in relation to the tangent plane through the point of interest  $m$ .
3. “*Convex local patch of umbilic kind*” of a real part surface  $P$ . A convex local patch of umbilic kind is schematically shown in Fig. 2.2c. Local surface patches of this kind feature positive “*Gaussian curvature*” ( $\mathcal{G}_P > 0$ ) and positive mean curvature ( $\mathcal{M}_P > 0$ ). At a point of interest  $m$ , the principal curvatures for a convex local patch of elliptic kind are not identified. All normal curvatures  $k_P$  of the surface are positive ( $k_P > 0$ ). The body side of a convex local patch of umbilic kind is entirely located on one side in relation to the tangent plane through the point of interest  $m$ . A convex local patch of umbilic kind can be viewed as a reduced case of the corresponding convex local patch of elliptic kind of a real part surface  $P$ .
4. “*Concave local patch of umbilic kind*” of a real part surface  $P$ . A concave local patch of umbilic kind is schematically shown in Fig. 2.2d. Local surface patches of this kind feature positive “*Gaussian curvature*” ( $\mathcal{G}_P > 0$ ) and negative mean curvature ( $\mathcal{M}_P < 0$ ). At a point of interest  $m$ , the principal curvatures for a concave local patch of umbilic kind are not identified. All normal curvatures  $k_P$  of the surface are negative ( $k_P < 0$ ). The body side of a concave local patch of umbilic kind is located on both sides in relation to the tangent plane through the point of interest  $m$ . A concave local patch of umbilic kind can be viewed as a reduced case of the corresponding concave local patch of elliptic kind of the real part surface  $P$ .
5. “*Convex local patch of parabolic kind*” of a real part surface  $P$ . Convex local patch of parabolic kind is schematically shown in Fig. 2.2e. Local surface patches of this kind feature zero “*Gaussian curvature*” ( $\mathcal{G}_P = 0$ ) and positive mean curvature ( $\mathcal{M}_P > 0$ ). At a point of interest  $m$ , the principal curvatures  $k_{1,P}$  and  $k_{2,P}$  for a convex local patch of parabolic kind relate to one another to fulfill the inequality  $k_{1,P} > k_{2,P}$ . Moreover, the second principal curvature  $k_{2,P}$  is zero ( $k_{2,P} = 0$ ). The body side of a convex local patch of parabolic kind is entirely located on one side in relation to the tangent plane through the point of interest  $m$ . A convex local patch of parabolic kind can be viewed as a degenerated case of the corresponding concave local patch of elliptic kind of a real part surface  $P$  assuming that the second principal curvature  $k_{2,P}$  is zero ( $k_{2,P} = 0$ ).

6. “*Concave local patch of parabolic kind*” of a real part surface  $P$ . A concave local patch of parabolic kind is schematically shown in Fig. 2.2f. Local surface patches of this kind feature zero “*Gaussian curvature*” ( $\mathcal{G}_P = 0$ ) and negative mean curvature ( $\mathcal{M}_P < 0$ ). At a point of interest  $m$ , the principal curvatures  $k_{1,P}$  and  $k_{2,P}$  for a concave local patch of parabolic kind relate to one another to meet the inequality  $k_{1,P} > k_{2,P}$ . Moreover, the first principal curvature  $k_{1,P}$  is zero ( $k_{1,P} = 0$ ). The body side of a concave local patch of parabolic kind is located on both sides in relation to the tangent plane through the point of interest  $m$ . A concave local patch of parabolic kind can be construed as a degenerated case of the corresponding concave local patch of elliptic kind of a real part surface  $P$  assuming that the first principal curvature  $k_{1,P}$  is zero ( $k_{1,P} = 0$ ).
7. “*Pseudo-convex (saddle) local patch of hyperbolic kind*” of a real part surface  $P$ . A pseudo-convex local patch of hyperbolic kind is schematically shown in Fig. 2.2g. Local surface patches of this kind feature negative “*Gaussian curvature*” ( $\mathcal{G}_P < 0$ ) and positive mean curvature ( $\mathcal{M}_P > 0$ ). At a point of interest  $m$ , the principal curvatures  $k_{1,P}$  and  $k_{2,P}$  for a pseudo-convex local patch of hyperbolic kind relate to one another to fulfill the inequality  $k_{1,P} > k_{2,P}$ . Moreover, the magnitude of the first principal curvature is greater than the magnitude of the second principal curvature ( $k_{1,P} > |k_{2,P}|$ ). The term “*pseudo-convex*” is due to this inequality. The body side of a pseudo-convex local patch of hyperbolic kind is located on both sides in relation to the tangent plane through the point of interest  $m$ .
8. “*Pseudo-concave (saddle) local patch of hyperbolic kind*” of a real part surface  $P$ . A pseudo-concave local patch of hyperbolic kind is schematically shown in Fig. 2.2h. Local surface patch of this kind features negative “*Gaussian curvature*” ( $\mathcal{G}_P < 0$ ) and negative mean curvature ( $\mathcal{M}_P < 0$ ). At a point of interest  $m$ , the principal curvatures  $k_{1,P}$  and  $k_{2,P}$  for pseudo-concave local patch of hyperbolic kind relate to one another to meet the inequality  $k_{1,P} > k_{2,P}$ . Moreover, the magnitude of the first principal curvature is smaller than the magnitude of the second principal curvature ( $k_{1,P} < |k_{2,P}|$ ). The term “*pseudo-concave*” is due to this inequality. The body side of a pseudo-concave local patch of hyperbolic kind is located on both sides in relation to the tangent plane through the point of interest  $m$ .
9. “*Minimal (saddle) local patch of hyperbolic kind*” of a real part surface  $P$ . A minimal local patch of hyperbolic kind is schematically shown in Fig. 2.2i. Local surface patches of this kind feature negative “*Gaussian curvature*” ( $\mathcal{G}_P < 0$ ) and zero mean curvature ( $\mathcal{M}_P = 0$ ). At a point of interest  $m$ , the principal curvatures  $k_{1,P}$  and  $k_{2,P}$  for minimal local patch of hyperbolic kind relate to one another to fulfill the inequality  $k_{1,P} > k_{2,P}$ . Moreover, magnitude of the first principal curvature is equal to the magnitude of the second principal curvature ( $k_{1,P} = |k_{2,P}|$ ). The body side of a minimal local patch of hyperbolic kind is located on both sides in relation to the tangent plane through the point of interest  $m$ .
10. “*Local patch of planar kind*” of a real part surface  $P$ . A local patch of planar kind is schematically shown in Fig. 2.2j. Local surface patches of this kind feature

zero “Gaussian curvature” ( $\mathcal{G}_P = 0$ ) and zero mean curvature ( $\mathcal{M}_P = 0$ ). At a point of interest  $m$ , the principal curvatures for a planar local patch are not identified. The body side of a local patch of planar kind is entirely located on one side in relation to the tangent plane through the point of interest  $m$ . A local patch of planar kind can be viewed either as a reduced case of the corresponding local patch of elliptic kind (either convex or concave), or as a degenerated case of corresponding local patch of parabolic kind (either convex or concave), or as a degenerated case of the corresponding local patch of hyperbolic kind (either pseudo-convex, or pseudo-concave, or minimal) of a real part surface  $P$ .

Local patches of sculptured part surfaces can be classified. Figure 2.3 is helpful for understanding the local topology of sculptured part surface. It also allows a scientific classification of local patches of smooth regular part surface  $P$  (Fig. 2.3). The classification includes ten kinds of local surface patches and is an accomplished one.

Based on the analysis of sculptured part surface geometry, as well as on the classification of local surface patches (Fig. 2.3), a profound scientific classification of all possible kinds of local surface patches is developed by Radzevich [1]. It is proven that the total number of possible kinds of local surface patches is limited (it is not an infinite). Hence, local surface patches of every kind can be investigated individually. Surface patches of no kind would be missed in such a consideration. The interested reader may wish to go to [2] for details on the developed classification of local surface patches and its use in surface generation.

The performed analysis of the geometry of local patches of a smooth regular part surface  $P$  (see Fig. 2.3) reveals that all the local patches can also be organized in another way. For a better understanding of how local surface patches of different geometry relate to one another, all of them are organized so as to form a circular

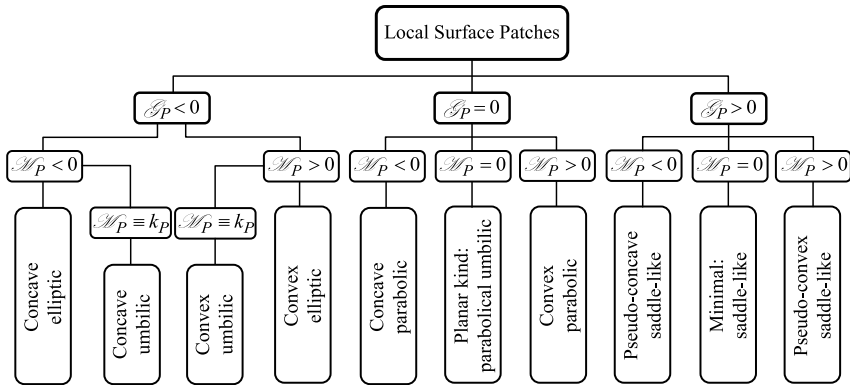


**Fig. 2.3** Ten kinds of local patches of a real smooth regular sculptured part surface  $P$  (adapted from [5])

chart.<sup>1</sup> Example of the chart is shown in Fig. 2.4. The transition from a local surface patch (see Fig. 2.4) to a nearby local surface patch, either in the radial direction of the circular chart or circumferentially shows how the normal curvatures of the local surface patch alter.

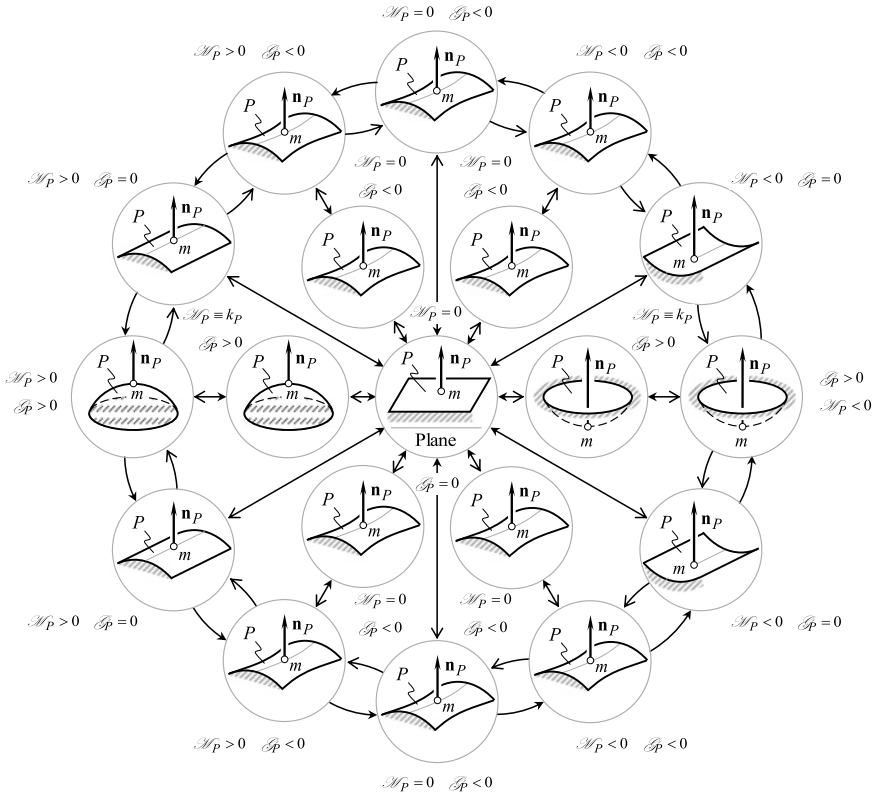


**Fig. 2.4** Circular chart comprised of ten different kinds of local patches of a real smooth regular part surface  $P$  (adapted from [5])

<sup>1</sup>The author would like to credit the idea of circular disposition of local surface patches of different kinds to *J. Koenderink*. To the best of the author's knowledge, *J. Koenderink* is the first (see Fig. 2.68 on p. 321 in [3]) to use circular disposition of "images" of local surface patches for the purpose of illustration of the relationship between local surface patches of different geometry. Reading the monograph by Koenderink [3] inspired the author to apply the concept of circular disposition of local surface patches of different kinds to the needs of surface geometry in mechanical engineering.

## 2.2 Planar Characteristic Images

For a more accurate analytical description of the geometry of a smooth regular part surface, the second-order parameters need to be incorporated into considered. The second-order analysis incorporates elements of both the first order and the second order.

### 2.2.1 Dupin Indicatrix

To perform the second-order analysis, familiarity with “*Dupin indicatrix*” is highly desired. The “*Dupin indicatrix*” is a perfect starting point for consideration of the second-order analysis.

The “*Dupin indicatrix,  $Dup(P)$* ” at a point of a smooth regular part surface  $P$  is a planar characteristic “*curve*” of the second order. This characteristic curve features both mirror symmetry and central symmetry.

Construction of the “*Dupin indicatrix,  $Dup(P)$* ” at a point of a smooth regular part surface  $P$  is illustrated in Fig. 2.5.

A plane  $W$  through the unit normal vector  $\mathbf{n}_P$  at a point of interest  $m$  of the part surface  $P$  spins about  $\mathbf{n}_P$ . When rotating, the plane occupies consecutive positions. Different positions of the plane  $W$  are denoted by  $W_1, W_2, W_3$ , and so forth. The radii

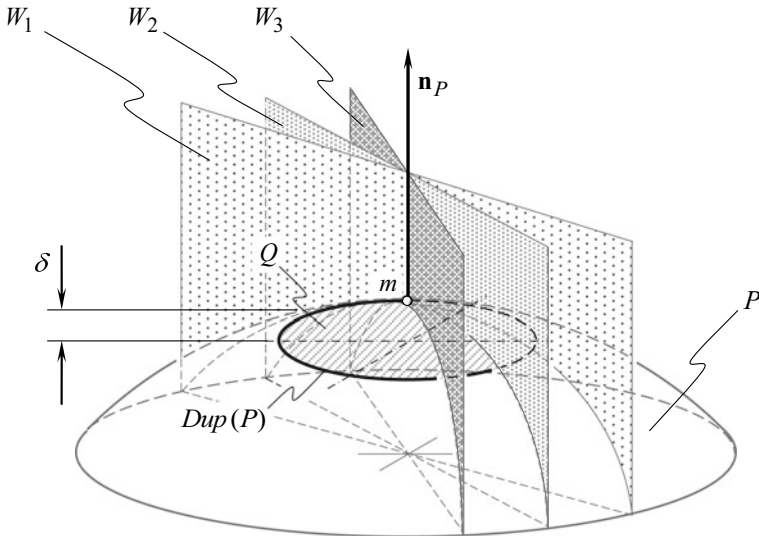


**Fig. 2.5** Geometrical interpretation of the “*Dupin indicatrix,  $Dup(P)$* ” at a point  $m$  of a part surface  $P$

of normal curvature of the lines of intersection of the surface  $P$  by normal planes  $W_1, W_2, W_3$ , and so forth are equal  $R_{P,1}, R_{P,2}, R_{P,3}$ , and so forth.

A plane  $Q$  is orthogonal to the unit normal vector  $\mathbf{n}_P$ . This plane is at a certain distance  $\delta$  from the point of interest  $m$ . The plane  $Q$  intersects the part surface  $P$ . When the distance  $\delta$  approaches zero ( $\delta \rightarrow 0$ ), and when the scale of the line of intersection of the part surface  $P$  by the plane  $Q$  approaches infinity, then the line of intersection of the surface  $P$  by the plane  $Q$  approaches a regular planar curve. This curve is called the “*Dupin indicatrix*” at a point of a smooth regular part surface  $P$ . Commonly, the “*Dupin indicatrix*” is designated as  $Dup(P)$ .

In differential geometry of surfaces, “*Dupin<sup>2</sup> indicatrices*” of the following five kinds are distinguished (Fig. 2.6):

- (a) elliptical [for which “*Gauss curvature*” is always positive ( $\mathcal{G}_P > 0$ )],
- (b) umbilical,
- (c) parabolical,
- (d) hyperbolical, and
- (e) minimal.

The “*Dupin indicatrix*” for a planar local patch of the surface  $P$  doesn’t exist. All points of this characteristic curve are remote to infinity.

Phantom branches of the characteristic curve  $Dup(P)$  in Fig. 2.6d through Fig. 2.6e are shown in dashed lines.

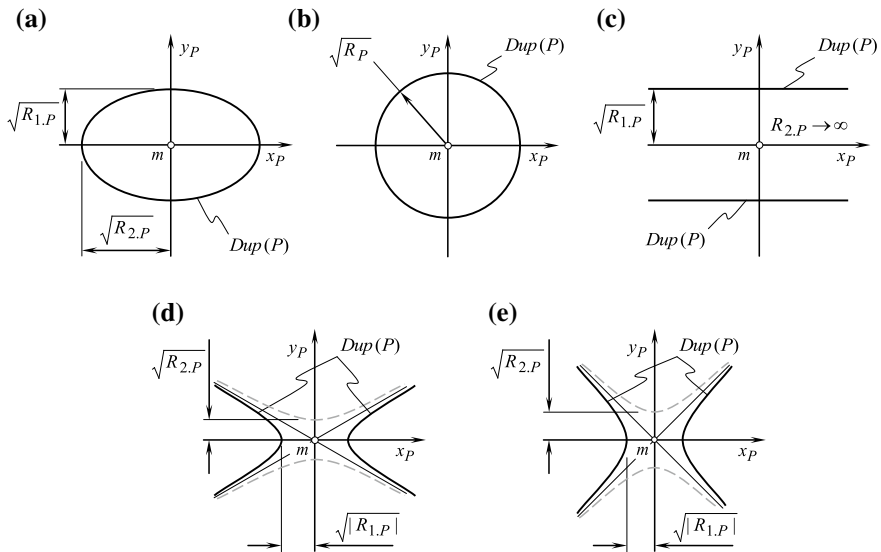


**Fig. 2.6** Five different kinds of “*Dupin indicatrix, Dup(P)*” at a point of interest of a perfect smooth regular part surface  $P$

<sup>2</sup>Fransua Pier Charles **Dupin** (October 6, 1784—January 18, 1873)—a French mathematician.

An easy way to derive an equation for the “*Dupin indicatrix*,  $Dup(P)$ ” at a point of a smooth regular part surface  $P$  is discussed immediately below.

“*Euler formula*” for surface normal curvature  $k_{1,P} \cos^2 \varphi + k_{2,P} \sin^2 \varphi = k_P$  can be represented in the form:

$$\frac{k_{1,P}}{k_P} \cos^2 \varphi + \frac{k_{2,P}}{k_P} \sin^2 \varphi = 1 \quad (2.1)$$

Transition from polar coordinates to “*Cartesian coordinates*” can be performed using the well-known formulae:

$$x_P = \rho \cos \varphi \quad (2.2)$$

$$y_P = \rho \sin \varphi \quad (2.3)$$

Equations (2.2) and (2.3) yield:

$$\cos^2 \varphi = \frac{x_P^2}{\rho^2} \quad (2.4)$$

$$\sin^2 \varphi = \frac{y_P^2}{\rho^2} \quad (2.5)$$

After substituting Eqs. (2.4) and (2.5) into Eq. (2.1), one can come up with the equation:

$$\frac{k_{1,P}}{k_P} \cdot \frac{x_P^2}{\rho^2} + \frac{k_{2,P}}{k_P} \cdot \frac{y_P^2}{\rho^2} = 1 \quad (2.6)$$

For further analysis, it is convenient to designate  $\rho = \sqrt{k_P^{-1}}$ .

Here, the principal curvatures at a point of a smooth regular part surface  $P$  are designated as  $k_{1,P}$  and  $k_{2,P}$ . They can be calculated as roots of the quadratic equation:

$$\begin{vmatrix} L_P - E_P k_P & M_P - F_P k_P \\ M_P - F_P k_P & N_P - G_P k_P \end{vmatrix} = 0 \quad (2.7)$$

Substituting the calculated values of the principal curvatures  $k_{1,P}$  and  $k_{2,P}$  into Eq. (2.6), and after performing the necessary formulae transformations, an equation for the “*Dupin indicatrix*,  $Dup(P)$ ” can be represented in the form:

$$k_{1,P} x_P^2 + k_{2,P} y_P^2 = 1 \quad (2.8)$$

That same equation of the “*Dupin indicatrix*” at a point of a smooth regular surface could be derived in another way. *Coxeter* [4] considers a pair of conics obtained by

expanding an equation in “*Monge form*”  $z = z(x, y)$  in a “*Maclauren series*”:

$$\begin{aligned} z &= z(0, 0) + z_1x + z_2y + \frac{1}{2}(z_{11}x_1^2 + 2z_{12}xy + z_{22}y^2) + \dots \\ &= \frac{1}{2}(b_{11}x^2 + 2b_{12}xy + b_{22}y^2) \end{aligned} \quad (2.9)$$

This gives the equation:

$$(b_{11}x^2 + 2b_{12}xy + b_{22}y^2) = \pm 1 \quad (2.10)$$

of the “*Dupin indicatrix*.”

The general form of equation for a “*Dupin indicatrix*”<sup>3</sup> is often represented as:

$$Dup(P) \Rightarrow \frac{L_P}{E_P}x_P^2 + \frac{2M_P}{\sqrt{E_P G_P}}x_P y_P + \frac{N_P}{G_P}y_P^2 = 1 \quad (2.11)$$

Equation (2.8) describes a particular case of the “*Dupin indicatrix*,” which is represented in “*Darboux frame*.”

Equation (2.11) for the position vector of a point  $\mathbf{r}_{dup}$  of the “*Dupin indicatrix*,  $Dup(P)$ ” at a point of interest of a smooth regular part surface  $P$  allows for matrix representation in the form:

$$Dup(P) \Rightarrow \mathbf{r}_{dup} = [x_P \ y_P \ 0 \ 0] \cdot \begin{bmatrix} \frac{L_P}{E_P} & \frac{2M_P}{\sqrt{E_P G_P}} & 0 & 0 \\ \frac{2M_P}{\sqrt{E_P G_P}} & \frac{N_P}{G_P} & 0 & 0 \\ 0 & 0 & \mp 1 & 0 \\ 0 & 0 & 0 & 1 \end{bmatrix} \cdot \begin{bmatrix} x_P \\ y_P \\ 0 \\ 0 \end{bmatrix} = \pm 1 \quad (2.12)$$

In “*Darboux*”<sup>4</sup> *trihedron*,” this equation reduces to:

$$Dup(P) \Rightarrow \mathbf{r}_{dup} = [x_P \ y_P \ 0 \ 0] \cdot \begin{bmatrix} L_P & M_P & 0 & 0 \\ M_P & N_P & 0 & 0 \\ 0 & 0 & \mp 1 & 0 \\ 0 & 0 & 0 & 1 \end{bmatrix} \cdot \begin{bmatrix} x_P \\ y_P \\ 0 \\ 0 \end{bmatrix} = \pm 1 \quad (2.13)$$

It is convenient to implement a matrix representation of the equation for the “*Dupin indicatrix*,” for instance, when developing software for machining sculptured surfaces on a multi-axis *NC* machine. In this particular case, multiple coordinate

<sup>3</sup>“*Dupin indicatrix*,  $Dup(P)$ ” is completely equivalent to the second fundamental form  $\Phi_{2,P}$  at a point of the surface  $P$ . The second fundamental form  $\Phi_{2,P}$  is also known as an operator of the surface shape. *Koenderink* [3] recommends to consider the characteristic curve  $Dup(P)$  as a rotation of operator of the surface shape  $\Phi_{2,P}$ .

<sup>4</sup>*Jean Gaston Darboux* (August 14, 1842—February 23, 1917), a French mathematician.



system transformations need to be performed. The matrix representation of equations is preferred in cases when multiple coordinate system transformations need to be performed.

The equation of the “*Dupin indicatrix*” can be also represented in the form:

$$r_{dup}(\varphi) = \sqrt{|R_P(\varphi)|} \cdot \text{sgn}\Phi_{2,P}^{-1} \quad (2.14)$$

Here, the angular parameter of a current point of the “*Dupin indicatrix, Dup(P)*” is denoted by  $\varphi$ . The angle  $\varphi$  is measured within a tangent plane through a point on the part surface  $P$ . The angle  $\varphi$  is measured from the first principal direction  $\mathbf{t}_{1,P}$  and between the direction  $\mathbf{t}_P$  in terms of which location of a current point of the “*Dupin indicatrix, Dup(P)*” is specified.

Analysis of Eq. (2.14) reveals that the position vector of a point of the “*Dupin indicatrix, Dup(P)*” in any direction on the part surface  $P$  is equal to square root of the normal radius of curvature taken in that same direction<sup>5</sup> on the part surface  $P$ .

### 2.2.2 Curvature Indicatrix

In engineering geometry of surfaces, the body side and void side of a part surface are distinguished [1, 2, 5, 6]. This feature of a part surface needs to be incorporated into a characteristic image that is used for analytical description of the distribution of normal curvature at a point of interest of the part surface.

“*Dupin indicatrix*” at a point of a convex part surface  $P$  can be identical to corresponding “*Dupin indicatrix*” of a concave part surface  $P$ ; in the both cases, the bounding “*mathematical surface*”  $P$  can be described with the same equation. Therefore, by means of “*Dupin indicatrix*,” no difference can be distinguished between convex and concave surfaces. The said above can be summarized by the following statement:

**Conclusion 2.1.** “*Dupin indicatrix, Dup(P)*” at a point of interest of a part surface  $P$  possesses no capability to distinguish whether the surface  $P$  is convex or concave.

For the purpose of distinguishing whether a part surface  $P$  is convex or concave, a planar characteristic image of another kind is used. This newly introduced characteristic image is referred to as the “*curvature indicatrix, Crv(P)*” at a point of part surface  $P$ .

The curvature indicatrix at a point of part surface  $P$  can be described analytically by the “*inequality*”:

---

<sup>5</sup>Similar to “*Dupin indicatrix, Dup(P)*,” a planar characteristic curve of another kind can be introduced as well. The equation of this characteristic curve can be postulated in the form  $r_{dup,k}(\varphi) = \sqrt{|k_P(\varphi)|} \cdot \text{sgn}\Phi_{2,P}^{-1}$ . Application of the curvature indicatrix in the form  $r_{dup,k}(\varphi)$  avoids uncertainty in cases of a plane. For a plane surface, the “*Dupin indicatrix, Dup(P)*” does not exist, while the characteristic curve  $r_{dup,k}(\varphi)$  exists. It is shrunk to the point  $m$ .

$$\text{Crv}(P) \Rightarrow \frac{L_P}{E_P} x_P^2 + \frac{2M_P}{\sqrt{E_P G_P}} x_P y_P + \frac{N_P}{G_P} y_P^2 \geq 1 \quad (2.15)$$

when the surface mean curvature is nonnegative ( $\tilde{M}_P \geq 0$ ), and by the “inequality”:

$$\text{Crv}(P) \Rightarrow \frac{L_P}{E_P} x_P^2 + \frac{2M_P}{\sqrt{E_P G_P}} x_P y_P + \frac{N_P}{G_P} y_P^2 \leq 1 \quad (2.16)$$

when the surface mean curvature is non-positive ( $\tilde{M}_P \leq 0$ ).

The inequalities (2.15) and (2.16) are composed on the premises of the “Dupin indicatrix,  $\text{Dup}(P)$ ” at a point of interest of the surface  $P$ .

Although the analytical description of the “curvature indicatrix,  $\text{Crv}(P)$ ” [see Eqs. (2.15) and (2.16)] resembles the analytical description of “Dupin indicatrix,  $\text{Dup}(P)$ ” [see Eq. (2.11)], these two characteristic images are different in nature.

“Dupin indicatrix,  $\text{Dup}(P)$ ” is a “planar curve” of the second order. Meanwhile, the “curvature indicatrix,  $\text{Crv}(P)$ ” is a “portion of a plane” that:

- (a) is bounded by the “Dupin indicatrix” and
- (b) is located either inside the characteristic curve  $\text{Dup}(P)$  (if  $\tilde{M}_{P(T)} \geq 0$ ) or outside the corresponding “Dupin indicatrix” (if  $\tilde{M}_{P(T)} \leq 0$ ).

When plotting the curvature indicatrix  $\text{Crv}(P)$  at a point of a part surface  $P$ , use of the “mean curvature,  $\mathcal{M}_P$ ” at a point of the surface along with its “Gaussian curvature,  $\mathcal{G}_P$ ” is helpful.

The performed analysis shows that there are as many as ten different kinds of the “curvature indicatrix,  $\text{Crv}(P)$ ” at a point of interest of a part surface  $P$ .

Curvature indicatrices at a point of interest of a part surface  $P$  of all possible kinds are depicted in Fig. 2.7. For the reader’s convenience, all the possible kinds of the “curvature indicatrix,  $\text{Crv}(P)$ ” at a point of interest of a smooth regular part surface  $P$  are listed below, together with corresponding sign of the “mean curvature,  $\mathcal{M}_P$ ” and of the “Gaussian curvature,  $\mathcal{G}_P$ ” (Fig. 2.7):

- convex elliptical ( $\mathcal{M}_P > 0$ ,  $\mathcal{G}_P > 0$ ) in Fig. 2.7a,
- concave elliptical ( $\mathcal{M}_P < 0$ ,  $\mathcal{G}_P > 0$ ) in Fig. 2.7b,
- convex umbilical ( $\mathcal{M}_P > 0$ ,  $\mathcal{G}_P > 0$ ) in Fig. 2.7c,
- concave umbilical ( $\mathcal{M}_P < 0$ ,  $\mathcal{G}_P > 0$ ) in Fig. 2.7d,
- convex parabolical ( $\mathcal{M}_P > 0$ ,  $\mathcal{G}_P = 0$ ) in Fig. 2.7e,
- concave parabolical ( $\mathcal{M}_P < 0$ ,  $\mathcal{G}_P = 0$ ) in Fig. 2.7f,
- pseudo-convex hyperbolic ( $\mathcal{M}_P > 0$ ,  $\mathcal{G}_P < 0$ ) in Fig. 2.7g,
- pseudo-concave hyperbolic ( $\mathcal{M}_P < 0$ ,  $\mathcal{G}_P < 0$ ) in Fig. 2.7h, and
- minimal hyperbolic ( $\mathcal{M}_P = 0$ ,  $\mathcal{G}_P < 0$ ) in Fig. 2.7i.

Phantom branches of the characteristic image in Fig. 2.7g–i are shown in dashed lines.

For a planar local patch of a part surface  $P$ , “curvature indicatrix,  $\text{Crv}(P)$ ” does not exist. All points of this characteristic image are remote to infinity.

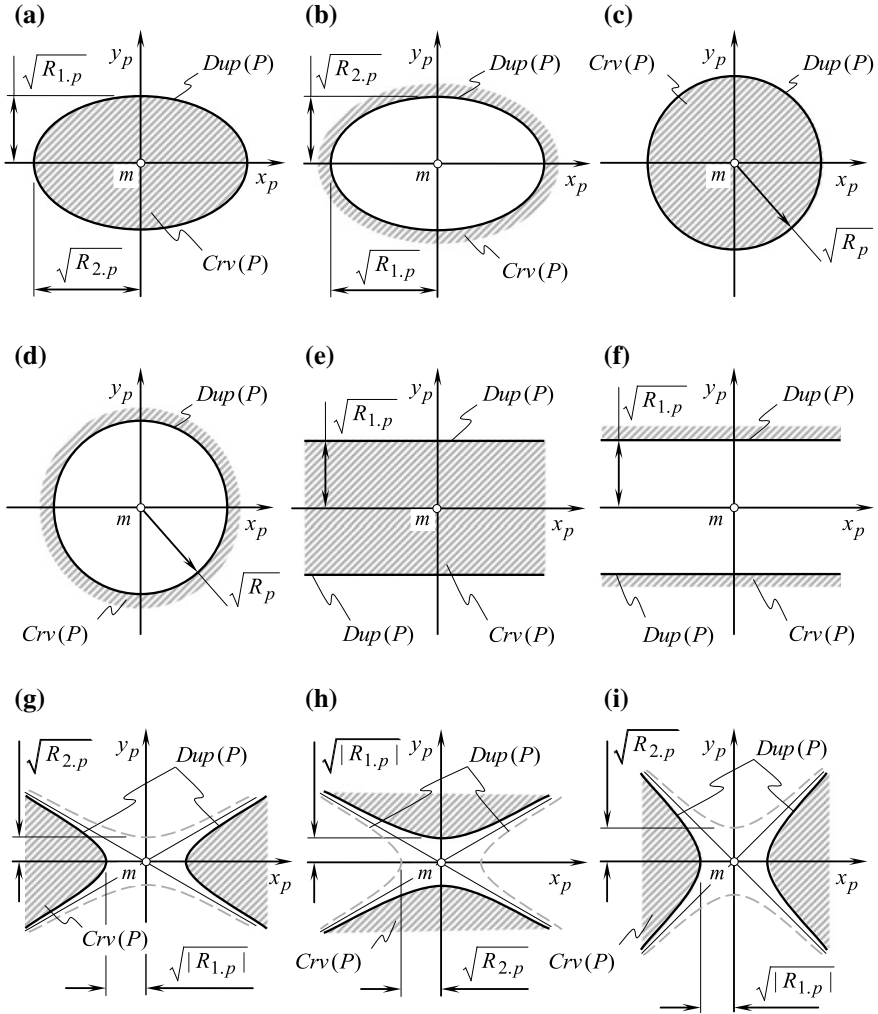


**Fig. 2.7** Kinds of “curvature indicatrices,  $Crv(P)$ ” at a point of real smooth regular part surface  $P$  (see Fig. 2.6) (After Prof. S. P. Radzevich, 1991)

### 2.2.3 Circular Chart of Curvature Indicatrices for Local Patches of Smooth Regular Part Surfaces

The analysis performed on the geometry of local patches of smooth regular part surface  $P$  (see Fig. 2.3) reveals that all of the local patches can also be organized in another way. For a better understanding of how local surface patches of different geometry relate to one another, they are placed as so to form a circular chat shown in Fig. 2.8. The transition from a local surface patch (see Fig. 2.8) to a nearby local

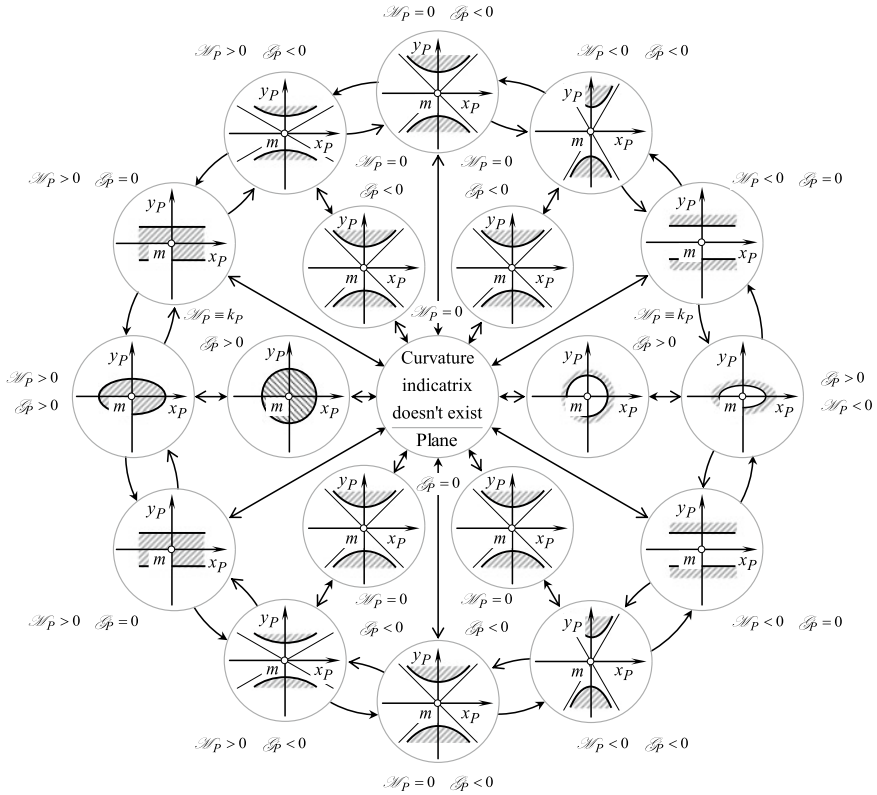


**Fig. 2.8** Circular chart comprised of ten different kinds of curvature indicatrices  $Crv(P)$  at a point of a real smooth regular part surface  $P$  (adapted from [5])

surface patch either in the radial direction of the circular chat or circumferentially shows how normal curvatures of the local surface patch change.

It is instructive to compare Fig. 2.8 with Fig. 2.4 discussed earlier. Implementation of the curvature indicatrix  $Crv(P)$  at a point of interest of a smooth regular part surface  $P$  makes it easier to distinguish local surface patch of one kind from those of another kind.

## 2.3 Circular Diagrams at a Surface Point

Another possibility for analytical description of the local geometry at a point of a smooth regular part surface  $P$  is associated with the so-called *circular diagrams*<sup>6</sup> at a point of interest within the surface patch.

Circular diagrams are a powerful tool for the analysis and in-depth understanding of the local geometry of a sculptured surface.

### 2.3.1 Circular Diagrams

Circular diagrams reflect the fundamental properties of a sculptured part surface in differential vicinity of a surface point.

“*Euler equation*” for normal surface curvature:

$$k_{\theta,P} = k_{1,P} \cos^2 \theta + k_{2,P} \sin^2 \theta \quad (2.17)$$

together with “*Germain equation*”<sup>7</sup> (or “*Bertrand equation*” in other interpretation)

$$t_{\theta,P} = (k_{2,P} - k_{1,P}) \sin \theta \cos \theta \quad (2.18)$$

served as a foundation of circular diagrams at a point of interest of a sculptured part surface. Here in Eq. (2.18),  $\tau_{\theta,P}$  designates the torsion of a curve on the surface at a point taken in the direction that is specified by the angle  $\theta$ .

Consider a *Cartesian* reference system  $k_P \tau_P$  as shown in Fig. 2.9. Here, the normal curvature at a point of a part surface  $P$  is designated as  $k_P$ , and the torsion of a curve through the point of interest  $m$  of the surface  $P$  is designated as  $\tau_P$ .

A circle of a diameter  $d_k = k_{1,P} - k_{2,P}$  is centering at a point  $(0, \mathcal{M}_P)$ , where  $\mathcal{M}_P$  is the mean curvature at the point  $m$  of the surface  $P$ . The circle intersects the  $k_P$ -axis at the points  $(0, k_{1,P})$  and  $(0, k_{2,P})$  accordingly. Constructed in this way, the circle is referred to as the “*circular diagram*” at a point of interest of a smooth regular part surface  $P$ .

---

<sup>6</sup>Initially proposed by *C.O. Mohr* (1835–1918) for the purposes of solving problems in the field of strength of materials, circular diagrams later achieved more extensive application. The origination of the application of circular diagrams for the purposes of differential geometry of surfaces can be traced back to the publications by *Miron* [7], and *Vaisman* (195–?). *Lowe* [8, 9] applied circular diagrams in studying surface geometry with special reference to twist, as well as in developing plate theory. A profound analysis of properties of circular diagrams can be found in publications by *Nutbourn* [10], and by *Nutbourn and Martin* [11]. Application of circular diagrams in the field of sculptured surface machining on a multi-axis *NC* machine is known from the monograph by *Radzevich* [2].

<sup>7</sup>*Marie-Sophie Germain* (April 1, 1776—June 27, 1831)—a French mathematician, physicist, and philosopher.

**Fig. 2.9** Example of a circular diagram constructed for a convex elliptical local patch of a smooth regular part surface  $P$

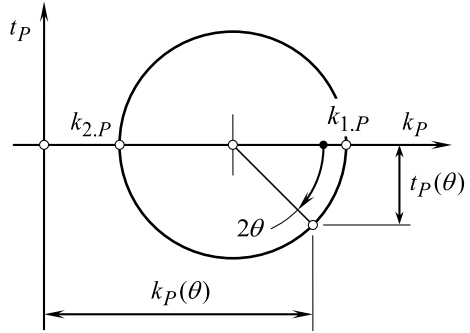


Figure 2.9 illustrates an example of circular diagram constructed for a convex local patch of elliptic kind. It is important to point out here that the algebraic value of the first principal curvature  $k_{1,P}$  always exceeds the algebraic value of the second principal curvature  $k_{2,P}$ ; thus, the circular diagram point with coordinates  $(0, k_{1,P})$  is always located at the far right relative to the circular diagram point with coordinates  $(0, k_{2,P})$ .

The application of circular diagrams enables one to easily identify the kind of a local surface patch<sup>8</sup> in differential vicinity of a point on a sculptured surface.

A brief discussion of the properties of vector diagrams of local patches at a point of a smooth regular part surface  $P$  is desired prior to proceeding with an in-depth analysis of circular diagrams of that same local patches of the surface  $P$ . The discussion below is based in much on the “*Euler equation*” [see Eq. (2.17)] together with “*Germain equation*” [see Eq. (2.18)]. The proof of these two equations is used in part for the construction of vector diagrams of local patches of a smooth regular part surface  $P$ .

Consider a unit vector  $\mathbf{t}_P(\theta)$  that is tangent to the part surface  $P$  at a point of interest  $m$ :

$$\mathbf{t}_P(\theta) = \mathbf{t}_{1,P} \cos \theta + \mathbf{t}_{2,P} \sin \theta \quad (2.19)$$

Here,  $\mathbf{t}_{1,P}$  and  $\mathbf{t}_{2,P}$  are unit tangent vectors in the principal directions at the surface point  $m$ .

The direction of the vector  $\mathbf{t}_P(\theta)$  in relation to the first principal direction is specified by the angle  $\theta$ .

A unit tangent vector  $\mathbf{t}_P^*(\theta)$  that is perpendicular to the unit tangent vector  $\mathbf{t}_P(\theta)$  can be analytically described by the equation:

$$\mathbf{t}_P^*(\theta) = \mathbf{t}_{2,P} \cos \theta - \mathbf{t}_{1,P} \sin \theta \quad (2.20)$$

<sup>8</sup>We refer to a sculptured surface area in the differential vicinity of a surface point as a “*local surface patch*,” and not as a “*surface point*.” The name of local surface patches corresponds to the name of surface points. However, from the standpoint of surface machining, treating local surface patches instead of surface points is preferred.

Owing to Eq. (2.19), the displacement  $\mathbf{t}_P(\theta) dS_P$  can be decomposed into two components as:

$$\mathbf{t}_P(\theta) dS_P = \mathbf{t}_{1,P} \cos \theta dS_P + \mathbf{t}_{2,P} \sin \theta dS_P \quad (2.21)$$

As the displacement  $\mathbf{t}_P(\theta) dS_P$  occurs in the principal directions  $\mathbf{t}_{1,P}$  and  $\mathbf{t}_{2,P}$  on the part surface  $P$ , the normal components of these displacements (namely, the components in the directions perpendicular to  $\mathbf{t}_{1,P}$  and  $\mathbf{t}_{2,P}$ ) are correspondingly equal to:

$$d\mathbf{N}_{1,P} = -k_{1,P} \mathbf{t}_{1,P} \cos \theta dS_P \quad (2.22)$$

$$d\mathbf{N}_{2,P} = -k_{2,P} \mathbf{t}_{2,P} \sin \theta dS_P \quad (2.23)$$

Combining these two equations, an expression for the resultant normal displacement  $d\mathbf{N}_P$  can be represented in the form:

$$d\mathbf{N}_P = d\mathbf{N}_{1,P} + d\mathbf{N}_{2,P} = \mathbf{N}'_P dS_P = -k_{1,P} \mathbf{t}_{1,P} \cos \theta dS_P - k_{2,P} \mathbf{t}_{2,P} \sin \theta dS_P \quad (2.24)$$

Equations (2.19) and (2.20) allow for the expressions for unit tangent vectors of principal directions  $\mathbf{t}_{1,P}$  and  $\mathbf{t}_{2,P}$  at a point  $m$  of a smooth regular part surface  $P$ :

$$\mathbf{t}_{1,P} = \mathbf{t}_P(\theta) \cos \theta - \mathbf{t}_P^*(\theta) \sin \theta \quad (2.25)$$

$$\mathbf{t}_{2,P} = \mathbf{t}_P(\theta) \sin \theta - \mathbf{t}_P^*(\theta) \cos \theta \quad (2.26)$$

Substituting these values for the  $\mathbf{t}_{1,P}$  and  $\mathbf{t}_{2,P}$  into Eq. (2.24), the infinitesimally small vector of normal displacement  $d\mathbf{N}_P$  can be derived as:

$$d\mathbf{N}_P = -(k_{1,P} \cos^2 \theta + k_{2,P} \sin^2 \theta) \mathbf{t}_P(\theta) dS_P - (k_{2,P} - k_{1,P}) \mathbf{t}_P^*(\theta) \sin \theta \cos \theta dS_P \quad (2.27)$$

It has been proven in differential geometry of surfaces that a displacement at a distance  $dS_P$  in the direction of a vector  $\mathbf{t}_P$  causes a corresponding displacement in the normal direction:

$$d\mathbf{N}_P = [-k_P \mathbf{t}_P(\theta) - t_P \mathbf{t}_P^*(\theta)] dS_P \quad (2.28)$$

Comparison of Eqs. (2.27) and (2.28) reveals that Eqs. (2.17) and (2.18) are valid.

For the purposes of investigation of the properties of circular diagrams at a point of smooth regular part surface  $P$ , vector diagrams in terms of the factors  $\mathbf{t}_P$  and  $\mathbf{N}'_P$  can be introduced. This is based mainly on the above proof of the validity of Eqs. (2.17) and (2.18).

For this purpose, Eq. (2.19) and slightly modified Eqs. (2.24) and (2.28) are rewritten below together:

$$\mathbf{t}_P(\theta) = \mathbf{t}_{1,P} \cos \theta + \mathbf{t}_{2,P} \sin \theta \quad (2.29)$$

$$\mathbf{N}'_P = -k_{1,P} \mathbf{t}_{1,P} \cos \theta - k_{2,P} \mathbf{t}_{2,P} \sin \theta \quad (2.30)$$

$$\mathbf{N}'_P = -k_P \mathbf{t}_P(\theta) - t_P \mathbf{t}_P^*(\theta) \quad (2.31)$$

An example of a vector diagram at a point of a smooth regular part surface  $P$  is shown in Fig. 2.10.

As the equalities  $d\mathbf{r}_P = \mathbf{t}_P dS_P$  and  $d\mathbf{N}_P = \mathbf{N}'_P dS_P$  hold, the vector diagram is scaled by a factor  $dS_P$ . This is due to the requirement that the vector diagram is referred to the parameters  $d\mathbf{r}_P$  and  $d\mathbf{N}_P$ .

The vectors  $\mathbf{N}'_P$  and  $\mathbf{t}_P$  (or opposite directions of these vectors) are pointed out in the same direction when either  $\theta = 0^\circ$  or  $\theta = 90^\circ$ . Otherwise, these vectors are of different directions (under another values of the angle  $\theta$  if  $k_{1,P} \neq k_{2,P}$ ).

Consider a line within the part surface  $P$ . The line is through the surface point  $m$ . As follows from Fig. 2.10, the torsion of the line is of negative value if the value of the angle  $\theta$  is within the interval  $0^\circ < \theta < 90^\circ$  ( $k_{1,P} > k_{2,P}$ ). Thus, the length shown in Fig. 2.10 as  $-\mathbf{t}_P$  is actually positive.

The use of “Pythagorean theorem” allows for an expression (see Fig. 2.10) for the magnitude of the vector  $\mathbf{N}'_P$  :

$$|\mathbf{N}'_P| = \sqrt{k_{1,P}^2 \cos^2 \theta + k_{2,P}^2 \sin^2 \theta} = \sqrt{k_P^2 + t_P^2} \quad (2.32)$$

**Fig. 2.10** Example of vector diagram of a local patch of a smooth regular part surface  $P$  in terms of the vectors  $\mathbf{t}_P$  and  $\mathbf{N}'_P$

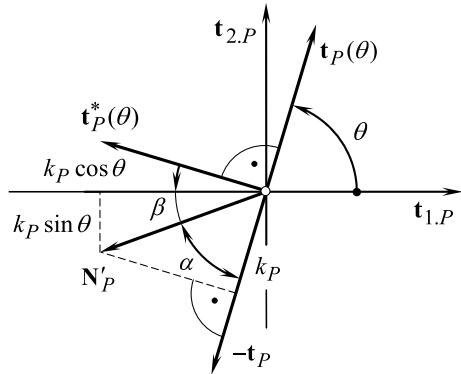
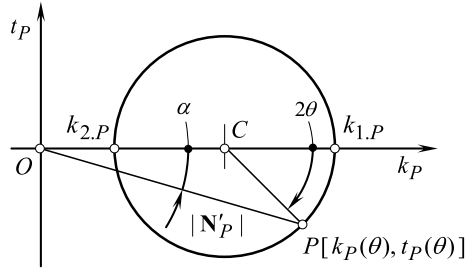




**Fig. 2.11** Example of circular diagram at a point of a smooth regular part surface  $P$  (angle  $\alpha$  and the magnitude of the normal vector  $\mathbf{N}'_P$  are shown)



The vectors  $\mathbf{N}'_P$  and  $-\mathbf{t}_P$  make an angle that is denoted by  $\alpha$  (see Fig. 2.10). The length  $|\mathbf{N}'_P|$  of the vector  $\mathbf{N}'_P$  along with an angle that is equal to  $\alpha$  is depicted on the circular diagram<sup>9</sup> of the local patch of the part surface  $P$  (see Fig. 2.11).

Let us discuss the behavior of the vector  $\mathbf{N}_P$  in a case the first principal curvature  $k_{1,P}$  at a point of the surface  $P$  at  $m$  is positive ( $k_{1,P} > 0$ ).

When the second principal curvature  $k_{2,P}$  is of positive value ( $k_{2,P} > 0$ ), the circular diagram does not intersect the  $t_P$ -axis. A circular diagram of this particular kind corresponds to a part surface  $P$  local patch, which is of elliptic kind.

The orientation of the vector  $\mathbf{N}'_P$  in relation to the vector  $-\mathbf{t}_P$  depends on the actual value of the angle  $\alpha_{\max}$ . The value of the angle  $\alpha_{\max}$  depends on the direction of  $OP$  when  $OP$  is in tangency to the circular diagram. The angle  $\alpha_{\max}$  can be calculated from the expression:

$$\alpha_{\max} = \sin^{-1} \left| \frac{k_{1,P} - k_{2,P}}{k_{1,P} + k_{2,P}} \right| \quad (2.33)$$

In this case, both principal curvatures are of positive value, which corresponds to a convex local patch of the part surface  $P$ .

When the second principal curvature  $k_{2,P}$  is of a negative value ( $k_{2,P} < 0$ ), the circular diagram intersects the axis  $t_P$ . A circular diagram of this particular kind corresponds to a hyperbolic local patch of the surface  $P$ , or, in other words, it corresponds to a local surface patch of saddle kind. The direction of the vector  $\mathbf{N}'_P$  is arbitrary. The principal curvatures are of opposite sign.

When the second principal curvature  $k_{2,P}$  is of a zero value ( $k_{2,P} = 0$ ), the circular diagram is in tangency to the axis  $t_P$ . Circular diagrams of this kind correspond to local part surface patches of parabolic kind. Permissible directions of the vector  $\mathbf{N}'_P$  are within the interval  $\pm 90^\circ$  in relation to the direction of  $-\mathbf{t}_P$ .

In cases if one of the principal curvatures is zero, then local part surface patch of this particular kind can be construed as a cylinder (as a “*surface of translation*,” in other words).

<sup>9</sup>The angle  $\theta$  cannot be depicted in the circular diagram Fig. 2.11 as a circular diagram is not equivalent to the vector diagram. The argument  $\theta$  of the vector  $\mathbf{N}'_P$  can be shown only on the corresponding vector diagram of local patch of the part surface  $P$ , as illustrated in Fig. 2.10.

Ultimately, once the principal curvatures are calculated for a certain point  $m$  on the part surface  $P$ , then all normal curvatures of the surface at the point  $m$ , as well as the torsion of a curve on the surface are known in all directions through the point  $m$ . The said is illustrated clearly in Fig. 2.11.

Theoretically, the behavior of the vector  $\mathbf{N}_P$  that is perpendicular to the surface  $P$  can also be determined from the circular diagram. However, as  $d\mathbf{N}_P (= \mathbf{N}'_P dS_P)$ , it is easier to derive the vector of displacement of the end of the unit normal vector to the part surface  $P$  from the corresponding vector diagram shown in Fig. 2.10.

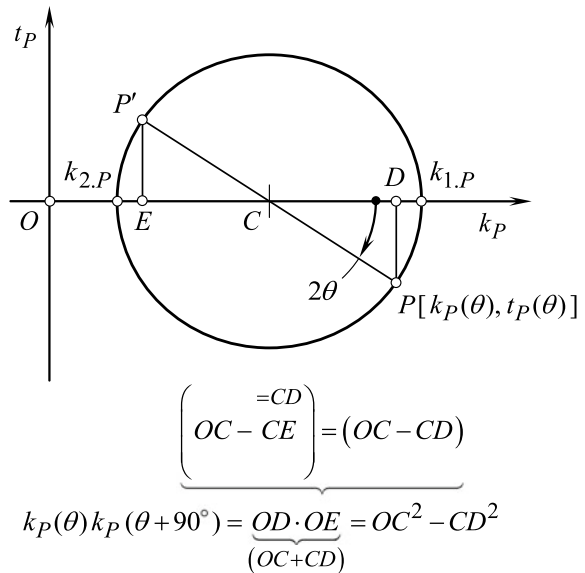
The mean curvature  $\mathcal{M}_P$  at a point of local patch of a smooth regular part surface  $P$  can easily be determined from the corresponding circular diagram. As a circle is always centered at a point at the middle of its diameter, the mean curvature  $\mathcal{M}_P$  is equal to the mean of any two normal curvatures taken in two directions, which are orthogonal to one another. Thus, for the purpose of determining the mean curvature, it is not necessary to determine the principal curvatures at a point of the surface  $P$  at  $m$ .

A statement similar to the above is not valid with respect to the “Gaussian curvature,  $\mathcal{G}_P$ ” at a point  $a$  of local surface patch. This infeasibility follows immediately from the geometrical interpretation of the mean curvature  $\mathcal{M}_P$  and of the full curvature  $\mathcal{G}_P$  of the part surface  $P$ , using the corresponding circular diagram of the surface  $P$  for this purpose. The following equality can be deduced (Fig. 2.12):

$$k_P(\theta) k_P(\theta + 90^\circ) = OD \cdot OE = OC^2 - CD^2 \quad (2.34)$$

The length of the straight-line segment  $CD$  depends on the value of the angle  $\theta$ , while the length of the straight-line segment  $OC$  is of a constant value.

**Fig. 2.12** Construction of a circular diagram at a point of the smooth regular part surface  $P$



Circular diagrams of convex ( $\mathcal{M}_P > 0, \mathcal{G}_P > 0$ ), and concave ( $\mathcal{M}_P < 0, \mathcal{G}_P > 0$ ) local surface patches of elliptic kind (Fig. 2.13a) are depicted as circles remote at a certain distance from  $t_P$ -axis. The circles are centered at a point at a distance  $\mathcal{M}_P$  from the  $t_P$ -axis. The diameter of a circle  $d_k$  is equal to the difference:

$$d_k = k_{1,P} - k_{2,P} \quad (2.35)$$

For local part surface patches of umbilic kind, the principal directions are not identified. Thus, the normal curvatures in all directions are of the same value. The result is that, for local surface patches of this particular kind, the circular diagram shrinks into points (Fig. 2.13b). The coordinates of the points are: (a) ( $k_P > 0$ ) for a convex ( $\mathcal{M}_P > 0, \mathcal{G}_P > 0$ ) local part surface patch and (b) ( $k_P < 0$ ) for a concave ( $\mathcal{M}_P < 0, \mathcal{G}_P > 0$ ) part surface patch accordingly.

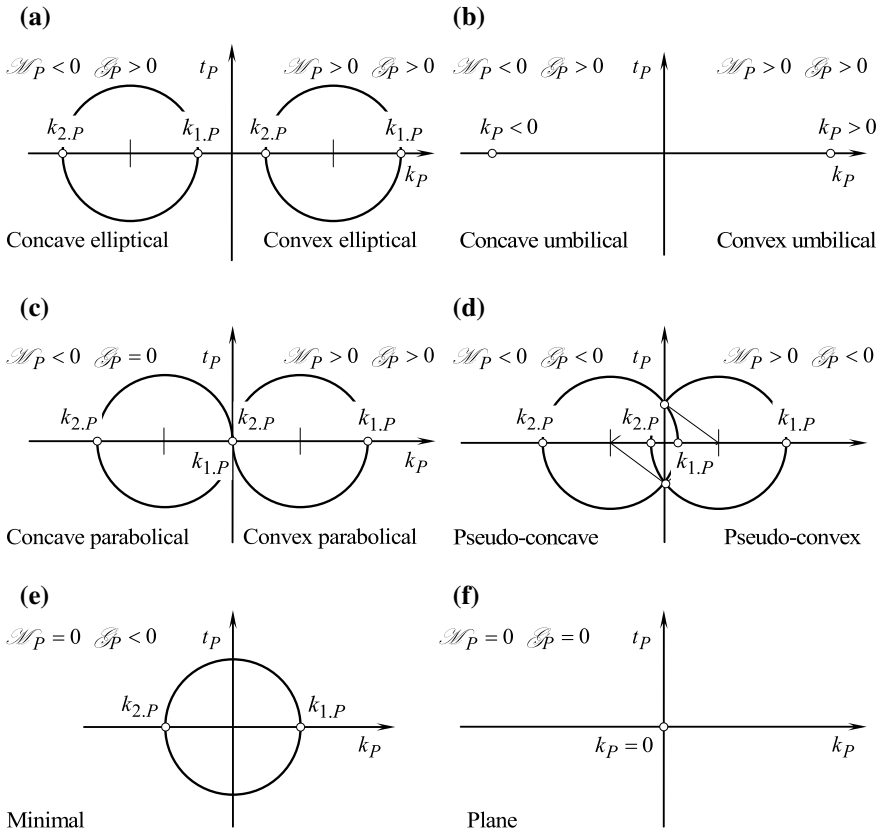


**Fig. 2.13** Circular diagrams at a point of smooth regular local patches of a part surface  $P$

Circular diagrams of convex ( $\mathcal{M}_P > 0, \mathcal{G}_P = 0$ ) and concave ( $\mathcal{M}_P < 0, \mathcal{G}_P = 0$ ) local part surface patches of a parabolic kind (Fig. 2.13c) pass through the origin of the coordinate system  $k_P t_P$ .

It is recommended to distinguish “pseudo-convex” ( $\mathcal{M}_P > 0$ ) from “pseudo-concave” ( $\mathcal{M}_P < 0$ ) kinds of local part surface patches when they are of hyperbolic type, that is, for saddle-like local surface patches ( $\mathcal{G}_P < 0$ ). Circular diagrams of saddle-like local surface patches intersect  $t_P$ -axis (Fig. 2.13d).

The particular case of a local part surface patch of saddle-like kind is distinguished for the hyperbolic surface local patch ( $\mathcal{G}_P < 0$ ) having zero mean curvature ( $\mathcal{M}_P = 0$ ). Local part surface patches of this particular kind are referred to as “minimal surface local patches” (Fig. 2.13e).

Finally, the circular diagram of a planar surface local patch ( $\mathcal{M}_P = 0, \mathcal{G}_P = 0$ ) is shrunk into the point that coincides with the origin of the coordinate system  $k_P \tau_P$  (Fig. 2.13f). All points of the plane can be considered as parabolic umbilics.

As it follows from Fig. 2.13, circular diagram clearly illustrates the major local properties of the geometry at a point of a smooth regular part surface. The principal curvatures, normal curvatures, and torsion of a curve on the surface can easily be deduced from the diagram. Moreover, the actual values of the mean  $\mathcal{M}_P$  and Gaussian  $\mathcal{G}_P$  curvatures can also be taken from the circular diagram. Figure 2.14 gives examples of how the mean  $\mathcal{M}_P$ , and the Gaussian  $\mathcal{G}_P$  curvatures can be constructed. The examples are given for convex and concave elliptic (Fig. 2.13a) local surface patches, as well as for pseudo-convex, and pseudo-concave saddle-like (Fig. 2.13a) local surface patches.

The above consideration yields a conclusion that circular diagram is a simple characteristic image that provides the researcher with comprehensive information on local topology at a point of a smooth regular part surface  $P$ . This data includes:

- the principal curvatures  $k_{1,P}$  and  $k_{2,P}$ ,
- the normal curvature  $k_P$  in a given direction on the surface,
- the extremum values of the torsion  $t_P^{\min}$  and  $t_P^{\max}$  of a curve on the surface,
- the torsion  $t_P$  of a curve on a surface in a given direction,
- the “mean curvature,  $\mathcal{M}_P$ ,” and
- the “Gaussian curvature,  $\mathcal{G}_P$ .”

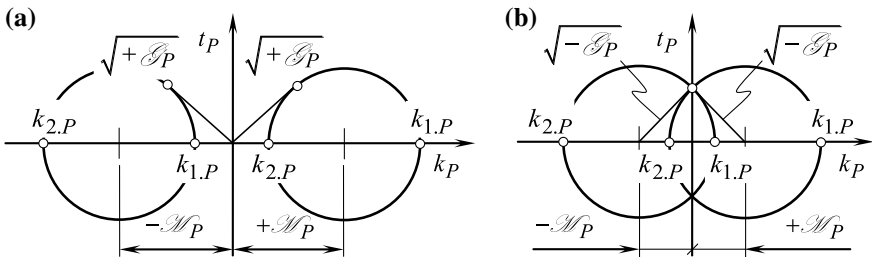


**Fig. 2.14** Geometric interpretation of mean  $\mathcal{M}_P$  and full  $\mathcal{G}_P$  (Gaussian) curvature at a point of a smooth regular part surface  $P$

No other characteristic image of such a simple nature (as the circular diagram is) provides the researcher with such comprehensive data on the local topology of a part surface. Circular diagrams are extensively used in engineering geometry of surfaces.

One such problem relates to the classification of surfaces. The classification of part surfaces is necessary for many practical purposes.

Let us take a brief look at surface classification from this standpoint.

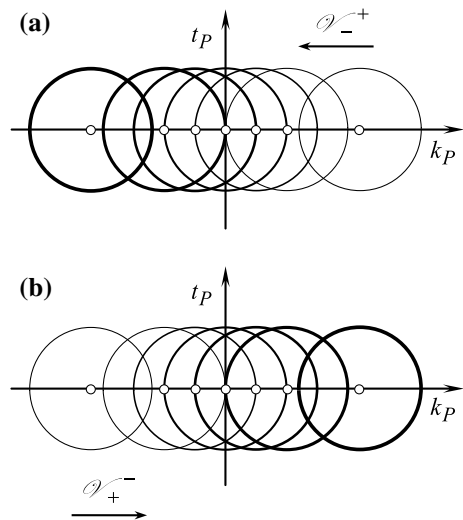
Sculptured surfaces are geometrical objects of a complex nature. It is shown [3] that no scientific classification of sculptured surfaces can be developed at all. It is recommended [3] to consider the classification of local surface patches instead of the classification of sculptured surfaces in a global sense. This recommendation is based on consideration of the point contact that a sculptured surface makes with the generating surface of a cutting tool when machining.

Figure 2.15 is insightful for understanding the relationship between local surface patches of different kinds. The shift of a circular diagram along  $k_P$ -axis either in the  $\mathcal{V}_-^+$  or in  $\mathcal{V}_+^-$  direction reflects a corresponding change in shape and kind of local part surface patch. On the premise of these changes, a classification of local part surface patches can be worked out.

Depicted in Fig. 2.15a, the initial circular diagram represents a convex elliptic local patch with certain values of the surface principal curvatures. Owing to the shift in the  $\mathcal{V}_-^+$ -direction, the shape of the convex elliptic surface patch alters; however, to some extent it remains of elliptic kind. When the circular diagram passes through the origin of the coordinate system  $k_P t_P$ , this results in a dramatic change in shape of the local surface patch. Instead of being of elliptic kind, it transforms to a local surface patch of parabolic kind.

A further shift of the circular diagram in the  $\mathcal{V}_+^-$ -direction results in a consequent change in shape of the local part surface patch to:

**Fig. 2.15** Various locations of the circular diagram correspond to local surface patches of different kinds



- (a) pseudo-convex saddle-like local surface patch and
- (b) minimal saddle-like local surface patch,

and so on up to a concave elliptic local surface patch of certain values of principal curvatures.

A similar change in shape and kind of local surface patch is observed when the circular diagram shifts in the direction of  $\mathcal{V}_+^-$ , which is opposite to the direction of  $\mathcal{V}_-^+$  (see Fig. 2.15b).

The diagram shown in Fig. 2.15 can be enhanced to the three-dimensional case. For this purpose, the  $k_P$ -axis and  $t_P$ -axis are complemented by the  $d_k$ -axis as illustrated in Fig. 2.16. Here,  $d_k$  is a parameter that specifies the diameter of the circular diagram at a part surface  $P$  current point  $m$  ( $d_k = k_{1,P} - k_{2,P}$ ). As an example, the diagram shown in Fig. 2.15,a is plotted in Fig. 2.16. As the circular diagram is centered at a point that travels,  $\mathcal{V}_+^+$ , parallel to the  $k_P$ -axis, the corresponding circular diagrams reflect the local geometry of surface patches of the following kinds:

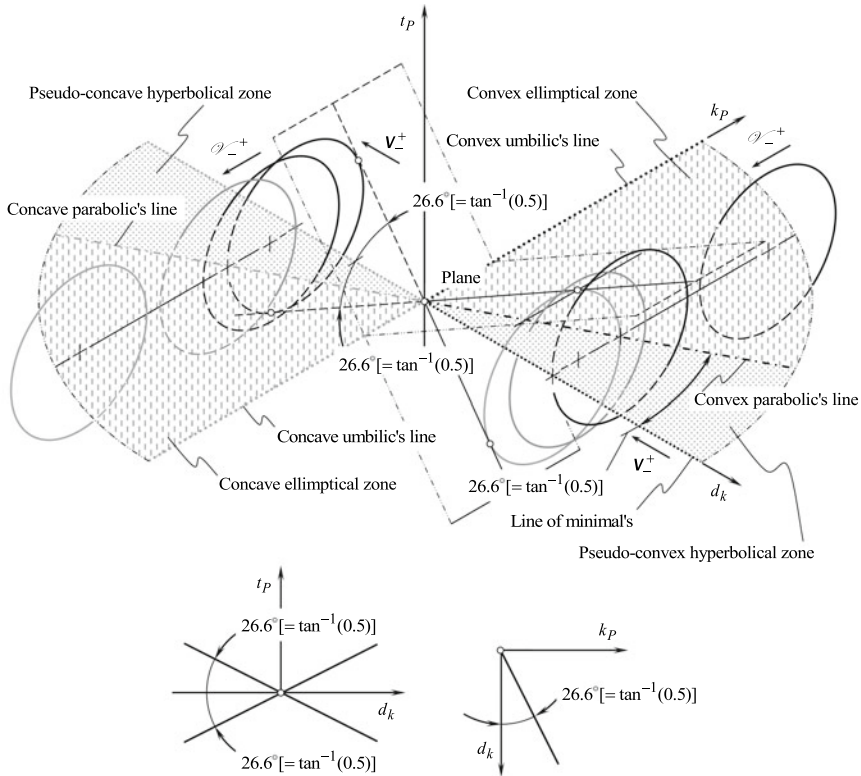


**Fig. 2.16** Diagram illustrating the variation of the geometry of a local patch of a smooth regular part surface  $P$  when the circular diagram is centered at different points within the coordinate plane  $k_P d_k$  (the concept of this schematic originates from the schematic shown in Fig. 1.26 on p. 99 of [2])

- (a) convex elliptical,
- (b) convex parabolical,
- (c) pseudo-convex hyperbolical,
- (d) minimal,
- (e) pseudo-concave hyperbolical,
- (f) concave parabolical, and
- (g) concave elliptical.

It should be pointed out here that the circular diagram at a part surface  $P$  current point  $m$  can be centered at any point within the two quadrants shaded in Fig. 2.16. So, in addition to traveling in the directions  $\mathcal{V}_-^+$  and  $\mathcal{V}_+^-$ , traveling in the directions  $V_-^+$  and  $V_+^-$  is permissible as well. The directions of traveling  $V_-^+$  and  $V_+^-$  are parallel to the  $d_k$ -axis of the reference system  $k_P d_k t_P$ .

An analysis performed on the schematic shown in Fig. 2.16 allows for the following conclusions.

First, several special boundary lines can be noticed within the coordinate plane  $k_P d_k$ .

“*Umbilic’s line*” is one of these special lines. This line can be construed as comprising two portions, namely, of “*convex umbilic’s line*” (for the points having coordinates  $\tau_P = 0$ ,  $d_k = 0$ ,  $0 < k_P < +\infty$ ) and “*concave umbilic’s line*” (for the points having coordinates  $\tau_P = 0$ ,  $d_k = 0$ ,  $-\infty < k_P < 0$ ). All points within umbilic’s line correspond to local surface patches of umbilic kind having different value of normal curvature  $k_P$ .

“*Line of minimal’s*” is the second of the special lines. This boundary line is aligned with the  $d_k$ -axis of the reference system  $k_P d_k t_P$ . The line can be split into two portions. Points having coordinates ( $t_P = 0$ ,  $0 < d_k < +\infty$ ,  $k_P = 0$ ) are located within the first portion of the “*line of minimal’s*.” Accordingly, points having coordinates ( $t_P = 0$ ,  $-\infty < d_k < 0$ ,  $k_P = 0$ ) are located within the second portion of the “*line of minimal’s*” as depicted in Fig. 2.16.

“*Parabolic’s line*” is the third of the special lines. This line can also be interpreted as comprising two portions, namely, of “*convex parabolic’s line*” [for the points having coordinates  $\tau_P = 0$ ,  $d_k = +k_P \cot^{-1}(0.5)$ ] and “*concave parabolic’s line*” [for the points having coordinates  $\tau_P = 0$ ,  $d_k = -k_P \cot^{-1}(0.5)$ ]. All points within the “*parabolic’s line*” correspond to local surface patches of parabolic kind having zero mean curvature ( $\mathcal{M}_P = 0$ ).

The said boundary straight lines form several sectors within the coordinate plane  $k_P d_k$ , within which circular diagrams for part surface of different kinds are centered. All of these zones, namely:

- convex elliptical zone,
- pseudo-convex hyperbolical zone,
- concave elliptical zone, and
- pseudo-concave hyperbolical zone,

are depicted in Fig. 2.16. As follows from the name of the zone, circular diagrams for convex local surface patches of elliptic kind are centered within the convex elliptic zone and similarly for the other three zones listed above.

The circular diagram for a plane is centered at the origin of the coordinate system  $k_P d_k t_P$ . In this particular case, the circular diagram is shrunk to a point that is coincident with origin of the coordinate system  $k_P d_k \tau_P$ .

When the center of a circular diagram travels within the coordinate plane  $k_P d_k$ , and in such travel approaches the origin of the coordinate system  $k_P d_k t_P$ , the local part surface patch gets more and more flatten. This is observed for local surface patches of all kinds: for local part surface patches of umbilic kind, elliptic kind, parabolic kind, and so forth. When approaching the origin of the coordinate system  $k_P d_k t_P$ , the corresponding circular diagram is reduced in diameter and ultimately shrunk to a point that is coincident with the origin of the coordinate system  $k_P d_k \tau_P$ . This means that the plane can be interpreted as a degenerated case not only of umbilics, but also as of all possible kinds of local part surface patches as well.

### 2.3.2 Circular Chart of Circular Diagrams for Local Patches of Smooth Regular Part Surfaces

As circular diagrams properly reflect the geometry of local part surface patches, a circular chart for local patches of smooth regular part surfaces can be constructed on the premise of the circular diagrams similar to that shown in Fig. 2.3 and in Fig. 2.8. An example of such a circular chart is depicted in Fig. 2.17.

The transition from a local surface patch (Fig. 2.17) to a nearby local surface patch either in the radial direction of the circular chat or circumferentially, shows how normal curvatures of the local surface patch change.

It is instructive to compare Fig. 2.17 with the earlier discussed Figs. 2.4 and 2.8. Implementation of the circular diagrams of a smooth regular part surface  $P$  makes it easier to differentiate between local surface patches of different kinds.

## 2.4 One More Useful Characteristic Curve

For the purpose of analytical description of the distribution of normal curvature in the differential vicinity of a point on a smooth regular surface, Prof. Böhm recommends [12] employing the following characteristic curve.

Setting  $\eta = \frac{dV_P}{dU_P}$  at a given point of a smooth regular part surface  $P$ , one can rewrite the equation:

$$k_P = \frac{\Phi_{2,P}}{\Phi_{1,P}} = \frac{L_P dU_P^2 + 2 M_P dU_P dV_P + N_P dV_P^2}{E_P dU_P^2 + 2 F_P dU_P dV_P + G_P dV_P^2} \quad (2.36)$$

for normal curvature in the form of:



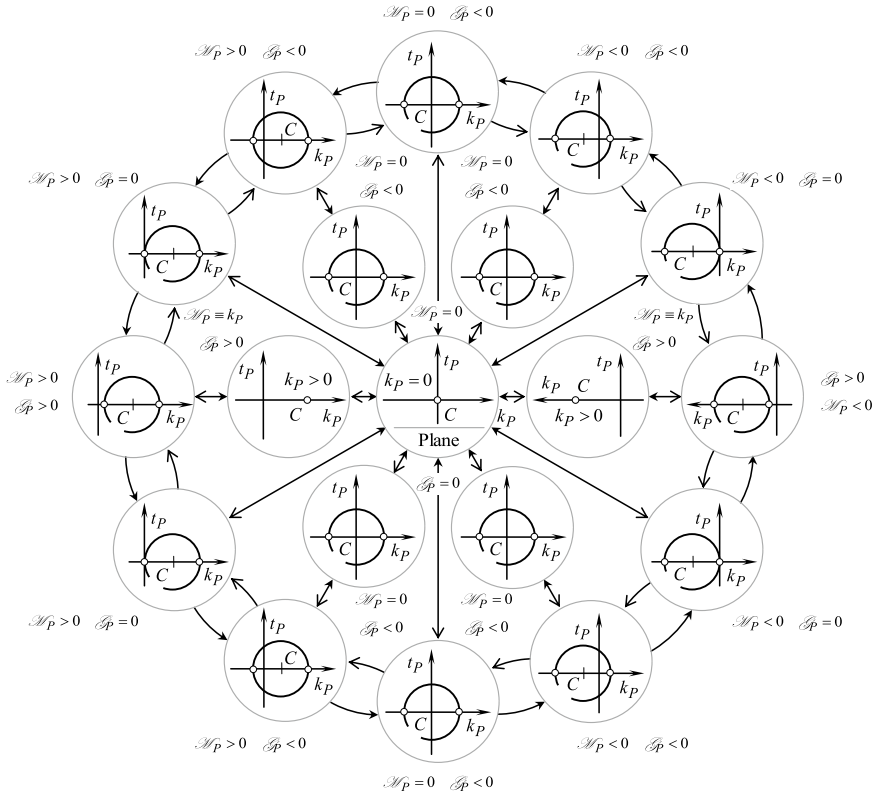


**Fig. 2.17** Circular chart comprised of circular diagrams for ten different kinds of local patches of a real smooth regular part surface  $P$  (adapted from [5])

$$k_P = \frac{L_P + 2M_P\eta + N_P\eta^2}{E_P + 2F_P\eta + G_P\eta^2} \quad (2.37)$$

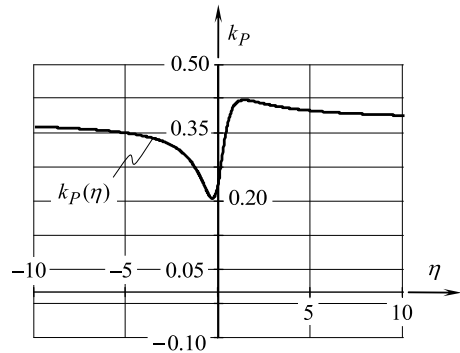
In the particular case when  $L_P : M_P : N_P = E_P : F_P : G_P$ , the normal curvature  $k_P$  is independent of  $\eta$ . Surface points with this property are known as umbilic points and flatten points.

In general cases when  $k_P$  changes as  $\eta$  changes, the function  $k_P = k_P(\eta)$  is a rational quadratic form, as illustrated in Fig. 2.18. The extreme values  $k_{1,P}$  and  $k_{2,P}$  of  $k_P = k_P(\eta)$  occur at the roots  $\eta_1$  and  $\eta_2$  of:

$$\begin{vmatrix} \eta^2 & -\eta & 1 \\ E_P & F_P & G_P \\ L_P & M_P & N_P \end{vmatrix} = 0 \quad (2.38)$$

It can be shown that  $\eta_1$  and  $\eta_2$  are always real.

**Fig. 2.18** An example of the characteristic curve  $k_P(\eta)$



The quantities  $\eta_1$  and  $\eta_2$  define directions that align with the principal directions on the part surface  $P$ .

The distribution of normal curvature  $k_P$  at an arbitrary point  $m$  of the part surface  $P$  (see Fig. 2.18) can be specified in terms of parameters of the characteristic curve  $k_P = k_P(\eta)$ . The function  $k_P = k_P(\eta)$  can be represented in polar coordinates having the pole at a current point  $m$  of the part surface  $P$ . Such a representation simplifies a comparison of the characteristic curve  $k_P = k_P(\eta)$  with other planar characteristic curves.

## References

1. Radzevich, S. P. (1988). *Classification of surfaces*, Monograph, Kiev, UkrNIINTI, No. 1440-YK88, 185p.
2. Radzevich, S. P. (2001). *Fundamentals of surface generation, monograph*, Kiev, Rastan, 592p.
3. Koenderink, J. J. (1990). *Solid Shape* (p. 699). Cambridge, Massachusetts: The MIT Press.
4. [http://www.math.hmc.edu/faculty/gu/curves\\_and\\_surfaces/surfaces/plucker.html](http://www.math.hmc.edu/faculty/gu/curves_and_surfaces/surfaces/plucker.html).
5. Radzevich, S. P. (1991). *Differential-geometrical method of surface generation* (Doctoral Thesis), Tula, Tula Polytechnic Institute, 300p.
6. Radzevich, S. P. (1991). *Sculptured Surface Machining on Multi-Axis NC Machine*, Monograph, Kiev, Vishcha Schola, 192p.
7. Miron, R. (1958). Observatii a Supra Unor Formule din Geometria Varietatilor Neonolome  $E_3^2$ .—*Bulletinul Institutului Politehnic din Iasi*.
8. Lowe, P. G. (1980). A note on surface geometry with special reference to twist. *Mathematical Proceedings of the Cambridge Philosophical Society*, 87, 481–487.
9. Lowe, P. G. (1982). *Basic principles of plate theory*. Surrey University.
10. Nutbourn, A. W. (1986). A circle diagram for local differential geometry. In J. Gregory (Ed.), *Mathematics of surfaces, conference proceedings, institute of mathematics and its application, 1984*. Oxford: Oxford University Press.
11. Nutbourn, A. W. & Martin, R. R. (1988). *Differential geometry applied to curve and surface design, Volume I: Foundations*. Chichester: Ellis Horwood Ltd. Publishers, 282p.
12. Böhm, W. (1990). *Differential geometry II*, In: *Curves and surfaces for computer aided geometric design. A practical guide* (2nd edn., pp. 367–383) Boston: Academic Press, Inc. 444p.

## Part II

# Contact Geometry of Part Surfaces

Surfaces such as investigated in engineering geometry are designed and produced to interact either with the environment, or with other parts of a mechanism.

In the first case, namely when the surfaces are interacting with the environment (either with gas, air, or fluids, and so forth), they should be designed and produced so as to meet the requirements specified by gas dynamics and/or hydrodynamics criteria. Designing the surfaces of this particular kind is beyond of the scope of this book and thus is not considered here.

In the second case, part surfaces interact with working surfaces of other parts of a mechanism. Surfaces of this particular kind should be designed and produced to meet the requirements specified by conditions of interaction of the surfaces in a higher kinematic pair. In order to design part surfaces properly, the contact geometry of the interacting part surfaces needs to be thoroughly investigated and properly understood. An analytical description of contact geometry of the interacting part surfaces is helpful for this purpose.

In this part of the book, the contact geometry of two smooth regular part surfaces in the first order of tangency, or simply “*contact geometry of part surfaces*,” is discussed in further detail.

Part II of the book is comprised of five chapters, namely:

Chapter 3 is titled “Early Works in the Field of Contact Geometry of Surfaces.”

Chapter 4 is titled “An Analytical Method Based on the Second Fundamental Forms of Contacting Part Surfaces.”

Chapter 5 is titled “Indicatrix of Conformity at Point of Contact of Two Smooth Regular Part Surfaces in the First Order of Tangency.”

Chapter 6 is titled “‘*Plücker Conoid*’: More Characteristic Curves.”

Chapter 7 is titled “Possible Kinds of Contact of Two Smooth Regular Part Surfaces in the First Order of Tangency.”

## Chapter 3

# Early Works in the Field of Contact Geometry of Surfaces



The investigation of the contact geometry of curves and surfaces can be traced back to the eighteenth century. The study of the contact of curves and surfaces was undertaken in considerable detail by *J.L. Lagrange*<sup>1</sup> in his “*Theorié des Fonctions Analytiques*” (1797) [1], and *A.L. Cauchy*<sup>2</sup> in his “*Leçons sur les Applications du Calcul Infinitésimal á la Geometrie*” (1826) [2]. Later, in the twentieth century, an investigation in the realm of contact geometry of curves and surfaces was undertaken by *J. Favard*<sup>3</sup> in his “*Course de Gèomètrie Diffèrentialle Locale*” (1957) [3]. A few more names of the researchers to be mentioned.

Contacts of curves and surfaces of two different kinds are distinguished. Speaking more generally, the contact of surfaces with “*different order of tangency*” is investigated in differential geometry of surfaces. As a particular case, the conditions of contact of two smooth regular part surfaces in the “*first order of tangency*” are investigated in engineering geometry of surfaces.

Let us begin the discussion from the analysis of the results of the research obtained so far in differential geometry of surfaces.

### 3.1 Order of Contact

Order of contact of two smooth regular surfaces can be specified in terms of the order of contact of two smooth regular planar curves. It is understood there that:

- the curves are within a common plane;
- the curves are passing through the point of contact of the surfaces; and

---

<sup>1</sup>*Joseph-Louis Lagrange* (January 25, 1736–April 10, 1813)—an Italian born [born *Giuseppe Lodovico (Luigi) Lagrangia*] famous French mathematician and mechanician.

<sup>2</sup>*Augustin-Louis Cauchy* (August 21, 1789–May 23, 1857)—a famous French mathematician.

<sup>3</sup>*Jean Favard* (August 28, 1902–January 21, 1965)—a French mathematician.

- the plane is through the direction of the common perpendicular to the contacting surfaces at a point of interest.

Under such an investigation scenario, the contact geometry of two surfaces can be reduced to investigation of the geometry of contact of the two curves when the section plane spins about the straight line along the common perpendicular to the contacting surfaces. One application of such an approach is in fitting a local model to a shape if we want the contact to be as tight as possible. This requirement can be formulated in other words, that is, if we want the highest possible degree of conformity of the contacting surfaces in a particular plane through the common perpendicular. Another application is in the interaction of probes with a shape. For instance, a light ray may graze a surface in many different ways, the degree of contact varying enormously from case to case.

Planar curves have no contact if they have no point in common. Contact of order zero is observed when two smooth regular curves have a common intersection. Then, the order-one contact of the curves occurs when—at the point in common—the tangents to the curves align with one another. Ultimately, it is said that two curves have contact of the order  $n$  if all their derivatives with respect to arc length up to the  $n$ th-order are aligned, whereas the  $(n + 1)$ th-order is different. The order thus amounts to the order of the common initial part of a *Taylor*<sup>4</sup> series.<sup>5</sup>

Similarly, it is said for the case of two surfaces that the order of contact is  $n$  if all mixed partial derivatives up to the  $n$ th-order for some mutual parameterization [ $\mathbf{r}_{P1}(U_P, V_P)$ , and  $\mathbf{r}_{P2}(U_P, V_P)$ ] align, whereas this is not the case for the  $(n + 1)$ th-order.

Thus, first-order contact means:

$$\frac{\partial \mathbf{r}_{P1}}{\partial U_P}(U_P, V_P) = \frac{\partial \mathbf{r}_{P2}}{\partial U_P}(U_P, V_P) \quad (3.1)$$

$$\frac{\partial \mathbf{r}_{P1}}{\partial V_P}(U_P, V_P) = \frac{\partial \mathbf{r}_{P2}}{\partial V_P}(U_P, V_P) \quad (3.2)$$

and at least one of the equalities:

$$\frac{\partial^2 \mathbf{r}_{P1}}{\partial U_P^2}(U_P, V_P) = \frac{\partial^2 \mathbf{r}_{P2}}{\partial U_P^2}(U_P, V_P) \quad (3.3)$$

$$\frac{\partial^2 \mathbf{r}_{P1}}{\partial U_P^2}(U_P, V_P) = \frac{\partial^2 \mathbf{r}_{P2}}{\partial U_P^2}(U_P, V_P) \quad (3.4)$$

$$\frac{\partial^2 \mathbf{r}_{P1}}{\partial U_P \partial V_P}(U_P, V_P) = \frac{\partial^2 \mathbf{r}_{P2}}{\partial U_P \partial V_P}(U_P, V_P) \quad (3.5)$$

---

<sup>4</sup>*Brook Taylor* (August 18, 1685–December 29, 1731)—a well known English mathematician.

<sup>5</sup>It can be found out in the book by *Favard* [3] that two curves having infinite degree of contact cannot be congruent to one another.

is not true; that is to say, the tangent planes coincide but the osculating quadrics differ.

In Eq. (3.1) through Eq. (3.5), the position vector of a point of the first of the contacting surfaces  $P_1$  is designated  $\mathbf{r}_{P1}$ , and the position vector of a point of the second of the contacting surface  $P_2$  is denoted  $\mathbf{r}_{P2}$ . Both the contacting surfaces  $P_1$  and  $P_2$  must be parameterized so as to have common “*Gaussian coordinates*”  $U_P$  and  $V_P$ . In a case the part surfaces  $P_1$  and  $P_2$  are expressed in different  $U_P$ - and  $V_P$ -coordinates, then it is required to re-parameterize them to common  $U_P$ - and  $V_P$ -parameters (see Appendix C).

A “*curve*” has contact of at least order  $n$  with a “*surface*” if there exists a curve in the surface, which has  $n$ th-order contact with the curve. One defines the contact of space curves in the same way as the contact of planar curves mentioned earlier.

## 3.2 Contact Geometry of Part Surfaces

When solving problems in engineering geometry of surfaces, an appropriate method for analytical description of the contact geometry of part surfaces—say of a part surface  $P_1$  and a part surface  $P_2$ —is required. The problem of analytical description of the contact geometry of two smooth regular part surfaces in the first order of tangency is a sophisticated one. It can be solved on the premise of analysis of geometry of the contacting surfaces in the differential vicinity of the point of their contact.

Various methods for analytical description of the contact geometry of smooth regular surfaces have been developed. An overview of the known methods can be found in the monograph by Prof. *Radzevich* [4]. The latest achievements in the field are discussed in the papers [5, 6] and in the monograph [7]. In these publications as well as in other works, two part surfaces  $P_1$  and  $P_2$  that make contact at a point  $K$  are considered. Locally, each of the contacting surfaces is represented by a corresponding quadric. Owing to the fact that only differential vicinity of the contacting surfaces is considered below, that same designation  $P_1$  and  $P_2$  is applied to the quadrics as to the surfaces  $P_1$  and  $P_2$  themselves.

Generally speaking, at the point of contact  $K$ , the contacting part surfaces  $P_1$  and  $P_2$  may feature an arbitrary configuration. Namely, the local part surface patches  $P_1$  and  $P_2$  may be turned around a common perpendicular through a certain angle. Thus, it makes sense to begin the discussion from the analytical description of local relative orientation of the part surfaces  $P_1$  and  $P_2$  (in the differential vicinity of the point of contact of the surfaces).

## 3.3 Local Relative Orientation of Contacting Part Surfaces

Consider two local part surface patches  $P_1$  and  $P_2$ , which make contact at a point  $K$  as illustrated in Fig. 3.1. At the contact point  $K$ , the surfaces  $P_1$  and  $P_2$  share a

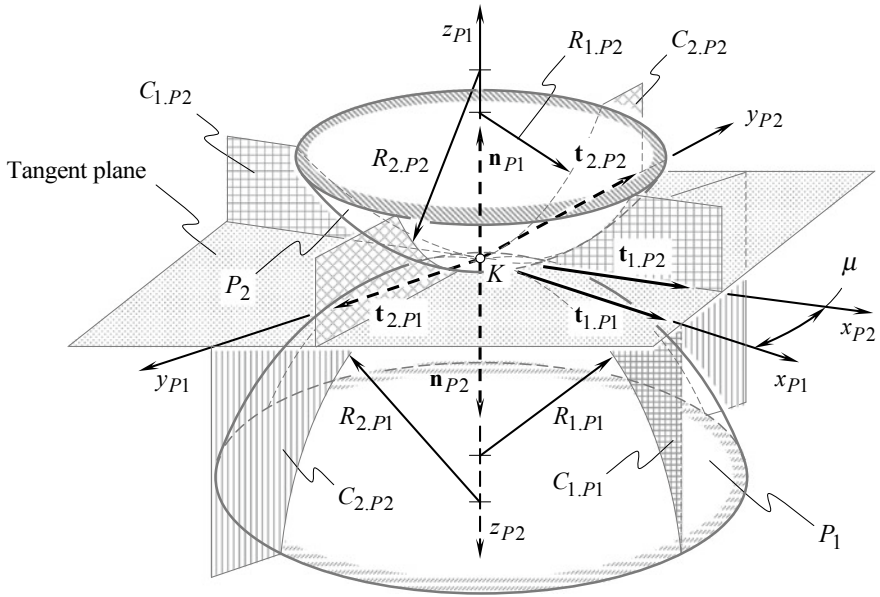


**Fig. 3.1** Local configuration of two smooth regular part surface patches  $P_1$  and  $P_2$  at a point  $K$  of their contact

common tangent plane. Tangency of the surfaces imposes a kind of restrictions on the relative configuration (location and orientation) of these surfaces, and on their relative motion, if any. In engineering geometry of surface generation, a quantitative measure of the surfaces  $P_1$  and  $P_2$  relative orientation is established.

Relative orientation of the contacting part surfaces  $P_1$  and  $P_2$  is specified by the angle  $\mu$  of the surfaces “local relative orientation”.<sup>6</sup> By definition [5, 8, and 9], the angle  $\mu$  is equal to the angle that the unit tangent vector  $\mathbf{t}_{1.P1}$  of the first principal direction of the part surface  $P_1$  forms with the unit tangent vector  $\mathbf{t}_{1.P2}$  of the first principal direction of the part surface  $P_2$ . That same angle  $\mu$  can also be specified as the angle made by the unit tangent vectors  $\mathbf{t}_{2.P1}$  and  $\mathbf{t}_{2.P2}$  of the second principal directions of the part surfaces  $P_1$  and  $P_2$  at a point  $K$  of their contact. This immediately yields the equations for the calculation of the angle  $\mu$  of the surfaces local relative orientation:

$$\sin \mu = |\mathbf{t}_{1.P1} \times \mathbf{t}_{1.P2}| = |\mathbf{t}_{2.P1} \times \mathbf{t}_{2.P2}| \quad (3.6)$$

$$\cos \mu = \mathbf{t}_{1.P1} \cdot \mathbf{t}_{1.P2} = \mathbf{t}_{2.P1} \cdot \mathbf{t}_{2.P2} \quad (3.7)$$

<sup>6</sup>Orientation of the surfaces  $P_1$  and  $P_2$  is “local” in nature as it is related only to the differential vicinity of point  $K$  of contact of the surfaces.

$$\tan \mu = \frac{|\mathbf{t}_{1,P1} \times \mathbf{t}_{1,P2}|}{\mathbf{t}_{1,P1} \cdot \mathbf{t}_{1,P2}} \equiv \frac{|\mathbf{t}_{2,P1} \times \mathbf{t}_{2,P2}|}{\mathbf{t}_{2,P1} \cdot \mathbf{t}_{2,P2}} \quad (3.8)$$

Here, we define:

- $\mathbf{t}_{1,P1}, \mathbf{t}_{2,P1}$  Are the unit vectors of principal directions on the first part surface  $P_1$  of two contacting surfaces
- $\mathbf{t}_{1,P2}, \mathbf{t}_{2,P2}$  Are the unit vectors of principal directions on the second part surface  $P_2$  of two contacting surfaces.

In case of point contact of the part surfaces  $P_1$  and  $P_2$ , the actual value of the angle  $\mu$  is calculated at the point  $K$  of contact of the surfaces. If the part surfaces  $P_1$  and  $P_2$  are in line contact, then the actual value of the angle  $\mu$  of the surfaces' local relative orientation can be calculated at every point within the line of contact.<sup>7</sup> The reason for why the angle  $\mu$  is referred to as the angle of “local” surfaces' orientation is clearly illustrated with this.

The determination of the angle  $\mu$  of the surfaces'  $P_1$  and  $P_2$  local relative orientation is illustrated in Fig. 3.2.

Unit tangent vectors of the principal directions  $\mathbf{t}_{1,P1}$  and  $\mathbf{t}_{1,P2}$  at a point of contact of the part surfaces  $P_1$  and  $P_2$  are employed for the purpose of calculation of the angle  $\mu$  of the surfaces' local relative orientation.

Consider two part surfaces  $P_1$  and  $P_2$  in point contact that are represented in a common reference system. The surfaces make contact at point  $K$ . For further analysis, an equation of the common tangent plane to the surfaces  $P_1$  and  $P_2$  at the point  $K$  is necessary (Figs. 3.1 and 3.3):

$$(\mathbf{r}_{tp} - \mathbf{r}_K) \cdot \mathbf{u}_{P1} \cdot \mathbf{v}_{P1} = 0 \quad (3.9)$$

Here, we define:

- $\mathbf{r}_{tp}$  Is the position vector of a point of the common tangent plane
- $\mathbf{r}_K$  Is the position vector of the contact point  $K$
- $\mathbf{u}_{P1}$  and  $\mathbf{v}_{P1}$  are the unit vectors tangent to  $U_{P1}$ - and  $V_{P1}$ -coordinate lines on the surface  $P_1$  at the point  $K$ .

An equation similar to Eq. (3.9) can also be expressed in terms of parameters of geometry of the other contacting surface  $P_2$ .

The actual value of the angle  $\omega_{P1}$  between the vectors  $\mathbf{v}_{P1}$  and  $\mathbf{v}_{P1}$  can be calculated from one of the following equations:

$$\sin \omega_{P1} = \frac{\sqrt{E_{P1}G_{P1} - F_{P1}^2}}{\sqrt{E_{P1}G_{P1}}} \quad (3.10)$$

---

<sup>7</sup>It is worth pointing out here that for line contact, the relative orientation of the surfaces  $P_1$  and  $P_2$  is predetermined in global sense. However, the actual value of the angle  $\mu$  of the surfaces'  $P_1$  and  $P_2$  “local” relative orientation at different points of the line of contact is different.



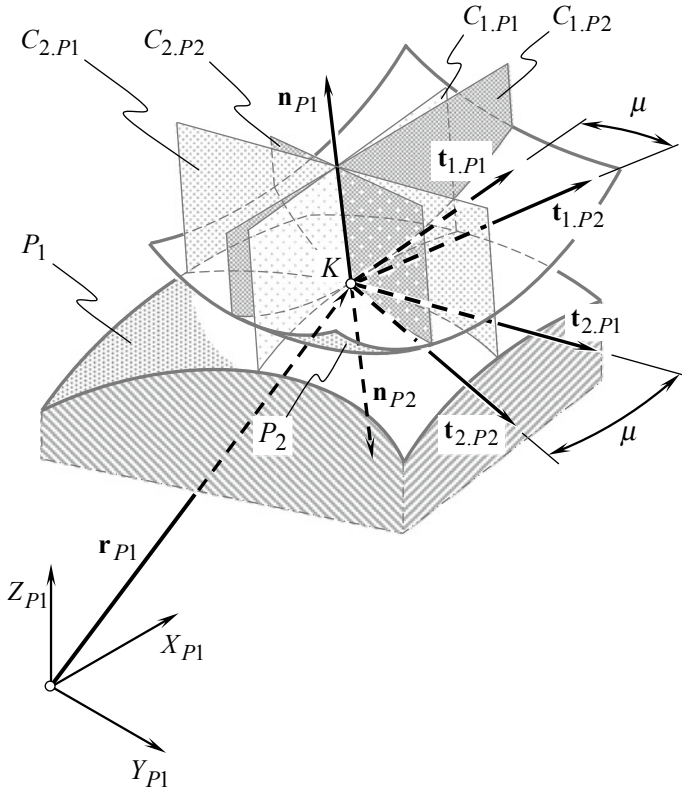


**Fig. 3.2** Specification of the angle  $\mu$  of the surfaces  $P_1$  and  $P_2$  local relative orientation

$$\cos \omega_{P1} = \frac{F_{P1}}{\sqrt{E_{P1}G_{P1}}} \quad (3.11)$$

$$\tan \omega_{P1} = \frac{\sqrt{E_{P1}G_{P1} - F_{P1}^2}}{F_{P1}} \quad (3.12)$$

Equations similar to Eq. (3.9) through Eq. (3.12) are also valid for the calculation of the angle  $\omega_{P2}$  of the other contacting surface  $P_2$ .

The unit tangent vectors  $\mathbf{u}_{P1}$  and  $\mathbf{v}_{P1}$ , which are tangent to the  $U_{P1}$ - and  $V_{P1}$ -coordinate lines on the part surface  $P_1$ , and the unit tangent vectors  $\mathbf{u}_{P2}$  and  $\mathbf{v}_{P2}$ , which are tangent to the  $U_{P2}$ - and  $V_{P2}$ -coordinate lines on the surface  $P_2$ , are specified by the angles  $\theta$  and  $\varepsilon$ . The actual values of the angles  $\theta$  and  $\varepsilon$  can be calculated from the following equations:

$$\cos \theta = \mathbf{u}_{P1} \cdot \mathbf{u}_{P2} \quad (3.13)$$

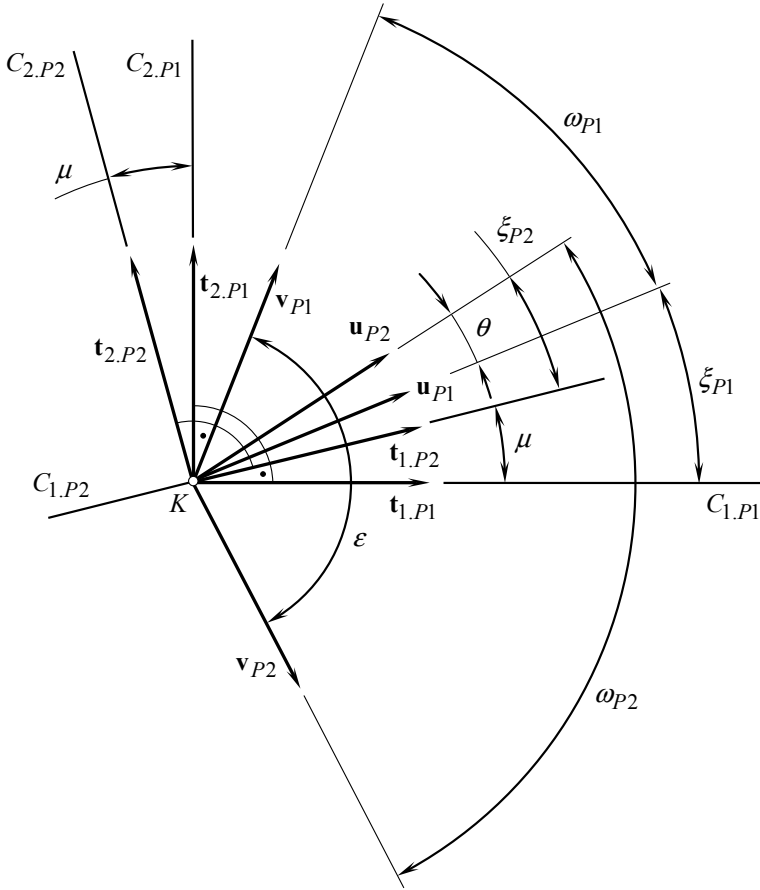


**Fig. 3.3** Local relative orientation of the contacting part surfaces  $P_1$  and  $P_2$ , considered in a common tangent plane

$$\cos \varepsilon = \mathbf{v}_{P1} \cdot \mathbf{v}_{P2} \quad (3.14)$$

Angle  $\xi_P$  is the angle that the first principal direction  $\mathbf{t}_{1,P}$  on the surface  $P$  forms with the unit tangent vector  $\mathbf{u}_P$  (see Fig. 3.3). The equation for the calculation of the actual value of the angle  $\xi_P$  is derived by Prof. Radzevich [5, 8, and 9]:

$$\sin \xi_{P1} = \frac{\eta_{P1}}{\sqrt{\eta_{P1}^2 - 2\eta_{P1} \cos \omega_{P1} + 1}} \sin \omega_{P1} \quad (3.15)$$

where the ratio  $\partial U_{P1}/\partial V_{P1}$  is denoted by  $\eta_{P1}$ , ( $\eta_{P1} = \partial U_{P1}/\partial V_{P1}$ ).

In the event  $F_{P1} = 0$ , the equality  $\tan \xi_{P1} = \eta_{P1}$  is observed. Here, the ratio  $\eta_{P1}$  is calculated as the root of the quadratic equation:

$$(F_{P1}L_{P1} - E_{P1}M_{P1})\eta_{P1}^2 + (G_{P1}L_{P1} - E_{P1}N_{P1})\eta_{P1} + (G_{P1}M_{P1} - F_{P1}N_{P1}) = 0 \quad (3.16)$$

that follows immediately from Eq. (1.68).

The equation for calculation of the actual value of the angle  $\xi_{P1}$  yields another representation. Following the chain rule,  $d\mathbf{r}_{P1}$  can be represented in the form:

$$d\mathbf{r}_{P1} = \mathbf{U}_{P1}dU_{P1} + \mathbf{V}_{P1}dV_{P1} \quad (3.17)$$

By definition,  $\tan \xi_{P1} = \frac{\sin \xi_{P1}}{\cos \xi_{P1}}$ . The functions  $\sin \xi_{P1}$  and  $\cos \xi_{P1}$  yield representation in the form:

$$\sin \xi_{P1} = \frac{|\mathbf{U}_{P1} \times d\mathbf{r}_{P1}|}{|\mathbf{U}_{P1}| \cdot |d\mathbf{r}_{P1}|} \quad (3.18)$$

$$\cos \xi_{P1} = \frac{\mathbf{U}_{P1} \cdot d\mathbf{r}_{P1}}{|\mathbf{U}_{P1}| \cdot |d\mathbf{r}_{P1}|} \quad (3.19)$$

The last expressions make it possible the formula:

$$\begin{aligned} \tan \xi_{P1} &= \frac{\sin \xi_{P1}}{\cos \xi_{P1}} = \frac{|\mathbf{U}_{P1} \times d\mathbf{r}_{P1}|}{\mathbf{U}_{P1} \cdot d\mathbf{r}_{P1}} = \frac{|\mathbf{U}_{P1} \times d\mathbf{r}_{P1}|}{\mathbf{U}_{P1} \cdot (\mathbf{U}_{P1}dU_{P1} + \mathbf{V}_{P1}dV_{P1})} \\ &= \frac{|\mathbf{U}_{P1} \times d\mathbf{r}_{P1}| \cdot dV_{P1}}{\mathbf{U}_{P1} \cdot \mathbf{U}_{P1}dU_{P1} + \mathbf{U}_{P1} \cdot \mathbf{V}_{P1}dV_{P1}} \end{aligned} \quad (3.20)$$

By definition,

$$\mathbf{U}_{P1} \cdot \mathbf{U}_{P1} = E_{P1} \quad (3.21)$$

$$\mathbf{U}_{P1} \cdot \mathbf{V}_{P1} = F_{P1} \quad (3.22)$$

$$\mathbf{V}_{P1} \cdot \mathbf{V}_{P1} = G_{P1} \quad (3.23)$$

$$|\mathbf{U}_{P1} \times \mathbf{V}_{P1}| = \sqrt{E_{P1}G_{P1} - F_{P1}^2} \quad (3.24)$$

Then, Eq. (3.17) through Eq. (3.24) yield the formula:

$$\tan \xi_{P1} = \frac{\sqrt{E_{P1}G_{P1} - F_{P1}^2}}{\eta_{P1} \cdot E_{P1} + F_{P1}} \quad (3.25)$$

for calculation of the actual value of the angle  $\xi_{P1}$ .

Equations, similar to those above Eqs. (3.15) and (3.25), are also valid for the calculation of the actual value of the angle  $\xi_{P_2}$  that the first principal direction  $\mathbf{t}_{1.P_2}$  on the part surface  $P_2$  makes with the unit tangent vector  $\mathbf{u}_{P_2}$ .

The analysis performed above yields the following equations for the calculation of the unit tangent vectors  $\mathbf{t}_{1.P_1}$ ,  $\mathbf{t}_{2.P_1}$  of the principal directions:

$$\mathbf{t}_{1.P_1} = \mathbf{Rt}(\xi_{P_1}, \mathbf{n}_{P_1}) \cdot \mathbf{u}_{P_1} \quad (3.26)$$

$$\mathbf{t}_{2.P_1} = \mathbf{Rt}\left[\left(\xi_{P_1} + \frac{\pi}{2}\right), \mathbf{n}_{P_1}\right] \cdot \mathbf{u}_{P_1} \quad (3.27)$$

for the first part surface  $P_1$ , and similar equations for the calculation of the unit tangent vectors  $\mathbf{t}_{1.T}$ ,  $\mathbf{t}_{2.T}$  of the principal directions:

$$\mathbf{t}_{1.P_2} = \mathbf{Rt}(\xi_{P_2}, \mathbf{n}_{P_2}) \cdot \mathbf{u}_{P_2} \quad (3.28)$$

$$\mathbf{t}_{2.P_2} = \mathbf{Rt}\left[\left(\xi_{P_2} + \frac{\pi}{2}\right), \mathbf{n}_{P_2}\right] \cdot \mathbf{u}_{P_2} \quad (3.29)$$

for the second part surface  $P_2$ .

See Appendix B for the calculation of the operators of rotation  $\mathbf{Rt}(\xi_{P_1}, \mathbf{n}_{P_1})$ ,  $\mathbf{Rt}\left[\left(\xi_{P_1} + \frac{\pi}{2}\right), \mathbf{n}_{P_1}\right]$ , and  $\mathbf{Rt}(\xi_{P_2}, \mathbf{n}_{P_2})$ ,  $\mathbf{Rt}\left[\left(\xi_{P_2} + \frac{\pi}{2}\right), \mathbf{n}_{P_2}\right]$  in Eq. (3.26) through Eq. (3.29) accordingly.

### 3.4 First-Order Analysis: Common Tangent Plane

Various methods can be implemented for analytical description of the contact geometry of two smooth regular part surfaces in the first order of tangency. The first-order analysis is the simplest among all of them.

First-order analysis is the simplest method used for the analysis of geometry of contact of two smooth regular part surfaces  $P_1$  and  $P_2$  at a point  $K$  of their contact. Implementation of the first-order analysis returns limited information on the contact geometry of the surfaces in the differential vicinity of the point of contact. Accurate analytical description of the geometry of contact of two smooth regular part surfaces is possible only when the first-order analysis is used together with a kind of higher-order analysis. Under such a scenario, the first-order analysis is incorporated as a first step of a higher-order analysis of the contact geometry of two smooth regular part surfaces  $P_1$  and  $P_2$ .

The common tangent plane can be defined as a plane through the contact point  $K$ . This plane is perpendicular to the common unit normal vector  $\mathbf{n}_P$  to the part surfaces  $P_1$  and  $P_2$  at  $K$ . For an analytical description of the common tangent plane, vector equation [see Eq. (1.15)]:

$$(\mathbf{r}_{tp} - \mathbf{r}_K) \cdot \mathbf{u}_{P1} \cdot \mathbf{v}_{P1} = 0 \quad (3.30)$$

can be employed.

Any pair of unit vectors chosen from the set of vectors, namely from the set of vectors  $\mathbf{u}_{P1}$ ,  $\mathbf{v}_{P1}$ ,  $\mathbf{u}_{P2}$ ,  $\mathbf{v}_{P2}$ ,  $\mathbf{t}_{1.P1}$ ,  $\mathbf{t}_{2.P1}$ ,  $\mathbf{t}_{1.P2}$ ,  $\mathbf{t}_{2.P2}$  can be used as a replacement for the unit tangent vectors  $\mathbf{u}_{P1}$  and  $\mathbf{v}_{P1}$  in Eq. (3.30).

The first-order analysis provides very limited information about the contact geometry of two smooth regular part surfaces in first order of tangency. Hence, the first-order analysis itself has limited application. However, the importance of the first-order analysis becomes valuable as it is incorporated into the second-order analysis, and/or into a higher-order analysis.

### 3.5 Second-Order Analysis

For a more accurate analytical description of the contact geometry of two part surfaces  $P_1$  and  $P_2$ , consideration of the second-order parameters is required. Elements of both of the first order and second order are taken into consideration when the second-order analysis undertaken. To perform the second-order analysis, familiarity with “*Dupin indicatrix*” is highly desirable. The “*Dupin indicatrix*” is a perfect starting point for consideration of the second-order analysis.

It makes sense to begin the discussion of the contact geometry of two smooth regular part surfaces in the first order of tangency from the assumptions those made by the founder of contact mechanics of materials, German physicist *Heinrich Hertz*. The theory proposed by *Hertz* is based on the implementation of an imaginary surface, which (after *Hertz*) is referred to as “*surface of relative curvature*.”

#### 3.5.1 Comments on Analytical Description of Local Geometry of Contacting Surfaces Loaded by a Normal Force: “Hertz Proportional Assumption”

Investigation of the geometry of interacting surfaces under an applied normal load can be traced back to the fundamental research by *H. Hertz*<sup>8</sup> on contact of solid elastic bodies (*Hertz*, 1881–1896).

In 1886–1889, *Hertz* published two articles on what was to become known as the field of “*contact mechanics*” of materials. His work basically summarizes how two axisymmetric objects placed in contact will behave under loading. The developed theory is based on *Hertz*’s observation of elliptical “*Newton’s rings*” formed upon placing a glass sphere upon a lens as the basis of assuming that the pressure exerted by the sphere follows an elliptical distribution.

---

<sup>8</sup>*Heinrich Rudolf Hertz* (February 22, 1857–January 1, 1894), a famous German physicist.

Interaction of an elastic sphere and a plane is illustrated schematically in Fig. 3.4a. Initial contact of the sphere of a certain radius,  $R_{\text{sphere}}$ , and of the plane can be assumed at a point,  $K$ . Then, after a normal load,  $F_n$ , is applied, the contact point,  $K$ , is spread to a round contact patch of radius,  $r_{pc}$ , as illustrated schematically in Fig. 3.4b.

It is of critical importance to stress here on the following two features of the theory developed by *Hertz*.

**First**, the theory developed by *Hertz* is based on the assumption that the radius of contact patch,  $r_{pc}$ , is much smaller than the radius of the sphere,  $R_{\text{sphere}}$ . The theory returns reasonable results of the calculation of contact stress if the radius,  $r_{pc}$ , is 10 (or more) times smaller than the radius of the sphere,  $R_{\text{sphere}}$ . If the inequality,  $R_{\text{sphere}} \gg r_{pc}$ , is not fulfilled, then the *Hertz* theory is not valid.

**Assumption 3.1** *The dimensions of the contact patch are much smaller than the corresponding radii of curvature of the contacting elastic bodies.*

An important intermediate conclusion that can be immediately drawn from that statement is as follows:

**Conclusion 3.1** *When applying the Hertz theory for calculation of contact stress in case of contact of elastic bodies bounded by a “convex” and “concave” surfaces it is necessary to be very careful, as in this particular case the inequality  $R_{\text{sphere}} \gg r_{pc}$  is commonly violated.*

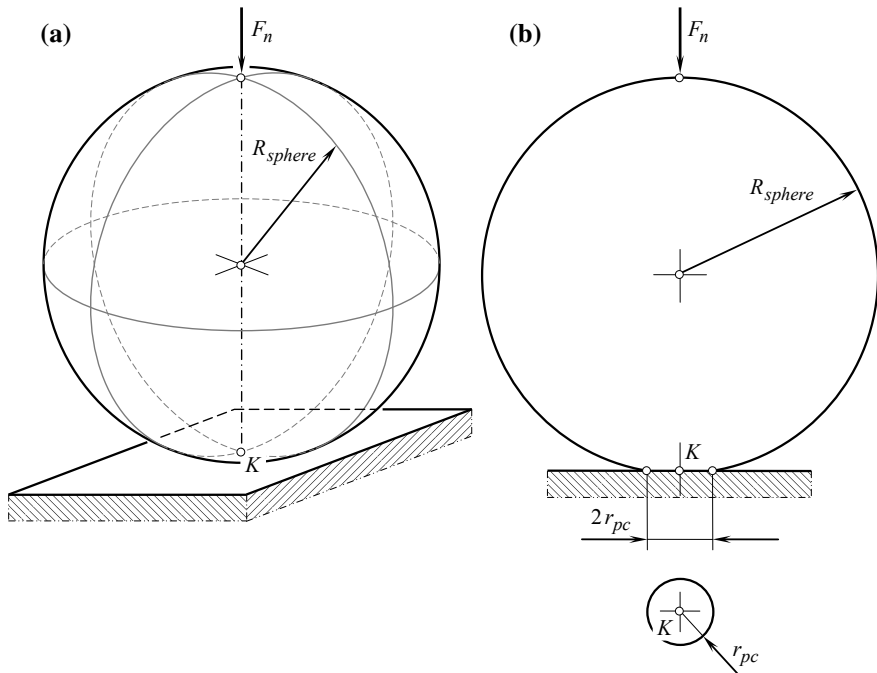


**Fig. 3.4** Interaction of a sphere of a radius,  $R_{\text{sphere}}$ , and of a plane under normal load,  $F_n$

**Second**, *Hertz* has considered the interaction of two elastic bodies having simple geometries of contacting surfaces. A plane, spheres of various radii, and so forth, are common in the research undertaken by *Hertz*. It should be pointed out here that for surfaces of that simple geometry, principal directions at the point of contact,  $K$ , are either not identified (as observed for a sphere, and for a plane), or they are aligned to one another. For surfaces of that simple geometry, the concept of “*surface of relative curvature is applicable*”.

In the simplest case of contact of a plane and a sphere (Fig. 3.5a), the radius of the sphere,  $R_{\text{sphere}}$ , is sufficient for an analytical description of geometry of contact of the sphere and the plane. No radius of relative curvature,  $R_{rl}$ , is required in this simplest case of the surfaces contact, as these two radii are identical to one another ( $R_{\text{sphere}} \equiv R_{rl}$ ). The results of the analytical description of the geometry of contact of a plane and a sphere can be enhanced to similar problems when two bodies with more complex geometries make contact, for example, the case of contact of two spheres of different radii. For this purpose, the concept of the “*radius of relative curvature*” is introduced. In the case of contact depicted in Fig. 3.5a, two points,  $a$  and  $b$ , are taken at a reasonably short distance,  $r$ , from a straight line through the point,  $K$ , that is, perpendicular to the plane. The points,  $a$  and  $b$ , are at a certain distance,  $\delta_{ab}$ , from one another.

In case of contact of two spheres,  $A$  and  $B$ , of radii,  $R_{\text{sphere}}^{(A)}$  and  $R_{\text{sphere}}^{(B)}$ , accordingly (see Fig. 3.5b), two points,  $c$  and  $d$ , are taken into consideration. These two points are equivalent to the points,  $a$  and  $b$ , in the aforementioned case of contact of a sphere and a plane. The distance,  $\delta_{cd}$  (not shown in Fig. 3.5b), between the points,  $c$  and  $d$ , significantly exceeds the distance,  $\delta_{ab}$ . A surface of relative curvature of a radius,  $R_{rl}$ , for the spheres,  $A$  and  $B$ , is designed to ensure equality of the distances,  $\delta_{ad}$ , with the distance,  $\delta_{ab}$ , in the case depicted in Fig. 3.5a. If the equality,  $\delta_{ad} = \delta_{ab}$  holds (and the equality  $ad = bc$  is met as well), then the problem of contact of two spheres of

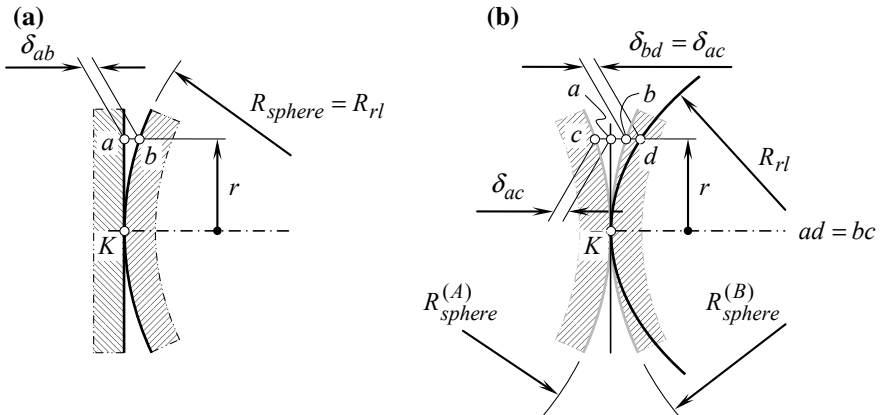


**Fig. 3.5** Definition of relative curvature,  $R_{rl}$ , of two smooth regular surfaces, 1 and 2, making point contact at  $K$

radii,  $R_{\text{sphere}}^{(A)}$  and  $R_{\text{sphere}}^{(B)}$  (Fig. 3.5b) can be substituted with the equivalent problem of contact of a plane and a sphere (Fig. 3.5a).

In order to construct a “*surface of relative curvature*,” the following manipulations with the radii of curvatures are required.

The geometry of contact of the two part surfaces can be expressed in terms of the curvature of the sphere. For a sphere of a radius,  $R_{\text{sphere}}$ , its curvature is expressed by the parameter inverse to the radius of the sphere,  $k_{\text{sphere}} = R_{\text{sphere}}^{-1}$ .

In order to accommodate the results obtained in the case of contact of two elastic bodies bounded by two spheres,  $A$  and  $B$ , the concept of the “*surface of relative curvature*” is used. For any normal section through the point of contact,  $K$ , of the bodies bounded by two spheres of radii,  $R_{\text{sphere}}^{(A)}$  and  $R_{\text{sphere}}^{(B)}$  (and having normal curvatures  $k_A$  and  $k_B$  accordingly), the normal curvature,  $k_r$ , of the surface of relative curvature can be calculated from the following formula:

$$k_r = k_A + k_B \quad (3.31)$$

This formula is composed under the assumption that the deviation,  $\delta_{ad}$ , of the surface of relative curvature from the plane in the case depicted in Fig. 3.5b, is equal to the deviation,  $\delta_{ab}$ , of the sphere from the plane as illustrated in Fig. 3.5a. The equality,  $\delta_{ad} = \delta_{ab}$ , holds (as well as the equality  $ad = bc$ ) when the deviations,  $\delta_{bd}$  and  $\delta_{ac}$ , are equal ( $\delta_{bd} = \delta_{ac}$ ). Such an equality,  $\delta_{ad} = \delta_{ab}$ , is reasonable if and only if the inequality  $R_{\text{sphere}} \gg r_{\text{pc}}$  is fulfilled. Otherwise, application of the “*Hertz theory*” is invalid.

Contact of two elastic bodies bounded by surfaces having more complex geometry has not been investigated by *Hertz*.

### 3.5.2 Surface of Normal Relative Curvature

The implementation of the surface of normal relative curvature for the purpose of analytical description of the contact geometry of two smooth regular part surfaces in the first order of tangency is a perfect example of the second-order analysis. This idea can be traced back to publications by *H. Hertz* (1881–1896).

Let us consider a “*Taylor expansion*” of equations of two part surfaces  $P_1$  and  $P_2$  at a point  $K$  of their contact. Implementation of “*Taylor expansion*” is convenient for the determination of the surface of relative normal curvature.

In a local reference system  $x_{P1}y_{P1}z_{P1}$ , the equation of the part surface  $P_1$  in the differential vicinity of the contact point  $K$  can be represented in the form:

$$P_1 \Rightarrow z_{P1} = \frac{x_{P1}^2}{2R_{1.P1}} + \frac{y_{P1}^2}{2R_{2.P1}} + \dots \quad (3.32)$$

where  $R_{1.P1}$  and  $R_{2.P1}$  are the principal radii of curvature of the part surface  $P_1$  at  $K$ . They are positive if the corresponding center of curvature is located within the body



bounded by the surface  $P_1$ , that is, the center of curvature is located on the negative portion of the  $z_{P1}$ -axis.

Similarly, in the local coordinate system  $x_{P2}y_{P2}z_{P2}$ , the equation of the part surface  $P_2$  in the differential vicinity of the contact point  $K$  yields a representation in the form:

$$P_2 \Rightarrow z_{P2} = \frac{x_{P2}^2}{2R_{1.P2}} + \frac{y_{P2}^2}{2R_{2.P2}} + \dots \quad (3.33)$$

The quantities  $R_{1.P2}$  and  $R_{2.P2}$  have the same meaning for the second part surface  $P_2$  as the quantities  $R_{1.P1}$  and  $R_{2.P1}$  for the part surface  $P_1$ .

A surface for which the equality  $z_{\mathcal{R}} = z_{P1} - z_{P2}$  is observed is referred to as the “*surface of relative normal curvature*.” Further, the surface of relative normal curvature is designated as  $\mathcal{R}$ .

In order to employ the equation  $z_{\mathcal{R}} = z_{P1} - z_{P2}$ , it is necessary to:

- (a) represent both the contacting part surfaces  $P_1$  and  $P_2$  in a common coordinate system having origin at the contact point  $K$  and
- (b) align the positive direction of  $z_{\mathcal{R}}$ -axis with the unit normal vector  $\mathbf{n}_{P1}$  to the surface  $P_1$  at  $K$ .

The local coordinate system  $x_{P1}y_{P1}z_{P1}$  is suitable for the purpose of analytical description of the surface of normal relative curvature. In this reference system, the equation of the surface of relative curvature  $\mathcal{R}$  yields representation in the form:

$$\mathcal{R} \Rightarrow z_{P1} = \frac{x_{P1}^2}{2R_{1.\mathcal{R}}} + \frac{y_{P1}^2}{2R_{2.\mathcal{R}}} + \dots \quad (3.34)$$

The local geometry of the contacting part surfaces  $P_1$  and  $P_2$ , and the contact geometry of these surfaces, is reflected by the surface of relative normal curvature locally, just in the differential vicinity of the contact point  $K$ . This yields only those terms in Eq. (3.32), which are written down explicitly. In the “*Darboux trihedron*,” this result yields the simplified equation for the surface of relative normal curvature:

$$\mathcal{R} \Rightarrow 2z_{P1} = k_{1.\mathcal{R}}x_{P1}^2 + k_{2.\mathcal{R}}y_{P1}^2 \quad (3.35)$$

Relative normal curvature is the major analytical tool used nowadays for the analytical description of the contact geometry in higher kinematic pairs. The relative normal curvature  $k_{\mathcal{R}}$  of two part surfaces  $P_1$  and  $P_2$  at a given contact point  $K$  is defined as the sum of normal curvatures  $k_{P1}$  and  $k_{P2}$  of both surfaces  $P_1$  and  $P_2$ . It is taken in a common normal plane section of surfaces  $P_1$  and  $P_2$ , and equal to:

$$k_{\mathcal{R}} = k_{P1} + k_{P2} \quad (3.36)$$

Here, the normal curvature of the surface of relative curvature  $\mathcal{R}$  is designated as  $k_{\mathcal{R}}$ ,  $k_{P1}$  is the normal curvature of the first part surface  $P_1$ , and finally  $k_{P2}$  is normal

curvature of the second part surface  $P_2$  in contact. All three curvatures are calculated in a common normal plane section of the surfaces  $P_1$ ,  $P_2$ , and  $\mathcal{R}$  through the contact point  $K$ .

Similarly, the relative normal radius of curvature  $R_{\mathcal{R}}$  of two smooth regular part surfaces  $P_1$  and  $P_2$  at a given contact point  $K$  could be defined as the difference of the normal radii of curvature  $R_{P_1}$  and  $R_{P_2}$ . The radii are taken in a common normal plane section of surfaces  $P_1$ ,  $P_2$ , and  $\mathcal{R}$  is equal to  $R_{\mathcal{R}} = R_{P_1} - R_{P_2}$ .

Consider a common normal plane section of two part surfaces  $P_1$  and  $P_2$  through the contact point  $K$ . This plane section makes a certain angle  $\varphi$  with the unit tangent vector  $\mathbf{t}_{1,P_1}$ . That same common normal plane section makes the angle  $(\varphi + \mu)$  with the unit tangent vector  $\mathbf{t}_{1,P_2}$ . Recall that the angle  $\mu$  of the surfaces' local relative orientation is the angle that make the first  $\mathbf{t}_{1,P_1}$  and  $\mathbf{t}_{1,P_2}$  (or, similarly, the second  $\mathbf{t}_{2,P_1}$  and  $\mathbf{t}_{2,P_2}$ ) principal directions of the part surfaces  $P_1$  and  $P_2$  (Fig. 3.2).

The “Euler equation” yields representation of the normal curvatures  $k_{P_1}$  and  $k_{P_2}$  in the form:

$$k_{P_1} = k_{1,P_1} \cos \varphi + k_{2,P_1} \sin \varphi \quad (3.37)$$

$$k_{P_2} = k_{1,P_2} \cos(\varphi + \mu) + k_{2,P_2} \sin(\varphi + \mu) \quad (3.38)$$

Here we define:

- $k_{1,P_1}$  and  $k_{2,P_1}$  Are the first and the second principal curvatures of the first part surface  $P_1$
- $k_{1,P_2}$  and  $k_{2,P_2}$  Are the first and the second principal curvatures of the second part surface  $P_2$
- $\varphi$  is the angular parameter
- $\mu$  Is the angle of the surfaces  $P_1$  and  $P_2$  local relative orientation.

It is of importance to point out here that the inequality  $k_{1,P_1} > k_{2,P_1}$  always holds.<sup>9</sup>

Thus, Eq. (3.36) yields an equation for the normal curvature  $k_{\mathcal{R}}$  of the surface  $\mathcal{R}$  at  $K$ :

$$k_{\mathcal{R}} = k_{1,P_1} \cos^2 \varphi + k_{2,P_1} \sin^2 \varphi + k_{1,P_2} \cos^2(\varphi + \mu) + k_{2,P_2} \sin^2(\varphi + \mu) \quad (3.39)$$

---

<sup>9</sup>This inequality is often representing in the form  $k_{1,P_1(P_2)} \geq k_{2,P_1(P_2)}$ , which is incorrect. In a case of equality, that is, if  $k_{1,P_1(P_2)} = k_{2,P_1(P_2)}$ , all normal curvatures of the contacting part surfaces  $P_1$  and  $P_2$  at  $K$  are of the same value (and of the same sign). The latter is observed for umbilics, as well as for plane surface. For this reason, at an umbilic point, the principal directions are undefined. Therefore, principal curvatures are also undefined. This means that the inequality  $k_{1,P_1(P_2)} > k_{2,P_1(P_2)}$  properly reflects the correspondence between the principal curvatures  $k_{1,P_1(P_2)}$  and  $k_{2,P_1(P_2)}$ .

This equation is expressed in terms of:

- (a) the principal curvatures  $k_{1.P1}$ ,  $k_{2.P1}$ ,  $k_{1.P2}$ , and  $k_{2.P2}$ ,
- (b) the angle  $\mu$  of the part surfaces  $P_1$  and  $P_2$  local relative orientation,
- (c) the angular parameter  $\varphi$ .

Equation (3.39) can be cast to:

$$k_{\mathcal{R}} = a \cdot \cos^2 \varphi + b \cdot \sin(2\varphi) + c \cdot \sin^2 \varphi \quad (3.40)$$

Here, in Eq. (3.40), the coefficients  $a$ ,  $b$ , and  $c$  are calculated from the following formulae:

$$a = k_{1.P1} + k_{1.P2} \cos^2 \mu + k_{2.P2} \sin^2 \mu \quad (3.41)$$

$$b = \frac{(k_{2.P2} - k_{1.P2})}{2} \cdot \sin(2\mu) \quad (3.42)$$

$$c = (k_{2.P1} + k_{1.P2} \sin^2 \mu + \cos^2 \mu) \quad (3.43)$$

The principal curvatures of the surface of relative normal curvature are the extreme values of the function  $k_{\mathcal{R}}(\varphi)$  [see Eq. (3.40)].

The principal directions of the surface  $\mathcal{R}$  can be determined from the equations those for which the equality:

$$\frac{\partial k_{\mathcal{R}}(\varphi)}{\partial \varphi} = 0 \quad (3.44)$$

is fulfilled. The last equation together with the Eq. (3.40) yield:

$$\tan(2\varphi) = \frac{2b}{c - a} \quad (3.45)$$

Two solutions for the angle  $\varphi$  are returned by the solution of Eq. (4.45). They are  $\varphi_1$  and  $\varphi_2 = \varphi_1 + 90^\circ$ . This means that there are two perpendicular directions for the principal directions of the surface of relative normal curvature. The principal curvatures of the surface of normal relative curvature can be calculated from:

$$k_{1,2,\mathcal{R}} = \frac{(a + c) \pm \sqrt{(a + c)^2 + 4b^2}}{2} \quad (3.46)$$

The surface of relative normal curvature  $\mathcal{R}$  is of importance for many engineering applications.

It is of importance to stress here again that all of three normal curvatures  $k_{\mathcal{R}}$ ,  $k_{P1}$ , and  $k_{P2}$  in Eq. (4.36) are taken in a common normal plane section through the point<sup>10</sup> of contact  $K$  of the surfaces  $P_1$ ,  $P_2$ , and  $\mathcal{R}$ .

Based on the calculated values of the principal curvatures  $k_{1,\mathcal{R}}$  and  $k_{2,\mathcal{R}}$ , the implicit equation of the surface of relative curvature yields representation in the form:

$$2Z_{\mathcal{R}} = k_{1,\mathcal{R}}X_{\mathcal{R}}^2 + k_{2,\mathcal{R}}Y_{\mathcal{R}}^2 \quad (3.47)$$

A characteristic surface similar to the surface  $\mathcal{R}$  of relative normal curvature can be defined as the surface for which the equality  $R_{\mathcal{R}} = R_{P1} - R_{P2}$  is observed. Evidently, this equality is similar in nature to the equality Eq. (4.36).

### 3.5.3 “Dupin Indicatrix” at a Point of Surface of Relative Normal Curvature

Consider an intersection of the surface of relative normal curvature by a plane, parallel to the tangent plane at the point  $K$ , but only at a small distance away from it. Then, project the intersection on the tangent plane. In the coordinate plane  $x_P y_P$ , principal part of the intersection will be given by the equation of “Dupin indicatrix”<sup>11</sup> [2]

$$\text{Dup}(\mathcal{R}) \Rightarrow \frac{L_{\mathcal{R}}}{E_{\mathcal{R}}}x_{\mathcal{R}}^2 + \frac{2M_{\mathcal{R}}}{\sqrt{E_{\mathcal{R}}G_{\mathcal{R}}}}x_{\mathcal{R}}y_{\mathcal{R}} + \frac{N_{\mathcal{R}}}{G_{\mathcal{R}}}y_{\mathcal{R}}^2 = \pm 1 \quad (3.48)$$

which describes the distribution of normal relative curvature within the differential vicinity of the point  $K$ .

Here,  $E_{\mathcal{R}}$ ,  $F_{\mathcal{R}}$ , and  $G_{\mathcal{R}}$  designate fundamental magnitudes of the first order, and  $L_{\mathcal{R}}$ ,  $M_{\mathcal{R}}$ , and  $N_{\mathcal{R}}$  designate fundamental magnitudes of the second order at the point  $K$  of the surface  $\mathcal{R}$ .

If the axes  $x_{\mathcal{R}}$  and  $y_{\mathcal{R}}$  of the local coordinate system  $x_{\mathcal{R}} y_{\mathcal{R}}$  align with the principal directions  $\mathbf{t}_{1,\mathcal{R}}$  and  $\mathbf{t}_{2,\mathcal{R}}$  of the surface of relative curvature  $\mathcal{R}$ , then Eq. (3.48) reduces to:

$$\text{Dup}(\mathcal{R}) \Rightarrow k_{1,\mathcal{R}}x_{\mathcal{R}}^2 + k_{2,\mathcal{R}}y_{\mathcal{R}}^2 = \pm 1 \quad (3.49)$$

<sup>10</sup>In a case of line contact of the surfaces  $P_1$  and  $P_2$ , point  $K$  is the point on the line of the surfaces' contact at which the normal curvatures  $k_{\mathcal{R}}$ ,  $k_{P1}$ , and  $k_{P2}$  are required to be calculated.

<sup>11</sup>To be more exact, the distribution of normal relative radii of curvature  $R_{\mathcal{R}}$ , and not of normal relative curvature  $k_{\mathcal{R}}$  itself, is reflected by the “Dupin indicatrix,  $\text{Dup}(\mathcal{R})$ ”. Thus, it could be designated as  $\text{Dup}_R(\mathcal{R})$ . However, the equation of the indicatrix  $\text{Dup}_k(\mathcal{R})$  of a surface normal curvature could also be composed.

Similarly, the corresponding equations for the normalized  $\text{Dup}_R(\mathcal{R})$  indicatrix of relative normal radius of curvature, and the indicatrix of normal curvature  $\text{Dup}_k(\mathcal{R})$  could also easily be derived.

An important intermediate conclusion follows immediately from Eq. (3.48):

**Conclusion 3.2** *The direction  $\mathbf{t}_{1,\mathcal{R}}$  for the maximum  $k_{1,\mathcal{R}}$ , and the direction  $\mathbf{t}_{2,\mathcal{R}}$  for the minimum  $k_{2,\mathcal{R}}$  values of normal curvature at a point of the surface of relative normal curvature  $\mathcal{R}$  are always orthogonal to one another; and, therefore, the condition  $\mathbf{t}_{1,\mathcal{R}} \perp \mathbf{t}_{2,\mathcal{R}}$  is always observed.*

The major axes of the “*Dupin indicatrix*,  $\text{Dup}(\mathcal{R})$ ” make the angles  $\varphi_{\min}$  and  $\varphi_{\max}$  with the principal directions  $\mathbf{t}_{1,\mathcal{R}}$  and  $\mathbf{t}_{2,\mathcal{R}}$ .

### 3.5.4 Matrix Representation of Equation of “*Dupin Indicatrix*” at a Point of Surface of Relative Normal Curvature

Like any other quadratic form, Eq. (3.48) of the “*Dupin indicatrix*” of the surface of normal relative curvature  $\mathcal{R}$  can be represented in matrix form

$$\text{Dup}(\mathcal{R}) \Rightarrow [x_P \ y_P \ 0 \ 0] \cdot \begin{bmatrix} \frac{L_{\mathcal{R}}}{E_{\mathcal{R}}} & \frac{2M_{\mathcal{R}}}{\sqrt{E_{\mathcal{R}}G_{\mathcal{R}}}} & 0 & 0 \\ \frac{2M_{\mathcal{R}}}{\sqrt{E_{\mathcal{R}}G_{\mathcal{R}}}} & \frac{N_{\mathcal{R}}}{G_{\mathcal{R}}} & 0 & 0 \\ 0 & 0 & \mp 1 & 0 \\ 0 & 0 & 0 & 1 \end{bmatrix} \cdot \begin{bmatrix} x_P \\ y_P \\ 0 \\ 0 \end{bmatrix} = \pm 1 \quad (3.50)$$

In “*Darboux trihedron*,” this equation reduces to:

$$\text{Dup}(\mathcal{R}) \Rightarrow [x_P \ y_P \ 0 \ 0] \cdot \begin{bmatrix} L_{\mathcal{R}} & M_{\mathcal{R}} & 0 & 0 \\ M_{\mathcal{R}} & N_{\mathcal{R}} & 0 & 0 \\ 0 & 0 & \mp 1 & 0 \\ 0 & 0 & 0 & 1 \end{bmatrix} \cdot \begin{bmatrix} x_P \\ y_P \\ 0 \\ 0 \end{bmatrix} = \pm 1 \quad (3.51)$$

It is convenient to implement matrix representation of the equation of the “*Dupin indicatrix*,  $\text{Dup}(\mathcal{R})$ ” (see above), for instance, when multiple coordinate system transformations need to be performed.

The equation of the “*Dupin indicatrix*,  $\text{Dup}(\mathcal{R})$ ” can be represented in the form:

$$r_{\text{Dup}}(\varphi) = \sqrt{|R_{\mathcal{R}}(\varphi)|} \cdot \text{sgn}\Phi_{2,\mathcal{R}}^{-1} \quad (3.52)$$

This last equation reveals that the position vector of a point of the indicatrix  $\text{Dup}(\mathcal{R})$  in any direction is equal to the square root of the radius of curvature in that same direction.<sup>12</sup>

<sup>12</sup>Similar to *Dupin indicatrix*  $\text{Dup}(\mathcal{R})$ , a planar characteristic curve of another kind can be introduced as well. The equation of this characteristic curve can be postulated in the form  $r_{\text{Dup},k}(\varphi) = \sqrt{|k_{\mathcal{R}}(\varphi)|} \cdot \text{sgn}\Phi_{2,\mathcal{R}}^{-1}$ . Application of curvature indicatrix in the form  $r_{\text{Dup},k}(\varphi)$  yields

### 3.5.5 Surface of Relative Normal Radii of Curvature

The normal curvature  $k_{\mathcal{R}}$  of the surface of normal relative curvature  $\mathcal{R}$ , the normal curvatures  $k_{P_1}$ , and  $k_{P_2}$  of the part surfaces  $P_1$  and  $P_2$  can be represented in the form:  $k_{\mathcal{R}} = R_{\mathcal{R}}^{-1}$ ,  $k_{P_1} = R_{P_1}^{-1}$ , and  $k_{P_2} = R_{P_2}^{-1}$  correspondingly, where  $R_{\mathcal{R}}$ ,  $R_{P_1}$ , and  $R_{P_2}$  are the corresponding radii of normal curvature of the surfaces  $\mathcal{R}$ ,  $P_1$ , and  $P_2$ . They are also taken in a common normal plane section through the point of contact  $K$  of these surfaces  $\mathcal{R}$ ,  $P_1$ , and  $P_2$ .

The radius of relative normal curvature is another widely known tool that is used in contemporary practice for the purposes of analytical description of the geometry of contact when performing second-order analysis. The radius  $R_{\mathcal{R}}$  of relative normal curvature can be defined by the expression:

$$R_{\mathcal{R}} = R_{P_1} - R_{P_2} \quad (3.53)$$

In many applications, Eq. (3.53) for the radius of relative normal of curvature  $R_{\mathcal{R}}$  is equivalent to Eq. (3.46) for the relative normal curvature  $k_{\mathcal{R}}$ .

### 3.5.6 Normalized Relative Normal Curvature

Usually, it is preferable to deal with unitless values when performing second-order analysis rather than with values having units. In order to eliminate unit values, it is recommended to use a normalized relative normal curvature  $\bar{k}_{\mathcal{R}}$  of the contacting surfaces  $P_1$  and  $P_2$ . The normalized relative normal curvature  $\bar{k}_{\mathcal{R}}$  of the surfaces  $P_1$  and  $P_2$  is referred to as the value determined by the equation

$$\bar{k}_{\mathcal{R}} = \frac{k_{P_1} + k_{P_2}}{|k_{1.P}|} \quad (3.54)$$

Similarly, the normalized radius of relative normal curvature  $\bar{R}_{\mathcal{R}}$  of the surfaces  $P_1$  and  $P_2$  can be introduced here based on Eq. (3.53). The normalized relative radius of normal curvature  $\bar{R}_{\mathcal{R}}$  of the surfaces  $P_1$  and  $P_2$  is referred to as the value determined by the equation:

$$\bar{R}_{\mathcal{R}} = \frac{R_{P_1} - R_{P_2}}{|R_{1.P1}|} \quad (3.55)$$

Implementation of the unitless parameters  $\bar{k}_{\mathcal{R}}$ ,  $\bar{R}_{\mathcal{R}}$ , as well as others makes it possible avoiding dealing with unit values. Equations comprised of unitless parameters are often more convenient in applications.

---

avoiding of uncertainty in cases of a plane. For a plane surface  $\text{Dup}(\mathcal{R})$  exists, while  $r_{\text{Dup},k}(\varphi)$  shrinks to the point  $K$ .

A corresponding “*Dupin indicatrix*” can be constructed for all of the above-considered characteristic surfaces. Namely for:

- (a) the surface of normal relative radii of curvature  $\text{Dup}_R(\mathcal{R})$ ,
- (b) the normalized surface of normal relative curvature  $\text{Dup}(\bar{\mathcal{R}})$ , and
- (c) the normalized surface of normal radii of relative curvature  $\text{Dup}_R(\bar{\mathcal{R}})$ .

### 3.5.7 Curvature Indicatrix of Surface of Relative Normal Curvature

The curvature indicatrix of the surface of relative normal curvature  $\mathcal{R}$  can be introduced similar to already done for a smooth regular part  $P$ . This planar characteristic curve is designated as  $\text{Crv}(\mathcal{R})$ . The curvature indicatrix  $\text{Crv}(\mathcal{R})$  can be implemented to make clear whether or not two smooth regular part surfaces  $P_1$  and  $P_2$  make physically feasible contact.

The curvature indicatrices  $\text{Crv}(\mathcal{R})$  those shown in Fig. 3.6 correspond to physically feasible kinds of contact of the part surfaces. Two part surfaces  $P_1$  and  $P_2$  can contact one another physically if the curvature indicatrix  $\text{Crv}(\mathcal{R})$  is either of convex elliptic type (Fig. 3.6a), or of convex umbilic type (Fig. 3.6b), or finally of convex parabolic type (Fig. 3.6c). Under such circumstances, the curvature indicatrix  $\text{Crv}(\mathcal{R})$  of the surface  $\mathcal{R}$  of relative normal curvature can be described analytically by the inequality:

$$\text{Crv}(\mathcal{R}) \Rightarrow \frac{L_{\mathcal{R}}}{E_{\mathcal{R}}} x_P^2 + \frac{2M_{\mathcal{R}}}{\sqrt{E_{\mathcal{R}}G_{\mathcal{R}}}} x_P y_P + \frac{N_{\mathcal{R}}}{G_{\mathcal{R}}} y_P^2 > 1 \quad (3.56)$$

In all of these cases, the mean curvature  $\mathcal{M}_{\mathcal{R}}$  of the surface  $\mathcal{R}$  of relative curvature is of a positive value ( $\mathcal{M}_{\mathcal{R}} > 0$ ).

In a particular case, the surface of relative normal curvature can be reduced either to a point or a line. These degenerated cases of the surface  $\mathcal{R}$  are illustrated schematically in Fig. 3.7a, b correspondingly.

In case contact of two smooth regular surfaces  $P_1$  and  $P_2$  is physically impossible, the curvature indicatrix  $\text{Crv}(\mathcal{R})$  of the surface of relative normal curvature  $\mathcal{R}$  is bounded by the corresponding “*Dupin indicatrix*  $\text{Dup}(\mathcal{R})$ ” position vector of a point of which has negative value [at least for one point for the characteristic curve  $\text{Dup}(\mathcal{R})$ ]. Curvature indicatrices  $\text{Crv}(\mathcal{R})$  for such cases are schematically illustrated in Fig. 3.8.

Curvature indicatrices  $\text{Crv}(\mathcal{R})$  of a surface of relative normal curvature  $\mathcal{R}$  are represented by three concave local patches of the surface  $\mathcal{R}$ , namely:

- (a) concave elliptic (Fig. 3.8a),
- (b) concave umbilic (Fig. 3.8b), and
- (c) concave parabolic (Fig. 3.8c)

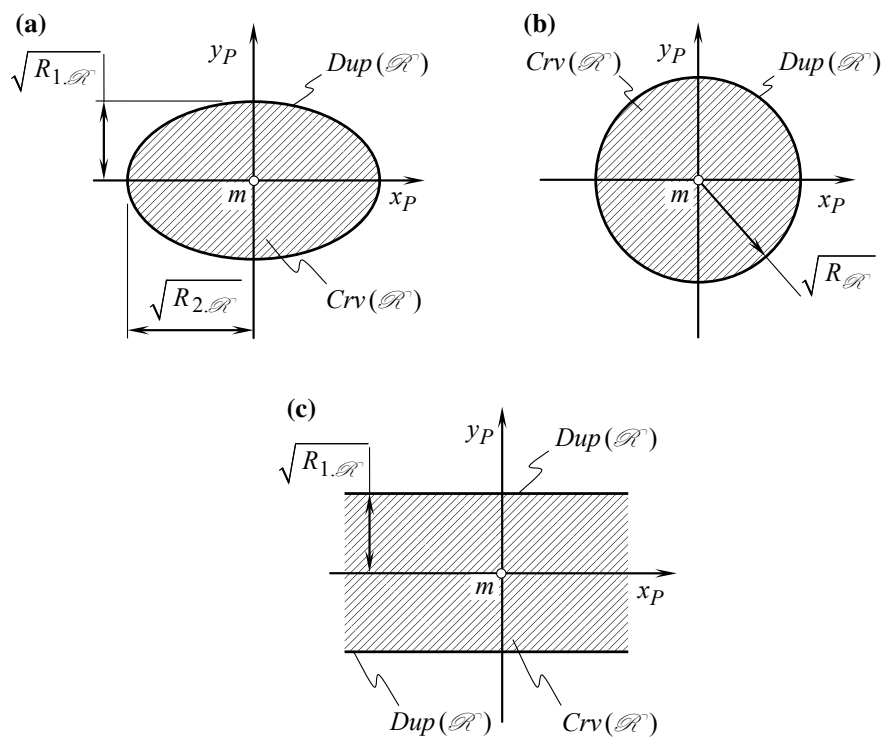


**Fig. 3.6** Three kinds of curvature indicatrices  $Crv(\mathcal{R})$  at a point  $m$  of a surface  $\mathcal{R}$  of relative normal curvature for the cases when physical contact of two smooth regular surfaces  $P_1$  and  $P_2$  is feasible

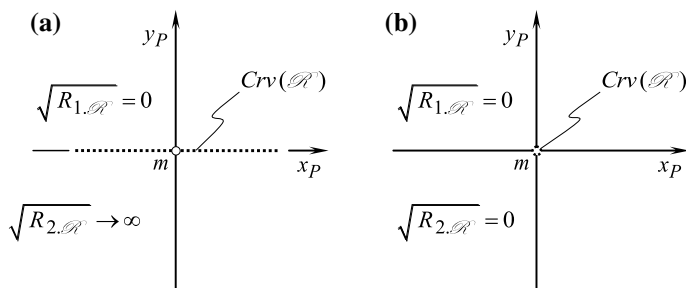


**Fig. 3.7** Two kinds of curvature indicatrices  $Crv(\mathcal{R})$  at a point  $m$  of a surface  $\mathcal{R}$  of relative normal curvature for the cases when physical contact of two smooth regular surfaces  $P_1$  and  $P_2$  is unidentified



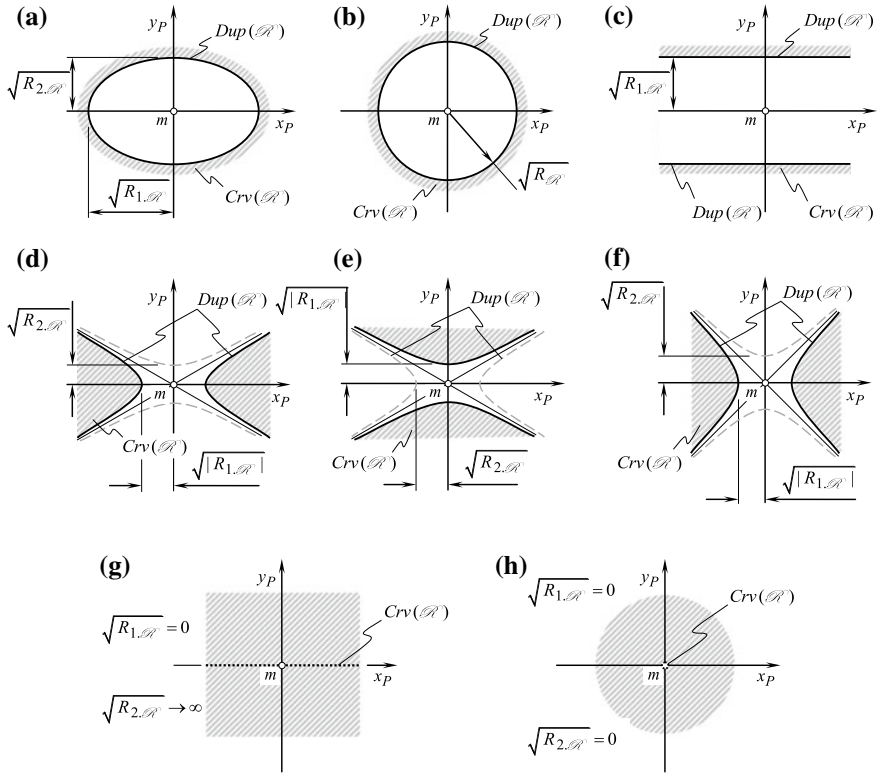


**Fig. 3.8** Curvature indicatrices  $\text{Crv}(\mathcal{R})$  at a point  $m$  of a surface  $\mathcal{R}$  of relative normal curvature for cases when physical contact of two smooth regular surfaces  $P_1$  and  $P_2$  is infeasible

local surface patches.

In addition to concave local patches, three saddle-like local patches of the surface of relative normal curvature  $\mathcal{R}$  are represented by three local patches having:

- (d) pseudo-convex (Fig. 3.8d),
- (e) minimal (Fig. 3.8e), and
- (f) pseudo-concave (Fig. 3.8f)

local surface patches.

Ultimately, two degenerate kinds of the curvature indicatrices  $\text{Crv}(\mathcal{R})$  of a surface of relative normal curvature  $\mathcal{R}$  are represented in Fig. 3.8g, h.

All the indicatrices  $\text{Crv}(\mathcal{R})$  in Fig. 3.8 fulfill the following inequality:

$$\text{Crv}(\mathcal{R}) \Rightarrow \frac{L_{\mathcal{R}}}{E_{\mathcal{R}}} x_P^2 + \frac{2M_{\mathcal{R}}}{\sqrt{E_{\mathcal{R}}G_{\mathcal{R}}}} x_P y_P + \frac{N_{\mathcal{R}}}{G_{\mathcal{R}}} y_P^2 < 1 \quad (3.57)$$

Again, the curvature indicatrices  $\text{Crv}(\mathcal{R})$  shown in Fig. 3.8 indicate that the surfaces  $P_1$  and  $P_2$  cannot contact one another physically.

### 3.6 A Characteristic Curve $\mathfrak{R}_K(\mathcal{R})$ of a Novel Kind

For the purpose of analytical description of the distribution of normal curvature in the differential vicinity of a point on a smooth regular surface, the following characteristic curve can be employed. This analysis is based on the results disclosed earlier in Chap. 2.

It is proven [see Eq. (2.37)] that for a part surface  $P_1$ , the first principal curvature,  $k_{P1}$ , can be calculated from the equation:

$$k_{P1} = \frac{L_{P1} + 2M_{P1}\eta_1 + N_{P1}\eta_1^2}{E_{P1} + 2F_{P1}\eta_1 + G_{P1}\eta_1^2} \quad (3.58)$$

A similar equation can be written for calculation of the first principal curvature,  $k_{P2}$ , of the contacting part surface  $P_2$ :

$$k_{P2} = \frac{L_{P2} + 2M_{P2}\eta_2 + N_{P2}\eta_2^2}{E_{P2} + 2F_{P2}\eta_2 + G_{P2}\eta_2^2} \quad (3.59)$$

It can be shown that  $\eta_1$  and  $\eta_2$  are always real.

The quantities  $\eta_1$  and  $\eta_2$  define directions that align with the principal directions on the surfaces  $P_1$  and  $P_2$ .

The distribution of normal curvature of the surface  $P_1$  (Fig. 2.19) at the contact point  $K$  is described by the characteristic curve  $k_{P1} = k_{P1}(\eta_1)$ . Another characteristic curve  $k_{P2} = k_{P2}(\eta)$  specifies the distribution of normal curvature of the generating surface  $P_2$  that makes contact with  $P_1$  at  $K$ . For the surfaces  $P_1$  and  $P_2$ , the surface of relative curvature  $\mathcal{R}$  can be constructed. The distribution of normal curvature of the surface  $\mathcal{R}$  at  $K$  is described by the characteristic curve  $k_{\mathcal{R}} = k_{\mathcal{R}}(\eta)$ .

The characteristic curve  $\mathfrak{R}_K(\mathcal{R})$  of this kind is defined here as:

$$\mathfrak{R}_K(\mathcal{R}) \Rightarrow k_{\mathfrak{R}} = k_{\mathcal{R}}(\eta) + k_{\mathcal{R}}(\eta + \mu) \quad (3.60)$$

Similarly, a characteristic curve  $\mathfrak{R}_R(\mathcal{R})$  of another sort is defined as:

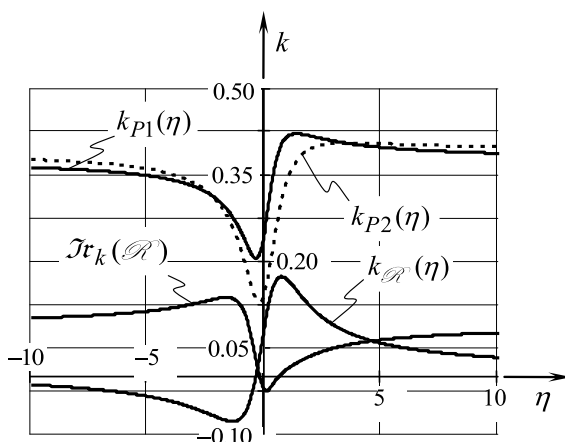
$$\mathfrak{R}_R(\mathcal{R}) \Rightarrow R_{\mathfrak{R}} = R_{\mathcal{R}}(\eta) - R_{\mathcal{R}}(\eta + \mu) \quad (3.61)$$

Examples of characteristic curves of both kinds are plotted in Fig. 3.9.

For orthogonally parameterized part surfaces  $P_1$  and  $P_2$ , Eqs. (3.60) and (3.61) can be expressed in simpler forms.

The methods developed for analytical description of the geometry of contact of two smooth regular surfaces in the first order of tangency are not limited to the methods disclosed above [4, 6, 10].

**Fig. 3.9** Derivation of equation of the characteristic curve  $\mathcal{I}r_k(\mathcal{R})$



The performed analysis of known methods of analytical description of the geometry of contact of two smooth regular surfaces has uncovered the poor capability of the methods for solving problems in the field of the optimal surface generation. Therefore, it is necessary to develop an accurate analytical method for analytical description of the geometry of contact of two smooth regular surfaces in first order of tangency that fits the nowadays needs of the engineering geometry of surfaces. Such a method has been worked out in Chap. 5.

## References

1. Lagrange, J. L. (1797). *Theorié des Fonctions Analytiques* (277p). Paris: Impr. De la République, prairial an V.
2. Cauchy, A. L. (1826). *Leçons sur les Applications du Calcul Infinitésimal à la Geometrie*. Paris: Imprimerie royale.
3. Favard, J. (1957). *Course de Gèométrie Diffèrentielle Locale* (viii + 553 p). Paris: Gauthier-Villars.
4. Radzevich, S.P. (1987). *Methods for investigation of the conditions of contact of surfaces, monograph* (103p). Kiev: UkrNIINTI, №759–Uk88.
5. Radzevich, S.P. (1991). *Differential-geometrical method of surface generation* (Doctoral thesis). Tula Polytechnic Institute, Tula (300p).
6. Radzevich, S. P. (2005). On analytical description of the geometry of contact of surfaces in highest kinematic pairs. *Theory for Mechanisms and Machines*, 3(5), 3–14.
7. Radzevich, S. P. (2008). *Kinematic Geometry of Surface Machining* (p. 536). Boca Raton, FL: CRC Press.
8. Radzevich, S. P. (2001). *Fundamentals of Surface Generation* (p. 592). Monograph: Kiev, Rastan.
9. Radzevich, S. P. (1991). *Sculptured surface machining on multi-axis NC machine* (p. 192). Monograph: Kiev, Vishcha Schola.
10. Radzevich, S. P. (2004). Mathematical modeling of contact of two surfaces in the first order of tangency. *Mathematical and Computer Modeling*, 39(9–10), 1083–1112.

# Chapter 4

## An Analytical Method Based on the Second Fundamental Forms of Contacting Part Surfaces



Known methods for analytical description of the contact geometry of two smooth regular part surface are applicable in degenerate cases of the surfaces contact, namely, either when the principal directions of one of the contacting surfaces align with the principal directions of the other or when the principal directions for one or both contacting surfaces are not identified (umbilics and/or planes).

In a more general case of contact of two smooth regular part surfaces, namely, either when the angle of the contacting surfaces' local relative orientation is not zero or when this angle differs from  $0.5\pi n$  (where  $n$  designates an integer number,  $n = 1, 2, 3, \dots$ ), known methods for analytical description of contact geometry of surfaces return approximate result.

Nowadays, engineering geometry of surfaces requires an accurate solution to the problem of analytical description of the contact geometry of two smooth regular part surfaces, which is valid for the most general cases of surface contact. A possible solution to the problem under consideration is discussed immediately below.

The second fundamental form at a point of a smooth regular surface was proposed by *Gauss* for analytical description of surface curvature at a point within a surface patch. Thus, it makes sense to begin the development of a method for analytical description of the contact geometry of two smooth regular part surfaces with an analysis of the second fundamental forms of both the surfaces at a point of their contact.

The second fundamental form  $\Phi_{2,P_1}$  at a point of a smooth regular part surface  $P_1$  is represented analytically by the expression [see Eq. (1.43)]:

$$\Phi_{2,P_1} \Rightarrow L_{P_1} dU_{P_1}^2 + 2M_{P_1} dU_{P_1} dV_{P_1} + N_{P_1} dV_{P_1}^2 \quad (4.1)$$

Here, we define:

- $L_{P_1}, M_{P_1}, N_{P_1}$  The fundamental magnitudes of the second order at a point of the part surface  $P_1$
- $U_{P_1}, V_{P_1}$  The *Gaussian* coordinate lines in the part surface  $P_1$ .

The geometrical interpretation of the second fundamental form  $\Phi_{2,P_1}$  at a point of a smooth regular part surface  $P_1$  is schematically depicted in Fig. 1.9. The deviation of the part surface  $P_1$  from the tangent plane in a specified direction is described analytically in terms of the fundamental form  $\Phi_{2,P_1}$ ; namely, the displacement is equal to  $\sqrt{\Phi_{2,P_1}}$ .

The above statement with regard to the part surface  $P_1$  is, of course, valid with regard to the second of two contacting part surface  $P_2$ . The second fundamental form  $\Phi_{2,P_2}$  of a point of the smooth regular part surface  $P_2$  is analytically represented by the expression:

$$\Phi_{2,P_2} \Rightarrow L_{P_2} dU_{P_2}^2 + 2M_{P_2} dU_{P_2} dV_{P_2} + N_{P_2} dV_{P_2}^2 \quad (4.2)$$

Here, we define:

$L_{P_2}, M_{P_2}, N_{P_2}$  The fundamental magnitudes of the second order of the part surface  $P_2$

$U_{P_2}, V_{P_2}$  The *Gaussian* coordinate lines in the part surface  $P_2$

With that said, consider two smooth regular part surfaces  $P_1$  and  $P_2$ , which contact each other at a point  $K$  (Fig. 4.1).

For the contacting part surfaces  $P_1$  and  $P_2$ , the second fundamental forms  $\Phi_{2,P_1}$  and  $\Phi_{2,P_2}$  are specified by Eq. (4.1) and Eq. (4.2). The common tangent plane is a

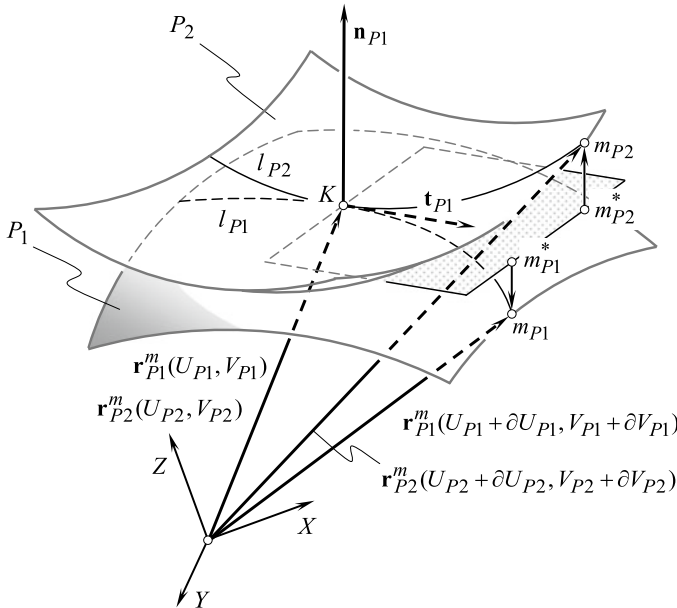


**Fig. 4.1** Definition of degree of conformity of two smooth regular part surfaces  $P_1$  and  $P_2$  at a point  $K$  of their contact

plane through the contact point  $K$ . In a direction within the tangent plane specified by unit tangent vector  $\mathbf{t}_{P1}$ , a line  $l_{P1}$  passes within the part surface  $P_1$ . A point  $m_{P1}$  within the curve  $l_{P1}$  deviates from the tangent plane at a distance  $m_{P1}m_{P1}^*$ . The deviation  $m_{P1}m_{P1}^*$  can be calculated from the formula:

$$m_{P1}m_{P1}^* = \sqrt{|\Phi_{2,P1}|} \operatorname{sgn} \Phi_{2,P1} \quad (4.3)$$

Owing to the torsion of the curve  $l_{P1}$ , the point  $m_{P1}^*$  within the common tangent plane is located aside of the straight line along the unit vector  $\mathbf{t}_{P1}$ . However, as the point  $m_{P1}$  approaches the contact point  $K$ , the displacement of the point  $m_{P1}^*$  from the straight line approaches zero [1]. Therefore, the torsion of the curve  $l_{P1}$  can be ignored.

Similarly, in the same direction specified by the unit tangent vector  $\mathbf{t}_{P1}$  (actually, this direction is specified by the unit tangent vector  $\mathbf{t}_{P2} \equiv \mathbf{t}_{P1}$ ), a line  $l_{P2}$  passes within the part surface  $P_2$ . A point  $m_{P2}$  within the curve  $l_{P2}$  deviates from the tangent plane at a distance  $m_{P2}m_{P2}^*$ . The deviation  $m_{P2}m_{P2}^*$  can be calculated from the formula:

$$m_{P2}m_{P2}^* = \sqrt{|\Phi_{2,P2}|} \operatorname{sgn} \Phi_{2,P2} \quad (4.4)$$

Owing to the torsion of the curve  $l_{P2}$ , the point  $m_{P2}^*$  within the common tangent plane is located aside of the straight line along the unit vector  $\mathbf{t}_{P1}$ . However, as the point  $m_{P2}$  approaches the contact point  $K$ , the displacement of the point  $m_{P2}^*$  from the straight line approaches zero [1]. Similar to the curve  $l_{P1}$ , the torsion of the curve  $l_{P2}$  can be ignored as well.

The deviation  $m_{P1}m_{P1}^*$  of the part surface  $P_1$  from the tangent plane together with the deviation  $m_{P2}m_{P2}^*$  of the part surface  $P_2$  from the tangent plane can be employed to quantify the deviation of the surfaces  $P_1$  and  $P_2$  from one another in a direction specified by the unit tangent vector  $\mathbf{t}_{P1}$ .

Refer to Fig. 4.2. Here, the section of the contacting part surfaces  $P_1$  and  $P_2$  by a

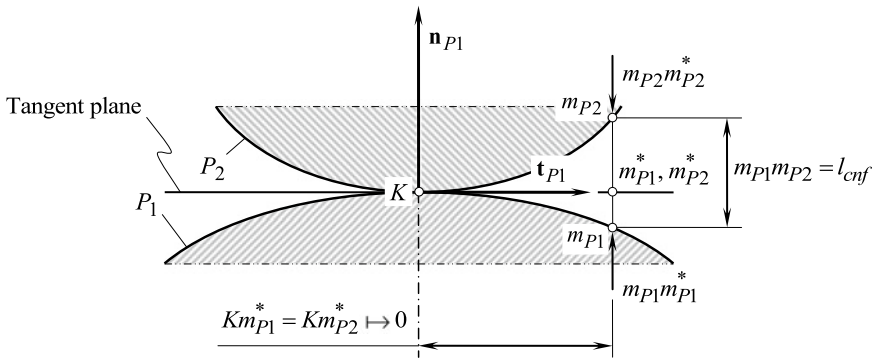


**Fig. 4.2** Specification of the deviation  $l_{cnf}$  in terms of the second fundamental forms  $\Phi_{2,P1}$  and  $\Phi_{2,P2}$  of the contacting part surfaces  $P_1$  and  $P_2$ , accordingly

plane through the unit vector of the common perpendicular  $\mathbf{n}_{P1}$  is shown schematically. Torsion of the lines  $l_{P1}$  and  $l_{P2}$  is ignored here as when the points  $m_{P1}$  and  $m_{P2}$  approach the contact point  $K$ , the corresponding projections  $m_{P1}^*$  and  $m_{P2}^*$  of these points onto the tangent plane approach the straight line along the unit tangent vector  $\mathbf{t}_{P1}$ .

Having calculated the distances  $m_{P1}m_{P1}^*$  [see Eq. (4.3)] and  $m_{P2}m_{P2}^*$  [see Eq. (4.4)], the distance  $l_{\text{cnf}} = m_{P1}m_{P2}$  between the contacting smooth regular part surfaces  $P_1$  and  $P_2$  can be expressed in terms of the second fundamental forms  $\Phi_{2,P1}$  and  $\Phi_{2,P2}$ , namely [1]:

$$l_{\text{cnf}} = \sqrt{|\Phi_{2,P1}|} \text{sgn } \Phi_{2,P1} + \sqrt{|\Phi_{2,P2}|} \text{sgn } \Phi_{2,P2} \quad (4.5)$$

For this purpose, both the fundamental forms,  $\Phi_{2,P1}$  and  $\Phi_{2,P2}$ , need to be represented in a common reference system.

The resultant deviation  $l_{\text{cnf}}$  can be employed as a quantitative measure of the deviation of two smooth regular part surfaces  $P_1$  and  $P_2$  from one another. It could be anticipated that the criterion of conformity  $l_{\text{cnf}}$  is the best possible criterion for evaluation of the degree of conformity of two smooth regular part surfaces in contact.

In order to implement the resultant deviation  $l_{\text{cnf}}$  in practice:

- (a) both fundamental forms,  $\Phi_{2,P1}$  and  $\Phi_{2,P2}$ , should be represented in a common reference system, and
- (b) both fundamental forms,  $\Phi_{2,P1}$  and  $\Phi_{2,P2}$ , should be expressed in that same  $U$ - and  $V$ -parameters.

For a second fundamental form  $\Phi_{2,P1}$  specified in the original reference system that is associated with the part surface  $P_1$ , a corresponding expression  $\Phi_{2,P1}^*$  in another reference system (which is common to the contacting surfaces  $P_1$  and  $P_2$ ) can be expressed as (see Appendix B):

$$[\Phi_{2,P1}^*] = \mathbf{Rs}^T(P_1 \rightarrow C) \cdot [\Phi_{2,P1}] \cdot \mathbf{Rs}(P_1 \rightarrow C) \quad (4.6)$$

The operator of the resultant coordinate system transformation, namely of the transformation from the original reference system associated with the part surface  $P_1$  to the common reference system (the reference system  $C$ ) in Eq. (4.6), is designated as  $\mathbf{Rs}(P_1 \rightarrow C)$ .

An expression similar to Eq. (4.6) is valid with respect to the second fundamental form  $\Phi_{2,P2}$  of the part surface  $P_2$  [1]:

$$[\Phi_{2,P2}^*] = \mathbf{Rs}^T(P_2 \rightarrow C) \cdot [\Phi_{2,P2}] \cdot \mathbf{Rs}(P_2 \rightarrow C) \quad (4.7)$$

Here, the operator of the resultant coordinate system transformation, namely of the transformation from the original reference system associated with the part surface  $P_2$  to the common reference system (the reference system  $C$ ), is designated as  $\mathbf{Rs}(P_2 \rightarrow C)$ .

Refer to Appendix C for details on change in surfaces parameters in order to express equations for both of the contacting surfaces  $P_1$  and  $P_2$  in terms of the same  $U$ - and  $V$ -parameters.

The discussed measure  $l_{\text{cnf}}$  of degree of conformity of two smooth regular part surfaces  $P_1$  and  $P_2$  in the first order of tangency is legitimate, but it is computationally inefficient. For practical applications, another quantitative measure of degree of conformity of two smooth regular part surfaces  $P_1$  and  $P_2$ , which make contact at a point  $K$ , needs to be developed [1].

## Reference

1. Radzevich, S. P. (1991). *Differential-geometrical method of surface generation*. (Doctoral thesis) (300p). Tula: Tula Polytechnic Institute.



## Chapter 5

# Indicatrix of Conformity at Point of Contact of Two Smooth Regular Part Surfaces in the First Order of Tangency



The accuracy of the earlier developed methods of the second-order analysis such as those discussed in Chap. 3 is often insufficient for the accurate analytical description of the contact geometry of two smooth regular part surfaces in the first order of tangency. In order to increase the accuracy of the analytical description of the contact geometry, higher-order analysis needs to be carried out.

The methods of higher-order analysis discussed below have been developed with the intent attaining an accurate analytical description of the degree of conformity of two smooth regular part surfaces  $P_1$  and  $P_2$  at a current point  $K$  of their contact. The higher the degree of conformity of the part surfaces  $P_1$  and  $P_2$ , the closer these surfaces to one another in the differential vicinity of the contact point  $K$ , and vice versa. This qualitative (or “*intuitive*,” in other words) definition of the degree of conformity at a point of contact of two smooth regular part surfaces in the first order of tangency needs in a corresponding quantitative measure.

### 5.1 Preliminary Remarks

The implementation of the total deviation  $l_{\text{cnf}}$  of two smooth regular part surfaces in contact form one another (see Chap. 4 for details) for the analytical description of the contact geometry of two part surfaces is a straightforward solution to the problem under consideration. This approach is proven to be computationally ineffective. However, the approach gives an insight into how an effective method for solving the problem under consideration can be developed.

As seen in Fig. 5.1, three geometrical parameters are interrelated. They are:

- (a) the measure of deviation of a part surface  $P$  from the tangent plane,  $l_{\text{cnf}}$ ,
- (b) the distance of a current point  $m_P$  from the contact point  $K$ , and
- (c) the radius of normal curvature  $R_P$  of the surface  $P$ .

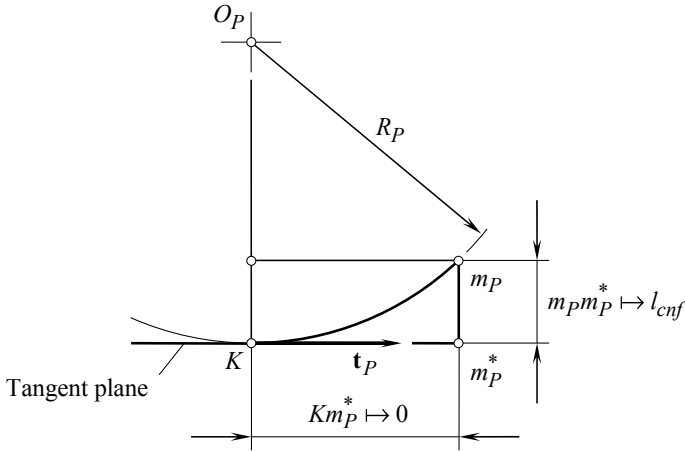


**Fig. 5.1** Transition from the resultant deviation,  $l_{\text{cnf}}$ , of two surfaces from one another to the indicatrix of conformity Cnf ( $P_1/P_2$ ) at a point of contact  $K$  of two smooth regular part surfaces  $P_1$  and  $P_2$  in the first order of tangency

As a consequence from this relationship among the parameters  $m_P m_P^*$ ,  $K m_P^*$ , and  $R_P$ , any of them can be used for quantitative evaluation of the degree of conformity of the contacting part surfaces  $P_1$  and  $P_2$ . As follows from Fig. 5.1:

$$m_P m_P^* = R_P - \sqrt{R_P^2 - (K m_P^*)^2} \Big|_{m_P \rightarrow K} \mapsto l_{\text{cnf}} \quad (5.1)$$

Inversely, for the radius of normal curvature  $R_P$  of the part surface  $P$ , the following expression is valid:

$$R_P = \frac{(m_P m_P^*)^2 + (K m_P^*)^2}{2 \cdot m_P m_P^*} \quad (5.2)$$

Ultimately, one may conclude that any legitimate analytical function of normal radii of curvature  $R_{P1}$  and  $R_{P2}$  of the part surfaces  $P_1$  and  $P_2$  in contact can be used for this particular purpose.

Consider two smooth regular part surfaces  $P_1$  and  $P_2$  in the first order of tangency that make contact at a point  $K$ . The degree of conformity of the part surfaces  $P_1$  and  $P_2$  can be construed as a function of the radii of normal curvature  $R_{P1}$  and  $R_{P2}$  of the surfaces. The radii of normal curvature  $R_{P1}$  and  $R_{P2}$  are taken in a common normal plane section through the contact point  $K$ . For a specified value of the radius of normal curvature  $R_{P1}$  of the surface  $P_1$ , the degree of conformity of the surfaces depends upon the corresponding value of the radius of normal curvature  $R_{P2}$  of the part surface  $P_2$ .

In most practical cases, the degree of conformity of the part surfaces  $P_1$  and  $P_2$  is not constant of a constant value, that is, the actual value of the degree of conformity: (a) depends on the orientation of the normal plane section through the point  $K$  and (b) alters as the normal plane section spins about the common perpendicular  $\mathbf{n}_{P1}$  to the contacting part surfaces. This statement immediately follows from the above conclusion that the degree of conformity at point of contact of the part surfaces  $P_1$  and  $P_2$  yields interpretation in terms of the radii of normal curvature  $R_{P1}$  and  $R_{P2}$ .

Figure 5.2 illustrates the change of degree of conformity at a point of contact of the part surfaces  $P_1$  and  $P_2$  to one another as the normal plane section spins about the common perpendicular  $\mathbf{n}_{P1}$ . Here, in Fig. 5.2, just two-dimensional examples are shown. In this example, that same normal plane section of the part surface  $P_1$  makes contact with different plane sections  $P_2^{(i)}$  of the part surface  $P_2$ .

In the example shown in Fig. 5.2a, the radius of normal curvature  $R_{P2}^{(1)}$  of the convex plane section  $P_2^{(1)}$  of the part surface  $P_2$  is of a positive value [ $R_{P2}^{(1)} > 0$ ]. The convex normal plane section of the part surface  $P_2$  makes contact with convex normal plane section ( $R_{P1} > 0$ ) of the part surface  $P_1$ . The degree of conformity of the part surface  $P_2$  to the part surface  $P_1$  at  $K$  in Fig. 5.2a is relatively low.

Another example is shown in Fig. 5.2b. The radius of normal curvature  $R_{P2}^{(2)}$  of the convex plane section  $P_2^{(2)}$  of the part surface  $P_2$  also is of a positive value [ $R_{P2}^{(2)} > 0$ ]. However, this value exceeds the value  $R_{P2}^{(1)}$  of the radius of normal curvature in the

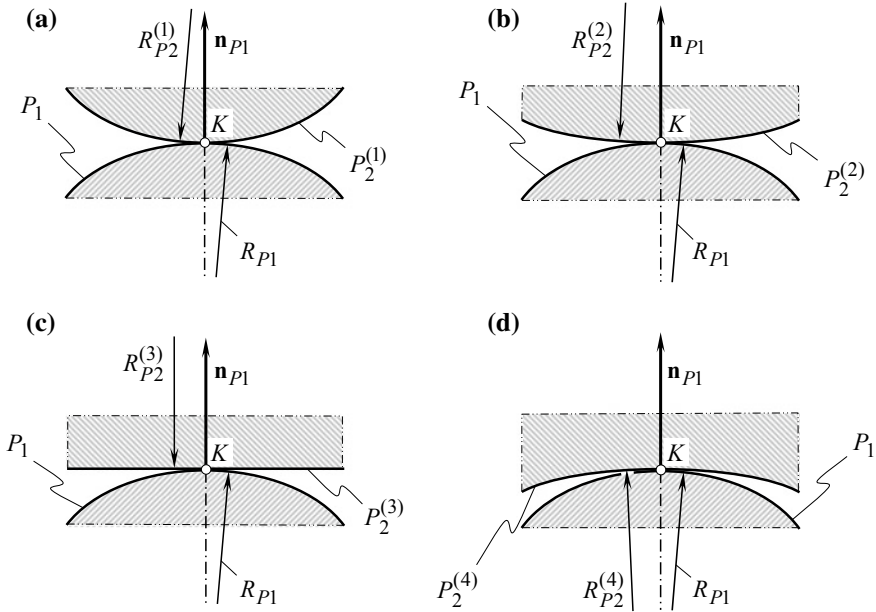


**Fig. 5.2** Sections of two smooth regular part surfaces  $P_1$  and  $P_2$  in contact by a plane through the common perpendicular  $\mathbf{n}_{P1}$

first example [i.e.,  $R_{P_2}^{(2)} > R_{P_2}^{(1)}$ ]. This results in that the degree of conformity of the part surface  $P_2$  to the surface part  $P_1$  at  $K$  (Fig. 5.2a) is greater compared to that shown in Fig. 5.2b.

In the next example (see Fig. 5.2c), the normal plane section  $R_{P_2}^{(3)}$  of the part surface  $P_2$  is represented with locally flattened section. The radius of normal curvature  $R_{P_2}^{(3)}$  of the flattened plane section  $P_2^{(3)}$  of the part surface  $P_2$  approaches infinity [ $R_{P_2}^{(3)} \rightarrow \infty$ ]. Thus, the inequality  $R_{P_2}^{(3)} > R_{P_2}^{(2)} > R_{P_2}^{(1)}$  holds. Therefore, the degree of conformity of the part surface  $P_2$  to the part surface  $P_1$  at  $K$  in Fig. 5.2c is also greater.

Finally, for a concave normal plane section  $P_2^{(4)}$  of the part surface  $P_2$  (see Fig. 5.2d), the radius of normal curvature  $R_{P_2}^{(4)}$  is of a negative value [ $R_{P_2}^{(4)} < 0$ ]. The degree of conformity of the part surface  $P_2$  to the part surface  $P_1$  at  $K$  is of the greatest value in all four examples considered in Fig. 5.2.

The examples shown in Fig. 5.2 illustrate qualitatively what we feel intuitively regarding the different degrees of conformity of two smooth regular part surfaces in the first order of tangency. Intuitively, one can realize that in the examples shown in Fig. 5.2a through Fig. 5.2d, the degree of conformity of two part surfaces  $P_1$  and  $P_2$  is rising from the case depicted in Fig. 5.2a to the case illustrated in Fig. 5.2d, and vice versa.

A similar is observed for a given pair of the contacting part surfaces  $P_1$  and  $P_2$  when different sections of the surfaces by a plane surface through the common perpendicular  $\mathbf{n}_{P_1}$  are considering (Fig. 5.3a). While rotating the plane section about the common perpendicular,  $\mathbf{n}_{P_1}$  one can observe that the degree of conformity of the part surfaces  $P_1$  and  $P_2$  is different in different directions (Fig. 5.3b).

The examples discussed above give an intuitive understanding of what the degree of conformity of two smooth regular part surfaces  $P_1$  and  $P_2$  in the first order of tangency stands for. They cannot be employed directly for a quantitative evaluation

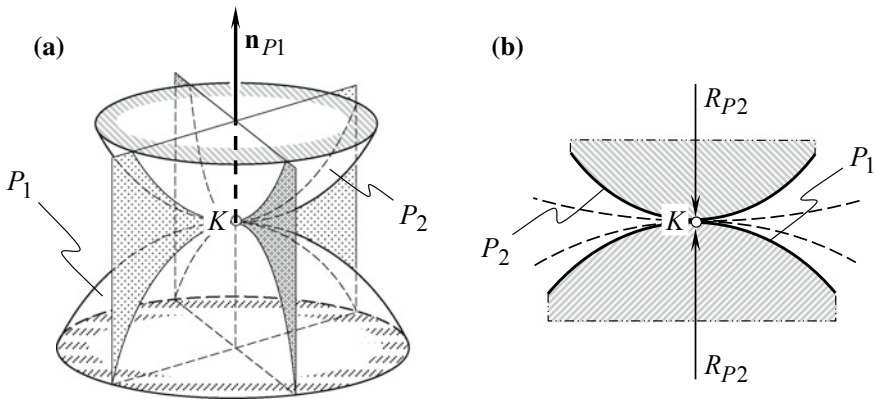


**Fig. 5.3** Analytical description of the contact geometry of two smooth regular part surfaces  $P_1$  and  $P_2$

of the degree of conformity of the surfaces  $P_1$  and  $P_2$ . The next step required is to introduce an appropriate quantitative evaluation of the degree of conformity of two smooth regular surfaces in the first order of tangency. In other words, it is necessary to make clear how a certain degree of conformity of two smooth regular surfaces can be described analytically.

## 5.2 “Indicatrix of Conformity” at Point of Contact of Two Smooth Regular Part Surfaces in the First Order of Tangency

This section aims to introduce a quantitative measure of the degree of conformity at a point of contact of two smooth regular part surfaces in the first order of tangency. The degree of conformity of two part surfaces  $P_1$  and  $P_2$  indicates how the part surface  $P_2$  is close to the part surface  $P_1$  in the differential vicinity of the point  $K$  of their contact; say how much the surface  $P_2$  is locally “congruent” to the surface  $P_1$  (i.e., in the differential vicinity of the point  $K$ ).

Quantitatively, the degree of conformity of a part surface  $P_2$  to another part surface  $P_1$  can be expressed in terms of the difference between the corresponding radii of normal curvature of the part surfaces. In order to develop a quantitative measure of the degree of conformity of the part surfaces  $P_1$  and  $P_2$ , it is convenient to implement the “Dupin indicatrices”  $\text{Dup}(P_1)$  and  $\text{Dup}(P_2)$  constructed at a point of contact of the surfaces  $P_1$  and  $P_2$ , respectively.

It is naturally to assume here that the larger the degree of conformity of the part surfaces  $P_1$  and  $P_2$ , the smaller the difference between the normal curvatures  $R_{P_1}$  and  $R_{P_2}$  of the surfaces  $P_1$  and  $P_2$  in a common section by a plane through the common unit normal vector  $\mathbf{n}_{P_1}$ .

The “Dupin indicatrix,  $\text{Dup}(P_1)$ ” indicates the distribution of radii of normal curvature  $R_{P_1}$  at a point of the part surface  $P_1$  as has been shown, for example, for a concave elliptic local patch of the part surface  $P_1$  (Fig. 5.4). For a surface  $P_1$ , the equation of this characteristic curve in polar coordinates can be represented in the form:

$$\text{Dup}(P_1) \Rightarrow r_{P_1}(\varphi_{P_1}) = \sqrt{|R_{P_1}(\varphi_{P_1})|} \quad (5.3)$$

where

$r_{P_1}$  is the position vector of a point of the “Dupin indicatrix,  $\text{Dup}(P_1)$ ” of the part surface  $P_1$

$\varphi_{P_1}$  is the polar angle of the “Dupin indicatrix,  $\text{Dup}(P_1)$ .”

Similarly, for the “Dupin indicatrix,  $\text{Dup}(P_2)$ ” at point of the part surface  $P_2$ , position vector of point can be constructed as has been shown, for instance, for a convex elliptical local patch of the part surface  $P_2$  (Fig. 5.4). The equation of this

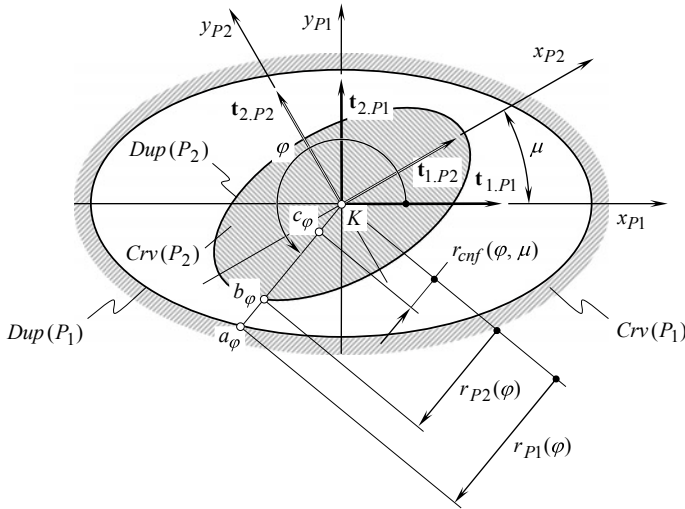


**Fig. 5.4** Derivation of equation of the indicatrix of conformity  $Cnf_R(P_1/P_2)$  at a point of contact of two smooth regular part surfaces  $P_1$  and  $P_2$  in the first order of tangency

characteristic curve in polar coordinates can be represented in the form:

$$\text{Dup}(P_2) \Rightarrow r_{P2}(\varphi_{P2}) = \sqrt{|R_{P2}(\varphi_{P2})|} \quad (5.4)$$

where

$r_{P2}$  is the position vector of a point of the “Dupin indicatrix,  $\text{Dup}(P_2)$ ” of the part surface  $P_2$

$\varphi_{P2}$  is the polar angle of the “Dupin indicatrix,  $\text{Dup}(P_2)$ .”

In the coordinate plane  $x_{P1}y_{P1}$  of the local coordinate system  $x_{P1}y_{P1}z_{P1}$ , the equalities  $\varphi_{P1} = \varphi$  and  $\varphi_{P2} = \varphi + \mu$  hold. Therefore, in the coordinate plane  $x_{P1}y_{P1}$ , Eq. (5.3) be casts into:

$$\text{Dup}(P_1) \Rightarrow r_{P1}(\varphi) = \sqrt{|R_{P1}(\varphi)|} \quad (5.5)$$

An equation similar to that above Eq. (5.5) is valid with respect to the other contacting surface  $P_2$ :

$$\text{Dup}(P_2) \Rightarrow r_{P2}(\varphi, \mu) = \sqrt{|R_{P2}(\varphi, \mu)|} \quad (5.6)$$

When the degree of conformity of the part surface  $P_2$  to the part surface  $P_1$  is greater, then the difference between the functions  $r_{P1}(\varphi)$  and  $r_{P2}(\varphi, \mu)$  is smaller. The latter makes valid the conclusion:

**Conclusion 5.1** The distance between the corresponding<sup>1</sup> points of the “Dupin indicatrices”  $\text{Dup}(P_1)$  and  $\text{Dup}(P_2)$  at a point of contact of the part surfaces  $P_1$  and  $P_2$  can be employed for an indication of the degree of conformity of the part surfaces  $P_1$  and  $P_2$  at that point  $K$  in the specified direction.

The equation of “indicatrix of conformity  $\text{Cnf}_R(P_1/R_2)$ ” at a point of contact of two part surfaces  $P_1$  and  $P_2$  is postulated to have the following structure:

$$\begin{aligned} \text{Cnf}_R(P_1/P_2) \Rightarrow r_{\text{cnf}}(\varphi, \mu) &= \sqrt{|R_{P1}(\varphi)|} \text{sgn} R_{P1}(\varphi) + \sqrt{|R_{P2}(\varphi, \mu)|} \text{sgn} R_{P2}(\varphi, \mu) \\ &= r_{P1}(\varphi) \text{sgn} R_{P1}(\varphi) + r_{P2}(\varphi, \mu) \text{sgn} R_{P2}(\varphi, \mu) \quad (5.7) \end{aligned}$$

Because of location of the point  $a_\varphi$  of the “Dupin indicatrix,  $\text{Dup}(P_1)$ ” of the part surface  $P_1$  is specified by position vector  $r_{P1}(\varphi)$ , and the location of the point  $b_\varphi$  of the “Dupin indicatrix,  $\text{Dup}(P_2)$ ” of the part surface  $P_2$  is specified by position vector  $r_{P2}(\varphi, \mu)$ , the location of a corresponding point  $c_\varphi$  (see Fig. 5.4) of the “indicatrix of conformity  $\text{Cnf}_R(P_1/R_2)$ ” at a point of contact of two part surfaces  $P_1$  and  $P_2$  is specified by position vector  $r_{\text{cnf}}(\varphi, \mu)$ . Therefore, the equality  $r_{\text{cnf}}(\varphi, \mu) = K c_\varphi$  holds, and the length of the straight line segment  $K c_\varphi$  is equal to the distance  $a_\varphi b_\varphi$ .

Here, we define:

$r_{P1} = \sqrt{|R_{P1}|}$  is the linear coordinate of a point of the “Dupin indicatrix” of the part surface  $P_1$   
 $r_{P2} = \sqrt{|R_{P2}|}$  is the linear coordinate of a corresponding point of the “Dupin indicatrix” of the part surface  $P_2$ .

Here, the multipliers  $\text{sgn} R_{P1}(\varphi)$  and  $\text{sgn} R_{P2}(\varphi, \mu)$  are assigned to each of the functions  $r_{P1}(\varphi) = \sqrt{|R_{P1}(\varphi)|}$  and  $r_{P2}(\varphi, \mu) = \sqrt{|R_{P2}(\varphi, \mu)|}$  just for the purpose of maintaining the corresponding sign of the functions, that is, that same sign that the radii of normal curvature  $R_{P1}(\varphi)$  and  $R_{P2}(\varphi, \mu)$  have.

Ultimately, one can come up with the conclusion that position vector  $r_{\text{cnf}}$  of a point of the “indicatrix of conformity  $\text{Cnf}_R(P_1/R_2)$ ” can be expressed in terms of the position vectors  $r_{P1}$  and  $r_{P2}$  of the “Dupin indicatrices”  $\text{Dup}(P_1)$  and  $\text{Dup}(P_2)$  of the contacting part surfaces  $P_1$  and  $P_2$ .

For the calculation of the value of the current radius of normal curvature  $R_{P1}(\varphi)$ , the equality:

$$R_{P1}(\varphi) = \frac{\Phi_{1.P1}}{\Phi_{2.P1}} \quad (5.8)$$

can be used.

Similarly, for the calculation of the value of the current radius of normal curvature  $R_{P2}(\varphi, \mu)$ , the equality:

<sup>1</sup> Corresponding points of the “Dupin indicatrices”  $\text{Dup}(P_1)$  and  $\text{Dup}(P_2)$  share the same straight line through the contact point  $K$  of the surfaces  $P_1$  and  $P_2$  and are located at the same side of the point  $K$ .

$$R_{P2}(\varphi, \mu) = \frac{\Phi_{1.P2}}{\Phi_{2.P2}} \quad (5.9)$$

can be employed.

Use of the angle  $\mu$  of the part surfaces'  $P_1$  and  $P_2$  local relative orientation indicates that the radii of normal curvature  $R_{P1}(\varphi)$  and  $R_{P2}(\varphi, \mu)$  are taken in a common normal plane section through the contact point  $K$ .

Further, it is well known that the inequalities  $\Phi_{1.P1} \geq 0$  and  $\Phi_{1.P2} \geq 0$  are always valid. Therefore, Eq. (5.7) can be rewritten in the form:

$$r_{\text{cnf}} = r_{P1}(\varphi) \text{sgn} \Phi_{2.P1}^{-1} + r_{P2}(\varphi, \mu) \text{sgn} \Phi_{2.P2}^{-1} \quad (5.10)$$

For the derivation of the equation of the “*indicatrix of conformity*,  $\text{Cnf}_R(P_1/R_2)$ ,” it is convenient to use “*Euler equation*” for the radius of normal curvature  $R_{P1}(\varphi)$  at a point of a part surface  $P_1$  [see Eq. (1.78)]:

$$R_{P1}(\varphi) = \frac{R_{1.P1} \cdot R_{2.P1}}{R_{1.P1} \cdot \sin^2 \varphi + R_{2.P1} \cdot \cos^2 \varphi} \quad (5.11)$$

Here, the radii of principal curvature  $R_{1.P1}$  and  $R_{2.P1}$  are the roots of the quadratic equation:

$$\begin{vmatrix} L_{P1} \cdot R_{P1} - E_{P1} & M_{P1} \cdot R_{P1} - F_{P1} \\ M_{P1} \cdot R_{P1} - F_{P1} & N_{P1} \cdot R_{P1} - G_{P1} \end{vmatrix} = 0 \quad (5.12)$$

Recall that the inequality  $R_{1.P1} < R_{2.P1}$  is always observed.

Equations (5.11) and (5.12) allow for an expression of the radius of normal curvature  $R_{P1}(\varphi)$  of the part surface  $P_1$  in terms of the fundamental magnitudes of the first order  $E_{P1}$ ,  $F_{P1}$ , and  $G_{P1}$ , and of the fundamental magnitudes of the second order  $L_{P1}$ ,  $M_{P1}$ , and  $N_{P1}$ .

A similar consideration is applicable with respect to the part surface  $P_2$ . Omitting routing analysis, one can reach the conclusion that the radius of normal curvature  $R_{P2}(\varphi, \mu)$  of the part surface  $P_2$  can be expressed in terms of the fundamental magnitudes of the first order  $E_{P2}$ ,  $F_{P2}$ , and  $G_{P2}$ , and of the fundamental magnitudes of the second order  $L_{P2}$ ,  $M_{P2}$ , and  $N_{P2}$ .

Finally, on the premise of the above-performed analysis, the following expression:

$$\begin{aligned} r_{\text{cnf}}(\varphi, \mu) = & \sqrt{\left| \frac{E_{P1}G_{P1}}{L_{P1}G_{P1}\cos^2\varphi - M_{P1}\sqrt{E_{P1}G_{P1}}\sin 2\varphi + N_{P1}E_{P1}\sin^2\varphi} \right|} \text{sgn} \Phi_{2.P1}^{-1} \\ & + \sqrt{\left| \frac{E_{P2}G_{P2}}{L_{P2}G_{P2}\cos^2(\varphi + \mu) - M_{P2}\sqrt{E_{P2}G_{P2}}\sin 2(\varphi + \mu) + N_{P2}E_{P2}\sin^2(\varphi + \mu)} \right|} \text{sgn} \Phi_{2.P2}^{-1} \end{aligned} \quad (5.13)$$

for the radial coordinate of a point of the “*indicatrix of conformity*,  $\text{Cnf}_R(P_1/P_2)$ ” at a point of contact of two part surfaces  $P_1$  and  $P_2$  can be derived.



For the first time ever, Eq. (5.13) of the characteristic curve<sup>2</sup>  $\text{Cnf}_R(P_1/P_2)$  is published in [1] and (in a hidden form) in [2].

The performed analysis of Eq. (5.13) reveals that the “*indicatrix of conformity*,  $\text{Cnf}_R(P_1/P_2)$ ” at the point of contact  $K$  of the part surfaces  $P_1$  and  $P_2$  is represented by a planar centro-symmetrical curve of the fourth order. In a particular case, this characteristic curve also possesses a property of mirror symmetry. Mirror symmetry of the indicatrix of conformity is observed, for example, when the angle  $\mu$  of the part surfaces’  $P_1$  and  $P_2$  local relative orientation is equal:

$$\mu = \pm \frac{\pi \cdot n}{2} \quad (5.14)$$

where  $n$  designates an integer number.

It is of importance to point out here that, even for the most general case of contact of part surface, the radial coordinate  $r_{\text{cnf}}(\varphi, \mu)$  of a point of the “*indicatrix of conformity*,  $\text{Cnf}_R(P_1/P_2)$ ” is not dependent of the fundamental magnitudes  $F_{P_1}$  and  $F_{P_2}$ . Independence of the characteristic curve  $\text{Cnf}_R(P_1/P_2)$  of the fundamental magnitudes  $F_{P_1}$  and  $F_{P_2}$  is due to the following.

The coordinate angle  $\omega_{P_1}$  can be calculated from the formula:

$$\omega_{P_1} = \arccos \frac{F_{P_1}}{\sqrt{E_{P_1} G_{P_1}}} \quad (5.15)$$

The radial coordinate  $r_{\text{cnf}}(\varphi, \mu)$  of a point of the “*indicatrix of conformity*,  $\text{Cnf}_R(P_1/P_2)$ ,” is not naturally a function of the coordinate angle  $\omega_{P_1}$ . Besides, the position vector  $r_{\text{cnf}}(\varphi, \mu)$  depends on the fundamental magnitudes  $E_{P_1}$ ,  $G_{P_1}$ , and  $E_{P_2}$ ,  $G_{P_2}$ ; the above analysis makes it clear why  $r_{\text{cnf}}(\varphi, \mu)$  is not dependent of the fundamental magnitudes  $F_{P_1}$  and  $F_{P_2}$ .

Two illustrative examples of the “*indicatrix of conformity*,  $\text{Cnf}_R(P_1/P_2)$ ” at a point of contact of two smooth regular part surfaces  $P_1$  and  $P_2$  are depicted schematically in Fig. 5.5. The first example (see Fig. 5.5a) relates to the cases of contact of a saddle-like local patch of the part surface  $P_1$  and of a convex elliptic-like local patch of the part surface  $P_2$ . The second one (see Fig. 5.5b) is for the case of contact of a convex parabolic-like local patch of the part surface  $P_1$  and of a convex elliptic-like local patch of the part surface  $P_2$ . For both cases (see Fig. 5.5), the corresponding curvature indicatrices  $\text{Crv}(P_1)$  and  $\text{Crv}(P_2)$  of the part surfaces  $P_1$  and  $P_2$  are depicted as well. The imaginary (phantom) branches of the “*Dupin indicatrix*,  $\text{Dup}(P_1)$ ” for the saddle-like local patch of the part surface  $P_1$  are shown in dashed line (see Fig. 5.5a).

<sup>2</sup> Equation of this characteristic curve is known from:

(a) Pat. No.1249787, USSR, *A Method of Sculptured Part Surface Machining on a Multi-Axis NC Machine*, S.P. Radzevich, B23C 3/16, Filed: December 27, 1984, [1] and (in a hidden form) from:

(b) Pat. No.1185749, USSR, *A Method of Sculptured Part Surface Machining on a Multi-Axis NC Machine*, S.P. Radzevich, B23C 3/16, Filed: October 24, 1983, [2].

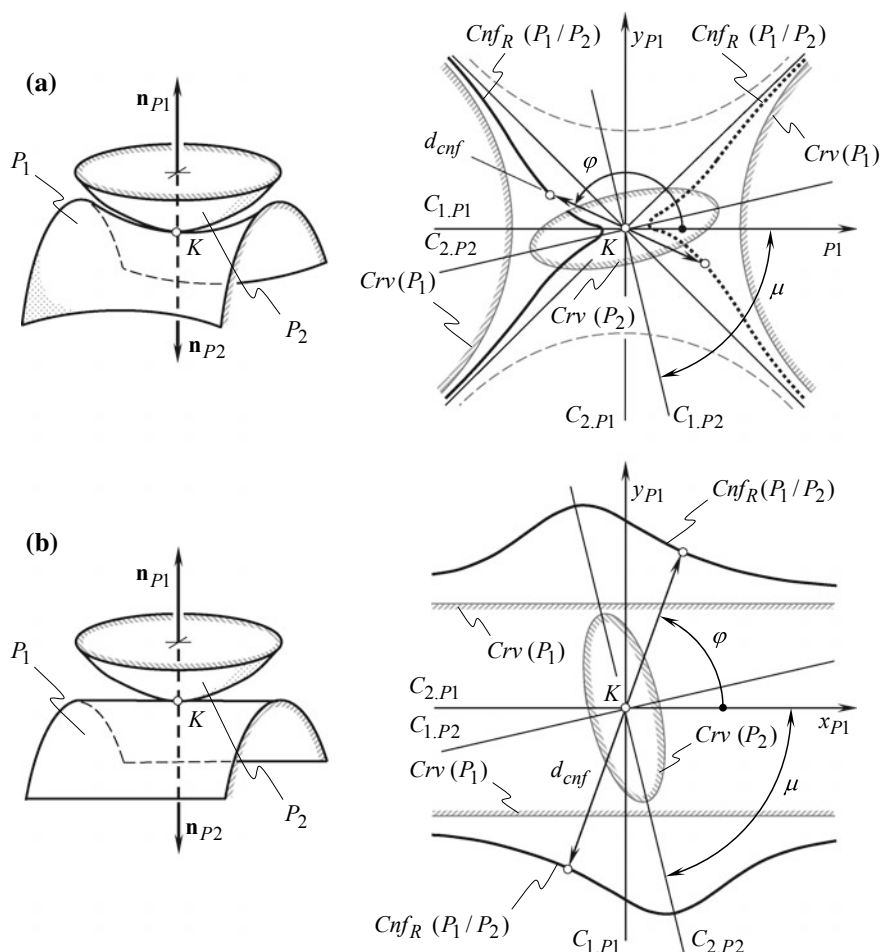


**Fig. 5.5** Examples of the indicatrix of conformity  $Cnf_R(P_1/P_2)$  at a point of contact of two smooth regular part surfaces  $P_1$  and  $P_2$  in the first order of tangency

Under certain circumstances, geometrical contact of two surfaces can be feasible, while physical conditions of contact of the part surfaces can be violated. Interference of the part surfaces  $P_1$  and  $P_2$  into one another is the result of violation of the physical condition of contact of the surfaces. Implementation of the “*indicatrix of conformity*  $Cnf_R(P_1/R_2)$ ” at a point of contact of the part surfaces  $P_1$  and  $P_2$  immediately uncovers the surfaces interference, if any. Three illustrative examples of violation of the physical condition of contact of the surfaces  $P_1$  and  $P_2$  are depicted schematically in Fig. 5.6. When a correspondence between the radii of normal curvature is inappropriate, then the “*indicatrix of conformity*  $Cnf_R(P_1/R_2)$ ” either intersects itself as illustrated in Fig. 5.6a, or all the diameters of this characteristic curve become negative as shown in Fig. 5.6b, c.

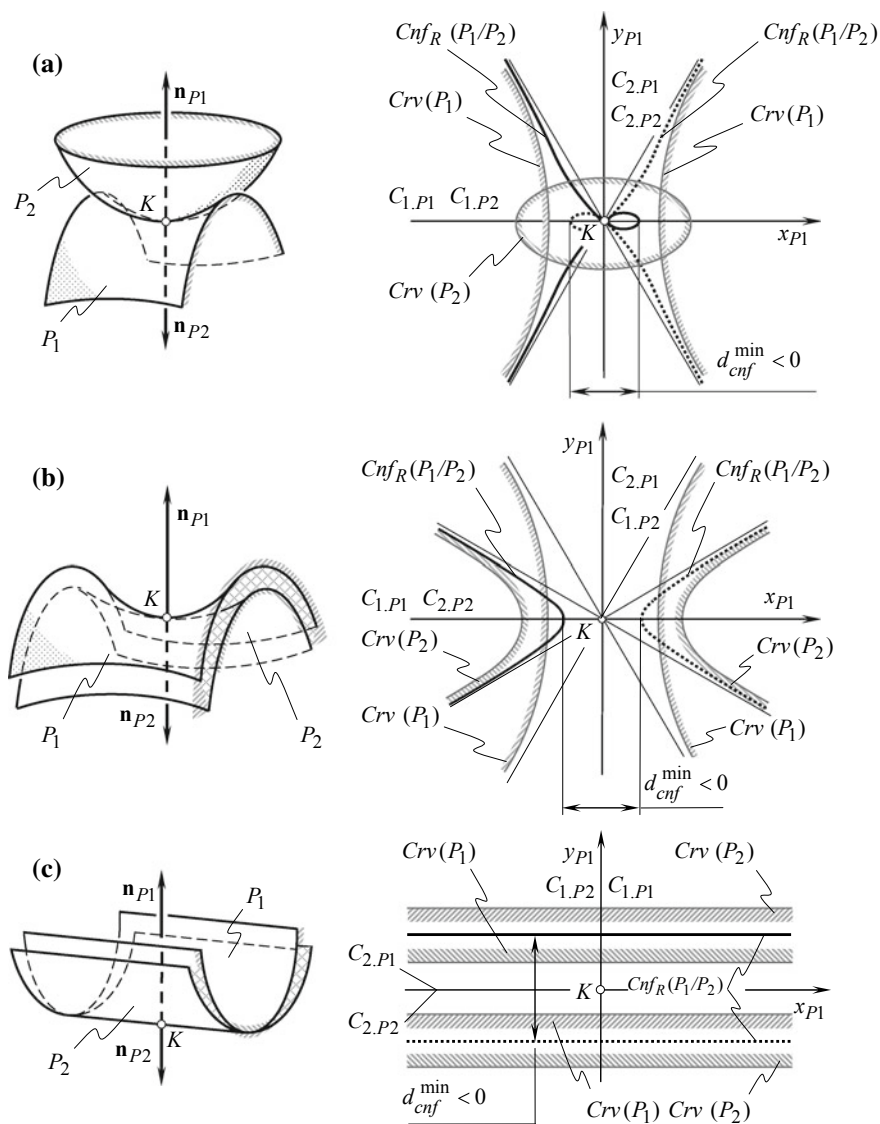


**Fig. 5.6** Examples of violation of condition of contact of two smooth regular part surfaces  $P_1$  and  $P_2$

The degree of conformity at a point of contact of two part surfaces  $P_1$  and  $P_2$  in a corresponding section of the surfaces by a plane through the common perpendicular  $\mathbf{n}_{P_1}$  can be evaluated by the length of the current diameter<sup>3</sup>  $d_{\text{cnf}}$  of the “*indicatrix of conformity*,  $\text{Cnf}_R(P_1/P_2)$ ” at a point of contact of the surfaces  $P_1$  and  $P_2$ . The orientation of the normal plane section with respect to the part surfaces  $P_1$  and  $P_2$  is specified by the corresponding central angle  $\varphi$ .

For the orthogonally parameterized part surfaces  $P_1$  and  $P_2$ , the equations of the “*Dupin indicatrices*”  $\text{Dup}(P_1)$  and  $\text{Dup}(P_2)$  are simplified to:

$$L_{P_1}x_{P_1}^2 + 2M_{P_1}x_{P_1}y_{P_1} + N_{P_1}y_{P_1}^2 = \pm 1 \quad (5.16)$$

$$L_{P_2}x_{P_2}^2 + 2M_{P_2}x_{P_2}y_{P_2} + N_{P_2}y_{P_2}^2 = \pm 1 \quad (5.17)$$

After been represented in a common coordinate system, Eq. (5.16) and Eq. (5.17) yield a simplified equation of the “*indicatrix of conformity*,  $\text{Cnf}_R(P_1/P_2)$ ” at a point of contact of the part surfaces  $P_1$  and  $P_2$ :

$$r_{\text{cnf}}(\varphi, \mu) = (L_{P_1} \cos^2 \varphi - M_{P_1} \sin 2\varphi + N_{P_1} \sin^2 \varphi)^{-\frac{1}{2}} \text{sgn } \Phi_{2,P_1}^{-1} \\ + [L_{P_2} \cos^2(\varphi + \mu) - M_{P_2} \sin 2(\varphi + \mu) + N_{P_2} \sin^2(\varphi + \mu)]^{-\frac{1}{2}} \text{sgn } \Phi_{2,P_2}^{-1} \quad (5.18)$$

Equation (5.13) of the “*indicatrix of conformity*,  $\text{Cnf}_R(P_1/R_2)$ ” yields an equation for one more characteristic curve. This characteristic curve is referred to as the “*curve of the minimum values of the radial coordinate*  $r_{\text{cnf}}$ ,” which is expressed in terms of  $\varphi$ . In the general case, the equation of this characteristic curve can be represented in the form:

$$r_{\text{cnf}}^{\min} = r_{\text{cnf}}^{\min}(\mu) \quad (5.19)$$

For the derivation of an expression for the characteristic curve  $r_{\text{cnf}}^{\min} = r_{\text{cnf}}^{\min}(\mu)$ , the following method can be employed.

A given relative orientation of the part surfaces  $P_1$  and  $P_2$  is specified by the angle  $\mu$  of the surfaces’  $P_1$  and  $P_2$  local relative orientation. The minimum value of the radial coordinate  $r_{\text{cnf}}^{\min}$  is observed when the angular parameter  $\varphi$  is equal to the root  $\varphi_1$  of the equation:

$$\frac{\partial}{\partial \varphi} r_{\text{cnf}}(\varphi, \mu) = 0 \quad (5.20)$$

The solution to Eq. (5.20) must also meet the requirement:

---

<sup>3</sup> The diameter of a centro-symmetrical curve can be defined as a distance between two points of the curve, measured along the corresponding straight line through the center of symmetry of the planar curve.

$$\frac{\partial^2}{\partial \varphi^2} r_{\text{cnf}}(\varphi, \mu) > 0 \quad (5.21)$$

In order to find the necessary value of the angle  $\varphi_1$ , it is required to solve Eq. (5.20) with respect to  $\mu$ . After substituting the obtained solution  $\mu^{\min}$  to Eq. (5.13) of the “*indicatrix of conformity*,  $\text{Cnf}_R(P_1/P_2)$ ,” one can derive an equation  $r_{\text{cnf}}^{\min} = r_{\text{cnf}}^{\min}(\varphi)$  of the curve of minimum diameters of the characteristic curve  $\text{Cnf}_R(P_1/P_2)$ .

In a similar way, one more characteristic curve:

$$r_{\text{cnf}}^{\max} = r_{\text{cnf}}^{\max}(\varphi) \quad (5.22)$$

can be derived. The distribution of the maximum values of the radial coordinate  $r_{\text{cnf}}$  in terms of  $\phi$  is reflected by the characteristic curve [see Eq. (5.22)].

### 5.3 Directions of Extremum Degree of Conformity of Two Part Surfaces in Contact

The directions along which the degree of conformity of two smooth regular part surfaces  $P_1$  and  $P_2$  is of extremum value, that is, the degree of the surfaces’ conformity reaches either a maximum or a minimum value, are of prime importance for many of engineering applications. This issue is especially important when designing blend surfaces, for computation of parameters of optimal tool paths for machining of sculptured part surface on a multi-axis *NC* machine, for improving the accuracy of solution to the problem of two elastic bodies in contact, and for many other applications in applied science and in engineering.

The directions of the extremum degree of conformity at a point of contact of the part surfaces  $P_1$  and  $P_2$  (i.e., the directions that are pointed along the extremum diameters  $d_{\text{cnf}}^{\min}$  and  $d_{\text{cnf}}^{\max}$  of the “*indicatrix of conformity*  $\text{Cnf}_R(P_1/R_2)$ ” at a point of contact of the part surfaces  $P_1$  and  $P_2$ ) can be derived from the equation for the “*indicatrix of conformity*  $\text{Cnf}_R(P_1/R_2)$ .” For the reader’s convenience, Eq. (5.13) of this characteristic curve is transformed and is represented in the form:

$$r_{\text{cnf}}(\varphi, \mu) = \sqrt{|r_{1.P1} \cos^2 \varphi + r_{2.P1} \sin^2 \varphi| \text{sgn} \Phi_{2.P1}^{-1}} + \sqrt{|r_{1.P2} \cos^2(\varphi + \mu) + r_{2.P2} \sin^2(\varphi + \mu)| \text{sgn} \Phi_{2.P2}^{-1}} \quad (5.23)$$

Two angles  $\varphi_{\min}$  and  $\varphi_{\max}$  specify two directions within the common tangent plane, along which the degree of conformity at a point of contact of the part surface  $P_2$  to the part surface  $P_1$  reaches its extremum values. These angles are the roots of the equation:

$$\frac{\partial}{\partial \varphi} r_{\text{cnf}}(\varphi, \mu) = 0 \quad (5.24)$$

It can easily be proven that in the general case of contact of two sculptured surfaces, the difference between the angles  $\varphi_{\min}$  and  $\varphi_{\max}$  is not equal to  $0.5\pi$ . This means that the equality  $\varphi_{\min} - \varphi_{\max} = \pm 0.5\pi n$  is not valid in the general case of the surfaces' contact. Instead, in most cases the inequality  $\varphi_{\min} - \varphi_{\max} \neq \pm 0.5\pi n$  is valid (here  $n$  is an integer number). The condition  $\varphi_{\min} = \varphi_{\max} \pm 0.5\pi n$  is fulfilled only in cases when the angle  $\mu$  of the part surfaces'  $P_1$  and  $P_2$  local relative orientation is equal to  $\mu = \pm 0.5\pi n$ . Thus, the principal directions  $\mathbf{t}_{1,P1}$  and  $\mathbf{t}_{2,P1}$  of the surface  $P_1$ , and the principal directions  $\mathbf{t}_{1,P2}$  and  $\mathbf{t}_{2,P2}$  of the surface  $P_2$  either align with each other or are directed oppositely.

This makes possible the following statement:

**Conclusion 5.2** *In general case of contact of two smooth regular part surfaces, the directions along which the degree of conformity at a point of contact of the surfaces  $P_1$  and  $P_2$  is of extremum value are not orthogonal to each other.*

This conclusion is of importance for many engineering applications.

The solution to Eq. (5.13) returns two extremum angles  $\varphi_{\min}$  and  $\varphi_{\max} = \varphi_{\min} + 90^\circ$ . Equation (5.24) allows for two solutions  $\varphi_{\min}^*$  and  $\varphi_{\max}^*$ . Therefore, it is easy to calculate the extremum differences:

$$\Delta\varphi_{\min} = \varphi_{\min} - \varphi_{\min}^* \quad (5.25)$$

$$\Delta\varphi_{\max} = \varphi_{\max} - \varphi_{\max}^* \quad (5.26)$$

Generally speaking, neither the extremum difference  $\Delta\varphi_{\min}$ , nor the extremum difference  $\Delta\varphi_{\max}$  is equal to zero. They are equal to zero only in particular cases, say when the angle  $\mu$  of the part surfaces  $P_1$  and  $P_2$  local relative orientation fulfills the relationship  $\mu = \pm 0.5\pi n$ .

**Example 5.1** *As an illustrative example, let's describe analytically the geometry of contact of two convex parabolical patches of the surfaces  $P_1$  and  $P_2$  (Fig. 5.7). In the example immediately below, the design parameters of the gear tooth flank (the surface  $P_1$ ) and of the shaving cutter tooth flank (the surface  $P_2$ ), together with the given the gear and the cutter configuration, yield the following numerical data for the calculations.*

At the contact point  $K$  of the surfaces  $P_1$  and  $P_2$ , the principal curvatures of the surface  $P_1$  are equal  $k_{1,P1} = 4 \text{ mm}^{-1}$  and  $k_{2,P1} = 0$ . The principal curvatures of the surface  $P_2$  are equal  $k_{1,P2} = 1 \text{ mm}^{-1}$  and  $k_{2,P2} = 0$ . The angle  $\mu$  of the surfaces  $P_1$  and  $P_2$  local relative orientation is set  $\mu = 45^\circ$ .

Two approaches can be implemented for the analytical description of the geometry of contact of the surfaces  $P_1$  and  $P_2$ . The first one is based on implementation of "Dupin indicatrix  $\text{Dup}(\mathcal{R})$ " of the surface of relative curvature  $\mathcal{R}$ . The second one



$\varphi_{\max}^* = 118^\circ$ . [Imaginary branches of the “*indicatrix of conformity*  $\text{Cnf}_R(P_1/R_2)$ ” at a point of contact of the surfaces  $P_1$  and  $P_2$  in Fig. 5.7 are depicted in dashed lines].

Two important conclusions can be drawn.

**First**, the extremum angles  $\varphi_{\min}$  and  $\varphi_{\max}$  calculated in the first approach are not equal to the corresponding extremum angles  $\varphi_{\min}^*$  and  $\varphi_{\max}^*$  computed using the second approach. The relationships  $\varphi_{\min} \neq \varphi_{\min}^*$  and  $\varphi_{\max} \neq \varphi_{\max}^*$  are generally observed.

**Second**, the difference  $\Delta\varphi^*$  between the extremum angles  $\varphi_{\min}^*$  and  $\varphi_{\max}^*$  is not equal to half of  $\pi$ . Therefore, the relationship  $\varphi_{\max}^* - \varphi_{\min}^* \neq 90^\circ$  between the extremum angles  $\varphi_{\min}^*$  and  $\varphi_{\max}^*$  holds. In the general case of contact of two smooth regular surfaces, the directions of their extremum degree of conformity are “**not (!)** orthogonal to one another.”

The example discussed reveals that in general cases of contact of two smooth regular part surfaces, “*indicatrix of conformity*  $\text{Cnf}_R(P_1/R_2)$ ” can be implemented for the purpose of accurate analytical description of the geometry of contact of the surfaces. The “*Dupin indicatrix*,  $\text{Dup}(\mathcal{R})$ ” of the surface of relative normal curvature can be implemented for this purpose only in particular cases of the surfaces’ configuration. Application of the “*Dupin indicatrix*,  $\text{Dup}(\mathcal{R})$ ” of the surface of relative curvature  $\mathcal{R}$  enables only approximate analytical description of the geometry of contact of the surfaces. The “*Dupin indicatrix*,  $\text{Dup}(\mathcal{R})$ ” of the surface of relative curvature could be equivalent to the indicatrix of conformity only in degenerated cases of contact of two surfaces. Advantages of the “*indicatrix of conformity*  $\text{Cnf}_R(P_1/R_2)$ ” over the “*Dupin indicatrix*,  $\text{Dup}(\mathcal{R})$ ” of the surface of relative curvature are due to the higher order of the “*indicatrix of conformity*  $\text{Cnf}_R(P_1/R_2)$ ” at a point of contact of two surfaces (the indicatrix of conformity is a planar curve of the “**fourth order**.”).

## 5.4 Asymptotes of the Indicatrix of Conformity $\text{Cnf}_R(P_1/P_2)$

In engineering geometry of surfaces, asymptotes of the “*indicatrix of conformity*  $\text{Cnf}_R(P_1/P_2)$ ” play an important role. The indicatrix of conformity could have asymptotes when a certain combination of parameters of shapes of the part surfaces  $P_1$  and  $P_2$  is observed.

Straight lines that possess the property of becoming and staying infinitely close to the curve as the distance from the origin increases to infinity are referred to as “*asymptotes*.” This definition of asymptotes is helpful for derivation of an equation of asymptotes of the indicatrix of conformity at a point of contact of part the surfaces  $P_1$  and  $P_2$ .

In polar coordinates, the “*indicatrix of conformity*  $\text{Cnf}_R(P_1/R_2)$ ” is analytically described by Eq. (5.13). For the readers’ convenience, the equation of this characteristic curve is represented below in the form  $r_{\text{cnf}} = r_{\text{cnf}}(\varphi, \mu)$ .



The derivation of an equation of the asymptote(s) of the characteristic curve  $r_{\text{cnf}} = r_{\text{cnf}}(\varphi, \mu)$  can be accomplished in just a few steps:

- (a) For a given indicatrix of conformity  $r_{\text{cnf}} = r_{\text{cnf}}(\varphi, \mu)$ , compose a function  $r_{\text{cnf}}^*(\varphi, \mu)$  that is equal to:

$$r_{\text{cnf}}^*(\varphi, \mu) = \frac{1}{r_{\text{cnf}}(\varphi, \mu)} \quad (5.29)$$

- (b) Solve the equation  $r_{\text{cnf}}^*(\varphi, \mu) = 0$  with respect to  $\varphi$ . A direction of the asymptote is specified by the solution  $\varphi_0$  to this equation.  
(c) Calculate the value of the parameter  $m_0$ . The value of the parameter  $m_0$  is equal to:

$$m_0 = \left( \frac{\partial g(\varphi, \mu)}{\partial \varphi} \right)^{-1} \quad (5.30)$$

under the condition  $\varphi = \varphi_0$ .

- (d) The asymptote(s) is the straight line through the point  $(m_0, \varphi_0 + 0.5\pi)$  and with the direction  $\varphi_0$ . Its equation is:

$$r(\varphi) = \frac{m_0}{\sin(\varphi - \varphi_0)} \quad (5.31)$$

In particular cases, the asymptotes of the “*indicatrix of conformity*  $\text{Cnf}_R(P_1/R_2)$ ” can align either with the asymptotes of the “*Dupin indicatrix*”  $\text{Dup}(P_1)$  of the surface  $P_1$ , or with the asymptotes of the “*Dupin indicatrix*”  $\text{Dup}(P_2)$  of the surface  $P_2$ , or finally with the asymptotes of the “*Dupin indicatrix*”  $\text{Dup}(\mathcal{R})$  of the surface of relative normal curvature  $\mathcal{R}$ .

## 5.5 Comparison of the Capabilities of the “*Indicatrix of Conformity* $\text{Cnf}_R(P_1/P_2)$ ” and of the “*Dupin Indicatrix* $\text{Dup}(R)$ ” of the Surface of Relative Curvature

Both characteristic curves, that is, the “*indicatrix of conformity*  $\text{Cnf}_R(P_1/R_2)$ ” at a point of contact of two part surfaces  $P_1$  and  $P_2$ , and the “*Dupin indicatrix*,  $\text{Dup}(\mathcal{R})$ ” of the surface of relative curvature  $\mathcal{R}$  can be used with the same goal of analytical description of the geometry of contact of two smooth regular part surfaces  $P_1$  and  $P_2$  in the first order of tangency. Therefore, it is important to compare the capabilities of these characteristic curves with one another.

A detailed analysis of the capabilities of the “*indicatrix of conformity*  $\text{Cnf}_R(P_1/R_2)$ ” at a point of contact of the part surfaces  $P_1$  and  $P_2$  [see Eq. (5.13)]

and of the “*Dupin indicatrix*,  $\text{Dup}(\mathcal{R})$ ” of the surface of relative curvature  $\mathcal{R}$  [see Eq. (3.39)] is performed. This analysis allows the following conclusions to be drawn.

From the viewpoint of completeness and effectiveness of analytical description of the geometry of contact of two smooth regular part surfaces in first order of tangency, the “*indicatrix of conformity*,  $\text{Cnf}_R(P_1/R_2)$ ” is more informative compared with the “*Dupin indicatrix*,  $\text{Dup}(\mathcal{R})$ ” of the surface of relative curvature. It reflects important features of the geometry of contact of the part surfaces  $P_1$  and  $P_2$  in the differential vicinity of the contact point  $K$  more accurately. Thus, implementation of the “*indicatrix of conformity*,  $\text{Cnf}_R(P_1/R_2)$ ” for scientific and engineering purposes has advantages over the “*Dupin indicatrix*,  $\text{Dup}(\mathcal{R})$ ” of the surface of relative curvature  $\text{Dup}(\mathcal{R})$ . This conclusion follows directly from the following:

- (a) The directions of extremum degree of conformity of two part surfaces  $P_1$  and  $P_2$  that are specified by the “*Dupin indicatrix*,  $\text{Dup}(\mathcal{R})$ ” are always orthogonal to one another. Actually, in the general case of contact of two smooth regular part surfaces, these directions are not orthogonal to each other. They could be orthogonal only in particular cases of the surfaces’ contact. The “*indicatrix of conformity*,  $\text{Cnf}_R(P_1/R_2)$ ” of the part surfaces  $P_1$  and  $P_2$  properly specifies the actual directions of the extremum degree of conformity of the part surfaces  $P_1$  and  $P_2$ . This is particularly (but not only) due to the fact that the characteristic curve  $\text{Cnf}_R(P_1/R_2)$  at a point of contact of the part surfaces  $P_1$  and  $P_2$  is a planar curve of the fourth order, while the “*Dupin indicatrix*,  $\text{Dup}(\mathcal{R})$ ” of the surface of relative curvature  $\mathcal{R}$  is a planar curve of the second order;
- (b) Accounting for higher-order members of in the equation of the “*Dupin indicatrix*,  $\text{Dup}(\mathcal{R})$ ” of the surface of relative curvature does not enhance the capabilities of this characteristic curve, and actually this is useless. Accounting for higher-order members in “*Taylor expansion*” of the equation of the “*Dupin indicatrix*” gives nothing more for a proper analytical description of the geometry of contact of two surfaces in the first order of tangency. The principal features of the equation of this characteristic curve cause a principal disadvantage of the *Dupin indicatrix*  $\text{Dup}(\mathcal{R})$  compared to the “*indicatrix of conformity*,  $\text{Cnf}_R(P_1/R_2)$ .” The disadvantage above is inherent to the “*Dupin indicatrix*,  $\text{Dup}(\mathcal{R})$ ” and it cannot be eliminated.

## 5.6 Important Properties of the Indicatrix of Conformity $\text{Cnf}_R(P/T)$ at Point of Contact of Two Smooth Regular Part Surfaces

A performed analysis of Eq. (5.13) of the “*indicatrix of conformity*,  $\text{Cnf}_R(P_1/R_2)$ ” at a point of contact of two smooth regular part surfaces in the first order of tangency reveals that this characteristic curve possesses the following important properties:

1. The “*indicatrix of conformity*,  $\text{Cnf}_R(P_1/R_2)$ ” at a point of contact of the part surfaces  $P_1$  and  $P_2$  is a planar characteristic curve of the fourth order. It possesses the property of central symmetry and, in particular cases, it also possesses the property of mirror symmetry.
2. The “*indicatrix of conformity*,  $\text{Cnf}_R(P_1/R_2)$ ” is closely related to the part surfaces’  $P_1$  and  $P_2$  second fundamental forms  $\Phi_{2,P1}$  and  $\Phi_{2,P2}$ . This characteristic curve is invariant with respect to the kind of parameterization of the part surfaces  $P_1$  and  $P_2$ , but its equation is not. A change in the surfaces  $P_1$  and  $P_2$  parameterization leads to the equation of the “*indicatrix of conformity*,  $\text{Cnf}_R(P_1/R_2)$ ” changing too, while the shape and parameters of this characteristic curve remain unchanged.
3. The characteristic curve  $\text{Cnf}_R(P_1/P_2)$  is independent on actual value of the coordinate angle  $\omega_{P1}$  between the coordinate lines  $U_{P1}$  and  $V_{P1}$  on the part surface  $P_1$ . It is also independent on the actual value of the coordinate angle  $\omega_{P2}$  between the coordinate lines  $U_{P2}$  and  $V_{P2}$  on the part surface  $P_2$ . However, the parameters of the “*indicatrix of conformity*  $\text{Cnf}_R(P_1/P_2)$ ” depend upon the angle  $\mu$  of the part surfaces’  $P_1$  and  $P_2$  local relative orientation. Therefore, for a given pair of part surfaces  $P_1$  and  $P_2$ , the degree of conformity of the surface varies corresponding to the variation of the angle  $\mu$ , while the part surface  $P_2$  is spinning around the unit vector  $\mathbf{n}_{P1}$  of the common perpendicular.

A few more items can be added to the above list of the important properties of the indicatrix of conformity  $\text{Cnf}_R(P_1/P_2)$  at a point of contact of two smooth regular part surfaces in the first order of tangency.

## 5.7 The “*Converse Indicatrix of Conformity*” at Point of Contact of Two Regular Part Surfaces in the First Order of Tangency

For the “*Dupin indicatrix*,  $\text{Dup}(\mathcal{R})$ ” at a point of the surface of relative curvature  $\mathcal{R}$  for the surfaces  $P_1$  and  $P_2$ , there exists a corresponding “*inverse Dupin indicatrix*,  $\text{Dup}_k(\mathcal{R})$ .” Similarly, for the “*indicatrix of conformity*,  $\text{Cnf}_R(P_1/P_2)$ ” at a point of contact of the part surfaces  $P_1$  and  $P_2$ , there exists a corresponding “*converse indicatrix of conformity*,  $\text{Cnf}_k(P_1/P_2)$ .” This characteristic curve can be expressed directly in terms of the part surfaces’  $P_1$  and  $P_2$  normal curvatures  $k_{P1}$  and  $k_{P2}$ :

$$\text{Cnf}_k(P_1/P_2) \Rightarrow r_{\text{cnf}}^{\text{cnv}}(\varphi, \mu) = \sqrt{|k_{P1}(\varphi)|} \cdot \text{sgn} \Phi_{2,P1}^{-1} - \sqrt{|k_{P2}(\varphi, \mu)|} \cdot \text{sgn} \Phi_{2,P2}^{-1} \quad (5.32)$$

For derivation of the equation of the converse “*indicatrix of conformity*,  $\text{Cnf}_k(P_1/P_2)$ ,” the “*Euler formula*” for a surface normal curvature is used. For this purpose, and for both of the contacting part surfaces  $P_1$  and  $P_2$ , this formula is represented in the form:

$$k_{P1}(\varphi) = k_{1.P1} \cos^2 \varphi + k_{2.P1} \sin^2 \varphi \quad (5.33)$$

$$k_{P2}(\varphi, \mu) = k_{1.P2} \cos^2(\varphi + \mu) + k_{2.P2} \sin^2(\varphi + \mu) \quad (5.34)$$

Here, the principal curvatures of the part surface  $P_1$  are designated as  $k_{1.P}$  and  $k_{2.P}$ , while  $k_{1.P2}$  and  $k_{2.P2}$  designate the principal curvatures of the part surface  $P_2$ .

After substituting of Eq. (5.33) and Eq. (5.34) into Eq. (5.32), one can come up with the expression:

$$r_{\text{Cnf}}^{\text{cnv}}(\varphi, \mu) = \sqrt{|k_{1.P1} \cos^2 \varphi + k_{2.P1} \sin^2 \varphi| \text{sgn} \Phi_{2.P1}^{-1}} - \sqrt{|k_{1.P2} \cos^2(\varphi + \mu) + k_{2.P2} \sin^2(\varphi + \mu)| \text{sgn} \Phi_{2.P2}^{-1}} \quad (5.35)$$

for the radial coordinate  $r_{\text{cnf}}^{\text{cnv}}$  of a point for the “*converse indicatrix of conformity*,  $\text{Cnf}_k(P_1/P_2)$ ” at a point of contact of the part surfaces  $P_1$  and  $P_2$  in the first order of tangency.

Here, the principal curvatures  $k_{1.P1}$ ,  $k_{2.P1}$ , and  $k_{1.P2}$ ,  $k_{2.P2}$  of the part surfaces  $P_1$  and  $P_2$ , accordingly, can be expressed in terms of the corresponding fundamental magnitudes  $E_{P1}$ ,  $F_{P1}$ ,  $G_{P1}$  of the first and  $L_{P1}$ ,  $M_{P1}$ ,  $N_{P1}$  of the second order of the part surface  $P_1$ , and in terms of the corresponding fundamental magnitudes  $E_{P2}$ ,  $F_{P2}$ ,  $G_{P2}$  of the first and  $L_{P2}$ ,  $M_{P2}$ ,  $N_{P2}$  of the second order of the part surface  $P_2$ . In this way, Eq. (5.35) of the inverse indicatrix of conformity  $\text{Cnf}_k(P_1/P_2)$  can be cast to a form similar to Eq. (5.13) of the ordinary “*indicatrix of conformity*,  $\text{Cnf}_R(P_1/P_2)$ ” of the contacting part surfaces  $P_1$  and  $P_2$ .

Similar to the “*indicatrix of conformity*,  $\text{Cnf}_R(P_1/P_2)$ ,” the characteristic curve  $\text{Cnf}_k(P_1/P_2)$  also possesses the property of central symmetry. In particular case of two surfaces in contact, this characteristic curve also possesses the property of mirror symmetry. The directions of the extremal rate conformity of the part surfaces  $P_1$  and  $P_2$  are orthogonal to one another only in degenerated cases of the surfaces’ contact.

Equation (5.35) of the “*converse indicatrix of conformity*  $\text{Cnf}_k(P_1/P_2)$ ” is convenient for implementation when:

- (a) either the surface  $P_1$ , or
- (b) the surface  $P_2$ , or
- (c) both of them (the surfaces  $P_1$  and  $P_2$  simultaneously)

have point(s) or line(s) of inflection. At the point(s) [or line(s)] of inflection, radii of normal curvature  $R_{P1}$  and  $R_{P2}$  of the surfaces  $P_1$  and  $P_2$  are equal to infinity. This causes indefiniteness when calculating the radial coordinate  $r_{\text{cnf}}(\varphi, \mu)$  of a point of the characteristic curve  $\text{Cnf}_k(P_1/P_2)$ . Equation (5.35) of the converse “*indicatrix of conformity*  $\text{Cnf}_k(P_1/P_2)$ ” is free from disadvantages of this kind, and therefore is recommended for practical applications.

## References

1. Pat. No. 1249787. (1984). *A method of sculptured surface machining on multi-axis NC machine*. S.P. Radzevich, Int. Cl. B23c 3/16, Filed: December 27, 1984.
2. Pat. No. 1185749. (1983). *A Method of sculptured surface machining on multi-axis NC machine*. S.P. Radzevich, Int. Cl. B23c 3/16, Filed: October 24, 1983.

## Chapter 6

# **“Plücker Conoid”: More Characteristic Curves**



It was shown earlier in Chap. 4 that numerous characteristic curves can be derived for the purpose of analytical description of contact geometry of two smooth regular part surfaces in the first order of tangency. One more characteristic curve of this sort can be derived on the premise of the “*Plücker conoid*”<sup>1</sup> [1], a conoid, which bears the name of *Julius Plücker*.<sup>2</sup> Prior to begin the derivation of a characteristic curve of novel kind, it makes sense to recall the main properties of “*Plücker conoid*”.

### **6.1 “Plücker Conoid”**

Several definitions for the “*Plücker conoid*” conoid are known.

Firstly, the “*Plücker conoid*” is a smooth regular ruled surface. A ruled surface is sometimes also called the “*cylindroid*,” which in another respect is the inversion of a cross-cap.

The “*Plücker conoid*” can also be considered as an example of a right conoid. A ruled surface is called a right conoid if it can be generated by moving a straight line intersecting a fixed straight line such that the lines are always perpendicular.

As with the “*cathenoid*,” another ruled surface, the “*Plücker conoid*,” must be re-parameterized to see the rulings. Illustrative examples of various “*Plücker conoids*” are considered in [2].

---

<sup>1</sup>“*Plücker conoid*” is a ruled surface, which bears the name of J. Plücker known for his research in the field of a new geometry of space [1].

<sup>2</sup>*Julius Plücker* (June 16, 1801—May 22, 1868), a famous German mathematician and physicist.

### 6.1.1 Basics

A ruled surface can be swept out by moving a line in space and therefore has a parameterization of the form:

$$\mathbf{x}(u, v) = \mathbf{b}(u) + v \boldsymbol{\delta}(u), \quad (6.1)$$

where  $\mathbf{b}$  is called the “*directrix*” (also referred to as the “*base curve*”) and  $\boldsymbol{\delta}$  is the “*director curve*.” The straight lines themselves are called “*rulings*.” The rulings of a ruled surface are asymptotic curves. Furthermore, the “*Gaussian curvature*” on a ruled regular surface is everywhere non-positive. The surface is known for the presence of two or more folds formed by the application of a cylindrical equation to the line during this rotation. This equation defines the path of the line along the axis of rotation.

### 6.1.2 Analytical Representation

For the “*Plücker conoid*,” von Seggern [3] gives the general functional form as:

$$a x^2 + b y^2 - z x^2 - z y^2 = 0 \quad (6.2)$$

whereas Fischer [4] and Gray [5] give:

$$z = \frac{2 x y}{x^2 + y^2} \quad (6.3)$$

Another form of “*Cartesian equation*”  $z = a \frac{x^2 - y^2}{x^2 + y^2}$  for twofold “*Plücker conoid*” is also known [6].

The latter equation yields the following matrix representation of non-polar parameterization of the “*Plücker conoid*”:

$$\mathbf{r}_{\text{pc}}(u, v) = \begin{bmatrix} u & v & \frac{2 u v}{u^2 + v^2} & 0 \end{bmatrix}^T \quad (6.4)$$

The “*Plücker conoid*” could be represented by the polar parameterization:

$$\mathbf{r}_{\text{pc}}(r, \theta) = \begin{bmatrix} r \cos \theta \\ r \sin \theta \\ 2 \cos \theta \sin \theta \\ 0 \end{bmatrix} \quad (6.5)$$

A more general form of the “*Plücker conoid*” is parameterized below, with “ $n$ ” folds instead of just two. A generalization of the “*Plücker conoid*” to  $n$  folds is given by [5]:

$$\mathbf{r}_{\text{pc}}(r, \theta) = \begin{bmatrix} r \cos \theta \\ r \sin \theta \\ \sin(n\theta) \\ 0 \end{bmatrix} \quad (6.6)$$

The difference between these two forms is the function in the  $z$  – axis. The polar form is a specialized function that outputs only one type of curvature with two undulations, while the generalized form is more flexible with the number of undulations of the outputted curvature being determined by the value of “ $n$ ”.

“*Cartesian parameterization*” of the equation of the multifold “*Plücker conoid*” [see Eq. (6.6)] therefore gives [6]:

$$z(\sqrt{x^2 + y^2})^n = \sum_{0 \leq k \leq \frac{n}{2}} (-1)^k C_n^{2k} x^{n-2k} y^{2k} \quad (6.7)$$

The surface appearance depends upon the actual number of folds [2].

In order to represent the “*Plücker conoid*” as a ruled surface, it is sufficient to represent Eq. (6.6) in the form of Eq. (6.7):

$$\mathbf{r}_{\text{pc}}(r, \theta) = \begin{bmatrix} r \cos \theta \\ r \sin \theta \\ \sin(n\theta) \\ 0 \end{bmatrix} = \begin{bmatrix} r \cos \theta \\ r \sin \theta \\ 2 \cos \theta \sin \theta \\ 0 \end{bmatrix} = \begin{bmatrix} 0 \\ 0 \\ 2 \cos \theta \sin \theta \\ 0 \end{bmatrix} + r \begin{bmatrix} \cos \theta \\ \sin \theta \\ 0 \\ 0 \end{bmatrix} \quad (6.8)$$

Taking the perpendicular plane as the  $xy$ -plane and taking the line to be the  $x$ -axis gives the parametric equation [5]:

$$\mathbf{r}_{\text{pc}} = \begin{bmatrix} v \cdot \cos v(u) \\ v \cdot \sin v(u) \\ h(u) \\ 0 \end{bmatrix} \quad (6.9)$$

In cylindrical coordinates [6]:

$$z = a \cos(n\theta) \quad (6.10)$$

which simplifies to:

$$z = a \cos 2\theta \quad \text{if } n = 2 \quad (6.11)$$



A few more kinds of parameterization of the “*Plücker conoid*” are to be considered.

### 6.1.3 Local Properties

Following the “*Bonnet theorem*” (see Chap. 1), local properties of the “*Plücker conoid*” could be expressed analytically in terms of the first and second fundamental forms of the surface. For practical application, some useful auxiliary formulas are also required.

The first and second fundamental forms [6] of the “*Plücker conoid*” could be represented as:

$$\Phi_1 \Rightarrow d s^2 = d \rho^2 + (\rho^2 + n^2 a^2 \sin^2(n \theta)) d \theta^2 \quad (6.12)$$

$$\Phi_2 \Rightarrow \frac{n a}{H} [\sin(n \theta) d \rho - n \rho \cos(n \theta) d \theta] d \theta \quad (6.13)$$

Asymptotes are given by the equation:

$$\rho^n = k a^n \sin(n \theta) \quad (6.14)$$

They correlate strictly to “*Bernoulli’s lemniscates*” [6].

For the simplified case of the “*Plücker conoid*”  $n = 2$ , the first and second fundamental forms reduce to [6]:

$$\Phi_1 \Rightarrow d s^2 = d \rho^2 + (\rho^2 + 4 a^2 \cos^2 2 \theta) d \theta^2 \quad (6.15)$$

$$E = 1 \quad (6.16)$$

$$F = 0 \quad (6.17)$$

$$G = \rho^2 + 4 a^2 \cos^2 2 \theta \quad (6.18)$$

$$H = \sqrt{G} \quad (6.19)$$

$$\Phi_2 \Rightarrow -\frac{4 a}{H} [\sin 2 \theta d \rho - n \rho \cos 2 \theta d \theta] d \theta \quad (6.20)$$

$$L = 0 \quad (6.21)$$

$$M = -\frac{2 a \cos 2 \theta}{H} \quad (6.22)$$

$$N = -\frac{4 a \rho \sin 2\theta}{H} \quad (6.23)$$

Because the consideration below is limited just to the case of  $n = 2$ , auxiliary formulae for this particular case of the “*Plücker conoid*” would be helpful.

### 6.1.4 Auxiliary Formulae

At  $u = u_0$ ,  $v = v_0$ , the tangent to the surfaces is parameterized by:

$$\mathbf{r}_{pc}(u, v) = \begin{bmatrix} u + u_0 \\ v + v_0 \\ \frac{2(-u u_0^2 v_0 + u v_0^3 + u_0 v_0^2(-v + v_0) + u_0^3(v + v_0))}{u_0^2 + v_0^2} \\ 0 \end{bmatrix} \quad (6.24)$$

The surface normal is its double line [2, 7].

The infinitesimal area of a patch on the surface is given by:

$$\Phi_1 \Rightarrow ds = \sqrt{1 + \frac{4(u-v)^2(u+v^2)}{(u^2+v^2)^3}} du dv \quad (6.25)$$

The “*Gaussian curvature*” of the “*Plücker conoid*” can be calculated from:

$$\mathcal{G}(u, v) = -\frac{4(u^4 - v^4)^2}{(u^6 + v^4(4 + v^2) + u^2 v^2(-8 + 3v^2) + u^4(4 + 3v^2))^2} \quad (6.26)$$

The mean curvature of the “*Plücker conoid*” is equal to:

$$\mathcal{M}(u, v) = -\frac{4 u v}{(u^2 + v^2)^2 \left(1 + \frac{4(u-v)^2(u+v)^2}{(u^2+v^2)^3}\right)^{\frac{3}{2}}} \quad (6.27)$$

Formulae such as those discussed in this subsection of the book are helpful for better understanding of “*Plücker conoid*” geometry.

## 6.2 On Analytical Description of Local Geometry of Smooth Regular Part Surface

For the consideration below, the following characteristics of a smooth regular part surface  $P_1$  are of prime importance:

- (a) the tangent plane to the part surface  $P_1$ ,
- (b) the unit normal  $\mathbf{n}_{P_1}$ ,
- (c) the surface  $P_1$  principal curvatures  $k_{1,P_1}$  and  $k_{2,P_1}$ , as well as
- (d) the surface  $P_1$  normal curvature  $k_{P_1}$  at a pre-specified direction.

The “*Plücker conoid*” could be used for visualization of the distribution of the surface  $P_1$  normal curvature at a given surface point. The corresponding “*Plücker conoid*” can be determined at “*every point*” of a smooth regular part surface  $P_1$ . The surface unit normal vector  $\mathbf{n}_{P_1}$  can be employed as the axis of the “*Plücker conoid*.” The rulings are the straight lines that intersect  $z$ -axis at a right angle. The generating straight-line segments of the “*Plücker conoid*” are always parallel to the tangent plane to the surface  $P_1$  at the point, at which the “*Plücker conoid*” is erected. In consideration below, other applications of the tangent plane to the surface  $P_1$  are of importance as well.

Consequently, the above-performed analysis makes it possible naturally to connect the “*Plücker conoid*” to the surface  $P_1$ .

### 6.2.1 Preliminary Remarks

An example of implementation of “*Plücker conoid*” is given by *Struik* [7]. He considers a “*cylindroid*,” which is represented by the locus of the curvature vectors at a point  $p_1$  of a part surface  $P_1$  belonging to all curves passing through  $p_1$ :

$$z(x^2 + y^2) = k_{1,P_1}x^2 + k_{2,P_1}y^2 \quad (6.28)$$

Here, the symbols  $k_{1,P_1}$  and  $k_{2,P_1}$  designate principal curvatures at a point of the part surface  $P_1$  (remember that the inequality  $k_{1,P_1} > k_{2,P_1}$  always holds).

The curvature vector is defined in the following way. According to [7], a proportionality factor  $k_{P_1}$  such that:

$$\mathbf{k}_{P_1} = d\mathbf{t}_{P_1}/dS = k_{P_1}\mathbf{n}_{P_1} \quad (6.29)$$

can be introduced.

The vector  $\mathbf{k}_{P_1} = d\mathbf{t}_{P_1}/dS$  expresses the rate of change of the tangent when we proceed along the curve. It is called the “*curvature vector*.” The factor  $k_P$  is called the “*curvature*”;  $|\mathbf{k}_P|$  is the length of the curvature vector. Although the sense of  $\mathbf{n}_{P_1}$  may be chosen arbitrarily, that of  $d\mathbf{t}_{P_1}/dS$  is perfectly determined by the curve, independent of its orientation; when  $S$  changes sign,  $\mathbf{t}_{P_1}$  also changes sign. When  $\mathbf{n}_{P_1}$  (as is often done) is taken in the sense of  $S$ , then  $k_P$  is always positive, but we shall note adhere to this convention.

### 6.2.2 The “Plücker Conoid”

In order to develop an appropriate graphical interpretation of the “*Plücker conoid*,  $\mathbf{Pl}_R(P_1)$ ” at a point of a part surface  $P_1$ , let us consider a smooth regular part surface  $P_1$  that is given by vector equation

$$\mathbf{r}_{P1} = \mathbf{r}_{P1}(U_{P1}, V_{P1}) \quad (6.30)$$

From the perspective of naturally connecting of the “*Plücker conoid*” to the part surface  $P_1$  itself, the axis of the “*Plücker conoid*,  $\mathbf{Pl}_R(P_1)$ ” aligns to the unit normal vector  $\mathbf{n}_{P1}$  to the part surface  $P_1$  at a point  $m$ .

For further consideration, the normal radii of curvature  $R_{P1} = k_{P1}^{-1}$  at the point  $m$  of the part surface  $P_1$  need to be calculated. In order to simplify the calculations, the equation:

$$R_{P1} = \frac{\Phi_{1.P1}}{\Phi_{2.P1}} \quad (6.31)$$

can be reduced to the “*Euler formula*” for radii of normal curvature of the part surface  $P_1$ :

$$R_P(\varphi) = (R_{1.P}^{-1} \cos^2 \varphi + R_{2.P}^{-1} \sin^2 \varphi)^{-1} \quad (6.32)$$

where we denote:

$R_{1.P1}$  and  $R_{2.P1}$  The principal radii of curvature at a point of interest  $m$  of the part surface  $P_1$

$\varphi$  The angle that the normal plane section  $R_{P1}(\varphi)$  makes with the first principal direction  $\mathbf{t}_{1.P1}$  of the part surface  $P_1$ .

Point  $C_1$  coincides with the curvature center of the surface  $P_1$  in the first principal plane section of  $P_1$  at a point  $m$ . It is located on the axis of the “*Plücker conoid*,  $\mathbf{Pl}_R(P_1)$ .” The straight-line segment of length  $R_{1.P1}$  extends from  $C_1$  in the direction of  $\mathbf{t}_{1.P1}$ . The unit tangent vector  $\mathbf{t}_{1.P1}$  indicates the first principal direction of the part surface  $P_1$  at the surface point  $m$ . It makes a right angle with the axis of the surface  $\mathbf{Pl}_R(P_1)$ . The straight-line segment of the same length  $R_{1.P}$  extends from  $C_1$  in the opposite direction  $-\mathbf{t}_{1.P1}$ .

Point  $C_2$  is coincident with the curvature center of the part surface  $P_1$  in the second principal plane section of  $P_1$  at the point  $m$ . It is remote from  $C_1$  at a distance  $(R_{1.P1} - R_{2.P1})$ . (remember that the radius of normal curvature  $R_{P1}$ , as well as the principal radii of curvature  $R_{1.P1}$  and  $R_{2.P1}$ , is algebraic values in nature). The straight-line segment of length  $R_{2.P1}$  extends from  $C_2$  in the direction of  $\mathbf{t}_{2.P1}$ . The unit tangent vector  $\mathbf{t}_{2.P1}$  indicates the second principal direction of the part surface  $P_1$  at the point  $m$ . It also makes a right angle with the axis of the “*Plücker conoid*,  $\mathbf{Pl}_R(P_1)$ .” The straight-line segment of the same length  $R_{2.P1}$  extends from  $C_2$  in the direction  $-\mathbf{t}_{2.P1}$ .

A certain point  $C$  coincides with the center of curvature of the part surface  $P_1$  in the normal plane section of  $P_1$  at a surface point  $m$  in arbitrary direction that is specified by the corresponding value of the central angle  $\varphi$ . The point  $C$  is located on the axis of the “Plücker conoid,  $\mathbf{PI}_R(P_1)$ .” The radius of normal curvature  $R_{P_1}(\varphi)$  corresponds to the principal radii of curvature  $R_{1,P_1}$  and  $R_{2,P_1}$  in the manner  $R_{1,P_1} < R_{P_1}(\varphi) < R_{2,P_1}$ .

The straight-line segment of length  $R_{P_1} = R_{P_1}(\varphi)$  spins about, and travels up and down along the axis of the “Plücker conoid,  $\mathbf{PI}_R(P_1)$ .” In such a way, the “Plücker conoid” could be represented as a locus of consecutive positions of the straight-line segment  $R_{P_1} = R_{P_1}(\varphi)$ .

Figure 6.1 reveals<sup>3</sup> that the “Plücker conoid” perfectly reflects the topology of the part surface  $P_1$  in the differential vicinity of a surface point  $m$ . Therefore, the surface  $\mathbf{PI}_R(P_1)$  can be implemented as a tool for the visualization of the change of parameters of its local geometry.

In order to plot the “Plücker conoid,  $\mathbf{PI}_R(P_1)$ ” together with the part surface  $P_1$  itself (Fig. 6.1), it is necessary to represent the equations of both the surfaces in a common coordinate system, for example in the coordinate system  $X_S Y_S Z_S$ . For this purpose, the operator of resultant coordinate system transformation  $\mathbf{Rs}(S \rightarrow P)$  needs to be composed (see Appendix B).

After been constructed at a point of the smooth regular part surface  $P_1$ , the characteristic surface  $\mathbf{PI}_R(P_1)$  clear indicates:

- the actual values of principal radii of curvature  $R_{1,P_1}$  and  $R_{2,P_1}$  of the part surface  $P_1$ ,
- the location of the curvature centers  $O_{1,P_1}$  and  $O_{2,P_1}$ ,
- the orientation of the principal plane sections  $C_{1,P_1}$  and  $C_{2,P_1}$  (that is, the directions of the unit tangent vectors  $\mathbf{t}_{1,P_1}$  and  $\mathbf{t}_{2,P_1}$  of the principal directions),
- the current value of the normal radii of curvature  $R_{P_1}(\varphi)$ , and
- the location of curvature center  $O_{P_1}$  for any given section by the normal plane  $C_{P_1}$  through the given direction  $\mathbf{t}_{P_1}(\varphi)$ .

Therefore, the “Plücker conoid” could be considered as an example of a “characteristic surface” that potentially could be used in engineering geometry of surfaces.

In addition to “Plücker conoid,  $\mathbf{PI}_R(P_1)$ ” of the kind described above (Fig. 6.1), a characteristic surface  $\mathbf{PI}_k(P_1)$  of inverse kind could be introduced as well.

When constructing the “Plücker conoid,  $\mathbf{PI}_R(P_1)$ ” (Fig. 6.1), a straight-line segment of length  $k_{P_1}(\varphi)$  is used instead of a straight-line segment of the length  $R_{P_1}(\varphi)$ . [Here,  $k_{P_1}(\varphi) = R_{P_1}^{-1}(\varphi)$  is the normal curvature of the surface  $P_1$  at the point  $K$  in the given normal plane section through the surface point  $m$ ]. This makes possible construction of the characteristic surface  $\mathbf{PI}_k(P_1)$  of inverse kind.

The characteristic surfaces  $\mathbf{PI}_R(P_1)$  and  $\mathbf{PI}_k(P_1)$  resemble one another from many aspects. They also appear similar, except of the cases, when  $R_{P_1}(\varphi)$  and/or  $k_{P_1}(\varphi)$  is equal to either zero (0) or infinity ( $\infty$ ).

<sup>3</sup>It is of importance to point out here, that for the reader’s convenience, the “Plücker conoid” (Fig. 6.1) is scaled along the axes of the local coordinate system (with the single goal for better visualization of the surface’  $P_1$  local geometrical properties).

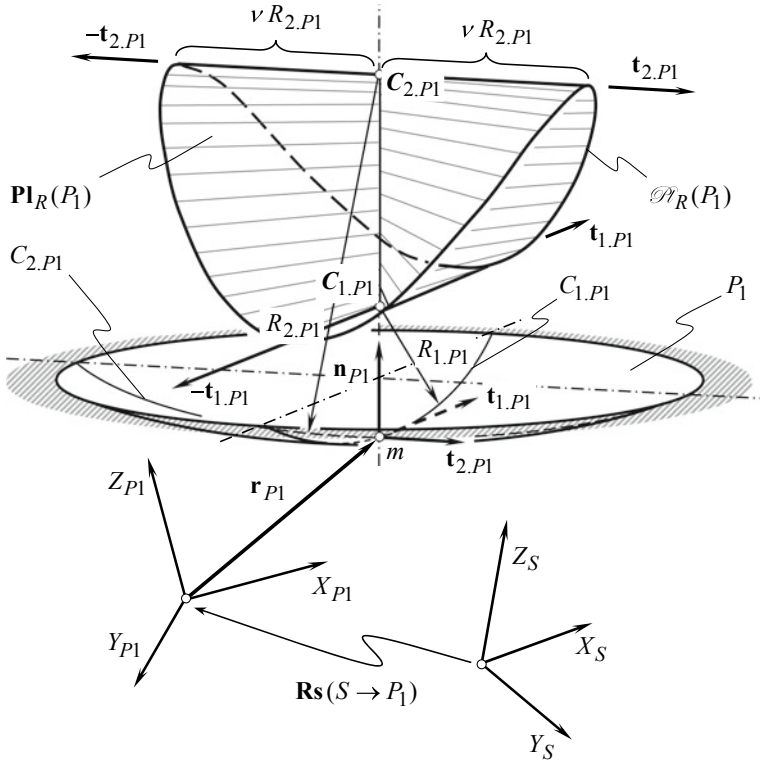


**Fig. 6.1** “Plücker conoid,  $\mathbf{Pl}_R(P_1)$ ,” and “Plücker curvature indicatrix,  $\mathcal{N}_R(P_1)$ ,” naturally connected to the concave patch of a smooth regular part surface  $P_1$

The characteristic surface  $\mathbf{Pl}_R(P_1)$  is referred to as the “*Plücker conoid of the first kind*,” while the characteristic surface  $\mathbf{Pl}_k(P_1)$  is referred to as the “*Plücker conoid of the second kind*.”

The conoids  $\mathbf{Pl}_R(P_1)$  and  $\mathbf{Pl}_k(P_1)$  are “*inverse*” to each other [ $\mathbf{Pl}_R(P_1) = \mathbf{Pl}_k^{inv}(P_1)$ , and vice versa].

“*Plücker conoids*,” that is,  $\mathbf{Pl}_R(P_1)$  and  $\mathbf{Pl}_k(P_1)$ , clearly indicate the change of parameters of the local topology in the differential vicinity of a point of smooth regular part surface  $P_1$ .

### 6.2.3 “Plücker Curvature Indicatrix”

The boundary curve of the “*Plücker conoid*” contains all the necessary information on the distribution of normal curvatures of the part surface  $P_1$  in the differential vicinity of a surface point  $m$ , while the surface  $\mathbf{Pl}_R(P_1)$  itself represents additional

information about the local topology of the surface  $P_1$ . This additional information is out of interest from the standpoint of its implementation in engineering geometry of surfaces. We remember here the rule often called “*Ockham’s razor*”<sup>4</sup>.

Thus, without loss of accuracy, the “*Plücker conoid*” itself could be replaced with the boundary curve of the surface  $\mathbf{PI}_R(P_1)$ . The boundary curve  $\mathbf{PI}_R(P_1)$  of the characteristic surface  $\mathbf{PI}_R(P)$  is referred to as the “*Plücker curvature indicatrix of the first kind*” of the part surface  $P_1$  at a surface point  $m$ .

“*Plücker curvature indicatrix*” is therefore represented therefore by the end-points of the position vector of length of  $R_{P_1}(\varphi)$  that is spinning about and is reciprocating up and down the axis of the surface  $\mathbf{PI}_R(P_1)$ .Eq This leads immediately to an equation of this characteristic curve:

$$\mathcal{P}_R(P_1) \Rightarrow \mathbf{r}_R(\varphi) = \begin{bmatrix} R_{P_1}(\varphi) \cos \varphi \\ R_{P_1}(\varphi) \sin \varphi \\ R_{P_1}(\varphi) \\ 0 \end{bmatrix} \quad (6.33)$$

where  $R_{P_1}(\varphi)$  is given by the “*Euler formula*” for the radius of normal curvature:

$$R_{P_1}(\varphi) = (R_{1,P_1}^{-1} \cos^2 \varphi + R_{2,P_1}^{-1} \sin^2 \varphi)^{-1} \quad (6.34)$$

The analysis performed [2] reveals that for most kinds of smooth regular part surfaces  $P_1$ , the “*Plücker curvature indicatrix,  $\mathcal{P}_R(P_1)$* ” of the first kind is a “*closed*” regular 3D curve. For the surface local patches of parabolic and of saddle-like type, “*Plücker curvature indicatrix,  $\mathcal{P}_R(P_1)$* ” is separated onto two and onto four branches correspondingly. In particular cases, it could be even reduced to a planar curve to a circle, for example, as observed for umbilic local patches of the part surface  $P_1$ .

An equation, similar to that above Eq. (6.33), is valid for the “*Plücker curvature indicatrix,  $\mathcal{P}_k(P_1)$* ” of the second kind:

$$\mathcal{P}_k(P_1) \Rightarrow \mathbf{r}_k(\varphi) = \begin{bmatrix} k_{P_1}(\varphi) \cos \varphi \\ k_{P_1}(\varphi) \sin \varphi \\ k_{P_1}(\varphi) \\ 0 \end{bmatrix} \quad (6.35)$$

where

$$k_{P_1}(\varphi) = k_{1,P_1} \cos^2 \varphi + k_{2,P_1} \sin^2 \varphi \quad (6.36)$$

---

<sup>4</sup>William of *Ockham*, also spelled *Occam* (b.c. 1285, Ockham, Surrey?, England– d. 1347/49, Munich, Bavaria [now in Germany]), is remembered mostly because he developed the tools of logic. He insisted that we should always look for the simplest explanation that fits all the facts, instead of inventing complicated theories. The rule, which said “plurality should not be assumed without necessity,” is called “*Ockham’s razor*.”

Usually, the “*Plücker curvature indicatrix*,  $\mathcal{P}_R(P_1)$ ” of the second kind is represented by a closed curve.

Further possible simplification of the analytical description of the local topology of a smooth regular part surface  $P_1$  could be based on the following consideration.

#### 6.2.4 $\mathcal{H}_R(P_1)$ -Indicatrix at a Point of a Part Surface

Aiming for further simplification of the analytical description of the local topology of two smooth regular part surfaces in the first order of tangency, “*Plücker curvature indicatrix*” could be replaced with a planar characteristic curve of novel kind.

As follows from Eq. (6.33), the first two elements  $R_{P_1}(\varphi) \cos \varphi$  and  $R_{P_1}(\varphi) \sin \varphi$  on the right-hand side of the above expression contain all the required information on the distribution of radii of normal curvature of the part surface  $P_1$  at a surface point  $m$ . Hence, instead of implementation of the “*Plücker curvature indicatrix*,  $\mathcal{P}_R(P_1)$ ” [see Eq. (6.33)] for the purpose of analytical description of the geometry of contact of two smooth regular part surfaces, a planar characteristic curve  $\mathcal{H}_R(P_1)$  of a simpler structure can be implemented instead. The equation of this characteristic curve yields representation in the form:

$$\mathcal{H}_R(P_1) \Rightarrow \mathbf{r}_{iR}(\varphi) = \begin{bmatrix} R_{P_1}(\varphi) \cos \varphi \\ R_{P_1}(\varphi) \sin \varphi \\ 0 \\ 0 \end{bmatrix} \quad (6.37)$$

This planar characteristic curve is referred to as the “ $\mathcal{H}_R(P_1)$ -indicatrix of the first kind” at a point  $m$  of the part surface  $P_1$ .

The distribution of normal curvature of the surface  $P_1$  at a surface point  $m$  could be given by another planar characteristic curve:

$$\mathcal{H}_k(P_1) \Rightarrow \mathbf{r}_{ik}(\varphi) = \begin{bmatrix} k_{P_1}(\varphi) \cos \varphi \\ k_{P_1}(\varphi) \sin \varphi \\ 0 \\ 0 \end{bmatrix} \quad (6.38)$$

This planar characteristic curve [see Eq. (6.38)] is referred to as the “ $\mathcal{H}_k(P_1)$  indicatrix of the second kind” of the part surface  $P_1$  at a surface point  $m$ .

An example of the “ $\mathcal{H}_k(P_1)$ -indicatrix of the second kind” is shown in Fig. 6.2. The parameters of the characteristic curve  $\mathcal{H}_R(P_1)$  are computed at a point of a part surface  $P_1$  having principal radii of curvature  $R_{1,P_1} = 3$  mm, and  $R_{2,P_1} = 15$  mm. It is of importance to point out here that the direction of minimal diameter  $d_R$  of the characteristic curve  $\mathcal{H}_R(P_1)$  is aligned with the first principal direction  $\mathbf{t}_{1,P_1}$ , and the direction of maximal diameter  $D_R$  of the characteristic curve  $\mathcal{H}_R(P_1)$  is aligned with the second principal direction  $\mathbf{t}_{2,P_1}$  on the part surface  $P_1$  at a point  $m$ . Therefore, the





curve of the second order. In the case under consideration, it is always convex with uniform change of curvature. The “ $\mathcal{H}_R(P_1)$ -indicatrix” is also a planar smooth regular curve. However, the points of inflection are inherent to this curve. This is due to the fact that the “ $\mathcal{H}_R(P_1)$ -indicatrix” is a curve of fourth order. The higher order enhances the capabilities of the characteristic curve  $\mathcal{H}_R(P_1)$ .

Owing to the higher order of the equation, the “ $\mathcal{H}_R(P_1)$ -indicatrix” reflects the distribution of normal radii of curvature, while the “Dupin indicatrix,  $Dup(P_1)$ ” reflects the distribution of square roots of normal radii of curvature of a part surface  $P_1$  at the surface point  $m$ . In order to make the difference clear, it is sufficient to represent the equation of the “Dupin indicatrix” in the form similar to that for “ $\mathcal{H}_R(P_1)$ -indicatrix” [see Eq. (6.37)]:

$$Dup(P_1) \Rightarrow \mathbf{r}_{Dup}(\varphi) = \begin{bmatrix} \sqrt{|R_{P1}(\varphi)|} \cos \varphi \operatorname{sgn} R_{P1}(\varphi) \\ \sqrt{|R_{P1}(\varphi)|} \sin \varphi \operatorname{sgn} R_{P1}(\varphi) \\ 0 \\ 0 \end{bmatrix} \quad (6.39)$$

It is evident from the above consideration that Eqs. (6.37) and (6.39) are similar.

### 6.3 Relative Characteristic Curve

The considered properties of the “Plücker conoid” can be employed for the derivation of the equation of a planar characteristic curve for analytical description of the contact geometry of two smooth regular part surfaces for the needs of engineering geometry of surfaces.

#### 6.3.1 On a Possibility of Implementation of Two “Plücker Conoids”

At first glimpse, implementation of two “Plücker conoids” sounds promising for the purpose of solving the problem of analytical description of contact geometry of two smooth regular part surfaces.

In order to develop an appropriate solution to the problem under consideration, the characteristic surface  $\mathbf{PI}_R(P_1/P_2)$  that reflects the “summa” of the corresponding normal radii of curvature at a point of contact of the part surfaces  $P_1$  and  $P_2$  could be introduced. The following matrix representation of the equation of the surface  $\mathbf{PI}_R(P_1/P_2)$  follows immediately:

$$\mathbf{Pl}_R(P_1/P_2) \Rightarrow \mathbf{R}_R^*(\varphi) = \begin{bmatrix} (R_{P1} + R_{P2}) \cos \varphi \\ (R_{P1} + R_{P2}) \sin \varphi \\ 2 \sin \varphi \cos \varphi \\ 0 \end{bmatrix} \quad (6.40)$$

The characteristic surface  $\mathbf{Pl}_R(P_1/P_2)$  is referred to as the “*Plücker relative conoid*.”

Because the centers  $C_{1.P1}$  and  $C_{2.P1}$  of the principal curvature of the part surfaces  $P_1$ , and the centers  $C_{1.P2}$  and  $C_{2.P2}$  of the principal curvatures of the part surface  $P_2$  in general case do not coincide with one another, the actual reciprocation of the straight-line segment of length  $(R_{P1} - R_{P2})$  could be restricted by different pairs of the limiting points  $C_{1.P1}$ ,  $C_{2.P1}$ ,  $C_{1.P2}$ ,  $C_{2.P2}$ . Various locations of the limiting points on the axis through the unit normal vector  $\mathbf{n}_{P1}$  result in “*deformation*” of the characteristic surface  $\mathbf{Pl}_R(P_1/P_2)$  in its axial direction. A deformation of such type does not affect the surface appearance in the direction of  $(R_{P1} + R_{P2})$  that is of critical importance for engineering geometry of surfaces.

The characteristic surface  $\mathbf{Pl}_R(P_1/P_2)$  is described analytically by Eq. (6.40). This indicates that the “*Plücker relative conoid*” correctly reflects the degree of conformity at a point of contact  $K$  of the part surfaces  $P_1$  and  $P_2$ . However, the surface  $\mathbf{Pl}_R(P_1/P_2)$  itself is inconvenient for implementation in engineering geometry of surfaces. In order to fix this undesired particular problem, the “*Plücker relative indicatrix*  $\mathbf{Pl}_R(P_1/P_2)$ ” at a point of contact  $K$  of two surfaces  $P_1$  and  $P_2$  is introduced. The equation of this 3D characteristic curve immediately follows immediately from Eq. (6.40):

$$\mathbf{Pl}_R(P_1/P_2) \Rightarrow \mathbf{R}_R(\varphi) = \begin{bmatrix} (R_{P1} + R_{P2}) \cos \varphi \\ (R_{P1} + R_{P2}) \sin \varphi \\ (R_{P1} + R_{P2}) \\ 0 \end{bmatrix} \quad (6.41)$$

Here, both radii of normal curvatures, namely  $R_{P1}$  and  $R_{P2}$ , are signed values. They are of positive values when the lines of intersection of the part surfaces  $P_1$  and  $P_2$  by a plane through the common perpendicular  $\mathbf{n}_{P1}$  are convex, and they are of negative values when the lines of intersection of the part surfaces by a plane through the common perpendicular are concave.

Further, the characteristic curve  $\mathbf{Pl}_R(P_1/P_2)$  can be reduced to a corresponding planar characteristic curve. Omitting the intermediate considerations, one may wish to go directly to the “*-relative indicatrix*” at a point of contact of the part surfaces  $P_1$  and  $P_2$ .

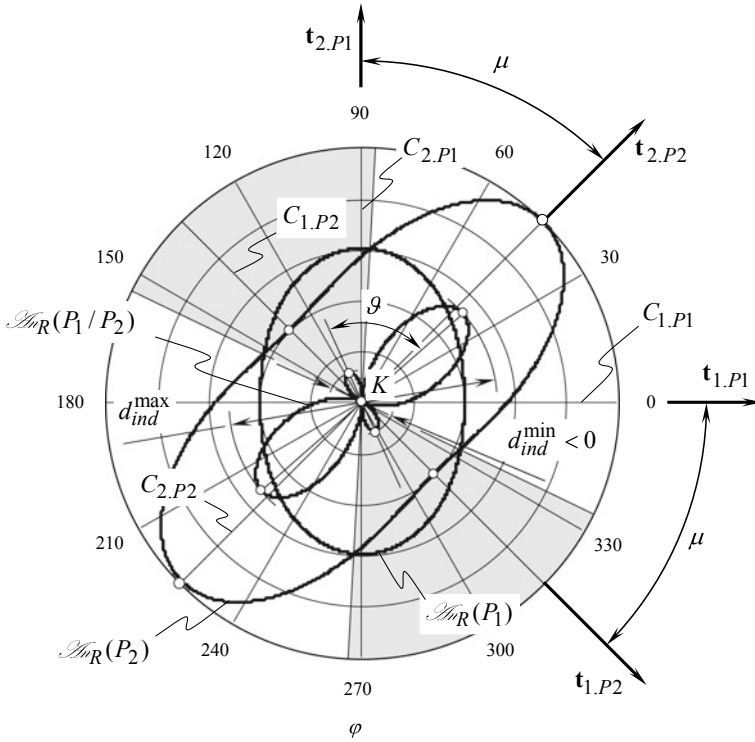


**Fig. 6.3** An example of the “ $\mathcal{H}_R(P_1/P_2)$ -relative indicatrix” at a point of contact  $K$  of two part surfaces  $P_1$  and  $P_2$  ( $R_{1.P1} = 2$  mm,  $R_{2.P1} = 3$  mm,  $R_{1.P2} = -2$  mm,  $R_{2.P2} = -5$  mm,  $\mu = 45^\circ$ ), plotted together with the corresponding “ $\mathcal{H}_R(P_1)$ -indicatrix” of the part surface  $P_1$ , and the “ $\mathcal{H}_R(P_2)$ -indicatrix” of the part surface  $P_2$  constructed at that same contact point  $K$

### 6.3.2 “ $\mathcal{H}_R(P_1/P_2)$ -Relative Indicatrix” at Point of Contact of Two Part Surfaces $P_1$ and $P_2$

Aiming for further simplification of the analytical description of the contact geometry of two part surfaces  $P_1$  and  $P_2$ , the “Plücker relative indicatrix,  $\mathcal{H}_R(P_1/P_2)$ ” can be replaced with the planar characteristic curve of a simpler structure. The equation of the 2D “ $\mathcal{H}_R(P_1/P_2)$ -relative indicatrix” at a point of contact of the part surfaces  $P_1$  and  $P_2$  can be derived from Eq. (6.41):

$$\mathcal{H}_R(P_1/P_2) \Rightarrow \mathbf{R}_{IR}(\varphi) = \begin{bmatrix} (R_{P1} + R_{P2}) \cos \varphi \\ (R_{P1} + R_{P2}) \sin \varphi \\ 0 \\ 0 \end{bmatrix} \quad (6.42)$$

This planar characteristic curve is referred to as the “ $\mathcal{H}_R(P_1/P_2)$ -relative indicatrix of the first kind.” The distribution of summa of normal radii of curvature at a point of contact  $K$  of the part surfaces  $P_1$  and  $P_2$  is described analytically by the “ $\mathcal{H}_R(P_1/P_2)$ -relative indicatrix of the first kind.”

In Eq. (6.42), the radii of normal curvature  $R_{P_1}$  and  $R_{P_2}$  can be expressed in terms of the corresponding principal radii of curvature  $R_{1,P_1}$ ,  $R_{2,P_1}$ , and  $R_{1,P_2}$ ,  $R_{2,P_2}$ , and in terms of the angle  $\mu$  of the part surfaces'  $P_1$  and  $P_2$  local relative orientation at the contact point  $K$ .

An example of the “ $\mathcal{H}_R(P_1/P_2)$ -relative indicatrix” at a point of contact of two part surfaces  $P_1$  and  $P_2$  is shown in Fig. 6.3. Parameters of the characteristic curve  $\mathcal{H}_R(P_1/P_2)$  are calculated at point of contact of the convex elliptic local patch of the part surface  $P_1$  ( $R_{1,P_1} = 3$  mm, and  $R_{2,P_1} = 15$  mm), and the concave elliptic local patch of the part surface  $P_2$  ( $R_{1,P_2} = -2$  mm, and  $R_{2,P_2} = -5$  mm). The part surfaces  $P_1$  and  $P_2$  are turned around the common perpendicular  $\mathbf{n}_{P_1}$  with respect to one another through the angle of local relative orientation  $\mu = 45^\circ$ . The corresponding “ $\mathcal{H}_R(P_1)$ -indicatrix” as well as the “ $\mathcal{H}_R(P_1)$ -indicatrix” is also plotted in Fig. 6.3. It is of importance to point out here that the direction of the minimum diameter  $d_{ind}^{\min}$  and the direction of the maximum diameter  $d_{ind}^{\max}$  of the characteristic curve  $\mathcal{H}_R(P_1/P_2)$  do not align either with the principal directions  $\mathbf{t}_{1,P_1}$  and  $\mathbf{t}_{2,P_1}$  on the part surface  $P_1$  or with the principal directions  $\mathbf{t}_{1,P_2}$  and  $\mathbf{t}_{2,P_2}$  on the part surface  $P_2$ . The extremal directions of the “ $\mathcal{H}_R(P_1/P_2)$ -relative indicatrix” are not orthogonal to one other. In the general case of two part surfaces in contact, they make a certain angle  $\vartheta \neq 90^\circ$ .

The following statement can be made at this point:

**Conclusion 6.1** *In the general case of part surfaces in contact, the directions of the extremal (i.e., of maximum minimum) degree of conformity of two surfaces  $P_1$  and  $P_2$  at the contact point  $K$  are not orthogonal to one another. The directions of the extremal degree of conformity of the part surface  $P_1$  and  $P_2$  could be orthogonal to one another only in a particular (degenerated) cases of the surfaces contact.*

The shape and parameters of the “ $\mathcal{H}_R(P_1/P_2)$ -relative indicatrix” depend upon the algebraic values of the principal radii of curvature  $R_{1,P_1}$ ,  $R_{2,P_1}$  and  $R_{1,P_2}$ ,  $R_{2,P_2}$  at a point of contact of the part surfaces  $P_1$  and  $P_2$ , as well as on the actual value of the angle  $\mu$  of the part surfaces  $P_1$  and  $P_2$  local relative orientation.

The “Dupin indicatrix  $Dup(\mathcal{H})$ ” at a point of the surface of relative curvature indicates that the directions of the extremum degree of conformity of the part surfaces  $P_1$  and  $P_2$  at the contact point  $K$  are always perpendicular to one another. The above consideration reveals that this is not correct and results in errors of calculations.

The characteristic curve  $\mathcal{H}_R(P_1/P_2)$  is of simpler structure rather than the “Plücker relative indicatrix,  $\mathcal{P}_R(P_1/P_2)$ ” itself. The “ $\mathcal{H}_R(P_1/P_2)$ -relative indicatrix” is always a kind of planar curve, while the “Plücker relative indicatrix,  $\mathcal{P}_R(P_1/P_2)$ ” is always a spatial 3D curve. This makes use of the characteristic curve  $\mathcal{H}_R(P_1/P_2)$ , preferred rather than the “Plücker relative indicatrix,  $\mathcal{P}_R(P_1/P_2)$ .”

The distribution of the differences between normal curvatures of the part surfaces  $P_1$  and  $P_2$  at the contact point  $K$  can be described analytically by a planar characteristic curve of another kind:

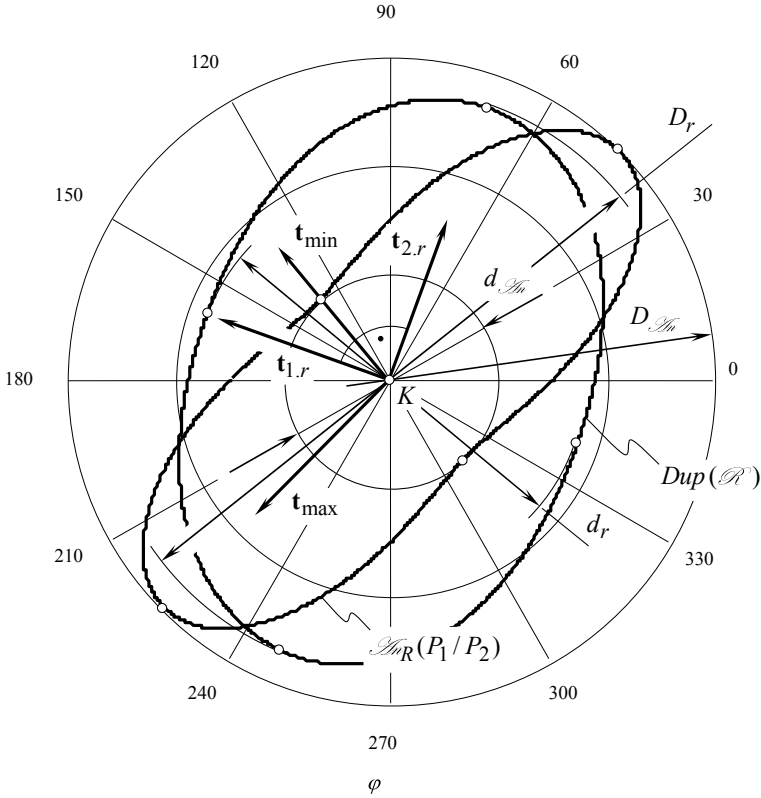


**Fig. 6.4** Comparison of the *-relative indicatrix* of two part surfaces  $P_1$  and  $P_2$  in contact with the *Dupin indicatrix*  $Dup(\mathcal{R})$  of the surface of relative curvature for that same part surfaces  $P_1$  and  $P_2$

$$\mathcal{M}_k(P_1/P_2) \Rightarrow \mathbf{R}_{ik}(\varphi) = \begin{bmatrix} (k_{P1} - k_{P2}) \cos \varphi \\ (k_{P1} - k_{P2}) \sin \varphi \\ 0 \\ 1 \end{bmatrix} \quad (6.43)$$

The characteristic curve [see Eq. (6.43)] is referred to as the “ $\mathcal{M}_k(P_1/P_2)$ -relative indicatrix of the second kind”.

Equation (6.43) of the “ $\mathcal{M}_k(P_1/P_2)$ -indicatrix” can be expressed in terms of radii of principal curvature of the contacting part surfaces  $P_1$  and  $P_2$ :

$$\mathcal{M}_k(P_1/P_2) \Rightarrow \mathbf{R}_{ik}(\varphi) = \begin{bmatrix} [k_{1,P1} \cos \varphi + k_{2,P1} \sin \varphi - k_{1,P2} \cos(\varphi + \mu) - k_{2,P2} \sin(\varphi + \mu)] \cos \varphi \\ [k_{1,P1} \cos \varphi + k_{2,P1} \sin \varphi - k_{1,P2} \cos(\varphi + \mu) - k_{2,P2} \sin(\varphi + \mu)] \sin \varphi \\ 0 \\ 1 \end{bmatrix} \quad (6.44)$$

The difference between the “ $\mathcal{H}_R(P_1/P_2)$ -relative indicatrix of the second kind” and between the “Dupin indicatrix,  $Dup(\mathcal{H})$ ” of the surface of relative curvature is clear illustrated in Fig. 6.4.

The planar characteristic curves  $\mathcal{H}_R(P_1)$  and  $\mathcal{H}_k(P_1)$ , as well as the characteristic curves  $\mathcal{H}_R(P_2)$  and  $\mathcal{H}_k(P_2)$  originate from the “Plücker conoid.” Equations (6.37), (6.38) and (6.42), (6.43) of the corresponding indicatrices,  $\mathcal{H}_R(P_1)$ ,  $\mathcal{H}_k(P_1)$  and,  $\mathcal{H}_R(P_2)$ ,  $\mathcal{H}_k(P_2)$  are derived on the premise of Eq. (6.8) of the surface of “Plücker conoid” (see [8], and Sect. 4.9, pp. 257–260 in [9]).

It is proven analytically that both planar characteristic curves, say the characteristic curve  $\mathcal{H}_R(P_1/P_2)$ , and the “indicatrix of conformity  $Cnf_R(P_1/P_2)$ ” at a point of contact of two smooth regular part surfaces  $P_1$  and  $P_2$  specify that same direction  $\mathbf{t}_{cnf}^{\max}$  at which the degree of conformity of the part surfaces  $P_1$  and  $P_2$  reaches its maximum value. Both the characteristic curves,  $Cnf_R(P_1/P_2)$  and  $\mathcal{H}_R(P_1/P_2)$ , are powerful tools in engineering geometry of surfaces. They are extensively used for the analysis of the geometry of contact of two smooth regular part surfaces  $P_1$  and  $P_2$ .

## References

1. Plücker, J. (1865). On a new geometry of space. *Philosophical Transactions of the Royal Society*, 155, 725–791.
2. Radzevich, S. P. (2004). A possibility of application of plücker conoid for mathematical modeling of contact of two smooth regular surfaces in the first order of tangency. *Mathematical and Computer Modeling*, 42, 999–1022.
3. von Seggern, D. (1993). *CRC standard curves and surfaces* (p. 288). Boca Raton, FL: CRC Press.
4. Fisher, G. (Ed.) (1986). *Mathematical models*. Braunachweig/Wiesbaden: Friedrich Vieweg & Sohn.
5. Gray, A. (1997). Plücker Conoid. *Modern differential geometry of curves and surfaces with mathematics* (2nd ed., pp. 435–437). Boca Raton, FL: CRC Press.
6. <http://www.mathcurve.com/surfaces/plucker/plucker.shtml>.
7. Struik, D. J. (1961). *Lectures on classical differential Geometry* (2nd ed., p. 232). Massachusetts: Addison-Wesley Publishing Company Inc.
8. Radzevich, S. P. (1991). *Sculptured Surface Machining on Multi-Axis NC Machine*, Monograph, Kiev, Vishcha Schola, 192 p.
9. Radzevich, S. P. (2001). *Fundamentals of surface Generation*, Monograph, Kiev, Rastan, 592 p.

## Chapter 7

# Possible Kinds of Contact of Two Smooth Regular Part Surfaces in the First Order of Tangency



Interaction of two part surfaces in contact is of tremendous importance for plurality of engineering applications. Therefore, analysis and classification of all possible kinds of contact of two smooth regular part surfaces  $P_1$  and  $P_2$  in the first order of tangency is a critical issue in engineering geometry of surfaces. Development of scientific classification of all possible kinds of contact of part surfaces  $P_1$  and  $P_2$  could be considered as the ultimate point in the analysis of the part surfaces  $P_1$  and  $P_2$  contact.

Prior to discussing this important issue, two more particular issues need to be mentioned.

The first issue relates to the possibility of implementation of the indicatrix of conformity for the identification of the actual kind of contact of two part surfaces  $P_1$  and  $P_2$ .

The second issue relates to the impact of the accuracy of the computations on the desired parameters of the indicatrix of conformity  $Cnf_R(P_1/P_2)$  at a point of contact of the part surfaces  $P_1$  and  $P_2$ , that is, onto the directions of extreme degree of their conformity.

### 7.1 On a Possibility of Implementation of the Indicatrix of Conformity for the Purposes of Identification of the Actual Kind of Contact of Two Smooth Regular Part Surfaces

Two regular part surfaces  $P_1$  and  $P_2$  can make contact either at a point, or along a line, or ultimately over a surface patch. Actually, the kind of contact of two part surfaces results in certain features in the shape and the parameters of the indicatrix of conformity  $Cnf_R(P_1/P_2)$  of the contacting part surfaces  $P_1$  and  $P_2$ .

As follows from Eqs. (6.34) and (6.35), special features in the shape and the parameters of the indicatrix of conformity  $Cnf_R(P_1/P_2)$  are inherited to every pos-



sible kind of contact of the part surfaces  $P_1$  and  $P_2$ . For example, when two smooth regular part surfaces  $P_1$  and  $P_2$  make contact:

(a) at a point  $K$  (Fig. 7.1a), then the minimum diameter  $d_{cnf}^{\min}$  of the indicatrix of

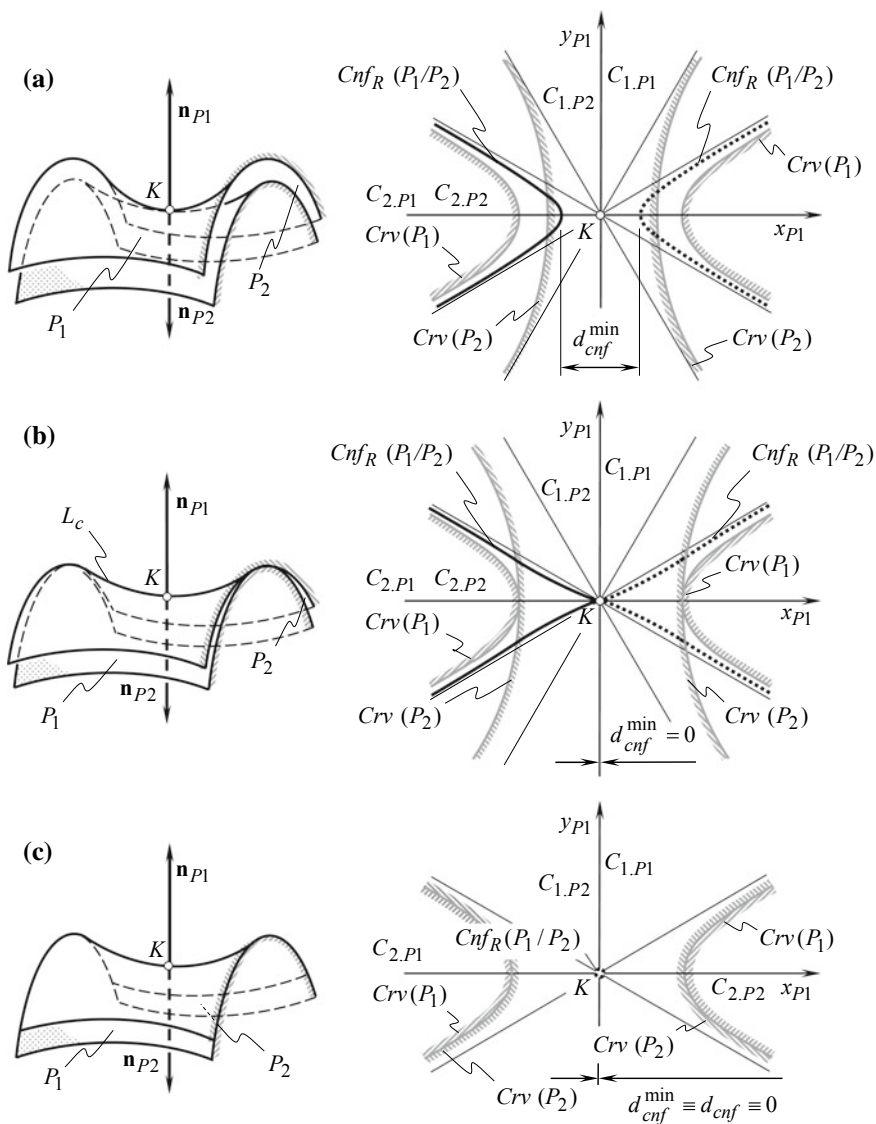


**Fig. 7.1** Correspondence between the shape of the indicatrix of conformity  $Cnf_R(P_1/P_2)$  and the kind of contact of two part surfaces  $P_1$  and  $P_2$ : **a** point contact, **b** line contact, and **c** surface contact

- conformity  $Cnf_R(P_1/P_2)$  at a point of contact (as well as all other diameters of this characteristic curve) is always of a positive value ( $d_{cnf}^{\min} > 0$ );
- (b) along a curve  $L_c$  (Fig. 7.1b), then the minimum diameter  $d_{cnf}^{\min}$  of the indicatrix of conformity  $Cnf_R(P_1/P_2)$  at a point of contact is always identical to zero ( $d_{cnf}^{\min} \equiv 0$ ), while all other diameters of this characteristic curve are of a positive value ( $d_{cnf} > 0$ ), and finally
- (c) over a surface patch (Fig. 7.1c), then the indicatrix of conformity at a point of contact of the part surfaces  $P_1$  and  $P_2$  shrinks to a point, which coincides with the point  $K$  of contact of the part surfaces  $P_1$  and  $P_2$ .

The above examples are worked out for the cases of the part surfaces  $P_1$  and  $P_2$  contact, when in the local vicinity of the contact point  $K$  both of the surfaces  $P_1$  and  $P_2$  are smooth regular surfaces of saddled type (having negative “Gauss curvature”  $\mathcal{G}_{P_1} < 0$ , and  $\mathcal{G}_{P_2} < 0$ ). A similarity is observed for all other types of local patches of part surfaces  $P_1$  and  $P_2$  as well.

In a case when the part surfaces  $P_1$  and  $P_2$  intersect one another, that is, the interference of the surfaces  $P_1$  and  $P_2$  into each other is observed as illustrated schematically in Fig. 5.6, then the minimum diameter of the indicatrix of conformity  $Cnf_R(P_1/P_2)$  at a point of contact of the part surfaces  $P_1$  and  $P_2$  is always of a negative value ( $d_{cnf}^{\min} < 0$ ).

It is of importance to make difference between partial and full interference of the part surfaces  $P_1$  and  $P_2$  in the differential vicinity of the contact point  $K$ .

For instance, in the differential vicinity of the point of contact  $K$ , a convex elliptical local patch of the part surface  $P_2$  can partially intersect a hyperbolic local patch of the part surface  $P_1$  (Fig. 5.6a). In this case, the minimum diameter  $d_{cnf}^{\min}$  of the indicatrix of conformity  $Cnf_R(P_1/P_2)$  is of a negative value ( $d_{cnf}^{\min} < 0$ ). Owing to this, the indicatrix of conformity  $Cnf_R(P_1/P_2)$  not only intersects itself, but intersection of each of its branches also occurs. Varying the angular parameter  $\varphi$  within the interval  $0 \leq \varphi \leq \pi$ , positive ( $d_{cnf} > 0$ ), as well as negative ( $d_{cnf} < 0$ ) values of the current diameter  $d_{cnf}$  of the characteristic curve  $Cnf_R(P_1/P_2)$  are observed.

Another example: In the differential vicinity of the contact point  $K$ , the local patch of the part surface  $P_2$  interferes into a local patch of the part surface  $P_1$  totally, as shown for two hyperbolic local patches (Fig. 5.6b) and for two parabolic (Fig. 5.6c) local patches of the part surfaces  $P_1$  and  $P_2$ . For the cases of total local interference of the part surfaces  $P_1$  and  $P_2$ , the minimum diameter  $d_{cnf}^{\min}$  of the indicatrix of conformity  $Cnf_R(P_1/P_2)$  is always of a negative value ( $d_{cnf}^{\min} < 0$ ), as well as all other diameters  $d_{cnf}$  of this characteristic curve  $Cnf_R(P_1/P_2)$  are also of a negative value, regardless of the actual value of the angular parameter  $\varphi$ .

The examples above show that every type of contact of the part surfaces  $P_1$  and  $P_2$  features important peculiarities in the shape and parameters of the indicatrix of conformity  $Cnf_R(P_1/P_2)$  at the point  $K$  of contact of the part surfaces  $P_1$  and  $P_2$ . The shape and the parameters of the characteristic curve  $Cnf_R(P_1/P_2)$  uniquely follow from the actual kind of contact of the part surfaces  $P_1$  and  $P_2$  and are completely

predetermined by the actual kind of contact of these surfaces. Here, it is natural to assume that the inverse statement could also be true. The question can be formulated as follows:

**Question 7.1** *Are the features in the shape and parameters of the indicatrix of conformity  $Cnf_R(P_1/P_2)$  at a point of contact of two part surfaces in contact  $P_1$  and  $P_2$  necessary and sufficient for drawing a conclusion regarding the kind of surfaces'  $P_1$  and  $P_2$  contact: contact at a point, along a curve  $L_c$ , or over a surface patch?*

Or, in another words, could the value and sign of the minimum diameter  $d_{cnf}^{\min}$  of the indicatrix of conformity  $Cnf_R(P_1/P_2)$  and the features in its shape be implemented as a criterion for determining uniquely the kind of contact of the part surfaces  $P_1$  and  $P_2$ ?

The detailed investigation of this particular sub-problem enables one to make the following statement:

**Conclusion 7.1** *The actual value and sign of the minimum diameter  $d_{cnf}^{\min}$  of the indicatrix of conformity  $Cnf_R(P_1/P_2)$  at a point of contact of two part surfaces  $P_1$  and  $P_2$ , as well as features in the shape of this characteristic curve, cannot be implemented as a sufficient criterion for determining uniquely the actual kind of contact of the part surfaces  $P_1$  and  $P_2$ .*

The positive value of the minimum diameter  $d_{cnf}^{\min}$  of the indicatrix of conformity  $Cnf_R(P_1/P_2)$  (that is,  $d_{cnf}^{\min} > 0$ ) is a sufficient but not a necessary requirement for contact of the part surfaces  $P_1$  and  $P_2$  at a point.

The indicatrix of conformity  $Cnf_R(P_1/P_2)$ , that is shrunk to the contact point  $K$ , is not sufficient to identify the kind of contact of the part surfaces  $P_1$  and  $P_2$  over a surface patch. However, if two part surfaces  $P_1$  and  $P_2$  are congruent to each other within a certain surface patch, then the indicatrix of conformity shrinks to a point, which coincides with the point of contact  $K$ . The inverse statement is not correct. In the event of the indicatrix of conformity  $Cnf_R(P_1/P_2)$  shrinking to a point, then the part surfaces  $P_1$  and  $P_2$  can be congruent to one another only "locally." Thus, if the indicatrix of conformity  $Cnf_R(P_1/P_2)$  shrinks to the contact point  $K$ , this indicates only a necessary but not a sufficient condition for the part surfaces  $P_1$  and  $P_2$  contact over a certain surface patch. In the case under consideration, the part surfaces  $P_1$  and  $P_2$  can make contact along a characteristic curve  $L_c$  and/or at a point  $K$  as well.

If the minimum diameter  $d_{cnf}^{\min}$  of the indicatrix of conformity  $Cnf_R(P_1/P_2)$  at a point of contact of the part surfaces  $P_1$  and  $P_2$  is equal to zero, this does not necessarily mean that the part surfaces  $P_1$  and  $P_2$  make contact along a curve  $L_c$ . This requirement is only a necessary but not a sufficient condition for the line contact of two smooth regular part surfaces. In the event  $d_{cnf}^{\min} = 0$ , the part surfaces  $P_1$  and  $P_2$  can make contact at a point.

As follows from the above discussion, in the event, the part surfaces  $P_1$  and  $P_2$  make contact along a line  $L_c$ , then the direction along the minimum diameter  $d_{cnf}^{\min}$  of the indicatrix of conformity  $Cnf_R(P_1/P_2)$  at a point of contact of the part surfaces  $P_1$  and  $P_2$  is aligned with the tangent line to the curve  $L_c$  at the contact

point  $K$ . This issue is of importance for engineering geometry of surfaces because it follows directly from the statement made above. According to this statement, in the differential vicinity of the point of contact  $K$ , the direction, along which minimum diameter  $d_{cnf}^{\min}$  can be measured, is aligned with the direction, along which the degree of conformity at a point of contact of the part surfaces  $P_1$  and  $P_2$  reaches a maximal value. Therefore, at the contact point  $K$ , the direction along the minimum diameter  $d_{cnf}^{\min}$  and the direction that is tangent to the line of contact  $L_c$  align to one another. Hence, contact point  $K$  is a point of tangency of:

- (a) the straight line that aligns with the direction in which the minimum diameter  $d_{cnf}^{\min}$  of the indicatrix of conformity  $Cnf_R(P_1/P_2)$  is measured, and
- (b) the line of contact  $L_c$  of the part surfaces  $P_1$  and  $P_2$ .

The statements above are also true for the inverse indicatrix of conformity  $Cnf_k(P_1/P_2)$  at a point of contact of the part surfaces  $P_1$  and  $P_2$  in the first order of tangency.

It is of critical importance to stress here that some of the conclusions similar to those listed above could be made based on other known approaches. This proves indirectly that the proposed novel approach for analytical description of the geometry of contact of two smooth regular part surfaces in the first order of tangency is in perfect agreement with the earlier developed approaches in the field. In a case when the contacting part surfaces are of a simple geometry (that is, planes, spheres, cylinders of revolution), implementation of the discussed approach, as well as implementation of known approaches for analytical description of contact geometry of two part surfaces returns identical results. If the contacting part surfaces are of a complex geometry, then implementation only of the indicatrix of conformity (of both kinds), or of the relative indicatrix (of both kinds), and not of any other characteristic curve, enable correct results of computation of parameters of the geometry of contact of two surfaces.

### ***7.1.1 Impact of Accuracy of Computation on the Parameters of the Indicatrices of Conformity $Cnf_R(P_1/P_2)$***

All the calculations, whether performed manually or by computer, are subject to errors of the computation. No calculations of any kind are performed with zero error. Errors of the calculation are unavoidable for many reasons.

The accuracy of calculation affects the desired parameters of the indicatrix of conformity  $Cnf_R(P_1/P_2)$  at a point of contact of the part surfaces  $P_1$  and  $P_2$ . For a predetermined error of the calculation, the optimal parameters of the characteristic curve  $Cnf_R(P_1/P_2)$  can be computed. As is known, the characteristic curve  $Cnf_R(P_1/P_2)$  is a function of the design parameters of two part surfaces  $P_1$  and  $P_2$  and of their relative orientation. Commonly, the design parameters of the given part

surfaces  $P_1$  and  $P_2$  cannot be changed (except for a scenario when elastic deformation of the contacting parts is encountered).

Figure 7.2 illustrates a portion of the indicatrix of conformity  $Cnf_R(P_1/P_2)$  for a certain kind of contact of the smooth regular part surfaces  $P_1$  and  $P_2$ . The actual arc of the indicatrix of conformity within the direction through the points  $A$  and  $B$  along which the minimum diameter  $d_{cnf}^{\min}$  of the indicatrix of conformity is measured and is approximated by a circular arc. The radius of the circular arc  $\rho_{r.cnf}$  is equal to the radius of curvature of the indicatrix of conformity  $Cnf_R(P_1/P_2)$  at the point  $B$ . The radius  $\rho_{r.cnf}$  can be calculated from the equation:

$$\rho_{r.cnf}(\varphi, \mu) = \frac{\left[ r_{cnf}^2 + \left( \frac{\partial r_{cnf}}{\partial \varphi} \right)^2 \right]^{\frac{3}{2}}}{r_{cnf}^2 + 2 \left( \frac{\partial r_{cnf}}{\partial \varphi} \right)^2 - r_{cnf} \cdot \frac{\partial^2 r_{cnf}}{\partial^2 \varphi}} \quad (7.1)$$

As follows from Fig. 7.2, the error  $\Delta d_{cnf}^{\min}$  of the calculation of the minimum diameter  $d_{cnf}^{\min}$  of the indicatrix of conformity  $Cnf_R(P_1/P_2)$  causes the deviation  $\Delta\varphi$  of the direction, along which the minimum diameter  $d_{cnf}^{\min}$  of the indicatrix of conformity is measured. The deviation  $\Delta\varphi$  can be computed from the equation:

$$\Delta\varphi = \cos^{-1} \left[ \frac{0.25 \cdot (d_{cnf}^{\min} + \Delta d_{cnf}^{\min})^2 + (0.5 \cdot d_{cnf}^{\min} + \rho_{r.cnf})^2}{2 \cdot (0.5 \cdot d_{cnf}^{\min} + \rho_{r.cnf}) \cdot (d_{cnf}^{\min} + \Delta d_{cnf}^{\min})} \right] \quad (7.2)$$

An example of the function  $\Delta\varphi = \Delta\varphi(\rho_{r.cnf})$  is plotted in Fig. 7.3. It is of

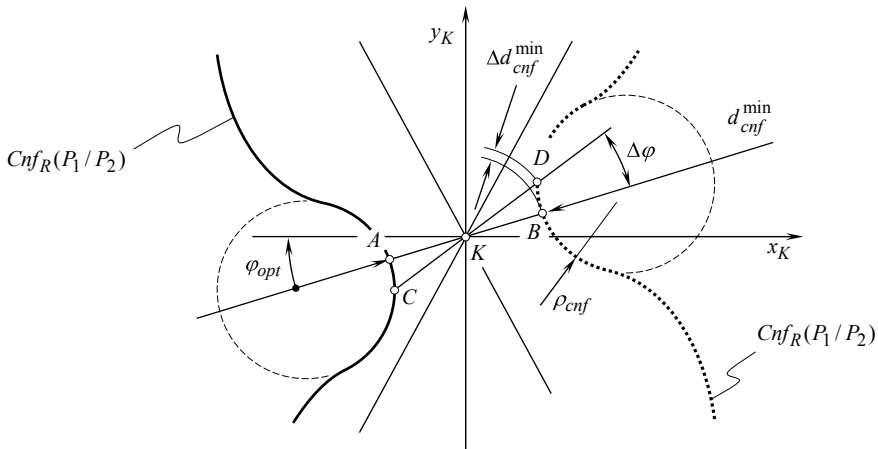


**Fig. 7.2** Local vicinity of the indicatrix of conformity  $Cnf_R(P_1/P_2)$  at a point of contact of two part surfaces  $P_1$  and  $P_2$

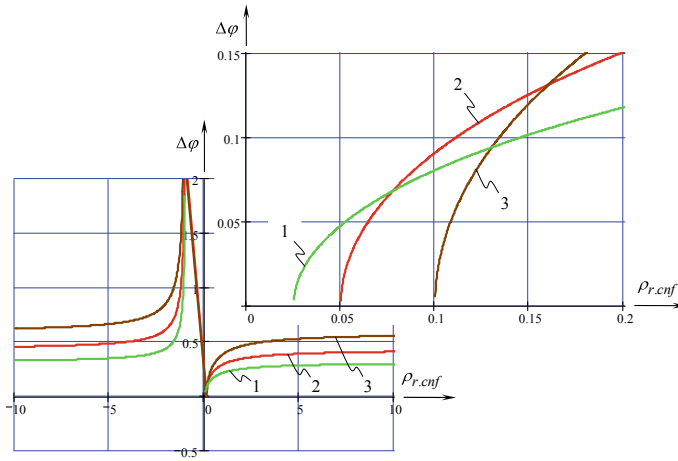


**Fig. 7.3** Illustration of the impact of the errors in the calculation on the direction of the maximum degree of conformity at a point of contact of two smooth regular part surfaces  $P_1$  and  $P_2$

importance to point out here that:

- firstly, the optimal value of the radius  $\rho_{r.cnf}$  is not equal to zero, and
- secondly, the optimal value of the radius  $\rho_{r.cnf}$  depends on the geometry of both, the part surfaces  $P_1$  and  $P_2$ , and on the surfaces' relative configuration.

Similar calculations can be performed with respect to the calculation of optimal parameters of the characteristic curves of other kinds as well.

The consideration above can be employed for the enhancement of the classification of possible kinds of contact of two smooth regular part surfaces  $P_1$  and  $P_2$  in the first order of tangency.

### 7.1.2 Classification of Possible Kinds of Contact of Two Smooth Regular Part Surfaces

Classification of possible kinds of contact of two smooth regular part surfaces in the first order of tangency is of importance for implementation of the methods those developed in engineering geometry of surfaces. The analysis discussed above makes possible the development of a scientific classification of all possible kinds of contact of two smooth regular surfaces  $P_1$  and  $P_2$ .

The following statement is implemented below as a postulate:

**Statement 7.1** *If two surfaces  $P_1$  and  $P_2$  make contact with one another, then there is at least one point of their contact.*

Two smooth regular part surfaces  $P_1$  and  $P_2$  can make contact:

- (a) at a point  $K$  (or at a certain number of distinct contact points  $K_i$ ),
- (b) along a line  $L_c$  (or along several lines of contact  $L_c^i$ ), or
- (c) within a certain surface patch.

No other kinds of part surfaces contact are feasible. This is mostly due to the fundamental properties of the 3D space we live in.

The following three kinds of part surfaces contact are evident. They are

- (a) Point contact
- (b) Line contact, and
- (c) Surface contact of two smooth regular part surfaces.

These three kinds of part surfaces contact are not only evident, but they are trivial.

In this point, we turn the readers' attention here to the following:

**1. Consider the *point kind of contact* of two part surfaces  $P_1$  and  $P_2$ .** When the part surfaces  $P_1$  and  $P_2$  make contact at a distinct point, then three different kinds of point contact can be recognized:

**1.1.** There are no normal plane sections through the contact point  $K$  of the part surfaces  $P_1$  and  $P_2$ , at which normal curvatures  $k_{P_1}$  and  $k_{P_2}$  of the part surfaces  $P_1$  and  $P_2$  are of the same magnitude and opposite sign. The equality  $k_{P_1} = -k_{P_2}$  is observed in no plane section of the part surfaces  $P_1$  and  $P_2$  through the common unit normal vector  $\mathbf{n}_{P_1}$ . This kind of the surface contact is referred to as the "*true point contact*" of two part surfaces. If two part surfaces make true point contact, then the expression  $k_{P_1}(\varphi) \neq -k_{P_2}(\varphi, \mu)$  is valid for any value of the angle  $\varphi$ .

**1.2.** There is only one normal plane section of the part surfaces  $P_1$  and  $P_2$  through the contact point  $K$ , at which the normal curvatures  $k_{P_1}$  and  $k_{P_2}$  of the part surfaces  $P_1$  and  $P_2$  are of the same magnitude and opposite sign. Thus, the equality  $k_{P_1} = -k_{P_2}$  is observed in a single plane section of the part surfaces  $P_1$  and  $P_2$  through the common unit normal vector  $\mathbf{n}_{P_1}$ . In this plane section, the part surfaces  $P_1$  and  $P_2$  make contact along infinitely short arc. The torsion of the part surfaces  $P_1$  and  $P_2$  along the infinitely short arc of contact is identical to one another, that is, geodesic (relative) torsions  $\tau_{g.P_1} \equiv \tau_{g.P_2}$  are identical. This kind of part surface contact is referred to as the "*locally line contact*" of the part surfaces. When two part surfaces are in "*locally line contact*," then the expression  $k_{P_1}(\varphi) = -k_{P_2}(\varphi, \mu)$  is valid for a certain value of  $\varphi$ .

As long as the second-order (and not a higher order) derivatives are considering, then the "*locally line contact*" of two part surfaces is identical to the "*true line contact*" of the surfaces.

**1.3.** Normal curvatures  $k_{P_1}$  and  $k_{P_2}$  of the part surfaces  $P_1$  and  $P_2$  are of the same magnitude and opposite sign in all normal plane section through the point of contact  $K$  of the surfaces  $P_1$  and  $P_2$ . Thus, the identity  $k_{P_1} \equiv -k_{P_2}$  holds in all plane sections through the common unit normal vector  $\mathbf{n}_{P_1}$  of the part surfaces  $P_1$  and  $P_2$ . In the case under consideration, the part surfaces  $P_1$  and  $P_2$  make contact within the infinitely small area. This kind of part surface contact is referred to as the "*locally surface contact of the first kind*."

As long as the second-order (and not a higher order) derivatives are considering, then the “*locally surface contact of the first kind*” is identical to the true surface contact of two part surfaces.

**2.** Consider the **line kind of contact** of two part surfaces  $P_1$  and  $P_2$ . When the part surfaces  $P_1$  and  $P_2$  make contact along a line, two different kinds of line contact can be distinguished.

**2.1.** There is only one normal plane section through the contact point  $K$  of the part surfaces  $P_1$  and  $P_2$ , at which the normal curvatures  $k_{P1}$  and  $k_{P2}$  of the part surfaces  $P_1$  and  $P_2$  are of the same magnitude and opposite sign. This normal plane section is congruent to the osculate plane of the line of contact  $L_c$  at the contact point  $K$  within the line  $L_c$ . Thus, the equality  $k_{P1} = -k_{P2}$  is observed in a single plane section of the part surfaces  $P_1$  and  $P_2$  through the common unit normal vector  $\mathbf{n}_{P1}$ . The torsion of the part surfaces  $P_1$  and  $P_2$  along the arc of contact is identical, that is, geodesic (relative) torsions  $\tau_{g.P1} \equiv \tau_{g.P2}$  are identical. This kind of two part surface contact is referred to as the “*true line contact*” of the surfaces. When two surfaces are in “*true line contact*,” then the expression  $k_{P1}(\varphi) = -k_{P2}(\varphi, \mu)$  is valid for a certain value of  $\varphi$ .

The geodesic (relative) torsion  $\tau_{g.P1}$  of the line of contact  $L_c$  determines the rate of rotation of the tangent plane to the part surface  $P_1$  about the line of contact  $L_c$ . It is assumed that the line of contact  $L_c$  and the part surface  $P_1$  are regular, and the rate of rotation of the tangent plane is a function of the length  $s$  of the line of contact  $L_c$ . The relative torsion can be defined by a point on the line of contact  $L_c$  and by a direction on the part surface  $P_1$ . It is equal to the torsion of the geodesic curve in that same direction:

$$\tau_{g.P1} = \left[ \frac{d\mathbf{r}_{Lc}}{ds_1} \times \mathbf{n}_{P1} \cdot \frac{d\mathbf{n}_{P1}}{ds_1} \right] = \tau_{Lc} + \frac{d\phi}{ds_1} = (k_{1.P1} - k_{2.P1}) \sin \kappa_1 \cos \kappa_1 \quad (7.3)$$

Here we denote:

$\mathbf{r}_{Lc}$	the position vector of a point of the line of contact $L_c$
$\mathbf{n}_{P1}$	the unit normal vector to the part surface $P_1$
$\tau_{Lc}$	the regular torsion of the line of contact $L_c$
$\phi$	the angle made by the osculating plane to $L_c$ and the tangent plane to $P_1$
$k_{1.P1}$ and $k_{2.P1}$	the principal curvatures of the part surface $P_1$ at the contact point $K$
$\kappa_1$	the angle made by the tangent to the line of contact $L_c$ at the contact point $K$ and the first principal direction $\mathbf{t}_{1.P1}$ of the part surface $P_1$

**2.2.** The normal curvatures  $k_{P1}$  and  $k_{P2}$  of the part surfaces  $P_1$  and  $P_2$  are of the same magnitude and opposite sign in all normal plane section of the part surfaces  $P_1$  and  $P_2$  at the contact point  $K$ . Thus, the identity  $k_{P1} \equiv -k_{P2}$  is observed in all plane sections through the common unit normal vector  $\mathbf{n}_{P1}$  of the part surfaces  $P_1$  and  $P_2$ . In the case under consideration, the part surfaces  $P_1$  and  $P_2$  make contact



within an infinitely small area. This kind of the surface contact is referred to as the “*locally surface contact of the second kind*.”

As long as the second-order (and not a higher order) derivatives are considering, then the “*locally surface contact of the second kind*” is identical to the true “*surface contact*” of the surfaces. In differential vicinity of the contact point  $K$ , the part surfaces  $P_1$  and  $P_2$  are locally congruent to each other.

**3.** Consider the **surface kind of contact** of two part surfaces  $P_1$  and  $P_2$ . When the part surfaces  $P_1$  and  $P_2$  make contact within a surface patch, just one kind of contact can be recognized.

**3.1.** The normal curvatures  $k_{P_1}$  and  $k_{P_2}$  of the part surfaces  $P_1$  and  $P_2$  are of the same magnitude and opposite sign in all normal plane sections at the point of contact  $K$  of the part surfaces  $P_1$  and  $P_2$ . Thus, the identity  $k_{P_1} \equiv -k_{P_2}$  is observed in all plane sections through the common unit normal vector  $\mathbf{n}_{P_1}$  of the part surfaces  $P_1$  and  $P_2$ . In the case under consideration, the part surfaces  $P_1$  and  $P_2$  make contact within a surface patch. This kind of part surfaces contact is referred to as the “*true surface contact*” of surfaces.

Without going into details, in many engineering applications, it is desired to maintain a kind of contact of two part surfaces  $P_1$  and  $P_2$ , which features the highest possible degree of conformity of the contacting part surfaces  $P_1$  and  $P_2$ .

In practice, when making calculations of the parameters of contact geometry of two part surfaces  $P_1$  and  $P_2$ , deviations in one of two part surfaces' relative location and orientation with respect to the other part surface are always observed. The deviations of the part surfaces  $P_1$  and  $P_2$  configuration are inevitable. Owing to the deviations, the desired “*locally extremal kind of contact*” is replaced with another kind of contact of the part surfaces  $P_1$  and  $P_2$ . Such a replacement can be achieved with the introduction of the pre-calculated deviations of principal radii of curvature  $R_{1,P_2}$  and  $R_{2,P_2}$  of one of the contacting part surfaces. In cases when the pre-calculated deviations are “*small*,” then the so-called *quasi-kind of contact* of two part surfaces  $P_1$  and  $P_2$  occurs, instead of the desired “*locally extremal kind of contact*” of the part surfaces. Several kinds of quasi-contact of two surfaces are distinguished below. They are as follows:

- (a) “*quasi-line contact*” of two part surfaces  $P_1$  and  $P_2$ ,
- (b) “*quasi-surface of the first kind*,” and
- (c) “*quasi-surface of the second kind*” contact of two part surfaces  $P_1$  and  $P_2$ .

The required pre-calculated values of “*small*” deviations of the actual normal curvatures from there initially calculated values can be determined on the premise of the following consideration. When the maximum deviations in the actual configuration of one of two part surfaces (location and orientation of one of the part surface relative to the other part surface) occur, then the degree of conformity of the part surface  $P_2$  with respect to the part surface  $P_1$  must not exceed the degree of their conformity in one of the “*locally extremal kind of contact*” of the part surface. When the actual deviations of the configuration of one of the contacting surfaces do not exceed the corresponding tolerances, then one of the feasible kinds of “*quasi-contact*” of the part surfaces  $P_1$  and  $P_2$  is observed.

Evidently, the larger the deviations in the part surfaces' configuration, the larger the pre-calculated corrections in normal curvature of one of two contacting surfaces and vice versa.

In the ideal case, when there are no deviations in the part surfaces configuration, it is recommended to assign normal curvatures of the values that enable one of the locally extremal kind of contact of the part surfaces  $P_1$  and  $P_2$ . Locally surface contact of the second kind is the most preferred kind of contact of the part surfaces  $P_1$  and  $P_2$ . The locally surface contact of the second kind yields the minimum value of the radius  $r_{cnf}^{\min} = 0$  of the indicatrix of conformity  $Cnf_R(P_1/P_2)$  at a point of contact of two smooth regular part surfaces  $P_1$  and  $P_2$  in the first order of tangency.

In reality, pure surface kind of contact of two part surfaces  $P_1$  and  $P_2$  (when the equality  $r_{cnf}^{\min} = 0$  is observed) is not feasible at all. Owing to the deviations in the part surfaces configuration maintaining pure surface contact of the part surfaces  $P_1$  and  $P_2$  would inevitably result in interference of the part surface  $P_2$  beneath the part surface  $P_1$ . Therefore, it is preferred to maintain a kind of quasi-surface contact of the second kind instead of a "pure surface contact" of two part surfaces  $P_1$  and  $P_2$ . A quasi-surface contact of the part surfaces  $P_1$  and  $P_2$  avoids an interference of the part surface  $P_2$  within the interior of the part surface  $P_1$ . Moreover, the minimum radius  $r_{cnf}^{\min}$  of the characteristic curve  $Cnf_R(P_1/P_2)$  at a point of contact of the part surfaces  $P_1$  and  $P_2$  in the first order of tangency could be as close to zero as possible ( $r_{cnf}^{\min} > 0, r_{cnf}^{\min} \rightarrow 0, r_{cnf}^{\min} \neq 0$ ). In this way, the desired geometry of contact of two part surfaces can be assured.

Quasi-contact of the part surfaces  $P_1$  and  $P_2$  is observed only when deviations in the part surfaces configuration are incorporated into consideration.

**Definition 7.1 Quasi-line contact** of two part surfaces  $P_1$  and  $P_2$  is a kind of point contact of the part surfaces under which the actual tangency of the part surfaces is within the true point contact and the locally line contact, and it varies as a function of the deviations in the part surfaces configuration.

**Definition 7.2 Quasi-surface (of the first kind) contact** of two part surfaces  $P_1$  and  $P_2$  is a kind of point contact of the part surfaces under which actual tangency of the part surfaces is within the true point contact and the locally surface (of the first kind) contact, and it varies as a function of deviations in the part surfaces configuration.

**Definition 7.3 Quasi-surface (of the second kind) contact** of two part surfaces  $P_1$  and  $P_2$  is a kind of point contact of the part surfaces under which actual tangency of the part surfaces is within the true point contact to locally surface (of the second kind) contact, and it varies as a function of deviations in the part surfaces configuration.

The difference between various kinds of the quasi-contact of two part surfaces  $P_1$  and  $P_2$ , as well as the difference between the corresponding kinds of locally extremal contact of the part surfaces can be recognized only under the limit values of the allowed deviations in the part surfaces' configuration. In the event, when the actual deviations are below the tolerances, then various possible kinds of quasi-contact of the part surfaces cannot be distinguished from other non-quasi-kinds of

their contact. The only difference is in actual location of the point  $K$  of contact of the surfaces. Owing to the deviations, it shifts from the original position to a certain other location.

There are only nine principally different kinds of contact of two part surfaces  $P_1$  and  $P_2$ . In addition to:

- (i) the “*true point contact*,”
- (ii) the “*true line contact*,” and
- (iii) the “*true surface contact*,”

the following three locally extremal kinds of contact are possible as well:

- (a) the “*locally line contact*,”
- (b) the “*locally surface of the first kind of contact*,” and
- (c) the “*locally surface of the second kind of contact*.”

Three kinds of quasi-contact of the surfaces are also possible. They are listed immediately below:

- (A) the “*quasi-line contact*,”
- (B) the “*quasi-surface of the first kind of contact*,” and
- (C) the “*quasi-surface of the second kind of contact*” of the part surfaces  $P_1$  and  $P_2$ .

Taking into consideration that there are only ten different kinds of local patches of smooth regular part surfaces  $P_1$  and  $P_2$  (see Chap. 2, Fig. 2.4), each of nine kinds of the part surfaces contact can be represented in details. For this purpose, a square morphological matrix of dimension  $10 \times 10 = 100$  is composed. This matrix covers all possible combinations of the part surfaces' contact. One axis of the morphological matrix is represented with ten kinds of local patches of the part surface  $P_1$ , while other axis is represented with ten kinds of local patches of the part surface  $P_2$ . The morphological matrix contains as many as:

$$\sum_{m=1}^9 C_9^m = \frac{9!}{m!(9-m)!} = \frac{100-10}{2} + 10 = 55 \quad (7.4)$$

different combinations of the local patches of the part surfaces  $P_1$  and  $P_2$ . Only 55 of them are required to be investigated more in detail. The analysis reveals that the following kinds of contact of two part surfaces  $P_1$  and  $P_2$  are feasible:

- (a) 29 kinds of the true point contact,
- (b) 23 kinds of the true line contact,
- (c) six kinds of the true surface contact,
- (d) 20 kinds of the locally line contact,
- (e) seven kinds of the locally surface (of the first kind) of contact,
- (f) eight kinds of the locally surface (of the second kind) of contact
- (g) 20 kinds of the quasi-line contact,
- (h) seven kinds of the quasi-surface (of the first kind) of contact,

- (i) eight kinds of the quasi-surface (of the second kind) of contact.

This means that only:

$$29 + 23 + 6 + 20 + 7 + 8 + 20 + 7 + 8 = 128 \quad (7.5)$$

kinds of contact of two smooth regular part surfaces  $P_1$  and  $P_2$  are possible in nature.

For some kinds of the part surface contact, no restrictions are imposed on the actual value of the angle  $\mu$  of the part surfaces'  $P_1$  and  $P_2$  local relative orientation. For the remaining kinds of the part surfaces contact, a corresponding interval of the permissible value of the angle  $\mu$ :  $[\mu_{\min}] \leq \mu \leq [\mu_{\max}]$  can be determined. For particular cases of the part surfaces contact, the only feasible value  $\mu = [\mu]$  is allowed.

On the premise of the above analysis, a scientific classification of all possible kinds of contact of two smooth regular part surfaces  $P_1$  and  $P_2$  is developed (Fig. 7.4).

The classification (Fig. 7.4) is a potentially complete one. It can be further developed and enhanced. It can be used, for example, for the purposes of analysis and qualitative evaluation of bearing capacity of the contacting surfaces. The classification indicates perfect correlation with the earlier developed classification (see Table 3.1 on pp. 230–243 in [1]).

Replacement of the true point contact of the part surfaces  $P_1$  and  $P_2$  with their locally line contact, and further with the locally surface of the first and/or of the second kind, and finally with the true surface contact results in significant alterations in the part surfaces' geometry of contact. Only locally extremal kinds of contact of the part surfaces  $P_1$  and  $P_2$  are considered here.

In order to attain the highest possible bearing capacity, it is preferred to maintain the true surface contact of the contacting part surfaces  $P_1$  and  $P_2$ .

Depending on the kind of contact of the part surfaces  $P_1$  and  $P_2$ , all possible kinds of contact of the part surface can be ranged in the following order (from the least efficient to the most efficient):

- (a) The true point kind of contact.
- (b) The locally line and/or quasi-line kind of contact.
- (c) The locally surface of the first kind and/or quasi-surface contact of the first kind.
- (d) The true line kind of contact.
- (e) The locally surface of the second kind contact and/or quasi-surface contact of the second kind.
- (f) The true surface kind of contact of the part surfaces  $P_1$  and  $P_2$ .

The bearing capacity of the contacting part surface  $P_1$  and  $P_2$  increases from (a) to (f).

The developed classification of all possible quasi-kinds of contact of two smooth regular part surfaces  $P_1$  and  $P_2$  in the first order of tangency can be extended and represented more in details.



## Part III

# Mapping of Contacting Part Surfaces

In engineering applications, it is often desired to design a pair of interacting part surfaces so, as to optimize the conditions of interaction between the two smooth regular part surfaces.

The conditions of interaction between two smooth regular part surfaces in contact can be specified in terms of:

- (a) contact stress,
- (b) conditions of lubrication, including but not limited to elastic-hydrodynamic (*EHD*) lubrication,
- (c) rolling/sliding conditions, and so forth.

Contact geometry of surfaces significantly influences the performance of the interacting part surfaces. This means that two part surfaces, which are featuring a certain contact geometry, demonstrate more favorable contact strength, lower surface wear, as well as others parameters that indicate high performance of the interacting part surfaces. In other words, for a given part surface, there exists a corresponding part surface geometry that ensures the highest possible bearing capacity of these two part surfaces in contact. It is of practical importance to determine a part surface that is corresponding to a given part surface, both of which in contact feature the most favorable performance. Engineering problems of this kind can be solved by means of mapping of one surface (of a given part surface) onto another surface (onto the part surface to be determined). Several useful kinds of surface mapping are considered in this section of the monograph.

Part III of the book is comprised of three chapters.

Chapter 8 is titled “ $\mathbb{R}$ -Mapping of Interacting Part Surfaces.”

Chapter 9 is titled “Generation of Enveloping Surfaces: General Consideration.”

Chapter 10 is titled “Generation of Enveloping Surfaces: Special Cases.”

## Chapter 8

# R-Mapping of Interacting Part Surfaces



The shape and parameters of the contacting part surfaces significantly affect the performance of the part surfaces bearing contact. In certain cases, one of the part surfaces can be specified, while the design engineer is free to pick the geometry of the other contacting part surfaces. Under such a scenario, it is possible to design the second part so as to ensure the highest possible performance of the contacting part surfaces.

The contact geometry of smooth regular part surfaces, as well as the problem of mapping one part surface onto another part surface, has received no detailed investigation yet. Selection of certain part surface geometry among its several available geometries is often recommended instead of determining the most favorable geometry of the contacting part surface. The selection of the part surface geometry usually targets the optimization of the contact geometry to meet certain requirements. This yields the conclusion that a robust mathematical method for determining of favorable geometry of the contacting part surface is necessary.

## 8.1 Preliminary Remarks

Many of the advanced sources are devoted to:

- (a) the investigation of contact stress between two interacting part surfaces,
- (b) the lubrication and wear of the contacting part surfaces, as well as
- (c) other output parameters for the interacting part surfaces.

However, the problem of the design of favorable part surfaces in contact still is not resolved yet.

In the general case of interaction of two smooth regular part surfaces, namely the part surfaces  $P_1$  and  $P_2$ , both of the surfaces should be considered as a kind of “free-form part surfaces” (or, as a kind of “sculptured part surfaces,” in different terminology). In order to avoid ambiguities in the consideration below, the following definition to the term “sculptured part surface” is adopted:

**Definition 8.1** A *sculptured part surface* is a smooth regular part surface, and the major parameters of local geometry at a point of which are not identical to the corresponding parameters of the local geometry of any other infinitesimally close point of the part surface.

It is instructive to point out here that sculptured surfaces do not allow for “*sliding over itself*.”

When interacting with one another, the part surfaces  $P_1$  and  $P_2$  can be either motionless in relation to one another, or they can move in relation to one another. In the second case, only those motions of the part surface  $P_2$  in relation to the part surface  $P_1$  are feasible, which fulfill the “*Shishkov equation of contact*” [1, 2]:

$$\mathbf{n}_{P_1} \cdot \mathbf{V}_\Sigma = 0 \quad (8.1)$$

Here, the unit vector of a common perpendicular to the contacting part surfaces  $P_1$  and  $P_2$  is denoted by  $\mathbf{n}_{P_1}$ . The linear velocity vector of the resultant relative motion of the interacting part surfaces is designated as  $\mathbf{V}_\Sigma$ .

In reality, the total number of part surfaces  $P_2$ , the geometry of which allows proper contact with the given part surface  $P_1$ , is endless. Use of all of them can meet the condition of contact that is specified by Eq. (8.1).

The performed retrospective analysis [3] reveals that Prof. V. A. *Shishkov* should be credited with the equation of contact in the form of the dot product  $\mathbf{n} \cdot \mathbf{V}_\Sigma = 0$  of the unit vector of the common perpendicular  $\mathbf{n}$  by the linear velocity vector of the resultant motion of the contacting part surfaces  $\mathbf{V}_\Sigma$ . Professor V. A. *Shishkov* was the first [1] to represent this equation in the form  $\mathbf{n} \cdot \mathbf{V}_\Sigma = 0$  (1948). It may be that the equation of contact  $\mathbf{n} \cdot \mathbf{V}_\Sigma = 0$  was published by Prof. V. A. *Shishkov* not in 1948 but even earlier, namely in his conference presentations, doctoral thesis, and so forth. Before Prof. V. A. *Shishkov*, the condition of contact was represented in a less elegant form.

While the unit normal vector  $\mathbf{n}_{P_1}$  to the part surfaces  $P_1$  and  $P_2$  is uniquely determined by geometry and relative orientation of the contacting part surfaces at a point of their contact, the total number of feasible vectors  $\mathbf{V}_\Sigma$  remains endless: any and all vectors  $\mathbf{V}_\Sigma$  through the contact point  $K$ , those within the common tangent plane, fulfill the equation of contact  $\mathbf{n}_{P_1} \cdot \mathbf{V}_\Sigma = 0$ . It is natural to assume that not all of them equivalent to each other from the standpoint of efficiency of the part surfaces interaction, and that some direction(s) of the linear velocity vector  $\mathbf{V}_\Sigma$  could be more favorable, moreover that there exists an optimal direction of the velocity vector  $\mathbf{V}_\Sigma$  within the common tangent plane for which efficiency of the part surfaces' interaction reaches its maximum degree. This makes the problem of designing the second part surface  $P_2$  largely indefinite. However, this indefiniteness is successfully overcome below by means of  $\mathbb{R}$ -mapping of part surfaces. Implementation of  $\mathbb{R}$ -mapping makes it possible to determine a unique part surface  $P_2$ . The part surface  $P_2$  so determined ensures the most favorable interaction with a given part surface  $P_1$ . It is noteworthy to mention here that the approach disclosed below can be enhanced to the determination of both smooth part surfaces  $P_1$  and  $P_2$  simultaneously.



When a part surface  $P_1$  is traveling in relation to  $P_2$ , the part surface  $P_2$  can be viewed as an enveloping surface to consecutive positions of the surface  $P_1$ .

## 8.2 On the Concept of $\mathbb{R}$ -Mapping of Interacting Part Surfaces

It is of critical importance to clarify from the very beginning what the term “*optimal contact geometry*” stands for. In the consideration below, the term “*optimal contact geometry*” means that the actual values of the design parameters of a certain part surface  $P_2$  are those under which the contacting part surfaces  $P_1$  and  $P_2$  feature an extremum (minimum/minimum) value of the desired criterion of optimality. Maximum bearing capacity and minimum contact stress between the part surfaces  $P_1$  and  $P_2$  are perfect examples of such criteria.

In engineering geometry of surfaces, only those criteria of optimization are applicable that can be expressed in terms of:

- (a) the geometry of the first part surface  $P_1$ ,
- (b) the geometry of the second part surface  $P_2$ , and
- (c) the kinematics of the relative motion of the part surfaces  $P_1$  and  $P_2$  with respect to one another.

The above consideration makes it a possible conclusion:

**Conclusion 8.1** *An appropriate alteration of shape of the part surface  $P_2$  can make possible improvement of contact geometry of two part surfaces  $P_1$  and  $P_2$ .*

This statement is of critical importance for further consideration.

At this point, we consider a more general example of part surfaces contact that supports in much the statement just made.

Consider a sculptured part surface  $P_1$  that makes point contact with another sculptured part surface  $P_2$ . Intersection of the contacting part surfaces  $P_1$  and  $P_2$  by a plane through the unit normal vector  $\mathbf{n}_{P_1}$  at the contact point  $K$  is illustrated schematically in Fig. 8.1.

The radius of normal curvature of the part surface  $P_1$  is of a certain positive value  $R_{P_1} > 0$ . The part surface  $P_1$  can make contact with another sculptured part surface  $P_2^a$  (see Fig. 8.1a). The radius of normal curvature of the part surface  $P_2^a$  has a certain positive value  $R_{P_2^a}^a > 0$ . The contact geometry of the part surfaces  $P_1$  and  $P_2^a$  depends strongly on the actual values of the radii of normal curvatures  $R_{P_1}$  and  $R_{P_2^a}^a$ .

That same part surface  $P_1$  can make contact with another sculptured part surface  $P_2^b$  as depicted schematically in Fig. 8.1b. The radius of normal curvature of the part surface  $P_2^b$  has a certain positive value  $R_{P_2^b}^b > 0$ . Again, the contact geometry of the part surfaces  $P_1$  and  $P_2^b$  depends strongly on the actual values of the radii of normal curvatures  $R_{P_1}$  and  $R_{P_2^b}^b$ . However, due to the inequality  $R_{P_2^b}^b > R_{P_2^a}^a > 0$  is valid,

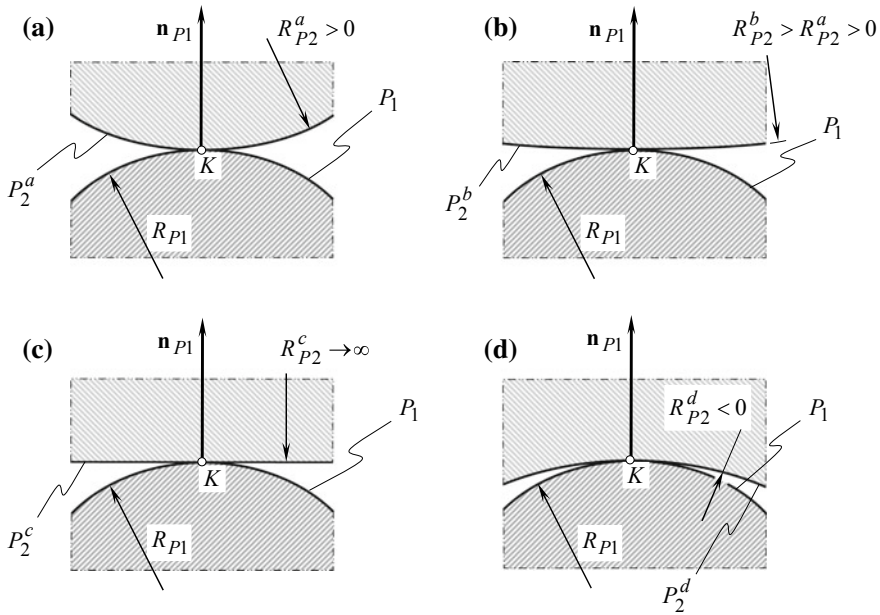


**Fig. 8.1** Examples of various degree of conformity at a point of contact of two smooth regular part surfaces  $P_1$  and  $P_2$  in the first order of tangency

then load capacity of contact of the part surfaces  $P_1$  and  $P_2^b$  exceeds that for the part surfaces  $P_1$  and  $P_2^a$ .

Further, that same part surface  $P_1$  can make contact with a sculptured part surface  $P_2^c$  as it is schematically shown in Fig. 8.1c. Radius of normal curvature of the part surface  $P_2^c$  is equal to infinity ( $R_{P_2}^c \rightarrow \infty$ ). Again, contact geometry of the part surfaces  $P_1$  and  $P_2^c$  strongly depends on actual values of the radii of normal curvatures  $R_{P_1}$  and  $R_{P_2}^c \rightarrow \infty$ . However, due to the inequality  $R_{P_2}^c > R_{P_2}^b > R_{P_2}^a > 0$ , the load capacity of contact of the part surfaces  $P_1$  and  $P_2^c$  exceeds that for the part surfaces  $P_1$  and  $P_2^b$ . Evidently, it also exceeds the load capacity of contact of the part surfaces  $P_1$  and  $P_2^a$ .

Ultimately, let us consider the part surface  $P_1$  that makes contact with a concave part surface  $P_2^d$ . The geometry of contact for this particular case is illustrated in Fig. 8.1d. The radius of normal curvature  $R_{P_2}^d$  of the part surface  $T^d$  is negative ( $R_{P_2}^d < 0$ ). In the case under consideration, the degree of conformity of the part surface  $P_2^d$  to the part surface  $P_1$  is the largest of all considered cases shown in Fig. 8.1. Thus, the load capacity of contact of the part surfaces  $P_1$  and  $P_2^d$  exceeds that for all the part surfaces (a)  $P_1$  and  $P_2^a$ , (b)  $P_1$  and  $P_2^b$ , and (c)  $P_1$  and  $P_2^c$ .

Summarizing the analysis of different geometries of contact of two smooth regular part surfaces illustrated in Fig. 8.1, the following conclusion can be formulated:

**Conclusion 8.2** An increase in degree of conformity of a part surface  $P_2$  to a surface  $P_1$  results in a corresponding increase in load capacity of the surfaces' contact.

This conclusion is of critical importance for engineering geometry of surfaces.

The degree of conformity at point of contact of a part surface  $P_2$  to a part surface  $P_1$  can be used as a quantitative criterion of load-carrying capacity of the part surfaces  $P_1$  and  $P_2$ . This issue is of prime importance to bypass all the major bottlenecks in designing optimal contacting surfaces, imposed by initial indefiniteness of the problem.

### 8.3 $\mathbb{R}$ -Mapping of a Part Surface $P_1$ onto Part Surface $P_2$

Engineering geometry of surfaces offers a method of mapping of one of the contacting part surfaces onto another contacting part surface so, as to ensure the most favorable performance of the part surfaces' contact.

The bearing performance of two part surfaces' contact depends significantly on the degree of conformity of the part surface  $P_2$  to a given sculptured part surface  $P_1$ .

In order to come up with the optimal contact of two part surfaces, the second part surface must be conformal to the first part surface as much as possible. For this purpose, the part surface  $P_2$  can be generated as a kind of mapping of the part surface  $P_1$ . The required kind of mapping of a part surface  $P_1$  onto the part surface  $P_2$  must ensure the required degree of conformity of the part surfaces  $P_1$  and  $P_2$  at every point of their contact. This kind of mapping of the part surface  $P_1$  onto the part surface  $P_2$  has been proposed initially by Prof. Radzevich [4–7]. It is referred to as “ $\mathbb{R}$ -mapping” of a part surface  $P_1$  onto another part surface  $P_2$ .

Consider an imaginary part surface  $P_2$  that makes contact with a smooth regular part surface  $P_1$  at a contact point  $K$ . The unit normal vector to the part surface  $P_1$  at  $K$  is designated as  $\mathbf{n}_{P_1}$ . A pencil of planes can be constructed using the unit vector  $\mathbf{n}_{P_1}$  as the directing vector of the axis of the pencil of planes. The maximum possible degree of conformity of a part surface  $P_2$  to the given part surface  $P_1$  is observed; when for every plane of the pencil of planes, the equality:

$$R_{P_2} = -R_{P_1} \quad (8.2)$$

is valid (in some cases, not the equality  $R_{P_2} = -R_{P_1}$  between the radii of normal curvature themselves, but the equivalent equality  $k_{P_2} = -k_{P_1}$  between normal curvatures can be used instead).

When the equality [see Eq. (8.2)] is met, then the contacting part surfaces  $P_1$  and  $P_2$  make either “*surface-to-surface contact*,” or they make a “*locally surface-to-surface contact*” [either the “*locally surface-to-surface contact of the first kind*,” or the “*locally surface-to-surface contact of the second kind*” (see Chap. 7)].

Actually, deviations in configuration of the part surface  $P_2$  with respect to the part surface  $P_1$  are inevitable. Hence, Eq. (8.2) cannot be fulfilled. This forces the replacement of Eq. (8.2) with an equality of the sort:

$$R_{P_2} = R_{P_2}(R_{P_1}) \quad (8.3)$$

instead.

The function  $R_{P_2}(R_{P_1})$  can be expressed in terms of the deviations/tolerances of the actual configuration of the part surface  $P_2$  in relation to the part surface  $P_1$ . It can be determined using either analytical methods or experimental methods.

Switching from the use of the function  $R_{P_2} = -R_{P_1}$  to use of the function  $R_{P_2} = R_{P_2}(R_{P_1})$  instead results in the perfect (ideal) locally extremal kind of contact of the part surfaces  $P_1$  and  $P_2$  being replaced with a kind of there quasi-kind of contact (Chap. 7).

Further, consider a part surface  $P_1$  that is described analytically by an equation in form vector from:

$$\mathbf{r}_{P_1} = \mathbf{r}_{P_1}(U_{P_1}, V_{P_1}) \quad (8.4)$$

In Eq. (8.4), the position vector of a point of the part surface  $P_1$  is designated as  $\mathbf{r}_{P_1}$ , and  $U_{P_1}$  and  $V_{P_1}$  are “Gaussian coordinates” of a point on the part surface  $P_1$ .

Use of Eq. (8.4) of the part surface  $P_1$  makes it possible to calculate the fundamental magnitudes  $E_{P_1}$ ,  $F_{P_1}$ , and  $G_{P_1}$  of the first order, and the fundamental magnitudes  $L_{P_1}$ ,  $M_{P_1}$ , and  $N_{P_1}$  of the second order of the part surface  $P_1$ .

The equation of the part surface  $P_2$  can be derived from the equation of the part surface  $P_1$  using for this purpose  $\mathbb{R}$ -mapping of surfaces. Initially, the equation of the part surface  $P_2$  is represented in the natural parameterized form. For the derivation of the equation of the part surface  $P_2$ , it necessary to express the first  $\Phi_{1,P_2}$  and the second  $\Phi_{2,P_2}$  fundamental forms of the part surface  $P_2$  in terms of the fundamental magnitudes  $E_{P_1}$ ,  $F_{P_1}$ ,  $G_{P_1}$  and  $L_{P_1}$ ,  $M_{P_1}$ ,  $N_{P_1}$  of the part surface  $P_1$ .

$\mathbb{R}$ -mapping of surfaces is capable of establishing the desired correspondence between points of the part surfaces  $P_1$  and  $P_2$ . Consider an arbitrary point on the part surface  $P_1$ . The principal radii of curvature  $R_{1,P_1}$  and  $R_{2,P_1}$  at this point of the part surface  $P_1$  are pre-calculated. A corresponding point exists on the part surface  $P_2$ . At this point of the part surface  $P_2$ , the desired principal radii of curvature  $R_{1,P_2}$  and  $R_{2,P_2}$  can be calculated on the premise of  $\mathbb{R}$ -mapping (but not mandatory vice versa). There could be one or more points on the part surface  $P_1$  that correspond to that same point of the part surface  $P_2$ .

When two part surfaces  $P_1$  and  $P_2$  are given, then one can easily calculate the degree of conformity of the surfaces at the given contact point  $K$ . In the case under consideration, a problem of another sort arises. This problem could be construed as an inverse problem to the problem of calculation of the actual degree of conformity of two part surface  $P_2$  and  $P_1$  in a prescribed direction on the part surface  $P_1$ .

$\mathbb{R}$ -mapping of surfaces establishes a functional relationship between the principal radii of curvature of the part surface  $P_1$  and of the corresponding part surface  $P_2$  in the differential vicinity of the contact point  $K$ . Use of  $\mathbb{R}$ -mapping makes it possible to compose two equations for determining six unknown fundamental magnitudes  $E_{P_2}$ ,  $F_{P_2}$ ,  $G_{P_2}$  of the first  $\Phi_{1,P_2}$  and  $L_{P_2}$ ,  $M_{P_2}$ ,  $N_{P_2}$  of the second  $\Phi_{2,P_2}$  fundamental forms of the part surface  $P_2$ .

The equation  $R_{P_2} = R_{P_2}(R_{P_1})$  can be split into the set of two equations:

$$\begin{cases} \mathcal{M}_{P_2} = \mathcal{M}_{P_2}(\mathcal{M}_{P_1}, \mathcal{G}_{P_1}) \\ \mathcal{G}_{P_2} = \mathcal{G}_{P_2}(\mathcal{M}_{P_1}, \mathcal{G}_{P_1}) \end{cases} \quad (8.5)$$

Here,  $\mathcal{M}_{P_1}$  and  $\mathcal{M}_{P_2}$  designate the “mean curvatures,” and  $\mathcal{G}_{P_1}$  and  $\mathcal{G}_{P_2}$  are the “Gaussian curvatures” of the contacting part surfaces  $P_1$  and  $P_2$  at a point of contact  $K$ , respectively.

The expression  $R_{P_2} = R_{P_2}(R_{P_1})$  gives an insight into the significance of a correlation between the radii of normal curvature  $R_{P_1}$  and  $R_{P_2}$ . In order to construct the function  $R_{P_2} = R_{P_2}(R_{P_1})$ , the “degree of conformity functions”  $\mathcal{F}_1$ ,  $\mathcal{F}_2$  and  $\mathcal{F}_3$  are implemented. The “degree of conformity functions”  $\mathcal{F}_1$ ,  $\mathcal{F}_2$ , and  $\mathcal{F}_3$  are of principal importance for the determination of the function  $R_{P_2} = R_{P_2}(R_{P_1})$ .

The required degree of conformity of a part surface  $P_2$  to a part surface  $P_1$  at every contact point of the surfaces is specified by the functions  $\mathcal{F}_1$ ,  $\mathcal{F}_2$ , and  $\mathcal{F}_3$ . This is the reason for they are referred as the “degree of conformity functions,  $\mathcal{F}_1$ ,  $\mathcal{F}_2$ , and  $\mathcal{F}_3$ .”

In order to meet the requirements of the set of two Eqs. (8.5), it is necessary to fulfill the following equalities:

$$L_{P_2}N_{P_2} - M_{P_2}^2 = \mathcal{F}_1(L_{P_1}N_{P_1} - M_{P_1}^2) \quad (8.6)$$

$$E_{P_2}N_{P_2} - 2F_{P_2}M_{P_2} + G_{P_2}L_{P_2} = \mathcal{F}_2(E_{P_1}N_{P_1} - 2F_{P_1}M_{P_1} + G_{P_1}L_{P_1}) \quad (8.7)$$

$$E_{P_2}G_{P_2} - F_{P_2}^2 = \mathcal{F}_3(E_{P_1}G_{P_1} - F_{P_1}^2) \quad (8.8)$$

In a particular case, Eq. (8.6) through Eq. (8.8) can be reduced to the form:

$$L_{P_2}N_{P_2} - M_{P_2}^2 = L_{P_1}N_{P_1} - M_{P_1}^2 \quad (8.9)$$

$$E_{P_2}N_{P_2} - 2F_{P_2}M_{P_2} + G_{P_2}L_{P_2} = E_{P_1}N_{P_1} - 2F_{P_1}M_{P_1} + G_{P_1}L_{P_1} \quad (8.10)$$

$$E_{P_2}G_{P_2} - F_{P_2}^2 = E_{P_1}G_{P_1} - F_{P_1}^2 \quad (8.11)$$

However, this does not necessarily mean that the part surfaces  $P_1$  and  $P_2$  are congruent to one another [see Eq. (8.9) through Eq. (8.11)].

Equation (8.6) through Eq. (8.8) describes analytically the vital link between the optimal design parameters of one of the contacting part surfaces and the given design parameters of the other of contacting surfaces. Use of these equations allows us to incorporate into the design of the part surface  $P_2$ , all important operating features of the contacting pair.

The degree of conformity functions  $\mathcal{F}_1$ ,  $\mathcal{F}_2$ , and  $\mathcal{F}_3$  are of prime importance for designing a smooth regular part surface  $P_2$  having a favorable geometry. They

can be determined, for instance, using the proposed [8] experimental method<sup>1</sup> of simulation of machining of a sculptured part surface. Other approaches for the determination of the degree of conformity functions  $\mathcal{F}_1$ ,  $\mathcal{F}_2$ , and  $\mathcal{F}_3$  can be used as well. There is much room for research in this area [9–16].

Three equations [that is, Eq. (8.6) through Eq. (8.8)] are necessary but not sufficient for determining the six unknown fundamental magnitudes  $E_{P2}$ ,  $F_{P2}$ ,  $G_{P2}$  of the first  $\Phi_{1,P2}$  and  $L_{P2}$ ,  $M_{P2}$ ,  $N_{P2}$  of the second  $\Phi_{2,P2}$  fundamental forms of the part surface  $P_2$  to be constructed. The equations of compatibility must be incorporated into the analyses in order to complete three Eq. (8.6) through Eq. (8.8) to a set of six equations of six unknowns.

Every smooth regular part surface  $P_2$  mandatory meets the “Gauss’ equation of compatibility” that follows from his famous “*theorem egregium*” [10, 17, 18]:

$$\begin{aligned} \tilde{G}_{P2}(E_{P2}G_{P2} - F_{P2}^2) = & \left[ \frac{\partial^2 F_{P2}}{\partial U_{P2} \partial V_{P2}} - \frac{1}{2} \left( \frac{\partial^2 E_{P2}}{\partial V_{P2}^2} + \frac{\partial^2 G_{P2}}{\partial U_{P2}^2} \right) \right] \cdot (E_{P2}G_{P2} - F_{P2}^2) \\ & + \begin{vmatrix} 0 & \frac{\partial F_{P2}}{\partial V_{P2}} - \frac{1}{2} \frac{\partial G_{P2}}{\partial U_{P2}} & \frac{1}{2} \frac{\partial G_{P2}}{\partial V_{P2}} \\ \frac{1}{2} \frac{\partial E_{P2}}{\partial U_{P2}} & E_{P2} & F_{P2} \\ \frac{\partial F_{P2}}{\partial U_{P2}} - \frac{1}{2} \frac{\partial E_{P2}}{\partial V_{P2}} & F_{P2} & G_{P2} \end{vmatrix} - \begin{vmatrix} 0 & \frac{1}{2} \frac{\partial E_{P2}}{\partial V_{P2}} & \frac{1}{2} \frac{\partial G_{P2}}{\partial U_{P2}} \\ \frac{1}{2} \frac{\partial E_{P2}}{\partial V_{P2}} & E_{P2} & F_{P2} \\ \frac{1}{2} \frac{\partial G_{P2}}{\partial U_{P2}} & F_{P2} & G_{P2} \end{vmatrix} \end{aligned} \quad (8.12)$$

Another two equations are the two “Mainardy-Codacci equations of compatibility” [10, 17, 18]:

$$\frac{\partial L_{P2}}{\partial V_{P2}} - \frac{\partial M_{P2}}{\partial U_{P2}} = L_{P2}\Gamma_{12}^1 + M_{P2} \cdot (\Gamma_{12}^2 - \Gamma_{11}^1) - N_{P2}\Gamma_{11}^2 \quad (8.13)$$

$$\frac{\partial M_{P2}}{\partial V_{P2}} - \frac{\partial N_{P2}}{\partial U_{P2}} = L_{P2}\Gamma_{22}^1 + M_{P2} \cdot (\Gamma_{22}^2 - \Gamma_{12}^1) - N_{P2}\Gamma_{12}^2 \quad (8.14)$$

Here, “Christoffel<sup>2</sup> symbols of the second kind” are used. “Christoffel symbols” can be calculated from the formulae [18]:

$$\Gamma_{11}^1 = \frac{G_u \frac{\partial E_u}{\partial U_u} - 2F_u \frac{\partial F_u}{\partial U_u} + F_u \frac{\partial E_u}{\partial V_u}}{2(E_u G_u - F_u^2)} \quad (8.15)$$

$$\Gamma_{11}^2 = \frac{2E_u \frac{\partial F_u}{\partial U_u} - E_u \frac{\partial E_u}{\partial V_u} + F_u \frac{\partial E_u}{\partial U_u}}{2(E_u G_u - F_u^2)} \quad (8.16)$$

$$\Gamma_{12}^1 = \frac{G_u \frac{\partial E_u}{\partial V_u} - F_u \frac{\partial G_u}{\partial U_u}}{2(E_u G_u - F_u^2)} = \Gamma_{21}^1 \quad (8.17)$$

<sup>1</sup>Pat. №1449246 (USSR). A Method of Experimental Simulation of Machining of a Sculptured Surface on a Multi-Axis NC Machine /S.P. Radzevich. Filed: February 17, 1987, Int. Cl. B 23 C, 3/16.

<sup>2</sup>Elwin Bruno Christoffel (November 10, 1829–March 15, 1900)—a German mathematician and physicist.

$$\Gamma_{12}^2 = \frac{E_u \frac{\partial G_u}{\partial U_u} - F_u \frac{\partial E_u}{\partial V_u}}{2(E_u G_u - F_u^2)} = \Gamma_{21}^2 \quad (8.18)$$

$$\Gamma_{22}^1 = \frac{2G_u \frac{\partial F_u}{\partial V_u} - G_u \frac{\partial G_u}{\partial U_u} + F_u \frac{\partial G_u}{\partial V_u}}{2(E_u G_u - F_u^2)} \quad (8.19)$$

$$\Gamma_{22}^2 = \frac{E_u \frac{\partial G_u}{\partial V_u} - 2F_u \frac{\partial F_u}{\partial V_u} + F_u \frac{\partial G_u}{\partial U_u}}{2(E_u G_u - F_u^2)} \quad (8.20)$$

Equations of compatibility are necessary to complete the set of three equations [Eq. (8.6) through Eq. (8.8)] to a set of six equations of six unknowns.

The set of three Eq. (8.6) through Eq. (8.8) together with the three equations of compatibility [Eq. (8.12) and Eq. (8.13)] describes completely the  $\mathbb{R}$ -mapping of two smooth regular part surfaces, that is, they describe the  $\mathbb{R}$ -mapping of a part surface  $P_1$  onto the part surface  $P_2$ , which is in contact with the surface  $P_1$ .

Thus, the fundamental magnitudes of the first  $\Phi_{1,P_2}$  and of the second  $\Phi_{2,P_2}$  fundamental forms of the part surface  $P_2$  can be determined using  $\mathbb{R}$ -mapping of the given part surface  $P_1$  onto the part surface  $P_2$  to be determined. A routing procedure can be used to solve the set of six equations of six unknowns, say of Eq. (8.6) through Eq. (8.8) and Eq. (8.12) through Eq. (8.13) with six unknowns  $E_{P_2}$ ,  $F_{P_2}$ ,  $G_{P_2}$  and  $L_{P_2}$ ,  $M_{P_2}$ ,  $N_{P_2}$ . Ultimately, the determined part surface  $P_2$  is represented in a natural parameterization.

Hence, the fundamental magnitudes  $E_{P_2}$ ,  $F_{P_2}$ ,  $G_{P_2}$  and  $L_{P_2}$ ,  $M_{P_2}$ ,  $N_{P_2}$  are considered below as known functions.

## 8.4 Reconstruction of Mapped Part Surface

Analytical representation of the mapped part surface  $P_2$  in a natural parameterization, namely in terms of fundamental magnitudes  $E_{P_2}$ ,  $F_{P_2}$ ,  $G_{P_2}$  of the first  $\Phi_{1,P_2}$  and  $L_{P_2}$ ,  $M_{P_2}$ ,  $N_{P_2}$  of the second  $\Phi_{2,P_2}$  fundamental forms are inconvenient for application in engineering practice. Natural parameterization of the mapped part surface  $P_2$  can be converted into parameterization in a convenient form, say to its representation in a *Cartesian* coordinate system, for example.

For the purposes of conversion of natural parameterization of the part surface  $P_2$  to representation in *Cartesian* coordinates, the set of two “*Gauss-Weingarten equations*” in tensor notation:

$$\text{Mapped part surface } P_2| \Leftrightarrow \begin{cases} \mathbf{r}_{ij} = \Gamma_{ij}^k \mathbf{r}_P + b_{ij} \mathbf{n}_P \\ \mathbf{n}_i = -b_{ik} g^{kj} \mathbf{r}_j \end{cases} \quad (8.21)$$

needs to be solved.

Solution to the set of two Eqs. (8.21) returns a matrix equation of the part surface  $P_2$ . Further, the initial conditions of integration of Eqs. (8.21) need to be chosen properly.

Here, we denote:

$$\mathbf{r}_i = \frac{\partial \mathbf{r}_{P_2}}{\partial U_{P_2}} \quad (8.22)$$

$$\mathbf{r}_{ij} = \frac{\partial^2 \mathbf{r}_{P_2}}{\partial U_{P_2} \partial V_{P_2}} \quad (8.23)$$

$$\mathbf{n}_i = \frac{\partial \mathbf{n}_{P_2}}{\partial U_{P_2}} \quad (8.24)$$

$$b_{ij} = \mathbf{r}_{ij} \cdot \mathbf{n}_{P_2} = -\mathbf{n}_i \mathbf{r}_j - \mathbf{n}_j \cdot \mathbf{r}_i \quad (8.25)$$

and  $g_{ij}$  is the metric tensor of the mapped part surface  $P_2$ ;  $g^{ij}$  is contravariant tensor of the part surface  $P_2$ .

Conventional methods [18] are used in order to solve the set of two Eqs. (8.21).

First, we need to establish certain initial conditions for integrating Eqs. (8.21). These conditions, for example, might include the coordinates of two points on the part surface  $P_2$  and direct cosines of the unit normal vector  $\mathbf{n}_{P_2}$  at one of these points.

The set of two differential equations in tensor notation [see Eqs. (8.21)] can be reduced either to a set of five differential equations in vector notation, or to a set of fifteen differential equations in parametric notation. Conventional mathematical methods can be implemented for solving of such a set of five differential equations or a set of fifteen differential equations with a corresponding number of unknowns. This is a kind of trivial mathematical problem that follows from the proposed theory of surface generation.

## 8.5 Illustrative Examples of Calculation of Design Parameters of Mapped Part Surface

Two illustrative examples of computations that do not require extensive application of a computer are presented below.

Instead of general demonstration of the approach developed, let us consider a scenario when all six fundamental magnitudes  $E_{P_2}$ ,  $F_{P_2}$ ,  $G_{P_2}$  and  $L_{P_2}$ ,  $M_{P_2}$ ,  $N_{P_2}$  of the part surface  $P_2$  have already been found from Eq. (8.6) through Eq. (8.8) and from equations of compatibility Eq. (8.12), Eq. (8.13), Eq. (8.14).

*Example 8.1* Given two differential forms:

$$\Phi_{1.P_2} \Rightarrow dU_{P_2}^2 + \cos^2 U_{P_2} dV_{P_2}^2 \quad (8.26)$$



and

$$\Phi_{2.P2} \Rightarrow dU_{P2}^2 + \cos^2 U_{P2} dV_{P2}^2, \quad (8.27)$$

find a smooth regular part surface  $P_2$ , for which  $\Phi_{1.P2}$  and  $\Phi_{2.P2}$  are the first and second fundamental forms.

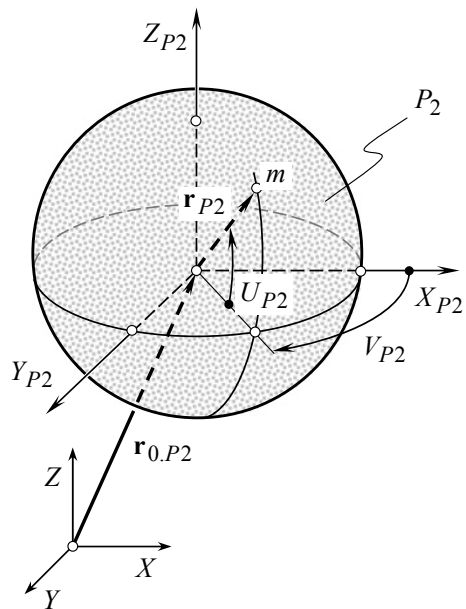
Since  $E_{P2} = 1$ ,  $F_{P2} = 0$ ,  $G_{P2} = \cos^2 U_{P2}$  and  $L_{P2} = 1$ ,  $M_{P2} = 0$ ,  $N_{P2} = \cos^2 U_{P2}$ , “*Christoffel symbols*”  $\Gamma_{11}^1 = \Gamma_{22}^2 = \Gamma_{12}^1 = \Gamma_{22}^2 = 0$ ,  $\Gamma_{12}^2 = -\tan U_{P2}$ ,  $\Gamma_{22}^1 = \sin U_{P2} \cos U_{P2}$ , that fulfill the “*Gauss-Codazzi equations of compatibility*,” can be found as the direct substitution shows.

The set of “*Gauss-Weingarten equations*” [Eq. (8.12) through Eq. (8.14)] returns the solution:

$$\tilde{\mathbf{r}}_{P2}(U_{P2}, V_{P2}) = \mathbf{r}_{0.P2} + \mathbf{r}_{P2}(U_{P2}, V_{P2}) = \mathbf{r}_{0.P2} + \begin{bmatrix} \cos V_{P2} \cos U_{P2} \\ \sin V_{P2} \cos U_{P2} \\ \sin U_{P2} \\ 1 \end{bmatrix} \quad (8.28)$$

which is the equation of a sphere (Fig. 8.2). The detailed derivation of Eq. (8.28) is not covered here. However, it is covered in all details in our paper [9]). Here  $\mathbf{r}_{0.P2}$  designates a vector that specifies the location of the part surface  $P_2$ . By the choice of  $\mathbf{r}_{0.P2}$ , one can place the part surface  $P_2$  in any position of space, selecting

**Fig. 8.2** Reconstructed spherical part surface  $P_2$



any orthogonal system of meridians and parallels for  $U_{P_2}$ – and  $V_{P_2}$ – curvilinear coordinates of an arbitrary point  $m$  on the part surface  $P_2$ .

*Example 8.2* In much the same way as is done above, for the fundamental forms:

$$\Phi_{1.P_2} \Rightarrow (r_{P_2} \cos \theta_{P_2} + R_{P_2})^2 dU_{P_2}^2 + (-r_{P_2} \sin \theta_{P_2} + R_{P_2})^2 + r_{P_2}^2 \cos^2 \theta_{P_2} dV_{P_2}^2 \quad (8.29)$$

and the corresponding:

$$\Phi_{2.P_2} \Rightarrow L_{P_2} dU_{P_2}^2 + 2M_{P_2} dU_{P_2} dV_{P_2} + N_{P_2} dV_{P_2}^2, \quad (8.30)$$

one can derive an equation of the part surface  $P_2$ .

Without going into details here, on solving Eq. (8.21), the following expression is derived:

$$\mathbf{r}_{P_2}(\theta_{P_2}, \varphi_{P_2}) = \begin{bmatrix} (r_{P_2} \cos \theta_{P_2} + R_{P_2}) \cos \varphi_{P_2} \\ (r_{P_2} \cos \theta_{P_2} + R_{P_2}) \sin \varphi_{P_2} \\ r_{P_2} \sin \theta_{P_2} \\ 1 \end{bmatrix} \quad (8.31)$$

and the surface  $P_2$  is a torus surface (Fig. 8.3).

The presented solution to the problem under consideration is grounded on a novel kind of surfaces mapping—the  $\mathbb{R}$ -mapping of a smooth regular part surface  $P_1$  onto the smooth regular part surface  $P_2$  [7, 10, 17] developed by the author. The idea and the general concept of implementation of the  $\mathbb{R}$ -mapping of surfaces can be traced back to 1987, when a method for designing optimal form-cutting tool for machining

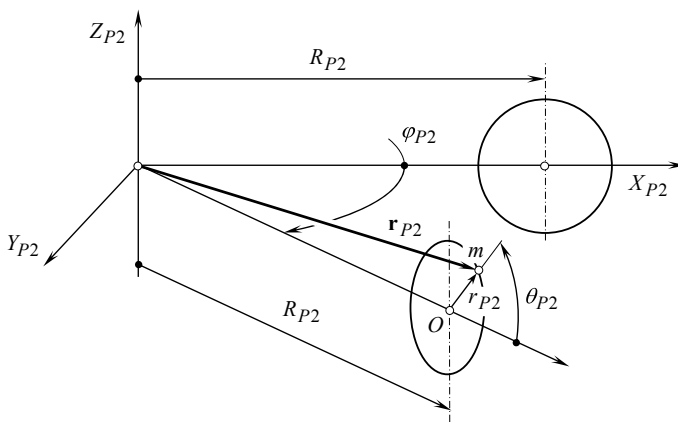


**Fig. 8.3** Toroidal part surface  $P_2$

a sculptured part surface on a multi-axis NC machine was proposed [4] by the author [5, 14].

## References

1. Shishkov, V. A. (1948). Elements of kinematics of generating and conjugating in gearing. In *Theory and Computation of Gears* (Vol. 6). Leningrad, LONITOMASH.
2. Shishkov, V. A. (1951). *Generation of surfaces using continuously indexing method* (p. 152). Moscow: Mashgiz.
3. Radzevich, S. P. (2010). Briefly about the kinematic method of surfaces generation and on history of equation of contact in the form  $\mathbf{n} \bullet \mathbf{V} = 0$ . *Theory of Mechanisms and Machines* 8(15), 42–51. <http://tmm.spbstu.ru>.
4. Radzevich, S. P. (1987). A method for designing of the optimal form-cutting-tool for machining of a given sculptured surface on multi-axis NC machine. Pat. No. 4242296/08 (USSR), Filed: March 31, 1987.
5. Radzevich, S. P. (1987). Profiling of the form cutting tools for sculptured surface machining on multi-axis NC machine. In *Proceedings of the Conference: Advanced Designs of Cutting Tools for Agile Production and Robotic Complexes, Moscow, MDNTP* (pp. 53–57).
6. Radzevich, S. P. (1989). Profiling of the form cutting tools for machining of sculptured surface on multi-axis NC machine. *Stanki i Instrument*, 7, 10–12.
7. Radzevich, S. P. (1991). *Sculptured surface machining on multi-axis NC machine* (Monograph) (192p). Kiev: Vishcha Schola.
8. Pat. No. 1449246 (USSR). A method of experimental simulation of machining of a sculptured surface on multi-axis NC machine. S.P.Radzevich. Filed: February 17, 1987, Int. Cl. B 23 C, 3/16.
9. Radzevich, S. P. (2007). A novel method for mathematical modeling of a form-cutting-tool of the optimum design. *Applied Mathematical Modeling*, 31, 2369–2654.
10. Radzevich, S. P. (2001). *Fundamentals of surface generation (Monograph)* (592p). Kiev: Rastan.
11. Radzevich, S. P. (2010). *Gear cutting tools: Fundamentals of design and computation* (p. 786). Boca Raton, Florida: CRC Press.
12. Radzevich, S. P. (2008). *Kinematic geometry of surface machining* (p. 536). Boca Raton, Florida: CRC Press.
13. Radzevich, S. P. (2004). Mathematical modeling of contact of two surfaces in the first order of tangency. *Mathematical and Computer Modeling*, 39(9–10), 1083–1112.
14. Radzevich, S. P. (2002).  $\mathbb{R}$ -mapping based method for designing of form cutting tool for sculptured surface machining. *Mathematical and Computer Modeling*, 36(7–8), 921–938.
15. Radzevich, S. P. (2012). *Theory of gearing: Kinematics, geometry, and synthesis* (856p). Boca Raton, Florida.
16. Radzevich, S. P. (2018). *Theory of gearing: Kinematics, geometry, and synthesis* (2nd Ed., 898p). Boca Raton, Florida.
17. Radzevich, S. P. (1991). *Differential-geometrical method of surface generation* (300p) (Doctoral thesis), Tula, Tula Polytechnic Institute.
18. Struik, D. J. (1961). *Lectures on classical differential geometry* (2nd ed., p. 232). Massachusetts: Addison-Wesley Publishing Company Inc.

## Chapter 9

# Generation of Enveloping Surfaces: General Consideration



Elements of the theory of enveloping lines and enveloping surfaces are extensively used in engineering geometry of surfaces. When a given smooth regular line or surface is traveling in space, an enveloping line/surface can be generated if the moving line/surface and parameters of its motion meet certain requirements. Many examples of application of elements of the theory of enveloping lines/surfaces can be found in current engineering practice.

For example, when machining a part surface, the part surfaces to be machined (part surface  $P$ ) and the generating surface of the cutting tool (the cutting tool surface  $T$ ) are two surfaces, which are in permanent tangency to one another. The generating surface of the cutting tool is an envelope for successive positions of the part surface to be machined when it is traveling in relation to a reference system associated with the cutting tool. This approach is commonly used when the problem of profiling a form-cutting tool is considered [1–5], as well as in many other cases.

### 9.1 Envelope for Successive Positions of a Moving Planar Curve

When a smooth regular planar curve is traveling within the plane through the curve, an envelope curve can exist when certain conditions are met.

Consider a planar curve that is traveling within the plane of location of the curve. If certain conditions are fulfilled, then an enveloping curve to consecutive positions of the moving curve exists [6]. As an example of a planar curve, a circle  $l$  of a radius  $r$  is shown in Fig. 9.1. All points of the circle  $l$  are within the coordinate plane  $XY$ . The circle  $l$  is traveling straightforward along the  $X$ -axis. When traveling, the circle  $l$  occupies consecutive positions. In this way, a family of circles is generated. Two straight lines  $l_1$  and  $l_2$  are the enveloping lines for the family of circles of radius  $r$ . These straight lines are parallel to the  $X$ -axis and are at a distance  $\pm r$  from the axis (and at a distance  $2r$  from each other).

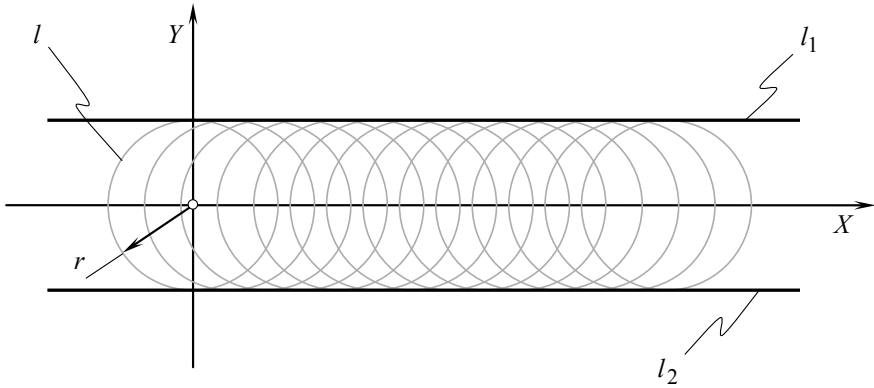


**Fig. 9.1** Generation of the enveloping lines  $l_1$  and  $l_2$  to successive positions of a circle  $l$  of a radius  $r$  that is traveling straightforward along the  $X$ -axis

The enveloping curve for a family of lines is tangent at every point of the line to one of the curves of the family of curves. Every circle shown in Fig. 9.1 has a common point with the enveloping line  $l_1$ , as well as a common point with another enveloping line  $l_2$ .

Consider a family  $\mathbf{r}^{\text{fm}}(u, \omega)$  of planar curves  $\mathbf{r}(u)$ :

$$\mathbf{r}^{\text{fm}}(u, \omega) = \begin{bmatrix} X(u, \omega) \\ Y(u, \omega) \\ 1 \end{bmatrix} \quad (9.1)$$

Here, the parameter of the initially given curve  $\mathbf{r}(u)$  is designated as  $u$ , and  $\omega$  designates the parameter of motion of the moving curve. In other words,  $\omega$  designates the parameter of the family of the curves  $\mathbf{r}^{\text{fm}}(u, \omega)$ .

Parallelism of the tangent vectors  $\frac{\partial \mathbf{r}}{\partial u}$  and  $\frac{\partial \mathbf{r}^{\text{fm}}}{\partial \omega}$  is the necessary condition for the existence of the enveloping curve. This condition is represented analytically in the form:

$$\frac{\partial \mathbf{r}}{\partial u} \times \frac{\partial \mathbf{r}^{\text{fm}}}{\partial \omega} = 0 \quad (9.2)$$

The inequality:

$$\frac{\partial \mathbf{r}}{\partial u} \cdot \frac{\partial \mathbf{r}^{\text{fm}}}{\partial \omega} - \frac{\partial \mathbf{r}}{\partial \omega} \cdot \frac{\partial \mathbf{r}^{\text{fm}}}{\partial u} \neq 0 \quad (9.3)$$

represents the sufficient condition for existence of the enveloping curve.

In order to derive an equation of the enveloping curve, Eq. (9.2) needs to be solved with respect to the enveloping parameter  $\omega$ . Then, the obtained solution for the parameter  $\omega$  is substituted into the equation for the family of the curves. Ultimately,

in this way the enveloping parameter  $\omega$  is excluded, and the position vector of a point  $\mathbf{r}^{\text{env}}$  of the enveloping curve can be expressed analytically as:

$$\mathbf{r}^{\text{env}} = \mathbf{r}^{\text{env}}(u) \quad (9.4)$$

Derivation of the equation of the enveloping curve is illustrated below by an example.

*Example 9.1* Consider a planar curve  $P_2$  that is given by the equation:

$$\mathbf{r}_{P_2}(\alpha, R) = \begin{bmatrix} (2 \cdot R + R \cdot \cos \alpha) \\ R \cdot \sin \alpha \\ 1 \end{bmatrix} \quad (9.5)$$

The partial derivatives of  $\mathbf{r}_{P_2}(\alpha, R)$  with respect to the parameters  $\alpha$  and  $R$  are equal:

$$\frac{\partial \mathbf{r}_{P_2}}{\partial \alpha} = \begin{bmatrix} -R \cdot \sin \alpha \\ R \cdot \cos \alpha \\ 1 \end{bmatrix} \quad (9.6)$$

and

$$\frac{\partial \mathbf{r}_{P_2}}{\partial R} = \begin{bmatrix} 2 + \cos \alpha \\ \sin \alpha \\ 1 \end{bmatrix} \quad (9.7)$$

accordingly.

Equations (9.6) and (9.7) reveal that the equality is valid:

$$\begin{vmatrix} -R \cdot \sin \alpha & R \cdot \cos \alpha \\ 2 + \cos \alpha & \sin \alpha \end{vmatrix} = 0 \quad (9.8)$$

From the determinant Eq. (9.8), one can come up with the expression:

$$-R \cdot (1 + 2 \cdot \cos \alpha) = 0 \quad (9.9)$$

Simple formula transformations yield a solution to Eq. (9.9):

$$\cos \alpha = -0.5, \quad \text{and} \quad \sin \alpha = \frac{\sqrt{3}}{2} \quad (9.10)$$

After substituting the last equalities into Eq. (9.5) of the family of curves, and after excluding the enveloping parameter  $R$ , the equation of the enveloping curve can be represented in the form:

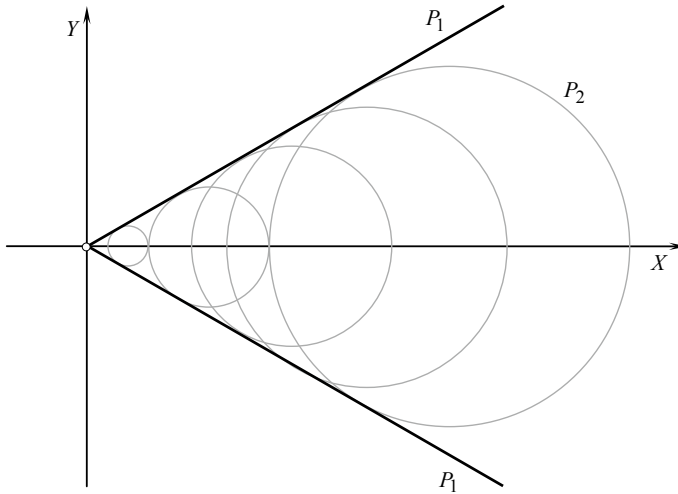


**Fig. 9.2** Enveloping curve for a family of planar curves

$$Y(X) = \frac{1}{\sqrt{3}} \cdot X \quad (9.11)$$

Therefore, in the case under consideration, the enveloping curve is a straight line at the angle  $\pm 30^\circ$  to the  $X$ -axis. The family of curves was a family of circles with centers on the  $X$ -axis (Fig. 9.2). The family of curves can be generated by a circle having translation along  $X$ -axis, radius of which increases accordingly to the distance from the origin of the coordinate system  $XY$  to the center of a movable circle.

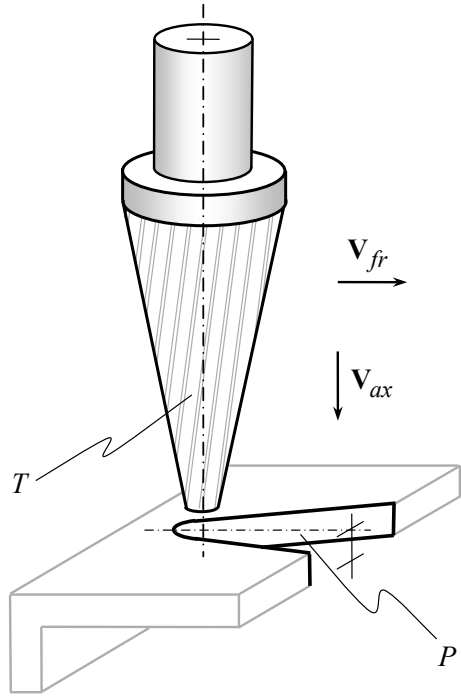
The considered example is of practical importance for machining of a sheet metal workpiece with a milling cutter having conical the generating surface  $T$  as illustrated schematically in Fig. 9.3. The milling cutter axis of rotation is traveling along the  $X$ -axis. The linear velocity vector  $\mathbf{V}_{fr}$  is the speed of this motion. Simultaneously with the motion  $\mathbf{V}_{fr}$ , the milling cutter is traveling along its axis of rotation (along the  $Z$ -axis; this axis is not shown in Fig. 9.3). The vector  $\mathbf{V}_{ax}$  is speed of this motion. The actual timing of the motions  $\mathbf{V}_{fr}$  and  $\mathbf{V}_{ax}$  depends upon the shape of the part surface  $P$ . The functional relation between the motions  $\mathbf{V}_{fr}$  and  $\mathbf{V}_{ax}$  can be either linear or nonlinear, as well.

In the considered example, the part surface  $P$  is generated as an envelope for successive positions of the generating surface  $T$  of the traveling cutting tool.

## 9.2 Envelope for Successive Positions of Moving Surface

The classical theory of enveloping surfaces encompasses the determination of an envelope for successive positions of a smooth regular surface that is performing

**Fig. 9.3** Example of practical implementation of the problem for determining an envelope for a family of planar curves



one-parametric motion in relation to a certain reference system. Later, this approach evolved to the case of determination of an envelope for successive positions of a smooth regular surface that is performing two-parametric motion in relation to a certain reference system. Both cases are discussed briefly below.

### 9.2.1 Envelope for One-Parametric Family of Surfaces

Consider a one-parametric family of smooth regular surfaces. The family of surfaces is dependent on a parameter of motion. The parameter of motion is designated as  $\omega$ . The enveloping surface is in tangency with every surface of the family of surfaces [6].

For example, the centers of all spheres of a family of spheres of a radius  $r$  are located within the  $X$ -axis of the *Cartesian* coordinate system  $XYZ$  (Fig. 9.4). The circular cylinder of radius  $r$  having the  $X$ -axis as the axis of its rotation represents the enveloping surface for the family of spheres of radius  $r$ .

Consider a family  $\mathbf{r}^{\text{fm}}(U, V, \omega)$  of surfaces  $\mathbf{r}(U, V)$ . The family of surfaces is specified by the equation:



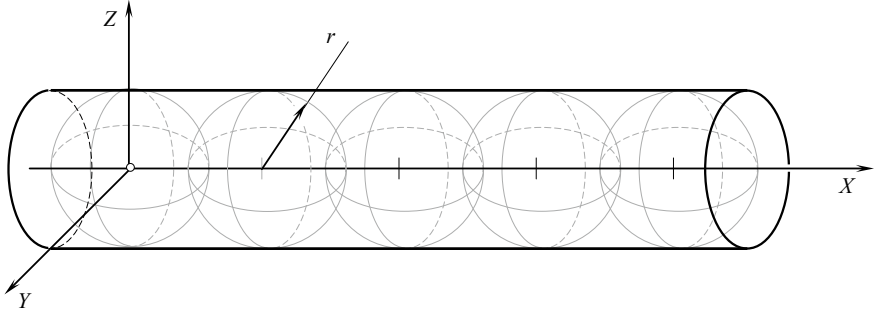


**Fig. 9.4** Generation of an enveloping surface to successive positions of a sphere of a radius  $r$  that is traveling straightforward along the  $X$ -axis

$$\mathbf{r}^{\text{fm}}(U, V, \omega) = \begin{bmatrix} X(U, V, \omega) \\ Y(U, V, \omega) \\ Z(U, V, \omega) \\ 1 \end{bmatrix} \quad (9.12)$$

for which the inequality:

$$\frac{\partial \mathbf{r}}{\partial U} \times \frac{\partial \mathbf{r}}{\partial V} \neq 0 \quad (9.13)$$

is valid. The necessary condition for existence of an enveloping surface is:

$$\mathbf{r}^{\text{fm}} = \mathbf{r}^{\text{fm}}(U, V, \omega) \quad (9.14)$$

$$\left( \frac{\partial \mathbf{r}}{\partial U} \frac{\partial \mathbf{r}}{\partial V} \frac{\partial \mathbf{r}}{\partial \omega} \right) = 0 \quad (9.15)$$

The line of tangency of a surface  $\mathbf{r}(U, V)$  of a family of surfaces  $\mathbf{r}^{\text{fm}}(U, V, \omega)$  with the enveloping surface is referred to as the “*characteristic line*  $\mathcal{E}$ .” The characteristic line  $\mathcal{E}$  meets the requirements specified by Eqs. (9.9) and (9.10). The enveloping surface yields representation in the form of a family of the characteristic lines.

When the enveloping surface is of the class of surfaces that allow “*sliding over itself*,” then Eq. (9.10) describes the profile of the enveloping surface.

Fulfillment of the condition  $\mathbf{r} \in \omega^2$  of relationships [see Eqs. (9.14) and (9.15)] together with the conditions:

$$\left| \begin{array}{ccc} \frac{\partial \Psi}{\partial U} & \frac{\partial \Psi}{\partial V} & \frac{\partial \Psi}{\partial \omega} \\ \left( \frac{\partial \mathbf{r}}{\partial U} \right)^2 & \frac{\partial \mathbf{r}}{\partial U} \cdot \frac{\partial \mathbf{r}}{\partial V} & \frac{\partial \mathbf{r}}{\partial U} \cdot \frac{\partial \mathbf{r}}{\partial \omega} \\ \frac{\partial \mathbf{r}}{\partial U} \cdot \frac{\partial \mathbf{r}}{\partial V} & \left( \frac{\partial \mathbf{r}}{\partial V} \right)^2 & \frac{\partial \mathbf{r}}{\partial V} \cdot \frac{\partial \mathbf{r}}{\partial \omega} \end{array} \right| \neq 0, \quad (9.16)$$

$$\left| \frac{\partial \Psi}{\partial U} \right| + \left| \frac{\partial \Psi}{\partial V} \right| \neq 0 \quad (9.17)$$

is the sufficient condition for the existence of the profile of the enveloping surface.

Violation of the first condition Eq. (9.16) is usually due to an edge of inversion observed on the surface.

Characteristic lines of the part surface  $P_1$  and of the generated part surface  $P_2$  meet the conditions:

$$\mathbf{r}_1 = \mathbf{r}_1(U_1, V_1, \omega), \quad f[U_1(\omega), V_1(\omega), \omega] = 0, \quad \omega = \text{Const} \quad (9.18)$$

$$\mathbf{r}_2 = \mathbf{r}_2(U_2, V_2, \omega), \quad f[U_2(\omega), V_2(\omega), \omega] = 0, \quad \omega = \text{Const} \quad (9.19)$$

In a stationary reference system, the family of the characteristic lines can be represented by the set of two equations:

$$\frac{\partial \mathbf{r}_2}{\partial f} = \frac{\partial \mathbf{r}_2}{\partial f}(U_2, V_2, \omega), \quad (9.20)$$

$$f(U_2, V_2, \omega) = 0 \quad (9.21)$$

Here, the equality:

$$\frac{\partial \mathbf{r}_2}{\partial f}(U_2, V_2, \omega) = \mathbf{Rs}(1 \rightarrow 2) \cdot \mathbf{r}_1(U_1, V_1) \quad (9.22)$$

is valid. The operator  $\mathbf{Rs}(1 \rightarrow 2)$  of the resultant coordinate system transformation is a function of the parameter of motion  $\omega$ .

It should be also pointed out here that theory of surface generation is dealing also with surfaces of the kind, for which the enveloping surface is congruent to the moving surface itself. Surfaces of this particular kind are referred to as the “*surfaces that allow for sliding over themselves*.”

### 9.2.2 Envelope for Two-Parametric Family of Surfaces

The theory of two-parametric enveloping surfaces is an extension of the theory of one-parametric enveloping surfaces.

A two-parametric enveloping surface is dependent on two parameters, say the parameters  $\omega_1$  and  $\omega_2$ . At every point, the enveloping surface makes tangency with one of the surfaces of the family of surfaces. The family of surfaces is specified by the parameters  $\omega_1(U, V)$  and  $\omega_2(U, V)$ . At every point of each surface of the family

of surfaces, the parameters  $\omega_1$  and  $\omega_2$  are of the same value. However, they are of different values at different points of the enveloping surface.

If the condition  $(\partial \mathbf{r} / \partial U) \times (\partial \mathbf{r} / \partial V) \neq 0$  is fulfilled, then the necessary condition for the existence of the enveloping surface for a family of surfaces  $\mathbf{r}(U, V, \omega_1, \omega_2)$  can be represented in the form [6]:

$$\psi_1 = \left( \frac{\partial \mathbf{r}}{\partial U} \frac{\partial \mathbf{r}}{\partial V} \frac{\partial \mathbf{r}}{\partial \omega_1} \right) = 0, \quad (9.23)$$

$$\psi_2 = \left( \frac{\partial \mathbf{r}}{\partial U} \frac{\partial \mathbf{r}}{\partial V} \frac{\partial \mathbf{r}}{\partial \omega_2} \right) = 0 \quad (9.24)$$

In order to get a sufficient set of conditions for the existence of the enveloping surface, the above conditions [see Eqs. (9.23) and (9.24)] need to be considered together with the conditions:

$$\begin{vmatrix} \frac{\partial \psi_1}{\partial \mu} & \frac{\partial \psi_1}{\partial v} & \frac{\partial \psi_1}{\partial A} & \frac{\partial \psi_1}{\partial B} \\ \frac{\partial \psi_2}{\partial \mu} & \frac{\partial \psi_2}{\partial v} & \frac{\partial \psi_2}{\partial A} & \frac{\partial \psi_2}{\partial B} \\ \left( \frac{\partial \mathbf{r}}{\partial U} \right)^2 & \frac{\partial \mathbf{r}}{\partial U} \cdot \frac{\partial \mathbf{r}}{\partial V} & \frac{\partial \mathbf{r}}{\partial U} \cdot \frac{\partial \mathbf{r}}{\partial \omega_1} & \frac{\partial \mathbf{r}}{\partial U} \cdot \frac{\partial \mathbf{r}}{\partial \omega_2} \\ \frac{\partial \mathbf{r}}{\partial V} \cdot \frac{\partial \mathbf{r}}{\partial U} & \left( \frac{\partial \mathbf{r}}{\partial V} \right)^2 & \frac{\partial \mathbf{r}}{\partial V} \cdot \frac{\partial \mathbf{r}}{\partial \omega_1} & \frac{\partial \mathbf{r}}{\partial V} \cdot \frac{\partial \mathbf{r}}{\partial \omega_2} \end{vmatrix} \neq 0, \quad (9.25)$$

$$\frac{D(\psi_1, \psi_2)}{D(\omega_1, \omega_2)} \neq 0 \quad (9.26)$$

If a surface  $\mathbf{r}(U, V)$ :

- (a) is performing a two-parametric motion [that is,  $\mathbf{r}(U, V, \omega_1, \omega_2)$ ],
- (b) with both the motions  $\omega_1$  and  $\omega_2$  independent from each other, and
- (c) the characteristics  $\mathcal{E}_1$  and  $\mathcal{E}_2$  are observed for each of the motions,

then the point of intersection of the characteristic lines  $\mathcal{E}_1$  and  $\mathcal{E}_2$  is a point of the enveloping surface. This point is referred to as “*characteristic point*.” At a characteristic point, the condition:

$$\mathbf{n} \cdot \mathbf{V}_{1-2}^{(\omega_1)} + \mathbf{n} \cdot \mathbf{V}_{1-2}^{(\omega_2)} = 0 \quad (9.27)$$

is always fulfilled. Here,  $\mathbf{n}$  designates unit normal vector to the enveloping surface.

Commonly written in the form:

$$\begin{cases} \mathbf{n} \cdot \mathbf{V}_{1-2}^{(\omega_1)} = 0 \\ \mathbf{n} \cdot \mathbf{V}_{1-2}^{(\omega_2)} = 0 \end{cases} \quad (9.28)$$

the enveloping condition is overconstrained.

The conditions  $\mathbf{n} \cdot \mathbf{V}_{1-2}^{(\omega_1)} = 0$  and  $\mathbf{n} \cdot \mathbf{V}_{1-2}^{(\omega_2)} = 0$  are derived for the cases when the linear velocity vector  $\mathbf{V}_\Sigma$  of the resultant relative motion of the surfaces is decomposed onto two components  $\mathbf{V}_{1-2}^{(\omega_1)}$  and  $\mathbf{V}_{1-2}^{(\omega_2)}$ , and both of the components are within

the common tangent plane. These conditions are definitely sufficient for the existence of the enveloping surface and are used, for example, when designing hobs for cutting gears, splines, pump rotors, and so forth.

Again, the conditions  $\mathbf{n} \cdot \mathbf{V}_{1-2}^{(\omega_1)} = 0$  and  $\mathbf{n} \cdot \mathbf{V}_{1-2}^{(\omega_2)} = 0$  are sufficient for the existence of the enveloping surface, but they are not mandatory. It is possible to decompose the resultant relative motion  $\mathbf{V}_\Sigma$  of the surfaces (which is entirely located within the common tangent plane) into two particular motions  $\mathbf{V}_{1-2}^{(\omega_1)}$  and  $\mathbf{V}_{1-2}^{(\omega_2)}$  that are not located within the common tangent plane. For example, the projections of the linear velocity vectors  $\mathbf{V}_{1-2}^{(\omega_1)}$  and  $\mathbf{V}_{1-2}^{(\omega_2)}$  onto a straight line along the unit normal vector  $\mathbf{n}$  can have equal magnitudes and can be pointed oppositely. However, the location of the resultant motion  $\mathbf{V}_\Sigma$  remained within the common tangent plane is the must.

The approach discussed can be employed for determination of an envelope (if any) of an arbitrary smooth regular part surface having motion of any desired kind. The interested reader may wish to go to [7] for the details on the solution to the problem of calculation of the parameters of the envelope of a sphere having screw motion as an example. Many practical examples in this regard are known from other sources.

Elements of the theory of enveloping surfaces are extensively used in kinematic geometry of surface generation [1–3, 8] and others.

As an example, Fig. 9.5 illustrates a problem that can be solved using elements of the theory of enveloping surfaces.

The generating surface of the first mill cutter is comprised of two portions, say of the cylindrical portion  $T_{11}$  and of the spherical portion  $T_{12}$ . When performing circular motion, the cylindrical portion  $T_{11}$  of the generating surface of the cutting

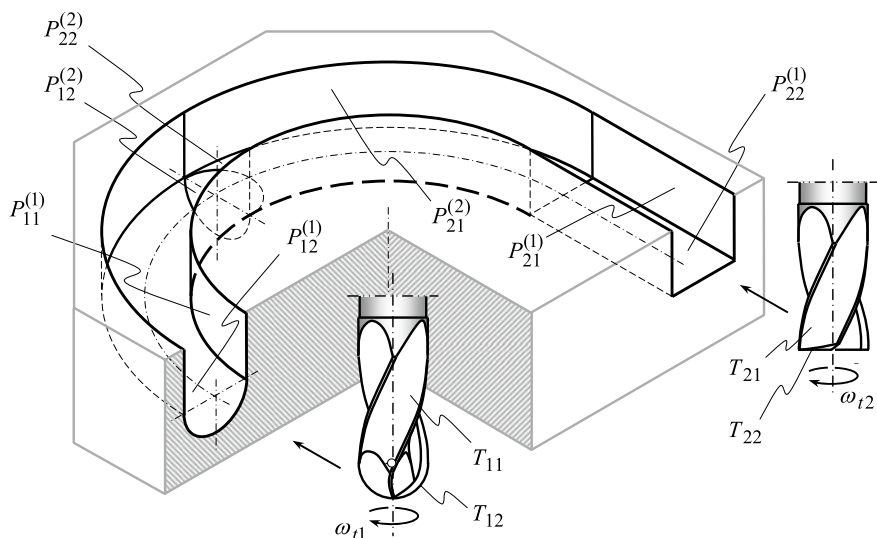


**Fig. 9.5** Illustrative example of implementation of elements of the theory of enveloping surfaces in kinematic geometry of surface generation

tool generates the part surface  $P_{11}^{(1)}$ . The spherical portion  $T_{12}$  of the generating surface of the mill cutter generates the surface  $P_{12}^{(1)}$ , which is a torus. When the circular feed-rate motion is halted, then the spherical portion  $P_{12}^{(2)}$  is machined on the part.

Similarly, the generating surface of the second mill cutter is comprised of two portions, say of the cylindrical portion  $T_{21}$  and of the flat portion  $T_{22}$ . The cylindrical portion  $T_{21}$  of the generating surface of the mill cutter generates the plane  $P_{21}^{(1)}$  and the circular cylinder  $P_{21}^{(2)}$ . The plane portion  $T_{22}$  of the generating surface generates the plane  $P_{22}^{(1)}$  and the plane  $P_{22}^{(2)}$ .

Use of the above formulae allows derivation of equations of all of the machined part surfaces if the dimensions of the mill cutters and the parameters of these motions relative to the work are known. This approach works perfectly in case the moving surfaces allow for “*sliding over themselves*.”

### 9.3 “Kinematic Method” for Determining Enveloping Surfaces

One more method for the determination of enveloping part surfaces is of critical importance in engineering applications. This method is commonly referred to as “*kinematic method*” for the determination of enveloping part surfaces. In 1940, Prof. V. A. Shishkov contributed much to the “*kinematic method*” for the determination of enveloping part surfaces. The method has been summarized in 1951 in the monograph [9].

The kinematic method is based on a particular location of the linear velocity vector  $\mathbf{V}_{1-2}$  of relative motion of the moving part surface and of the enveloping part surface. Vector  $\mathbf{V}_{1-2}$  is located within the common tangent plane to the part surfaces. This condition follows immediately from the following consideration. Motions only of two kinds are feasible for the moving part surface and the part enveloping surface. The part surfaces can either roll over each other or slide over each other. The component of the resultant relative motion  $\mathbf{V}_{1-2}$  in the direction of common perpendicular to the part surfaces is always equal to zero (Fig. 9.6).

A part surface  $P_2$  is performing certain motion relative to a reference system (the reference system is not shown here), which the enveloping part surface  $P_1$  will be associated with. The part surface  $P_1$  is generated as an enveloping surface for successive positions of the moving part surface  $P_2$ . Points of three different kinds can be distinguished on the moving part surface  $P_2$ .

Consider points of the first kind, for example a point  $A$  (see Fig. 9.6). The linear velocity vector of the resultant motion of the part surface  $P_2$  with respect to the work at the point  $A$  is designated as  $\mathbf{V}_{\Sigma}^{(A)}$ . Projection  $\text{Pr}_{\mathbf{n}} \mathbf{V}_{\Sigma}^{(A)}$  of the vector  $\mathbf{V}_{\Sigma}^{(A)}$  onto the unit normal vector  $\mathbf{n}_{P_2}^{(A)}$  to the moving part surface  $P_2$  is pointed to interior of the body of the work ( $\text{Pr}_{\mathbf{n}} \mathbf{V}_{\Sigma}^{(A)} > 0$ ). Therefore, in the vicinity of the point  $A$ , the part

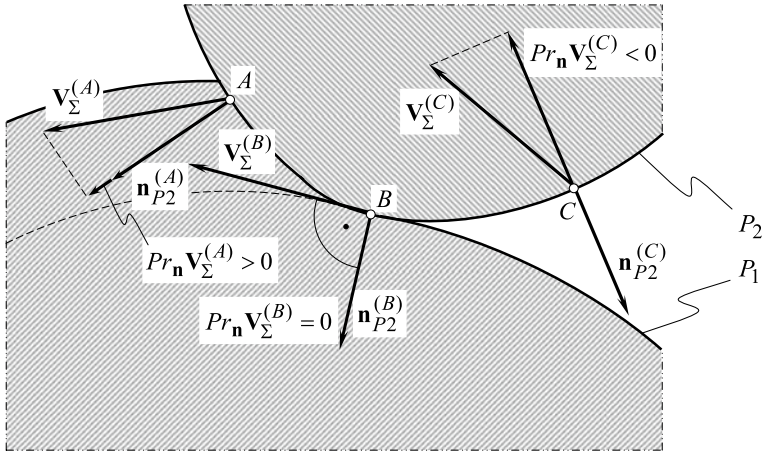


**Fig. 9.6** To the concept of the *kinematic method* for determining an enveloping part surface

surface  $P_2$  penetrates body of the work. The part surface  $P_1$  is not generating in the vicinity of the point  $A$  by the part surface  $P_2$ .

Further, consider points of the second kind, for example a point  $B$  as it is shown schematically in Fig. 9.6. The vector of resultant motion of the part surface  $P_2$  with respect to the work at the point  $B$  is designated as  $\mathbf{V}_\Sigma^{(B)}$ . The projection  $\text{Pr}_n \mathbf{V}_\Sigma^{(B)}$  of the linear velocity vector  $\mathbf{V}_\Sigma^{(B)}$  onto the unit normal vector  $\mathbf{n}_{P_2}^{(B)}$  to the moving part surface  $P_2$  is perpendicular to this unit normal vector; that is, it is tangential to the part surface  $P_1$  ( $\text{Pr}_n \mathbf{V}_\Sigma^{(B)} = 0$ ). Therefore, in the vicinity of the point  $B$  the part surface  $P_2$  does not penetrate the part body. The moving part surface  $P_2$  is generating the part surface  $P_1$  in the vicinity of the point  $B$ . In addition to the resultant instant linear motion  $\mathbf{V}_\Sigma^{(B)}$ , an additional motion is permissible at the point  $B$ . Spinning  $\pm \omega_{n.B}$  about an axis along the common perpendicular  $\mathbf{n}_{P_2}^{(B)}$  is this motion. The spinning  $\pm \omega_{n.B}$  can be performed simultaneously with the translation  $\mathbf{V}_\Sigma^{(B)}$ . The spinning within a certain angle  $\pm \theta \leq 360^\circ$  either is allowed or can be performed through the angle of  $360^\circ$ . The latter depends on the parameters of the local geometry of the interacting part surfaces in the differential vicinity of the contact point  $B$ .

Ultimately, consider points of the third kind, for example a point  $C$  (see Fig. 9.6). The linear velocity vector of resultant motion of the part surface  $P_2$  with respect to the work at the point  $C$  is designated  $\mathbf{V}_\Sigma^{(C)}$ . The projection  $\text{Pr}_n \mathbf{V}_\Sigma^{(C)}$  of the vector  $\mathbf{V}_\Sigma^{(C)}$  onto the unit normal vector  $\mathbf{n}_{P_2}^{(C)}$  to the traveling part surface  $P_2$  is pointed outside the part body ( $\text{Pr}_n \mathbf{V}_\Sigma^{(C)} < 0$ ). Therefore, in the vicinity of the point  $C$ , the part surface  $P_2$  is departing from the generated part surface  $P_1$ .

The nature of the kinematic method for determining enveloping part surfaces becomes clear from the considered example (see Fig. 9.6).

For a family of part surfaces  $\mathbf{r} = \mathbf{r}(U, V, \omega)$ , the equation of the characteristic curve  $\mathcal{C}$  yields representation in the form:

$$\mathbf{r} = \mathbf{r}(U, V, \omega) \quad (9.29)$$

$$\mathbf{n} \cdot \mathbf{V}_{1-2} = 0 \quad (9.30)$$

Here and below, the linear velocity vector  $\mathbf{V}_{1-2}$  is equal to the linear velocity vector  $\mathbf{V}_\Sigma$ .

The perpendicular  $\mathbf{n}$  to a smooth regular part surface  $\mathbf{r}$  can be expressed analytically by the equation in the form:

$$\mathbf{n} = \frac{\frac{\partial \mathbf{r}}{\partial U} \times \frac{\partial \mathbf{r}}{\partial V}}{\left| \frac{\partial \mathbf{r}}{\partial U} \times \frac{\partial \mathbf{r}}{\partial V} \right|} \quad (9.31)$$

This means that the dot product  $\mathbf{n} \cdot \mathbf{V}_{1-2}$  yields representation in the form of a triple product

$$\mathbf{n} \cdot \mathbf{V}_{1-2} = \frac{\partial \mathbf{r}}{\partial U} \times \frac{\partial \mathbf{r}}{\partial V} \cdot \mathbf{V}_{1-2} \quad (9.32)$$

of three vectors. Here, the speed  $\mathbf{V}_{1-2}$  of the relative motion with a certain parameter  $\omega$  is equal to:

$$\mathbf{V}_{1-2}^{(\omega)} = \frac{\partial \mathbf{r}}{\partial \omega} = \begin{bmatrix} \frac{\partial X}{\partial \omega} \\ \frac{\partial Y}{\partial \omega} \\ \frac{\partial Z}{\partial \omega} \\ 1 \end{bmatrix} \quad (9.33)$$

Ultimately, the equation of the characteristic curve  $\mathcal{E}$ :

$$\begin{aligned} & \frac{\partial X}{\partial U} \left( \frac{\partial Y}{\partial V} \cdot \frac{\partial Z}{\partial \omega} - \frac{\partial Y}{\partial \omega} \cdot \frac{\partial Z}{\partial V} \right) \\ & - \frac{\partial Y}{\partial U} \left( \frac{\partial X}{\partial V} \frac{\partial Z}{\partial \omega} - \frac{\partial X}{\partial \omega} \frac{\partial Z}{\partial V} \right) \\ & + \frac{\partial Z}{\partial U} \left( \frac{\partial X}{\partial V} \frac{\partial Y}{\partial \omega} - \frac{\partial X}{\partial \omega} \frac{\partial Y}{\partial V} \right) = 0 \end{aligned} \quad (9.34)$$

can be derived for the equation of contact:

$$\mathbf{n} \cdot \mathbf{V}_{1-2}^{(\omega)} = \frac{\partial \mathbf{r}}{\partial U} \times \frac{\partial \mathbf{r}}{\partial V} \cdot \mathbf{V}_{1-2}^{(\omega)} = 0 \quad (9.35)$$

When the kinematic method is used, then the sufficient condition for the existence of the enveloping part surface can be obtained in the following way.

Consider a smooth regular part surface  $\mathbf{r}$  that is given in a *Cartesian* coordinate system  $XYZ$ . The equation for the position vector of a point  $\mathbf{r}$  of the part surface is

represented in the form  $\mathbf{r} = \mathbf{r}(U, V) \in C^2$ . The family  $\mathbf{r}^\omega$  of successive positions of this part surface in another *Cartesian* coordinate system  $X_0Y_0Z_0$  is given in the form  $\mathbf{r}^\omega = \mathbf{r}^\omega(U, V, \omega)$ , where the inequality  $\omega^{\min} \leq \omega \leq \omega^{\max}$  is observed. The reference system  $X_0Y_0Z_0$  can be considered as a stationary reference system.

Then, if at a certain point either the condition:

$$\left( \frac{\partial \mathbf{r}(\omega)}{\partial U(\omega)} \times \frac{\partial \mathbf{r}(\omega)}{\partial V(\omega)} \right) \cdot \frac{\partial \mathbf{r}(\omega)}{\partial \omega} = f[U(\omega), V(\omega), \omega] = 0, \quad f \in C^1 \quad (9.36)$$

or the conditions:

$$\left( \frac{\partial \mathbf{r}(\omega)}{\partial U(\omega)} \times \frac{\partial \mathbf{r}(\omega)}{\partial V(\omega)} \right) \cdot \mathbf{V}_{1-2} = f[U(\omega), V(\omega), \omega] = 0, \quad \left( \frac{\partial f}{\partial U} \right)^2 + \left( \frac{\partial f}{\partial V} \right)^2 \neq 0 \quad (9.37)$$

$$g[U(\omega), V(\omega), \omega] = \begin{vmatrix} \frac{\partial f}{\partial U} & \frac{\partial f}{\partial V} & \frac{\partial f}{\partial \omega} \\ \left( \frac{\partial \mathbf{r}}{\partial U} \right)^2 & \left( \frac{\partial \mathbf{r}}{\partial U} \right) \cdot \left( \frac{\partial \mathbf{r}}{\partial V} \right) & \left( \frac{\partial \mathbf{r}}{\partial U} \right) \cdot \mathbf{V}_{1-2} \\ \left( \frac{\partial \mathbf{r}}{\partial V} \right) \cdot \left( \frac{\partial \mathbf{r}}{\partial U} \right) & \left( \frac{\partial \mathbf{r}}{\partial V} \right)^2 & \left( \frac{\partial \mathbf{r}}{\partial V} \right) \cdot \mathbf{V}_{1-2} \end{vmatrix} \neq 0 \quad (9.38)$$

are fulfilled, the enveloping part surface exists and can be represented by the set of two equations:

$$\begin{cases} \mathbf{r} = \mathbf{r}(U, V, \omega) \\ \frac{\partial \mathbf{r}}{\partial \omega} = 0 \end{cases} \quad (9.39)$$

Consider an example of implementation of the kinematic method for determination of enveloping part surface for successive positions of a moving smooth regular surface.

*Example 9.2* Consider a plane  $P_2$  having a screw motion. The plane  $P_2$  forms a certain angle  $\tau_b$  with the  $X$ -axis of the Cartesian coordinate system  $X_0Y_0Z_0$ . The reduced pitch  $p$  of the screw motion is given. Axis  $X_0$  is the axis of the screw motion.

The auxiliary reference system  $X_1Y_1$  is rigidly associated with the plane  $P_2$  illustrated schematically in Fig. 9.7.

The equation of the plane  $P_2$  can be represented in the form:

$$Y_1 = X_1 \cdot \tan \tau_b \quad (9.40)$$

The auxiliary coordinate system  $X_1Y_1Z_1$  is performing the screw motion together with the plane  $P_2$  with respect to the motionless coordinate system  $X_0Y_0Z_0$ . In the coordinate system  $X_1Y_1Z_1$ , the unit normal vector  $\mathbf{n}_{P_2}$  to the plane  $P_2$  can be expressed by a column matrix as:



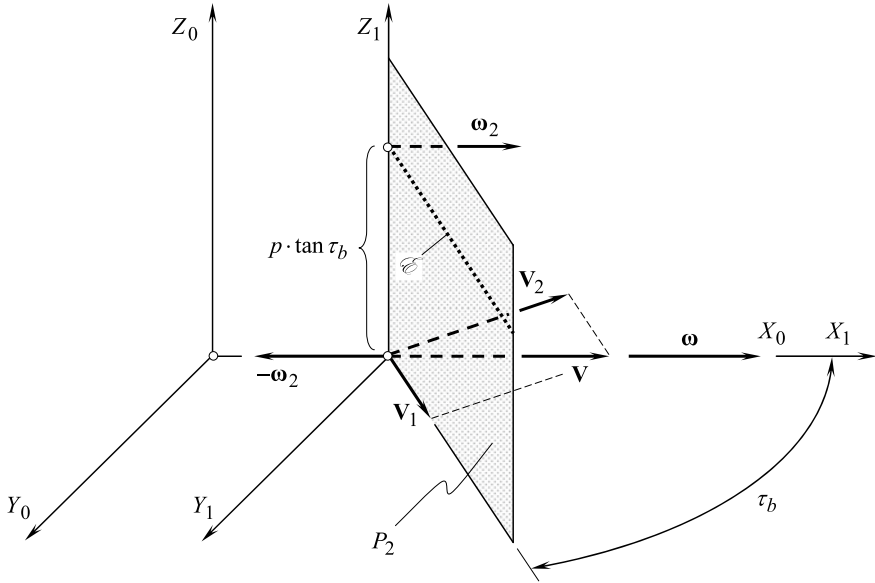


**Fig. 9.7** Generation of a screw involute part surface  $P_1$  as an enveloping surface for successive positions of a plane  $P_2$  that is performing a screw motion

$$\mathbf{n}_{P2} = \begin{bmatrix} 1 \\ -\tan \tau_b \\ 0 \\ 1 \end{bmatrix} \quad (9.41)$$

The position vector  $\mathbf{r}_{P2}$  of an arbitrary point  $m$  of the plane  $P_2$  can be represented in the form:

$$\mathbf{r}_{P2} = \begin{bmatrix} X_{P2} \\ Y_{P2} \\ Z_{P2} \\ 1 \end{bmatrix} \quad (9.42)$$

The speed of the point of interest  $m$  in its screw motion can be calculated from the expression:

$$\mathbf{v}_m = \mathbf{v} + [\boldsymbol{\omega} \times \mathbf{R}] \quad (9.43)$$

Here, we denote:

- $\mathbf{v}$  The speed of the translational motion
- $\boldsymbol{\omega}$  The speed of the rotational motion.

To determine the characteristic  $\mathcal{E}$ , the direction of the unit vector  $\mathbf{v}_m$  is of importance while the magnitude of this vector is not important. Hence, it can be assumed that  $|\boldsymbol{\omega}| = 1$ . Therefore:

$$\boldsymbol{\omega} = \mathbf{i} \quad (9.44)$$

$$\mathbf{v} = \mathbf{i} \cdot p \quad (9.45)$$

Equation (9.45) and Eq. (9.46) allow for an expression:

$$\mathbf{v}_m = \mathbf{i} \cdot p + \begin{vmatrix} \mathbf{i} & \mathbf{j} & \mathbf{k} \\ 1 & 0 & 0 \\ X_1 & Y_1 & Z_1 \end{vmatrix} \quad (9.46)$$

and

$$\mathbf{v}_m = \mathbf{i} \cdot p - \mathbf{j} \cdot Y_1 + \mathbf{k} \cdot Z_1 \quad (9.47)$$

or

$$\mathbf{v}_m = \begin{bmatrix} p \\ Y_1 \\ Z_1 \\ 0 \end{bmatrix} \quad (9.48)$$

The dot product of the unit normal vector  $\mathbf{n}_{P_2}$  and of the speed  $\mathbf{v}_m$  of the translational motion can be expressed analytically as:

$$\mathbf{n}_{P_2} \cdot \mathbf{v}_m = p \cdot \tan \tau_b - Z_1 = 0 \quad (9.49)$$

Thus, for the case under consideration, the “*Shishkov equation of contact*,  $\mathbf{n} \cdot \mathbf{V}_\Sigma = 0$ ” can be represented in the form:

$$Z_1 = p \cdot \tan \tau_b \quad (9.50)$$

The above equation of contact together with equation of the plane  $P_2$  represents the characteristic  $\mathcal{E}$ . Position vector of a point  $\mathbf{r}_\mathcal{E}$  of the characteristic  $\mathcal{E}$  can be expressed as:

$$\mathbf{r}_\mathcal{E}(t) = \begin{bmatrix} y \\ t \cdot \tan \tau_b \\ p \cdot \tan \tau_b \\ 1 \end{bmatrix} \quad (9.51)$$

Here, the parameter of the characteristic  $\mathcal{E}$  is denoted by  $t$ .

In the example under consideration, the characteristic  $\mathcal{E}$  is the straight line of intersection of these two planes. It is parallel to the coordinate plane  $X_1Z_1$  and distanced from the plane at  $p \cdot \tan \tau_b$ .

For a specified screw motion, the characteristic  $\mathcal{E}$  remains its location within the plane  $P_2$  in the initial coordinate system  $X_0Y_0Z_0$ .

The angle of rotation of the coordinate system  $X_1Y_1Z_1$  about the  $X_0$ -axis is designated  $\varepsilon$ . The translation of the coordinate system  $X_1Y_1Z_1$  with respect to the reference system  $X_0Y_0Z_0$  that corresponds to the angle  $\varepsilon$  can be expressed in terms of the reduced pitch  $p$  as  $p \cdot \varepsilon$ . This makes it possible to compose an equation for the operator  $\mathbf{Rs}(1 \rightarrow 0)$  of the resultant coordinate system transformation:

$$\mathbf{Rs}(1 \rightarrow 0) = \begin{bmatrix} 1 & 0 & 0 & p \cdot \varepsilon \\ 0 & \cos \varepsilon & \sin \varepsilon & 0 \\ 0 & -\sin \varepsilon & \cos \varepsilon & 0 \\ 0 & 0 & 0 & 1 \end{bmatrix} \quad (9.52)$$

In order to represent analytically the enveloping part surface  $P_1$ , we need to consider the equation  $\mathbf{r}_{\mathcal{E}}(t)$  of the characteristic line  $\mathcal{E}$  together with the operator  $\mathbf{Rs}(1 \rightarrow 0)$  of the resultant coordinate system transformation. Ultimately, the position vector of a point  $\mathbf{r}_{P_1}$  of the part surface  $P_1$  can be expressed by the column matrix:

$$\mathbf{r}_{P_1}(X_1, \varepsilon) = \begin{bmatrix} X_1 + p \cdot \varepsilon \\ X_1 \cdot \tan \tau_b \cdot \cos \varepsilon + p \cdot \tan \tau_b \cdot \sin \varepsilon \\ -X_1 \cdot \tan \tau_b \cdot \sin \varepsilon + p \cdot \tan \tau_b \cdot \cos \varepsilon \\ 1 \end{bmatrix} \quad (9.53)$$

Consider the intersection of the enveloping part surface  $P_1$  by the plane:

$$X_0 = X_1 + p \cdot \varepsilon = 0 \quad (9.54)$$

It is convenient to represent the last equation in the form:

$$X_1 = -p \cdot \varepsilon \quad (9.55)$$

Therefore:

$$\mathbf{r}_{X_0}(\varepsilon) = \begin{bmatrix} 0 \\ p \cdot \tan \tau_b \cdot (\sin \varepsilon - p \cdot \varepsilon \cdot \cos \varepsilon) \\ p \cdot \tan \tau_b \cdot (\cos \varepsilon + p \cdot \varepsilon \cdot \sin \varepsilon) \\ 1 \end{bmatrix} \quad (9.56)$$

An involute of a circle is analytically described by Eq. (9.56).

The radius of the base circle of the involute curve can be calculated from the equation:

$$r_b = p \cdot \tan \tau_b \quad (9.57)$$

Therefore, the enveloping part surface  $P_1$  for successive positions of a plane  $P_2$  having a screw motion is a screw involute surface. The reduced pitch of the involute screw surface equals  $p$ , and the radius of the base cylinder equals  $r_b = p \cdot \tan \tau_b$ . The screw involute surface intersects the base cylinder. The line of intersection is a helix. Tangent to the helix makes the angle  $\omega_b$  with the axis of screw motion:

$$\tan \omega_b = \frac{r_b}{p} \quad (9.58)$$

It can be deduced from this that  $\tan \omega_b = \tan \tau_b$  and, thus,  $\omega_b = \tau_b$ . The straight-line characteristic  $\mathcal{E}$  is tangent to the helix of intersection of the enveloping part surface  $P_1$  with the base cylinder. This means that if a plane  $A$  is tangent to the base cylinder, then:

- (i) a straight line  $\mathcal{E}$  within a plane  $A$  forms an angle  $\tau_b$  with the axis of the screw motion,
- (ii) the plane  $A$  is rolling over the base cylinder without sliding, so the enveloping surface  $P_1$  can be represented as a locus of successive positions of the straight line  $\mathcal{E}$  that rolls without sliding over the base cylinder together with the plane  $A$ . The enveloping surface is a screw involute surface.

Another solution to the problem of determining the envelope for a plane having screw motion can be found in the monograph by Cormac [7].

Implementation of the kinematic method for determining the enveloping part surface for successive positions of a given smooth regular part surface that is moving in space in relation to a motionless reference system is especially beneficial in cases when:

- (a) the geometry of the moving part surface is simple (a plane, a cylinder of revolution, a cone of revolution, a sphere, many surfaces of translation, many surfaces of rotation, as well as many screw surfaces), and
- (b) the motion of the given surface in relation to the motionless reference system is simple (straight motion, rotation, or a combination of these elementary motions).

Owing to the simplicity of the surface geometry, the unit normal vector  $\mathbf{n}$  to the moving surface can be determined directly, with no need to differentiate the equation of the part surface with respect to the surface parameters. Similarly, the simplicity of the relative motion makes it possible determination of an expression for the linear velocity vector  $\mathbf{V}_\Sigma$  of the resultant motion of the part surface in relation to the stationary reference system without differentiation.

Consider an example.

*Example 9.3* Given the screw involute surface  $\mathcal{G}$  shown in Fig. 1.10, the position vector of a point  $\mathbf{r}_g$  of the surface  $\mathcal{G}$  can be expressed in matrix form [see Eq. (1.52)]:

$$\mathbf{r}_g(U_g, V_g) = \begin{bmatrix} 0.5d_{b,g} \cos V_g + U_g \sin \psi_{b,g} \sin V_g \\ 0.5d_{b,g} \sin V_g - U_g \cos \psi_{b,g} \sin V_g \\ 0.5d_{b,g} \tan \psi_{b,g} - U_g \cos \psi_{b,g} \\ 1 \end{bmatrix} \quad (9.59)$$

where

$U_g, V_g$  Is the *Gaussian* (curvilinear) coordinates on the screw involute surface  $\mathcal{G}$   
 $d_{b,g}$  Is the diameter of the base cylinder of the screw involute surface  $\mathcal{G}$   
 $\psi_{b,g}$  Is the base helix angle of the screw involute surface  $\mathcal{G}$ .

Once an equation of the part surface  $\mathcal{G}$  is known, the tangent vectors  $\mathbf{U}_g$  and  $\mathbf{V}_g$  can be derived [see Eqs. (1.53) and (1.54)]:

$$\mathbf{U}_g(U_g, V_g) = \frac{\partial \mathbf{r}_g}{\partial U_g}(U_g, V_g) = \begin{bmatrix} \sin \psi_{b,g} \sin V_g \\ -\cos \psi_{b,g} \sin V_g \\ -\cos \psi_{b,g} \\ 0 \end{bmatrix} \quad (9.60)$$

$$\mathbf{V}_g(U_g, V_g) = \frac{\partial \mathbf{r}_g}{\partial V_g}(U_g, V_g) = \begin{bmatrix} -0.5d_{b,g} \sin V_g + U_g \sin \psi_{b,g} \cos V_g \\ 0.5d_{b,g} \cos V_g - U_g \cos \psi_{b,g} \cos V_g \\ 0 \\ 0 \end{bmatrix} \quad (9.61)$$

The expressions derived for the tangent vectors  $\mathbf{U}_g$  and  $\mathbf{V}_g$  [see Eqs. (9.60) and (9.61)] make possible the derivation of an expression for the unit normal vector  $\mathbf{n}_g$  to the moving part surface  $\mathcal{G}$  [see Eq. (1.17)]:

$$\mathbf{n}_g = \frac{\mathbf{U}_g \times \mathbf{V}_g}{|\mathbf{U}_g \times \mathbf{V}_g|} \quad (9.62)$$

After substituting Eqs. (9.60) and (9.61) into Eq. (9.62), and after making necessary formula transformations, one can come up with an expression for the unit normal vector  $\mathbf{n}_g$ :

$$\mathbf{n}_g(U_g, V_g) = \begin{bmatrix} -\cos \psi_{b,g} \cos V_g \\ \cos \psi_{b,g} \sin V_g \\ \sin \psi_{b,g} \\ 0 \end{bmatrix} \quad (9.63)$$

The problem of derivation of an equation for the unit normal vector to a surface is simple in nature; however in particular cases, it can be inconvenient technically. Let's

consider how an expression for that same unit normal vector  $\mathbf{n}_g$  [see Eq. (9.63)] can be obtained from the analysis of features of geometry of the part surface  $\mathcal{G}$ , namely what the kinematic method is focused on and where implementation of the method can be beneficial.

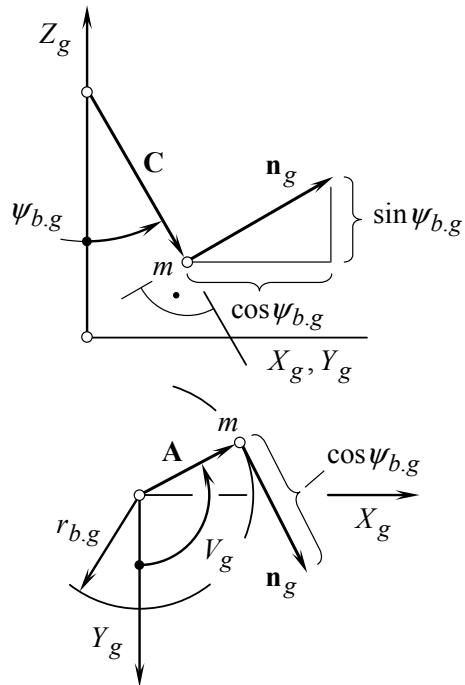
Refer to Fig. 9.8 for a more detailed analysis. A straight line along the unit normal vector  $\mathbf{n}_g$  is tangent to the base cylinder of diameter  $d_{b.g}$ . Moreover, this straight line is crossing with the axis of the screw involute surface  $\mathcal{G}$  at an angle that is equal to  $(90^\circ - \psi_{b.g})$ . This immediately yields an expression for the unit normal vector  $\mathbf{n}_g$ :

$$\mathbf{n}_g(U_g, V_g) = \begin{bmatrix} -\cos \psi_{b.g} \cos V_g \\ \cos \psi_{b.g} \sin V_g \\ \sin \psi_{b.g} \\ 0 \end{bmatrix} \quad (9.64)$$

It is of critical importance to stress here that Eqs. (9.63) and (9.64) are identical to one another. However, no derivatives are used for the derivation of Eq. (9.64). This advantage of the second approach is utilized when “kinematic method” for the determination of enveloping part surface is used.

For the purposes of determination of the linear velocity vector  $\mathbf{V}_\Sigma$  of the resultant relative motion of the screw involute part surface  $\mathcal{G}$  and of the part surface to be

**Fig. 9.8** Determination of the unit normal vector  $\mathbf{n}_g$  to a screw involute part surface  $\mathcal{G}$  based on the analysis of the features of the part surface geometry (in a case when the “kinematic method” for the determination of enveloping part surfaces is used)



determined, let's consider the case when both the surfaces are rotating about parallel axes.

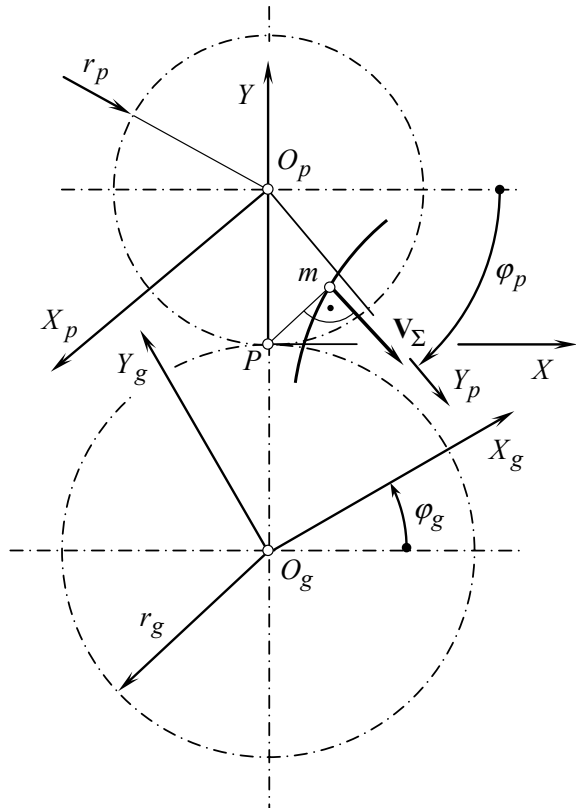
The given screw involute part surface  $\mathcal{G}$  is rotating about the axis  $O_g$  as it is shown schematically in Fig. 9.9. A reference system  $X_p Y_p Z_p$  of an enveloping part surface to be determined (the surface  $\mathcal{P}$ , not shown in Fig. 9.9) is rotating about the axis  $O_p$ . The axes  $O_g$  and  $O_p$  are parallel to one another. The angle of rotation  $\varphi_p$  of the reference system  $X_p Y_p Z_p$  corresponds to an angle of rotation  $\varphi_g$  of the reference system  $X_g Y_g Z_g$  associated with the part surface  $\mathcal{G}$ . The current value of the angle  $\varphi_p$  can be calculated from the expression:

$$\varphi_p = \varphi_g \frac{r_g}{r_p} \quad (9.65)$$

Here, the radii of pitch circles of the part surfaces  $\mathcal{G}$  and  $\mathcal{P}$  are designated as  $r_g$  and  $r_p$  accordingly.

The origin of a stationary reference system  $XYZ$  is placed at the point of tangency of the pitch circles of radii  $r_g$  and  $r_p$ , namely at the pitch point  $\mathcal{P}$ .

**Fig. 9.9** Determination of the linear velocity vector  $\mathbf{V}_\Sigma$  of the resultant motion of the part surface  $\mathcal{G}$  in relation to a reference system of the enveloping part surface  $\mathcal{P}$



An arbitrary point  $m$  is located within the part surface  $\mathcal{G}$ . In a particular case, this point can be located within the coordinate plane  $X_g = 0$ . The coordinates of the point  $m$  are denoted by  $X_m$  and  $Y_m$  (remember that in the example under consideration, it is assumed that  $Z_g = 0$ ).

The linear velocity vector  $\mathbf{V}_\Sigma$  of the resultant relative motion of the screw involute part surface  $\mathcal{G}$  and of the part surface to be determined can be analytically expressed by equation:

$$\mathbf{V}_\Sigma = \mathbf{i} \cdot Y_m + \mathbf{j} \cdot X_m \quad (9.66)$$

It is of critical importance to stress here that no operation of differentiation is used when composing Eq. (9.66).

At this point, the determined vectors  $\mathbf{n}_g$  [see Eq. (9.64)] and  $\mathbf{V}_\Sigma$  [see Eq. (9.66)] are represented in different reference systems. The vector  $\mathbf{n}_g$  is represented in the coordinate system  $X_g Y_g Z_g$  associated with the screw involute part surface  $\mathcal{G}$ , while the vector  $\mathbf{V}_\Sigma$  is analytically expressed in the motionless coordinate system  $XYZ$ . As the vectors  $\mathbf{n}_g$  and  $\mathbf{V}_\Sigma$  should be considered together, we need to represent both of them in a common reference system. Then, we can allow substitution of the derived equations for the vectors  $\mathbf{n}_g$  and  $\mathbf{V}_\Sigma$  into the “*Shishkov equation of contact*,”  $\mathbf{n}_g \cdot \mathbf{V}_\Sigma = 0$ ,” Further analysis is trivial and, therefore, is beyond the scope of this monograph. The interested reader may exercise himself/herself on the required formula transformations in this particular example.

The discussed example reveals the possibility of determination of the unit normal vector  $\mathbf{n}_g$ , as well as of the linear velocity vector  $\mathbf{V}_\Sigma$  of the resultant relative motion using no operation of differentiation for particular surfaces, which are performing certain relatively simple motions in relation to one another. Under such a scenario, namely when no operations of differentiation are used, implementation of the “*kinematic method*” for determining enveloping surfaces is reasonable. In this case, implementation of the equation of contact in *Shishkov’s* form:

$$\mathbf{n} \cdot \mathbf{V}_\Sigma = 0 \quad (9.67)$$

makes sense.

When expressions for either the unit normal vector  $\mathbf{n}$ , or the linear velocity vector  $\mathbf{V}_\Sigma$  of the resultant relative motion, or for both are derived based on derivatives of the moving part surface [see Eqs. (9.60) and (9.61)], then the “*kinematic method*” is less beneficial. In cases when expressions for the unit normal vector  $\mathbf{n}$ , and/or for the linear velocity vector  $\mathbf{V}_\Sigma$  of the resultant relative motion, are derived based on derivatives, then the “*kinematic method*” reduces to conventional method that is extensively used in differential geometry of surfaces. In order to illustrate the last statement, the “*Shishkov equation of contact*” [see Eq. (9.67)] is rewritten in the form:



$$\left[ \underbrace{\frac{\partial \mathbf{r}}{\partial U}}_{\mathbf{n}} \quad \frac{\partial \mathbf{r}}{\partial V} \quad \frac{\partial \mathbf{r}}{\partial \omega} \right]^T = 0 \quad (9.68)$$

As in the equation of contact [see Eq. (9.67)], the dot product of the vectors  $\mathbf{n}$  and  $\mathbf{V}_\Sigma$  is equalized to zero, and the multiplier  $\left| \frac{\partial \mathbf{r}}{\partial U} \times \frac{\partial \mathbf{r}}{\partial V} \right|^{-1}$  is omitted in the expression for the unit normal vector  $\mathbf{n}$ .

#### 9.4 Peculiarities of Implementation of the “Kinematic Method” in Cases of Multi-parametric Relative Motion of Surfaces

The resultant motion of the moving smooth regular part surface  $P_1$  in relation to the motionless reference surface of the part surface  $P_2$  to be generated can be decomposed onto several,  $n$ , elementary motions (here,  $n$  is an integer number). The “*Shishkov equation of contact*” [see Eq. (9.67)] is still valid when the resultant motion  $\mathbf{V}_\Sigma$  is considered (Fig. 9.10):

$$\mathbf{n} \cdot \sum_{i=1}^n \mathbf{V}_i = 0 \quad (9.69)$$

However, it is wrong to demand that any and all of the elementary motions  $\mathbf{V}_i$  fulfill this requirement; namely, the equality:

$$\mathbf{n} \cdot \mathbf{V}_i = 0 \quad (9.70)$$

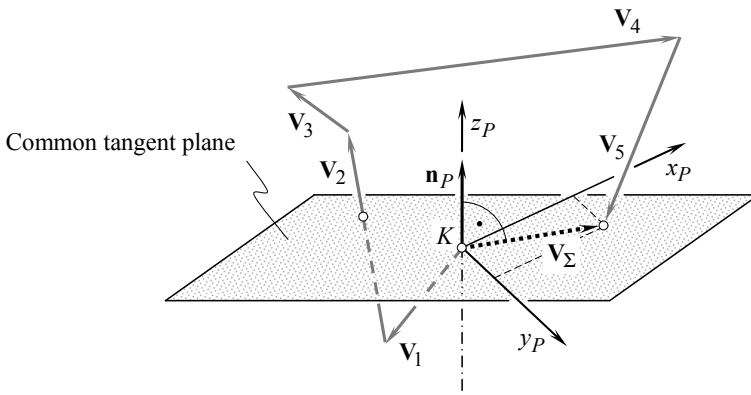


**Fig. 9.10** Linear velocity vector of the resultant motion  $\mathbf{V}_\Sigma$  of two smooth regular part surfaces  $P_1$  and  $P_2$  in a case of multi-parametric relative motion of the surfaces

describes the sufficient condition for the enveloping surface’s existence, which is not mandatory. The projection  $\text{Pr}_{\mathbf{n}} \mathbf{V}_i$  of a linear velocity vector  $\mathbf{V}_i$  of elementary motion onto direction of the common perpendicular,  $\mathbf{n}$ , can differ from zero ( $\text{Pr}_{\mathbf{n}} \mathbf{V}_i \neq 0$ ). The summa of all the projections  $\text{Pr}_{\mathbf{n}} \mathbf{V}_i$  is mandatorily equal to zero:

$$\sum_{i=1}^n \text{Pr}_{\mathbf{n}} \mathbf{V}_i = 0 \quad (9.71)$$

In practice, the “kinematic method” for the determination of enveloping part surface is used, for example, when the first method by *Theodore Olivier*<sup>1</sup> [10] is implemented [1, 3, 8] and many others.

## References

1. Radzevich, S. P. (1991). Differential-geometrical method of surface generation. *Doctoral Thesis, Tula, Tula Polytechnic Institute*, 300p.
2. Radzevich, S. P. (2008). *Kinematic geometry of surface machining* (p. 536). Boca Raton, Florida: CRC Press.
3. Radzevich, S. P. (1991). *Sculptured surface machining on multi-axis NC machine, Monograph* (p. 192). Kiev: Vishcha Schola.
4. Radzevich, S. P. (2012). *Theory of gearing: Kinematics, geometry, and synthesis* (p. 856). Boca Raton, Florida: CRC Press.
5. Radzevich, S. P. (2018). *Theory of gearing: Kinematics, geometry, and synthesis* (2nd ed., p. 898). Boca Raton, Florida: CRC Press.
6. L’ukshin, V. S. (1968). *Theory of screw surfaces in cutting tool design* (p. 372p). Moscow: Mashinostroyeniye.
7. Cormac, P. (1936). *A treatise on screws and worm gear, their mills and hobs* (p. 138). London: Chapman & Hall Ltd.
8. Radzevich, S. P. (2001). *Fundamentals of surface generation, Monograph* (p. 592). Kiev: Rastan.
9. Shishkov, V. A. (1951). *Generation of surfaces using continuously indexing method* (p. 152). Moscow: Mashgiz.
10. Olivier, T. (1842). *Théorie Géométrique des Engrenages destinés* (p. 118). Paris: Bachelier.

---

<sup>1</sup> *Theodore Olivier* (January 21–August 5, 1853)—French Mathematician and Engineer.

# Chapter 10

## Generation of Enveloping Surfaces: Special Cases



When considering enveloping surface in general, it should be noticed that an enveloping surface is generated by a smooth regular part surface, which is performing a certain motion in relation to a reference system the generated part surface (the envelope) will be associated with. This makes it possible to conclude that three components in total are involved in the enveloping process, namely:

- (a) a moving smooth regular part surface,
- (b) a certain motion of the given part surface in relation to a reference system, and
- (c) the generated part surface associated with the reference system.

In cases, when two of the three components are known, the third one can be derived from the two known ones. In common practice, item (c) can be determined on the premise of the items (a) and (b). However, item (b) can be derived from the item (a) and (c) as well.

A few special cases of enveloping are distinguished. From this perspective, it makes sense to begin with consideration of one special case of enveloping, namely, with the case when the envelope allows for “*sliding over themselves*.”

### 10.1 Part Surfaces that Allow for “*Sliding Over Themselves*”

Generally speaking, all part surfaces fall in one of two groups. First, these are part surfaces those allow for “*sliding over themselves*.” Second, these are sculptured part surfaces or, in other words, part surfaces that do not allow for “*sliding over themselves*.”

In practice, a small number of kinds of surfaces with relatively simple geometry are extensively used. Surfaces of this particular kind allow for “*sliding over themselves*.” The property of a surface to allow for “*sliding over themselves*” means that for a certain part surface  $P$  there exists a corresponding motion of a special kind. While performing this motion, the enveloping surface to successive position of the moving

surface  $P$  is congruent to the surface  $P$  itself. With that said, those surfaces that allow for “*sliding over themselves*” can be interpreted as a kind of enveloping surfaces.

The above-mentioned motion can be of the following three kinds: either

- (a) mono-parametric, or
- (b) bi-parametric, or
- (c) tri-parametric.

All possible kinds of part surfaces that allow for “*sliding over themselves*” are schematically depicted in Fig. 10.1. Part surfaces of this particular kind are invariant with respect to a group of elementary motions. A group of elementary motions can be comprised of either just one motion or two motions; ultimately, a group of motions can be comprised of three motions. In cases of two and three motions in a group of motions, these motions are not synchronized with one another.

A screw surface of a constant axial pitch ( $p_x = \text{Const}$ ) is the most general kind of surfaces allowing for “*sliding over themselves*.” While performing a screw motion having that same axial pitch  $p_x$  as the axial pitch of the part surface, the surface  $P$  is sliding over itself similar to that observed in a pair “*bolt-and-nut*.”

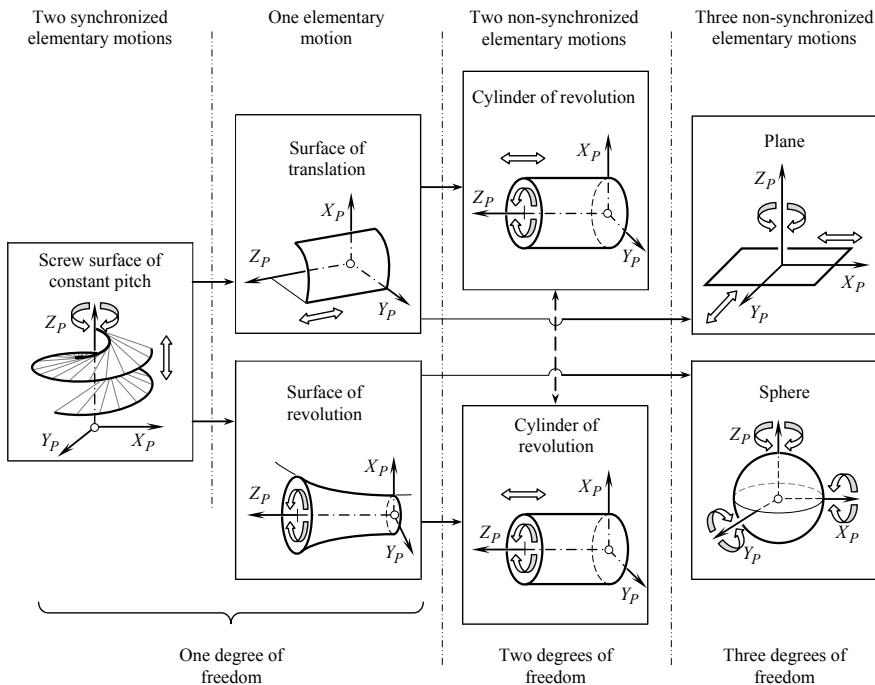


**Fig. 10.1** Part surfaces  $P$  invariant with respect to a group of motions. Adopted from Prof. Radzevich [1]

When the axial pitch of a screw surface reduces to zero ( $p_x = 0$ ), the screw surface degenerates to a surface of revolution. Every surface of revolution is sliding over itself when rotating about the axis of rotation of the surface.

When the axial pitch of a screw surface is increased and equal to infinity, the screw surface degenerates to a surface of translation, that is, to a cylinder of general kind (not mandatory to a cylinder of revolution). Surfaces of that kind allow for a straight motion along straight generating lines of the part surface  $P$ .

The above-considered motions of surfaces are of three kinds, namely:

- (a) a screw motion of constant axial pitch  $p_x = \text{Const}$ ,
- (b) a rotation about the axis of rotation of a surface of revolution, and
- (c) a translation along straight generating line of a general cylinder correspondingly.

All of these motions are mono-parametric.

In addition to part surfaces that allow for a mono-parametric motion, a part surface of certain geometry allows for sliding when the surface motion is either a two-parametric or a three-parametric.

Surfaces like a cylinder of revolution allow for rotation about, as well as translation along, the axis of rotation of the cylinder of revolution. In this case, the surface motion is bi-parametric (rotation and translation can be performed independently).

A sphere allows for rotations about three axes independently. A plane surface allows for translations in two different directions as well as for a rotation about an axis that is orthogonal to the plane. The surface motion in the last two cases (for a sphere and a plane) is tri-parametric.

Ultimately, one can summarize the surfaces that allow for sliding over themselves, as being limited to:

- (a) screw surfaces of constant axial pitch,
- (b) surfaces of translation (cylinders of general kind),
- (c) surfaces of revolution,
- (d) cylinders of revolution,
- (e) spheres, and
- (f) planes.

It is proven [1–4] that surfaces of no other kinds those that allow for “*sliding over themselves*” are feasible.

It is also being proven that those part surfaces that allow for “*sliding over themselves*” are very convenient for machining, as well as for other engineering applications. Most of the surfaces being machining in various industries are surfaces of this nature.

Unfortunately, more in detail classification of part surfaces those allow for “*sliding over themselves*” is not developed to this end.

## 10.2 Reversibly Enveloping Surfaces: Introductory Remarks

Reversibly enveloping part surfaces are another special kind of enveloping surfaces.

In engineering applications, these smooth regular part surfaces are of particular interest, as they allow for reproducing the desired motion of the driven component to be reproduced. Moreover, it is necessary to reproduce the desired relative motion when that motion is transmitting from the driving element to the driven element, as well as in cases where the driving component is turned to be driven, and when the driven element is turned to be driving component accordingly. This important property of enveloping surfaces can be formulated as follows.

**A desired property of enveloping surfaces:** *For a particular application, it is required to design the driving and the driven elements so as to make the enveloping surfaces capable of reproducing the desired relative motion in both directions, namely, when one of the part surfaces is driving, and another one is driven, as well as the motion is transmitting in opposite direction.*

Enveloping part surfaces that possess this property are referred to as the “*reversibly enveloping surfaces*” or just “*R<sub>e</sub>-surfaces*” for simplicity (or “*R<sub>e</sub>-profiles*” if the two-dimensional case is considered). “*R<sub>e</sub>-surfaces*” are of prime importance for engineering applications.

Not all of smooth regular part surfaces meet this requirement.

For example, consider a case when a steady rotation at constant angular velocity of one of two parallel shafts (namely the driving shaft) is transmitting to a steady rotation at constant angular velocity of another two shafts (namely the driven shaft). The example is illustrated in Fig. 10.2.

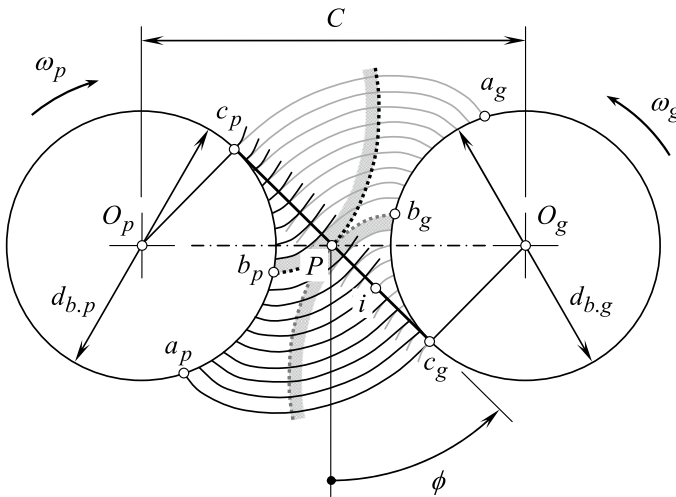


**Fig. 10.2** Involute tooth profiles are profiles of the only geometry capable of transmitting a steady rotation from one shaft to another parallel shaft

The driving shaft is rotating about the axis  $O_p$  at an angular velocity  $\omega_p$ . The driven shaft is rotating about the axis  $O_g$  at an angular velocity  $\omega_g$ . The axes of the rotations are parallel to one another. The distance between the axes  $O_g$  and  $O_p$  is designated as  $C$ . The distance  $C$  is commonly referred to as the “center distance.” In a general case of crossing axes of rotation, the center distance  $C$  is measured along the closest distance of approach between the axes of rotations  $O_g$  and  $O_p$ .

Involute profiles of the interacting part surfaces are developed from the base circles of diameters  $d_{b,g}$  and  $d_{b,p}$ , accordingly. The base circles are centered at the axes of the rotations  $O_g$  and  $O_p$ .

The pitch point  $P$  is located within the centerline  $\mathcal{L}$ , that is, within the straight line along the closest distance of approach between the axes of rotations  $O_g$  and  $O_p$ . The location of the pitch point  $P$  fulfills the ratio  $O_p P / O_g P = \omega_g / \omega_p$ . A straight line that is tangent to the base circles of diameters  $d_{b,g}$  and  $d_{b,p}$  is a straight line through the pitch point  $P$ . This straight line is the line through the points  $c_g$  and  $c_p$ , and forms an angle  $\phi$  with the perpendicular through the pitch point  $P$  to the centerline  $\mathcal{L}$ .

Multiple involutes can be developed from each of two base circles. Involute profiles constructed from the base circle of diameter  $d_{b,g}$  start at the points  $a_g, b_g, c_g$ , and others. Similarly, involute profiles constructed from the base circle of diameter  $d_{b,p}$  start at the points  $a_p, b_p, c_p$ , and others.

Reversibly enveloping involute profiles of the gear and the pinion can be traced by an arbitrary point  $i$  within the straight line  $c_g c_p$ . This conclusion is based on the analogy between gear pairs and between the corresponding “pulley-and-belt transmissions.”

Ultimately, it should be realized from the analysis of Fig. 10.2 that only gears with “involute” tooth profile are capable of transmitting a rotation smoothly: Tooth profiles of no other geometry are capable of doing this. In other words, in the case of parallel axes of rotations of the interacting part surfaces only involutes developed of the base circles of diameters  $d_{b,g}$  and  $d_{b,p}$  represent “ $R_e$ -profiles,” and no other profile can be a kind of “ $R_e$ -profile.” Profiles of any and all other geometries are not capable of transmitting a steady rotation smoothly.

If an arbitrary tooth profile is used in design of the driving gear, then the tooth profile of the driven gear can be generated as an envelope to successive positions of the driving tooth profile. However, this does not mean that arbitrary teeth profiles are capable of transmitting the rotation smoothly. As is well known, non-involute tooth profiles are not capable of transmitting the rotation smoothly as they are not reversibly enveloping to one another.

The interaction of non-involute profiles is illustrated by an example considered below. This example is adapted from the widely used practice of designing a hob for cutting straight-sided splines. This example perfectly illustrates the widely spread poor understanding of generation of enveloping surfaces.

A straight profile is associated with a pitch circle, while the corresponding profile of the rack is associated with the straight pitch line of the rack.

The hob design is based on an auxiliary rack, the teeth of which are engaged in mesh with splines of the spline-shaft. The tooth profile of the rack is commonly generated as an envelope for successive positions of the spline profile when the pitch

circle of the spline is rolling with no sliding over the pitch line associated with the rack.

The determination of coordinates of points of the tooth profile of a rack to machine a spline-shaft is executed in practice using the “*method of common perpendiculars*.” The tooth profile of a spline hob is generated as an envelope to successive positions of the spline profile when the pitch line of the hob is rolling with no slipping over the pitch circle of the spline-shaft. An example of solving a problem of this kind is illustrated in Fig. 10.3.

The profile of the spline is associated with the pitch circle of certain radius  $r_{w.sp}$ . The pitch line of the rack to be determined,  $P_{ln}$ , is in tangency with the pitch circle of the spline-shaft. The point of tangency of the pitch line,  $P_{ln}$ , and of the pitch circle,  $r_{w.sp}$ , is the pitch point in rolling motion of the spline-shaft and of the rack. The pitch point is designated as  $P$ .

The spline-shaft is rotated about its axis of rotation,  $O_{sp}$ . The angular velocity of the rotation is designated as  $\omega_{sp}$ . The rack is associated with the pitch line,  $P_{ln}$ . The rack is traveling straight forward together with the pitch line. The linear velocity of the rack is designated as  $V_{rc}$ .

Let us assume that at the initial configuration of the pitch circle and the pitch line, the profile of the spline passes through the pitch point,  $P$ . This profile is at a distance  $r_{sp}$  from the axis of rotation,  $O_{sp}$ , of the spline-shaft. Practically, the straight-line profile is tangent to a circle of certain radius  $r_{sp}$ . The radius  $r_{sp}$  is equal to a half of spline thickness of the spline-shaft.

When the spline-shaft rotates, the lateral spline profile is rotated together with the spline-shaft. The spline-shaft lateral profile consequently passes through the points

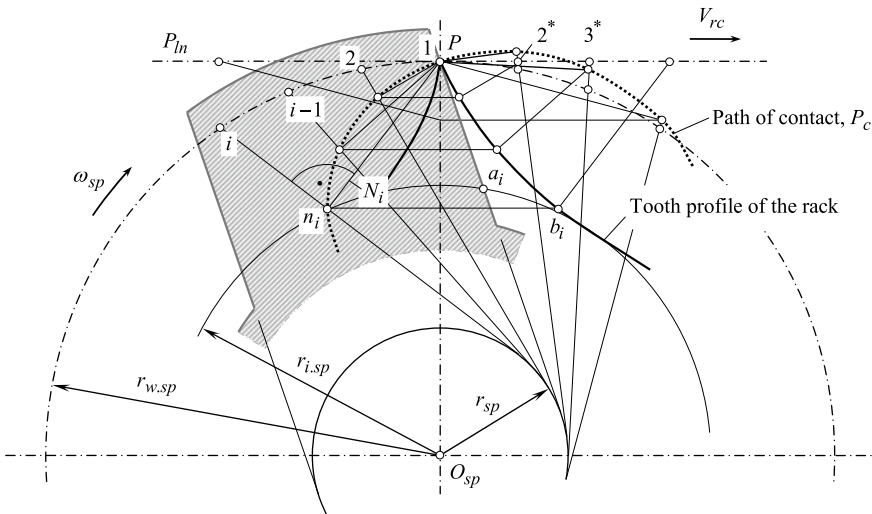


**Fig. 10.3** Interaction between a straight-sided spline profile associated with a pitch circle and a non-involute profile associated with the pitch line



1, 2, ...,  $(i - 1)$ ,  $i$ . The point 1 is coincident with the pitch point,  $P$ . The pitch line is traveling straightforward. In this motion, the pitch point consequently occupies positions  $1^*$ ,  $2^*$ ,  $3^*$ , ... . The distances  $1^* - 2^*$ ,  $2^* - 3^*$  between consequent locations of the pitch point are equal to lengths of the arcs  $\smile 1 - 2$ ,  $\smile 2 - 3$ , ... of the pitch circle of the spline-shaft. This is because the pitch line of the rack is rolling with no slipping over the pitch circle of the spline-shaft.

At every chosen location of the lateral profile of the spline, perpendiculars to the profile are constructed so that all of them are through the pitch point,  $P$ . For example, a perpendicular  $N_i$  is normal to the spline profile in its  $i$ th location (Fig. 10.3). The point  $n_i$  is the point of tangency of the lateral profile of the spline and of the rack tooth profile.

The plurality of points constructed in this way for various configurations of the lateral spline profile is located within the path of contact  $P_c$ , in rolling motion of the given spline-shaft and of the rack to be determined. The path of contact  $P_c$  is constructed in a stationary reference system.

It is anticipated that in a reference system associated with the spline-shaft, all the points are located within the lateral spline profile of the spline-shaft.

When the spline-shaft is rotating, points of the lateral profile consequently pass through the path of contact  $P_c$ . It is supposed that in these instants of time, these points coincide with the corresponding points of the rack tooth profile. If an arbitrary point  $n_i$  within the path of contact, corresponding to the point of contact in  $i$ th location of the lateral profile of the spline, is returned back to the initial position of the spline by means of rotation through the angle of the arc  $Pi$ , then this point will occupy the position of the point  $a_i$ .

It is assumed similarly that in a reference system associated with the rack, contact points are located within tooth profile of the rack to be determined.

Let us assume that an arbitrary point  $n_i$  within the path of contact  $P_c$  is associated with the pitch line,  $P_{in}$ . In order to determine the location of this point in the initial instant of time, the pitch line together with the point  $n_i$  travels through a distance that is equal to the arc length  $Pi$  in the direction opposite to the direction of straight motion of the rack tooth in its rolling motion. After this transition is complete, the point  $n_i$  occupies the position of the point  $b_i$ . The point  $b_i$  is located on tooth profile of the rack. All points of the rack tooth profile are constructed in a way similar to the point  $b_i$ . Connecting the constructed points by a smooth curve, the rack tooth profile can be constructed.

The above-discussed approach for determining tooth profile of a rack is commonly adopted. However, this method is inaccurate in nature.

When the method is used, it is assumed that the generated tooth profile of the rack can generate the spline profile of the spline-shaft when an inverse problem is solving. This is not correct at all. As the tooth profiles are not involutes, no straight spline profile can be obtained using inverse rolling of the rack in relation to the spline-shafts. In practice, instead of straight spline profile a certain curved profile of the splines is obtained (Fig. 10.4).

When the constructed hob tooth profile is rolling in relation to the spline-shaft, the original straight-sided spline profile is not generated; instead, spline profile of other

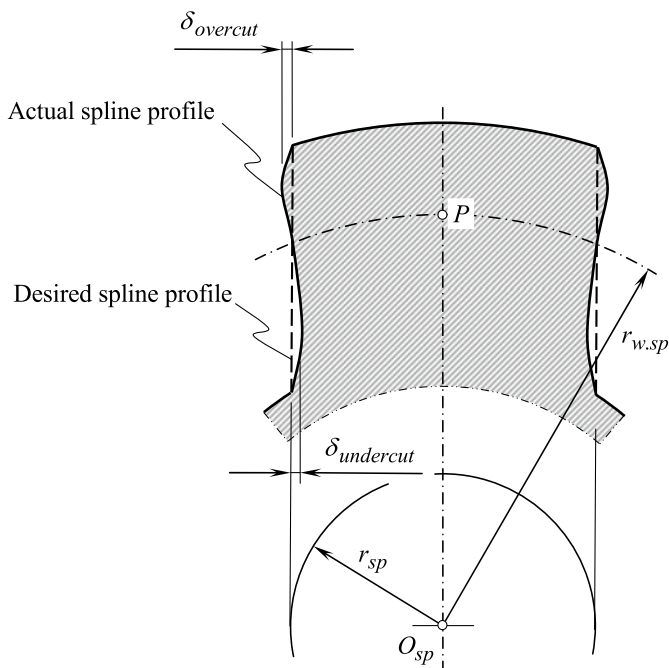


**Fig. 10.4** Deviation of the actual straight profile of the spline (generated as shown in Fig. 10.2) from its desired profile

geometries is generated. Then, we roll the “new” spline profile in relation to the hob, then the hob in relation to the spline, and so on. Under such a scenario, divergence rather than the convergence of the spline profile to the ideal profile is observed. This is valid for a general case of relative motion of two smooth regular part surfaces.

A following conclusion can be drawn from the above consideration.

**Conclusion 10.1** *For the purpose of transmitting a steady rotation from a driving shaft to a driven shaft by means of tooth profiles, non-involute tooth profiles are not applicable at all.*

In the example discussed in Fig. 10.3, the spline tooth profile and the hob tooth profile are not reversibly enveloping tooth profiles. The path of contact,  $P_c$ , is loosely assumed as the line of action,  $LA$ , which is not correct at all—the line of action can be only a straight line and never a curved line. For a pair of reversibly enveloping tooth profiles, a straight tangent at any and all points to the path of contact,  $P_c$ , “*must*” pass through the pitch point,  $P$ . This condition is not met in Fig. 10.3. This is the root cause for the spline tooth profile, and the hob tooth profiles are not reversibly enveloping tooth profiles. Ultimately, the spline tooth profile and the hob tooth profile are enveloping to one another, but they are not reversibly enveloping to one another.

Another approach needs to be implemented for the purpose of derivation of the required teeth profile geometry in order to have them reversibly enveloping to one



In the example discussed in Fig. 10.5, the path of contact,  $P_c$ , and the line of action,  $LA$ , are two straight lines that “align with one another.” At any and all points of the path of contact,  $P_c$ , the line of action,  $LA$ , passes through the pitch point,  $P$  (as these two lines,  $P_c$  and  $LA$ , align with one another). Consequently, the tooth flanks,  $\mathcal{G}$  and  $\mathcal{P}$ , represent a kind of reversibly enveloping tooth surfaces. This is owing to the tooth profiles,  $\mathcal{G}$  and  $\mathcal{P}$ , that are conjugate to one another.

It should be mentioned here that not just straight line can be used for the generation of “reversibly enveloping surfaces.” Planar curves of other geometries (arcs of a circle, arcs of a spiral curve, and so forth) can be used for this purpose as well. Initially specified, the line of contact,  $LC$ , does not change its shape when traveling together with the plane of action,  $PA$ . The line of contact,  $LC$ , remains the same for any and all instant configurations of the axis of instant rotations. The interested reader is referred to [5, 6] for more details on generation of reversibly enveloping part surfaces.

Another example is also pertinent to the field of gearing.

Consider the centroles of a pair of non-circular gears as it is illustrated schematically in Fig. 10.6.

In the example shown in Fig. 10.6, the pinion centrole is shaped in the form of an ellipse. The axis of rotation of the pinion  $O_p$  is the straight line through one of two focuses of the ellipse. The pinion is rotating about the axis  $O_p$  with a certain angular velocity  $\omega_p$ .

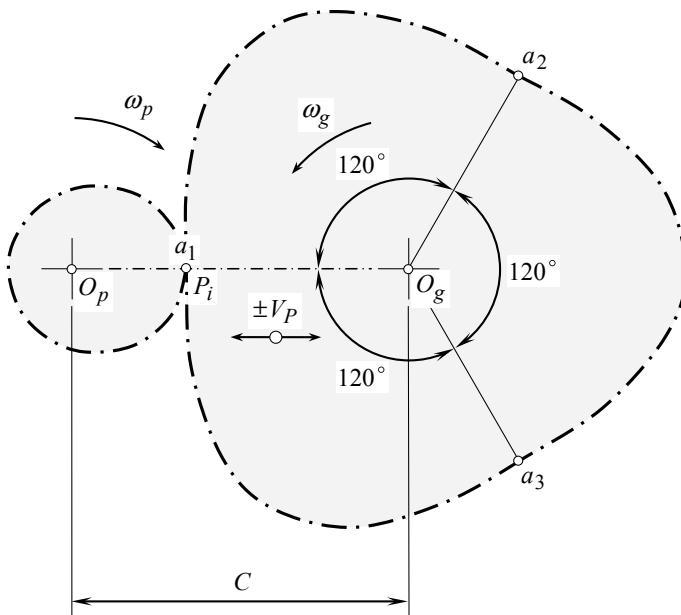


**Fig. 10.6** Example of centroles for a non-circular gearing: the centrole for the one-lobe pinion and the centrole for the three-lobe gear

The axis of rotation of the mating gear  $O_g$  is parallel to the axis  $O_p$  and is remote at a certain center distance  $C$  from the pinion axis of rotation  $O_p$ . Rotation of the gear is denoted by  $\omega_g$ . In the particular case under consideration, the one-lobe pinion is engaged in mesh with a three-lobe gear. This means that the arc lengths  $a_1a_2$ ,  $a_2a_3$ , and  $a_1a_3$  of the gear centrode are equal to one another ( $a_1a_2 = a_2a_3 = a_1a_3$ ), and all of them are equal to perimeter of the pinion centrode. Each of the arc lengths  $a_1a_2$ ,  $a_2a_3$ , and  $a_1a_3$  spans a central angle of  $120^\circ$ . The perimeter of the gear centrode is triple of the pinion centrode.

The instant value of the angular velocity of the driven gear  $\omega_g$  depends on the current value of the angle of rotation,  $\varphi_g$ , of the driving pinion (here,  $\varphi_g = t \omega_g$ , and time is designated  $t$ ). The pitch point  $P$  in the gear pair reciprocates along the centerline,  $\mathcal{L}$ . The linear velocity  $\pm V_P$  is the velocity of the reciprocation. The instant location of the pitch point  $P$  within the centerline,  $\mathcal{L}$ , is designated as  $P_i$ .

When designing non-circular gears, it is commonly assumed that one of the centrodes is specified (in the case under consideration, it is assumed that the pinion centrode is shaped in the form of an ellipse). The corresponding centrode of the mating member is generated as an envelope to successive positions of the given centrode (in the above-considered example illustrated in Fig. 10.6, this is the gear centrode). Unfortunately, in most cases this is not correct as the centrodes are not reversibly enveloping curves—therefore, the centrodes do not exist at all. Therefore, when a driving member having a specified centrode is rotating with a specified constant angular velocity, the centrode of the driven member cannot be generated as an envelope for successive positions of the centrode of the driving member. Unfortunately, if the driven member is turned to be a driving member, and, correspondingly, the driving member is turned to be a driven member, the transmitting rotation is not the inverse one to the original rotation.

**Conclusion 10.2** *It is the wrong way trying to design a non-circular gear so as to generate a centrode on one member of a gear pair as an envelope for successive positions of a pre-specified centrode of another member of the gear pair.*

Unless the pitch lines are in permanent tangency to each other, the required function of the transmitting rotation cannot be reproduced.

For the purposes of designing non-circular gears, another approach should be used when determining the geometry of the tooth flank geometry. The tooth flank geometry should be derived from the required transmission function of the non-circular gear pair [5, 6]. No centrodes are used for this purpose, as no centrodes exist at all.

In order to design the tooth flank for a pair of non-circular gears, two considerations are of critical importance. The first one relates to migration of the pitch point along the centerline,  $\mathcal{L}$ , when the transverse pressure angle is considered constant. The second one relates to variation of the transverse pressure angle when the pitch point considered motionless. These two considerations are used to construct the unique path of contact for a desired non-circular gear pair.

Both of the cases are considered immediately below.

Let us assume that the transverse pressure angle  $\phi$  is of a constant value ( $\phi = \text{const}$ ). The pitch point  $P$  is migrating within the line of centers depending upon the

current value of the rotation angle,  $\varphi_p$ , of the pinion (or of the rotation angle,  $\varphi_g$ , of the gear) as illustrated schematically in Fig. 10.7. The pitch point  $P$  is migrating with a certain angular velocity  $\pm V_P$  in the direction parallel to the line of centers. Under such a scenario, for any instant line of action  $LA_i$ , an instant base circles of the corresponding radii  $r_{b.g}^{(i)}$  and  $r_{b.p}^{(i)}$  can be constructed. The base curve for non-involute gearing can be specified in terms of instant lines of action  $LA_{(i-1)}$ ,  $LA_i$ , and  $LA_{(i+1)}$ , and of radii  $r_{b.p}^{(i-1)}$ ,  $r_{b.p}^{(i)}$ , and  $r_{b.p}^{(i+1)}$  (and  $r_{b.g}^{(i-1)}$ ,  $r_{b.g}^{(i)}$ , and  $r_{b.g}^{(i+1)}$ ) of instant base circles.

It should be pointed out here that in a case of constant transverse pressure angle ( $\phi = \text{const}$ ), and variable position of the pitch point,  $P$ , as illustrated schematically in Fig. 10.7, no reversibly enveloping profiles can be constructed. Moreover, even regular enveloping tooth flanks cannot be generated in this case.

The path of contact,  $P_c$ , for non-involute gearing is a segment of a curve (not shown in Fig. 10.7). A straight line that is tangent to the curved path of contact,  $P_c$ , can be drawn at any point of the path of contact. The tangent can be interpreted as an instant line of action,  $LA_{\text{inst}}$ .

The concept of an instant line of action is helpful for better understanding the kinematics and geometry of gearing, especially of non-circular gearing, as well as non-involute gears.

In non-circular gearing, the straight-line tangent to the path of contact should pass through the pitch point  $P$ . The pitch point  $P$  is located within the centerline,  $\mathcal{L}$ , of the gear pair. The actual location of the point  $P$  can be expressed in terms of the rotations  $\omega_g$  and  $\omega_p$ . The instant line of action,  $LA_i$ , makes a certain angle  $\phi_i$  with

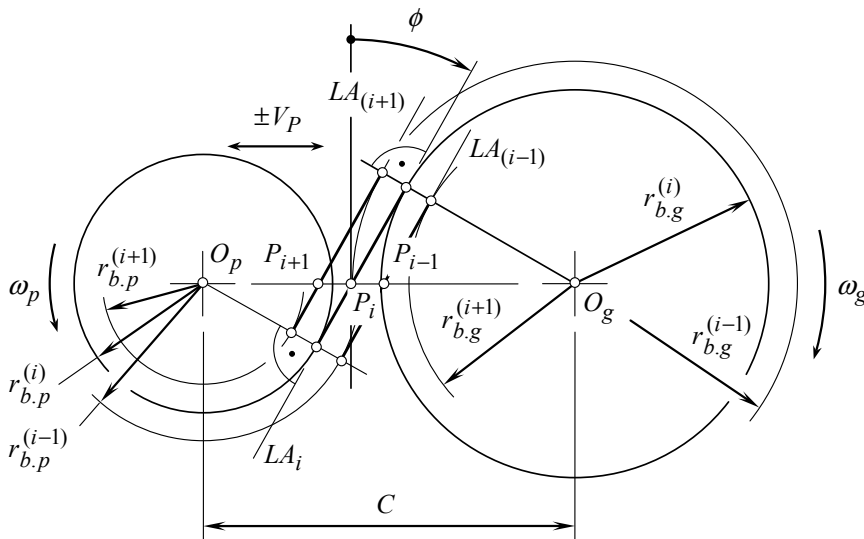


**Fig. 10.7** Schematic of the case of gearing when the pitch point,  $P$ , is migrating within the centerline, and the instant value of the transverse pressure angle  $\phi$  is of a constant value

the perpendicular through  $P$  to the line of center  $\mathcal{L}$ , as illustrated in Fig. 10.8. The angle  $\phi_i$  can be expressed in terms of the rotation angle  $\varphi_p$  (or  $\varphi_g$ ):  $\phi = \phi(\varphi_p)$ .

Under any value of the rotation angle,  $\varphi_p$ , of the pinion (or of the rotation angle,  $\varphi_g$ , of the gear), the instant line of action is tangent to the corresponding instant base circles of radii  $r_{b,p}^{(i)}$  and  $r_{b,g}^{(i)}$ . The base curve for non-involute gearing is an analogy of base circle for involute gearing. The base curve for non-involute gearing can be specified in terms of instant lines of action  $LA_{(i-1)}$ ,  $LA_i$ , and  $LA_{(i+1)}$ , and of radii  $r_{b,p}^{(i-1)}$ ,  $r_{b,p}^{(i)}$ , and  $r_{b,p}^{(i+1)}$  (and  $r_{b,g}^{(i-1)}$ ,  $r_{b,g}^{(i)}$ , and  $r_{b,g}^{(i+1)}$ ) of instant base circles.

It should be pointed out here that in a case of variable transverse pressure angle,  $[\phi = \phi(t)]$ , and stationary pitch point,  $P$ , as illustrated schematically in Fig. 10.8, no reversibly enveloping profiles can be constructed. Moreover, even regular enveloping tooth flanks cannot be generated in this case.

However, both:

- (a) the migration of the pitch point within the centerline and
- (b) the rotation of the instant line of action  $LA_i$  about the pitch point

are feasible for certain non-circular profiles if both of these motions are properly timed with one another. Proper timing of the motions in this sense means that the velocity of the resultant motion of the contact point along the path of contact  $P_c$  must always be perpendicular to the common tangent to the mating profiles at the contact point.

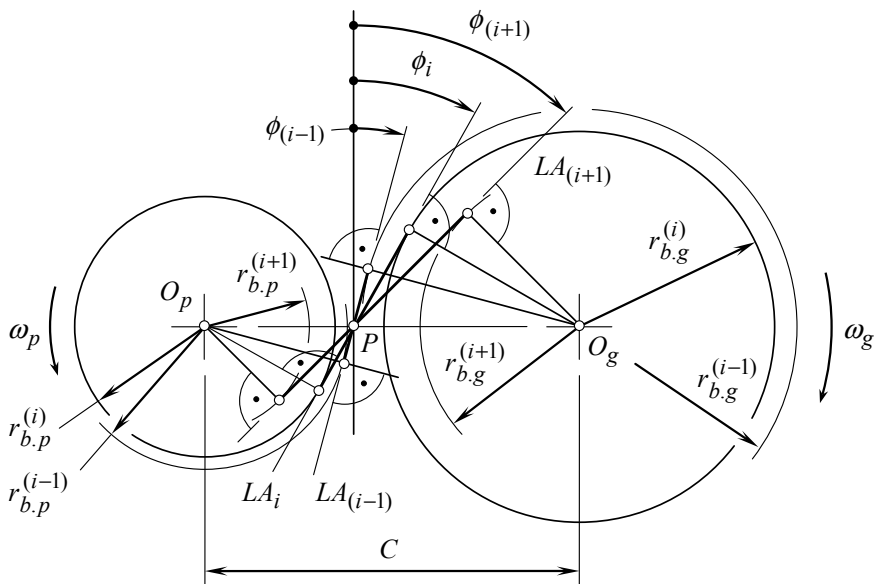


**Fig. 10.8** Schematic of the case when the pitch point,  $P$ , is considered motionless and the instant value of the transverse pressure angle  $\phi$  depends on the angle of rotation of the driving member

The possibility of migration of the pitch point within the centerline along with rotation of the instant line of action about the pitch point is illustrated with an example of the required timing of the motions when determining the geometry of centrodes in non-circular gear.

In this example, depicted schematically in Fig. 10.9, two non-circular gears to be designed are rotating about axes of rotations  $O_g$  and  $O_p$  at angular velocities  $\omega_g$  and  $\omega_p$  accordingly. The axes  $O_g$  and  $O_p$  are parallel to one another and are remote from one another at a certain center distance  $C$ . The example in Fig. 10.9 resembles a “pulley-and-belt transmission” when “non-circular pulleys” are considered.

Consider a case where the pinion is rotating at a constant angular velocity,  $\omega_p$ . Then, the angular velocity of the gear,  $\omega_g$ , in the non-circular gearing to be designed is a function of  $\omega_p$ ,  $\omega_g = \omega_g(\omega_p)$ . As the current value of angle of rotation of the pinion  $\varphi_{p,i}$  can be expressed in terms of time  $t$  and pinion angular velocity  $\omega_p$ , namely  $\varphi_{p,i} = \omega_p t$ , the instant ratio  $r_{p,i}/r_{g,i}$  of the pitch radii of the pinion and the gear is reciprocal to  $\omega_{g,i}/\omega_p$ , where  $\omega_{g,i}$  is the instant rotation of the gear.

Consider a point of contact between the gear and the pinion tooth flanks. This point is designated  $K$ . The contact point is located within a straight line through the axis  $O_p$ . The angular location of the straight line is specified by the central angle  $\varphi_{p,i}$ . The point  $K$  is remote from the axis  $O_p$  at a certain distance  $r_{p,K}$ .

The linear velocity vector  $\mathbf{V}_{p,i}$  of the contact point in its rotation with the pinion is perpendicular to the straight line through the axis  $O_p$  and the contact point  $K$ . This linear velocity  $V_{p,i} = |\mathbf{V}_{p,i}|$  is equal to  $V_{p,i} = \omega_p r_{p,K}$ . The vector  $\mathbf{V}_{p,i}$  of

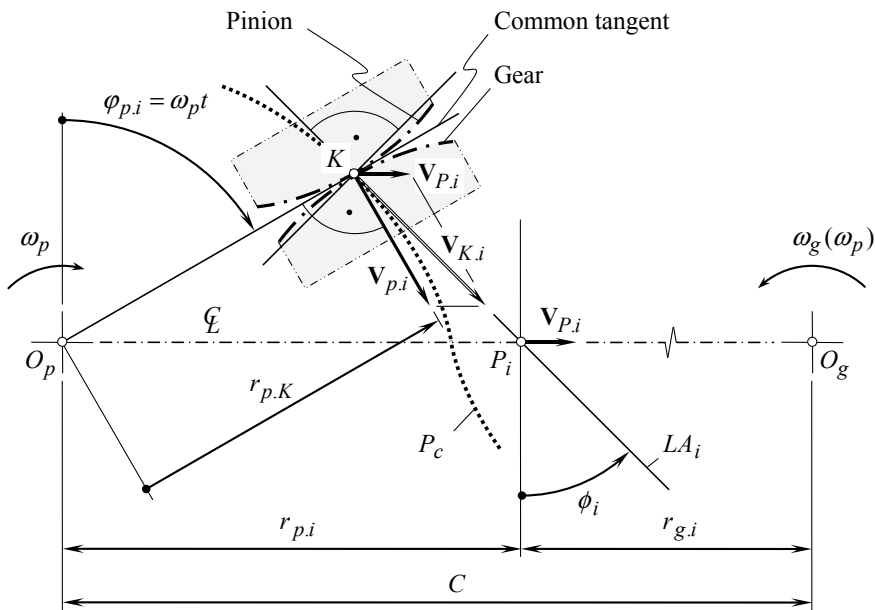


Fig. 10.9 Construction of the tooth flanks in a reversibly enveloping non-circular gear pair



the required instant linear velocity of the pitch point  $P_i$  can be determined from a pre-specified angular velocity ratio:

$$u = \frac{\omega_p}{\omega_g(\omega_p)} = \frac{\varphi_{p,i}}{t} \cdot \frac{t}{\varphi_{g,i}} = u(\varphi_{p,i}) \quad (10.1)$$

Ultimately, vector  $\mathbf{V}_{K,i}$  of the resultant linear velocity of the contact point  $K$  is a superposition of the linear velocities  $\mathbf{V}_{p,i}$  and  $\mathbf{V}_{P,i}$ :

$$\mathbf{V}_{K,i} = \mathbf{V}_{p,i} + \mathbf{V}_{P,i} \quad (10.2)$$

The vector  $\mathbf{V}_{K,i}$  of the resultant linear velocity goes through the instant pitch point,  $P_i$ . Therefore, the instant pitch point in a non-circular gearing can be determined as the point of intersection between the centerline and the straight line along the vector  $\mathbf{V}_{K,i}$ . This straight line is referred to as the “*instant line of action*” and is designated as  $LA_i$ . The common tangent for contacting centrodes is a straight line through the contact point,  $K$ , that is perpendicular to the instant line of action.

The path of contact  $P_c$  is a planar curve that can be interpreted as a family of instant contact points considered in a motionless reference system. The path of contact  $P_c$  (see Fig. 10.9):

- passes through a current contact point  $K$ ,
- at every instant of time is tangent to the instant line of action,  $LA_i$ , and
- is perpendicular to the common tangent through  $K$ .

Based on the schematic depicted in Fig. 10.9, the tooth flanks for a gear pair having pre-specified angular velocity ratio  $u(\varphi_{p,i})$  can be determined. The tooth flanks in this case are a kind of reversibly enveloping curves (that is, “ $R_e$ -curves”). The desired geometries of both tooth flanks, namely the tooth flank of the gear and the tooth flank of the pinion, can be determined following common practice:

- the tooth flank of the gear is loci of the instant contact point represented in a reference system associated with the gear, and
- the tooth flank of the pinion is loci of the instant contact point represented in a reference system associated with the pinion.

Determined in this way, a pair of tooth flanks is the only possible kind of the tooth flanks that meets the pre-specified angular velocity ratio  $u(\varphi_{p,i})$ . Tooth flanks of no other geometry are capable of to fulfill this requirement.

It should be clearly understood that the concept of “*reversibly enveloping surfaces*” can be easily enhanced to the cases of interaction of two smooth regular part surfaces rotating about intersected axes of rotation, as well as those rotating about crossing axes of rotation. Moreover, the rotation to be transmitted is not necessarily steady: It should follow a prescribed time-dependant function.

### 10.3 Generation of Reversibly Enveloping Surfaces

It is convenient to discuss generation of “*reversibly enveloping surfaces*” (or just “ $R_e$ -surfaces”) following an example of generation of tooth flanks in perfect (that is, geometrically accurate) “*crossed-axes gearing*” (or just “ $C_a$ -gearing”, for simplicity) having line contact between the interacting tooth flanks as proposed earlier by Prof. Radzevich [5, 6]. Gearing of this particular kind is known as “*R-gearing*.” Under such a scenario, one of two smooth regular part surfaces,  $P_1$ , is assumed to be a gear tooth flank,  $\mathcal{G}$ , while another smooth regular part surface  $P_2$  is assumed to be the pinion tooth flank,  $\mathcal{P}$ . The consideration below targets generation of reversibly enveloping smooth regular tooth flanks  $\mathcal{G}$  and  $\mathcal{P}$  having line contact with one another at every instant of time and capable of transmitting a uniform rotation from the driving shaft to the driven shaft. The most general case of configuration of the axes of rotation of the gear and of the pinion is considered.

#### 10.3.1 Kinematics of Crossed-Axes Gearing

Gear pairs used for the transmission of rotation between two shafts having crossing axes of rotation are referred to as “*crossed-axes gear pairs*.”

Every feasible kind of crossed-axes gear pairs can be specified by a corresponding vector diagram. Use of the vector diagrams together with the developed classification of possible kinds of vector diagrams of gear pairs [5, 6] makes possible a comprehensive analysis of gearing of this particular kind.

The rotation of the input shaft as well as the rotation of the output shaft can be easily represented by corresponding rotation vectors,  $\omega_g$  and  $\omega_p$ , of the gear and the pinion accordingly.<sup>1</sup> The rotation vectors,  $\omega_g$  and  $\omega_p$ , are along straight lines, which cross one another. The closest distance of approach between the lines of action of the rotation vectors,  $\omega_g$  and  $\omega_p$ , is denoted by  $C$ . This distance is commonly referred to as the “*center distance*”  $C$ .

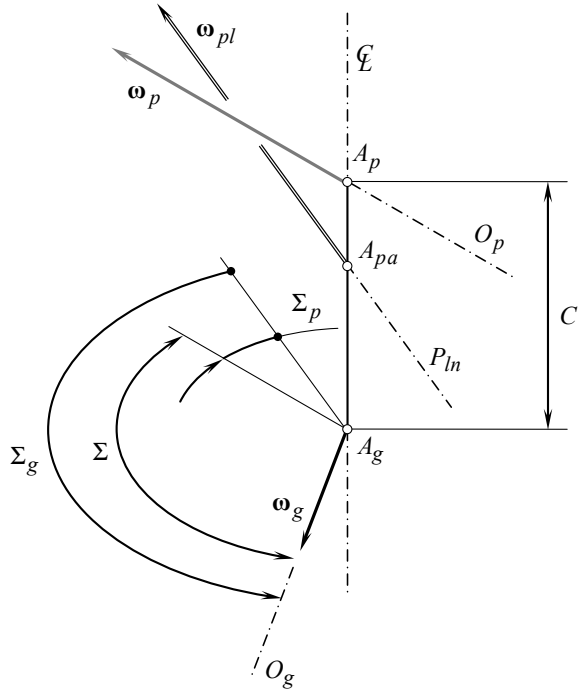
Consider a vector diagram constructed for an arbitrary configuration of the rotation vectors  $\omega_g$  and  $\omega_p$ . The vector diagram is depicted in Fig. 10.10, and it corresponds to an external crossed-axes gearing.

The vector diagram shown in Fig. 10.10 features an obtuse gear angle,  $\Sigma_g$ , between the rotation vector,  $\omega_g$ , of the gear and the vector of instant rotation,  $\omega_{pl}$ . The gear angle,  $\Sigma_g$ , can be expressed in terms of the shaft angle,  $\Sigma$ , and the magnitudes,  $\omega_g$  and  $\omega_p$ , of the rotation vectors,  $\omega_g$  and  $\omega_p$ :

---

<sup>1</sup>It is of importance to stress here that angular velocity is considered in this monograph as a vector directed along the axis of rotation in a direction defined by the right-hand screw rule. It is understood here and below that rotations are not vectors in nature. Therefore, special care is required when treating rotations as vectors.

**Fig. 10.10** Example of a vector diagram for a crossed-axes gear pair



$$\Sigma_g = \tan^{-1} \left( \frac{\sin \Sigma}{\omega_p / \omega_g + \cos \Sigma} \right) \quad (10.3)$$

A similar formula is valid for calculation of the pinion angle,  $\Sigma_p$ .

The center distance,  $C$ , can be interpreted as the summa of the pitch radii of the gear,  $r_g$ , and that of the pinion,  $r_p$ ,

$$C = r_g + r_p \quad (10.4)$$

Both the pitch radii,  $r_g$  and  $r_p$ , can be expressed in terms of magnitudes  $\omega_g$  and  $\omega_p$  of the rotation vectors  $\omega_g$  and  $\omega_p$ , and of the center distance,  $C$ :

$$r_g = \frac{1 + \omega_p - \omega_g}{1 + \omega_p} \cdot C \quad (10.5)$$

$$r_p = \frac{1 + \omega_g - \omega_p}{1 + \omega_g} \cdot C \quad (10.6)$$

The considered elements of kinematics of crossed-axes gearing make possible determination of the design parameters of the base cones in crossed-axes gear pairs.

### 10.3.2 Base Cones in Crossed-Axes Gear Pairs

Perfect crossed-axes gear pairs (or, in other words, “*geometrically accurate*”, or “*ideal*” crossed-axes gear pairs) are capable of transmitting an input steady rotation smoothly.

It should be noted here that in the case of crossing axes of rotation of the driving shaft and the driven shaft, there is no freedom in choosing a configuration of the axis of instant rotation,  $P_{in}$ , in relation to the rotation vectors  $\omega_g$  and  $\omega_p$ . Once the rotation vectors,  $\omega_g$  and  $\omega_p$ , are specified, the configuration of the axis of instant rotation,  $P_{in}$ , can be expressed in terms of the rotations  $\omega_g$  and  $\omega_p$ , and the center distance,  $C$ .

It is well known that perfect parallel-axes gear pairs feature two base cylinders. Smooth and synchronized rotation of the base cylinders allows for interpretation as a corresponding “*pulley-and-belt mechanism*.” Similar to the base cylinders in parallel-axes gearing, two base cones are associated with the gear and the pinion in an intersected axes gearing. Smooth rotation of the base cones can be interpreted as a “*pulley-and-belt mechanism*” having the belt in the form of a round tape. The similar is valid with respect to perfect crossed-axes gearing.

A base cone can be associated with the gear, and another base cone can be associated with the pinion of any and all perfect crossed-axes gear pairs. This concept is illustrated schematically in Fig. 10.11. The axis of rotation of the gear,  $O_g$ , and the axis of rotation of the pinion,  $O_p$ , cross each other at a shaft angle,  $\Sigma$ . The closest distance of approach of the axes of the rotation,  $O_g$  and  $O_p$ , is denoted by  $C$ . An orthogonal intersected axes gear pair is shown here just for illustrative purposes. Without going into details of the analysis, it should be stated here that the same approach is applicable with respect to angular bevel gears having shaft angle  $\Sigma \neq 90^\circ$ , namely either an obtuse or an acute shaft angle  $\Sigma$ .

The schematic shown in Fig. 10.11 is constructed starting from the rotation vectors,  $\omega_g$  and  $\omega_p$ , of the gear and of the pinion, accordingly. The gear and the pinion are rotating about their axes,  $O_g$  and  $O_p$ , respectively. The rotation vectors,  $\omega_g$  and  $\omega_p$ , allow for the construction of the vector,  $\omega_{pl}$ , of instant relative rotation. The rotation vector,  $\omega_{pl}$ , meets the requirement  $\omega_{pl} = \omega_p - \omega_g$ . The axis of instant rotation,  $P_{in}$ , is aligned with the vector of instant rotation,  $\omega_{pl}$ .

The vector of instant rotation,  $\omega_{pl}$ , is the vector through a point,  $A_{pa}$ , that is located within the centerline  $\mathcal{L}$ . The endpoints of the center distance,  $C$ , are labeled as  $A_g$  and  $A_p$ . The first of them, namely  $A_g$ , is the point of intersection of the centerline  $\mathcal{L}$  (the closest distance of approach,  $C$ , is a straight-line segment of the centerline  $\mathcal{L}$ ) and the gear axis of rotation,  $O_g$ . The second one,  $A_p$ , is the point of intersection of the centerline,  $\mathcal{L}$ , and the pinion axis of rotation,  $O_p$ .

The point,  $A_{pa}$ , is at a certain distance,  $r_g$ , from the axis of rotation,  $O_g$ . At that same time, the point,  $A_{pa}$ , is at a certain distance,  $r_p$ , from the axis of rotation,  $O_p$ . The following expression:

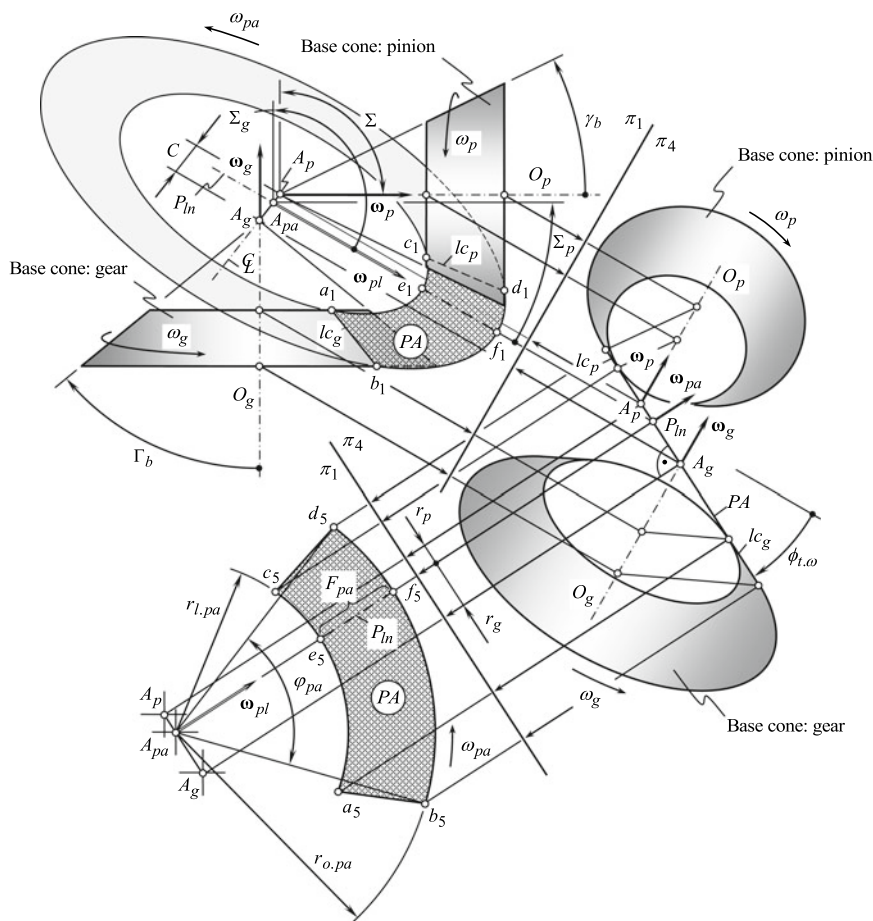


**Fig. 10.11** Base cones and the plane of action,  $PA$ , in an orthogonal crossed-axes gear pair (After Prof. S. P. Radzevich, 2008)

$$r_g + r_p = C \quad (10.7)$$

is valid.

Here, in Eq. (10.7) the distances  $r_g$  and  $r_p$  are signed values. The distances,  $r_g$  and  $r_p$ , are of positive values ( $r_g > 0, r_p > 0$ ) when the point,  $A_{pa}$ , is located within the center distance,  $C$ . When the point,  $A_{pa}$ , is located outside the center distance,  $C$ , the distance,  $r_g$ , is of a negative value ( $r_g < 0$ ), while the distance,  $r_p$ , is remained of positive value ( $r_p > 0$ ).

The equation:

$$\frac{r_g}{r_p} = \frac{\omega_p^{rl}}{\omega_g^{rl}} \quad (10.8)$$

makes possible calculation of the distances,  $r_g$  and  $r_p$ :

$$r_g = \frac{1 + \omega_p - \omega_g}{1 + \omega_p} \cdot C \quad (10.9)$$

and

$$r_p = \frac{1 + \omega_g - \omega_p}{1 + \omega_g} \cdot C \quad (10.10)$$

For a pair of rotation vectors  $\omega_g$  and  $\omega_p$ , the ratio  $\tan \Sigma_g / \tan \Sigma_p$  can be calculated:

$$\frac{r_p}{r_g} = \frac{\tan \Sigma_g}{\tan \Sigma_p} \quad (10.11)$$

The plane of action,  $PA$ , is a plane through the axis of instant rotation,  $P_{ln}$ . The plane of action,  $PA$ , is in tangency with both base cones, namely, with the base cone of the gear, as well as with that of the pinion. Hence, the plane of action,  $PA$ , makes a certain transverse pressure angle,  $\phi_{t,\omega}$ , in relation to a perpendicular to a plane associated with the axis of instant rotation,  $P_{ln}$ . The perpendicular is constructed to the plane through the vector of instant rotation,  $\omega_{pl}$ , and through the centerline along  $\mathcal{L}$ . The transverse pressure angle,  $\phi_{t,\omega}$ , is measured within a plane that is perpendicular to the axis of instant rotation,  $P_{ln}$ .

The portion of the schematic plotted in the upper left corner in Fig. 10.11 is constructed within the plane of projections,  $\pi_1$ . Two other main planes of projections,  $\pi_2$  and  $\pi_3$ , of the standard set of planes of projections,  $\pi_1\pi_2\pi_3$ , are not used in this particular consideration. Therefore, these planes,  $\pi_2$  and  $\pi_3$ , are not shown in Fig. 10.11. Instead, two auxiliary planes of projections, namely the plane of projections,  $\pi_4$  and  $\pi_5$ , are used. The axis of projections,  $\pi_1/\pi_4$ , is constructed so as to be perpendicular to the axis of instant rotation,  $P_{ln}$ . The axis of projections,  $\pi_4/\pi_5$ , is constructed so as to be parallel to the trace of the plane of action,  $PA$ , within the plane of projections,  $\pi_4$ . The plane of action,  $PA$ , is projected with no distortions onto the plane of projections  $\pi_4$ .

The plane of action can be construed as a flexible zero-thickness film. The film is free to wrap/unwrap from and onto the base cones of the gear and of the pinion. The plane of action,  $PA$ , is not allowed for any bending about an axis perpendicular to the plane  $PA$  itself. Under uniform rotation of the gears, the plane of action,  $PA$ , is rotating about the axis,  $O_{pa}$  (in Fig. 10.11, the axis,  $O_{pa}$ , is projected into the point,  $A_{pa}$ , that is referred to as the “plane-of-action apex,  $A_{pa}$ ”). The rotation vector,  $\omega_{pa}$ ,

is along the axis,  $O_{pa}$ . The rotation vector,  $\omega_{pa}$ , is perpendicular to the plane of action,  $PA$ .

As the axis of instant rotation,  $P_{ln}$ , and the axes of rotations of the gear,  $O_g$ , and the pinion,  $O_p$ , cross one another, then not pure rolling of the base cones of the gear and the pinion over the pitch plane,  $PA$ , is observed, but rolling together with sliding of  $PA$  over the base cones is observed instead. This is because the axes of rotations  $O_g$  and  $O_p$  cross one another.

For crossed-axes gearing, the plane of action,  $PA$ , can be construed as a round cone having  $90^\circ$  cone angle. As  $\sin 90^\circ = 1$ , the magnitude,  $\omega_{pa}$ , of the rotation vector,  $\omega_{pa}$ , can be calculated from the formula:

$$\omega_{pa} = \frac{\omega_g}{\sin \Gamma_b} = \frac{\omega_p}{\sin \gamma_b} \quad (10.12)$$

where we denote:

$\omega_g$  is the rotation of the gear.

$\omega_p$  is the rotation of the pinion.

$\Gamma_b$  is the base cone angle of the gear.

$\gamma_b$  is the base cone angle of the pinion.

For crossed-axes gear pairs, the base cone angles,  $\Gamma_b$  and  $\gamma_b$ , vary within the intervals  $0^\circ < \Gamma_b < 180^\circ$  and  $0^\circ < \gamma_b < (180^\circ - \Gamma_b)$  accordingly.

A desired working portion, or, in other words, a functional portion of the plane of action,  $PA$ , can be constructed in the following way.

Consider a straight-line segment,  $ef$ , within the axis of instant rotation,  $P_{ln}$  (Fig. 10.11). When the gears rotate, the straight-line segment,  $ef$ , is traveling together with the plane of action,  $PA$ . The point,  $f$ , traces a circular arc of radius,  $r_{o.pa}$ , while the point,  $e$ , traces a circular arc of radius,  $r_{l.pa}$ . The face width of the plane of action,  $F_{pa}$ , or, in other words, the working (functional) portion of the plane of action is located between two circles of radii  $r_{o.pa}$  and  $r_{l.pa}$ .

The straight-line segments,  $lc_g$  and  $lc_p$ , are along the corresponding lines of contact of the plane of action,  $PA$ , with the base cones of the gear and the pinion.

In angular directions, the functional portion of the plane of action,  $PA$ , spans within central angle:

$$\Phi_{pa} = \varphi_{pa} + \Delta\varphi_{pa.g} + \Delta\varphi_{pa.p} \quad (10.13)$$

The components,  $\Delta\varphi_{pa.g}$  and  $\Delta\varphi_{pa.p}$ , are due to the gear axis of rotation,  $O_g$ , and the pinion axis of rotation,  $O_p$ , being the straight lines not through the “plane-of-action apex,  $A_{pa}$ .”

### 10.3.3 Tooth Flanks in Perfect Crossed-Axes Gear Pairs

The conjugate tooth flanks of a gear and a mating pinion in a crossed-axes gear pair are in line contact with one another. As the gears rotate, the line of contact is traveling with respect to:

- (a) the gear,
- (b) the pinion, as well as
- (c) the gearing housing.

The tooth flank of the gear,  $\mathcal{G}$ , can be construed as the loci of successive positions of the line of contact,  $LC$ , when the line of contact is traveling in relation to a reference system associated with the gear. Similarly, the tooth flank of the pinion,  $\mathcal{P}$ , can be viewed as the loci of successive positions of that same line of contact,  $LC$ , when the line of contact is traveling in relation to a reference system associated with the pinion. Ultimately, the loci of successive positions of that same line of contact,  $LC$ , when the line of contact is traveling in relation to a stationary reference system associated with the gearing housing represent the surface of action. Therefore, once the line of contact is known, the kinematics of a crossed-axes gearing (Fig. 10.11) can be employed for the derivation of an analytical representation of the tooth flank of the gear,  $\mathcal{G}$ , and of the pinion,  $\mathcal{P}$ . For this purpose, several reference systems need to be introduced.

*The applied coordinate systems and linear transformations.* For convenience, several reference systems are introduced. These reference systems are associated with the gear, with the pinion, with the housing, and so forth. Auxiliary coordinate systems are also used when necessary.

*The main reference systems.* First, a *Cartesian* coordinate system,  $X_g Y_g Z_g$ , is associated with the gear as shown in Fig. 10.12. Second, a *Cartesian* coordinate system,  $X_p Y_p Z_p$ , is associated with the pinion (Fig. 10.12). Third, a *Cartesian* coordinate system,  $X_r Y_r Z_r$ , is associated with auxiliary round rack, which is engaged in mesh simultaneously with both, namely with the gear and with the pinion. Fourth, a *Cartesian* coordinate system,  $X_{pa} Y_{pa} Z_{pa}$ , is associated with the plane of action. Finally, a stationary *Cartesian* coordinate system,  $X_h Y_h Z_h$ , is associated with the gearing housing. A few more auxiliary reference systems are used below as well.

The origin of the coordinate system,  $X_r Y_r Z_r$ , coincides with the plane-of-action apex,  $A_{pa}$ . The orientation of the coordinate system,  $X_r Y_r Z_r$ , is defined by the rotation vectors,  $\omega_g$ ,  $\omega_p$ , and  $\omega_{pl}$ . The  $X_r$ -axis is aligned with the vector,  $\omega_{pl}$ , of instant rotation. The axis  $Y_r$  aligns with the vector defined by the cross product  $\omega_p \times \omega_g$  of the rotation vectors of the gear and pinion. Ultimately, the  $Z_r$ -axis is along the vector that is defined by the triple vector product,  $\omega_p \times \omega_g \times \omega_{pl}$ , of the rotation vectors of the gear and the pinion, and of the vector of instant rotation.

The coordinate system,  $X_{pa} Y_{pa} Z_{pa}$ , shares the origin with the reference system,  $X_r Y_r Z_r$ . The axis,  $X_{pa}$ , is located within the plane of action,  $PA$ , and forms a certain angle,  $\theta_{pa}$ , with the vector,  $\omega_{pl}$ , of instant rotation. The  $Y_{pa}$ -axis is located also within the plane of action,  $PA$ , and is perpendicular to the  $X_{pa}$ -axis (here  $\theta_{pa} = \omega_{pa} \cdot t$ , and



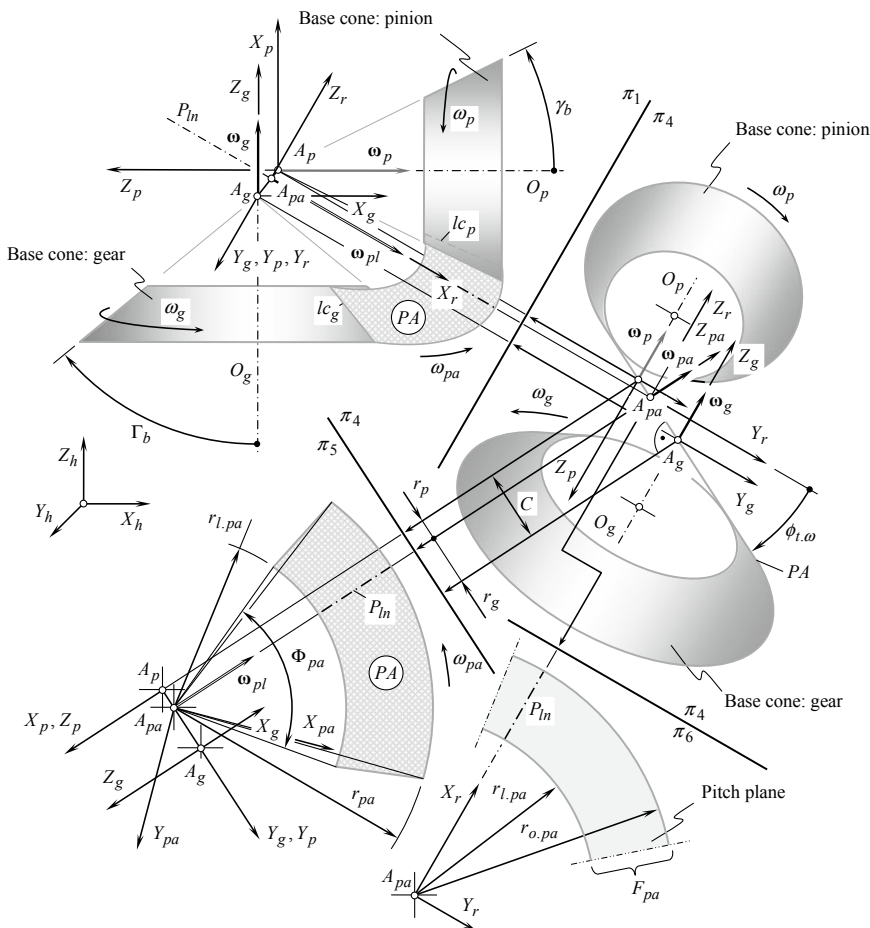


**Fig. 10.12** Reference systems those used for the derivation of an analytical expression for a gear tooth flank,  $\mathcal{G}$ , and a pinion tooth flank,  $\mathcal{P}$ , in a crossed-axes gear pair (After Prof. S. P. Radzevich, 2008)

time is denoted  $t$ ). Finally, the axis  $Z_{pa}$  compliments the axes  $X_{pa}$  and  $Y_{pa}$  to the left-hand oriented *Cartesian* coordinate system,  $X_{pa}Y_{pa}Z_{pa}$ .

The line of contact,  $LC$ , between the gear tooth flank,  $\mathcal{G}$ , and the pinion tooth flank,  $\mathcal{P}$ , is conveniently specified in the coordinate system,  $X_{pa}Y_{pa}Z_{pa}$ . Then, the representation of the current position of the moving line of contact,  $LC$ , in the reference systems,  $X_gY_gZ_g$  and  $X_pY_pZ_p$ , will return analytical expressions for the tooth flanks,  $\mathcal{G}$  and  $\mathcal{P}$ , of the gear and pinion. Similarly, the representation of the current position of the moving line of contact,  $LC$ , in the motionless reference system,  $X_hY_hZ_h$ , will return an equation for the surface of action in crossed-axes gearing.

*The operators of rolling/sliding.* For the derivation of an equation of the gear tooth flank,  $\mathcal{G}$ , an operator,  $\mathbf{Rs} (PA \mapsto \mathcal{G})$ , of the resultant coordinate system transforma-

tion needs to be composed. The operator,  $\mathbf{Rs} (PA \mapsto \mathcal{G})$ , can be expressed in terms of the following:

- (a) The operator of rotation,  $\mathbf{Rt} (pa \mapsto pa_0)$ , of the coordinate system,  $X_{pa}Y_{pa}Z_{pa}$ , about the  $Z_{pa}$ -axis through a certain angle,  $\theta_{pa}$ . When the axis,  $X_{pa}$ , is aligned with the vector of instant rotation,  $\omega_{pl}$ , the reference system,  $X_{pa}Y_{pa}Z_{pa}$ , occupies a particular configuration,  $X_{pa}^0Y_{pa}^0Z_{pa}^0$  (the coordinate system,  $X_{pa}^0Y_{pa}^0Z_{pa}^0$ , is not depicted in Fig. 10.12). The operator of rotation,  $\mathbf{Rt} (pa \mapsto pa_0)$ , can be expressed in the form:

$$\mathbf{Rt} (pa \mapsto pa_0) = \begin{bmatrix} \cos \theta_{pa} & 0 & -\sin \theta_{pa} & 0 \\ 0 & 1 & 0 & 0 \\ \sin \theta_{pa} & 0 & \cos \theta_{pa} & 0 \\ 0 & 0 & 0 & 1 \end{bmatrix} \quad (10.14)$$

- (b) The operator of the translation,  $\mathbf{Tr} (-r_g, Y_g)$ , of the reference system,  $X_{pa}^0Y_{pa}^0Z_{pa}^0$ , at a distance,  $-r_g$ , along the centerline,  $P_{a.g}O_{pa}$ , to a position of the coordinate system,  $X_g^0Y_g^0Z_g^0$ , is:

$$\mathbf{Tr} (-r_g, Y_g) = \begin{bmatrix} 1 & 0 & 0 & 0 \\ 0 & 1 & 0 & -r_g \\ 0 & 0 & 1 & 0 \\ 0 & 0 & 0 & 1 \end{bmatrix} \quad (10.15)$$

- (c) The operator of rotation,  $\mathbf{Rt} (pa_0 \mapsto r)$ , of the coordinate system,  $X_g^0Y_g^0Z_g^0$ , about the vector of instant rotation,  $\omega_{pl}$ , through the transverse profile angle,  $\phi_{l,\omega}$  (the transverse profile angle,  $\phi_{l,\omega}$ , is measured within a plane that is perpendicular to the vector,  $\omega_{pl}$ ), is:

$$\mathbf{Rt} (pa_0 \mapsto r) = \begin{bmatrix} 1 & 0 & 0 & 0 \\ 0 & \cos \phi_{l,\omega} & -\sin \phi_{l,\omega} & 0 \\ 0 & \sin \phi_{l,\omega} & \cos \phi_{l,\omega} & 0 \\ 0 & 0 & 0 & 1 \end{bmatrix} \quad (10.16)$$

- (d) The operator of rotation,  $\mathbf{Rt} (r \mapsto g)$ , of the coordinate system,  $X_rY_rZ_r$ , about the  $Y_r$ -axis through an angle,  $\angle(\omega_r, \omega_p)$ . Note that the angle  $\angle(\omega_r, \omega_p)$  is equal to the angle  $\angle(\omega_p, \omega_{pl}) = \Sigma_p$ . The operator of rotation,  $\mathbf{Rt} (r \mapsto g)$ , can be represented in the form:

$$\mathbf{Rt} (r \mapsto g) = \begin{bmatrix} \cos \Sigma_p & 0 & \sin \Sigma_p & 0 \\ 0 & 1 & 0 & 0 \\ -\sin \Sigma_p & 0 & \cos \Sigma_p & 0 \\ 0 & 0 & 0 & 1 \end{bmatrix} \quad (10.17)$$

The operator,  $\mathbf{Rs} (PA \mapsto \mathcal{G})$ , of the resultant coordinate system transformation is equal to the product:

$$\mathbf{Rs} (PA \mapsto \mathcal{G}) = \mathbf{Rt} (r \mapsto g) \cdot \mathbf{Rt} (pa_0 \mapsto r) \cdot \mathbf{Tr} (-r_g, Y_g) \cdot \mathbf{Rt} (pa \mapsto pa_0) \quad (10.18)$$

This operator allows for matrix representation in the form:

$$\begin{aligned} \mathbf{Rs} (PA \mapsto \mathcal{G}) &= \begin{bmatrix} \cos \Sigma_p \cos \theta_{pa} + \sin \Sigma_p \cos \phi_{t,\omega} \sin \theta_{pa} & & & \\ & -\sin \phi_{t,\omega} \sin \theta_{pa} & & \\ \cos \Sigma_p \cos \phi_{t,\omega} \sin \theta_{pa} - \sin \Sigma_p \cos \theta_{pa} & & & \\ & 0 & & \end{bmatrix} \\ &\quad \begin{bmatrix} \sin \Sigma_p \sin \phi_{t,\omega} \sin \Sigma_p \cos \phi_{t,\omega} \cos \theta_{pa} - \cos \Sigma_p \sin \theta_{pa} - r_g \sin \Sigma_p \sin \phi_{t,\omega} & & \\ \cos \phi_{t,\omega} & -\sin \phi_{t,\omega} \cos \theta_{pa} & -r_g \cos \phi_{t,\omega} \\ \cos \Sigma_p \sin \phi_{t,\omega} \sin \Sigma_p \sin \theta_{pa} + \cos \Sigma_p \cos \phi_{t,\omega} \cos \theta_{pa} - r_g \cos \Sigma_p \sin \phi_{t,\omega} & & \\ 0 & 0 & 1 \end{bmatrix} \end{aligned} \quad (10.19)$$

The operator,  $\mathbf{Rs} (PA \mapsto \mathcal{P})$ , of the resultant coordinate system transformation, that is, the operator of the transition from the coordinate system,  $X_{pa}Y_{pa}Z_{pa}$ , associated with the plane of action,  $PA$ , to the coordinate system,  $X_pY_pZ_p$ , associated with the pinion is equal to the product:

$$\mathbf{Rs} (PA \mapsto \mathcal{P}) = \mathbf{Rt} (r \mapsto p) \cdot \mathbf{Rt} (pa_0 \mapsto r) \cdot \mathbf{Tr} (r_p, Y_p) \cdot \mathbf{Rt} (pa \mapsto pa_0) \quad (10.20)$$

Here, the operator of rotation,  $\mathbf{Rt} (r \mapsto p)$ , can be composed similar to that the operator of rotation,  $\mathbf{Rt} (r \mapsto g)$  [see Eq. (10.20)] is composed. The similarity allows for the following expression for the operator of rotation,  $\mathbf{Rt} (r \mapsto p)$ :

$$\mathbf{Rt} (r \mapsto p) = \begin{bmatrix} \cos \Sigma_g & 0 & \sin \Sigma_g & 0 \\ 0 & 1 & 0 & 0 \\ -\sin \Sigma_g & 0 & \cos \Sigma_g & 0 \\ 0 & 0 & 0 & 1 \end{bmatrix} \quad (10.21)$$

Substituting into Eq. (10.20), Eq. (10.21) together with the Eq. (10.14) and Eq. (10.16) returns an expression for the operator,  $\mathbf{Rs} (PA \mapsto \mathcal{P})$ , of the resultant coordinate system transformation:

$$\begin{aligned}
& \mathbf{Rs}(PA \mapsto \mathcal{P}) \\
&= \begin{bmatrix} \cos \Sigma_g \cos \theta_{pa} + \sin \Sigma_g \cos \phi_{t,\omega} \sin \theta_{pa} & & & \\ & -\sin \phi_{t,\omega} \sin \theta_{pa} & & \\ \cos \Sigma_g \cos \phi_{t,\omega} \sin \theta_{pa} - \sin \Sigma_g \cos \theta_{pa} & & & \\ & & 1 & \\ \sin \Sigma_g \sin \phi_{t,\omega} \sin \Sigma_g \cos \phi_{t,\omega} \cos \theta_{pa} - \cos \Sigma_g \sin \theta_{pa} r_p \sin \Sigma_g \sin \phi_{t,\omega} & & & \\ & \cos \phi_{t,\omega} & & -\sin \phi_{t,\omega} \cos \theta_{pa} r_p \cos \phi_{t,\omega} \\ \cos \Sigma_g \sin \phi_{t,\omega} \sin \Sigma_g \sin \theta_{pa} + \cos \Sigma_g \cos \phi_{t,\omega} \cos \theta_{pa} r_p \cos \Sigma_g \sin \phi_{t,\omega} & & & \\ & 0 & & 0 & & 1 \end{bmatrix} \quad (10.22)
\end{aligned}$$

The operators,  $\mathbf{Rs}(PA \mapsto \mathcal{G})$  and  $\mathbf{Rs}(PA \mapsto \mathcal{P})$ , are both a kind of rolling/sliding operator. Transformation of rolling/sliding is extensively used in the theory of gearing, particularly in the investigation of crossed-axes gearing. As the operators of transformation of the kind [see  $\mathbf{Rs}(PA \mapsto \mathcal{G})$  and  $\mathbf{Rs}(PA \mapsto \mathcal{P})$ ] got an extensive application in the theory of gearing, for crossed-axes gears in particular, it makes sense to introduce a special designation. That is, for convenience the operators of the linear transformations,  $\mathbf{Rc}(PA \mapsto \mathcal{G})$  and  $\mathbf{Rc}(PA \mapsto \mathcal{P})$ , can be designated:

$$\mathbf{Rs}(PA \mapsto \mathcal{G}) = \mathbf{Rc}(PA \mapsto \mathcal{G}) \quad (10.23)$$

$$\mathbf{Rs}(PA \mapsto \mathcal{P}) = \mathbf{Rc}(PA \mapsto \mathcal{P}) \quad (10.24)$$

As the operators of rolling/sliding,  $\mathbf{Rc}(PA \mapsto \mathcal{G})$  and  $\mathbf{Rc}(PA \mapsto \mathcal{P})$ , are known, the operator of rolling,  $\mathbf{Rc}(\mathcal{P} \mapsto \mathcal{G})$ , of the pinion over the gear can be calculated from the formula:

$$\mathbf{Rc}(\mathcal{P} \mapsto \mathcal{G}) = \mathbf{Rc}(PA \mapsto \mathcal{G}) \cdot \mathbf{Rc}^{-1}(PA \mapsto \mathcal{P}) \quad (10.25)$$

Similarly, the operator of rolling,  $\mathbf{Rc}(\mathcal{G} \mapsto \mathcal{P})$ , of the gear over the pinion can be calculated either as reciprocal to the operator,  $\mathbf{Rc}(\mathcal{P} \mapsto \mathcal{G})$ , or the expression:

$$\mathbf{Rc}(\mathcal{G} \mapsto \mathcal{P}) = \mathbf{Rc}^{-1}(\mathcal{P} \mapsto \mathcal{G}) = \mathbf{Rc}(PA \mapsto \mathcal{P}) \cdot \mathbf{Rc}^{-1}(PA \mapsto \mathcal{G}) \quad (10.26)$$

can be used for the calculation of the operator of rolling,  $\mathbf{Rc}(\mathcal{G} \mapsto \mathcal{P})$ .

*The operators associated with gear housing.* A stationary reference system,  $X_h Y_h Z_h$ , is associated with housing of the gear pair. The choice of the coordinate system,  $X_h Y_h Z_h$ , depends mostly on convenience. In a particular case, either stationary *Cartesian* coordinate system,  $X_g^0 Y_g^0 Z_g^0$ , or stationary *Cartesian* coordinate system,  $X_p^0 Y_p^0 Z_p^0$ , can be used for this purpose.

The coordinate system,  $X_g^0 Y_g^0 Z_g^0$ , shares a common  $Z_g$ -axis with the coordinate system,  $X_g Y_g Z_g$ , associated with the gear. The coordinate system,  $X_g Y_g Z_g$ , is turned in relation to the motionless coordinate system,  $X_g^0 Y_g^0 Z_g^0$ , through a certain angle,  $\varphi_g$ .

Similarly, the reference system,  $X_p^0 Y_p^0 Z_p^0$ , shares a common  $Z_p$ -axis with the coordinate system,  $X_p Y_p Z_p$ , associated with the pinion. The coordinate system,  $X_p Y_p Z_p$ , is turned in relation to the motionless coordinate system,  $X_p^0 Y_p^0 Z_p^0$ , through a certain angle,  $\varphi_p$ .

It is of importance to note here that the rotation angles,  $\varphi_g$  and  $\varphi_p$ , correspond to one another by the relation  $\varphi_p = u \varphi_g$ , and  $u$  designates tooth ratio of the gear pair. For crossed-axes gearing, the following expression for  $u$ :

$$u = \frac{\omega_p^{rl}}{\omega_g^{rl}} = \frac{\omega_p \cos \Sigma_p}{\omega_g \cos \Sigma_g} \quad (10.27)$$

is valid.

Here, the rolling components of the rotations,  $\omega_g$  and  $\omega_p$ , are designated as  $\omega_g^{rl}$  and  $\omega_p^{rl}$  accordingly, and the gear and the pinion angles,  $\Sigma_g$  and  $\Sigma_p$ , are calculated from:

$$\Sigma_g = \frac{1 - \omega_g + \omega_p}{1 + \omega_p} \Sigma \quad (10.28)$$

$$\Sigma_p = \frac{1 + \omega_g - \omega_p}{1 + \omega_g} \Sigma \quad (10.29)$$

and  $\Sigma$  is the angle between the rotation vectors of the gear,  $\omega_g$ , and of the pinion,  $\omega_p$ .

Rotation of the reference system,  $X_g Y_g Z_g$ , about the  $Z_g$ -axis through an angle,  $\varphi_g$ , can be analytically described by the operator of rotation,  $\mathbf{Rt} (\mathcal{G} \mapsto h)$ . This operator can be expressed in the form:

$$\mathbf{Rt} (\mathcal{G} \mapsto h) = \begin{bmatrix} \cos \varphi_g & \sin \varphi_g & 0 & 0 \\ -\sin \varphi_g & \cos \varphi_g & 0 & 0 \\ 0 & 0 & 1 & 0 \\ 0 & 0 & 0 & 1 \end{bmatrix} \quad (10.30)$$

Equation (10.30) allows for an expression for the operator of the resultant coordinate system transformation, that is, for the operator of the transition,  $\mathbf{Rs} (pa \mapsto h)$ , from the coordinate system,  $X_{pa} Y_{pa} Z_{pa}$ , associated with the plane of action,  $PA$ , to the stationary coordinate system,  $X_h Y_h Z_h$ . This operator of linear transformation can be represented as the product:

$$\mathbf{Rs} (pa \mapsto h) = \mathbf{Rt} (\mathcal{G} \mapsto h) \cdot \mathbf{Rc} (PA \mapsto \mathcal{G}) \quad (10.31)$$

Equation (10.31) is not represented in matrix form as it is bulky.

Rotation of the reference system,  $X_p Y_p Z_p$ , about the  $Z_p$ -axis through an angle,  $\varphi_p = -u \varphi_g$ , can be analytically described by the operator of rotation,  $\mathbf{Rt} (\mathcal{P} \mapsto h_p)$ . This operator can be expressed in the form:

$$\mathbf{Rt} (\mathcal{P} \mapsto h_p) = \begin{bmatrix} \cos \varphi_p & \sin \varphi_p & 0 & 0 \\ -\sin \varphi_p & \cos \varphi_p & 0 & 0 \\ 0 & 0 & 1 & 0 \\ 0 & 0 & 0 & 1 \end{bmatrix} \quad (10.32)$$

Equation (10.32) allows for an expression for the operator of the resultant coordinate system transformation, that is, for the operator of transition  $\mathbf{Rs} (pa \mapsto h_p)$  from the coordinate system,  $X_{pa} Y_{pa} Z_{pa}$ , associated with the plane of action,  $PA$ , to the stationary coordinate system,  $X_{h.p} Y_{h.p} Z_{h.p}$ . This operator can be represented as the product:

$$\mathbf{Rs} (pa \mapsto h_p) = \mathbf{Rt} (\mathcal{G} \mapsto h) \cdot \mathbf{Rc} (PA \mapsto \mathcal{G}) \quad (10.33)$$

Equation (10.33) is not represented in matrix form as it is bulky.

Both reference systems, namely the coordinate systems,  $X_h Y_h Z_h$  and  $X_{h.p} Y_{h.p} Z_{h.p}$ , are stationary reference systems somehow associated with housing of the gear pair. The relation between these two coordinate systems can be analytically described by the expression:

$$\mathbf{Rs} (h_p \mapsto h) = \mathbf{Rs} (pa \mapsto h) \cdot \mathbf{Rs}^{-1} (pa \mapsto h_p) \quad (10.34)$$

The expressions derived above for the operators of the coordinate system transformations make it possible to obtain corresponding expressions of any and all geometrical features:

- (a) of the gear,
- (b) of the pinion, as well as
- (c) of the “gear-to-pinion” mesh represented in a common reference system.

Ultimately, both the kinematics and the geometry of a gear pair can be expressed analytically this way.

### 10.3.4 Tooth Flank of a Gear in Crossed-Axes Gear Pair

The tooth flank of a gear in a crossed-axes gear pair allows for interpretation as loci of successive positions of the line of contact,  $LC$ , when the plane of action,  $PA$ , is either wrapping on or unwrapping from the base cone of the gear. For this purpose, the line of contact should be represented in a reference system associated with the gear.

Any planar curve of a reasonable geometry can be employed as the line of contact of tooth flanks. The geometry of tooth flanks of the gear,  $\mathcal{G}$ , and of the pinion,  $\mathcal{P}$ , depends on the shape of the line of contact. In any case, the line of contact,  $LC$ , is entirely located within the coordinate plane,  $X_{pa}Y_{pa}$ , of the reference system,  $X_{pa}Y_{pa}Z_{pa}$ , associated with the plane of action,  $PA$ , as it is illustrated schematically in Fig. 10.13.

Generally speaking, the position vector of a point,  $\mathbf{r}_{lc}$ , of the line of contact,  $LC$ , can be described analytically by an expression in matrix form:

$$\mathbf{r}_{lc}(v) = \begin{bmatrix} X_{lc}(v) \\ Y_{lc}(v) \\ 0 \\ 1 \end{bmatrix} \quad (10.35)$$

In order to represent Eq. (10.35) for the position vector of a point,  $\mathbf{r}_{lc}$ , of the line of contact,  $LC$ , in the reference system,  $X_gY_gZ_g$ , the operator of the resultant coordinate system transformation,  $\mathbf{Rs}(PA \mapsto \mathcal{G})$ , can be employed. This makes possible an expression:

$$\mathbf{r}_g(v, \theta_{pa}) = \mathbf{r}_{lc}^g(v, \theta_{pa}) = \mathbf{Rs}(PA \mapsto \mathcal{G}) \cdot \mathbf{r}_{lc}(v) \quad (10.36)$$

When the axis,  $X_{pa}$ , is pointed along one side of the face advance angle,  $\vartheta_{adv}$ , then the central angle,  $\theta_{pa}$ , is within the domain  $\varphi_{pl}^p + \vartheta_{adv} \leq \theta_{pa} \leq \varphi_{pl}^g - \vartheta_{adv}$  (see Fig. 10.12) (the angles,  $\varphi_{pl}^g$  and  $\varphi_{pl}^p$ , are of opposite signs). Other than these

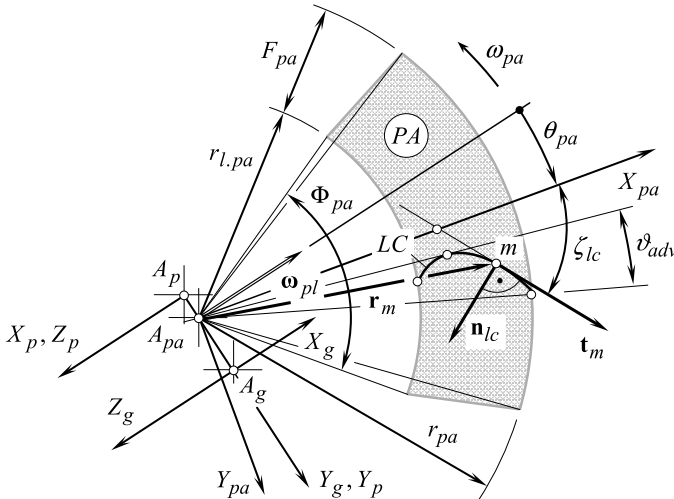


**Fig. 10.13** Geometry of an arbitrary line of contact,  $LC$ , between a gear tooth flank,  $\mathcal{G}$ , and a pinion tooth flank,  $\mathcal{P}$ , in a crossed-axes gear pair

angles, those the  $X_{pa}$ -axis makes with sides of the face advance angle,  $\vartheta_{adv}$ , should be incorporated into consideration.

Substituting  $\mathbf{r}_{lc}$  [Eq. (10.35)] and  $\mathbf{R}_s(PA \mapsto \mathcal{G})$  [see Eq. (10.19)] into Eq. (10.36), an expression for the calculation of the position vector of a point,  $\mathbf{r}_g$ , of the gear tooth flank,  $\mathcal{G}$ :

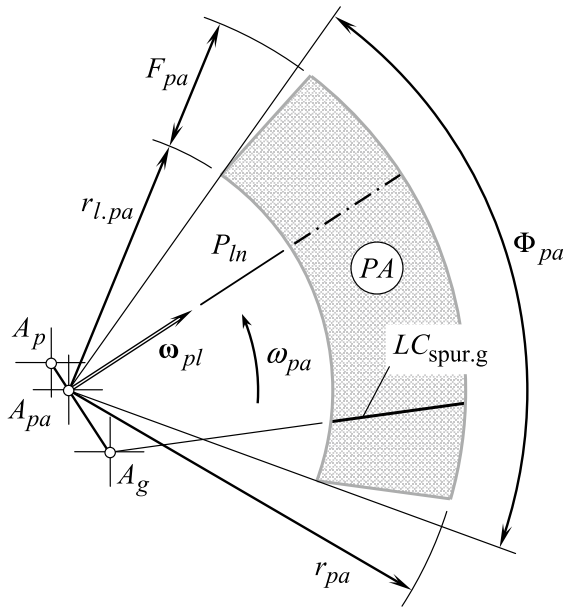
$$\mathbf{r}_g(v, \theta_{pa}) = \begin{bmatrix} (\cos \Sigma_p \cos \theta_{pa} + \sin \Sigma_p \cos \phi_{t,\omega} \sin \theta_{pa}) \cdot X(v) + \sin \Sigma_p \sin \phi_{t,\omega} \cdot Y(v) + r_p \sin \Sigma_p \sin \phi_{t,\omega} \\ -X(v) \sin \phi_{t,\omega} \sin \theta_{pa} + Y(v) \cos \phi_{t,\omega} + r_p \cos \phi_{t,\omega} \\ -(\sin \Sigma_p \cos \theta_{pa} - \cos \Sigma_p \cos \phi_{t,\omega} \sin \theta_{pa}) \cdot X(v) + \cos \Sigma_p \sin \phi_{t,\omega} \cdot Y(v) + r_p \cos \Sigma_p \sin \phi_{t,\omega} \end{bmatrix} \quad (10.37)$$

can be derived.

Lines of contact of various geometries can be used for the purpose of generation of tooth flanks of the gear and pinion in crossed-axes gearing. In a particular case, the tooth flanks of the gear and of the pinion in a crossed-axes gear pair can be designed so that the line of contact,  $LC$ , of the tooth flanks,  $\mathcal{G}$  and  $\mathcal{P}$ , is aligned with a line through the gear apex  $A_g$ . This case is schematically depicted in Fig. 10.14. Straight bevel gear tooth flank,  $\mathcal{G}$ , is generated by the line of contact,  $LC_{spur.g}$ , of this geometry. Tooth flank,  $\mathcal{P}$ , of the mating pinion is a kind of screw surface.

In the particular case of a straight line of contact (see Fig. 10.15), the position vector of a point,  $\mathbf{r}_{lc}$ , of the line of contact,  $LC$ , can be represented as the sum:

**Fig. 10.14** Example of a possible kind of the line of contact,  $LC$ , between a gear tooth flank,  $\mathcal{G}$ , and a pinion tooth flank,  $\mathcal{P}$ , in a crossed-axes gear pair





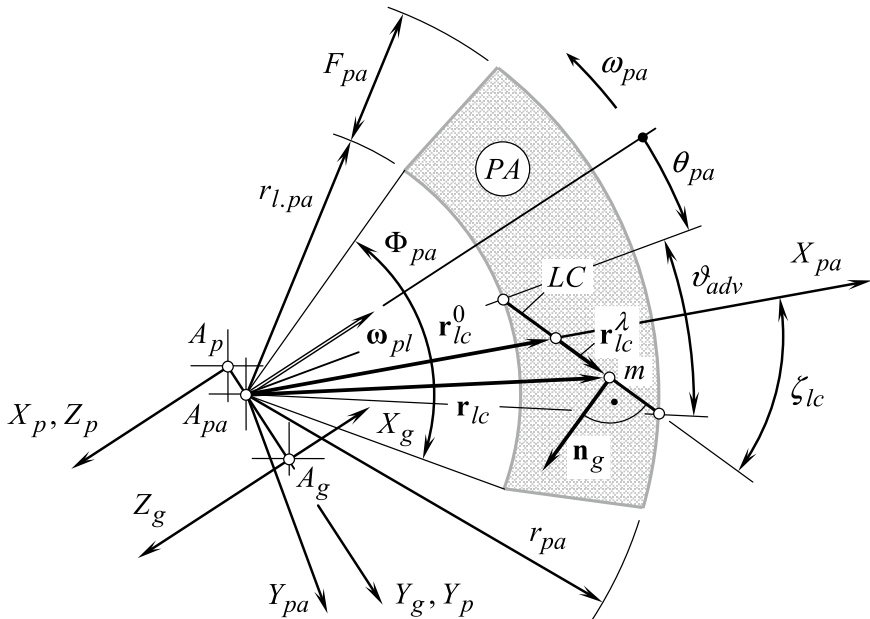


**Fig. 10.15** Line of contact,  $LC$ , between the tooth flank,  $\mathcal{G}$ , of the gear and the tooth flank,  $\mathcal{P}$ , of the mating pinion for a skew crossed-axes gearing

$$\mathbf{r}_{lc} = \mathbf{r}_{lc}^0 + \mathbf{r}_{lc}^\lambda \quad (10.38)$$

Here, the vector  $\mathbf{r}_{lc}^0$  is of constant length,  $\mathbf{r}_{lc}^0 = \mathbf{i} \cdot r_{lc}^0$ , where  $r_{lc}^0 = |\mathbf{r}_{lc}^0|$ . Another component of the position vector of a point,  $\mathbf{r}_{lc}$ , namely the vector  $\mathbf{r}_{lc}^\lambda$ , can be represented in the form:

$$\mathbf{r}_{lc}^\lambda(\lambda) = \mathbf{i} \cdot \lambda \cos \zeta_{cl} + \mathbf{j} \cdot \lambda \sin \zeta_{cl} \quad (10.39)$$

where:

$\lambda$  is the magnitude of the vector  $\mathbf{r}_{lc}^\lambda$ .

$\zeta_{cl}$  is the angle of inclination of the line of contact,  $LC$ , in relation to  $X_{pa}$ -axis of the coordinate system  $X_{pa}Y_{pa}Z_{pa}$  (see Fig. 10.15).

Ultimately, the position vector of a point,  $\mathbf{r}_{lc}$ , of the line of contact,  $LC$ , allows for representation in matrix form:

$$\mathbf{r}_{lc}(\lambda) = \begin{bmatrix} r_{lc}^0 + \lambda \cos \zeta_{cl} \\ \lambda \sin \zeta_{cl} \\ 0 \\ 1 \end{bmatrix} \quad (10.40)$$

Equation (10.40) considered together with the operator,  $\mathbf{Rs}(PA \mapsto \mathcal{G})$  [see Eq. (10.19)], of the resultant coordinate system transformation makes possible calculation of the position vector of a point,  $\mathbf{r}_g$ , of the tooth flank of a bevel gear that is featuring an inclined line of contact:

$$\mathbf{r}_g(v, \theta_{pa}) = \mathbf{r}_{lc}^g(\lambda, \theta_{pa}) = \mathbf{Rs}(PA \mapsto \mathcal{G}) \cdot \mathbf{r}_{lc}(\lambda) \quad (10.41)$$

An expanded form of the expression for the calculation of the position vector of a point of the gear tooth flank,  $\mathbf{r}_{lc}^g$ , can be derived after substituting of the position vector,  $\mathbf{r}_{lc}$ , and the operator of the resultant coordinate system transformation,  $\mathbf{Rs}(PA \mapsto \mathcal{G})$ , into Eq. (10.41):

$$\begin{aligned} \mathbf{r}_g(\lambda, \theta_{pa}) &= \begin{bmatrix} (\cos \Sigma_p \cos \theta_{pa} + \sin \Sigma_p \cos \phi_{t,\omega} \sin \theta_{pa}) \cdot (r_{l,c}^0 + \lambda \cos \zeta_{lc}) + \lambda \sin \Sigma_p \sin \phi_{t,\omega} \sin \zeta_{lc} - r_g \sin \Sigma_p \sin \phi_{t,\omega} \\ (\lambda \cos \phi_{t,\omega} \sin \zeta_{lc} - \sin \phi_{t,\omega} \sin \theta_{pa}) \cdot (r_{l,c}^0 + \lambda \cos \zeta_{lc}) - r_g \cos \phi_{t,\omega} \\ -(\sin \Sigma_p \cos \theta_{pa} - \cos \Sigma_p \cos \phi_{t,\omega} \sin \theta_{pa}) \cdot (r_{l,c}^0 + \lambda \cos \zeta_{lc}) + \lambda \cos \Sigma_p \sin \phi_{t,\omega} \sin \zeta_{lc} - r_g \cos \Sigma_p \sin \phi_{t,\omega} \end{bmatrix} \\ &\quad 1 \end{aligned} \quad (10.42)$$

Expressions:

- (a) for the unit normal vector,  $\mathbf{n}_g$ , to the gear tooth flank,  $\mathcal{G}$ ,
- (b) for the unit normal vector,  $\mathbf{n}_p$ , to the mating pinion tooth flank,  $\mathcal{P}$ , as well as
- (c) for the unit normal vector,  $\mathbf{n}_r$ , to tooth flank of the auxiliary generating round rack,  $\mathcal{R}$ ,

can be derived based on the unit normal vector,  $\mathbf{n}_{lc}$ , to the line of contact,  $LC$ , which is constructed within the plane of action,  $PA$ . For this purpose, the unit normal vector,  $\mathbf{n}_{lc}$ , should be considered together with the corresponding operators of the coordinate system transformations. The vector,  $\mathbf{n}_{lc}$ , in nature, is perpendicular to a planar curve. So, this perpendicular is located entirely within the plane where the line of contact,  $LC$ , is located.

The above-considered approach for determination of the geometry of the gear tooth flank,  $\mathcal{G}$ , and of the pinion tooth flank,  $\mathcal{P}$ , is based on generation of the tooth flanks in the form of a family of successive positions of the line of contact,  $LC$ , that is traveling together with the plane of action,  $PA$ . This approach does not require specification of the tooth flanks in the form of enveloping surfaces to successive positions of the generating basic rack. Thus, the proposed method for the generation of the tooth flanks,  $\mathcal{G}$  and  $\mathcal{P}$ , does not require implementation of the elements of the theory of enveloping surfaces. This is a significant advantage of the disclosed method for the generation of tooth flank,  $\mathcal{G}$ , of the gear, and tooth flank,  $\mathcal{P}$ , of the pinion in an intersected axes gearing over conventional methods used for this purpose (over the “kinematic method” in particular).

Crossed-axes gearing having tooth flanks of the proposed geometry (which is generated by the line of contact,  $LC$ , traveling together with the plane of action,  $PA$ ) is the most general kind of perfect gearing having “line contact” of the tooth

flanks,  $\mathcal{G}$  and  $\mathcal{P}$ . In a particular case, when the center distance is reduced to zero ( $C = 0$ ), the crossed-axes gearing of the proposed geometry simplifies intersected axes gearing having line contact of the tooth flanks. Under another scenario, namely, when the crossed-axes angle is equal to either 0 or  $\pi$ , the crossed-axes gearing of the proposed geometry simplifies parallel-axes gearing having line contact of the tooth flanks.

The crossed-axes gearing, tooth flanks of the gear and of the pinion which are generated as loci of consequent positions of the line of contact,  $LC$ , that is traveling together with the plane of action,  $PA$ , is a novel kind of gearing. This novel kind of gearing ensures line contact of the tooth flanks of the gear and of the pinion. This kind of gearing is referred to as the “ $R$ -gearing”<sup>2</sup> (patent pending).

The concept of “ $R$ -gearing” has been evolved later to the more general concept of the “ $S_{pr}$ -gearing.” The interested reader may wish to go to original source [5, 6] for details.

## 10.4 On Looseness of Two “Olivier Principles”

The generation of “*reversibly enveloping surfaces*” by means of a line that is associated with the plane of action shows that this is the only way to generate “ $R_e$ -surfaces.” No other approach for generation enveloping surfaces is capable of to generate “ $R_e$ -surfaces.”

With that said, the well-known principles for generation of enveloping surfaces those proposed by Olivier [7] as early as 1842 need to be carefully investigated one more time.

**First Olivier Principle:** *The first Olivier principle states that both conjugate surfaces can be generated with an arbitrarily chosen auxiliary generating surface.*

The generating surface in this case differs from both the conjugate surfaces. According to *T. Olivier*, there is much freedom in selection of the auxiliary generating surface.

**Second Olivier Principle:** *The second Olivier principle states that in a particular case the auxiliary generating surface can be congruent to one of the conjugate surfaces.*

---

<sup>2</sup>It should be stressed here that “ $R$ -gearing” is the only kind of crossed-axes gearing that ensures line contact of the worm threads with the tooth flanks of the worm gear. No other kind of gearing features line contact of this kind. Many efforts have been undertaken by Dr. *J. Fillips* to develop a kind of spatial gearing having line contact between the tooth flanks. In the design of spatial gearing proposed by Dr. *J. Fillips* (2003), both tooth flanks of the gear and of the pinion are generated by a plane that is traveling in relation to the axis of rotation of the gear,  $\mathcal{G}$ , and to the axis of rotation of the pinion (when the pinion tooth flank,  $\mathcal{P}$ , is generated). In  $R$ -gearing, neither tooth flanks of a gear, nor of a mating pinion can be generated by a plane. Therefore, it becomes evident that in the spatial gearing proposed by Dr. *J. Fillips*, the tooth flanks of the mating gears never make line contact. Research in this area was later carried out by Dr. *Stachel* (circa 2006, and others) to determine a special combination of the design parameters of the gearing under which the tooth flanks make line contact.

As it follows from the title of the book by *T. Olivier* (“*Théorie Géométrique des Engrenages destinés*” that can be translated to English as “*Geometrical Theory of Gearing*”), both the “*Olivier principles*” are developed first of all for the needs of the theory of gearing. In perfect gearings of all kinds, the tooth flanks of a gear and that of a mating pinion are conjugate to one another; that is, they are a kind of “*reversibly enveloping surfaces*.”

Conjugacy is a specific property of the tooth flanks of a gear,  $\mathcal{G}$ , and a mating pinion,  $\mathcal{P}$ . Only surfaces that roll over one another can feature this unique property. Let us briefly analyze the property of conjugacy of two interacting surfaces. A crossed-axes gearing is used below as an example for this purpose.

In crossed-axes gearing, when a gear and a mating pinion rotate steadily, the gear tooth flank,  $\mathcal{G}$ , can be viewed as an envelope to consecutive positions of the mating pinion tooth flank,  $\mathcal{P}$ . The gear tooth flank,  $\mathcal{G}$ , generated in this way, can be used to generate the mating pinion tooth flank. If the tooth flanks,  $\mathcal{G}$  and  $\mathcal{P}$ , are conjugate (that is, they are “*reversibly enveloping surfaces*”), then the original pinion tooth flank,  $\mathcal{P}$ , and the pinion tooth flank,  $\mathcal{P}_g$ , generated by the gear tooth flank,  $\mathcal{G}$ , are identical to one another ( $\mathcal{P}_g \equiv \mathcal{P}$ ).

Tooth flanks not of many geometries can be referred to as the “*conjugate surfaces*” or, the same, “*reversibly enveloping surfaces*”. For “*reversibly enveloping surfaces*,” all instant lines of action intersect the axis of instant rotation  $P_{\text{In}}$ , and it is a must to fulfill this requirement by a pair of “*reversibly enveloping surfaces*.”

A criterion to be fulfilled by two teeth flanks,  $\mathcal{G}$  and  $\mathcal{P}$ , of a crossed-axes gear pair in order to possess the property of conjugacy can be expressed analytically.

When a gear,  $\mathcal{G}$ , and a mating pinion,  $\mathcal{P}$ , teeth flanks interact with one another, straight lines that align to common perpendiculars,  $\mathbf{n}_g$ , through points within a current line of contact,  $LC$ , must always intersect the axis of instant rotation,  $P_{\text{In}}$ . The condition of conjugacy must be met at all points of a (desired) line of contact,  $LC_{\text{des}}$ , between the interacting teeth flanks,  $\mathcal{G}$  and  $\mathcal{P}$ . This is a key requirement to be fulfilled by conjugate tooth flanks,  $\mathcal{G}$  and  $\mathcal{P}$ , when the gears rotate.

At an arbitrary point,  $m$ , within a desired line of contact,  $LC_{\text{des}}$ , an instant line of action,  $LA_{\text{inst}}$ , forms an angle with the axis of instant rotation,  $P_{\text{In}}$ . At every instant of time, every instant line of action,  $LA_{\text{inst}}$ , intersects the axis of instant rotation,  $P_{\text{In}}$ , of a gear and a mating pinion teeth flanks,  $\mathcal{G}$  and  $\mathcal{P}$ —this is a must for conjugate tooth flanks.

A component of the instant motion that is parallel to the axis of instant rotation,  $P_{\text{In}}$ , does not affect the conjugate action between the interacting teeth flanks,  $\mathcal{G}$  and  $\mathcal{P}$ . Therefore, this component of the relative motion is not considered here.

The other component of the relative motion is along a straight line through a point,  $P$ , that is located within the axis of instant rotation,  $P_{\text{In}}$ . The conjugate action between the interacting teeth flanks,  $\mathcal{G}$  and  $\mathcal{P}$ , is considered for this component of the relative motion.

Three vectors,  $\mathbf{p}_{\text{In}}$ ,  $\mathbf{V}_m$ , and  $\mathbf{n}_g$ , are constructed in Fig. 10.16 [8].

Two vectors,  $\mathbf{p}_{\text{In}}$  and  $\mathbf{V}_m$ , are located within the plane of action,  $PA$ .

The unit vector,  $\mathbf{p}_{\text{In}}$ , is along the axis of instant rotation,  $P_{\text{In}}$ . Therefore, in the plane-of-action “*Cartesian*” coordinate system,  $X_{pa}Y_{pa}Z_{pa}$ , it can be analytically

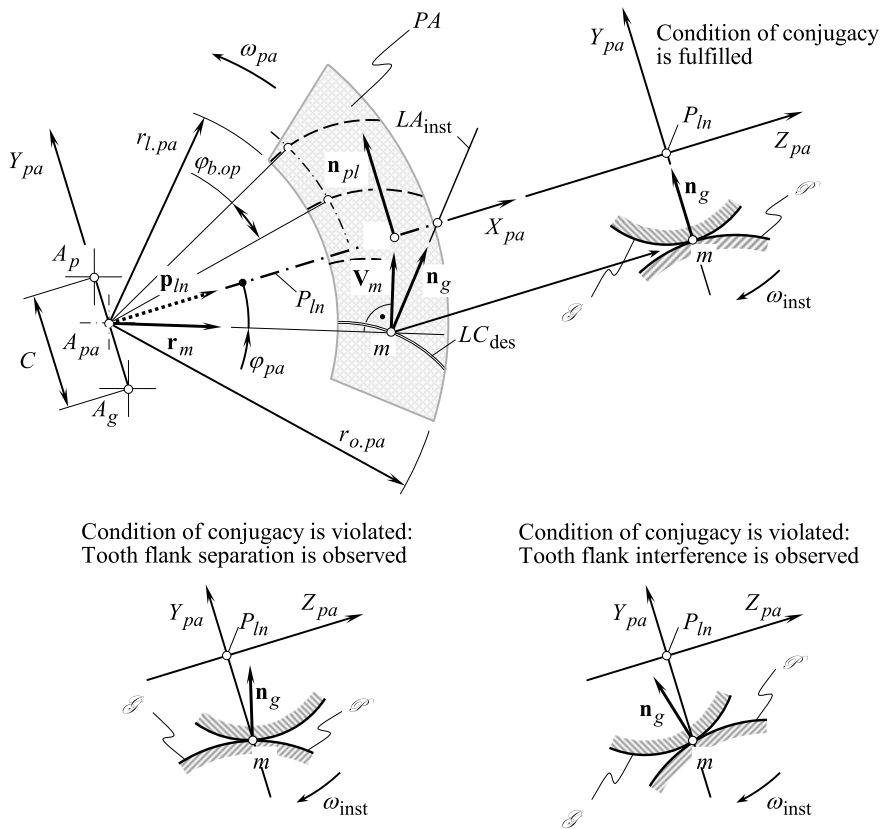


**Fig. 10.16** Condition of conjugacy of a gear,  $\mathcal{G}$ , and a mating pinion,  $\mathcal{P}$ , tooth flanks in a pair of “reversibly enveloping surfaces” (After Prof. S. P. Radzevich, 2008)

represented in a form:

$$\mathbf{p}_{ln} = \mathbf{i} \quad (10.43)$$

The linear velocity vector,  $\mathbf{V}_m$ , is along an instant line of action,  $LA_{inst}$ , through the point of interest,  $m$ . In the plane-of-action “Cartesian” coordinate system,  $X_{pa}Y_{pa}Z_{pa}$ , the velocity vector,  $\mathbf{V}_m$ , can be analytically described as:

$$\mathbf{V}_m = \mathbf{i} \cdot V_m \sin \varphi_{pa} + \mathbf{j} \cdot V_m \cos \varphi_{pa} \quad (10.44)$$

The magnitude,  $V_m$ , of the linear velocity vector,  $\mathbf{V}_m$ , is omitted from the further analysis as it does not affect the direction of the vector,  $\mathbf{V}_m$ .

The third unit vector,  $\mathbf{n}_g$ , is perpendicular to the gear tooth flank,  $\mathcal{G}$ . Therefore, it can be calculated from the equation:

$$\mathbf{n}_g = \frac{\frac{\partial \mathbf{r}_g}{\partial U_g} \times \frac{\partial \mathbf{r}_g}{\partial V_g}}{\left| \frac{\partial \mathbf{r}_g}{\partial U_g} \times \frac{\partial \mathbf{r}_g}{\partial V_g} \right|} \quad (10.45)$$

where

$\mathbf{r}_g$  is the position vector of a point of a gear tooth flank,  $\mathcal{G}$ .

$U_g$  and  $V_g$  are the curvilinear (the “*Gaussian*”) coordinates of a point of a gear tooth flank,  $\mathcal{G}$ .

The unit vector,  $\mathbf{n}_{pl}$ , is entirely located within the plane of action,  $PA$ , and is perpendicular to the axis of instant rotation,  $P_{ln}$ . Therefore, in the plane-of-action “*Cartesian*” coordinate system,  $X_{pa}Y_{pa}Z_{pa}$ , it can be analytically represented in a form:

$$\mathbf{n}_{pl} = \mathbf{j} \quad (10.46)$$

A gear,  $\mathcal{G}$ , and a mating pinion,  $\mathcal{P}$ , tooth flanks are conjugate if a straight line along the unit normal vector,  $\mathbf{n}_g$ , intersects the axis of instant rotation,  $P_{ln}$ , at any point of the line of contact,  $LC$ . To meet this requirement, the unit normal vectors,  $\mathbf{n}_{pl}$  and  $\mathbf{n}_g$ , must be coplanar,<sup>3</sup> and they must not be perpendicular to one another (here, the unit normal vector to the axis of instant rotation,  $P_{ln}$ , is designated as  $\mathbf{n}_{pl}$ . This vector is entirely located within the plane of action,  $PA$ ).

When a gear,  $\mathcal{G}$ , and a mating pinion,  $\mathcal{P}$ , tooth flanks are conjugate, then the three unit vectors,  $\mathbf{p}_{ln}$ ,  $\mathbf{V}_m$ , and  $\mathbf{n}_g$ , must be coplanar. The unit vectors,  $\mathbf{p}_{ln}$ ,  $\mathbf{V}_m$ , and  $\mathbf{n}_g$ , are coplanar if and only if the triple scalar product,  $\mathbf{p}_{ln} \times \mathbf{V}_m \cdot \mathbf{n}_g$ , is zero, that is, if the equality [8]:

$$\mathbf{p}_{ln} \times \mathbf{V}_m \cdot \mathbf{n}_g = 0 \quad (10.47)$$

is valid. The triple scalar product,  $\mathbf{p}_{ln} \times \mathbf{V}_m \cdot \mathbf{n}_g$ , can be represented in the form of a determinant:

$$\mathbf{p}_{ln} \times \mathbf{V}_m \cdot \mathbf{n}_g = \begin{vmatrix} X_{pl} & Y_{pl} & Z_{pl} \\ V_{x,m} & V_{y,m} & V_{z,m} \\ X_g & Y_g & Z_g \end{vmatrix} = 0 \quad (10.48)$$

In addition to Eq. (10.48), the condition:

$$\mathbf{n}_{pl} \cdot \mathbf{n}_g \neq 0 \quad (10.49)$$

must also be fulfilled. The parallelism of the directions specified by the unit normal vectors,  $\mathbf{n}_{pl}$  and  $\mathbf{n}_g$ , is eliminated by this condition. No rotation transmission by

---

<sup>3</sup>In the case under consideration, the angular velocity vector,  $\boldsymbol{\omega}_{pl}$ , can be used instead of the unit vector,  $\mathbf{p}_{ln}$ .

means of gears is possible when the unit normal vector,  $\mathbf{n}_g$ , is parallel to the axis of instant rotation,  $P_{\text{In}}$ .

An expression:

$$\mathbf{p}_{\text{In}} \times \mathbf{n}_g \neq 0 \quad (10.50)$$

is an alternative representation of the condition specified by Eq. (10.49).

A gear,  $\mathcal{G}$ , and a mating pinion,  $\mathcal{P}$ , tooth flanks are said to be conjugate if and only if the conditions, those specified by Eq. (10.47) [or Eq. (10.48)] and Eq. (10.49) [or Eq. (10.50)], are fulfilled for any and all points within the line of contact,  $LC$ , for any possible configurations of the gear and the pinion in relation to one another [8]:

$$\begin{cases} \mathbf{p}_{\text{In}} \times \mathbf{V}_m \cdot \mathbf{n}_g = 0 \\ \mathbf{p}_{\text{In}} \times \mathbf{n}_g \neq 0 \end{cases} \quad (10.51)$$

Equation (10.51) analytically describes the condition of conjugacy of a gear,  $\mathcal{G}$ , and a mating pinion,  $\mathcal{P}$ , tooth flanks.

As shown clearly in the previous section of the book, there is no freedom in selection of enveloping surfaces if the configuration of the rotation vectors is specified. Once the configuration of the rotation vectors is specified, a limited number of “*reversibly enveloping surfaces*” can be generated. They differ from one another only by the value of the transverse pressure angle in relative motion of the surfaces. Thus, in general, an arbitrary auxiliary surface cannot be used for generation of a pair of “*R<sub>e</sub>-surfaces*.” Further, if one of the moving surfaces is given, and a configuration of the rotation vectors is specified, then, in general, an enveloping surface does not exist at all.

This makes it possible to conclude that in general, it is a huge mistake trying to generate “*reversibly enveloping surfaces*” as envelopes either to an auxiliary generating surface or to another traveling surface. The “*Olivier principles*” are useless for solving this particular problem as reverse enveloping is feasible only in particular cases where the interacting surfaces are a kind of tooth flank of “*R-gearing*.”

When a pair of “*R<sub>e</sub>-surfaces*” is generated, then both “*Olivier principles*” are valid for a pair of the already existing smooth regular “*reversibly enveloping surfaces*.” However, under such a scenario these principles become useless.

Nothing is said by *T. Olivier* about the necessity to fulfill the condition of conjugacy of two interacting surfaces when using the “*Olivier principles*” (see (14.71) in [7]). The “*Olivier principles*” are equivalent to enveloping conditions in bi-parametric (“*the first Olivier principle*”) and mono-parametric (“*the second Olivier principle*”) enveloping surfaces. Ultimately, the “*Olivier principles*” for generation of enveloping surfaces in general cases are either incorrect or useless when they are valid.

Summarizing, one can conclude that both of *Olivier’s principles* are valid for:

- involute tooth profiles when the axes of rotation are parallel to one another,
- Spherical involute tooth profiles when the axes of rotation intersect one another,
- “*R-gearing*” when the axes of rotation cross one another.

The “*Olivier principles*” are not valid for the tooth flanks of all the rest geometries. Thus, these two principles are useless, as only approximate enveloping part surfaces can be generated using them.

The application of “*Olivier principles*” is valid in degenerate cases, when one of the part surfaces allows for “*sliding over itself*” in the direction of the enveloping motion. Such simple examples of generation of enveloping part surface are illustrated in the examples immediately following.

#### ***10.4.1 An Example of Implementation of the “First Olivier Principle” for Generation of Enveloping Surfaces in a Degenerate Case***

The resultant motion of a smooth regular part surface  $P_2$  with respect to a smooth regular part surface  $P_1$  can be complex in nature. For the purpose of simplification, it can be decomposed on two elementary motions, each of which is simple. Elementary motions are usually represented with a rotational motion and with a translational motion.

As an example of implementation of the “*first Olivier principle*” for generation of enveloping surfaces in a degenerate case, consider generation of a smooth regular part surface  $P_2$  by means of a smooth regular part surface  $P_1$ . The geometry or the part surface  $P_1$  is specified, as well as the motion of this surface in relation to a certain reference system which the part surface  $P_2$  (to be generated) will be associated with. The schematic of generation of the part surface  $P_2$  as an enveloping surface to consecutive positions of the moving part surface  $P_1$  is depicted in Fig. 10.17.

The part surface  $P_1$  is rotating about the axis  $O_{P1}$  (see Fig. 10.17) with a certain angular velocity  $\omega_{P1}$ . The surface  $P_2$  coordinate system  $X_{P2}Y_{P2}Z_{P2}$  is rotating with a certain angular velocity  $\omega_{P2}$  about the axis  $O_{P2}$ . The axes of rotations  $O_{P1}$  and  $O_{P2}$  are at a right angle.

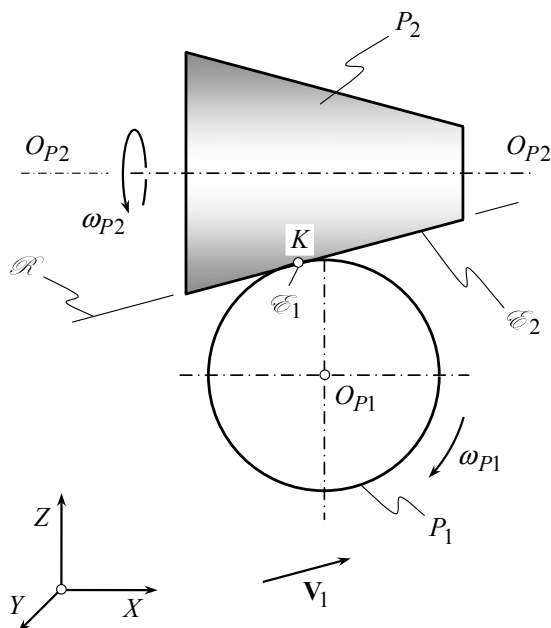
The resultant generating motion  $\mathbf{V}_\Sigma$  is decomposed into two elementary linear motions  $\mathbf{V}_1$  and  $\mathbf{V}_2$  (here, the equality  $\mathbf{V}_\Sigma = \mathbf{V}_1 + \mathbf{V}_2$  is observed).

First, an auxiliary generating surface  $\mathcal{R}$  needs to be determined. The auxiliary surface  $\mathcal{R}$  is an enveloping surface to successive positions of the part surface  $P_1$  in its motion with the linear velocity  $\mathbf{V}_1$  of the first elementary motion. Further, the part surface  $P_2$  is represented in the coordinate system  $X_{P2}Y_{P2}Z_{P2}$  with the enveloping surface to consecutive positions of the auxiliary generating surface  $\mathcal{R}$  in its motion with the velocity  $\mathbf{V}_2$  of the second elementary motion. Here, the vector  $\mathbf{V}_2$  designates linear velocity of rotational motion of the auxiliary generating surface  $\mathcal{R}$  about the axis  $O_{P1}$  with the angular velocity  $\omega_{P2}$ .

The part surface  $P_2$  that is determined following the two-parametric approach usually makes point contact with the part surface  $P_1$ . This occurs for the following reason.



**Fig. 10.17** Example of implementation of the “first Olivier principle” for generation of enveloping surfaces in a degenerate case



The line  $\mathcal{E}_1$  is the characteristic line for the part surface  $P_1$  and the auxiliary generating surface  $\mathcal{R}$ . The auxiliary generating surface  $\mathcal{R}$  and the generated surface  $P_2$  make line contact, and the line  $\mathcal{E}_2$  is the characteristic to the surfaces  $\mathcal{R}$  and  $P_2$ . The characteristic line  $\mathcal{E}_1$  and the characteristic line  $\mathcal{E}_2$  both are within the auxiliary generating surface  $\mathcal{R}$ . Generally speaking, the characteristics  $\mathcal{E}_1$  and  $\mathcal{E}_2$  intersect each other at a point. At least, one common point of the characteristics  $\mathcal{E}_1$  and  $\mathcal{E}_2$  is observed—otherwise, the surfaces  $P_1$  and  $P_2$  cannot make contact. The point  $K$  is the point of intersection of the characteristics  $\mathcal{E}_1$  and  $\mathcal{E}_2$ . In particular cases, the characteristic lines  $\mathcal{E}_1$  and  $\mathcal{E}_2$  can be congruent to each other, which is not common. As a result, the part surfaces  $P_1$  and  $P_2$  make line contact instead of point contact even in the case when a smooth regular part surface  $P_2$  is generated by a smooth regular part surface  $P_1$  according to the “first Olivier principle.”

When the part surfaces  $P_1$  and  $P_2$  move relative to each other with the velocity of  $\mathbf{V}_1$ , the characteristic line  $\mathcal{E}_1$  occupies stationary location on the part surface  $P_1$ , but travels over the part surface  $P_2$ . When the plane  $\mathcal{R}$  is rotating about the axis  $O_{P2}$ , the characteristic curve  $\mathcal{E}_2$  on the auxiliary surface  $\mathcal{R}$  is stationary, but it is traveling over the part surface  $P_2$ . Therefore, in the case of surface generation (see Fig. 10.17), the point  $K$  of intersection of the characteristic lines  $\mathcal{E}_1$  and  $\mathcal{E}_2$  is moveable.

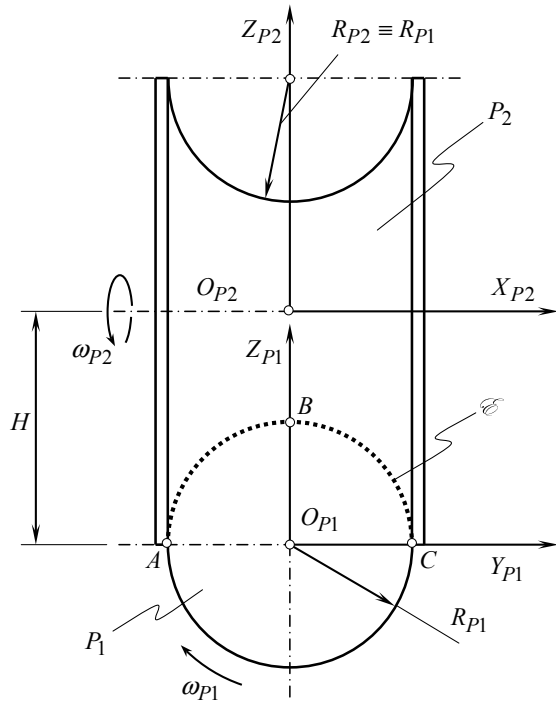
The part surface  $P_2$  that is determined using the first “Olivier principle” for generation of enveloping surfaces makes point contact with the part surface  $P_1$ . This means that no perfect generated surface  $P_1$  is feasible. Cusps on the machined part surface  $P_1$  are inevitable under such a scenario [9].

### 10.4.2 An Example of Implementation of the “Second Olivier Principle” for Generation of Enveloping Surfaces in a Degenerate Case

As an example of implementation of the “*second Olivier principle*” for generation of enveloping surfaces in a degenerate case, consider generation of a smooth regular part surface  $P_2$  by means of a smooth regular part surface  $P_1$ . The geometry or the part surface  $P_1$  is specified, as well as the motion of this surface in relation to a certain reference system which the part surface  $P_2$  (to be generated) will be associated with. The schematic of generation of the part surface  $P_2$  as an enveloping surface to consecutive positions of the moving part surface  $P_1$  is depicted in Fig. 10.18.

When generating a circular cylinder of radius  $R_{P1}$  (see Fig. 10.18) [9], the part is rotating about its axis  $O_{P1}$  with a certain angular velocity  $\omega_{P1}$ . A coordinate system  $X_{P2}Y_{P2}Z_{P2}$  is rotating with a certain angular velocity  $\omega_{P2}$ . The axis of this rotation  $O_{P2}$  crosses at a right angle of the axis of rotation  $O_{P1}$  of surface  $P_1$ . Simultaneously, the coordinate system  $X_{P2}Y_{P2}Z_{P2}$  is traveling along the axis  $O_{P1}$  with a certain velocity (not shown in Fig. 10.18). The part surface  $P_2$  in this case can be represented as an enveloping surface to successive positions of the part surface  $P_1$  in the coordinate system  $X_{P2}Y_{P2}Z_{P2}$ . Remember that the coordinate

**Fig. 10.18** Example of implementation of the “*second Olivier principle*” for generation of enveloping surfaces in a degenerate case



system  $X_{P_2}Y_{P_2}Z_{P_2}$  is the reference system at which the generating surface  $P_2$  can be determined.

After it has been determined, the part surface  $P_2$  and the part surface  $P_1$  make tangency along the characteristic line  $\mathcal{E}$ . In the case under consideration, the characteristic line  $\mathcal{E}$  is represented with a circular arc  $ABC$  of the radius  $R_{P_1}$ .

### 10.4.3 Concluding Remarks

An enveloping surface is specified by the equation of contact ( $\mathbf{n} \cdot \mathbf{V} = 0$ ) only in cases when the envelope exists. Under such a scenario, the “*Shishkov equation of contact*,  $\mathbf{n} \cdot \mathbf{V} = 0$ ,” is helpful to derive an equation of the enveloping surface. Generally speaking, this equation is fulfilled only in differential vicinity of a point within the characteristic line, but either before or after the point the properly generated portion of the enveloping surface can be cut off. Once a portion of the generated envelope is cut off, then the envelope (in a global sense) does not exist. Prior to implement the equation of contact, it must be verified whether or not the envelope exists. Such verification is of critical importance. The conditions of existence of the envelope are not investigated thoroughly yet.

The following theorem can be proven:

**Theorem 10.1** *For a specified traveling surface, an enveloping surface, if any, can be generated when the given surface is performing not an arbitrary motion, but a certain unique (in a certain sense) motion.*

From the standpoint of this theorem, in the general case of enveloping there is no freedom in choosing either kinematics of the relative motion or the geometry of the traveling surface. Namely:

- (a) For a specified kinematics of the relative motion, there could be a unique family of pairs of “ $R_e$ -surfaces” having a different transverse profile angle,  $\phi_{t,\omega}$ , and having line of contact,  $LC$ , of various geometries.
- (b) If the geometry of the traveling part surface is specified, then there is no freedom in choosing the enveloping motion or the geometry of the generated part surface.

The correctness of the theorem is clearly illustrated by the kinematics and geometry of tooth flanks in “ $R$ -gearing.” From the standpoint of “ $R$ -gearing,” the generation of “*reversibly enveloping surfaces*” is feasible for a limited number of cases. All kinds of “ $R_e$ -surfaces” are pre-specified:

- by a given configuration of the rotation vectors,  $\omega_g$  and  $\omega_p$ , and
- by the transverse pressure angle,  $\phi_{t,\omega}$ .

Part surfaces of other kinds cannot be referred to as “ $R_e$ -surfaces.” Therefore, as the total number of “*reversibly enveloping surfaces*” is limited, what is the purpose of the two principles proposed by *T. Olivier*? As there is no freedom to pick an arbitrary kind of an auxiliary generating surface, both the “*Olivier principles*” become useless.

They can be implemented only in case of approximate generation of enveloping surfaces.

**Conclusion 10.3** *In the general case of generation of enveloping surfaces, the first as well as the second Olivier principles are not valid.*

The discussion in this section can be enhanced to more general cases of an arbitrary relative motion of the given surface in relation to a reference system that the enveloping surface will be associated with.

Further development in the field of generation of enveloping surfaces results in generation of surfaces applied in spatial gearing (“ $C_a$ -gearing”) featuring variably disposed axes of rotation of the moving part surface, and of the enveloping part surface. Reversibly enveloping part surfaces of this particular kind are used as tooth flanks in perfect “ $S_{pr}$ -gearing” [5, 6]. They feature point contact of the interacting smooth regular part surfaces  $P_1$  and  $P_2$ .

## References

1. Radzevich, S. P. (1991). *Differential-geometrical method of surface generation* (Doctoral thesis) (300p). Tula: Tula Polytechnic Institute.
2. Radzevich, S. P. (2001). *Fundamentals of surface generation, monograph* (592p). Kiev, Rastan.
3. Radzevich, S. P. (1991). *Sculptured surface machining on multi-axis NC machine* (192p). Monograph, Kiev, Vishcha Schola.
4. Radzevich, S. P., & Petrenko, T. Yu. (1999). Part and tool surfaces that allow sliding over themselves. *Mechanika ta Mashinobuduvann'a* (Vol. 1, pp. 231–240). Kharkiv, Ukraine.
5. Radzevich, S. P. (2012). *Theory of gearing: Kinematics, geometry, and synthesis* (856p). Boca Raton, FL.
6. Radzevich, S. P. (2018). *Theory of gearing: Kinematics, geometry, and synthesis* (2nd ed., 898p). Boca Raton, FL.
7. Olivier, T. (1842). *Théorie Géométrique des Engrenages destinés* (118p). Paris: Bachelier.
8. Radzevich, S. P. (2018). Three fundamental laws of gearing: For gear design and gear production. In *Proceedings of the VIII International Conference “Complex Assurance of Quality of Technological Processes & Systems”* (Vol. 1, pp. 21–23). Chernihiv, Ukraine, May 10–12, 2018.
9. Radzevich, S. P. (2008). *Kinematic geometry of surface machining* (536p). Boca Raton FL: CRC Press.

## Conclusion

This book has been written by a mechanical engineer, and for mechanical engineers involved in design, production, and implementation parts interacting with one another. An in-depth investigation of geometry of smooth regular part surfaces has been undertaken in this book. The new discoveries those disclosed in the book are briefly outlined immediately below.

Principal features of “*Engineering Geometry of Surfaces*” are stated at the beginning of the book. This analysis is based largely on results of analytical description of the local geometry of smooth regular part surfaces, and on the natural representation of part surfaces in terms of fundamental magnitudes of first and second order. The natural representation of part surfaces is based on the main theorem of the theory of surfaces, which is commonly referred to as “*Bonnet theorem*”.

In addition to the “*Dupin indicatrix*,  $Dup(P)$ ” at a point of a part surface  $P$ , a novel planar characteristic image is introduced. This is the so-called “*curvature indicatrix*,  $Crv(P)$ ”, at a point of a smooth regular part surface. Introduction of the curvature indicatrix makes it possible to distinguish not 5 (as known earlier) but 10 different kinds of local patches of smooth regular part surfaces.

On the premise of the curvature indicatrix, a circular chart for local patches of smooth regular part surfaces is developed. The circular chart can be interpreted as a kind of classification of local part surface patches. It reveals the inherent relationship among surface local patches of different geometry.

Further, circular diagrams for local patches of smooth regular part surfaces are employed. Use of planar characteristic image of this particular kind allows to enhance the circular chart for local patches of smooth regular part surfaces.

Earlier works in the realm of geometry of contact of two smooth regular surfaces are reviewed briefly.

The possibility of an analytical method for description of the contact geometry of two surfaces, based on the second fundamental forms of the contacting smooth regular part surfaces, is discussed briefly.

For analytical description of the contact geometry at a point of contact of two smooth regular part surfaces, a planar characteristic of a novel kind curve is introduced. This is the so-called *indicatrix of conformity*,  $Cnf_R(P_1/R_2)$  at a point of contact of two smooth regular part surfaces. The indicatrix of conformity is a planar centro-symmetrical characteristic curve of the fourth order. In particular cases, it also possesses the property of mirror symmetry. Then, the concept of the indicatrix of conformity is enhanced to another planar characteristic curve, which is constructed with implementation of “*Plücker conoid*” for each of two contacting surfaces. The performed analysis makes it possible to distinguish all possible kinds of contact of two smooth regular part surfaces in the first order of tangency. Ultimately, a classification of all possible kinds of contact of two smooth regular part surfaces in the first order of tangency is developed.

For the purposes of designing optimal contacting pairs, a novel kind of surfaces mapping is proposed. This kind of surfaces mapping is referred to as “*R-mapping of the interacting part surfaces*.”

Further, methods for generation of enveloping surfaces are discussed. Here, both single-parametric enveloping and bi-parametric enveloping are analyzed. The results are generalized to the case of an arbitrary number of enveloping parameters.

The principal features of the “*kinematic method*” for determining of enveloping surfaces are outlined. In the nowadays interpretation, this method is based largely on the “*Shishkov equation of contact*,  $\mathbf{n} \cdot \mathbf{V} = 0$ ”, proposed by Prof. V. A. Shishkov as early as in 1948 (or even earlier). This consideration is complemented by the equation of conjugacy:

$$\begin{cases} \mathbf{p}_{ln} \times \mathbf{V}_m \cdot \mathbf{n}_g = 0 \\ \mathbf{p}_{ln} \times \mathbf{n}_g \neq 0 \end{cases}$$

Special cases of enveloping are investigated thoroughly. Smooth regular part surfaces those allow for “*sliding over themselves*” are covered by this analysis.

“*Reversibly enveloping surfaces*” (or just “*R<sub>e</sub>-surfaces*”, for simplicity) are introduced in the analysis. It is shown here that there is no freedom in picking the geometry of an auxiliary generating surface. In the general case of enveloping process, three components are included. These are:

- a pre-specified generating smooth regular part surfaces,  $P_1$ , that is traveling in relation to a certain reference system;
- the kinematics of the relative motion of the smooth regular part surface  $P_1$ ;
- the generated envelope for successive positions of the traveling part surface  $P_2$ .

If not two, but just one of the above-listed three components is known, then the others two can be derived from the condition of enveloping. On this principle, a novel kind of gearing is invented.<sup>1</sup> For convenience, this novel kind of gearing is referred to as “*R-gearing*.” It is proven based on the concept of “*R-gearing*” that in

---

<sup>1</sup>Paten pending.

the general case of enveloping process, two fundamental principles proposed by *Theodore Olivier* (1842) are invalid. Both the “*Olivier principles*” were developed first of all for the needs of the theory of gearing. In perfect gearings of all kinds the tooth flanks of a gear and that of a mating pinion are conjugate to one another, that is, they are a kind of “*reversibly enveloping surfaces*.” These two principles are valid in degenerate cases only, when they become useless. This is mostly due to the condition of conjugacy of interacting part surfaces is ignored when the two “*Olivier principles*” for generation part surfaces were elaborated.

It is shown that the concept of enveloping that is used in design of “*R-gearing*” can be enhanced to a more general case of enveloping process that features point contact of the traveling part surface, and of the enveloping part surfaces; thus, having an additional degree of freedom. A novel kind of gearing, the so-called *S<sub>pr</sub>-gearing* is developed on this enhanced concept of enveloping surfaces.<sup>2</sup>

---

<sup>2</sup>See Footnote 1.

## Appendix A

### Elements of Vector Calculus

Vector calculus is a powerful tool for solving many of geometrical and kinematical problems those pertain to the design and generation of part surfaces. In this book, *vectors are understood as quantities that have magnitude and direction and obey the law of addition.*

#### A.1 Fundamental Properties of Vectors

The distance-and-direction interpretation suggests a powerful way to visualize a vector, and that is, as a directed line segment or arrow. The length of the arrow (at some predetermined scale) represents magnitude of the vector, and the orientation of the segment and placement of the arrowhead (at one end of the segment or the another) represents its direction.

Vectors possess certain properties, the set of which is commonly interpreted as the set of fundamental properties of vectors.

**Addition.** Given two vectors **a** and **b**, their sum (**a** + **b**) is graphically defined by joining the tail of **b** to the head of **a**. Then, the line from the tail of **a** to the head of **b** is the sum **c** = (**a** + **b**).

**Equality.** Two vectors are equal when they have the same magnitude and direction. Position of the vectors is unimportant for equality.

**Negation.** The vector **-a** has the same magnitude as **a** but opposite direction.

**Subtraction.** From the properties of “addition” and “negation,” the following **a** – **b** = **a** + (**-b**) can be defined.

**Scalar multiplication.** The vector **ka** has the same direction as **a**, with a magnitude *k* times that of **a**. *k* is called a scalar as it changes the scale of the vector **a**.



## A.2 Mathematical Operations Over Vectors

The following rules and mathematical operations can be determined from the above-listed fundamental properties of vectors.

Let us assume that a set of three vectors  $\mathbf{a}$ ,  $\mathbf{b}$ , and  $\mathbf{c}$  and two scalars  $k$  and  $t$  are given. Then, vector addition and scalar multiplication have the following properties:

$$\mathbf{a} + \mathbf{b} = \mathbf{b} + \mathbf{a} \quad (\text{A.1})$$

$$\mathbf{a} + (\mathbf{b} + \mathbf{c}) = (\mathbf{a} + \mathbf{b}) + \mathbf{c} \quad (\text{A.2})$$

$$k(t\mathbf{a}) = kt\mathbf{a} \quad (\text{A.3})$$

$$(k + t)\mathbf{a} = k\mathbf{a} + t\mathbf{a} \quad (\text{A.4})$$

$$k(\mathbf{a} + \mathbf{b}) = k\mathbf{a} + k\mathbf{b} \quad (\text{A.5})$$

Magnitude  $a$  of a vector  $\mathbf{a}$  is

$$a = |\mathbf{a}| = \sqrt{a_x^2 + a_y^2 + a_z^2} \quad (\text{A.6})$$

where  $a_x$ ,  $a_y$ , and  $a_z$  are the scalar components of  $\mathbf{a}$ .

A unit vector  $\bar{\mathbf{a}}$  in the direction of a vector  $\mathbf{a}$  is

$$\bar{\mathbf{a}} = \frac{\mathbf{a}}{|\mathbf{a}|} = \frac{\mathbf{a}}{a} \quad (\text{A.7})$$

The components  $\bar{a}_x$ ,  $\bar{a}_y$ , and  $\bar{a}_z$  of a unit vector  $\bar{\mathbf{a}}$  are also the direction cosines of the vector  $\bar{\mathbf{a}}$ :

$$\cos \alpha = \bar{a}_x \quad (\text{A.8})$$

$$\cos \beta = \bar{a}_y \quad (\text{A.9})$$

$$\cos \gamma = \bar{a}_z \quad (\text{A.10})$$

It is common practice to denote the components  $\bar{a}_x$ ,  $\bar{a}_y$ , and  $\bar{a}_z$  by  $l$ ,  $m$  and  $n$  accordingly.

**Scalar product (or dot product) of vectors:** The formula

$$\mathbf{a} \cdot \mathbf{b} = a_x b_x + a_y b_y + a_z b_z = |\mathbf{a}| |\mathbf{b}| \cos \angle(\mathbf{a}, \mathbf{b}) \quad (\text{A.11})$$

is commonly used for calculation of scalar product of two vectors  $\mathbf{a}$  and  $\mathbf{b}$ .

Equation (A.11) can also be represented in the form

$$\mathbf{a} \cdot \mathbf{b} = [\mathbf{a}]^T \cdot [\mathbf{b}] = \begin{bmatrix} a_x & a_y & a_z \end{bmatrix} \cdot \begin{bmatrix} b_x \\ b_y \\ b_z \end{bmatrix} \quad (\text{A.12})$$

Angle  $\angle(\mathbf{a}, \mathbf{b})$  between two vectors  $\mathbf{a}$  and  $\mathbf{b}$  is calculated from

$$\angle(\mathbf{a}, \mathbf{b}) = \cos^{-1} \left( \frac{\mathbf{a} \cdot \mathbf{b}}{|\mathbf{a}| |\mathbf{b}|} \right) \quad (\text{A.13})$$

Scalar product of two vectors  $\mathbf{a}$  and  $\mathbf{b}$  features the following properties:

$$\mathbf{a} \cdot \mathbf{a} = |\mathbf{a}|^2 \quad (\text{A.14})$$

$$\mathbf{a} \cdot \mathbf{b} = \mathbf{b} \cdot \mathbf{a} \quad (\text{A.15})$$

$$\mathbf{a} \cdot (\mathbf{b} + \mathbf{c}) = \mathbf{b} \cdot \mathbf{a} + \mathbf{b} \cdot \mathbf{c} \quad (\text{A.16})$$

$$(k\mathbf{a}) \cdot \mathbf{b} = \mathbf{a} \cdot (k\mathbf{b}) = k(\mathbf{a} \cdot \mathbf{b}) \quad (\text{A.17})$$

If  $\mathbf{a}$  is perpendicular to  $\mathbf{b}$ , then

$$\mathbf{a} \cdot \mathbf{b} = 0 \quad (\text{A.18})$$

**Vector product (or cross product) of two vectors:** Vector product of two vectors can be calculated from the formula

$$\mathbf{a} \times \mathbf{b} = (a_y b_z - a_z b_y) \mathbf{i} + (a_z b_x - a_x b_z) \mathbf{j} + (a_x b_y - a_y b_x) \mathbf{k} \quad (\text{A.19})$$

Here, in Eq. (A.19),  $\mathbf{i}$ ,  $\mathbf{j}$ , and  $\mathbf{k}$  are unit vectors in the  $X$ -,  $Y$ -, and  $Z$ -directions of the reference system  $XYZ$ , in which the vectors  $\mathbf{a}$  and  $\mathbf{b}$  are specified.

Vector product possesses the following property: in case  $\mathbf{a} \times \mathbf{b} = \mathbf{c}$ , then the vector  $\mathbf{c}$  is perpendicular to a plane through the vectors  $\mathbf{a}$  and  $\mathbf{b}$ .

Vector product of two vectors  $\mathbf{a}$  and  $\mathbf{b}$  features the following properties:

$$\mathbf{a} \times \mathbf{b} = \begin{vmatrix} \mathbf{i} & \mathbf{j} & \mathbf{k} \\ a_x & a_y & a_z \\ b_x & b_y & b_z \end{vmatrix} \quad (\text{A.20})$$

$$\mathbf{a} \times \mathbf{b} = |\mathbf{a}| |\mathbf{b}| \mathbf{n} \sin \angle(\mathbf{a}, \mathbf{b}) \quad (\text{A.21})$$

where unit normal vector to the plane through the vectors  $\mathbf{a}$  and  $\mathbf{b}$  is denoted by  $\mathbf{n}$ .

$$|\mathbf{a} \times \mathbf{b}| = |\mathbf{a}| |\mathbf{b}| \sin \angle(\mathbf{a}, \mathbf{b}) \quad (\text{A.22})$$

Coordinates of the vector product  $\mathbf{a} \times \mathbf{b}$  can also be expressed in the form

$$|\mathbf{a} \times \mathbf{b}| = \begin{bmatrix} 0 & -a_z & a_y \\ a_z & 0 & -a_x \\ -a_y & a_x & 0 \end{bmatrix} \cdot \begin{bmatrix} b_x \\ b_y \\ b_z \end{bmatrix} = \begin{bmatrix} -a_z b_y + a_y b_z \\ -a_x b_z + a_z b_x \\ -a_y b_x + a_x b_y \end{bmatrix} \quad (\text{A.23})$$

$$\mathbf{a} \times \mathbf{b} = -\mathbf{b} \times \mathbf{a} \quad (\text{A.24})$$

$$\mathbf{a} \times (\mathbf{b} + \mathbf{c}) = \mathbf{a} \times \mathbf{b} + \mathbf{a} \times \mathbf{c} \quad (\text{A.25})$$

$$(k\mathbf{a}) \times \mathbf{b} = \mathbf{a} \times (k\mathbf{b}) = k(\mathbf{a} \times \mathbf{b}) \quad (\text{A.26})$$

$$\mathbf{i} \times \mathbf{j} = \mathbf{k}, \mathbf{j} \times \mathbf{k} = \mathbf{i}, \mathbf{k} \times \mathbf{i} = \mathbf{j} \quad (\text{A.27})$$

If  $\mathbf{a}$  is parallel to  $\mathbf{b}$ , then

$$\mathbf{a} \times \mathbf{b} = \mathbf{0} \quad (\text{A.28})$$

**Triple scalar product of three vectors:** The product  $(\mathbf{a} \times \mathbf{b}) \cdot \mathbf{c}$  is commonly referred to as *triple scalar product* of three vectors  $\mathbf{a}$ ,  $\mathbf{b}$ , and  $\mathbf{c}$ .

Triple scalar product of three vectors  $\mathbf{a}$ ,  $\mathbf{b}$ , and  $\mathbf{c}$  features the following properties:

$$(\mathbf{a} \times \mathbf{b}) \cdot \mathbf{c} = (\mathbf{b} \times \mathbf{c}) \cdot \mathbf{a} = (\mathbf{c} \times \mathbf{a}) \cdot \mathbf{b} \quad (\text{A.29})$$

$$(\mathbf{b} \times \mathbf{c}) \cdot \mathbf{a} = \mathbf{a} \cdot (\mathbf{b} \times \mathbf{c}) \quad (\text{A.30})$$

$$(\mathbf{a} \times \mathbf{b}) \cdot \mathbf{c} = \mathbf{a} \cdot (\mathbf{b} \times \mathbf{c}) \quad (\text{A.31})$$

$$\mathbf{a} \cdot (\mathbf{b} \times \mathbf{c}) = \begin{vmatrix} a_x & a_y & a_z \\ b_x & b_y & b_z \\ c_x & c_y & c_z \end{vmatrix} \quad (\text{A.32})$$

**Triple vector product of three vectors:** The product  $(\mathbf{a} \times \mathbf{b}) \times \mathbf{c}$  is commonly referred to as *triple vector product* of three vectors  $\mathbf{a}$ ,  $\mathbf{b}$ , and  $\mathbf{c}$ .

The product  $(\mathbf{a} \times \mathbf{b}) \times \mathbf{c}$  can be evaluated by two vector products. However, it also can be evaluated in a more simple way by use of the identity

$$(\mathbf{a} \times \mathbf{b}) \times \mathbf{c} = (\mathbf{a} \cdot \mathbf{c})\mathbf{b} - (\mathbf{b} \cdot \mathbf{c})\mathbf{a} \quad (\text{A.33})$$

It should be mentioned here that in general, the triple vector products  $(\mathbf{a} \times \mathbf{b}) \times \mathbf{c}$  and  $\mathbf{a} \times (\mathbf{b} \times \mathbf{c})$  are not equal

$$(\mathbf{a} \times \mathbf{b}) \times \mathbf{c} \neq \mathbf{a} \times (\mathbf{b} \times \mathbf{c}) \quad (\text{A.34})$$

Analytical interpretation of many problems and results in the field of geometry of surfaces are getting much simpler when vector calculus is used.

***Lagrange equation for vectors:*** For the purposes of calculation of mixed product of vectors **a** and **b** an equation

$$(\mathbf{a} \times \mathbf{b}) \cdot (\mathbf{a} \times \mathbf{b}) = (\mathbf{a} \cdot \mathbf{a})(\mathbf{b} \cdot \mathbf{b}) - (\mathbf{a} \cdot \mathbf{b})^2 \quad (\text{A.35})$$

can be used.

Equation (A.35) is due to *Lagrange*.<sup>3</sup>

---

<sup>3</sup>*Joseph-Louis Lagrange* (January 25, 1736–April 10, 1813), a famous French mathematician, astronomer and mechanician.

## Appendix B

# Applied Coordinate Systems and Linear Transformations

Consequent coordinate systems transformations can be easily described analytically with implementation of matrices. The use of matrices for the coordinate system transformation<sup>4</sup> can be traced back to the mid of 1940s<sup>5</sup> when Dr. *S. S. Mozhayev*<sup>6</sup> began describing of coordinate system transformations by means of matrices.

Below, coordinate system transformation is briefly discussed from the standpoint of its implementation in the theory of gearing.

### B.1 Coordinate System Transformation

Homogeneous coordinates utilize a mathematical trick to embed three-dimensional coordinates and transformations into a four-dimensional matrix format. As a result, inversions or combinations of linear transformations are simplified to inversions or multiplication of the corresponding matrices.

---

<sup>4</sup>Matrices were introduced into mathematics by *A. Cayley* in 1857. They provide a compact and flexible notation particularly useful in dealing with linear transformations, and they presented an organized method for the solution of systems of linear differential equations.

<sup>5</sup>Application of matrices for the purposes of analytical representation of coordinate system transformation should be credited to Dr. *S. S. Mozhayev* [Mozhayev, S. S., *General Theory of Cutting Tools*, Doctoral Thesis, Leningrad, Leningrad Polytechnic Institute, 1951, 295 pages]. Dr. *S. S. Mozhayev* began using matrices for this purpose in the mid of 1940s. Later on, matrix approach for coordinate system transformation has been used by *Denavit and Hartenberg* [13], as well as by many other researchers.

<sup>6</sup>*S. S. Mozhayev*—is a soviet scientist mainly known for his accomplishments in the theory of cutting tool design.

### ***B.1.1 Homogeneous Coordinate Vectors***

Instead of representing each point  $\mathbf{r}(x, y, z)$  in three-dimensional space with a single three-dimensional vector,

$$\mathbf{r} = \begin{bmatrix} x \\ y \\ z \end{bmatrix} \quad (\text{B.1})$$

homogeneous coordinates allow each point  $\mathbf{r}(x, y, z)$  to be represented by any of an infinite number of four-dimensional vectors:

$$\mathbf{r} = \begin{bmatrix} T \cdot x \\ T \cdot y \\ T \cdot z \\ T \end{bmatrix} \quad (\text{B.2})$$

The three-dimensional vector corresponding to any four-dimensional vector can be calculated by dividing the first three elements by the fourth, and a four-dimensional vector corresponding to any three-dimensional vector can be created by simply adding a fourth element and setting it equal to one.

### ***B.1.2 Homogeneous Coordinate Transformation Matrices of the Dimension $4 \times 4$***

Homogeneous coordinate transformation matrices operate on four-dimensional homogeneous vector representations of traditional three-dimensional coordinate locations. Any three-dimensional linear transformation (translation, rotation, and so forth) can be represented by a  $4 \times 4$  homogeneous coordinate transformation matrix. In fact, because of the redundant representation of three-space in a homogeneous coordinate system, an infinite number of different  $4 \times 4$  homogeneous coordinate transformation matrices are available to perform any given linear transformation. This redundancy can be eliminated to provide a unique representation by dividing all elements of a  $4 \times 4$  homogeneous transformation matrix by the last element (which will become equal to one). This means that a  $4 \times 4$  homogeneous transformation matrix can incorporate as many as 15 independent parameters. The generic format representation of a homogeneous transformation equation for mapping the three-dimensional coordinate  $(x_1, y_1, z_1)$  to the three-dimensional coordinate  $(x_2, y_2, z_2)$  is:

$$\begin{bmatrix} T^* \cdot x_2 \\ T^* \cdot y_2 \\ T^* \cdot z_2 \\ T^* \end{bmatrix} = \begin{bmatrix} T^* \cdot a & T^* \cdot b & T^* \cdot c & T^* \cdot d \\ T^* \cdot e & T^* \cdot f & T^* \cdot g & T^* \cdot h \\ T^* \cdot i & T^* \cdot j & T^* \cdot k & T^* \cdot m \\ T^* \cdot n & T^* \cdot p & T^* \cdot q & T^* \end{bmatrix} \cdot \begin{bmatrix} T \cdot x_2 \\ T \cdot y_2 \\ T \cdot z_2 \\ T \end{bmatrix} \quad (\text{B.3})$$

If any two matrices or vectors of this equation are known, the third matrix (or vector) can be calculated, and then the redundant  $T$  element in the solution can be eliminated by dividing all elements of the matrix by the last element.

Various transformation models can be used to constrain the form of the matrix to transformations with fewer degrees of freedom.

### B.1.3 Translations

Translation of a coordinate system is one of the major linear transformations used in the theory of part surface generation. Translations of the coordinate system  $X_2Y_2Z_2$  along axes of the coordinate system  $X_1Y_1Z_1$  are depicted in Fig. B.1. Translations can be analytically described by the homogeneous transformation matrix of dimension  $4 \times 4$ .

For an analytical description of translation along coordinate axes, the operators of translation  $\mathbf{Tr}(a_x, X)$ ,  $\mathbf{Tr}(a_y, Y)$ , and  $\mathbf{Tr}(a_z, Z)$  are used. These operators yield matrix representation in the form:

$$\mathbf{Tr}(a_x, X) = \begin{bmatrix} 1 & 0 & 0 & a_x \\ 0 & 1 & 0 & 0 \\ 0 & 0 & 1 & 0 \\ 0 & 0 & 0 & 1 \end{bmatrix} \quad (\text{B.4})$$

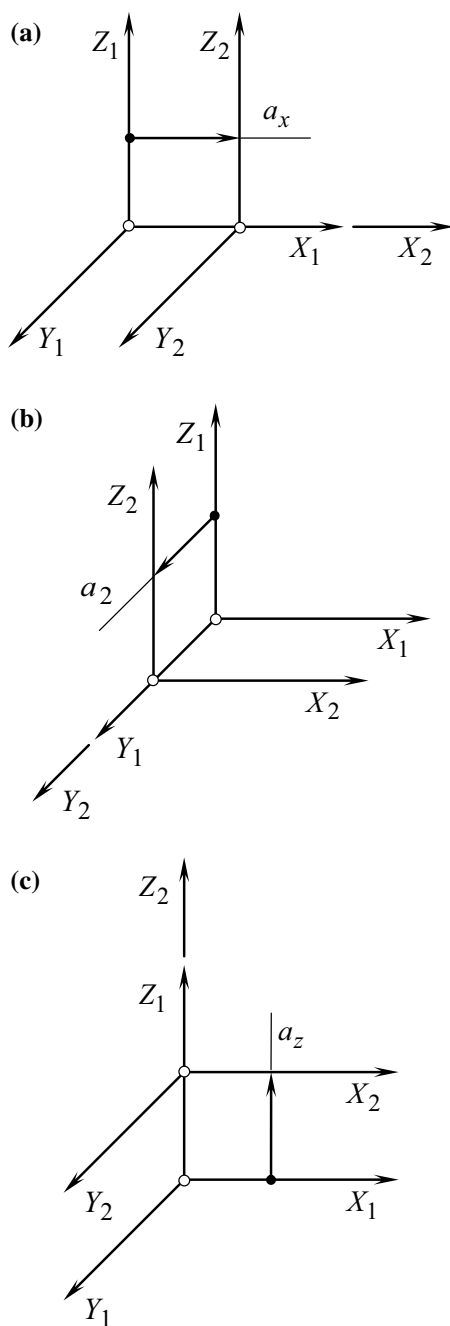
$$\mathbf{Tr}(a_y, Y) = \begin{bmatrix} 1 & 0 & 0 & 0 \\ 0 & 1 & 0 & a_y \\ 0 & 0 & 1 & 0 \\ 0 & 0 & 0 & 1 \end{bmatrix} \quad (\text{B.5})$$

$$\mathbf{Tr}(a_z, Z) = \begin{bmatrix} 1 & 0 & 0 & 0 \\ 0 & 1 & 0 & 0 \\ 0 & 0 & 1 & a_z \\ 0 & 0 & 0 & 1 \end{bmatrix} \quad (\text{B.6})$$

Here, in Eqs. (B.4)–(B.6), the parameters  $a_x$ ,  $a_y$ , and  $a_z$  are signed values that denote the distance of translation along the corresponding axis.

Consider two coordinate systems,  $X_1Y_1Z_1$  and  $X_2Y_2Z_2$ , displaced along the  $X_1$ -axis at a distance  $a_x$  as schematically depicted in Fig. B.1a. A point  $m$  in the reference system  $X_2Y_2Z_2$  is given by the position vector  $\mathbf{r}_2(m)$ . In the coordinate

**Fig. B.1** Analytical description of the operators of translations  $\mathbf{Tr}(a_x, X)$ ,  $\mathbf{Tr}(a_y, Y)$ ,  $\mathbf{Tr}(a_z, Z)$  along the coordinate axes of a “Cartesian” reference system  $XYZ$





system,  $X_1Y_1Z_1$ , that same point  $m$  can be specified by the position vector  $\mathbf{r}_1(m)$ . Then the position vector  $\mathbf{r}_1(m)$  can be expressed in terms of the position vector  $\mathbf{r}_2(m)$  by the equation:

$$\mathbf{r}_1(m) = \mathbf{Tr}(a_x, X) \cdot \mathbf{r}_2(m) \quad (\text{B.7})$$

Equations similar to Eq. (B.7) are valid for the operators  $\mathbf{Tr}(a_y, Y)$  and  $\mathbf{Tr}(a_z, Z)$  of the coordinate system transformation. The latter is schematically illustrated in Fig. B.1b, c.

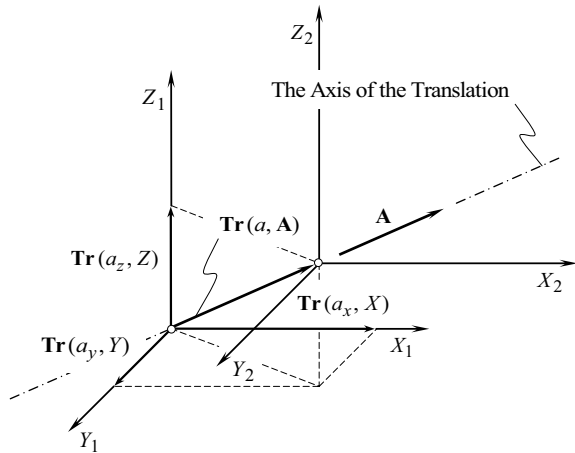
Use of the operators of translation  $\mathbf{Tr}(a_x, X)$ ,  $\mathbf{Tr}(a_y, Y)$ , and  $\mathbf{Tr}(a_z, Z)$  makes it possible an introduction of an operator  $\mathbf{Tr}(a, \mathbf{A})$  of a combined transformation. Suppose that point,  $p$ , on a rigid body goes through a translation describing a straight line from a point  $p_1$  to a point  $p_2$  with a change of coordinates of  $(a_x, a_y, a_z)$ . This motion of the point,  $p$ , can be analytically described with a resultant translation operator  $\mathbf{Tr}(a, \mathbf{A})$ :

$$\mathbf{Tr}(a, \mathbf{A}) = \begin{bmatrix} 1 & 0 & 0 & a_x \\ 0 & 1 & 0 & a_y \\ 0 & 0 & 1 & a_z \\ 0 & 0 & 0 & 1 \end{bmatrix} \quad (\text{B.8})$$

The operator  $\mathbf{Tr}(a, \mathbf{A})$  of the resultant coordinate system transformation can be interpreted as the operator of translation along an arbitrary axis having the vector  $\mathbf{A}$  as the direct vector.

An analytical description of translation of the coordinate system  $X_1Y_1Z_1$  in the direction of an arbitrary vector  $\mathbf{A}$  to the position of  $X_2Y_2Z_2$  can be composed from Fig. B.2. The operator of translation  $\mathbf{Tr}(a, \mathbf{A})$  of that particular kind can be expressed in terms of the operators  $\mathbf{Tr}(a_x, X)$ ,  $\mathbf{Tr}(a_y, Y)$ , and  $\mathbf{Tr}(a_z, Z)$  of elementary translations:

**Fig. B.2** Analytical description of an operator,  $\mathbf{Tr}(a, \mathbf{A})$ , of translation along an arbitrary axis (vector  $\mathbf{A}$  is the direct vector of the axis)



$$\mathbf{Tr}(a, \mathbf{A}) = \mathbf{Tr}(a_z, Z) \cdot \mathbf{Tr}(a_y, Y) \cdot \mathbf{Tr}(a_x, X) \quad (\text{B.9})$$

Evidently, the axis along the vector  $\mathbf{A}$  is always the axis through the origins of both the reference systems  $X_1Y_1Z_1$  and  $X_2Y_2Z_2$ .

Any and all coordinate system transformations that do not change the orientation of a geometrical object are referred to as “*orientation-preserving transformation*,” or “*direct transformation*.” Therefore, transformation of translation is an example of a direct transformation.

### B.1.4 Rotation About a Coordinate Axis

Rotation of a coordinate system about a coordinate axis is another major linear transformation used in the theory of part surface generation. A rotation is specified by an axis of rotation and the angle of the rotation. It is a fairly simple trigonometric calculation to obtain a transformation matrix for a rotation about one of the coordinate axes.

Possible rotations of the coordinate system  $X_2Y_2Z_2$  about the axis of the coordinate system  $X_1Y_1Z_1$  are illustrated in Fig. B.3.

For analytical description of rotation about a coordinate axis, the operators of rotation  $\mathbf{Rt}(\varphi_x, X_1)$ ,  $\mathbf{Rt}(\varphi_y, Y_1)$ , and  $\mathbf{Rt}(\varphi_z, Z_1)$  are used. These operators of linear transformations yield representation in the form of homogeneous matrices:

$$\mathbf{Rt}(\varphi_x, X_1) = \begin{bmatrix} 1 & 0 & 0 & 0 \\ 0 & \cos \varphi_x & \sin \varphi_x & 0 \\ 0 & -\sin \varphi_x & \cos \varphi_x & 0 \\ 0 & 0 & 0 & 1 \end{bmatrix} \quad (\text{B.10})$$

$$\mathbf{Rt}(\varphi_y, Y_1) = \begin{bmatrix} \cos \varphi_y & 0 & \sin \varphi_y & 0 \\ 0 & 1 & 0 & 0 \\ -\sin \varphi_y & 0 & \cos \varphi_y & 0 \\ 0 & 0 & 0 & 1 \end{bmatrix} \quad (\text{B.11})$$

$$\mathbf{Rt}(\varphi_z, Z_1) = \begin{bmatrix} \cos \varphi_z & \sin \varphi_z & 0 & 0 \\ -\sin \varphi_z & \cos \varphi_z & 0 & 0 \\ 0 & 0 & 1 & 0 \\ 0 & 0 & 0 & 1 \end{bmatrix} \quad (\text{B.12})$$

Here,  $\varphi_x$ ,  $\varphi_y$ , and  $\varphi_z$  are signed values that denote the corresponding angles of rotations about a corresponding coordinate axis:  $\varphi_x$  is the angle of rotation around the  $X_1$ -axis (pitch) of the “*Cartesian*” coordinate system  $X_1Y_1Z_1$ ;  $\varphi_y$  is the angle of rotation around the  $Y_1$ -axis (roll), and  $\varphi_z$  is the angle of rotation around the  $Z_1$ -axis (yaw) of that same “*Cartesian*” reference system  $X_1Y_1Z_1$ .

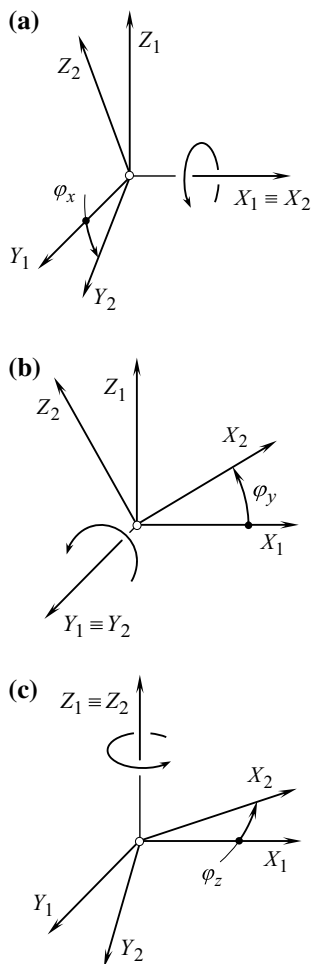


**Fig. B.3** Analytical description of the operators of rotation  $\mathbf{Rt}(\varphi_x, X)$ ,  $\mathbf{Rt}(\varphi_y, Y)$ , and  $\mathbf{Rt}(\varphi_z, Z)$  about a coordinate axis of a reference system  $X_1Y_1Z_1$

Rotation about a coordinate axis is illustrated in Fig. B.3.

Consider two coordinate systems  $X_1Y_1Z_1$  and  $X_2Y_2Z_2$ , which are turned about  $X_1$ -axis through an angle  $\varphi_x$  as shown in Fig. B.3a. In the reference system  $X_2Y_2Z_2$ , a point  $m$  is given by a position vector  $\mathbf{r}_2(m)$ . In the coordinate system  $X_1Y_1Z_1$ , that same point  $m$  can be specified by the position vector  $\mathbf{r}_1(m)$ . Then, the position vector  $\mathbf{r}_1(m)$  can be expressed in terms of the position vector  $\mathbf{r}_2(m)$  by the equation:

$$\mathbf{r}_1(m) = \mathbf{Rt}(\varphi_x, X) \cdot \mathbf{r}_2(m) \quad (\text{B.13})$$

Equations those similar to that above Eq. (B.13) are also valid for other operators  $\mathbf{Rt}(\varphi_y, Y)$  and  $\mathbf{Rt}(\varphi_z, Z)$  of the coordinate system transformation. These elementary coordinate system transformations are schematically illustrated in Fig. B.3b, c accordingly.

### ***B.1.5 Rotation About an Arbitrary Axis Through the Origin***

When a rotation is to be performed around an arbitrary vector based at the origin, the transformation matrix must be assembled from a combination of rotations about the “*Cartesian*” coordinate.

Two different approaches for analytical description of a rotation about an arbitrary axis through the origin are discussed below.

#### **B.1.5.1 Conventional Approach**

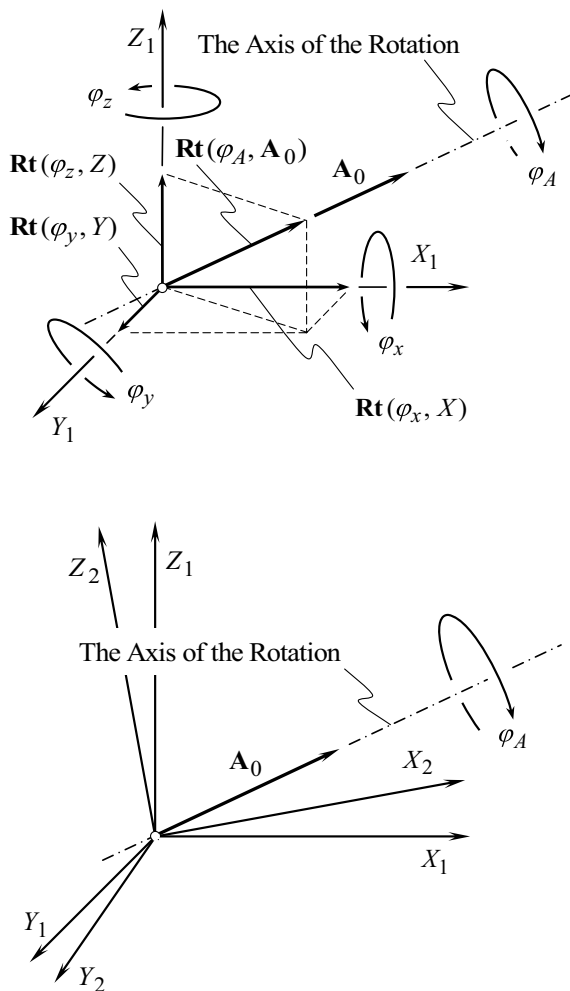
Analytical description of rotation of the coordinate system  $X_1Y_1Z_1$  about an arbitrary axis through the origin to the position of a reference system  $X_2Y_2Z_2$  is illustrated in Fig. B.4. It is assumed here that the rotation is performed about the axis having a vector  $\mathbf{A}_0$  as the direction vector. The operator  $\mathbf{Rt}(\varphi_A, \mathbf{A}_0)$  of rotation of that kind can be expressed in terms of the operators  $\mathbf{Rt}(\varphi_x, X)$ ,  $\mathbf{Rt}(\varphi_y, Y)$ , and  $\mathbf{Rt}(\varphi_z, Z)$  of elementary rotations:

$$\mathbf{Rt}(\varphi_A, \mathbf{A}_0) = \mathbf{Rt}(\varphi_z, Z) \cdot \mathbf{Rt}(\varphi_y, Y) \cdot \mathbf{Rt}(\varphi_x, X) \quad (\text{B.14})$$

Evidently, the axis of rotation (a straight line along the vector  $\mathbf{A}_0$ ) is always an axis through the origin.

The operators of translation and of rotation also yield linear transformations of other kinds as well.

**Fig. B.4** Analytical description of the operator  $\mathbf{Rt}(\varphi_A, \mathbf{A})$  of rotation about an arbitrary axis through the origin of a “Cartesian” coordinate system  $X_1Y_1Z_1$  (the vector  $\mathbf{A}$  is the directing vector of the axis of rotation)

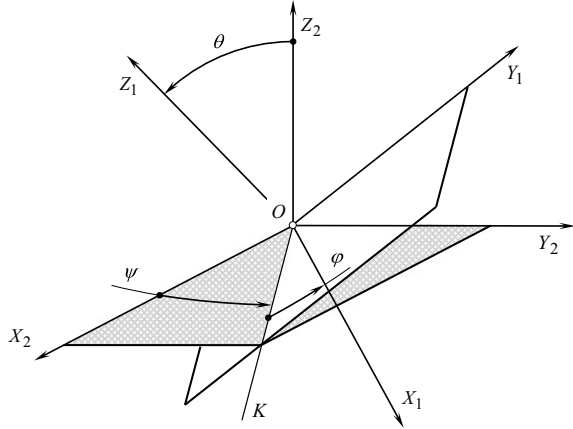


### B.1.5.2 “Eulerian Transformation”

“Eulerian transformation” is a well-known kind of linear transformations used widely in mechanical engineering. This kind of the linear transformations is analytically described by the operator  $\mathbf{Eu}(\psi, \theta, \varphi)$  of “Eulerian<sup>7</sup> transformation”.

The operator  $\mathbf{Eu}(\psi, \theta, \varphi)$  is expressed in terms of three “Euler angles” (or “Eulerian angles”)  $\psi$ ,  $\theta$ , and  $\varphi$ . Configuration of an orthogonal “Cartesian” coordinate system  $X_1Y_1Z_1$  in relation to another orthogonal “Cartesian” coordinate

<sup>7</sup>Leonhard **Euler** (April 15, 1707–September 18, 1783), a famous Swiss mathematician and physicist who spent most of his life in Russia and Germany.

**Fig. B.5** “Euler angles”

system  $X_2Y_2Z_2$  is defined by the “Euler angles”  $\psi$ ,  $\theta$ , and  $\varphi$ . These angles are shown in Fig. B.5.

The line of intersection of the coordinate plane  $X_1Y_1$  of the first reference system by the coordinate plane  $X_2Y_2$  of the second reference system is commonly referred to as “line of nodes.” In Fig. B.5, the line  $OK$  is the line of nodes. It is assumed here and below that the line of nodes,  $OK$ , and the axes  $Z_1$  and  $Z_2$  form a frame of that same orientation as the reference systems  $X_1Y_1Z_1$  and  $X_2Y_2Z_2$  do.

The “Euler angle,  $\varphi$ ” is referred to as the “angle of pure rotation.” This angle is measured between the  $X_1$ -axis and the line of nodes,  $OK$ . The angle of pure rotation,  $\varphi$ , is measured within the coordinate plane  $X_1Y_1$  in the direction of shortest rotation from the axis  $X_1$  to the axis  $Y_1$ .

The “Euler angle,  $\theta$ ” is referred to as the “angle of nutation.” The angle of nutation,  $\theta$ , is measured between the axes  $Z_1$  and  $Z_2$ . Actual value of this angle never exceeds  $180^\circ$ .

The “Euler angle,  $\psi$ ” is referred to as the “angle of precession.” The angle of precession,  $\psi$ , is measured in the coordinate plane  $X_2Y_2$ . This is the angle between the line of nodes,  $OK$ , and the  $X_2$ -axis. Direction of the shortest rotation from the axis  $X_2$  to the axis  $Y_2$  is the direction in which the angle of precession is measured.

In case, when the angle of nutation is equal either  $\theta = 0^\circ$  or  $\theta = 180^\circ$ , then the “Euler angles” are not defined.

Operator  $\mathbf{Eu}(\psi, \theta, \varphi)$  of “Eulerian transformation” allows for the following matrix representation:

$$\mathbf{Eu}(\psi, \theta, \varphi) = \begin{bmatrix} -\sin \psi \cos \theta \sin \varphi + \cos \psi \cos \varphi & \cos \psi \cos \theta \sin \varphi + \sin \psi \cos \varphi & \sin \theta \sin \varphi & 0 \\ -\sin \psi \cos \theta \cos \varphi - \cos \psi \sin \varphi & \cos \psi \cos \theta \cos \varphi - \sin \psi \cos \varphi & \sin \theta \cos \varphi & 0 \\ \sin \theta \sin \varphi & -\cos \psi \cos \theta & \cos \theta & 0 \\ 0 & 0 & 0 & 1 \end{bmatrix} \quad (\text{B.15})$$

It is important to stress here on difference between the operator  $\mathbf{Eu}(\psi, \theta, \varphi)$  of “*Eulerian transformation*,” and between the operator  $\mathbf{Rt}(\psi_A, \mathbf{A}_0)$  of rotation about an arbitrary axis through the origin.

The operator  $\mathbf{Rt}(\psi_A, \mathbf{A})$  of rotation about an arbitrary axis through the origin can result in that same final orientation of the coordinate system  $X_2Y_2Z_2$  in relation to the coordinate system  $X_1Y_1Z_1$  as the operator  $\mathbf{Eu}(\psi, \theta, \varphi)$  of “*Eulerian transformation*” does. However, the operators of linear transformations  $\mathbf{Rt}(\psi_A, \mathbf{A}_0)$  and  $\mathbf{Eu}(\psi, \theta, \varphi)$  are the operators of completely different nature. They can result in identical coordinate system transformation, but they are not equal to one another.

### B.1.6 *Rotation About an Arbitrary Axis not Through the Origin*

The transformation corresponding to rotation of an angle  $\varphi$  around an arbitrary vector not through the origin cannot readily be written in a form similar to the rotation matrices about the coordinate axes.

The desired transformation matrix is obtained by combining a sequence of elementary translation and rotation matrices. (Once a single  $4 \times 4$  matrix has been obtained representing the composite transformations it can be used in the same way as any other transformation matrix.)

Rotation of the coordinate system  $X_1Y_1Z_1$  to a configuration, which the coordinate system  $X_2Y_2Z_2$  possesses, can be performed about a corresponding axis that features an arbitrary configuration in space (see Fig. B.6). The vector  $\mathbf{A}$  is the direction vector of the axis of the rotation. The axis of the rotation is not a line through the origin.

The operator of linear transformation of this particular kind  $\mathbf{Rt}(\psi_A, \mathbf{A})$  can be expressed in terms of the operator  $\mathbf{Tr}(a, \mathbf{A})$  of translation along, and of the operator  $\mathbf{Rt}(\psi_A, \mathbf{A}_0)$  of rotation about an arbitrary axis through the origin:

$$\mathbf{Rt}(\varphi_A, \mathbf{A}) = \mathbf{Tr}(-b, \mathbf{B}^*) \cdot \mathbf{Rt}(\varphi_A, \mathbf{A}_0) \cdot \mathbf{Tr}(b, \mathbf{B}) \quad (\text{B.16})$$

Here, Eq. (B.16) is designated:

$\mathbf{Tr}(b, \mathbf{B})$ —is the operator of translation along the shortest distance of approach of the axis of rotation and origin of the coordinate system

$\mathbf{Tr}(-b, \mathbf{B}^*)$ —is the operator of translation in the direction opposite to the translation  $\mathbf{Tr}(b, \mathbf{B})$  after the rotation  $\mathbf{Rt}(\psi_A, \mathbf{A})$  is completed.

In order to determine the shortest distance of approach,  $B$ , of the axis of rotation (that is, the axis along the directing vector  $\mathbf{B}$ ) and origin of the coordinate system, consider the axis ( $\mathbf{B}$ ) through two given points  $\mathbf{r}_{B.1}$  and  $\mathbf{r}_{B.2}$ .

The shortest distance between a certain point  $\mathbf{r}_0$ , and the straight line through the points  $\mathbf{r}_{B.1}$  and  $\mathbf{r}_{B.2}$  can be calculated from the following formula:

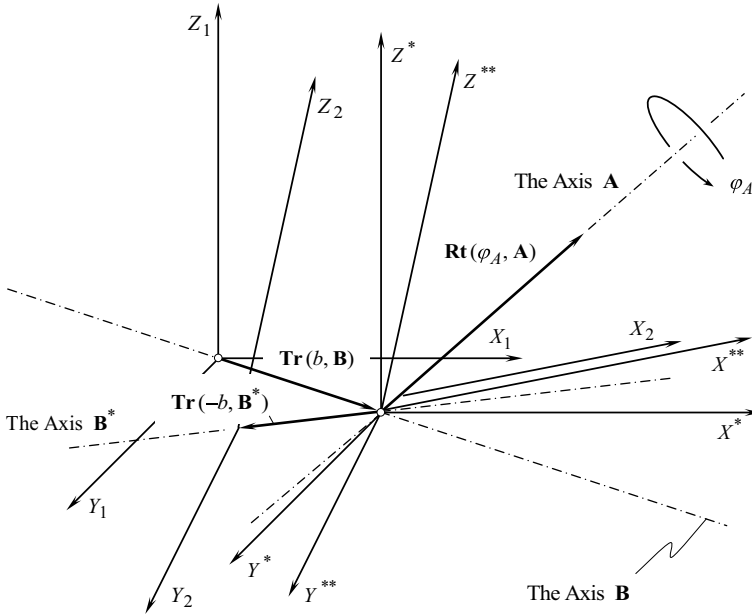


**Fig. B.6** Analytical description of the operator,  $\mathbf{Rt}(\varphi_A, \mathbf{A})$ , of rotation about an arbitrary axis not through the origin (vector  $\mathbf{A}$  is the direct vector of the axis of the rotation)

$$B = \frac{|(\mathbf{r}_2 - \mathbf{r}_1) \times (\mathbf{r}_1 - \mathbf{r}_0)|}{|\mathbf{r}_2 - \mathbf{r}_1|} \quad (\text{B.17})$$

For the origin of the coordinate system, the equality  $\mathbf{r}_0 = 0$  is observed. Then,

$$B = |\mathbf{r}_1| \cdot \sin \angle [\mathbf{r}_1, (\mathbf{r}_2 - \mathbf{r}_1)] \quad (\text{B.18})$$

Matrix representation of the operators of translation  $\mathbf{Tr}(a_x, X)$ ,  $\mathbf{Tr}(a_y, Y)$ ,  $\mathbf{Tr}(a_z, Z)$  along the coordinate axes, together with the operators of rotation  $\mathbf{Rt}(\varphi_x, X)$ ,  $\mathbf{Rt}(\varphi_y, Y)$ ,  $\mathbf{Rt}(\varphi_z, Z)$  about the coordinate axes is convenient for implementation in the theory of part surface generation. Moreover, use of the operators is the simplest possible way to analytically describe the linear transformations.

### ***B.1.7 Resultant Coordinate System Transformation***

The operators of translation  $\mathbf{Tr}(a_x, X)$ ,  $\mathbf{Tr}(a_y, Y)$ , and  $\mathbf{Tr}(a_z, Z)$  together with the operators of rotation  $\mathbf{Rt}(\varphi_x, X)$ ,  $\mathbf{Rt}(\varphi_y, Y)$ , and  $\mathbf{Rt}(\varphi_z, Z)$  are used for the purpose of composing the operator  $\mathbf{Rs}(1 \mapsto 2)$  of the resultant coordinate system



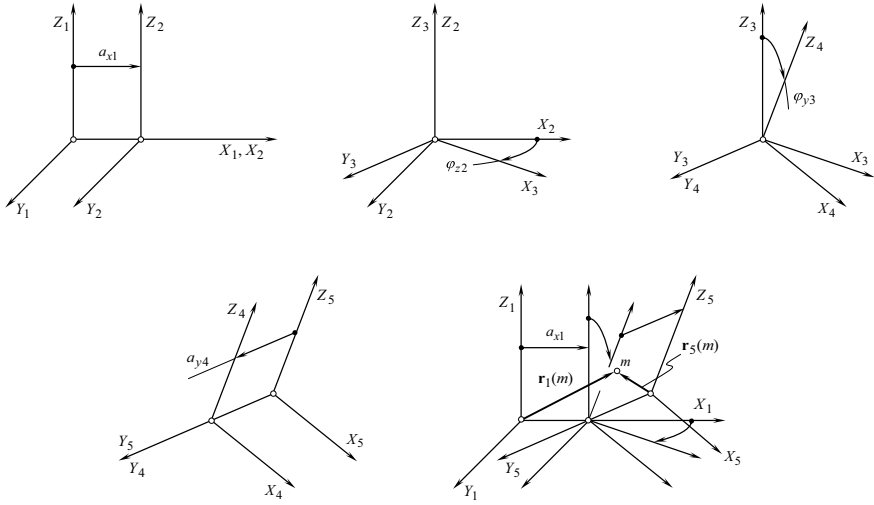


**Fig. B.7** An example of the resultant coordinate system transformation is analytically expressed by the operator  $\mathbf{Rs}(1 \mapsto 5)$

transformation. The transition from the initial “*Cartesian*” reference system  $X_1 Y_1 Z_1$  to other “*Cartesian*” reference system  $X_2 Y_2 Z_2$  is analytically described by the operator  $\mathbf{Rs}(1 \mapsto 2)$  of the resultant coordinate system transformation.

For example, the expression:

$$\mathbf{Rs}(1 \mapsto 5) = \mathbf{Tr}(a_x, X) \cdot \mathbf{Rt}(\varphi_z, Z) \cdot \mathbf{Rt}(\varphi_x, X) \cdot \mathbf{Tr}(a_y, Y) \quad (\text{B.19})$$

indicates that the transition from the coordinate system  $X_1 Y_1 Z_1$  to the coordinate system  $X_5 Y_5 Z_5$  is executed in the following four steps (see Fig. B.7):

- translation  $\mathbf{Tr}(a_y, Y)$  followed by
- rotation  $\mathbf{Rt}(\varphi_x, X)$ , followed by
- second rotation  $\mathbf{Rt}(\varphi_z, Z)$ , and finally followed by the
- translation  $\mathbf{Tr}(a_x, X)$ .

Ultimately, the equality:

$$\mathbf{r}_1(m) = \mathbf{Rs}(1 \mapsto 5) \cdot \mathbf{r}_5(m) \quad (\text{B.20})$$

is valid.

When the operator  $\mathbf{Rs}(1 \mapsto t)$  of the resultant coordinate system transformation is specified, then the transition in the opposite direction can be performed by means of the operator  $\mathbf{Rs}(t \mapsto 1)$  of the inverse coordinate system transformation. The following equality can be easily proven:

$$\mathbf{Rs}(t \mapsto 1) = \mathbf{Rs}^{-1}(1 \mapsto t) \quad (\text{B.21})$$

In the above example illustrated in Fig. B.7, the operator  $\mathbf{Rs}(5 \mapsto 1)$  of the inverse resultant coordinate system transformation can be expressed in terms of the operator  $\mathbf{Rs}(1 \mapsto 5)$  of the direct resultant coordinate system transformation. Following Eq. (B.21), one can come up with the equation:

$$\mathbf{Rs}(5 \mapsto 1) = \mathbf{Rs}^{-1}(1 \mapsto 5) \quad (\text{B.22})$$

It is easy to show that the operator  $\mathbf{Rs}(1 \mapsto t)$  of the resultant coordinate system transformation allows for representation in the following form:

$$\mathbf{Rs}(1 \mapsto t) = \mathbf{Tr}(a, A) \cdot \mathbf{Eu}(\psi, \theta, \varphi) \quad (\text{B.23})$$

The linear transformation  $\mathbf{Rs}(1 \mapsto t)$  [see Eq. (B.23)] can also be expressed in terms of rotation about an axis  $\mathbf{Rt}(\varphi_A, A)$ , not through the origin [see Eq. (B.16)].

## B.2 Complex Coordinate System Transformation

In particular cases of complex coordinate system transformations that are repeatedly used in practice, special purpose operators of coordinate system transformation can be composed of elementary operators of translation and operators of rotation.

### B.2.1. Linear Transformation Describing a Screw Motion About a Coordinate Axis

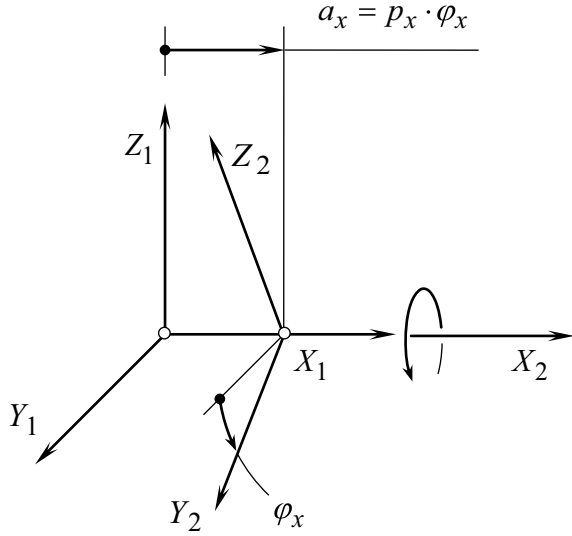
Operators for the analytical description of screw motions about an axis of the “*Cartesian*” coordinate system are a particular case of the operators of the resultant coordinate system transformation.

By definition (see Fig. B.8), the operator  $\mathbf{Sc}_x(\varphi_x, p_x)$  of a screw motion about  $X$ – axis of the “*Cartesian*” coordinate system  $XYZ$  is equal to:

$$\mathbf{Sc}_x(\varphi_x, p_x) = \mathbf{Rt}(\varphi_x, X) \cdot \mathbf{Tr}(a_x, X) \quad (\text{B.24})$$

After substituting of the operator of translation  $\mathbf{Tr}(a_x, X)$  [see Eq. (3.4)–(3.6)], and the operator of rotation  $\mathbf{Rt}(\varphi_x, X)$  [see Eq. (B.10)], Eq. (B.24) casts into the expression:

**Fig. B.8** On analytical description of the operator of screw motion,  $\mathbf{Sc}_x(\varphi_x, p_x)$



$$\mathbf{Sc}_x(\varphi_x, p_x) = \begin{bmatrix} 1 & 0 & 0 & p_x \cdot \varphi_x \\ 0 & \cos \varphi_x & \sin \varphi_x & 0 \\ 0 & -\sin \varphi_x & \cos \varphi_x & 0 \\ 0 & 0 & 0 & 1 \end{bmatrix} \quad (\text{B.25})$$

for the calculation of the operator of the screw motion  $\mathbf{Sc}_x(\varphi_x, p_x)$  about  $X$ -axis.

The operators of screw motions  $\mathbf{Sc}_y(\varphi_y, p_y)$  and  $\mathbf{Sc}_z(\varphi_z, p_z)$  about  $Y$ - and  $Z$ -axes correspondingly are defined in the way similar to that, the operator of the screw motion  $\mathbf{Sc}_x(\varphi_x, p_x)$  is defined:

$$\mathbf{Sc}_y(\varphi_y, p_y) = \mathbf{Rt}(\varphi_y, Y) \cdot \mathbf{Tr}(a_y, Y) \quad (\text{B.26})$$

$$\mathbf{Sc}_z(\varphi_z, p_z) = \mathbf{Rt}(\varphi_z, Z) \cdot \mathbf{Tr}(a_z, Z) \quad (\text{B.27})$$

Using Eqs. (B.5) and (B.6) together with Eqs. (B.11) and (B.12), one can come up with the expressions:

$$\mathbf{Sc}_y(\varphi_y, p_y) = \begin{bmatrix} \cos \varphi_y & 0 & -\sin \varphi_y & 0 \\ 0 & 1 & 0 & p_y \cdot \varphi_y \\ \sin \varphi_y & 0 & \cos \varphi_y & 0 \\ 0 & 0 & 0 & 1 \end{bmatrix} \quad (\text{B.28})$$

$$\mathbf{Sc}_z(\varphi_z, p_z) = \begin{bmatrix} \cos \varphi_z & \sin \varphi_z & 0 & 0 \\ -\sin \varphi_z & \cos \varphi_z & 0 & 0 \\ 0 & 0 & 1 & p_z \cdot \varphi_z \\ 0 & 0 & 0 & 1 \end{bmatrix} \quad (\text{B.29})$$

for the calculation of the operators of the screw motion  $\mathbf{Sc}_y(\varphi_y, p_y)$  and  $\mathbf{Sc}_z(\varphi_z, p_z)$  about  $Y$ - and  $Z$ -axes.

Screw motions about a coordinate axis and screw surfaces are common in the theory of part surface generation. This makes it practical to use the operators of the screw motion  $\mathbf{Sc}_x(\varphi_x, p_x)$ ,  $\mathbf{Sc}_y(\varphi_y, p_y)$  and  $\mathbf{Sc}_z(\varphi_z, p_z)$  in the theory of part surface generation.

In case of necessity, an operator of the screw motion about an arbitrary axis either through the origin of the coordinate system or not through the origin of the coordinate system can be derived following the method similar to that used for the derivation of the operators  $\mathbf{Sc}_x(\varphi_x, p_x)$ ,  $\mathbf{Sc}_y(\varphi_y, p_y)$  and  $\mathbf{Sc}_z(\varphi_z, p_z)$ .

## ***B.2.2 Linear Transformation Describing Rolling Motion of a Coordinate System***

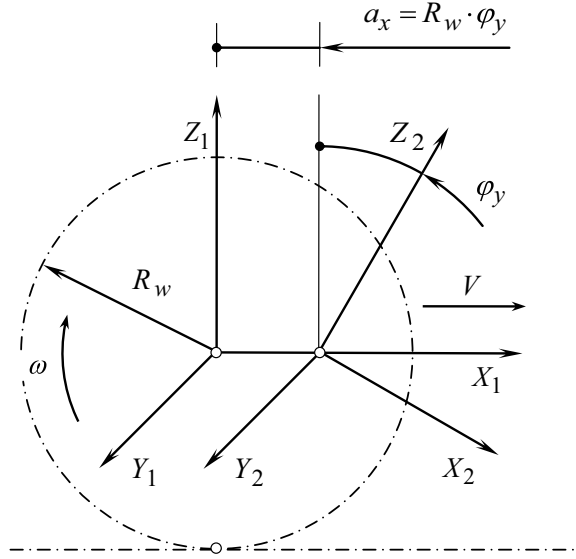
One more practical combination of a rotation and of a translation is often used in the theory of part surface generation.

Consider a “*Cartesian*” coordinate system  $X_1Y_1Z_1$  (see Fig. B.9). The coordinate system  $X_1Y_1Z_1$  is traveling in the direction of  $X_1$ -axis. Velocity of the translation is denoted by  $V$ . The coordinate system  $X_1Y_1Z_1$  is rotating about its  $Y_1$ -axis simultaneously with the translation. Speed of the rotation is denoted as  $\omega$ . Assume that the ratio  $V/\omega$  is constant. Under such a scenario, the resultant motion of the reference system  $X_1Y_1Z_1$  to its arbitrary position  $X_2Y_2Z_2$  allows interpretation in the form of rolling with no sliding of a cylinder of radius  $R_w$  over the plane. The plane is parallel to the coordinate  $X_1Y_1$ -plane, and it is remote from it at the distance  $R_w$ . For the calculation of radius of the rolling cylinder, the expression  $R_w = V/\omega$  can be used.

Due to rolling of the cylinder of a radius,  $R_w$ , over the plane is performed with no sliding, a certain correspondence between the translation and the rotation of the coordinate system is established. When the coordinate system turns through a certain angle  $\varphi_y$ , then the translation of origin of the coordinate system along  $X_1$ -axis is equal to  $a_x = \varphi_y \cdot R_w$ .

Transition from the coordinate system  $X_1Y_1Z_1$  to the coordinate system  $X_2Y_2Z_2$  can be analytically described by the operator of the resultant coordinate system transformation  $\mathbf{Rs}(1 \mapsto 2)$ . The  $\mathbf{Rs}(1 \mapsto 2)$  is equal:

**Fig. B.9** Illustration of the transformation of rolling,  $\mathbf{Rl}_x(\varphi_y, Y)$ , of a coordinate system



$$\mathbf{Rs}(1 \mapsto 2) = \mathbf{Rt}(\varphi_y, Y_1) \cdot \mathbf{Tr}(a_x, X_1) \quad (\text{B.30})$$

Here,  $\mathbf{Tr}(a_x, X_1)$  designates the operator of the translation along  $X_1$ -axis, and  $\mathbf{Rt}(\varphi_y, Y_1)$  is the operator of the rotation about  $Y_1$ -axis.

Operator of the resultant coordinate system transformation of the kind [see Eq. (B.30)] is referred to as the “operator of rolling motion over a plane.”

When the translation is performed along the  $X_1$ -axis and the rotation is performed about the  $Y_1$ -axis, the operator of rolling is denoted as  $\mathbf{Rl}_x(\varphi_y, Y)$ . In this particular case, the equality  $\mathbf{Rl}_x(\varphi_y, Y) = \mathbf{Rs}(1 \mapsto 2)$  [see Eq. (B.30)] is valid. Based on this equality, the operator of rolling over a plane  $\mathbf{Rl}_x(\varphi_y, Y)$  can be calculated from the equation:

$$\mathbf{Rl}_x(\varphi_y, Y) = \begin{bmatrix} \cos \varphi_y & 0 & -\sin \varphi_y & a_x \cdot \cos \varphi_y \\ 0 & 1 & 0 & 0 \\ \sin \varphi_y & 0 & \cos \varphi_y & a_x \cdot \sin \varphi_y \\ 0 & 0 & 0 & 1 \end{bmatrix} \quad (\text{B.31})$$

While rotation remains about the  $Y_1$ -axis, the translation can be performed not along the  $X_1$ -axis, but along the  $Z_1$ -axis instead. For rolling of this kind, the operator of rolling is equal:

$$\mathbf{Rl}_z(\varphi_y, Y) = \begin{bmatrix} \cos \varphi_y & 0 & -\sin \varphi_y & -a_z \cdot \sin \varphi_y \\ 0 & 1 & 0 & 0 \\ \sin \varphi_y & 0 & \cos \varphi_y & a_z \cdot \cos \varphi_y \\ 0 & 0 & 0 & 1 \end{bmatrix} \quad (\text{B.32})$$

For the cases when the rotation is performed about the  $X_1$ -axis, the corresponding operators of rolling are as follow:

$$\mathbf{Rl}_y(\varphi_x, X) = \begin{bmatrix} 1 & 0 & 0 & 0 \\ 0 & \cos \varphi_x & \sin \varphi_x & a_y \cdot \cos \varphi_x \\ 0 & -\sin \varphi_x & \cos \varphi_x & -a_y \cdot \sin \varphi_x \\ 0 & 0 & 0 & 1 \end{bmatrix} \quad (\text{B.33})$$

for the case of rolling along the  $Y_1$ -axis, and

$$\mathbf{Rl}_z(\varphi_x, X) = \begin{bmatrix} 1 & 0 & 0 & 0 \\ 0 & \cos \varphi_x & \sin \varphi_x & a_z \cdot \sin \varphi_x \\ 0 & -\sin \varphi_x & \cos \varphi_x & a_z \cdot \cos \varphi_x \\ 0 & 0 & 0 & 1 \end{bmatrix} \quad (\text{B.34})$$

for the case of rolling along the  $Z_1$ -axis.

Similar expressions can be derived for the case of rotation about the  $Z_1$ -axis:

$$\mathbf{Rl}_x(\varphi_z, Z) = \begin{bmatrix} \cos \varphi_z & \sin \varphi_z & 0 & a_x \cdot \cos \varphi_z \\ -\sin \varphi_z & \cos \varphi_z & 0 & a_x \cdot \sin \varphi_z \\ 0 & 0 & 1 & 0 \\ 0 & 0 & 0 & 1 \end{bmatrix} \quad (\text{B.35})$$

$$\mathbf{Rl}_y(\varphi_z, Z) = \begin{bmatrix} \cos \varphi_z & \sin \varphi_z & 0 & a_y \cdot \sin \varphi_z \\ -\sin \varphi_z & \cos \varphi_z & 0 & a_y \cdot \cos \varphi_z \\ 0 & 0 & 1 & 0 \\ 0 & 0 & 0 & 1 \end{bmatrix} \quad (\text{B.36})$$

Use of the operators of rolling Eqs. (B.31)–(B.36) significantly simplifies analytical description of the coordinate system transformations.

### ***B.2.3 Linear Transformation Describing Rolling of Two Coordinate Systems***

In the theory of part surface generation, combinations of two rotations about parallel axes are of particular interest.

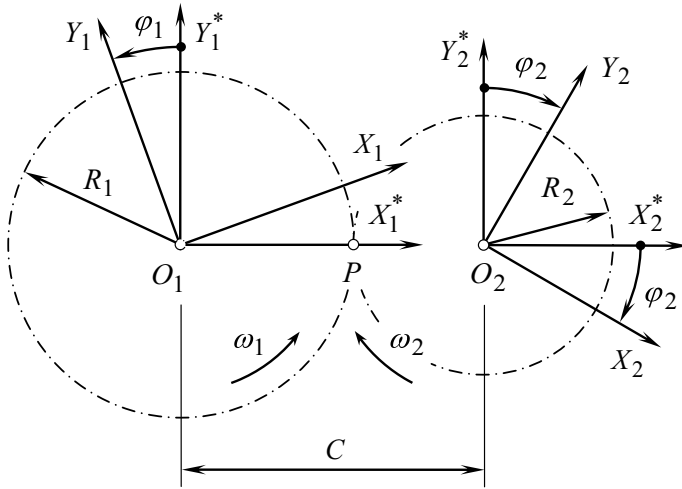


**Fig. B.10** On derivation of the operator of rolling,  $\mathbf{Rr}_u(\varphi_1, Z_1)$ , of two coordinate systems

As an example, consider two “Cartesian” coordinate systems  $X_1Y_1Z_1$  and  $X_2Y_2Z_2$  shown in Fig. B.10. The coordinate systems  $X_1Y_1Z_1$  and  $X_2Y_2Z_2$  are rotated about their axes  $Z_1$  and  $Z_2$ . The axes of the rotations are parallel to each other ( $Z_1 \parallel Z_2$ ). The rotations  $\omega_1$  and  $\omega_2$  of the coordinate systems can be interpreted so that a circle of a certain radius  $R_1$  that is associated with the coordinate system  $X_1Y_1Z_1$ , is rolling with no sliding over a circle of the corresponding radius  $R_2$  that is associated with the coordinate system  $X_2Y_2Z_2$ . When the center distance  $C$  is known, then radii,  $R_1$  and  $R_2$ , of the circles (that is, of centrodes) can be expressed in terms of the center distance,  $C$ , and of the given rotations,  $\omega_1$  and  $\omega_2$ . For the calculations, the following formulae:

$$R_1 = C \cdot \frac{1}{1+u} \quad (\text{B.37})$$

$$R_2 = C \cdot \frac{u}{1+u} \quad (\text{B.38})$$

can be used. Here, the ratio  $\omega_1/\omega_2$  is denoted by  $u$ .

In the initial configuration, the  $X_1$ - and  $X_2$ -axes align to each other. The  $Y_1$ - and  $Y_2$ -axes are parallel to each other. As shown in Fig. B.10, the initial configuration of the coordinate systems  $X_1Y_1Z_1$  and  $X_2Y_2Z_2$  is labeled as  $X_1^*Y_1^*Z_1^*$  and  $X_2^*Y_2^*Z_2^*$ .

When the coordinate system  $X_1Y_1Z_1$  turns through a certain angle  $\varphi_1$ , then the coordinate system  $X_2Y_2Z_2$  turns through the corresponding angle  $\varphi_2$ . When the angle  $\varphi_1$  is known then the corresponding angle  $\varphi_2$  is equal to  $\varphi_2 = \varphi_1/u$ .

Transition from the coordinate system  $X_2Y_2Z_2$  to the coordinate system  $X_1Y_1Z_1$  can be analytically described by the operator of the resultant coordinate system

transformation  $\mathbf{Rs}(1 \mapsto 2)$ . In the case under consideration, the operator  $\mathbf{Rs}(1 \mapsto 2)$  can be expressed in terms of the operators of the elementary coordinate system transformations:

$$\mathbf{Rs}(1 \mapsto 2) = \mathbf{Rt}(\varphi_1, Z_1) \cdot \mathbf{Rt}(\varphi_1/u, Z_1) \cdot \mathbf{Tr}(-C, X_1) \quad (\text{B.39})$$

Other equivalent combinations of the operators of elementary coordinate system transformations can result in that same operator  $\mathbf{Rs}(1 \mapsto 2)$  of the resultant coordinate system transformation. The interested reader may wish to exercise on his or her own deriving the equivalent expressions for the operator  $\mathbf{Rs}(1 \mapsto 2)$ .

The operator of the resultant coordinate system transformations of the kind [see Eq. (B.39)] are referred to as the “*operators of rolling motion over a cylinder*.”

When rotations are performed around the  $Z_1$ - and the  $Z_2$ -axis, the operator of rolling motion over a cylinder is designated as  $\mathbf{Rr}_u(\varphi_1, Z_1)$ . In this particular case, the equality  $\mathbf{Rr}_u(\varphi_1, Z_1) = \mathbf{Rs}(1 \mapsto 2)$  [see Eq. (B.39)] is valid. Based on this equality, the operator of rolling  $\mathbf{Rr}_u(\varphi_1, Z_1)$  over a cylinder can be calculated from the equation:

$$\mathbf{Rr}_u(\varphi_1, Z_1) = \begin{bmatrix} \cos(\varphi_1 \cdot \frac{u+1}{u}) & \sin(\varphi_1 \cdot \frac{u+1}{u}) & 0 & -C \\ -\sin(\varphi_1 \cdot \frac{u+1}{u}) & \cos(\varphi_1 \cdot \frac{u+1}{u}) & 0 & 0 \\ 0 & 0 & 1 & 0 \\ 0 & 0 & 0 & 1 \end{bmatrix} \quad (\text{B.40})$$

is derived.

For the inverse transformation, the inverse operator of rolling of two coordinate systems  $\mathbf{Rr}_u(\varphi_2, Z_2)$  can be used. It is equal to  $\mathbf{Rr}_u(\varphi_2, Z_2) = \mathbf{Rr}_u^{-1}(\varphi_1, Z_1)$ . In terms of the operators of the elementary coordinate system transformations, the operator  $\mathbf{Rr}_u(\varphi_2, Z_2)$  can be expressed as follows:

$$\mathbf{Rr}_u(\varphi_2, Z_2) = \mathbf{Rt}(\varphi_1/u, Z_2) \cdot \mathbf{Rt}(\varphi_1, Z_2) \cdot \mathbf{Tr}(C, X_1) \quad (\text{B.41})$$

Other equivalent combinations of the operators of elementary coordinate system transformations can result in that same operator  $\mathbf{Rr}_u(\varphi_2, Z_2)$  of the resultant coordinate system transformation. The interested reader may wish to exercise on his or her own deriving the equivalent expressions for the operator  $\mathbf{Rr}_u(\varphi_2, Z_2)$ .

For the calculation of the operator of rolling of two coordinate systems  $\mathbf{Rr}_u(\varphi_2, Z_2)$ , the equation:

$$\mathbf{Rr}_u(\varphi_2, Z_2) = \begin{bmatrix} \cos(\varphi_1 \cdot \frac{u+1}{u}) & -\sin(\varphi_1 \cdot \frac{u+1}{u}) & 0 & C \\ \sin(\varphi_1 \cdot \frac{u+1}{u}) & \cos(\varphi_1 \cdot \frac{u+1}{u}) & 0 & 0 \\ 0 & 0 & 1 & 0 \\ 0 & 0 & 0 & 1 \end{bmatrix} \quad (\text{B.42})$$

can be used.



Similar to that the expression [see Eq. (B.40)] is derived for the calculation of the operator of rolling  $\mathbf{Rr}_u(\varphi_1, Z_1)$  around the  $Z_1$ - and  $Z_2$ -axis, corresponding formulae can be derived for the calculation of the operators of rolling  $\mathbf{Rr}_u(\varphi_1, X_1)$  and  $\mathbf{Rr}_u(\varphi_1, Y_1)$  about parallel axes  $X_1$  and  $X_2$ , as well as about parallel axes  $Y_1$  and  $Y_2$ .

Use of the operators of rolling about two axes  $\mathbf{Rr}_u(\varphi_1, X_1)$ ,  $\mathbf{Rr}_u(\varphi_1, Y_1)$  and  $\mathbf{Rr}_u(\varphi_1, Z_1)$  substantially simplifies analytical description of the coordinate system transformations.

## B.2.4 Coupled Linear Transformation

It is right point to notice here that a translation,  $\mathbf{Tr}(a_x, X)$ , along the  $X$ - axis of a “*Cartesian*” reference system,  $XYZ$ , and a rotation,  $\mathbf{Rt}(\varphi_x, X)$ , about the axis  $X$  of that same coordinate system,  $XYZ$ , obey the commutative law, that is, these two coordinate system transformations can be performed in different order equally. It makes no difference whether the translation,  $\mathbf{Tr}(a_x, X)$ , is initially performed, which is followed by the rotation,  $\mathbf{Rt}(\varphi_x, X)$ , or the rotation,  $\mathbf{Rt}(\varphi_x, X)$ , is initially performed, which is followed by the translation,  $\mathbf{Tr}(a_x, X)$ . This is because of the dot products  $\mathbf{Rt}(\varphi_x, X) \cdot \mathbf{Tr}(a_x, X)$  and  $\mathbf{Tr}(a_x, X) \cdot \mathbf{Rt}(\varphi_x, X)$  are identical to one another:

$$\mathbf{Rt}(\varphi_x, X) \cdot \mathbf{Tr}(a_x, X) \equiv \mathbf{Tr}(a_x, X) \cdot \mathbf{Rt}(\varphi_x, X) \quad (\text{B.43})$$

This means that the translation from the coordinate system  $X_1Y_1Z_1$  to the intermediate coordinate system  $X^*Y^*Z^*$  followed by the rotation from the coordinate system  $X^*Y^*Z^*$  to the finale coordinate system  $X_2Y_2Z_2$  produces that same reference  $X_2Y_2Z_2$  as in a case when the rotation from the coordinate system  $X_1Y_1Z_1$  to the intermediate coordinate system  $X^*Y^*Z^*$  followed by the translation from the coordinate system  $X^*Y^*Z^*$  to the finale coordinate system  $X_2Y_2Z_2$ .

The validity of Eq. (B.43) is illustrated in Fig. B.11. The translation,  $\mathbf{Tr}(a_x, X)$ , that is followed by the rotation,  $\mathbf{Rt}(\varphi_x, X)$ , as shown in Fig. B.11a, is equivalent to the rotation,  $\mathbf{Rt}(\varphi_x, X)$ , that is followed by the translation,  $\mathbf{Tr}(a_x, X)$  as shown in Fig. B.11b.

Therefore, the two linear transformations,  $\mathbf{Tr}(a_x, X)$  and  $\mathbf{Rt}(\varphi_x, X)$ , can be coupled into a linear transformation:

$$\mathbf{Cp}_x(a_x, \varphi_x) = \mathbf{Rt}(\varphi_x, X) \cdot \mathbf{Tr}(a_x, X) \equiv \mathbf{Tr}(a_x, X) \cdot \mathbf{Rt}(\varphi_x, X) \quad (\text{B.44})$$

The operator of linear transformation,  $\mathbf{Cp}_x(a_x, \varphi_x)$ , can be expressed in matrix form (see Fig. B.12a):

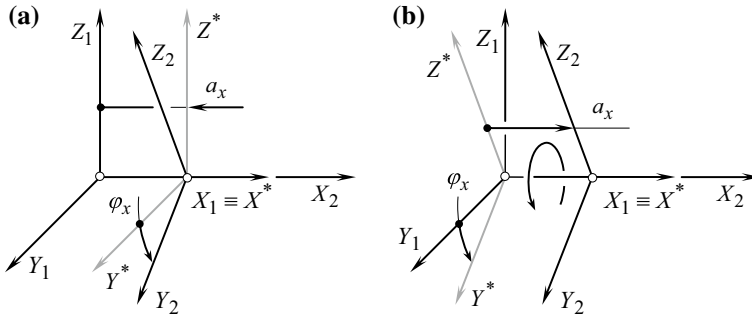


**Fig. B.11** On the equivalency of the linear transformations,  $\mathbf{Rt}(\varphi_x, X) \cdot \mathbf{Tr}(a_x, X)$  and  $\mathbf{Tr}(a_x, X) \cdot \mathbf{Rt}(\varphi_x, X)$ , in the operator,  $\mathbf{Cp}_x(a_x, \varphi_x)$ , of coupled linear transformation of a “Cartesian” reference system  $XYZ$

$$\mathbf{Cp}_x(a_x, \varphi_x) = \begin{bmatrix} 1 & 0 & 0 & a_x \\ 0 & \cos \varphi_x & \sin \varphi_x & 0 \\ 0 & -\sin \varphi_x & \cos \varphi_x & 0 \\ 0 & 0 & 0 & 1 \end{bmatrix} \quad (\text{B.45})$$

This expression is composed based on Eq. (B.4) for the linear transformation  $\mathbf{Tr}(a_x, X)$ , and on Eq. (B.10) that describes the linear transformation  $\mathbf{Rt}(\varphi_x, X)$ .

Two reduced cases of operator of the linear transformation,  $\mathbf{Cp}_x(a_x, \varphi_x)$ , are distinguished.

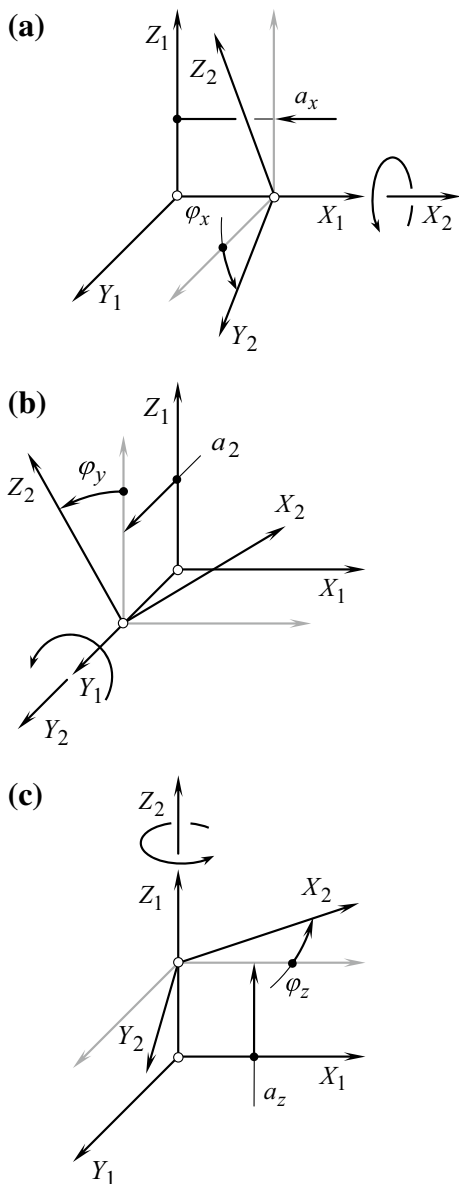
First, it could happen that in a particular case the component,  $a_x$ , of the translation is zero, that is  $a_x = 0$ . Under such a scenario, the operator of linear transformation,  $\mathbf{Cp}_x(a_x, \varphi_x)$ , reduces to the operator of rotation,  $\mathbf{Rt}(\varphi_x, X)$ , and the equality  $\mathbf{Cp}_x(a_x, \varphi_x) = \mathbf{Rt}(\varphi_x, X)$  is observed in the case under consideration.

Second, it could happen that in a particular case the component,  $\varphi_x$ , of the rotation is zero, that is  $\varphi_x = 0^\circ$ . Under such a scenario the operator of linear transformation,  $\mathbf{Cp}_x(a_x, \varphi_x)$ , reduces to the operator of translation,  $\mathbf{Tr}(a_x, X)$ , and the equality  $\mathbf{Cp}_x(a_x, \varphi_x) = \mathbf{Tr}(a_x, X)$  is observed in the case under consideration.

The said is valid with respect to the translations and the rotations along and about the axes  $Y$  and  $Z$  of a “Cartesian” reference system  $XYZ$ . The corresponding coupled operators,  $\mathbf{Cp}_y(a_y, \varphi_y)$  and  $\mathbf{Cp}_z(a_z, \varphi_z)$ , for linear transformations of these kinds can also be composed (see Fig. B.12b, c):

$$\mathbf{Cp}_y(a_y, \varphi_y) = \begin{bmatrix} \cos \varphi_y & 0 & \sin \varphi_y & 0 \\ 0 & 1 & 0 & a_y \\ -\sin \varphi_y & 0 & \cos \varphi_y & 0 \\ 0 & 0 & 0 & 1 \end{bmatrix} \quad (\text{B.46})$$

**Fig. B.12** Analytical description of the operators  $\mathbf{Cp}_x(a_x, \varphi_x)$ ,  $\mathbf{Cp}_y(a_y, \varphi_y)$ , and  $\mathbf{Cp}_z(a_z, \varphi_z)$ , of linear transformation of a “Cartesian” reference system  $XYZ$



$$\mathbf{Cp}_z(a_z, \varphi_z) = \begin{bmatrix} \cos \varphi_z & \sin \varphi_z & 0 & 0 \\ -\sin \varphi_z & \cos \varphi_z & 0 & 0 \\ 0 & 0 & 1 & a_z \\ 0 & 0 & 0 & 1 \end{bmatrix} \quad (\text{B.47})$$

In the operators of linear transformations,  $\mathbf{Cp}_x(a_x, \varphi_x)$ ,  $\mathbf{Cp}_y(a_y, \varphi_y)$ , and  $\mathbf{Cp}_z(a_z, \varphi_z)$ , values of the translations  $a_x$ ,  $a_y$ , and  $a_z$ , as well as values of the rotations  $\varphi_x$ ,  $\varphi_y$ , and  $\varphi_z$ , are finite values (and not continuous). The linear and angular displacements do not correlate to one another in time, thus, they are not screws. They are just a kind of couples of a translation along, and a rotation about a coordinate axis of a “*Cartesian*” reference system.

Introduction of the operators of linear transformation,  $\mathbf{Cp}_x(a_x, \varphi_x)$ ,  $\mathbf{Cp}_y(a_y, \varphi_y)$ , and  $\mathbf{Cp}_z(a_z, \varphi_z)$ , makes the linear transformations easier as all the operators of the linear transformations become uniform.

The operators of linear transformation  $\mathbf{Cp}_x(a_x, \varphi_x)$ ,  $\mathbf{Cp}_y(a_y, \varphi_y)$ , and  $\mathbf{Cp}_z(a_z, \varphi_z)$ , do not obey the commutative law. This is because rotations are not vectors in nature. Therefore, special care should be undertaken when treating rotations as vectors—when implementing coupled operators of linear transformations in particular.

The operators of coupled linear transformations  $\mathbf{Cp}_x(a_x, \varphi_x)$ ,  $\mathbf{Cp}_y(a_y, \varphi_y)$ , and  $\mathbf{Cp}_z(a_z, \varphi_z)$ , [see Eqs. (B.45)–(B.47)] can be used for the purpose of analytical description of a resultant coordinate system transformation. Under such the scenario, the operator,  $\mathbf{Rs}(1 \mapsto t)$ , of a resultant coordinate system transformation can be expressed in terms of all the operators  $\mathbf{Cp}_x(a_x, \varphi_x)$ ,  $\mathbf{Cp}_y(a_y, \varphi_y)$ , and  $\mathbf{Cp}_z(a_z, \varphi_z)$  by the following expression:

$$\mathbf{Rs}(1 \mapsto t) = \prod_{i=1, j=x,y,z}^{t-1} \mathbf{Cp}_j^i(a_j^i, \varphi_j^i) \quad (\text{B.48})$$

In Eq. (B.48), only operators of coupled linear transformations are used.

### B.2.5 An Example of Non-orthogonal Linear Transformation

Consider a non-orthogonal reference system  $X_1Y_1Z_1$  having certain angle  $\omega_1$  between the axes  $X_1$  and  $Y_1$ . Axis  $Z_1$  is perpendicular to the coordinate plane  $X_1Y_1$ . Another reference system  $X_2Y_2Z_2$  is identical to the first coordinate system  $X_1Y_1Z_1$ , and is turned about  $Z_1$ -axis through a certain angle  $\varphi$ . Transition from the reference system  $X_1Y_1Z_1$  to the reference system  $X_2Y_2Z_2$  can be analytically described by the operator of linear transformation:

$$\mathbf{Rt}_\omega(1 \rightarrow 2) = \begin{bmatrix} \frac{\sin(\omega_1 + \varphi)}{\sin \omega_1} & \frac{\sin \varphi}{\sin \omega_1} & 0 & 0 \\ -\frac{\sin \varphi}{\sin \omega_1} & \frac{\sin(\omega_1 - \varphi)}{\sin \omega_1} & 0 & 0 \\ 0 & 0 & 1 & 0 \\ 0 & 0 & 0 & 1 \end{bmatrix} \quad (\text{B.49})$$

In order to distinguish the operator of rotation in the orthogonal linear transformation  $\mathbf{Rt}(1 \rightarrow 2)$  from the similar operator of rotation in a non-orthogonal linear transformation  $\mathbf{Rt}_\omega(1 \rightarrow 2)$ , the subscript “ $\omega$ ” is assigned to the last.

When  $\omega = 90^\circ$ , Eq. (B.49) casts into Eq. (B.12).

### B.2.6 Conversion of a Coordinate System Hand

Application of matrix method of coordinate system transformation presumes that both of the reference systems “ $i$ ” and “ $(i \pm 1)$ ” are of the same hand. This means that it assumed from the very beginning that both of them are either right-hand-, or left-hand-oriented “*Cartesian*” coordinate systems. In the event the coordinate systems  $i$  and  $(i \pm 1)$  are of opposite hand, say one of them is the right-hand-oriented coordinate system while another one is left-hand-oriented coordinate system, then one of the coordinate systems must be converted into the oppositely oriented “*Cartesian*” coordinate system.

For the conversion of a left-hand-oriented “*Cartesian*” coordinate system into a right-hand-oriented coordinate system or vice versa, the operators of reflection are commonly used.

In order to change the direction of  $X_i$  axis of the initial coordinate system  $i$  to the opposite direction (in this case in the new coordinate system  $(i \pm 1)$  the equalities  $X_{i\pm 1} = -X_i$ ,  $Y_{i\pm 1} \equiv Y_i$  and  $Z_{i\pm 1} \equiv Z_i$  are observed) the operator of reflection  $\mathbf{Rf}_x(Y_i Z_i)$  can be applied. The operator of reflection yields representation in matrix form:

$$\mathbf{Rf}_x(Y_i Z_i) = \begin{bmatrix} -1 & 0 & 0 & 0 \\ 0 & 1 & 0 & 0 \\ 0 & 0 & 1 & 0 \\ 0 & 0 & 0 & 1 \end{bmatrix} \quad (\text{B.50})$$

Similarly, implementation of the operators of reflections  $\mathbf{Rf}_y(X_i Z_i)$  and  $\mathbf{Rf}_z(X_i Y_i)$  changes the directions of  $Y_i$  axis and  $Z_i$  axes onto opposite directions. The operators of reflections  $\mathbf{Rf}_y(X_i Z_i)$  and  $\mathbf{Rf}_z(X_i Y_i)$  can be expressed analytically in the form:

$$\mathbf{Rf}_y(X_i Z_i) = \begin{bmatrix} 1 & 0 & 0 & 0 \\ 0 & -1 & 0 & 0 \\ 0 & 0 & 1 & 0 \\ 0 & 0 & 0 & 1 \end{bmatrix} \quad (\text{B.51})$$

$$\mathbf{Rf}_z(X_i Y_i) = \begin{bmatrix} 1 & 0 & 0 & 0 \\ 0 & 1 & 0 & 0 \\ 0 & 0 & -1 & 0 \\ 0 & 0 & 0 & 1 \end{bmatrix} \quad (\text{B.52})$$

A linear transformation that reverses direction of the coordinate axis is an “*opposite transformation*”. Transformation of reflection is an example of “*orientation-reversing transformation*”.

## B.3 Useful Equations

The sequence of the successive rotations can vary depending on the intention of the researcher. Several special types of successive rotations are known, including “*Eulerian transformation*,” “*Cardanian transformation*,” two kinds of “*Euler-Krylov transformations*,” and so forth. The sequence of the successive rotations can be chosen from a total of 12 different combinations. Even though the “*Cardanian transformation*” is different from the “*Eulerian transformation*” in terms of the combination of the rotations, they both use a similar approach to calculate the orientation angles.

### B.3.1 RPY-Transformation

A series of rotations can be performed in the order “*roll matrix, (R)*,” by “*pitch matrix (P)*,” and finally by “*yaw matrix, (Y)*.” The linear transformation of this kind is commonly referred to as “*RPY-transformation*.” The resultant transformation of this kind can be represented by the homogenous coordinate transformation matrix:

$$\mathbf{RPY}(\varphi_x, \varphi_y, \varphi_z) = \begin{bmatrix} \cos \varphi_y \cos \varphi_z + \sin \varphi_x \sin \varphi_y \sin \varphi_z & \cos \varphi_y \sin \varphi_z - \sin \varphi_x \sin \varphi_y \cos \varphi_z & \cos \varphi_x \sin \varphi_y & 0 \\ -\cos \varphi_x \sin \varphi_z & \cos \varphi_x \cos \varphi_z & \sin \varphi_x & 0 \\ \sin \varphi_x \cos \varphi_y \sin \varphi_z - \sin \varphi_y \cos \varphi_z & -\sin \varphi_x \cos \varphi_y \cos \varphi_z - \cos \varphi_y \sin \varphi_z & \cos \varphi_x \cos \varphi_y & 0 \\ 0 & 0 & 0 & 1 \end{bmatrix} \quad (\text{B.53})$$

The “*RPY-transformation*” can be used for solving problems in the field of part surface generation.

### B.3.2 Operator of Rotation About an Axis in Space

A spatial rotation operator for the rotational transformation of a point about a unit axis  $\mathbf{a}_0(\cos \alpha, \cos \beta, \cos \gamma)$  passing through the origin of the coordinate system can

be described as follows, with  $\mathbf{a}_0 = \mathbf{A}_0/|\mathbf{A}_0|$  designating the unit vector along the axis of rotation  $\mathbf{A}_0$ .

Suppose the angle of rotation of the point about  $\mathbf{a}_0$  is  $\theta$ , the “rotation operator” is expressed by:

$$\mathbf{Rt}(\theta, \mathbf{a}_0) = \begin{bmatrix} (1 - \cos \theta) \cos^2 \alpha + \cos \theta & (1 - \cos \theta) \cos \alpha \cos \beta - \sin \theta \cos \gamma & (1 - \cos \theta) \cos \alpha \cos \gamma + \sin \theta \cos \beta & 0 \\ (1 - \cos \theta) \cos \alpha \cos \beta + \sin \theta \cos \gamma & (1 - \cos \theta) \cos^2 \beta + \cos \theta & (1 - \cos \theta) \cos \beta \cos \gamma - \sin \theta \cos \alpha & 0 \\ (1 - \cos \theta) \cos \alpha \cos \gamma - \sin \theta \cos \beta & (1 - \cos \theta) \cos \beta \cos \gamma + \sin \theta \cos \alpha & (1 - \cos \theta) \cos^2 \gamma + \cos \theta & 0 \\ 0 & 0 & 0 & 1 \end{bmatrix} \quad (\text{B.54})$$

Solution to a problem in the field of part surface generation can be significantly simplified by implementation of the rotational operator  $\mathbf{Rt}(\theta, \mathbf{a}_0)$  [see Eq. (B.54)].

### B.3.3 Combined Linear Transformation

Suppose a point,  $p$ , on a rigid body rotates with an angular displacement,  $\theta$ , about an axis along a unit vector,  $\mathbf{a}_0$ , passing through the origin of the coordinate system at first, and then followed by a translation at a distance,  $B$ , in the direction of a unit vector,  $\mathbf{b}$ . The linear transformation of this kind can be analytically described by the homogenous matrix

$$\mathbf{Rt}(\theta_{\mathbf{a}_0}, B_{\mathbf{b}}) = \begin{bmatrix} (1 - \cos \theta) \cos^2 \alpha + \cos \theta & (1 - \cos \theta) \cos \alpha \cos \beta - \sin \theta \cos \gamma & (1 - \cos \theta) \cos \alpha \cos \gamma + \sin \theta \cos \beta & B \cos \alpha \\ (1 - \cos \theta) \cos \alpha \cos \beta + \sin \theta \cos \gamma & (1 - \cos \theta) \cos^2 \beta + \cos \theta & (1 - \cos \theta) \cos \beta \cos \gamma - \sin \theta \cos \alpha & B \cos \beta \\ (1 - \cos \theta) \cos \alpha \cos \gamma - \sin \theta \cos \beta & (1 - \cos \theta) \cos \beta \cos \gamma + \sin \theta \cos \alpha & (1 - \cos \theta) \cos^2 \gamma + \cos \theta & B \cos \gamma \\ 0 & 0 & 0 & 1 \end{bmatrix} \quad (\text{B.55})$$

More operators of particular linear transformations can be found out in the literature.

## B.4 Chains of Consequent Linear Transformations and a Closed Loop of Consequent Coordinate Systems Transformations

Consequent coordinate system transformations form chains (circuits) of linear transformations. The elementary chain of coordinate system transformation is composed of two consequent transformations. Chains of linear transformations play an important role in the theory of part surface generation.

Two different kinds of chains of consequent coordinate system transformations are distinguished.

**First**, transition from the coordinate system  $X_gY_gZ_g$  associated with the gear tooth flank,  $\mathcal{G}$ , to the local “*Cartesian*” coordinate system  $x_gy_gz_g$  having the origin at a point,  $K$ , of contact of the gear tooth flank,  $\mathcal{G}$ , and of the pinion tooth flank,  $\mathcal{P}$ . This linear transformation is also made up of numerous operators of intermediate coordinate system transformations ( $X_{in}Y_{in}Z_{in}$ ). It forms a chain of direct consequent coordinate system transformations illustrated in Fig. B.13a.

The local coordinate system,  $x_gy_gz_g$ , is associated with the gear tooth flank,  $\mathcal{G}$ . The operator  $\mathbf{Rs}(\mathcal{G} \rightarrow K_g)$  of the resultant coordinate system transformation for a direct chain of the linear transformations can be composed using for this purpose a certain number of the operators of translations [see Eqs. (B.4)–(B.6)], and a corresponding number of the operators of rotations [see Eqs. (B.10)–(B.12)].

**Second**, transition from the coordinate system,  $X_gY_gZ_g$ , to the local “*Cartesian*” coordinate system,  $x_py_pz_p$ , with the origin at a point  $K$  of contact of the tooth flanks,  $\mathcal{G}$  and  $\mathcal{P}$ . The local coordinate system,  $x_py_pz_p$ , is associated to pinion tooth flank,  $\mathcal{P}$ . This linear transformation is also made up of numerous intermediate coordinate system transformations ( $X_jY_jZ_j$ ), for example, transitions from the coordinate system  $X_hY_hZ_h$  associated with gear housing, to numerous intermediate coordinate system  $X_iY_iZ_i$ . The linear transformation of this kind forms a chain of inverse consequent coordinate system transformations shown in Fig. B.13b. The operator  $\mathbf{Rs}(\mathcal{G} \rightarrow K_p)$  of the resultant coordinate system transformations for the inverse chain of transformations can be composed using for this purpose a certain number of the operators of translations [see Eqs. (B.4)–(B.6)], and a corresponding number of the operators of rotations [see Eq. (B.10)–(B.12)].

Chains of the direct and of the reverse consequent coordinate system transformations together with the operator of transition from the local coordinate system,  $x_py_pz_p$ , to the local coordinate system,  $x_gy_gz_g$ , form a closed loop (a closed circuit) of the consequent coordinate system transformations depicted in Fig. B.13c.

If a closed loop of the consequent coordinate system transformations is complete, implementation of a certain number of the operators of translations [see Eqs. (B.4)–(B.6)], and a corresponding number of the operators of rotations [see Eq. (B.10)–(B.12)] returns a result that is identical to the input data. This means that an analytical description of a meshing process specified in the original



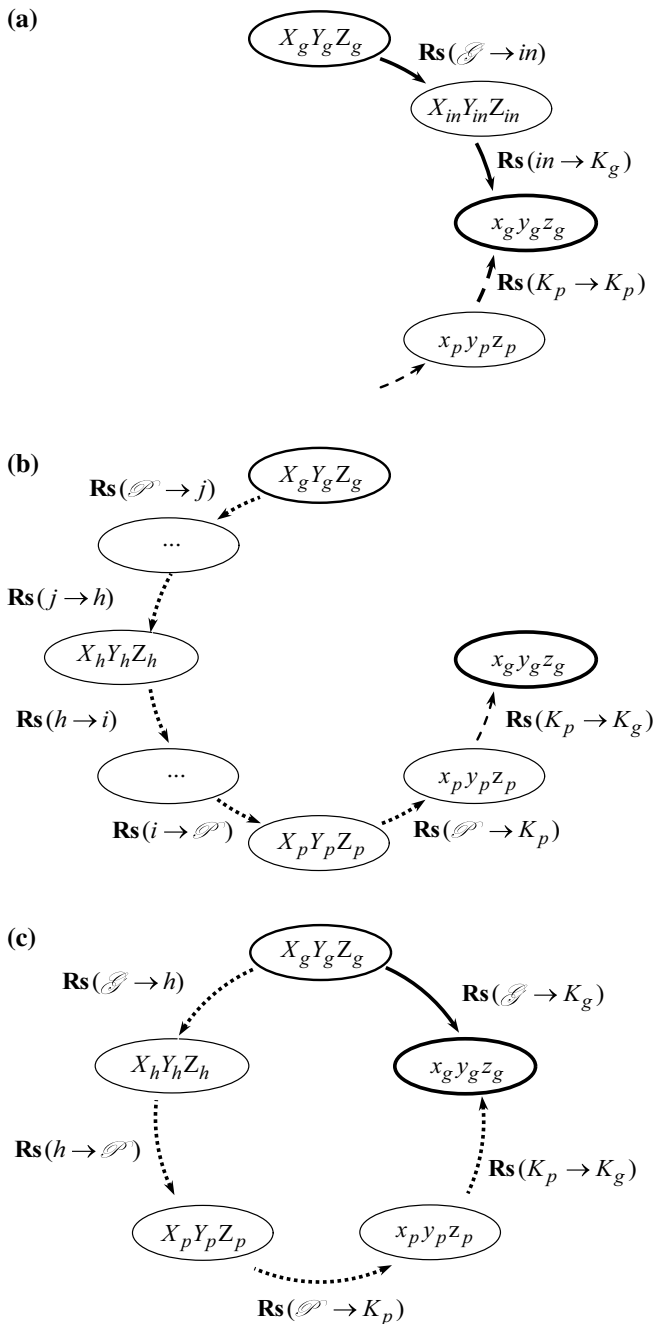


**Fig. B.13** An example of direct chain (a), of reverse chain (b), and a closed loop (c) of consequent coordinate system transformations

coordinate system remains the same after implementation of the operator of the resultant coordinate system transformations. This condition is the necessary and sufficient condition for existence of a closed loop of consequent coordinate system transformations.

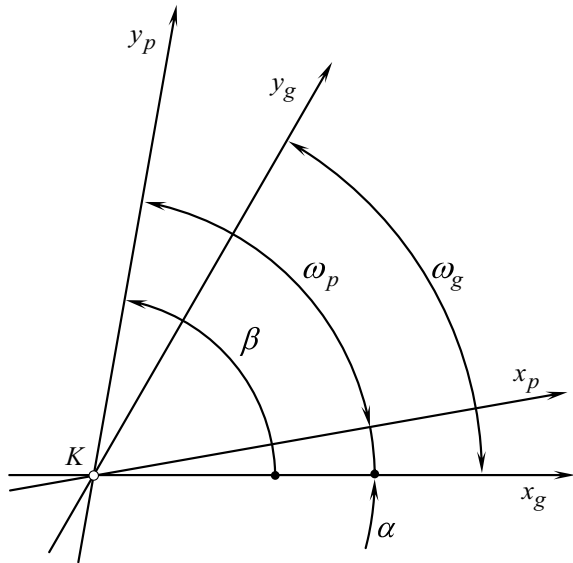
Implementation of the chains and the closed loops of consequent coordinate system transformations make it possible consideration of the meshing process of the teeth flanks,  $\mathcal{G}$  and  $\mathcal{P}$ , in any and all of reference systems that make up the loop. Therefore, for consideration of a particular problem of part surface generation, the most convenient reference system can be chosen.

In order to complete the construction of a closed loop of a consequent coordinate system transformations, an operator of transformation from the local coordinate system,  $x_p y_p z_p$ , to the local coordinate system,  $x_g y_g z_g$ , must be composed. Usually, the local reference systems,  $x_g y_g z_g$  and  $x_p y_p z_p$ , are the kind of semi-orthogonal coordinate systems. This means that the axis,  $z_p$ , is always orthogonal to the coordinate plane,  $x_g y_g$ , while the axes,  $x_g$  and  $y_g$ , can be either orthogonal or not orthogonal to each other. The same is valid with respect to the local coordinate system,  $x_p y_p z_p$ .

Two possible ways for performing the required transformation of the local reference systems,  $x_g y_g z_g$  and  $x_p y_p z_p$ , are considered below.

Following the first way, the operator  $\mathbf{Rt}_\omega(p \rightarrow g)$  of the linear transformation of semi-orthogonal coordinate systems (see Fig. B.14) must be composed. The operator  $\mathbf{Rt}_\omega(p \rightarrow g)$  can be represented in the form of the homogenous matrix:

**Fig. B.14** Local coordinate systems,  $x_g y_g z_g$  and  $x_p y_p z_p$ , with the origin at contact point,  $K$



$$\mathbf{Rt}_\omega(p \rightarrow g) = \begin{bmatrix} \frac{\sin(\omega_p + \alpha)}{\sin \omega_p} & -\frac{\sin(\omega_g - \omega_p - \alpha)}{\sin \omega_p} & 0 & 0 \\ -\frac{\sin \alpha}{\sin \omega_p} & \frac{\sin(\omega_g - \alpha)}{\sin \omega_p} & 0 & 0 \\ 0 & 0 & -1 & 0 \\ 0 & 0 & 0 & 1 \end{bmatrix} \quad (\text{B.56})$$

Here is designated:

$\omega_g$ —the angle that make  $U_g$  and  $V_g$  coordinate lines on the gear tooth flank,  $\mathcal{G}$   
 $\omega_p$ —the angle that make  $U_p$  and  $V_p$  coordinate lines on the pinion tooth flank,  $\mathcal{P}$   
 $\alpha$ —the angle that make the axes,  $x_g$  and  $x_p$ , of the local coordinate systems  $x_g y_g z_g$  and  $x_p y_p z_p$ .

The auxiliary angle  $\beta$  in Fig. B.14 is equal to  $\beta = \omega_T + \alpha$ .

The inverse coordinate system transformation, that is, the transformation from the local coordinate system,  $x_g y_g z_g$ , to the local coordinate system,  $x_p y_p z_p$ , can be analytically described by the operator  $\mathbf{Rt}_\omega(g \rightarrow p)$  of the inverse coordinate system transformation. The operator  $\mathbf{Rt}_\omega(g \rightarrow p)$  can be represented in the form of the homogenous matrix:

$$\mathbf{Rt}_\omega(g \rightarrow p) = \begin{bmatrix} \frac{\sin(\omega_g - \alpha)}{\sin \omega_g} & \frac{\sin(\omega_g - \omega_p - \alpha)}{\sin \omega_g} & 0 & 0 \\ \frac{\sin \alpha}{\sin \omega_g} & \frac{\sin(\omega_p + \alpha)}{\sin \omega_g} & 0 & 0 \\ 0 & 0 & -1 & 0 \\ 0 & 0 & 0 & 1 \end{bmatrix} \quad (\text{B.57})$$

Following the second way of transformation of the local coordinate systems, the auxiliary orthogonal local coordinate system must be constructed.

Let us consider an approach, according to which a closed loop (a closed circuit) of the consequent coordinate system transformations can be composed.

In order to construct an orthogonal normalized basis of the coordinate system  $x_g y_g z_g$ , an intermediate coordinate system  $x_1 y_1 z_1$  is used. Axis  $x_1$  of the coordinate system  $x_1 y_1 z_1$  is pointed out along the unit vector  $\mathbf{u}_g$  that is tangent to the  $U_g$ -coordinate curve (see Fig. B.15). Axis  $y_1$  is directed along vector  $\mathbf{v}_g$  that is tangent to the  $V_g$ -coordinate line on the gear tooth flank,  $\mathcal{G}$ . The axis,  $z_1$ , aligns with unit normal vector,  $\mathbf{n}_g$ , and is pointed outward the gear tooth body.

For a gear tooth flank,  $\mathcal{G}$ , having orthogonal parameterization (for which  $F_g = 0$ , and therefore  $\omega_g = \pi/2$ ), analytical description of coordinate system transformations is significantly simpler. Further simplification of the coordinate system transformation is possible when the coordinate  $U_g$ - and  $V_g$ -lines are congruent to the lines of curvature on the part surface  $\mathcal{G}$ . Under such a scenario, the local coordinate system is represented by “*Darboux frame*”.

In order to construct “*Darboux frame*,” principal directions on the gear tooth flank,  $\mathcal{G}$ , must be calculated. Determination of the unit tangent vectors,  $\mathbf{t}_{1,g}$  and  $\mathbf{t}_{2,g}$ , of the principal directions on the gear tooth flank,  $\mathcal{G}$ , is considered in Chap. 1.

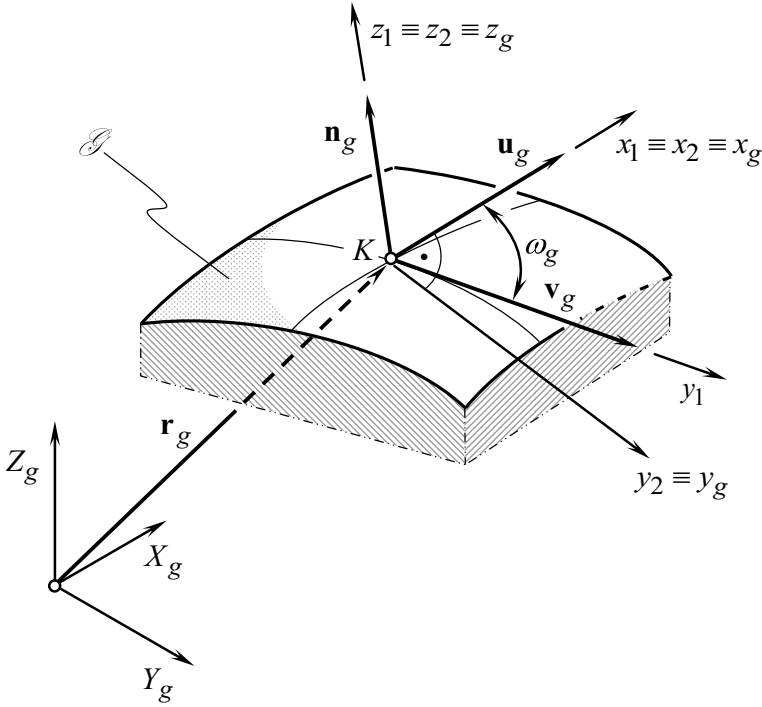


**Fig. B.15** Local coordinate system,  $x_g, y_g, z_g$ , associated with the gear tooth flank,  $\mathcal{G}$

In the common tangent plane, orientation of the unit vector,  $\mathbf{t}_{1.g}$ , of the first principal direction on the gear tooth flank,  $\mathcal{G}$ , can be uniquely specified by the included angle,  $\xi_{1.g}$ , that the unit vector,  $\mathbf{t}_{1.g}$ , forms with the  $U_g$ -coordinate curve. This angle depends on both, on the gear tooth flank,  $\mathcal{G}$ , geometry, and on the gear tooth flank,  $\mathcal{G}$ , parameterization. Depicted in Fig. B.16 is the relationship between the tangent vectors  $\mathbf{U}_g$  and  $\mathbf{V}_g$ , and the included angle  $\xi_{1.g}$ . From the law of sine's,

$$\frac{\sqrt{G_g}}{\sin \xi_{1.g}} = \frac{\sqrt{E_g}}{\sin[\pi - \xi_{1.g} - (\pi - \omega_g)]} = \frac{\sqrt{F_g}}{\sin(\omega_g - \xi_{1.g})} \quad (\text{B.58})$$

Here,  $\omega_g = \cos^{-1}(F_g/\sqrt{E_g G_g})$ .

Solving the expression above for the included angle,  $\xi_{1.g}$ , results in:

$$\xi_{1.g} = \tan^{-1} \frac{\sqrt{E_g G_g - F_g^2}}{E_g + F_g} \quad (\text{B.59})$$

Another possible way of constructing of orthogonal local basis of the local “Cartesian” coordinate system,  $x_P, y_P, z_P$ , is based on the following consideration.

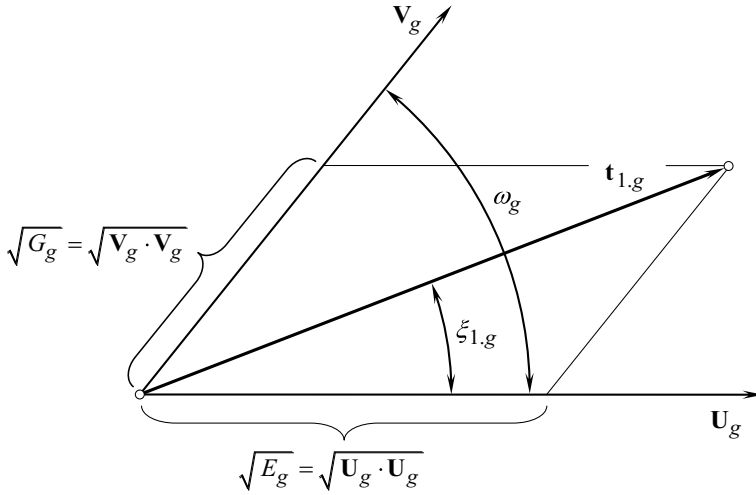


**Fig. B.16** Differential relationships between the tangent vectors,  $U_g$  and  $V_g$ , the fundamental magnitudes of the first order, the included the angle,  $\xi_{1,g}$ , and the direction of the unit tangent vector,  $t_{1,g}$

Consider an arbitrary non-orthogonal and not normalized basis,  $\mathbf{x}_1\mathbf{x}_2\mathbf{x}_3$  (see Fig. B.17a). Let us construct an orthogonal and normalized basis based on the initial given basis,  $\mathbf{x}_1\mathbf{x}_2\mathbf{x}_3$ .

Cross product of any two of three vectors,  $\mathbf{x}_1$ ,  $\mathbf{x}_2$ , and  $\mathbf{x}_3$ , for example, cross product of the vectors  $\mathbf{x}_1 \times \mathbf{x}_2$ , determines a new vector,  $\mathbf{x}_4$  (see Fig. B.17b). Evidently, the vector,  $\mathbf{x}_4$ , is orthogonal to the coordinate plane,  $\mathbf{x}_1\mathbf{x}_2$ . Then, use the calculated vector,  $\mathbf{x}_4$ , and one of two original vectors,  $\mathbf{x}_1$  or  $\mathbf{x}_2$ , for instance, use the vector,  $\mathbf{x}_2$ . This yields calculation of a new vector,  $\mathbf{x}_5 = \mathbf{x}_4 \times \mathbf{x}_2$  (see Fig. B.17c). The calculated basis,  $\mathbf{x}_1\mathbf{x}_4\mathbf{x}_5$ , is orthogonal. In order to convert it into a normalized basis, each of the vectors,  $\mathbf{x}_1$ ,  $\mathbf{x}_4$ , and  $\mathbf{x}_5$  must be divided by its magnitude:

$$\mathbf{e}_1 = \frac{\mathbf{x}_1}{|\mathbf{x}_1|} \quad (\text{B.60})$$

$$\mathbf{e}_4 = \frac{\mathbf{x}_4}{|\mathbf{x}_4|} \quad (\text{B.61})$$

$$\mathbf{e}_5 = \frac{\mathbf{x}_5}{|\mathbf{x}_5|} \quad (\text{B.62})$$

The resultant basis  $\mathbf{e}_1\mathbf{e}_4\mathbf{e}_5$  (see Fig. B.17d) is always orthogonal, as well as it is always normalized.

In order to complete the analytical description of a closed loop of consequent coordinate system transformations, it is necessary to compose the operator

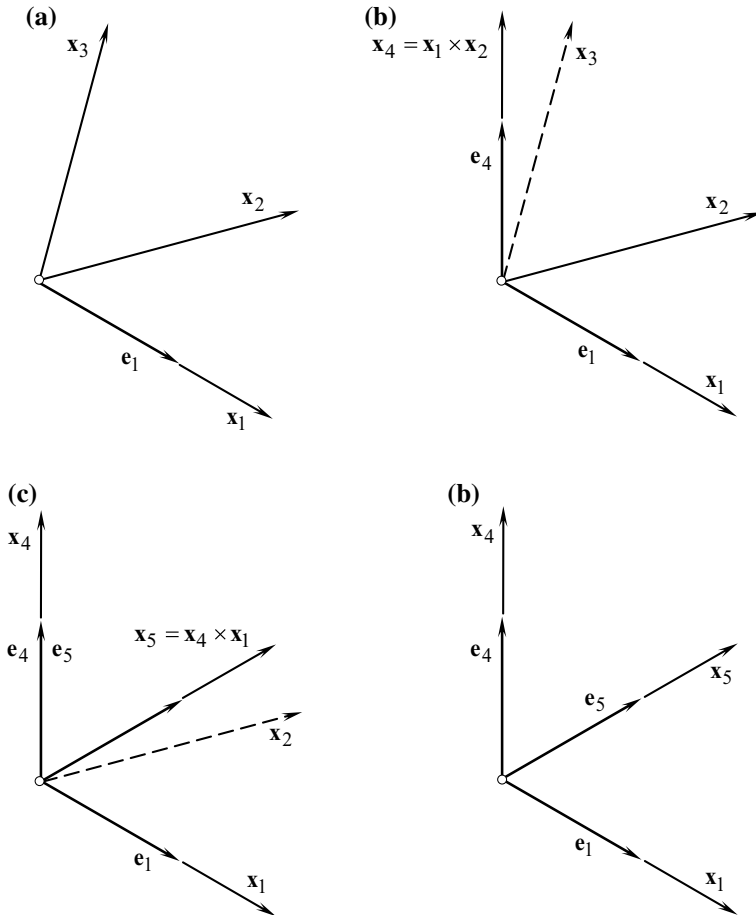


**Fig. B.17** A normalized and orthogonally parameterized basis,  $e_1 e_4 e_5$ , that is constructed from an arbitrary basis,  $x_1 x_2 x_3$

$\mathbf{Rs}(K_p \rightarrow K_g)$  of transformation from the local reference system,  $x_p y_p z_p$ , to the local reference system,  $x_g y_g z_g$  (see Fig. B.13c).

In the case under consideration, the axes,  $z_g$  and  $z_p$ , align with the common unit normal vector,  $\mathbf{n}_g$ . The axis,  $z_g$ , is pointed out from the bodily side to the void side of the gear tooth flank,  $\mathcal{G}$ . The axis,  $z_p$ , is pointed oppositely. Due to that, the following equality is observed:

$$\mathbf{Rs}(K_p \rightarrow K_g) = \mathbf{Rt}(\varphi_z, z_p) \quad (\text{B.63})$$

The inverse coordinate system transformation can be analytically described by the operator:

$$\mathbf{Rs}(K_g \rightarrow K_p) = \mathbf{Rs}^{-1}(K_p \rightarrow K_g) = \mathbf{Rt}(-\varphi_z, z_p) \quad (\text{B.64})$$

Implementation of the discussed results allows for:

- (a) representation of the gear tooth flank,  $\mathcal{G}$ , and the pinion tooth flank,  $\mathcal{P}$ , of the form cutting tool, as well as their relative motion in a common coordinate system, and
- (b) consideration meshing of the gear tooth flank,  $\mathcal{G}$ , in any desired coordinate systems that is a component of the chain and/or the closed loop of consequent coordinate system transformations.

Transition from one coordinate system to another coordinate system can be performed in both of two feasible directions, say in direct as well as in inverse directions.

## B.5 Impact of the Coordinate Systems Transformations on Fundamental Forms of the Surface

Every coordinate system transformation results in a corresponding change to equation of the gear tooth flank,  $\mathcal{G}$ , and/or pinion tooth flank,  $\mathcal{P}$ . Because of this, it is often necessary to re-calculate coefficients of the first  $\Phi_{1,g}$  and of the second  $\Phi_{2,g}$  fundamental forms of the gear tooth flank,  $\mathcal{G}$  (as many times as the coordinate system transformation is performed). This routing and time-consuming operation can be eliminated if the operators of coordinate system transformations are used directly to the fundamental forms  $\Phi_{1,g}$  and  $\Phi_{2,g}$ .

After been calculated in an initial reference system, the fundamental magnitudes  $E_g$ ,  $F_g$ , and  $G_g$  of the first,  $\Phi_{1,g}$ , and the fundamental magnitudes  $L_g$ ,  $M_g$ , and  $N_g$  of the second,  $\Phi_{2,g}$ , fundamental forms can be determined in any new coordinate system using for this purpose, the operators of translation, of rotation, and of resultant coordinate system transformation [106]. Transformation of such kind of the fundamental magnitudes,  $\Phi_{1,g}$  and  $\Phi_{2,g}$ , becomes possible due to implementation of a formula, that can be found out immediately below.

Let us consider a gear tooth flank,  $\mathcal{G}$ , that is given by equation  $\mathbf{r}_g = \mathbf{r}_g(U_g, V_g)$ , where  $(U_g, V_g) \in G$ .

For the analysis below, it is convenient to use the equation of the first fundamental form,  $\Phi_{1,g}$ , of the gear tooth flank,  $\mathcal{G}$ , represented in matrix form:

$$[\Phi_{1,g}] = [dU_g \quad dV_g \quad 0 \quad 0] \cdot \begin{bmatrix} E_g & F_g & 0 & 0 \\ F_g & G_g & 0 & 0 \\ 0 & 0 & 1 & 0 \\ 0 & 0 & 0 & 1 \end{bmatrix} \cdot \begin{bmatrix} dU_g \\ dV_g \\ 0 \\ 0 \end{bmatrix} \quad (\text{B.65})$$

Similarly, equation of the second fundamental form  $\Phi_{2,g}$  of the gear tooth flank,  $\mathcal{G}$ , can be given by:

$$[\Phi_{2,g}] = [dU_g \quad dV_g \quad 0 \quad 0] \cdot \begin{bmatrix} L_g & M_g & 0 & 0 \\ M_g & N_g & 0 & 0 \\ 0 & 0 & 1 & 0 \\ 0 & 0 & 0 & 1 \end{bmatrix} \cdot \begin{bmatrix} dU_g \\ dV_g \\ 0 \\ 0 \end{bmatrix} \quad (\text{B.66})$$

The coordinate system transformation that is performed by the operator of linear transformation  $\mathbf{Rs}(1 \rightarrow 2)$  transfers the equation  $\mathbf{r}_g = \mathbf{r}_g(U_g, V_g)$  of the gear tooth flank,  $\mathcal{G}$ , initially given in  $X_1Y_1Z_1$ , to the equation  $\mathbf{r}_g^* = \mathbf{r}_g^*(U_g^*, V_g^*)$  of that same gear tooth flank,  $\mathcal{G}$ , in a new coordinate system  $X_2Y_2Z_2$ . It is clear that  $\mathbf{r}_g \neq \mathbf{r}_g^*$ .

In the new coordinate system, the gear tooth flank,  $\mathcal{G}$ , is analytically described by the following expression:

$$\mathbf{r}_g^*(U_g^*, V_g^*) = \mathbf{Rs}(1 \rightarrow 2) \cdot \mathbf{r}_g(U_g, V_g) \quad (\text{B.67})$$

The operator of the resultant coordinate system transformation  $\mathbf{Rs}(1 \rightarrow 2)$  casts the column matrices of variables in Eqs. (B.65) and (B.66) to the form:

$$[dU_g^* \quad dV_g^* \quad 0 \quad 0]^T = \mathbf{Rs}(1 \rightarrow 2) \cdot [dU_g \quad dV_g \quad 0 \quad 0]^T. \quad (\text{B.68})$$

Substitution of Eq. (B.68) into Eq. (B.65) and Eq. (B.66) makes it possible the expressions for the fundamental forms,  $\Phi_{1,g}^*$  and  $\Phi_{2,g}^*$ , in the new coordinate system:

$$\begin{aligned} [\Phi_{1,g}^*] &= [\mathbf{Rs}(1 \rightarrow 2) \cdot [dU_g \quad dV_g \quad 0 \quad 0]^T]^T \cdot [\Phi_{1,g}] \cdot \\ &\quad \mathbf{Rs}(1 \rightarrow 2) \cdot [dU_g \quad dV_g \quad 0 \quad 0]^T \end{aligned} \quad (\text{B.69})$$

$$\begin{aligned} [\Phi_{2,g}^*] &= [\mathbf{Rs}(1 \rightarrow 2) \cdot [dU_g \quad dV_g \quad 0 \quad 0]^T]^T \cdot [\Phi_{2,g}] \cdot \\ &\quad \mathbf{Rs}(1 \rightarrow 2) \cdot [dU_g \quad dV_g \quad 0 \quad 0]^T \end{aligned} \quad (\text{B.70})$$

The following equation is valid for multiplication:

$$[\mathbf{Rs}(1 \rightarrow 2) \cdot [dU_g \quad dV_g \quad 0 \quad 0]^T]^T = \mathbf{Rs}^T(1 \rightarrow 2) \cdot [dU_g \quad dV_g \quad 0 \quad 0] \quad (\text{B.71})$$

Therefore,

$$\begin{aligned} [\Phi_{1,g}^*] &= [dU_g \quad dV_g \quad 0 \quad 0]^T \cdot \{ \mathbf{Rs}^T(1 \rightarrow 2) \cdot [\Phi_{1,g}] \cdot \mathbf{Rs}(1 \rightarrow 2) \} \\ &\quad \cdot [dU_g \quad dV_g \quad 0 \quad 0] \end{aligned} \quad (\text{B.72})$$



$$\begin{bmatrix} \Phi_{2,g}^* \end{bmatrix} = \begin{bmatrix} dU_g & dV_g & 0 & 0 \\ dU_g & dV_g & 0 & 0 \end{bmatrix}^T \cdot \{ \mathbf{Rs}^T(1 \rightarrow 2) \cdot [\Phi_{2,g}] \cdot \mathbf{Rs}(1 \rightarrow 2) \} \quad (\text{B.73})$$

It can be easily shown that the matrices  $[\Phi_{1,g}^*]$  and  $[\Phi_{2,g}^*]$  in Eq. (B.72) and Eq. (B.73) represent quadratic forms with respect to  $dU_g$  and  $dV_g$ .

The operator of transformation  $\mathbf{Rs}(1 \rightarrow 2)$  of the gear tooth flank,  $\mathcal{G}$ , having the first,  $\Phi_{1,g}$ , and the second,  $\Phi_{2,g}$ , fundamental forms from the initial coordinate system  $X_1Y_1Z_1$  to the new coordinate system,  $X_2Y_2Z_2$ , results in that in the new coordinate system the corresponding fundamental forms are expressed in the form:

$$[\Phi_{1,g}^*] = \mathbf{Rs}^T(1 \rightarrow 2) \cdot [\Phi_{1,g}] \cdot \mathbf{Rs}(1 \rightarrow 2) \quad (\text{B.74})$$

$$[\Phi_{2,g}^*] = \mathbf{Rs}^T(1 \rightarrow 2) \cdot [\Phi_{2,g}] \cdot \mathbf{Rs}(1 \rightarrow 2) \quad (\text{B.75})$$

Equations (B.74) and (B.75) reveal that after the coordinate system transformation is completed, the first  $\Phi_{1,g}^*$  and the second  $\Phi_{2,g}^*$  fundamental forms of the gear tooth flank,  $\mathcal{G}$ , in the coordinate system  $X_2Y_2Z_2$  are expressed in terms of the first,  $\Phi_{1,g}$ , and the second,  $\Phi_{2,g}$ , fundamental forms initially represented in the coordinate system  $X_1Y_1Z_1$ . In order to do that, the corresponding fundamental form (either the form,  $\Phi_{1,g}$ , or the form,  $\Phi_{2,g}$ ) must be pre-multiplied by  $\mathbf{Rs}(1 \rightarrow 2)$  and after that, it been post-multiplied by  $\mathbf{Rs}^T(1 \rightarrow 2)$ .

Implementation of Eqs. (B.74) and (B.75) significantly simplifies formulae transformations.

Equations similar to those above Eqs. (B.74) and (B.75) are valid with respect to pinion tooth flank,  $\mathcal{P}$ .

In case of use of the third,  $\Phi_{3,g}$ , and of the fourth,  $\Phi_{4,g}$ , fundamental forms, their coefficients can be expressed in terms of the fundamental magnitudes of the first and of the second order.

## Appendix C

### Change of Surface Parameters

When solving problems in the field of engineering geometry, it is often necessary to treat two or more surfaces simultaneously. For example, cutting edge of the cutting tool can be considered as the line of intersection of the generating surface  $T$  of the gear cutting tool by the rake surface  $R_s$ . Equation of the cutting edge cannot be derived on the premises of equations of the surfaces  $T$  and  $R_s$  as long as the initial parameterization of the surfaces is improper.

When two surfaces  $\mathbf{r}_i$  and  $\mathbf{r}_j$  are necessary been treated simultaneously, then they have not just been represented in a common reference system but the  $U_i$ - and  $V_i$ -parameters of one of the surfaces  $\mathbf{r}_i = \mathbf{r}_i(U_i, V_i)$  have to be synchronized with the corresponding  $U_j$ - and  $V_j$ -parameters of another surface  $\mathbf{r}_j = \mathbf{r}_j(U_j, V_j)$ . The procedure of changing of surface parameters is used for this purpose. Use of the procedure allows representation of one of the surfaces, for example, of the surface  $\mathbf{r}_j = \mathbf{r}_j(U_j, V_j)$  in the terms of the  $U_i$ - and  $V_i$ -parameters, say as  $\mathbf{r}_j = \mathbf{r}_j(U_i, V_i)$ .

If the parameterization of a surface is transformed by the equations  $U^* = U^*(U, V)$  and  $V^* = V^*(U, V)$ , we obtain the new derivatives

$$\frac{\partial \mathbf{r}}{\partial U^*} = \frac{\partial \mathbf{r}}{\partial U} \cdot \frac{\partial U}{\partial U^*} + \frac{\partial \mathbf{r}}{\partial V} \cdot \frac{\partial V}{\partial U^*} \quad (\text{C.1})$$

$$\frac{\partial \mathbf{r}}{\partial V^*} = \frac{\partial \mathbf{r}}{\partial U} \cdot \frac{\partial U}{\partial V^*} + \frac{\partial \mathbf{r}}{\partial V} \cdot \frac{\partial V}{\partial V^*} \quad (\text{C.2})$$

so that

$$\mathbf{A}^* = \left[ \frac{\partial \mathbf{r}}{\partial U^*} \middle| \frac{\partial \mathbf{r}}{\partial V^*} \right] = \mathbf{A} \cdot \mathbf{J} \quad (\text{C.3})$$

where

$$\mathbf{J} = \begin{bmatrix} \frac{\partial U}{\partial U^*} & \frac{\partial U}{\partial V^*} \\ \frac{\partial V}{\partial U^*} & \frac{\partial V}{\partial V^*} \end{bmatrix} \quad (\text{C.4})$$

is called the *Jacobian matrix* of the transformation.

It can be shown that the new fundamental matrix  $\mathbf{G}^*$  is given by

$$\mathbf{G}^* = \mathbf{A}^{*T} \mathbf{A}^* = \mathbf{J}^T \mathbf{A}^T \mathbf{A} \mathbf{J} = \mathbf{J}^T \mathbf{G} \mathbf{J} \quad (\text{C.5})$$

From this equation, we see by the properties of determinants that  $|\mathbf{G}^*| = |\mathbf{J}|^2 |\mathbf{G}|$ . Using this result, and Eq. (C.2), we can show that the unit surface normal  $\mathbf{n}$  is invariant under the transformation, as we could expect.

The transformation of the second fundamental matrix can similarly be shown to be given by

$$\mathbf{D}^* = \mathbf{J}^T \mathbf{D} \mathbf{J} \quad (\text{C.6})$$

by differentiating equations (C.2) and using the invariance of  $\mathbf{n}$ . From Eqs. (C.5) and (C.6), it can be shown that the principal curvatures and directions are invariant under the transformation.

We conclude that the unit normal vector  $\mathbf{n}$  and the principal directions and curvatures are independent of the parameters used, and are therefore geometric properties of the surface itself. They should be continuous if the surface is to be tangent and curvature continuous.

## Appendix D

### Closest Distance of Approach Between Two Part Surfaces

Generally, the problem of the calculation of the closest distance of approach between two smooth regular part surfaces is a sophisticated and challenging one. As per the author's knowledge, no general solution to the problem of calculation of the closest distance of approach between two smooth regular surfaces is available in the public domain. For the purpose of calculation of the deviation,  $\delta_g$ , of the actual part surface,  $P_{1.ac}$ , with respect to the desired (nominal) part surface,  $P_{1.nom}$ , the problem under consideration can be reduced to the problem of computation of the closest distance of approach between two torus surfaces,  $Tr_{p.1}$  and  $Tr_{p.2}$ .

Consider a smooth regular part surface,  $P_1$ , and an interacting smooth regular part surface,  $P_2$ , that initially are given in a common stationary coordinate system,  $X_h Y_h Z_h$ , as illustrated in Fig. D.1. The part surfaces,  $P_1$  and  $P_2$ , are locally approximated by portions of torus surfaces,  $Tr_{p.1}$  and  $Tr_{p.2}$ , respectively.<sup>8</sup> Again, not all points of the torus surfaces,  $Tr_{p.1}$  and  $Tr_{p.2}$ , can be used for the local approximation of the gear and the pinion tooth flanks,  $P_1$  and  $P_2$ . Only points that are located either within the biggest meridian or within the smallest meridian of the torus surface are employed for this purpose.

The points,  $K_{p.1}$  and  $K_{p.2}^*$ , are chosen as the first guess points on the torus surfaces,  $Tr_{p.1}$  and  $Tr_{p.2}$ . For the analysis below, it is convenient to relabel the points,  $K_{p.1}$  and  $K_{p.2}^*$ , to  $g_i$  and  $p_i$  accordingly.

For a given configuration of the torus surfaces,  $Tr_{p.1}$  and  $Tr_{p.2}$ , the closest distance of approach between these surfaces can be used as a first approximation to

---

<sup>8</sup>Surfaces of the second order are less preferred for the purposes of local approximation as they possess a lower approximative capability compared to the torus surfaces.

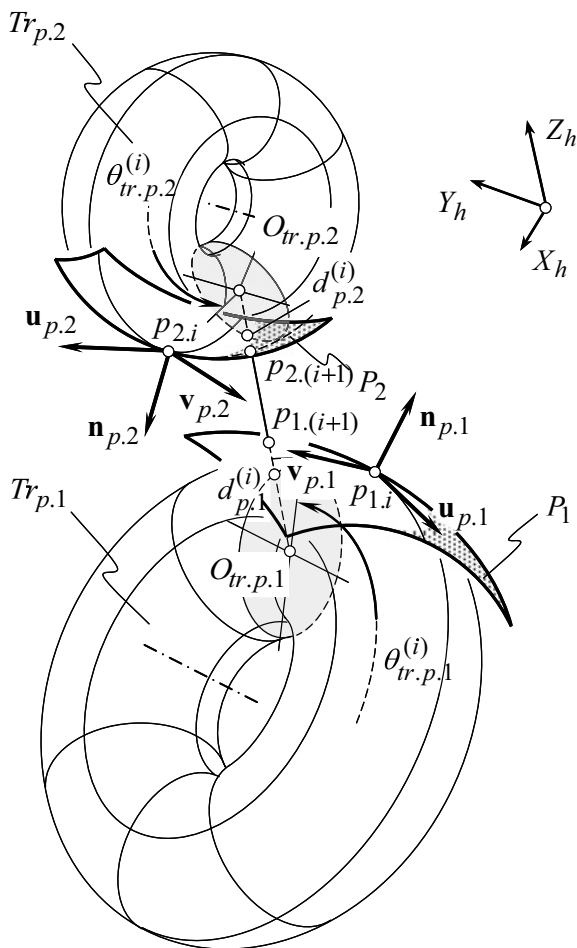


**Fig. D.1** Calculation of the closest distance of approach between two smooth regular part surfaces  $P_1$  and  $P_2$

the closest distance of approach between the original gear and the pinion tooth flanks,  $P_1$  and  $P_2$ .

The closest distance of approach between the torus surfaces,  $Tr_{p,1}$  and  $Tr_{p,2}$ , is measured along the common perpendicular to these surfaces. The following equations can be composed on the premises of this property of the closest distance of approach.

Unit normal vector,  $\mathbf{n}_{Tr,p,1}$ , to the torus surface,  $Tr_{p,1}$ , is located within a plane through the axis of rotation of the surface,  $Tr_{p,1}$ . In the coordinate system  $X_{tr,p,1}Y_{tr,p,1}Z_{tr,p,1}$  associated with the torus surface,  $Tr_{p,1}$ , the equation of a plane through the axis of rotation of the torus surface,  $Tr_{p,1}$ , can be expressed in the form:

$$[\mathbf{r}_{\text{tp},1} - \mathbf{r}_{\text{tr},p,1}^{(0)}] \times \mathbf{k}_{\text{tr},p,1} \times \mathbf{R}_{\text{tr},p,1} = 0 \quad (\text{D.1})$$

were is designated:

$\mathbf{r}_{\text{tp},1}$ —is the position vector of point of the plane through the axis of rotation of the torus,  $Tr_{p,1}$

$\mathbf{r}_{\text{tr},p,1}^{(0)}$ —is the position vector of point within the plane,  $\mathbf{r}_{\text{tp},1}$  (it is assumed below that this point coincides with the origin of the coordinate system,  $X_{\text{tr},p,1} Y_{\text{tr},p,1} Z_{\text{tr},p,1}$ )

$\mathbf{k}_{\text{tr},p,1}$ —is the unit vector of the  $Z_{\text{tr},p,1}$ -axis.

Equation (D.1) is expressed in terms of the radius,  $\mathbf{R}_{\text{tr},p,1}$ . This indicates that the set of all planes through the fixed  $Z_{\text{tr},p,1}$ -axis forms a pencil of planes. The equation of the pencil of planes,  $\mathbf{r}_{\text{tp},1}$ , in the common coordinate system,  $X_h Y_h Z_h$ , can be represented in the form:

$$\mathbf{r}_{\text{tp},1}(Z_{\text{tr},p,1}, V_{\text{tr},p,1}, \theta_{\text{tr},p,1}) = \mathbf{Rs}(Tr_{p,1} \mapsto h) \cdot \begin{bmatrix} V_{\text{tr},p,1} \cdot \cos \theta_{\text{tr},p,1} \\ V_{\text{tr},p,1} \cdot \sin \theta_{\text{tr},p,1} \\ Z_{\text{tr},p,1} \\ 1 \end{bmatrix} \quad (\text{D.2})$$

The unit normal vector,  $\mathbf{n}_{\text{tr},p,2}$ , to the torus surface,  $Tr_{p,2}$ , is located within a plane through the axis of rotation of the surface,  $Tr_{p,2}$ . In the coordinate system,  $X_{\text{tr},p,2} Y_{\text{tr},p,2} Z_{\text{tr},p,2}$ , that is associated with the surface,  $Tr_{p,2}$ , equation of a plane through the axis of rotation of the torus surface,  $Tr_{p,2}$ , can be represented in the form:

$$[\mathbf{r}_{\text{tp},2} - \mathbf{r}_{\text{tr},p,2}^{(0)}] \times \mathbf{k}_{\text{tr},p,2} \times \mathbf{R}_{\text{tr},p,2} = 0 \quad (\text{D.3})$$

Here is designated:

$\mathbf{r}_{\text{tp},2}$ —is the position vector of point of the plane through the torus,  $Tr_{p,2}$ , axis of rotation

$\mathbf{r}_{\text{tr},p,2}^{(0)}$ —is the position vector of point within the plane,  $\mathbf{r}_{\text{tp},2}$  (it is assumed below that this point coincides with the origin of the coordinate system,  $X_{\text{tr},p,2} Y_{\text{tr},p,2} Z_{\text{tr},p,2}$ )

$\mathbf{k}_{\text{tr},p,2}$ —is the unit vector of the  $Z_{\text{tr},p,2}$ -axis

Equation (D.3) is expressed in terms of the radius,  $\mathbf{R}_{\text{tr},p,2}$ . This indicates that the set of all planes through the fixed  $Z_{\text{tr},p,2}$ -axis forms a pencil of planes. The equation of this pencil of planes,  $\mathbf{r}_{\text{tp},2}$ , in the common coordinate system,  $X_h Y_h Z_h$ , can be represented in the form:

$$\mathbf{r}_{tp.2}(Z_{tr.p.2}, V_{tr.p.2}, \theta_{tr.p.2}) = \mathbf{Rs}(Tr_{p.2} \mapsto h) \cdot \begin{bmatrix} V_{tr.p.2} \cdot \cos \theta_{tr.p.2} \\ V_{tr.p.2} \cdot \sin \theta_{tr.p.2} \\ Z_{tr.p.2} \\ 1 \end{bmatrix} \quad (D.4)$$

A straight line through the points,  $d_{p.1}^{(i)}$  and  $d_{p.2}^{(i)}$ , along which the shortest distance of approach,  $d_{p.1/2}^{\min}$ , of the torus surfaces,  $Tr_{p.1}$  and  $Tr_{p.2}$ , is measured, is the line of intersection of the planes,  $\mathbf{r}_{tp.1}$  and  $\mathbf{r}_{tp.2}$ . Therefore, this line,  $d_{p.1/2}^{\min}$ , must be aligned with both unit normal vectors,  $\mathbf{n}_{tr.p.1}$  and  $\mathbf{n}_{tr.p.2}$ .

In the coordinate system,  $X_h Y_h Z_h$ , the equation for the unit normal vector,  $\mathbf{n}_{tr.p.1}$ , to the torus surface,  $Tr_{p.1}$ , yields representation in matrix form:

$$\mathbf{n}_{tr.p.1} = \mathbf{Rs}(Tr_{p.1} \mapsto h) \cdot \begin{bmatrix} (C_{tr.p.1} + \cos \varphi_{tr.p.1}) \cdot \cos \varphi_{tr.p.1} \cdot \cos \theta_{tr.p.1} \\ (C_{tr.p.1} + \cos \varphi_{tr.p.1}) \cdot \cos \varphi_{tr.p.1} \cdot \sin \theta_{tr.p.1} \\ (C_{tr.p.1} + \cos \varphi_{tr.p.1}) \cdot \sin \varphi_{tr.p.1} \\ 1 \end{bmatrix} \quad (D.5)$$

where  $C_{tr.p.1}$  designates the parameter  $C_{tr.p.1} = 1 - \frac{R_{2.p.1}}{R_{1.p.1}}$ .

Similarly, in the coordinate system,  $X_h Y_h Z_h$ , the equation for the unit normal vector,  $\mathbf{n}_{tr.p.2}$ , to the torus surface,  $Tr_{p.2}$ , yields matrix representation in the form:

$$\mathbf{n}_{tr.p.2} = \mathbf{Rs}(Tr_{p.2} \mapsto h) \cdot \begin{bmatrix} (C_{tr.p.2} + \cos \varphi_{tr.p.2}) \cdot \cos \varphi_{tr.p.2} \cdot \cos \theta_{tr.p.2} \\ (C_{tr.p.2} + \cos \varphi_{tr.p.2}) \cdot \cos \varphi_{tr.p.2} \cdot \sin \theta_{tr.p.2} \\ (C_{tr.p.2} + \cos \varphi_{tr.p.2}) \cdot \sin \varphi_{tr.p.2} \\ 1 \end{bmatrix} \quad (D.6)$$

where  $C_{tr.p.2}$  designates the parameter  $C_{tr.p.2} = 1 - \frac{R_{2.p.2}}{R_{1.p.2}}$ .

Evidently, the points  $O_{tr.p.1}$ ,  $O_{tr.p.2}$ ,  $d_{p.1}^{(i)}$ , and  $d_{p.2}^{(i)}$  (see Fig. D.1) are located within the straight line through the centers,  $O_{tr.p.1}$  and  $O_{tr.p.2}$ . The position vector,  $\mathbf{r}_{cd}$ , of this straight line can be calculated from the equation:

$$(\mathbf{r}_{cd} - \mathbf{r}_{cg}) \times (\mathbf{r}_{cp} - \mathbf{r}_{cg}) = 0 \quad (D.7)$$

where is designated:

$\mathbf{r}_{cg}$ —is the position vector of a point on the circle of a radius,  $R_{tr.p.1}$

$\mathbf{r}_{cp}$ —is the position vector of a point on the circle of a radius,  $R_{tr.p.2}$

It is necessary that the straight line,  $\mathbf{r}_{cd}$ , be along the unit normal vectors,  $\mathbf{n}_{tp.1}$  and  $\mathbf{n}_{tp.2}$ , to the torus surfaces,  $Tr_{p.1}$  and  $Tr_{p.2}$ .

Considered together, Eqs. (D.2), (D.4), and (D.7), make possible calculation of the closest distance of approach between the torus surfaces,  $Tr_{p.1}$  and  $Tr_{p.2}$ . Then, the straight line,  $d_{p.1/2}^{\min}$ , intersects the part surface,  $P_1$ , and the part surface,  $P_2$ , at the

points,  $g_{i+1}$  and  $p_{i+1}$ , correspondingly. The points,  $g_{i+1}$  and  $p_{i+1}$ , serve as the second guess to the closest distance of approach between the surfaces,  $P_1$  and  $P_2$ .

The cycle of the recursive calculations is repeated as many times, as necessary for making the deviation of the calculation of the closest distance of approach between the surfaces,  $P_1$  and  $P_2$ , smaller than the maximal permissible value.

There is an alternative approach for the calculation of the closest distance of approach between two torus surfaces. The direction of the unit normal vector to an offset surface to,  $Tr_{p,1}$ , is identical to the direction of the unit normal vector,  $\mathbf{n}_{tr,p,1}$ , to the torus surface,  $Tr_{p,1}$ . This statement is also valid for the unit normal vector  $\mathbf{n}_{tr,p,2}$  to the torus surface,  $Tr_{p,2}$ . This property of the unit normal vectors,  $\mathbf{n}_{tr,p,1}$  and  $\mathbf{n}_{tr,p,2}$ , can be used for the modification of the method of calculation of the closest distance of approach between two torus surfaces.

The equation of the circle of radius,  $R_{tr,p,1}$ , yields matrix representation:

$$\mathbf{r}_{cg}(\theta_{tr,p,1}) = \mathbf{Rs}(P_1 \mapsto h) \cdot \begin{bmatrix} R_{tr,p,1} \cdot \cos \theta_{tr,p,1} \\ R_{tr,p,1} \cdot \sin \theta_{tr,p,1} \\ 0 \\ 1 \end{bmatrix} \quad (D.8)$$

The equation of the circle of radius,  $R_{tr,p,2}$ , can be analytically described in the similar way:

$$\mathbf{r}_{cp}(\theta_{tr,p,2}) = \mathbf{Rs}(P_2 \mapsto h) \cdot \begin{bmatrix} R_{tr,p,2} \cdot \cos \theta_{tr,p,2} \\ R_{tr,p,2} \cdot \sin \theta_{tr,p,2} \\ 0 \\ 1 \end{bmatrix} \quad (D.9)$$

The distance,  $d_{gp}$ , between two arbitrary points on the circles,  $\mathbf{r}_{cp,1}(\theta_{tr,p,1})$  and  $\mathbf{r}_{cp,2}(\theta_{tr,p,2})$ , equals:

$$d_{gp}(\theta_{tr,p,1}, \theta_{tr,p,2}) = |\mathbf{r}_{cp,1}(\theta_{tr,p,1}) - \mathbf{r}_{cp,2}(\theta_{tr,p,2})| \quad (D.10)$$

The distance,  $d_{gp}$ , is minimal for a specific (optimal) combination of the parameters,  $\theta_{tr,p,1}$  and  $\theta_{tr,p,2}$ . The favorable values of the parameters,  $\theta_{tr,p,1}$  and  $\theta_{tr,p,2}$ , can be calculated on solution of the set of two equations:

$$\frac{\partial}{\partial \theta_{tr,p,1}} \mathbf{r}_{cp,1}(\theta_{tr,p,1}) = 0 \quad (D.11)$$

$$\frac{\partial}{\partial \theta_{tr,p,2}} \mathbf{r}_{cp,2}(\theta_{tr,p,2}) = 0 \quad (D.12)$$



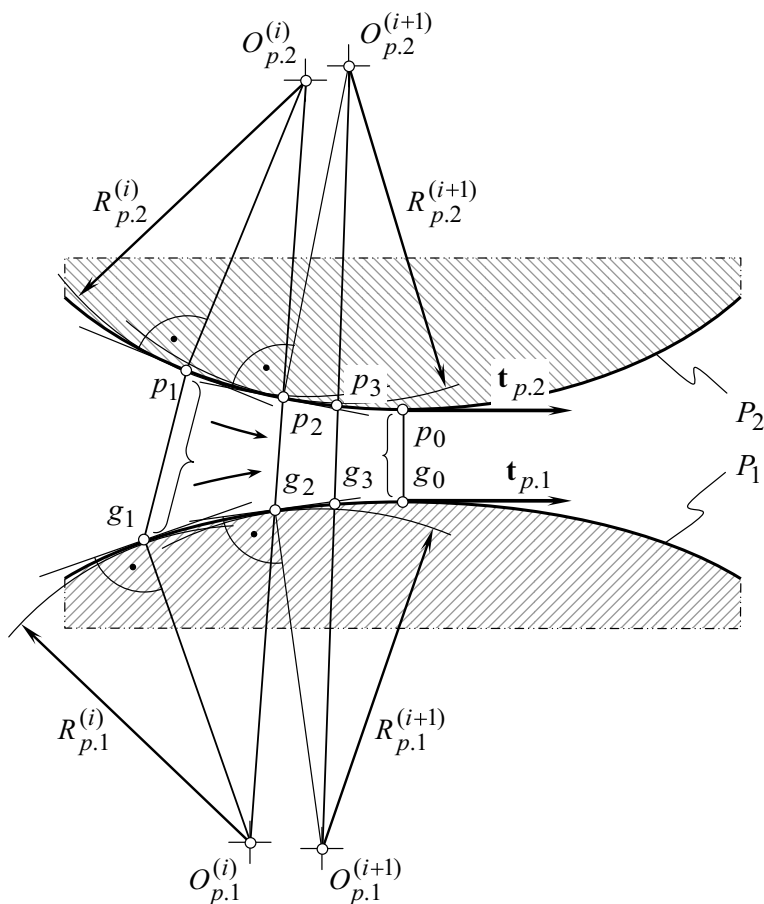


**Fig. D.2** Convergence of the methods of calculation of the closest distance of approach between two smooth regular part surfaces  $P_1$  and  $P_2$

On solution of Eqs. (D.11) and (D.12), the optimal values,  $\theta_{tr,p,1}^{(opt)}$  and  $\theta_{tr,p,2}^{(opt)}$ , can be determined. These angles specify the direction of the closest distance of approach of the torus surfaces,  $Tr_{p,1}$  and  $Tr_{p,2}$ .

Following this method, the three-dimensional problem of calculation of the closest distance of approach of two torus surfaces is reduced to the problem of calculation of the closest distance of approach between two circles. Under a certain scenario, the last approach could possess an advantage over the previous approach.

Convergence of the disclosed algorithms for the computation of the closest distance of approach between two smooth regular surfaces is illustrated in Fig. D.2. The computation procedure is convergent regardless of the actual location of the first guess points on the surfaces,  $P_1$  and  $P_2$ .

It is instructive to draw attention here to the similarities between the disclosed iterative method for the computation of the closest distance of approach between two smooth regular surfaces, and between the “*Newton-Raphson’s method*,” the iterative method of chords, and so forth. Many similarities can be found out on this comparison.

## Uncited References

1. Olivier T. (1839). *Théorie Géométrique des Engrenages destinés à transmettre le mouvement de rotation entre deux axes ou non situés dans un même plan*, Bulletin de la soc d’Encouragement etc. (Vol. xxviii, p. 430).
2. Radzevich, S. P. (1988). *Advanced technological processes of sculptured surface machining* (56 p), Moscow: VNIITEMR.
3. Radzevich, S. P. (2008). *CAD/CAM of sculptured surfaces on multi-axis NC machine: The DG/K-based approach* (114 p). San Rafael, CA: M&C Publishers.
4. Radzevich, S. P. (1989). *Methods of milling of sculptured surfaces* (72 p). Moscow: VNIITEMR.
5. Radzevich, S. P. (1987). *New achievements in the field of sculptured surface machining on multi-axis NC machine* (48 p). Moscow: VNIITEMR.
6. Rodin, P. R. (1961). *Issues of theory of cutting tool design* (Doctoral dissertation) (373 p). Odessa: Odessa Polytechnic Institute.
7. Rodin, P. R., Linkin, G. A., & Tatarenko, G. A. (1976). *Machining of sculptured surfaces on NC machines* (200 p). Kiev: Technica.

# Glossary

We list, alphabetically, the most commonly used terms in engineering geometry of surfaces. In addition, most of the newly introduced terms are listed below as well.

**Auxiliary generating surface  $R$**  A smooth regular surface that is used as an intermediate (auxiliary) surface when an envelope for successive position of a moving surface is determined.

**$C_a$ -gearing** Crossed-axes gearing or a gearing having axes of rotation of the gear and of the pinion that are skewed in relation to one another.

**Cartesian coordinate system** A reference system comprised of three mutually perpendicular straight axes through the common origin. Determination of the location of a point in a Cartesian coordinate system is based on the distances along the coordinate axes. Commonly, the axes are labeled as  $X$ ,  $Y$ , and  $Z$ . Often, either a subscript or a superscript is added to the designation of the reference system  $XYZ$ .

**Center distance** This is the closest distance of approach between the two axes of rotation. In the particular case of hypoid gearing, the center distance is often referred to as the “*offset*”.

**Characteristic line** This is a limit configuration of the line of intersection of a moving surface that occupies two distinct positions when the distance between the surfaces in these positions is approaching zero. In the limit case, a characteristic line,  $E$ , aligns with the line of tangency of the moving surface and with the envelope for successive positions of the moving surface.

**“Darboux frame”** In the differential geometry of surfaces, this is a local moving *Cartesian* reference system constructed on a surface. The origin of a “*Darboux frame*” is located at a current point of interest on the surface. The axes of the “*Darboux frame*” are along three unit vectors, namely along the unit normal vector to the surface and two unit tangent vectors along principal directions on

the gear tooth flank. The “*Darboux frame*” is analogous to the “*Frenet-Serret frame*” as applied to the geometry of spatial curves. A “*Darboux frame*” exists at any non-umbilic point of a surface. It is named after the French mathematician *Jean Gaston Darboux*.

**Degree of conformity** This is a qualitative parameter to evaluate how the part surface of one member of a kinematic pair is close to part surface of another member of the kinematic pair at a point of their contact (or at a point within the line of contact of the part surfaces).

**Dynamic surface** This is a part surface that is interacting with the environment.

**Engineering surface** This is a part surface that can be reproduced on a solid using for this purpose any production method.

**Free-form surface** This is a kind of part surfaces (see: “*sculptured part surface*” for more details).

**Indicatrix of conformity** This is a planar centro-symmetrical characteristic curve of the fourth order that is used for the purpose of analytical description of the contact geometry of two part surfaces. In particular cases, the indicatrix of conformity also possesses the property of mirror symmetry.

**Natural kind of surface representation** Specification of a surface in terms of the first and second fundamental forms commonly referred to as a “*natural kind of a surface representation*”.

**Part surface** This is one of the numerous surfaces that bound a solid.

**Point of contact** This is any point at which two tooth profiles touch each other.

**“*R-gearing*”** A perfect crossed-axes gearing that features line contact between tooth flanks of the gear and pinion.

**$\mathbb{R}$ -mapping of the interacting part surfaces** A kind of mapping of one smooth regular part surface onto another smooth regular part surface, under which normal curvatures at every point of the mapped surface correspond to normal curvatures at a corresponding point of a given surface.

**“*Reversibly enveloping surfaces*” (or just “*R<sub>e</sub>-surfaces*”)** A pair of smooth regular part surfaces that are enveloping to one another regardless of which one of the surfaces is traveling, and which of them is the enveloping. All instant lines of action in “*reversibly enveloping surfaces*” intersect the axis of instant rotation.

**Rotation vector** A vector along an axis of rotation having magnitude that is equal to the rotation about the axis. The direction of the rotation vector depends upon direction of the rotation. Commonly, the rotation vector is designated  $\boldsymbol{\omega}$ . The magnitude of the rotation vector is commonly denoted  $\omega$ . Therefore, the equality  $\omega = |\boldsymbol{\omega}|$  is always valid. The rotation vector of a gear is designated  $\boldsymbol{\omega}_g$ , the rotation vector of a mating pinion is designated  $\boldsymbol{\omega}_p$ , and rotation vector of the

plane of action is designated as  $\omega_{pa}$ . Formally, the “*rotation vector*” is not a vector, as no rotation can be expressed by a vector. Therefore, special care is necessary when treating a rotation as a vector: the order of multipliers is important when coordinate system transformations are performed (no alteration of the multipliers is allowed).

**Sculptured part surface** This is a kind of part surfaces parameters of local geometry where every two neighboring infinitesimally small patches differ from one another. “*Free form surface*” is another terminology that is used for part surfaces of this particular kind.

**“*S<sub>pr</sub>-gearing*”** A kind of real crossed-axes gearing that features equal base pitches, that is, (a) an angular base pitch of a gear, (b) an angular base pitch of a mating pinion, and (c) an angular operating base pitch of the gear pair, are equal to one another under various values of the axes misalignment. Gearing of this kind is capable of to accommodate for the axes misalignment, is noiseless, and features the highest possible power density.

**Surface that allow for “*sliding over itself*”** A smooth regular surfaces, for which there exists a motion, that results in the envelope for successive position of the moving surface being congruent to the surface itself.

**Vector of instantaneous rotation** A vector along the axis of instant rotation of one part surface in relation to another part surface. The magnitude of the vector of instant rotation is a signed value and is equal to the difference of the rotations of these two part surfaces (depending on which of the surfaces,  $P_1$  and  $P_2$ , is assumed motionless, either the equation  $\omega_{p1} = \omega_{P1} - \omega_{P2}$  or the equation  $\omega_{p1} = \omega_{P2} - \omega_{P1}$  is valid). Commonly, the rotation vector is designated as  $\omega_{p1}$ .

# Bibliography

- Akivis, M. A., & Goldberg, V. V. (1972). *An introduction to linear algebra and tensors*. New York: Dover.
- Artobolevskii, I. I. (1965). *Theory of mechanisms* (776 p). Moscow: Nauka.
- Ball, R. S. (1998). *A treatise on the theory of screws* (544 p). Cambridge (Eng.): Printed by J. and C. P. Clay, at the University Press, 1900, 544p. Cambridge, New York: Cambridge University Press, 588p. ISBN 0521636507.
- Ball, R. S. (1876). *The theory of screws*. Dublin: Hodges & Foster.
- Barnhill, R. E., & Riesenfeld, R. F. (1974). *Computer-aided geometric design*. NY: Academic Press.
- Bezier, P. E. (1970). *Emploi les Machines a Commande* (p. 456). Numirique. Paris: Massonet Cie.
- Bezier, P. (1972). *Numerical control: Mathematics and applications* (240 p). In: (A. R. Forrest & A. F. Pankhurst, Trans.). London: Wiley.
- Bezier, P. (1986). *The mathematical basis of the UNISURF CAD system*. London: Butterworths.
- Bezier, P. E. (1973). Uniserf system. In *Proceedings of IFIP-IFAC Conference PROLOMAT-73* (pp. 417–442).
- Blashke, V. (1957). *Introduction into differential geometry* (224 p). Moscow: GITTL.
- Boehm, W., & Prautzsch, H. (1994). *Geometric concepts for geometric design* (402 p). A K Peters: Wellesley, Massachusetts.
- Boltyanskii, V. G. (1964). *Envelopes* (76 p). NY: McMillan Co.
- Bringing line geometry together with CAGD: computational line geometry* (563 p.). (2001). In H. Pottmann & J. Wallner (Eds.) Berlin: Springer. ISBN 3-540-42058-4.
- Bruce, J. W., & Giblin, P. J. (1984). *Curves and singularities*. Cambridge: Cambridge University Press.
- Burke, W. L. (1985). *Applied differential geometry*. Cambridge: Cambridge University Press.
- B'ushgens, S. S. (1940). *Differential geometry* (300 p). Moscow, GTTI.
- Choi, B. K. (1991). *Surface modeling for CAD/CAM* (389 p) Elsevier.
- Clar, L., & Hart, J. A. (1980). *Calculus with analytic geometry for the technologies*. Englewood Cliffs, NJ: Prentice-Hall.
- da Vinci, L. (1974). *The madrid codices* (Vol. 1, p. 1493). Facsimile Edition of “*Codex Madrid 1*”, original Spanish title: *Tratado de Estatica y Mechanica en Italiano*, McGraw Hill Book Company.
- Darboux, G. (1896). *Lecons Sur la Théorie Générale des Surfaces* (Vol. 4). Paris: Gauthier-Villars.

- Darboux, G. (1887). *Lecons Sur la Théorie Générale des Surfaces et ses Applications geometrie infinitesimal* (Vol. 1). Paris: Gauthier-Villars.
- Denavit, J., & Hartenberg, R. S. (1955). A kinematics notation for lower-pair mechanisms based on matrices. *ASME Journal of Applied Mechanics*, 77, 215–221.
- doCarmo, M. P. (1976). *Differential geometry of curves and surfaces* (503 p). Englewood Cliffs, NJ: Prentice-Hall.
- Eisenhart, L. P. (1909). *A treatise on the differential geometry of curves and surfaces* (474 p). London: Dover Publications, Inc., New York (reprint 1960).
- Farin, G. E. (1990). *Curves and surfaces for computer aided design. A practical guide* (444 p). New York: Academic Press.
- Farin, G. E. (2001). *Curves and surfaces for CAGD. A practical guide* (5th ed. 499 p.). San Francisco: Morgan Kaufmann Publishers. ISBN 1-55860-737-4 (Publication date: October 1, 2001).
- Farin, G. E. (1999). *NURBS from projective geometry to practical use* (267 p). A K Peters: Natick, Massachusetts.
- Farin, G. E., & Hansford, D. (2000). *The essential of CAGD* (229 p). A K Peters: Natick, Massachusetts.
- Farin, G. E., & Hansford, D. *The geometry toolbox for graphics and modeling* (288 p). Natick, Massachusetts: A K Peters. ISBN 1-56881-074-1.
- Faux, L. D., & Pratt, M. J. (1987). *Computational geometry for design and manufacture* (331 p). Chichester, NY: Ellis Horwood Limited Publishers, Wiley.
- Favard, J. (1957). *Course de Géométrie Différentielle Locale* (viii + 553 p). Paris: Gauthier-Villars.
- Ferguson, R. S. (2001). *Practical algorithms for 3D computer graphics* (539 p). A K Peters: Natick, Massachusetts.
- Finikov, S. P. (1961). *Differential geometry* (158 p). Moscow: Moscow State University Publishers.
- Finikov, S. P. (1934). *Theory of surfaces* (200 p). Moscow: GTTI.
- Fisher, G. (Ed.). (1986). *Mathematical models*. Braunachweig/Wiesbaden: Friedrich Vieweg & Sohn.
- Flanders, H. (1963). *Differential forms*. New York: Academic Press.
- Flaquer, J., Garate, G., & Pargade, M. (1992). Envelopes of moving quadric surface. *Computer-Aided Geometric Design*, 9, 299–312.
- Foley, J. D., & Van Dam, A. (1982). *Foundations of interactive computer graphics* (664 p). Addison-Wesley Publishing Company.
- Forrest, A. R. (1971). Computational geometry. *Proceedings of Royal Society of London*, A321, 187–195.
- Forsyth, A. R. (1912). *Lectures on the differential geometry of curves and surfaces* (525 p). Cambridge: at the University Press.
- Fuller, L. E. (1962). *Basic matrix theory* (245 p). Englewood Cliffs, NJ.
- Fundamental developments of computer-aided geometric modeling* (414 p). (1993). In L. Piegl (Ed.) New York, NY: Academic Press. ISBN 0-12-554765-X.
- Gantmakher, F. (1967). *Theory of matrices* (575 p). Moscow: Nauka.
- Gasson, P. C. (1983). *Geometry of spatial forms* (601 p). Chichester: Ellis Horwood.
- Gauss, K.-F. (1902). *Disquisitiones Generales Circa Superficies Curvas*, Gottingen, 1828. (In J. C. Morehead & A. M. Hildebrandt (Eds.), English translation: *General investigation of curved surfaces*, Princeton). Reprinted with introduction. New York: Courant, Raven Press, Hewlett, 1965, 119 p.
- Geometric and algorithmic aspects of computer-aided design and manufacturing*. (2005). In J. Ravi, M. Smid, & D. Dutta (Eds.), *DIMACS Workshop. Computer-Aided Design and Manufacturing*, October 7–9, 2003, Piscataway, NJ. *DIMACS series in discrete mathematics and theoretical computer science* (Vol. 67, 345 p). American Mathematical Society. ISBN 0821836285.

- Geotz, A. (1970). *Introduction to differential geometry*. Reading: Addison-Wesley.
- Gilbert, D., & Cohn-Vossen, S. (1999). *Geometry and the imagination* (357 p). Providence, Rhode Island: Ams Chelsea Publishing.
- Giusti, E. (1978). On the equation of surfaces of prescribed mean curvature. *Inventiones Mathematicae*, 46, 111–137.
- Graphic gems* (834 p). (1990). In A. S Glassner (Ed.), Palo Alto, California, Boston: Xerox Palo Alto Research Center, Academic Press, Inc., Harcourt Brace Jovanovich, Publishers.
- Graustein, W. C. (1935). *Differential geometry*. New York: MacMillan.
- Guggenheimer, H. W. (1963). *Differential geometry*. New York: McGraw-Hill.
- Hamilton, W. R. (1969). In C. J. Joly (Ed.), *Elements of quaternions* (Vol. I, 3rd ed., 594 p). New York, NY: Chelsea Publication Company.
- Hamilton, W. R. (1969). In C. J. Joly (Ed.), *Elements of quaternions* (Vol. I, 3rd ed., 502 p). New York, NY: Chelsea Publication Company.
- Hamilton, W. R. (1844). On quaternions: Or on a new system of imaginaries in algebra. *Philosophical Magazine*, 25, 10–14.
- Hamilton, W. R. (1884). On quaternions: Or on a new system of imaginaries in algebra. *Philosophical Magazine*, 3rd Series, 25, 489–495.
- Hausdorff, F. (1914). *Grundzüge der Mengenlehre*. New York: Leipzig: Veit & Comp. Reprint Chelsea, 1949.
- Held, M. (1991). *On the computational geometry of pocket machining*. Springer.
- Hertz, H. (1981). Über die Berührung Fester Elastischer Körper (The Contact of Solid Elastic Bodies). *Journal für die Reine und Angewandte Mathematik (Journal for Pure and Applied Mathematics)*, 156–171 (Berlin); *Über die Berührung Fester Elastischer Körper und Über die Härte (The Contact of Solid Elastic Bodies and Their Harnesses)*, Berlin, 1882; Reprinted in: H. Hertz (Ed.), *Gesammelte Werke (Collected works)* (Vol. 1, pp. 155–173 and pp. 174–196), Leipzig, 1895, D. E. Jones & G. A. Schottor Trans. The English translation: *Miscellaneous papers*, pp. 146–162, 163–183), London: McMillan and Co., Ltd., 1896.
- Hertz, Heinrich. (1881). On contact of solid elastic bodies and on hardness. *J. Math.*, 92, 156–171.
- Hilbert, D., & Cohn-Vossen, S. (1952). *Geometry and the imagination* (357 p). NY: Chelsea Publishing Company.
- Hohn, F. E. (1973). *Elementary matrix algebra* (3rd ed.). NY: McMillan.
- Hopf, H. (1955). *Lectures on differential geometry in the large* (155 p) (USA: Typewritten, Copy: The Library of Brown University).
- Hoschek, J., & Laser, D. (1993). *Fundamentals of Computer aided geometric design* (727 p). A K Peters: Wellesley, Massachusetts.
- Jeffreys, H. (1961). *Cartesian tensors* (p. 93 p). Cambridge: University Press.
- Karelin, N. M. (1966). *Guideless machining of cylindrical surfaces* (1987 p). Moscow: Mashinostroyeniye.
- Kartan, E. (1962). *Extrinsic differential systems and their geometrical applications* (238 p). Moscow: Moscow State University Publishers.
- Kartan, E. (1963). *Theory of finite continuous groups and differential geometry disclosed by means of mobil trihedron method* (368 p). Moscow: Moscow State University Publishers.
- Kells, L. M., Kern, W. F., & Bland, J. R. (1951). *Plane and spherical trigonometry* (3rd ed., 318 p). NY: McGraw Hill.
- Kliot-Dashinskii, M. I. (1974). *Algebra of matrices and vectors* (160 p). Leningrad: Leningrad State University Publishers.
- Koenderink, J. J. (1990). *Solid shape* (699 p). Cambridge, Massachusetts: The MIT Press.
- Korneychuk, N. P. (1984). *Splines in the theory of approximation* (352 p). Moscow: Nauka.
- Kreyszig, E. (1959). *Differential geometry* (352 p). Toronto: University of Toronto Press.
- Kreyszig, E. (1991). *Differential geometry*. New York: Dover.
- Korn, G. A., & Korn, T. M. (1968). *Mathematical handbook for scientists and engineers. Definitions, theorems and formulas for reference and review* (2nd, enlarged and revised ed., 832 p). NY: McGraw-Hill Book Company.



- Kvason, B. I. (2000). *Methods of shape-preserving spline approximation* (338 p.). NJ, London, Hong Kong: World Scientific Publishing Co. Pte. Ltd. ISBN 981-02-4010-4.
- Liming, R. (1944). *Practical analytical geometry with application to aircraft*, Macmillan.
- Liming, R. (1979). *Mathematics for computer graphics*, Aero Publishers (1979).
- Lowe, P. G. (1980). A note on surface geometry with special reference to twist. *Mathematical Proceedings of the Cambridge Philosophical Society*, 87, 481–487.
- L'ukshin, V. S. (1968). *Theory of screw surfaces in designing of cutting tools* (372 p). Moscow: Mashinostroyeniye.
- Makhanov, S. S., & Anotaipaiboon, W. (2007). *Advanced numerical methods to optimize cutting operations of five-axis milling machines* (206 p). Berlin, Heidelberg: Springer. ISBN 978-3-540-71120-9.
- Marciniak, K. (1985). *Podstawy Geometryczne Obróbki Powierzchni Krzywoliniowych na Frezarzach Sterowanych Numericznie* (177 p). Wydawnictwa Politechniki Warszawskiej: Warszawa.
- Marciniak, K. (1991). *Geometric modeling for numerically controlled machining* (245 p). NY: Oxford University Press.
- Milinskii, V. I. (1934). *Differential geometry* (332 p). Leningrad: Kubuch.
- Miron, R. (1958). *Observatii a Supra Unor Formule din Geometria Varietatilor Neonolonne  $E_3^2$* . *Buletinul Institutului Politehnic din Iasi*.
- Monge, G. (1850). *Application de l'Analyse à la Géométrie*. Paris: Bachalier.
- Monge, G. (1811). *Géométrie descriptive* (Nouvelle ed.). Paris: J. Klostermann Fils.
- Monge, G. (1799). *Leçons de Géométrie Descriptive*, Paris.
- Montaldi, J. A. (1986). Surfaces in 3-space and their contact with circles. *Journal of Differential Geometry*, 23, 109–126.
- Mortenson, M. (1990). *Computer graphics handbook* (259 p). New York: Industrial Press Inc.
- Mortenson, M. E. (1985). *Geometric modeling* (763 p). NY: Wiley. ISBN 0-471-882279-8.
- Mortenson, M. (1995). *Geometric transformations* (357 p). New York: Industrial Press Inc.
- Mortenson, M. (1999). *Mathematics for computer graphics application* (2nd ed., 354 p). New York: Industrial Press Inc.
- Norden, A. P. (1956). *Theory of surfaces* (259 p). Moscow: GTTI.
- Nutbourn, A. W. (1986). A circle diagram for local differential geometry. In J. Gregory (Ed.), *Mathematics of surfaces.*, Conference Proceedings, Institute of Mathematics and its Application, 1984 Oxford: Oxford University Press.
- Nutbourn, A. W., & Martin, R. R. (1988). *Differential geometry applied to curve and surface design* (Vol. 1, 282 p). Chichester: Foundations, Ellis Horwood Ltd. Publishers.
- O'Neil, B. (1966). *Elementary differential geometry* (411 p). New York and London: Academic Press.
- Patrikalakis, N. M., & Maekawa, T. (2002). *Shape interrogation for computer aided design and manufacturing* (480 p). New York: Springer. ISBN 3-540-42454-7.
- Paul, P. R. (1981). *Robot manipulators: mathematics, programming, and control. The computer control of robot manipulators* (279 p.). Cambridge, Massachusetts and London, England: The M I T Press (Second Printing, 1982).
- Piegl, L., & Tiller, W. (1995). *The NURBS book (monographs in visual communications)* (2nd ed., 1997, 646 p). New York: Springer, ISBN 3-540-35069-0, ISBN 3-540-61545-8.
- Plücker, J. (1865). On a new geometry of space. *Philosophical Transactions, titled Philosophical Transactions of the Royal Society*, 155, 725–791.
- Radzevich, S.P. (1988). A quantitative measure of degree of conformity between a part surface and the generating surface of the cutting tool. In *Investigation in the field of production of cutting tool, and in metal cutting* (pp. 19–29). Tula: Tula Polytechnic Institute.
- Radzevich, S.P. (1988). Part Surfaces those allow for Sliding over themselves. In *Investigation in the field of part surface generation* (pp. 29–53). Dneprodzerzhinsk: Dneprodzerzhinsk Industrial Institute. Department In UkrNIINTI on 02.01.1989, No. 65-Uk89/.

- Rogers, D. F., & Adams, J. A. (1976). *Mathematical elements for computer graphics* (239 p). NY: McGraw-Hill Book Company.
- Stechkin, S. V., & Subbotin, Yu N. (1976). *Splines in computational mathematics* (248 p). Moscow: Nauka.
- Stoker, J. J. (1969). *Differential geometry* (404 p). New York: Wiley-Interscience.
- Stout, K. J. (1988). Engineering surfaces—a philosophy of manufacture (a proposal for good manufacturing practice). *Journal of Engineering Manufacture*, 212(B3), 169–174.
- Strang, G. (1986). *Introduction to applied mathematics* (758 p). Massachusetts: Wellesley-Cambridge Press.
- Struik, D. J. (1961). *Lectures on classical differential geometry* (2nd ed., 232 p). Massachusetts: Addison-Wesley Publishing Company Inc.
- Trudinger, N. S. (1990). A priori bounds and necessary conditions for solvability of prescribed curvature equations. *Manuscripta Mathematica*, 67, 99–117.
- Trudinger, N. S., & Urbas, J. I. E. (1983). The Dirichlet problem for the equation of prescribed gauss curvature. *Bulletin of Australian Mathematical Society*, 28, 217–231.
- Urbas, J. I. E. (1984). The equation of prescribed gauss curvature without boundary conditions. *Journal of Differential Geometry*, 20, 311–327.
- Vaisman, I. Unele Observatii Privind Suprafetele si Varietatile Neonolonome din  $S_3$  Euclidian. *Mathematica*, Academia R.P.R., Filila Iasi, Studii si Cercetari Stiintifice, 10(1), 195
- Willmore, T. J. (1959). *An introduction to differential geometry* (317 p.). London E.C.4, 1959: Oxford University Press, Amen House.
- Woodsford, P. A. (1971). Mathematical methods in computer graphics—a survey. In *Gessellschaft fur Informatike* (Vol. 5), Symposium on Computer Graphics, Berlin.
- Wildhaber, E. (1948). *Fundamentals of meshing of bevel and hypoid gearing* (176 p). Moscow: Mashgiz.
- Yamaguchi, F. (1988). *Curves and surfaces in computer aided design* (378 p). Berlin, Heidelberg, New York, London, Paris, Tokyo: Springer.
- Yerikhov, M. L. (1965). *Application of the double enveloping principle for the purposes of analysis and synthesis of gears* (Ph.D. thesis). Leningrad: Leningrad Polytechnic Institute.
- Yerikhov, M. L. (1972). *Principles of systematic, methods of analysis and issues of synthesis of schemes of gearing* (Doctoral thesis). Khabarovsk: Khabarovsk Polytechnic Institute, 373 p.
- Zalgaller, V. A. (1975). *Theory of envelopes* (104 p). Moscow: Nauka.
- Zav'alov, Y.S., Leus, V. A., & Skorospelov, V. A. (1985). *Splines in engineering geometry* (224 p). Moscow: Mashinostroyeniye.

# Index

## A

Absolute curvature at a surface point, 31  
 Actual surface, 16, 17  
 $\mathcal{H}_R(P_1)$  indicatrix of the first kind, 129  
 $\mathcal{H}_k(P_1)$ -indicatrix of the second kind, 129  
 $\mathcal{H}_R(P_1/P_2)$ -relative indicatrix of the first kind, 134  
 $\mathcal{H}_k(P_1/P_2)$ -relative indicatrix of the second kind, 135, 136  
 Asymptotes, 112, 113, 122  
 Axis of instant rotation, 208, 210, 211, 224, 226, 227

## B

Base cylinder, 23, 183–185  
 Base helix angle, 23, 184, 199  
 Bernoulli's lemniscates, 122  
 Bertrand equation (*Sophie Germain equation*), 29  
**Bertrand**, Joseph Louise François (1822–1900), 29  
**Bonnet**, Pierre Ossian (1819–1892), 18  
 Bonnet theorem, 18, 122, 233  
 Boundary surface, 15, 17

## C

$C_a$ -gearing (Crossed-Axes Gearing), 206–208, 211–213, 216, 217, 219, 220, 222–224  
*Cartesian coordinates* of a point, 6  
**Cauchy**, Augustin-Louis (1789–1857), 67  
**Christoffel**, Ervin Bruno (1829–1900), 160  
 Christoffel symbols, 160, 163  
 Circular chart, 42, 49, 50, 62, 63, 233  
 Circular diagram, 51–53, 55–62  
 Classical differential geometry, 11, 12, 17

Closed side of a part surface, 12  
**Codazzi**, Delfino (1824–1873), 18  
*Codazzi-Mainardi* equations of compatibility, 18  
 Computer-Aided Design/Computer-Aided Machining (CAD/CAM), 12, 19, 22  
 Contact geometry, 67–69, 75, 76, 79, 80, 91, 97, 100, 119, 131, 133, 141, 146, 153, 155, 156, 233, 234  
 Converse indicatrix of conformity, 115, 116  
 Coordinate angle, 105, 115  
 Coordinate Measuring Machine (CMM), 17  
 Curvature indicatrix, 47, 48, 50, 84, 86, 127–129, 233  
 Curvature vector, 124  
 Curvilinear (*Gaussian*) coordinates of a point, 226  
 Cylindroid, 119, 124

## D

**Darboux**, Jean Gaston (1842–1917), 27, 46  
*Darboux* trihedron (*Darboux* frame), 80, 84  
 Degree of conformity functions, 159, 160  
 Deviation of a point, 13  
 Discriminant of the first fundamental form, 19, 24, 29  
**Dupin**, François Pier Charles (1784–1873), 44  
 Dupin indicatrix, 43–48, 76, 83, 84, 86, 101–103, 105, 110–115, 130, 131, 134–136, 233  
 Dynamic surfaces, 35

## E

Engineering geometry, 11–13, 15, 17, 18, 21, 27, 47, 59, 67, 69, 70, 90, 91, 112, 126,

- 128, 131, 132, 136, 137, 141, 143, 155, 157, 167, 233, 281
- Enveloping surfaces, 167, 170–176, 183, 187, 189, 191, 192, 194, 195, 199, 200, 222–225, 227–232, 234, 235
- Euler equation, 51, 52, 81, 104
- F**
- Favard, Jean** (1902–1965), 67
- First fundamental form of a surface, 18, 19, 24
- First *Olivier* principle, 223, 227–229
- First order analysis, 75, 76
- First order contact, 68
- First principal plane section, 27, 29, 125
- Free-form surface, 3
- Full (*Gaussian*) curvature at a surface point, 30
- Functional surfaces, 35
- Fundamental magnitudes of the first order, 19, 20, 24, 27, 83, 104
- Fundamental magnitudes of the second order, 22, 25, 83, 91, 92, 104
- G**
- Gaussian* (curvilinear) coordinates of a point, 184
- Gaussian* (full) curvature at a surface point, 30
- Gauss, Johann Carl Friedrich** (1777–1855), 18
- Gauss* map, 32
- Gauss-Weingarten* equations, 161, 163
- Germain equation, 51, 52
- Germain, Marie-Sophie** (1776–1831), 51
- H**
- Hertz, Heinrich Rudolf** (1857–1894), 76
- I**
- Indicatrix of conformity, 101–106, 108–116, 136–142, 147, 234
- J**
- Jacobian* matrix, 282
- K**
- Kinematic method, 176–179, 183, 185, 187–189, 222, 234
- Koenderink, J.J.**, 42
- L**
- Lagrange equation for vectors, 241
- Lagrange, Joseph-Louis** (1736–1813), 67
- Local relative orientation, 69–73, 81, 82, 91, 104, 105, 108, 110, 115, 134, 149
- Local surface patch, 35, 37, 40, 42, 49, 50, 52, 55, 56, 59, 60, 62
- M**
- Machine element, 12
- Machine part, 12
- Mainardi, Gaspard** (1800–1879), 18
- Mean curvature at a surface point, 30
- Method of common perpendiculars, 196
- Meusnier, de La Place Jean Baptist Marie** (1754–1793), 29
- Mohr, Christian Otto** (1835–1918), 51
- N**
- Newton's* rings, 76
- Normal curvature, 27, 29, 30, 37, 39, 42, 44, 45, 47, 50, 51, 56–58, 61–64, 79–89, 98, 99, 101, 103, 104, 106, 112, 113, 115, 116, 124–127, 129, 132, 134, 144–147, 157, 159
- Normal plane section, 29, 80, 81, 83, 85, 98–100, 104, 108, 125, 126, 144–146
- O**
- Ockham's* razor, 128
- Ockham, William** (1285–1347/49), 128
- Olivier* principles, 189, 223, 224, 227, 228, 231, 232, 235
- Olivier, Theodore** (1793–1853), 189
- Open side of a part surface, 12
- Operator of resultant coordinate system transformation, 126, 278
- Operator of rolling/sliding, 3, 33, 35, 154, 172, 173, 176, 183, 191–193, 192, 193, 196, 211, 213, 216, 228, 234, 258, 259, 261–263
- Operator of rotation, 214, 215, 217, 218, 256, 264, 267, 268
- Operator of screw motion, 256–258
- Operator of translation, 247, 253, 256, 264
- Order of contact, 67, 68
- P**
- Perpendicular, 10, 11, 13, 27, 52, 53, 56, 68, 69, 75, 78, 82, 94, 99, 100, 108, 115, 119, 121, 132, 134, 154, 176–178, 189, 195, 197, 203–205, 210–212, 214, 222, 225, 226, 239, 266, 284
- Plücker* conoid, 119–128, 131, 136, 234
- Plücker* indicatrix, 128, 129
- Plücker, Julius** (1801–1868), 119
- Plücker* relative conoid, 132
- Plücker* relative indicatrix, 119, 132–134

Position vector of a point, 46, 47, 69, 71, 84, 86, 101, 102, 145, 158, 169, 178, 181, 182, 184, 219–222, 226, 286

Principal curvatures, 28–33, 36, 37, 39–41, 45, 55, 56, 58–60, 81–83, 110, 116, 124, 132, 135, 145, 282

Principal directions of a surface, 27, 28, 33, 37, 52, 64, 70, 71, 75, 81, 82, 89, 91, 110, 125, 134, 282

Principal radii of curvature, 28, 79, 125, 126, 129, 134, 146, 158

Pythagorean theorem, 54

## R

$\mathbb{R}$ -mapping, 154, 155, 158, 161, 164

Radius of normal curvature, 85, 97–100, 103, 104, 125, 126, 128, 155, 156

Radius of principal curvature, 28, 47, 79, 81, 83, 84, 125, 126, 129, 134, 142, 146, 158

Radius of relative curvature, 78

Relative characteristic curve, 131

Reversibly enveloping surfaces ( $R_c$ -surfaces), 194, 195, 198–200, 205, 206, 223, 224, 227, 231, 232, 234, 235

## S

Sculptured part surface, 3, 10, 11, 16, 33, 35, 36, 41, 51, 105, 109, 153, 155–157, 160, 165, 191

Second fundamental form of a surface, 17, 18, 20–22, 24, 25, 32, 91, 92, 94, 122, 163

Second *Olivier* principle, 223, 227, 230, 232

Second order analysis, 43, 76, 79, 85

Second plane section, 27

Second principal curvature, 37, 39, 40, 52, 55

Shape index, 31

Shape operator, 31–33

*Shishkov* equation of contact, 154, 181, 187, 188, 231, 234

*Shishkov*, V.A., 154, 176, 234

*Sophie Germain* equation (*Bertrand* equation), 29

$S_{pr}$ -gearing (crossed-axes gearing), 235

Surface curvedness, 33

Surface of lower tolerance, 17

Surface of relative curvature, 76, 78–80, 83, 89, 110–115, 134–136

Surface of upper tolerance, 16, 17

## T

Tangent plane, 10, 21, 27, 39–41, 47, 69–71, 73, 75, 83, 92–94, 97, 109, 124, 145, 154, 175, 176, 274

Tangent vector, 7, 8, 11, 23, 26, 27

*Taylor*, Brook (1685–1731), 68

Tolerance band, 15

Torsion at a surface point, 29, 51, 56, 93

## U

Unit normal vector, 10, 11, 16, 27, 43, 44, 56, 75, 80, 101, 124, 125, 132, 144–146, 154, 155, 157, 162, 174–177, 179, 181, 183–185, 187, 188, 222, 226, 227, 239, 273, 276, 282, 284–287

Unit tangent, 6, 7, 10, 11, 26, 27, 29, 52, 53, 70–73, 75, 76, 81, 93, 94, 125, 126, 273

Unit vector of principal directions, 94, 154

## V

Van *Dorn*, 32

Von *Seggern*, 120

## W

*Weingarten* equations, 32

*Weingarten*, Julius (1836–1910), 31

*Weingarten* map, 31